frontiers | Research Topics

Immunity and inflammatory responses in kidney disease: From mechanisms to novel therapeutic strategies

Edited by
Wei Jing Liu and Xu-jie Zhou

Coordinated by
Qingguo Liu

Published in
Frontiers in Immunology

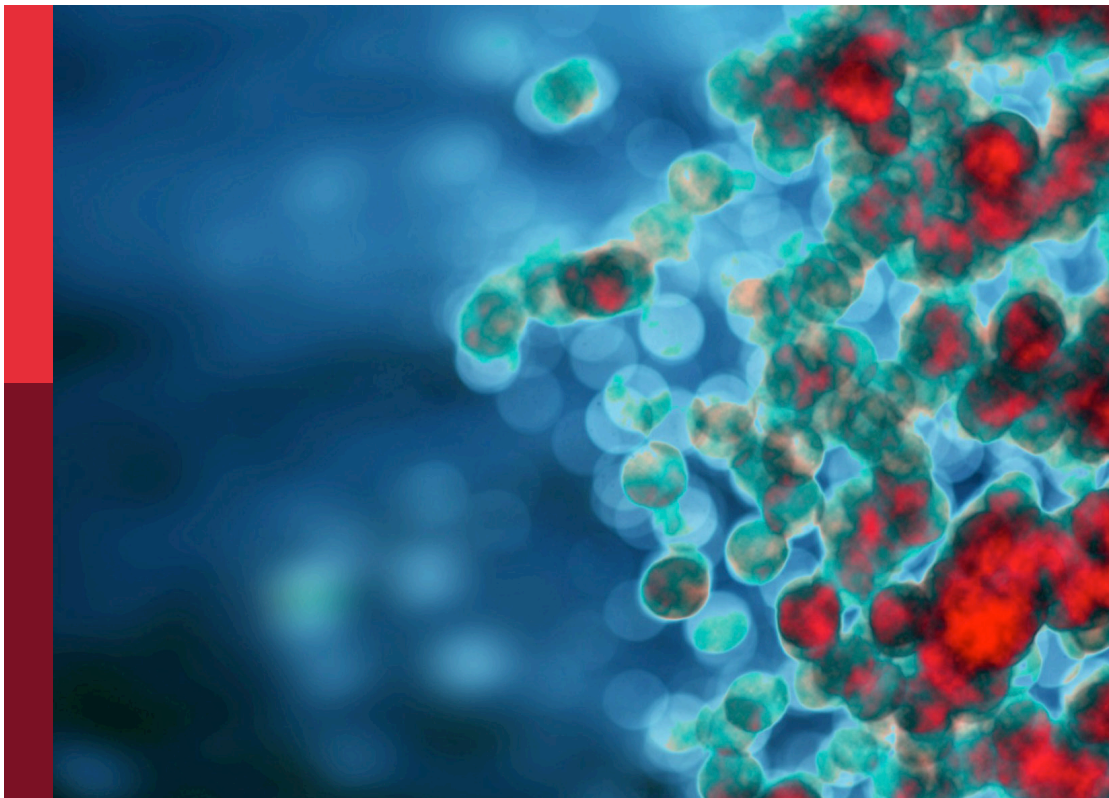

ISSN 1664-8714
ISBN 978-2-8325-5364-0
DOI 10.3389/978-2-8325-5364-0

About Frontiers

Frontiers is more than just an open access publisher of scholarly articles: it is a pioneering approach to the world of academia, radically improving the way scholarly research is managed. The grand vision of Frontiers is a world where all people have an equal opportunity to seek, share and generate knowledge. Frontiers provides immediate and permanent online open access to all its publications, but this alone is not enough to realize our grand goals.

Frontiers journal series

The Frontiers journal series is a multi-tier and interdisciplinary set of open-access, online journals, promising a paradigm shift from the current review, selection and dissemination processes in academic publishing. All Frontiers journals are driven by researchers for researchers; therefore, they constitute a service to the scholarly community. At the same time, the *Frontiers journal series* operates on a revolutionary invention, the tiered publishing system, initially addressing specific communities of scholars, and gradually climbing up to broader public understanding, thus serving the interests of the lay society, too.

Dedication to quality

Each Frontiers article is a landmark of the highest quality, thanks to genuinely collaborative interactions between authors and review editors, who include some of the world's best academicians. Research must be certified by peers before entering a stream of knowledge that may eventually reach the public - and shape society; therefore, Frontiers only applies the most rigorous and unbiased reviews. Frontiers revolutionizes research publishing by freely delivering the most outstanding research, evaluated with no bias from both the academic and social point of view. By applying the most advanced information technologies, Frontiers is catapulting scholarly publishing into a new generation.

What are Frontiers Research Topics?

Frontiers Research Topics are very popular trademarks of the *Frontiers journals series*: they are collections of at least ten articles, all centered on a particular subject. With their unique mix of varied contributions from Original Research to Review Articles, Frontiers Research Topics unify the most influential researchers, the latest key findings and historical advances in a hot research area.

Find out more on how to host your own Frontiers Research Topic or contribute to one as an author by contacting the Frontiers editorial office: frontiersin.org/about/contact

Immunity and inflammatory responses in kidney disease: From mechanisms to novel therapeutic strategies

Topic editors
Wei Jing Liu — Beijing University of Chinese Medicine, China
Xu-jie Zhou — Peking University, China

Topic coordinator
Qingguo Liu — Beijing University of Chinese Medicine, China

Citation
Liu, W. J., Zhou, X.-j., Liu, Q., eds. (2024). *Immunity and inflammatory responses in kidney disease: From mechanisms to novel therapeutic strategies*.
Lausanne: Frontiers Media SA. doi: 10.3389/978-2-8325-5364-0

Table of contents

frontiers | Frontiers in Immunology

TYPE Original Research
PUBLISHED 09 October 2023
DOI 10.3389/fimmu.2023.1252347

OPEN ACCESS

EDITED BY
Henry Liu,
Penn State Milton S. Hershey Medical Center, United States

REVIEWED BY
Zhongda Jin,
Guangdong Provincial Hospital of Chinese Medicine, China
Xueqin Zhang,
Hebei University of Chinese Medicine, China

*CORRESPONDENCE
Xiaojun Xiang
xxj7563@sina.com
Kezhen Yang
767299632@qq.com
Hongbo Chen
chenhb521@126.com

†These authors have contributed equally to this work

RECEIVED 03 July 2023
ACCEPTED 21 September 2023
PUBLISHED 09 October 2023

CITATION
Zhang P, Geng Y, Tang J, Cao Z, Xiang X, Yang K and Chen H (2023) Identification of biomarkers related to immune and inflammation in membranous nephropathy: comprehensive bioinformatic analysis and validation. *Front. Immunol.* 14:1252347. doi: 10.3389/fimmu.2023.1252347

Identification of biomarkers related to immune and inflammation in membranous nephropathy: comprehensive bioinformatic analysis and validation

Pingna Zhang[1†], Yunling Geng[2†], Jingyi Tang[2†], Zijing Cao[2], Xiaojun Xiang[1*], Kezhen Yang[3*] and Hongbo Chen[1*]

[1]Department of Nephrology, The First Affiliated Hospital of Zhejiang Chinese Medical University (Zhejiang Provincial Hospital of Chinese Medicine), Hangzhou, China, [2]Renal Research Institution of Beijing University of Chinese Medicine, and Key Laboratory of Chinese Internal Medicine of Ministry of Education and Beijing, Dongzhimen Hospital Affiliated to Beijing University of Chinese Medicine, Beijing, China, [3]Department of Rehabilitation Medicine, Sir Run Run Shaw Hospital, Zhejiang University School of Medicine, Hangzhou, China

Background: Membranous nephropathy (MN) is an autoimmune glomerular disease that is predominantly mediated by immune complex deposition and complement activation. The aim of this study was to identify key biomarkers of MN and investigate their association with immune-related mechanisms, inflammatory cytokines, chemokines and chemokine receptors (CCRs).

Methods: MN cohort microarray expression data were downloaded from the GEO database. Differentially expressed genes (DEGs) in MN were identified, and hub genes were determined using a protein-protein interaction (PPI) network. The relationships between immune-related hub genes, immune cells, CCRs, and inflammatory cytokines were examined using immune infiltration analysis, gene set enrichment analysis (GSEA), and weighted gene co-expression network analysis (WGCNA). Finally, the immune-related hub genes in MN were validated using ELISA.

Results: In total, 501 DEGs were identified. Enrichment analysis revealed the involvement of immune- and cytokine-related pathways in MN progression. Using WGCNA and immune infiltration analysis, 2 immune-related hub genes (*CYBB* and *CSF1R*) were identified. These genes exhibited significant correlations with a wide range of immune cells and were found to participate in B cell/T cell receptor and chemokine signaling pathways. In addition, the expressions of 2

immune-related hub genes were positively correlated with the expression of *CCR1*, *CX3CR1*, *IL1B*, *CCL4*, *TNF*, and *CCR2*.

Conclusion: Our study identified *CSF1* and *CYBB* as immune-related hub genes that potentially influence the expression of CCRs and pro-inflammatory cytokines (*CCR1*, *CX3CR1*, *IL1B*, *CCL4*, *TNF*, and *CCR2*). *CSF1* and *CYBB* may be potential biomarkers for MN progression, providing a perspective for diagnostic and immunotherapeutic targets of MN.

KEYWORDS

membranous nephropathy, immune, inflammatory cytokines, biomarkers, bioinformatics

1 Introduction

Membranous nephropathy (MN) is an autoimmune glomerular disease and is the most frequent cause of nephrotic syndrome (NS) in adults, accounting for approximately 30% of the cases, with individuals aged 30–50 years reaching the peak incidence rate (1, 2). Specific lesions of MN are the results of thickening of the glomerular capillary walls that results from the formation of immune deposits on the capillary wall (3). This immunological conflict is predominantly mediated by immune complex deposition and complement activation, which contribute to the impairment of glomerular filtration barrier, leading to nonselective proteinuria (4). Approximately 80% of MN cases occur without a specific cause (primary MN [pMN]), whereas 20% are associated with other diseases such as lupus erythematosus, infections (hepatitis B), malignancies, or drug intoxication (5).

The organ-specific autoimmune nature of pMN was determined in 2009 with the identification of phospholipase A2 receptor (PLA2R) in podocytes (6). Glomerular deposition of IgG on PLA2R is specific for pMN and is found in approximately 70% of cases reported in adults. This discovery has improved our understanding of the pathophysiology of pMN, in which circulating autoantibodies directly target podocyte antigens (7). This has opened a paradigm shift in the pathophysiological pattern, diagnosis, and targeted intervention for MN. Meanwhile, the mechanisms of autoimmunity initiation, exposure to antigens, and antibody pathogenicity have attracted much attention, revealing the significance of the immune system in the progression of MN (8). The initiation of MN may involve the cooperation of multiple factors, including genetic and environmental factors, as well as epigenetic and immune predispositions that result in the loss of immune system tolerance to develop MN (9). B and T cells, autoantibodies, cytokines, and complement system activation contribute to MN pathogenesis. A disordered proportion of regulatory T cells has been suggested to be the main characteristic of patients with MN without treatment (10). Some patients with MN display an increase in the $CD4^+/CD8^+$ subset ratio (11), which might be associated with the clinical response to immunosuppressive therapy; however, this was not confirmed in patients with MN treated with rituximab (12). In addition, the number of plasma cells and regulatory B cells in patients with MN was significantly higher than those in healthy individuals, and the number of PLA2R-specific memory B cells amplified *in vitro* may be related to circulating PLA2R antibody titers (13). Chemokines and chemokine receptors (CCRs) could recruit immune cells into tissues and are involved in inflammatory response (14). However, many aspects of the molecular mechanisms of immunity and chemokines involved in MN pathogenesis remain unclear.

Bioinformatics analysis has been widely utilized to reveal molecular pathogenesis of diseases and identify disease biomarkers (15). Microarray technology has been used in a range of bioinformatics analyses in the biomedical field to provide novel insights and help discover critical factors in the etiopathogenesis of diseases (16). In this study, gene expression profiles of MN were obtained using the Gene Expression Omnibus (GEO) database and differentially expressed genes (DEGs) were identified from them. Notably, weighted co-expression network analysis (WGCNA) and Gene Set Enrichment Analysis (GSEA) analyses were performed to explore immune cell infiltration in MN and further reveal immune-related pathways and identify potential biomarkers for MN. In addition, correlations between immune-related central genes and pro-inflammatory cytokines were analyzed. A flowchart of this study is shown in Figure 1.

2 Materials and methods

2.1 Data acquirement and preprocessing

Microarray expression data for the MN cohorts were obtained from the GEO database (http://www.ncbi.nlm.nih.gov/geo/). The GSE108113 dataset containing data of 44 cases of MN and six healthy controls was used as a training set. For validation, microarray expression data from an additional 51 patients with MN and 6 healthy controls were obtained from another dataset, GSE200828. The "ggord" and "yyplot" packages in R were used to perform principal component analysis (PCA) between samples. In this analysis, the sample separation among different groups were checked. Meanwhile, the "GEOquery" package was used to perform

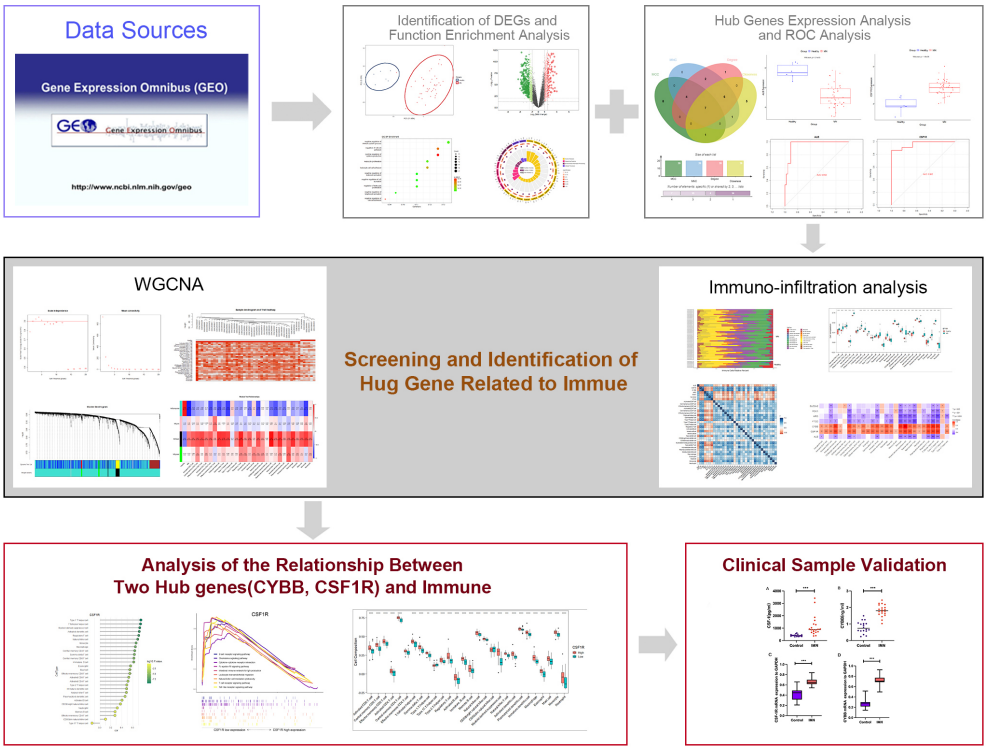

FIGURE 1
Technology roadmap for this study.

probe annotation and normalization of gene expression using the obtained datasets. When a gene corresponded to multiple probe IDs, only the ID with the highest average expression level was retained. The standardized matrix file was used for all subsequent downstream analyses.

2.2 Identification of DEGs, construction of PPI network, and screening of hub genes

Differential expression analysis was conducted using the 'limma' package in R software, employing a screening criterion of P-value < 0.05 and |log fold change (FC)| > 1.5 (17, 18). The resulting DEGs were visualized using various approaches including PCA, Venn diagrams, and volcano plots. To identify hub genes, a protein-protein interaction (PPI) network of DEGs was constructed using the STRING database (https://cn.string-db.org/). The PPI information was extracted with an interaction score of 0.4, specifically focusing on "Homo sapiens" as the species. Subsequently, the PPI network analysis results were exported to Cytoscape 3.9.1, for further investigation. The CytoHubba plug-in was employed to sort and filter the nodes within the network based on the network characteristics, aiding in the identification of core elements within this complex network. Core genes were identified using the degree, MNC, closeness, and MCC methods available in the CytoHubba plug-in. Common genes among the top 20 genes identified by each method were identified to determine the hub genes.

2.3 Functional enrichment analysis

GO and KEGG analyses of the DEGs were conducted using the Metascape database (https://metascape.org/). The analysis was limited to the species "Homo sapiens," and the KEGG screening conditions included a minimum overlap of 3, a P-value threshold of 0.01, and a minimum enrichment of 1.5. The DEG list was used for GO and KEGG enrichment analysis (19), and the results were visualized using the 'clusterprofiler' packages of R software and the OmicShare tools (https://www.omicshare.com/tools).

2.4 Validation of hub genes

The levels of different hub genes in patients with MN and healthy individuals were assessed by box plots, which were processed by the "ggplot2" package of R software. To further evaluate the predictive accuracy of the hub genes, receiver operating characteristic (ROC) curve analysis was performed to distinguish patients with MN from healthy individuals. Based on the obtained expression profile of hub genes and its high-throughput sequencing data, the ROC curves of hub genes were plotted using the "pROC " software package. The area under the curve (AUC) was used to compare the diagnostic value of the hub genes. Meanwhile, the independent external GSE200828 dataset was used to validate the expression levels and diagnostic value of the hub

genes in distinguishing patients with MN and healthy individuals.

2.5 Immune cell infiltration analysis and its correlation with hub genes

The ssGSEA algorithm (20) was utilized to quantify the infiltration levels of 28 immune cells in the selected samples from the GSE108113 dataset. The abundance of these 28 types of infiltrating immune cells in the GSE108113 samples was estimated using the "GSVA" package. The proportion of 22 immune cell types in the GSE108113 samples was estimated using CIBERSORTx. The relationship between hub genes and immune cell infiltration was estimated by the "GSVA" package, which was visualized using the "ggplot2" package. KEGG pathway datasets from different expression groups performed functional enrichment analyses by using "GSVA" package.

2.6 Weighted gene co-expression network analysis and its correlation with hub genes

To construct a gene co-expression network of the GSE108113 dataset, WGCNA was performed using the WGCNA package in R software. Genes with the highest absolute deviation of 25% from the median were selected for analysis (21). The quality of the analyzed data was evaluated by "goodSampleGenes" function, followed by clustering of samples and elimination of outlier samples. An ideal soft threshold was selected, and the "pickSoftThreshold" function was used to transform the matrix data into an adjacency matrix. This was followed by cluster analysis and modules were identified according to topological overlap. The results of immune infiltration obtained as phenotypic data were combined with WGCNA results to perform module analysis, which aimed to explore the relationship between the modules and immune cells. The genes in the module most closely related to immunity that overlapped with the hub genes were selected for further analysis.

2.7 Correlation of immune-related hub genes with chemokines and pro-inflammatory cytokines

To further analyze the correlation between immune-related hub genes, CCRs, and pro-inflammatory cytokines, lists of CCRs and pro-inflammatory cytokines were collected (Supplementary Table S1). Spearman correlation coefficients between immune-related hub genes, CCRs, and pro-inflammatory cytokines were analyzed. Thereafter, scatter plots depicting their relations were generated using the "ggstatsplot" package, presenting the linear relationship between them generated using the statistical method "lm.".

2.8 Enzyme-linked immunosorbent assay

To measure the protein levels of CSF-1 and CYBB/NOX2, we used specific ELISA kits for human CSF-1 (KE00184; Proteintech, USA) and CYBB/NOX2 (EK13559; Signalway Antibody, USA). Serum samples were collected from 20 patients with MN and 18 healthy controls (the clinical characteristics of the patients with MN and healthy controls are provided in Supplementary Table S2). ELISA was performed according to the manufacturer's instructions. Briefly, the standard samples and samples from both experimental groups were transferred to a 96-well plate. An equal volume of the kit reagent was added to each well, and the plate was incubated for 30 min. The stop solution was added, and the absorbance signal was measured at 450 nm using a plate reader.

2.9 RT-PCR

To test the gene expression level of CSF1R and CYBB in patients with MN and healthy controls, quantitative real-time polymerase chain reaction (RT–PCR) analysis of the mRNA levels of the genes from serum of patients was performed (Applied Biosystems, USA). The mRNA was reverse transcribed to cDNA using an Omniscript RT kit (Vazyme, China). RT-qPCR analysis was performed using the AceQ Universal SYBR qPCR Master Mix. After GAPDH normalization, the relative expression levels of the target gene were carried out with the $2^{-\triangle\triangle}$CT approach. The primer sequences are listed in Table 1.

2.10 Ethics approval and consent to participate

All patients came from Dongzhimen Hospital. Studies involving human participants were reviewed and approved by the Ethics Committee of Beijing Dongzhimen Hospital, First Clinical Medical College of Beijing University of Chinese Medicine. All the patients/participants provided written informed consent to participate in the study.

TABLE 1 Sequences of the primers designed for RT-qPCR.

Gene	Forward sequence	Reverse sequence
CYBB	TGGAAACCCTCCTATGACTTGG	AAACCGAACCAACCTCTCACAAA
CSF1R	GCTGCTTCACCAAGGATTATG	GGGTCACTGCTAGGGATG
GAPDH	GCACCGTCAAGGCTGAGAAC	TGGTGAAGACGCCAGTGGA

3 Results

3.1 Sorting of sample data, identification of DEGs and screening of hub genes

PCA distinctly indicated the separation of patients with MN from healthy controls (Figure 2A). A total of 501 DEGs were identified during differential expression analysis based on adjusted P-value < 0.05 and |logFC| > 1.5. Among these DEGs, 133 were upregulated and 368 were downregulated (Figure 1) (Supplementary Table S3). Using the STRING database, a PPI network of DEGs was constructed, comprising 273 nodes and 840 edges. The scores for degree, MNC, closeness, and MCC were calculated using the CytoHubba plug-in, and the top 20 genes from each method were intersected to identify seven hub genes: *SLC2A2*, *HRG*, *CYBB*, *PCK1*, *CSF1R*, *FTCD*, and *ALB*. The Venn diagram in Figure 2B shows the overlap between DEGs.

3.2 GO and KEGG enrichment analysis of DEGs

During KEGG enrichment analysis, the upregulated KEGG pathways were related to the MAPK signaling pathway, cytokine-cytokine receptor interactions, and NK cell-mediated cytotoxicity (Figures 3A-C). During GO analysis, the upregulated genes were mainly involved in the negative regulation of the immune system process, endocytic vesicles, and heme binding (Figure 3D). Among the downregulated genes, the most relevant downregulated KEGG pathways were those related to metabolism of xenobiotics by cytochrome P450, drug metabolism, and chemical carcinogenesis-receptor activation (Figures 3E-G). The genes downregulated in MN were mostly related to amino acid metabolic process, apical part of cell, and transmembrane transporter activity (Figure 3H). Detailed information is provided in Supplementary Table S4.

3.3 Validation of hub gene expression and diagnostic efficacy

Box plots were constructed to assess the expression levels of the seven hub genes between patients with MN and healthy controls (Figure 4A). The expression levels of *ALB* (P=2.1e-05), *FTCD* (P=6.3e-05), *HRG* (P=1.6e-05), *PCK1* (P=8.1e-06), and *SLC2A2* (P=0.0019) in MN were significantly lower than those in healthy controls. However, the expression levels of *CSF1R* (P=1.6e-05) and *CYBB* (P=2.1e-05) in patients with MN were significantly higher than those in healthy controls (Figure 4B). Furthermore, to validate the expression levels of these seven hub genes in patients with MN and healthy controls, an independent external dataset, GSE200828, was used, and the results were consistent with those from the GSE108113 dataset (Figure 5A). The diagnostic ability of these seven hub genes was validated using GSE200828 dataset. The values of AUC of the seven hub genes showed that all seven hub genes indicated favorable diagnostic value for MN, with an AUC of 0.958 (95%CI 90.52%-100%) for *ALB*, AUC of 0.962 (95%CI 90.53%-100%) for *CSF1R*, AUC of 0.958 (95%CI 90.23%-100%) for *CYBB*, AUC of 0.943 (95%CI 87.22%-100%) for *FTCD*, AUC of 0.962 (95% CI 91.1%-100%) for *HRG*, AUC of 0.970 (95%CI 92.44%-100%) for *PCK1*, and AUC of 0.871 (95%CI 73.74%-100%) for *SLC2A2* (Figure 5B). Thus, all seven hub genes exhibited high diagnostic values, with AUC values > 0.85.

3.4 Immune cell infiltration and association between hub genes

To investigate the relative level of immune cell infiltration between patients with MN and healthy controls, the CIBERSORT algorithm was used. The distribution of the 22 immune cell infiltrations in GSE108113 is presented as a bar plot (Figure 6A). Immune cell infiltration analysis revealed that the numbers of $CD4^+$

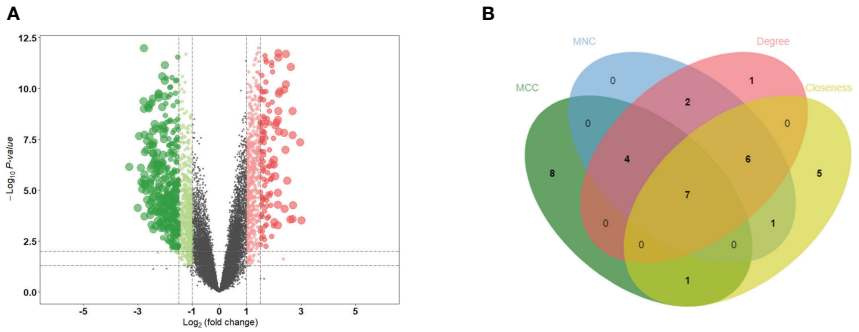

FIGURE 2
Identification of DEGs and hub genes. **(A)** Volcano diagram of DEGs. Red indicates upregulated genes and green indicates downregulated genes. **(B)** Venn diagram for screening hub genes. DEGs, differentially expressed genes.

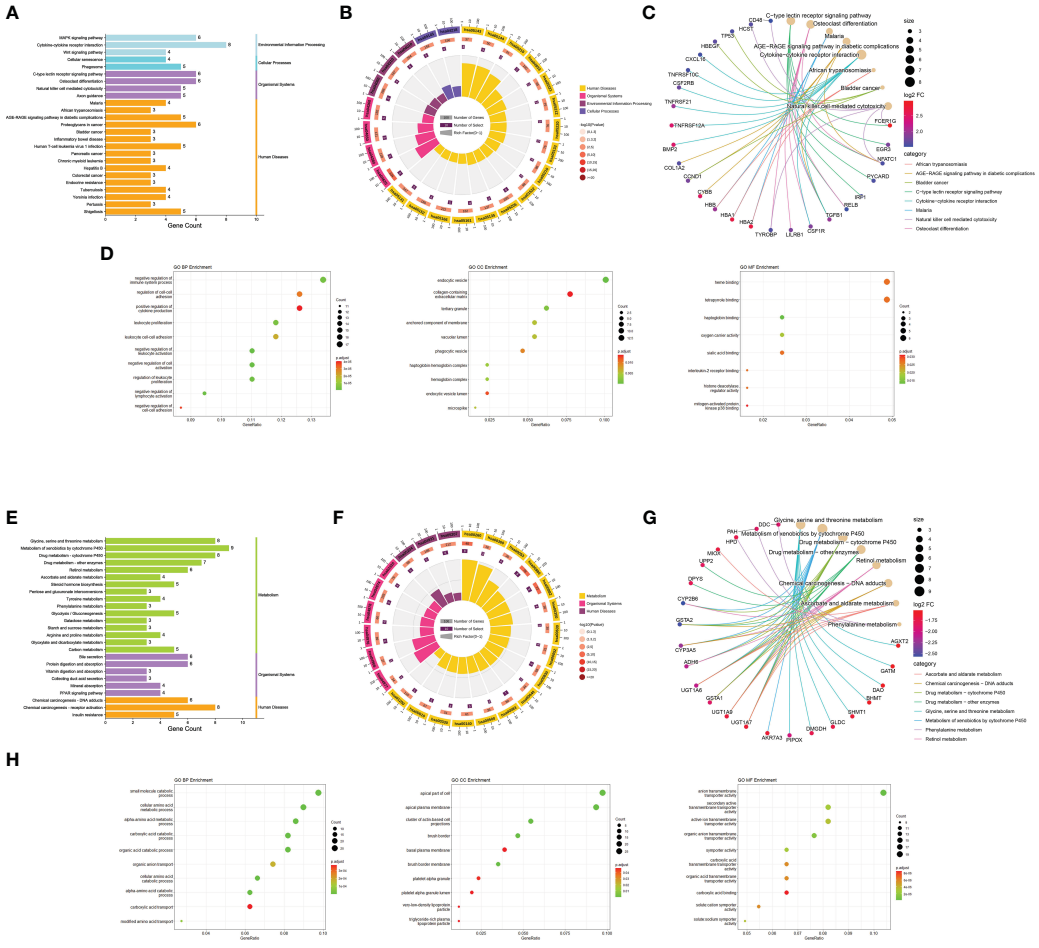

FIGURE 3
Functional enrichment analysis. **(A)** Bar graph of KEGG pathway enrichment analysis of upregulated genes. The horizontal coordinate indicates the number of genes annotated to the pathway, and different colors represent different pathway classifications. **(B)** Circle diagram of KEGG pathway enrichment analysis of upregulated genes. The first circle indicates the number of the pathway; the second circle indicates the number of genes and P-value of the pathway; the third circle indicates the number of genes annotated to the pathway; and the fourth circle indicates the enrichment coefficient for each pathway. **(C)** Network diagram of KEGG pathway enrichment analysis of upregulated genes indicate the specific target distribution on the pathway. **(D)** Bubble plot of GO enrichment analysis of upregulated genes, including BP, CC, and MF. The size of the dots indicates the number of genes, and the color corresponds to the P-value. **(E-H)** GO and KEGG pathway enrichment analysis of downregulated genes. BP: biological process, CC: cell component, MF: molecular function.

T cells, $CD8^+$ T cells, natural killer (NK) cells, monocytes, and macrophages were significantly higher in MN tissues than in healthy tissues ($P < 0.001$) (Figure 6B). Furthermore, the correlation between the seven hub genes and 28 immune cells was assessed. *CYBB* and *CSF1R* exhibited positive correlations with several immune cells, particularly central memory $CD4^+$ T cells (cor = 0.70, $P < 0.001$; cor = 0.640, $P < 0.001$), monocyte (cor = 0.776, $P < 0.001$; cor = −0.640, $P < 0.001$), activated dendritic cell (cor = 0.750, $P < 0.001$; cor = 0.724, $P < 0.001$), T follicular helper cell (cor = 0.782, $P < 0.001$; cor = 0.744, $P < 0.001$) and regulatory T cell (cor = 0.737, $P < 0.001$; cor = 0.715, $P < 0.001$). In addition, *SLC2A2, PCK1, HRG, FTCD*, and *ALB* levels were negatively correlated with most immune cells, including central memory $CD4^+$ T cells, monocytes, NK cells, and follicular helper T cells ($P < 0.05$) (Figures 6C, D).

3.5 Co-expression network construction and hub module identification

For WGCNA, 6,221 genes were selected. The appropriate soft threshold was determined to be $\beta = 2$, indicating a scale-free network (Figure 7A). Combining the results of immune infiltration with WGCNA, the correlation between each sample and the 28 immune cells is shown in Figure 7B. Four gene modules were obtained by merging similar modules (Figure 7C). As revealed by heat maps, the correlations between multiple modules of 28 immune cells associated with patients with MN and healthy controls are presented in Figure 7D, which shows that immune cells are closely associated with genes in the black module. Within the black module, two immune-related hub genes, *CSF1R* and *CYBB*, were selected by intersecting the genes in the module with previously identified hub genes.

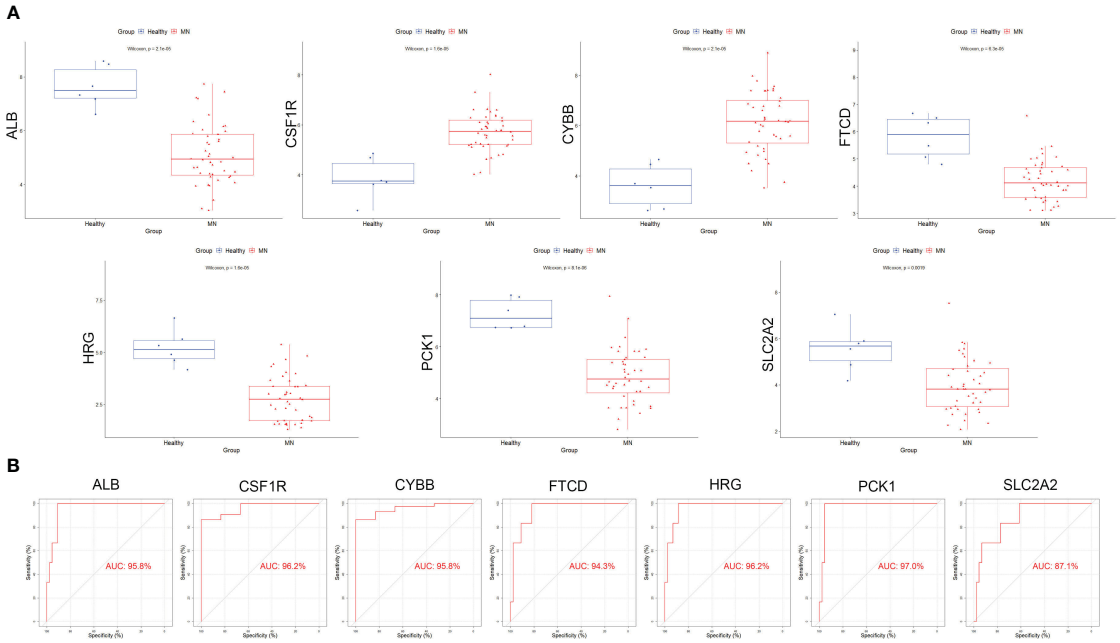

FIGURE 4
Validation of hub genes in the exploration cohort. **(A)** The expression of each hub gene in different subgroups. **(B)** AUC values for each hub gene in the ROC curve. AUC: area under the curve. ROC: receiver operating characteristic.

3.6 Correlation analysis between two hub genes and immune cell infiltration

To further explore the correlation between two hub genes and immune cells infiltration, the "GSVA" and "ggplot" packages were used for analysis and visualization. As shown in Figures 8A, D, both *CSF1* and *CYBB* displayed a significant positive correlation with 28 immune cells, except type 17 helper cells (P <0.005). In Figures 8C, F, the boxplot shows the abundance of 28 immune cells corresponding to hub genes at different expression levels. Due to

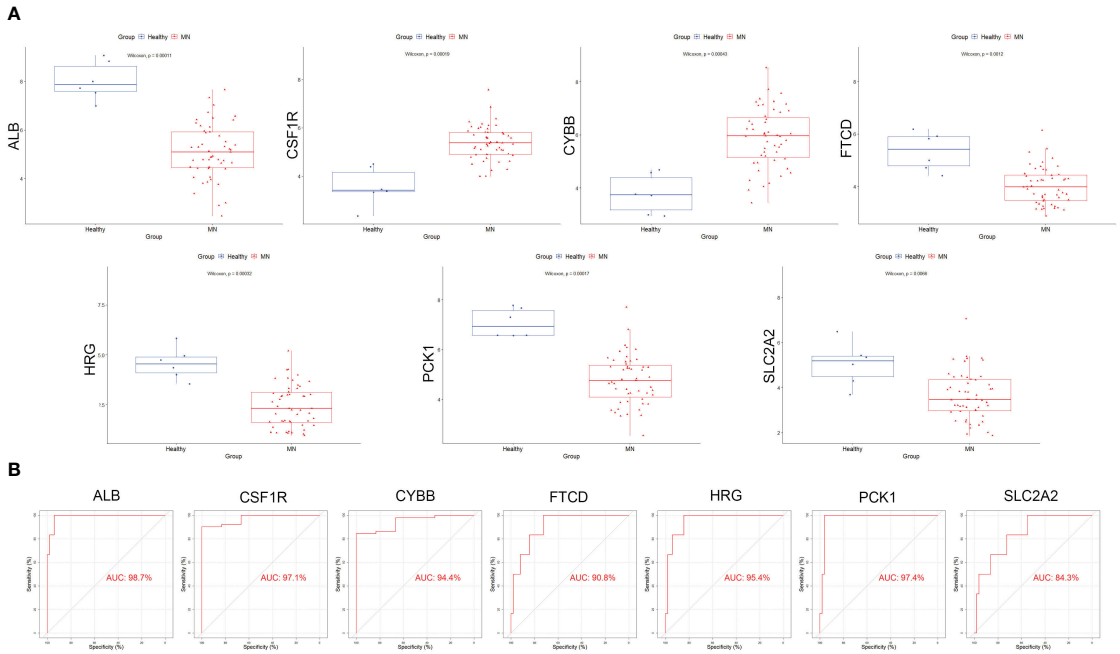

FIGURE 5
Validation of the hub genes in the validation cohort. **(A)** The expression of each hub gene in different subgroups. **(B)** AUC values for each hub gene in the ROC curve.

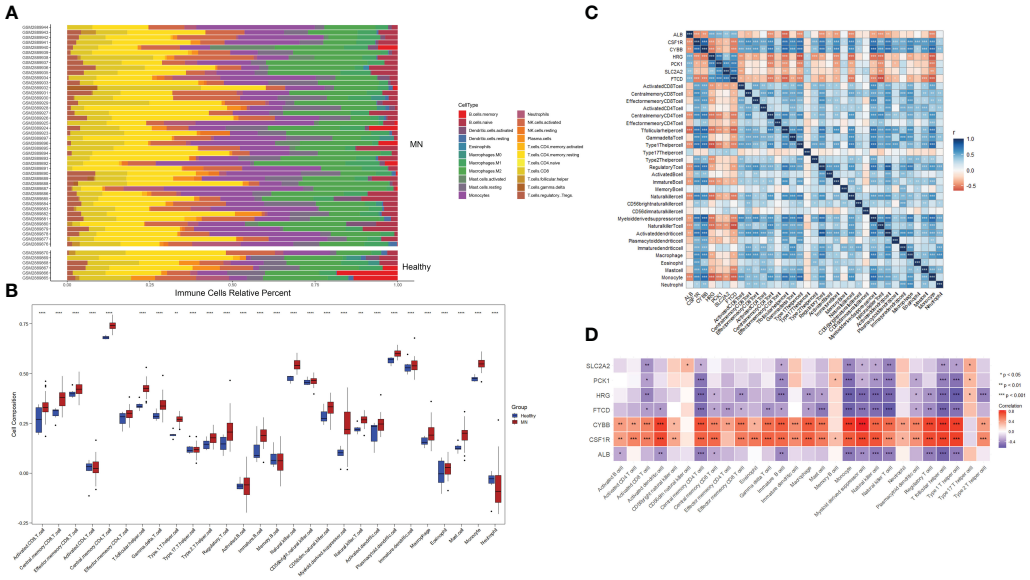

FIGURE 6
Immune cell infiltration analysis. **(A)** Plot of the percentage of 22 immune cells in each sample. Different colors represent different immune cells. **(B)** The distribution of 28 immune cells in different groups. **(C, D)** Correlation between 28 immune cells and hub genes. The color indicates the correlation size. *P <0.05, **P <0.01, ***P <0.001, ****P <0.0001.

the similarity in the grouping of these two genes at different expression levels, the results of immune cell infiltration analysis are also similar, but they are actually different. $CD4^+$ T cells, $CD8^+$ T cells, NK cells, monocytes, and macrophages evidently exhibited high immune scores for high *CYBB* and *CSF1R* expression (P < 0.001), which further verified that the two hub genes were responsible for the pathogenesis of immune-mediated MN.

The GSEA of DEGs that take the canonical pathways gene sets (c2.cp.kegg.v7.5.1.symbols) in the MsigDB database as a reference was performed with the criteria of | normalized enriched score

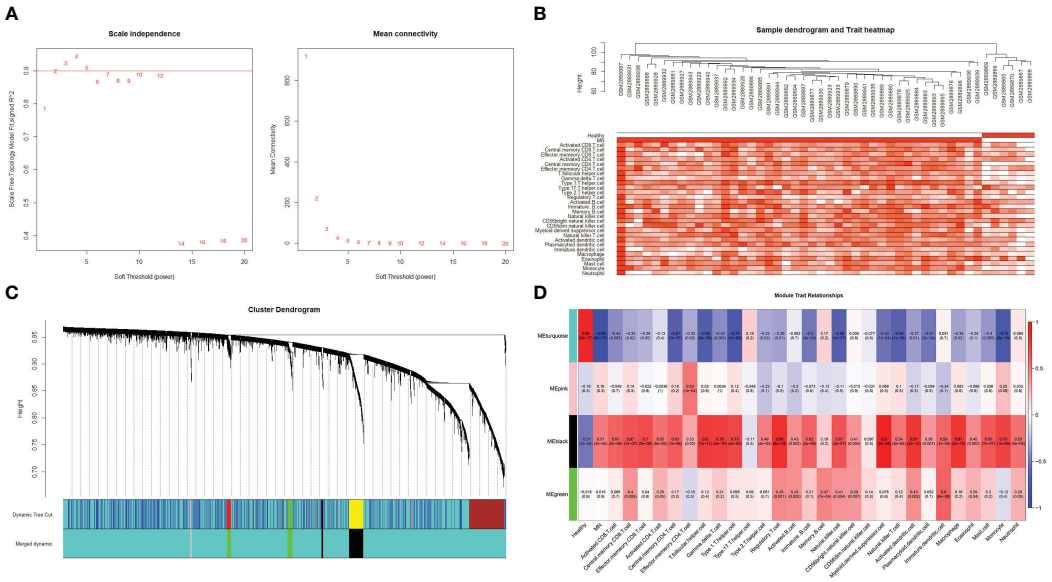

FIGURE 7
Weighted gene co-expression network analysis **(A)** Determination of the soft threshold value. The red line indicates the soft threshold value corresponding to a correlation coefficient of 0.9. **(B)** The samples were analyzed for clustering, observed for the presence of outliers, and combined with the results of immune cell infiltration. **(C)** Clustered dendrogram of the top 25% absolute deviations of the median, with each branch representing one gene. Each color at the bottom indicates one module, and the modules after merging are shown below. **(D)** Heat map of the relationship between modules and traits. The black modules in the graph clearly correlate more strongly with multiple immune cells than other modules.

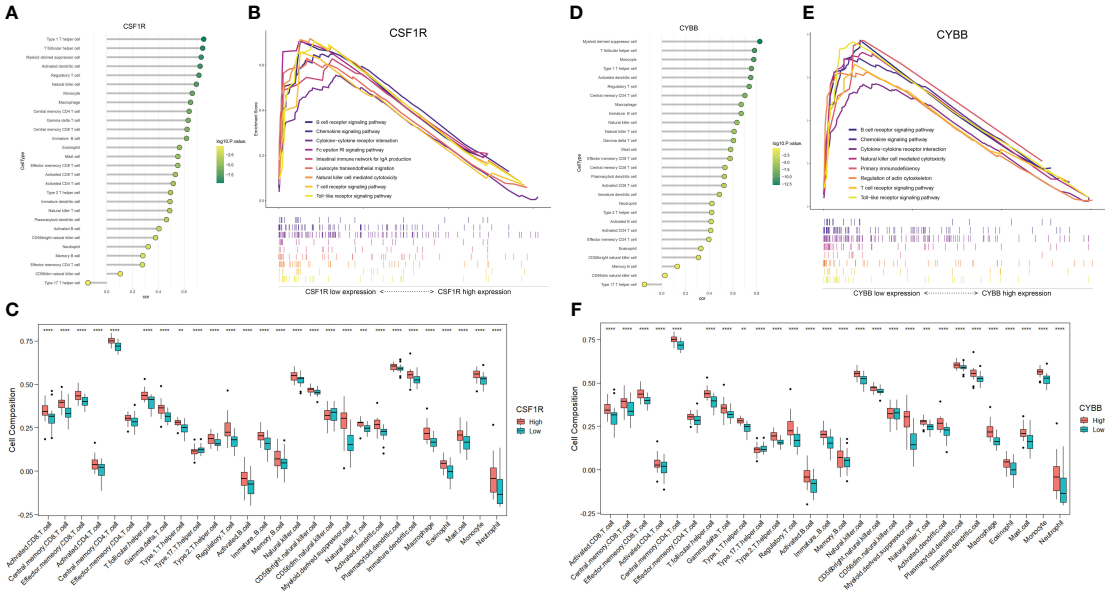

FIGURE 8
Analysis of immune-associated hub genes. **(A)** Lollipop plot of CSF1R correlation with 28 immune cells. The horizontal coordinate indicates the correlation size, and the color indicates the P-value. **(B)** Immune-related GSEA analysis of CSF1R with different expression levels. **(C)** Distribution of 28 immune cells in CSF1R with different expression levels. **(D-F)** Analysis of CYBB. **P <0.01, ***P <0.001, ****P <0.0001.

(NES)| > 1 and FDR < 0.25 (Supplementary Table S5). The samples were divided into high- and low-expression groups based on the expression levels of *CYBB* and *CSF1R* (Figures 8B, E). Overexpression of *CSF1R* was enriched in pathways involved in B cell/T cell receptor signaling pathways, chemokine signaling pathway, NK cell-mediated cytotoxicity, and cytokine-cytokine receptor interactions ($P < 0.05$). In addition, the pathways altered by *CYBB* were related to B cell/T cell receptor signaling pathways, chemokine signaling pathway, and primary immunodeficiency ($P < 0.05$). These results confirmed that *CYBB* and *CSF1R* play crucial roles in immune-related signaling pathways during MN development.

3.7 Correlation analysis of immune-related hub genes with ccrs and pro-inflammatory cytokines

To further analyze the effect of immune-related hub genes on CCRs and pro-inflammatory cytokines, six CCRs and pro-inflammatory cytokines were obtained from the black modules: *CCR1*, *CX3CR1*, *IL1B*, *CCL4*, *TNF*, and *CCR2*. The correlation between *CYBB* and *CSF1R* and the six CCRs and pro-inflammatory cytokines is shown in Figure 9A. There was a significant positive correlation with a significant difference ($P < 0.01$). The correlation between *CSF1R* and *CYBB* was further demonstrated using scatter plots (Figures 9B, C). As the expression of *CYBB* and *CSF1R* increased, the expression of the six CCRs and proinflammatory cytokines also increased. This showed that *CYBB* and *CSF1R* influenced the expression of CCRs and pro-inflammatory cytokines to promote inflammation.

3.8 Validation of CSF-1 and CYBB in clinical samples

The experimental results of serum levels of *CSF-1* in patients with MN were significantly higher than those in healthy controls (Figure 10A), which is consistent with the results of our bioinformatic prediction. Similarly, increased *CYBB* expression was observed in patients with MN compared to that in healthy controls (Figure 10B). qPCR analysis showed that mRNA expression of *CSF1R* and *CYBB* was increased in patients with MN compared to healthy controls (Figures 10C, D). These experimental findings validate and reinforce the predictive value of bioinformatic analysis, further supporting the involvement of *CSF1R* and *CYBB* in MN pathogenesis.

4 Discussion

In this study, GO analysis revealed that the upregulated genes were primarily enriched in immune system processes, endocytic vesicles, and heme-binding. The pathogenesis of MN involves the formation of circulating immune network complexes and activation of autoreactive immune cells targeting glomerular cells, encompassing both innate and adaptive immune responses. The upregulated genes mainly participated in multiple immune-related diseases and immune pathways according to KEGG, such as the C-type lectin (CTL) receptor (CLR) signaling pathway, cytokine-cytokine receptor interaction, and NK cell-mediated cytotoxicity. The accumulation of subepithelial immunocomplexes induces complement activation and disruption events that lead to the release of pathogen-associated molecular patterns (PAMP) and

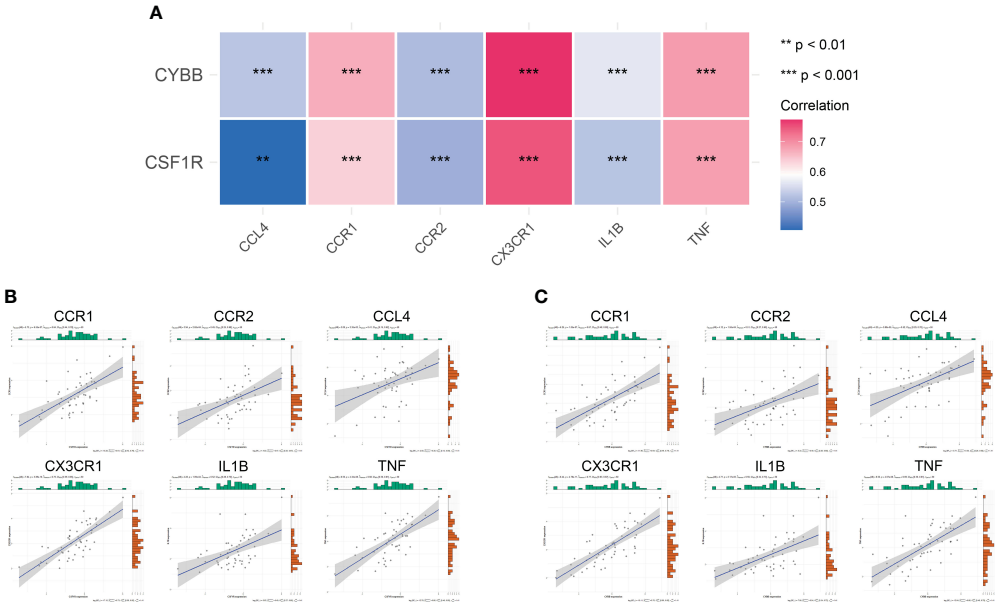

FIGURE 9
Correlation between immune-related hub genes and inflammatory factors and CCRs. **(A)** Correlation heat map. The different colors represent the magnitude of the correlation. **(B, C)** Correlation scatter plot. $^{**}P < 0.01$, $^{***}P < 0.001$.

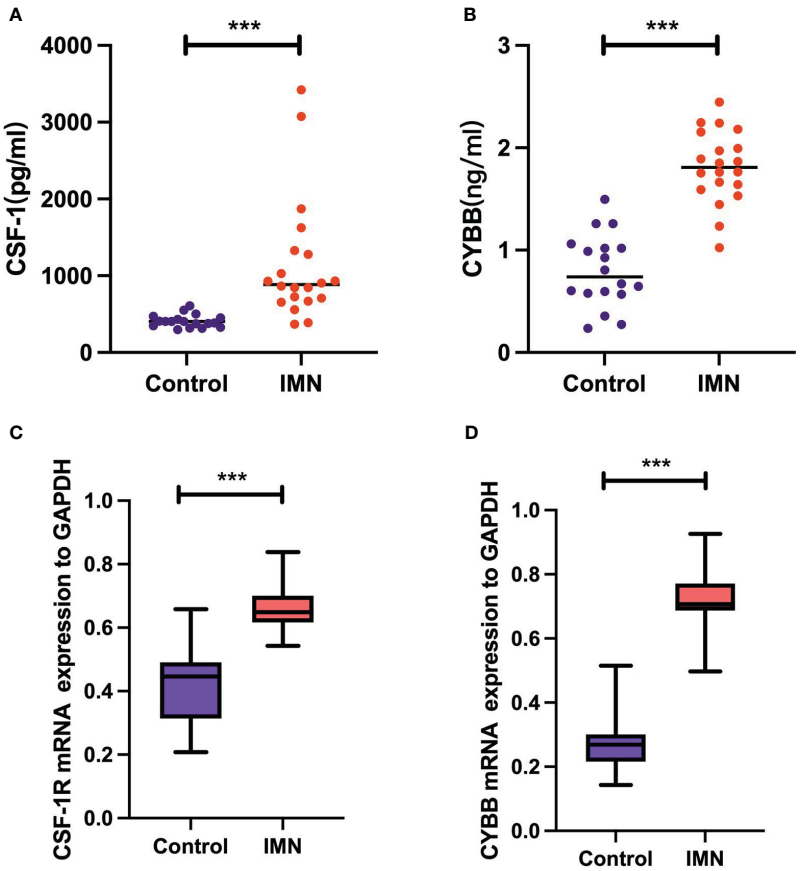

FIGURE 10
Validation of CSF-1 and CYBB. Each point represents a sample. **(A, B)** ELISA measurement of CSF-1 and CYBB. **(C, D)** mRNA expression of CSF1R and CYBB was analyzed by RT-qPCR. $^{***}P < 0.001$, vs Control.

damage-associated molecular patterns (DAMP). CTLs are pattern recognition receptors that recognize these molecules and play vital roles in the immune system. CLRs on the surface of dendritic cells can promote the expression of costimulatory molecules and enhance their ability to present antigens to $CD4^+$ and $CD8^+$ T cells after binding to ligands, thus regulating the adaptive immune response. After recognizing ligands, CLRs on the surface of lymphocytes can induce the expression of pro-inflammatory factors and facilitate the binding of lymphocytes to major histocompatibility complex I (MHC I) or MHC class I molecules on target cells to induce inflammation and cytotoxicity. The concordance between these findings and the enrichment of upregulated genes suggests the presence of key genes involved in the immune response networks associated with MN.

Growing evidence regarding the pathogenic role of the impaired immune system and the molecular mechanism of MN progression has been widely revealed. Autoantibodies, immune complexes, and cytokines induced by T cells, B cells, monocytes, and other immune cells are involved in the progression of MN. Immune complex deposition within the GBM leads to the release of DAMP, which activate innate immune cells and trigger antigen-presenting cell (APC) activation. Antigen presentation by APCs to T cells leads to their activation and differentiation into subsets, such as Th1 and Th2, which involve key signaling pathways in patients with idiopathic MN (8). T cell-derived cytotoxicity contributes to the inflammatory response and tissue infiltration by immune cells (22). Autoreactive T-cells recruit, activate, and proliferate B-cells, resulting in the production of autoantibodies that cause barrier disruption and irreversible kidney damage. Indeed, basic and clinical research has indicated that the deposition of IgG along the glomerular basement membrane secreted by B cells is a hallmark of MN, which results in a sequence of events that impair the glomerular filtering barrier and induce proteinuria (23). In addition, B cells are present in renal biopsy specimens of MN, which shows that B lymphocytes are related to the pathogenesis of the disease (24). Rituximab treatment reduces glomerular IgG4 and C3 deposition by suppressing autoantibody generation, improving proteinuria in MN (25). Monocytes and macrophages are critical drivers of the innate immune system and are responsible for tissue regeneration and regulation immune (26). A recent study showed that $CD14^+CD163^+CD206^+$M2 monocytes positively correlated with 24 h urine albumin and PLA2R levels in MN (27). Tubulointerstitial injury is mediated by macrophage migration, which is a common finding during the early phase of MN progression. M2-like monocytes are considered potential indicators of MN severity (28). We employed computational approaches such as CIBERSORTx or the ssGSEA algorithm to analyze immune infiltration. The results of the present study are consistent with previous findings, confirming an altered distribution of immune cells in MN.

Based on the genes closely associated with MN, as identified by PPI network analysis, seven hub genes were identified, namely, *ALB, FTCD, HRG, PCK1*, and *SLC2A2* (upregulated genes) and *CSF1R* and *CYBB* (downregulated genes). To identify genes closely related to MN progression, WGCNA was used to identify core molecules. Furthermore, combined with immune cell infiltration analysis, the results of WGCNA revealed that the black module was closely related to immune response in MN, which was further intersected with seven hub genes to obtain the overlapping genes *CSF1R* and *CYBB*. These results strongly suggest that the regulation of *CSF1R* and *CYBB* may influence MN pathogenesis through the immune system. Based on the immune infiltration analysis, both *CSF1R* and *CYBB* were significantly and positively associated with most immune cells, which further confirmed that these two genes play a central role in the autoimmune pathology of MN.

The identification of the roles of *CSF1R* and *CYBB* in MN advances our strategies for disease diagnosis and treatment. As a central receptor on the macrophage surface, *CSF1R* binds to CSF-1 or IL-34 to regulate the development, activation, and function of macrophages (29). Furthermore, the CSF-1R signaling pathway is responsible for migration and multiply of macrophage (30). Several studies have identified CSF-1R as a pharmacological target for alleviating disease progression, including those of rheumatoid arthritis, Alzheimer's disease, and cancer. Particularly, CSF-1 acted as a "master switch" and contributed to monocyte and macrophage phenotypes that was positively related with lupus activity in kidney diseases (31). Further, the treatment with CSF-1R inhibitor was confirmed to significantly ameliorate renal injury in murine lupus (32). Pharmacological inhibition of CSF-1R with GW2580 alleviated ischemia-induced renal injury by reducing M2 macrophage infiltration (33). Recently, MALDI–MSI analysis was performed to detect proteomic alterations in renal biopsies, and macrophage migration inhibitory factor was identified as a valuable biomarker for response to therapy in MN (34). In addition, renal biopsies from patients with MN showed that monocytes/macrophages predominate the interstitial infiltrate, suggesting that macrophages may be key regulators of the pathogenesis of MN (35). Based on these studies, *CSF1R* was predicted to contribute to the disturbance of the immune balance associated with MN. *CYBB* (also called NOX2) is considered the central component of NADPH oxidase, which is responsible for the bactericidal activity within macrophages and neutrophils involved in respiratory bursts (36). When CYBB/NOX2, the terminal component of the respiratory chain, is activated, it enters the plasma membrane to form phagosomes, which are necessary for triggering superoxide production activity of the complex (37). A recent study showed that CYBB/NOX2 in cDCs promotes antigen presentation to activate $CD4^+$ T cells and leads to TH cell-induced tissue damage (38). In a model of hyperhomocysteinemia-induced renal injury, NADPH oxidase-mediated redox signaling was responsible for switching on NLRP3 inflammasome activation, which recruited immune cell infiltration, ultimately leading to glomerular injury and sclerosis (39). These results are further supported by our study. To explore the possible mechanism by which *CSF1* and *CYBB* act on immune cells in MN, GSEA was used to determine the immune function of DEGs. The results revealed that *CSF1R* and *CYBB* were significantly correlated with B cell/T cell receptor signaling pathways, which are involved in MN immunopathogenesis. Furthermore, using ELISA, CSF1 and CYBB/NOX2 were found to be overexpressed in patients with MN, and the dependability of their diagnostic values was confirmed by ROC curve analysis, which further verified our bioinformatics analysis results.

Chemokines could promote differentiation of immune cells and induce tissue extravasation (40). Notably, studies have found that podocytes can be stimulated by the inflammatory setting of glomerulonephritis, which is mediated by CCRs (41). The expression of IL-10 and CCR1 mRNA were observed in polarized Mφ, and M-CSF restored the synthesis of IL-10 through M1 Mφ (42). CCL2/MCP-1 coordinates inflammatory monocyte transport between bone marrow, circulation and atherosclerotic plaque by binding to CCR2 (43).The distribution pattern of CX3CR1 was consistent with the expression of T cells and monocytes/macrophages, and it was distributed in both renal interstitial and glomerular infiltrated leukocytes (44). In our study, CCR1, CX3CR1, IL1B, CCL4, TNF, and CCR2 were activated by CSF1 and CYBB/NOX2, which are closely related to the inflammatory response. These results reveal that CSF1 and CYBB/NOX2 could be potential diagnostic biomarkers and immunotherapy targets for MN.

Our study has some limitations. First, the sample size of healthy controls was small, which may have influenced the study results. Second, through validation using sera from patients with MN, gene expression levels in renal tissues need to be further explored, and experimental studies are warranted to utilize our results in clinical settings. Third, there was little clinical information in the included dataset, which resulted in further correlation analyses that could not be conducted.

5 Conclusion

Through comprehensive bioinformatics analysis, we identified two hub genes (*CSF1R* and *CYBB*) that are closely involved in the progression of MN. The results of this preliminary study highlight the significance of immune infiltration and the relationship between the two hub genes and most immune cells with potential immune mechanisms in MN. *CSF1R* and *CYBB* influenced the expression of CCRs and proinflammatory cytokines (*CCR1*, *CX3CR1*, *IL1B*, *CCL4*, *TNF*, and *CCR2*). *CSF1R* and *CYBB* may be potential biomarkers for MN progression, providing a perspective for diagnostic and immunotherapeutic targets of MN.

Data availability statement

The original contributions presented in the study are included in the article/Supplementary Material. Further inquiries can be directed to the corresponding authors.

Ethics statement

The studies involving humans were approved by the Ethics Committee of Beijing Dongzhimen Hospital, First Clinical Medical College of Beijing University of Chinese Medicine. All the patients/participants provided written informed consent to participate in the study. The studies were conducted in accordance with the local legislation and institutional requirements. The participants provided their written informed consent to participate in this study.

Author contributions

PZ: Writing – original draft. YG: Data curation. JT: Formal analysis. ZC: Software. XX: Validation. KY: Methodology. HC: Project administration. All authors contributed to the article and approved the submitted version.

Funding

This study was supported by the Major project jointly constructed by the State Administration of Traditional Chinese Medicine and Zhejiang Provincial Administration of Traditional Chinese Medicine (GZY-ZJ-KJ-23013) and the Zhejiang natural science foundation of China (Y23H270009).

Conflict of interest

The authors declare that the research was conducted in the absence of any commercial or financial relationships that could be construed as a potential conflict of interest.

Publisher's note

Supplementary material

The Supplementary Material for this article can be found online at: https://www.frontiersin.org/articles/10.3389/fimmu.2023.1252347/full#supplementary-material

References

1. Ronco P, Debiec H. Molecular pathogenesis of membranous nephropathy. *Annu Rev Pathol* (2020) 15:287–313. doi: 10.1146/annurev-pathol-020117-043811

2. Francis JM, Beck LH Jr., Salant DJ. Membranous nephropathy: A journey from bench to bedside. *Am J Kidney Dis* (2016) 68(1):138–47. doi: 10.1053/j.ajkd.2016.01.030

3. Membranous nephropathy. *Nat Rev Dis Primers* (2021) 7(1):70. doi: 10.1038/s41572-021-00310-0

4. Beck LH Jr., Salant DJ. Membranous nephropathy: from models to man. *J Clin Invest* (2014) 124(6):2307–14. doi: 10.1172/JCI72270

5. Couser WG. Primary membranous nephropathy. *Clin J Am Soc Nephrol* (2017) 12 (6):983–97. doi: 10.2215/CJN.11761116

6. Beck LH Jr., Bonegio RG, Lambeau G, Beck DM, Powell DW, Cummins TD, et al. M-type phospholipase A2 receptor as target antigen in idiopathic membranous nephropathy. *N Engl J Med* (2009) 361(1):11–21. doi: 10.1056/NEJMoa0810457

7. Ronco P, Beck L, Debiec H, Fervenza FC, Hou FF, Jha V, et al. Membranous nephropathy. *Nat Rev Dis Primers* (2021) 7(1):69. doi: 10.1007/978-3-642-27843-3_94-1

8. Motavalli R, Etemadi J, Kahroba H, Mehdizadeh A, Yousefi M. Immune system-mediated cellular and molecular mechanisms in idiopathic membranous nephropathy pathogenesis and possible therapeutic targets. *Life Sci* (2019) 238:116923. doi: 10.1016/j.lfs.2019.116923

9. van de Logt AE, Fresquet M, Wetzels JF, Brenchley P. The anti-PLA2R antibody in membranous nephropathy: what we know and what remains a decade after its discovery. *Kidney Int* (2019) 96(6):1292–302. doi: 10.1016/j.kint.2019.07.014

10. Motavalli R, Etemadi J, Soltani-Zangbar MS, Ardalan MR, Kahroba H, Roshangar L, et al. Altered Th17/Treg ratio as a possible mechanism in pathogenesis of idiopathic membranous nephropathy. *Cytokine* (2021) 141:155452. doi: 10.1016/j.cyto.2021.155452

11. Kuroki A, Iyoda M, Shibata T, Sugisaki T. Th2 cytokines increase and stimulate b cells to produce IgG4 in idiopathic membranous nephropathy. *Kidney Int* (2005) 68 (1):302–10. doi: 10.1111/j.1523-1755.2005.00415.x

12. Fervenza FC, Abraham RS, Erickson SB, Irazabal MV, Eirin A, Specks U, et al. Rituximab therapy in idiopathic membranous nephropathy: a 2-year study. *Clin J Am Soc Nephrol* (2010) 5(12):2188–98. doi: 10.2215/CJN.05080610

13. Cantarelli C, Jarque M, Angeletti A, Manrique J, Hartzell S, O'Donnell T, et al. A comprehensive phenotypic and functional immune analysis unravels circulating anti-phospholipase A2 receptor antibody secreting cells in membranous nephropathy patients. *Kidney Int Rep* (2020) 5(10):1764–76. doi: 10.1016/j.ekir.2020.07.028

14. Jiang BC, Liu T, Gao YJ. Chemokines in chronic pain: cellular and molecular mechanisms and therapeutic potential. *Pharmacol Ther* (2020) 212:107581. doi: 10.1016/j.pharmthera.2020.107581

15. Cortes-Ciriano I, Gulhan DC, Lee JJ, Melloni GEM, Park PJ. Computational analysis of cancer genome sequencing data. *Nat Rev Genet* (2022) 23(5):298–314. doi: 10.1038/s41576-021-00431-y

16. Abbott TR, Dhamdhere G, Liu Y, Lin X, Goudy L, Zeng L, et al. Development of CRISPR as an antiviral strategy to combat SARS-CoV-2 and influenza. *Cell* (2020) 181 (4):865–76 e12. doi: 10.1016/j.cell.2020.04.020

17. Ritchie ME, Phipson B, Wu D, Hu Y, Law CW, Shi W, et al. Limma powers differential expression analyses for RNA-sequencing and microarray studies. *Nucleic Acids Res* (2015) 43(7):e47. doi: 10.1093/nar/gkv007

18. Davis S, Meltzer PS. GEOquery: a bridge between the gene expression omnibus (GEO) and BioConductor. *Bioinformatics* (2007) 23(14):1846–7. doi: 10.1093/bioinformatics/btm254

19. Huang da W, Sherman BT, Lempicki RA. Systematic and integrative analysis of large gene lists using DAVID bioinformatics resources. *Nat Protoc* (2009) 4(1):44–57. doi: 10.1038/nprot.2008.211

20. Bindea G, Mlecnik B, Tosolini M, Kirilovsky A, Waldner M, Obenauf AC, et al. Spatiotemporal dynamics of intratumoral immune cells reveal the immune landscape in human cancer. *Immunity* (2013) 39(4):782–95. doi: 10.1016/j.immuni.2013.10.003

21. Langfelder P, Horvath S. WGCNA: an r package for weighted correlation network analysis. *BMC Bioinf* (2008) 9:559. doi: 10.1186/1471-2105-9-559

22. Suarez-Fueyo A, Bradley SJ, Klatzmann D, Tsokos GC. T cells and autoimmune kidney disease. *Nat Rev Nephrol* (2017) 13(6):329–43. doi: 10.1038/nrneph.2017.34

23. Glassock RJ. Human idiopathic membranous nephropathy–a mystery solved? *N Engl J Med* (2009) 361(1):81–3. doi: 10.1056/NEJMe0903343

24. Cohen CD, Calvaresi N, Armelloni S, Schmid H, Henger A, Ott U, et al. CD20-positive infiltrates in human membranous glomerulonephritis. *J Nephrol* (2005) 18 (3):328–33.

25. Ruggenenti P, Fervenza FC, Remuzzi G. Treatment of membranous nephropathy: time for a paradigm shift. *Nat Rev Nephrol* (2017) 13(9):563–79. doi: 10.1038/nrneph.2017.92

26. Laria A, Lurati A, Marrazza M, Mazzocchi D, Re KA, Scarpellini M. The macrophages in rheumatic diseases. *J Inflammation Res* (2016) 9:1–11. doi: 10.2147/JIR.S82320

27. Hou J, Zhang M, Ding Y, Wang X, Li T, Gao P, et al. Circulating CD14(+)CD163 (+)CD206(+) M2 monocytes are increased in patients with early stage of idiopathic membranous nephropathy. *Mediators Inflamm* (2018) 2018:5270657. doi: 10.1155/2018/5270657

28. Mezzano SA, Droguett MA, Burgos ME, Ardiles LG, Aros CA, Caorsi I, et al. Overexpression of chemokines, fibrogenic cytokines, and myofibroblasts in human membranous nephropathy. *Kidney Int* (2000) 57(1):147–58. doi: 10.1046/j.1523-1755.2000.00830.x

29. Buechler MB, Fu W, Turley SJ. Fibroblast-macrophage reciprocal interactions in health, fibrosis, and cancer. *Immunity* (2021) 54(5):903–15. doi: 10.1016/j.immuni.2021.04.021

30. Sehgal A, Irvine KM, Hume DA. Functions of macrophage colony-stimulating factor (CSF1) in development, homeostasis, and tissue repair. *Semin Immunol* (2021) 54:101509. doi: 10.1016/j.smim.2021.101509

31. Ruacho G, Lira-Junior R, Gunnarsson I, Svenungsson E, Bostrom EA. Inflammatory markers in saliva and urine reflect disease activity in patients with systemic lupus erythematosus. *Lupus Sci Med* (2022) 9(1):e000607. doi: 10.1136/lupus-2021-000607

32. Chalmers SA, Wen J, Shum J, Doerner J, Herlitz L, Putterman C. CSF-1R inhibition attenuates renal and neuropsychiatric disease in murine lupus. *Clin Immunol* (2017) 185:100–8. doi: 10.1016/j.clim.2016.08.019

33. Deng X, Yang Q, Wang Y, Zhou C, Guo Y, Hu Z, et al. CSF-1R inhibition attenuates ischemia-induced renal injury and fibrosis by reducing Ly6C(+) M2-like macrophage infiltration. *Int Immunopharmacol* (2020) 88:106854. doi: 10.1016/j.intimp.2020.106854

34. L'Imperio V, Smith A, Ajello E, Piga I, Stella M, Denti V, et al. MALDI-MSI pilot study highlights glomerular deposits of macrophage migration inhibitory factor as a possible indicator of response to therapy in membranous nephropathy. *Proteomics Clin Appl* (2019) 13(3):e1800019. doi: 10.1002/prca.201800019

35. Alexopoulos E, Seron D, Hartley RB, Nolasco F, Cameron JS. Immune mechanisms in idiopathic membranous nephropathy: The role of the interstitial infiltrates. *Am J Kidney Diseases* (1989) 13(5):404–12. doi: 10.1016/S0272-6386(89)80024-1

36. Weaver CJ, Leung YF, Suter DM. Expression dynamics of NADPH oxidases during early zebrafish development. *J Comp Neurol* (2016) 524(10):2130–41. doi: 10.1002/cne.23938

37. Rastogi R, Geng X, Li F, Ding Y. NOX activation by subunit interaction and underlying mechanisms in disease. *Front Cell Neurosci* (2016) 10:301. doi: 10.3389/fncel.2016.00301

38. Keller CW, Kotur MB, Mundt S, Dokalis N, Ligeon LA, Shah AM, et al. CYBB/NOX2 in conventional DCs controls t cell encephalitogenicity during neuroinflammation. *Autophagy* (2021) 17(5):1244–58. doi: 10.1080/15548627.2020.1756678

39. Abais JM, Zhang C, Xia M, Liu Q, Gehr TW, Boini KM, et al. NADPH oxidase-mediated triggering of inflammasome activation in mouse podocytes and glomeruli during hyperhomocysteinemia. *Antioxid Redox Signal* (2013) 18(13):1537–48. doi: 10.1089/ars.2012.4666

40. Markl F, Huynh D, Endres S, Kobold S. Utilizing chemokines in cancer immunotherapy. *Trends Cancer* (2022) 8(8):670–82. doi: 10.1016/j.trecan.2022.04.001

41. Popovic ZV, Bestvater F, Krunic D, Kramer BK, Bergner R, Loffler C, et al. CD73 overexpression in podocytes: A novel marker of podocyte injury in human kidney disease. *Int J Mol Sci* (2021) 22(14):7642. doi: 10.3390/ijms22147642

42. Nakano H, Kirino Y, Takeno M, Higashitani K, Nagai H, Yoshimi R, et al. GWAS-identified CCR1 and IL10 loci contribute to M1 macrophage-predominant inflammation in behcet's disease. *Arthritis Res Ther* (2018) 20(1):124. doi: 10.1186/s13075-018-1613-0

43. Georgakis MK, Bernhagen J, Heitman LH, Weber C, Dichgans M. Targeting the CCL2-CCR2 axis for atheroprotection. *Eur Heart J* (2022) 43(19):1799–808. doi: 10.1093/eurheartj/ehac094

44. Segerer S, Hughes E, Hudkins KL, Mack M, Goodpaster T, Alpers CE. Expression of the fractalkine receptor (CX3CR1) in human kidney diseases. *Kidney Int* (2002) 62(2):488–95. doi: 10.1046/j.1523-1755.2002.00480.x

frontiers | Frontiers in Immunology

TYPE Original Research
PUBLISHED 02 November 2023
DOI 10.3389/fimmu.2023.1251452

OPEN ACCESS

EDITED BY
Xu-jie Zhou,
Peking University, China

REVIEWED BY
Kenta Moriwaki,
Toho University, Japan
Zhigao Wang,
University of South Florida, United States
Zilong Deng,
Southern Medical University, China

*CORRESPONDENCE
Peter J. Cowan
Peter.Cowan@svha.org.au

RECEIVED 01 July 2023
ACCEPTED 19 October 2023
PUBLISHED 02 November 2023

CITATION
Pefanis A, Bongoni AK, McRae JL, Salvaris EJ, Fisicaro N, Murphy JM, Ierino FL and Cowan PJ (2023) Dynamics of necroptosis in kidney ischemia-reperfusion injury.
Front. Immunol. 14:1251452.
doi: 10.3389/fimmu.2023.1251452

Dynamics of necroptosis in kidney ischemia-reperfusion injury

Aspasia Pefanis[1,2,3], Anjan K. Bongoni[1], Jennifer L. McRae[1], Evelyn J. Salvaris[1], Nella Fisicaro[1], James M. Murphy[4,5,6], Francesco L. Ierino[2,3] and Peter J. Cowan[1,2]*

[1]Immunology Research Centre, St Vincent's Hospital, Melbourne, VIC, Australia, [2]Department of Medicine, The University of Melbourne, Melbourne, VIC, Australia, [3]Department of Nephrology, St Vincent's Hospital, Melbourne, VIC, Australia, [4]Walter and Eliza Hall Institute of Medical Research, Parkville, VIC, Australia, [5]Department of Medical Biology, The University of Melbourne, Parkville, VIC, Australia, [6]Drug Discovery Biology, Monash Institute of Pharmaceutical Sciences, Monash University, Parkville, VIC, Australia

Necroptosis, a pathway of regulated necrosis, involves recruitment and activation of RIPK1, RIPK3 and MLKL, leading to cell membrane rupture, cell death and release of intracellular contents causing further injury and inflammation. Necroptosis is believed to play an important role in the pathogenesis of kidney ischemia-reperfusion injury (IRI). However, the dynamics of necroptosis in kidney IRI is poorly understood, in part due to difficulties in detecting phosphorylated MLKL (pMLKL), the executioner of the necroptosis pathway. Here, we investigated the temporal and spatial activation of necroptosis in a mouse model of unilateral warm kidney IRI, using a robust method to stain pMLKL. We identified the period 3-12 hrs after reperfusion as a critical phase for the activation of necroptosis in proximal tubular cells. After 12 hrs, the predominant pattern of pMLKL staining shifted from cytoplasmic to membrane, indicating progression to the terminal phase of necroptotic cell death. *Mlkl*-ko mice exhibited reduced kidney inflammation at 12 hrs and lower serum creatinine and tubular injury at 24 hrs compared to wild-type littermates. Interestingly, we observed increased apoptosis in the injured kidneys of *Mlkl*-ko mice, suggesting a relationship between necroptosis and apoptosis in kidney IRI. Together, our findings confirm the role of necroptosis and necroinflammation in kidney IRI, and identify the first 3 hrs following reperfusion as a potential window for targeted treatments.

KEYWORDS

necroptosis, ischemia-reperfusion, necroinflammation, mlkl, acute kidney injury, chronic kidney disease

1 Introduction

Ischemia-reperfusion injury (IRI) is a pathological process that occurs when the blood supply to an organ is temporarily reduced and then restored (1). Cellular damage occurs during both the ischemic period and subsequent reperfusion of the kidney. During ischemia, there is a switch from aerobic to anaerobic metabolism (2), resulting in acidosis (3). Cellular ion transport mechanisms are compromised, with increased intracellular calcium, sodium and water causing cellular oedema (4–6). During reperfusion aerobic metabolism is restored and pH is normalised, but reactive oxygen species (ROS) are generated, damaging functional cellular components and ultimately inducing cell death (7–9). The kidney, a highly vascular and metabolically active organ, is particularly susceptible to IRI which may occur during episodes of hypotension, vascular surgery, sepsis, cardiac events or during kidney retrieval for transplantation (10). Kidney IRI causes inflammation (11, 12), immune system activation (13–15), microvascular dysfunction (16–19) and fibrosis (20, 21). IRI has both immediate and early clinical consequences (acute kidney failure) (22, 23) and contributes to progressive long term fibrosis and chronic kidney disease (CKD) (24). Kidney IRI causes significant patient morbidity and mortality, contributing to increasing healthcare costs (25–31). One of the hallmarks of kidney IRI is acute tubular necrosis, which occurs predominantly in the proximal tubules (9).

Recent studies have established that necrosis can occur in a regulated manner via several pathways including necroptosis (32), ferroptosis (33), pyroptosis (34, 35), mitochondrial permeability transition (MPT)-driven necrosis (36), and parthanatos (37, 38). In contrast to apoptosis, these forms of regulated necrosis lead to cell membrane rupture and release of damage-associated molecular patterns (DAMPs), resulting in inflammation and immune activation [reviewed in (39)]. Necroptosis is a caspase-independent regulated necrosis pathway triggered by a range of extracellular stimuli, including death receptor ligands (e.g. TNF) or pathogen patterns (e.g. LPS) binding to their respective cell surface receptors, or intracellular stimuli such as viral nucleic acids binding to the intracellular receptor ZBP1 (reviewed in (40, 41). In scenarios where the pro-NF-κB activity of the cIAP E3 ubiquitin ligase family and the pro-apoptotic function of Caspase-8 protease are diminished, the intracellular kinases Receptor Interacting Protein Kinase 1 (RIPK1) and Receptor Interacting Protein Kinase 3 (RIPK3) assemble into a high molecular weight intracellular platform termed the necrosome via their RIP homology interaction motifs (RHIMs) (42, 43). Recruitment of subcomplexes comprising RIPK3 and the terminal effector in the pathway – the Mixed lineage kinase domain-like (MLKL) pseudokinase – from the cytosol to the necrosome prompts RIPK3-mediated phosphorylation of the MLKL pseudokinase domain at T357/S358 in human MLKL and S345 in mouse MLKL (44–46). Phosphorylation is the critical step in MLKL activation, inducing MLKL to undergo a conformational change, disengage from the necrosome, and assemble into pro-necroptotic oligomers (47–50). MLKL oligomers are trafficked from the necrosome to the plasma membrane, where they accumulate in hotspots that perturb the membrane to kill cells once a phospho-MLKL (pMLKL) threshold is exceeded (50). Accordingly, phosphorylation of MLKL has become synonymous with necroptosis pathway and MLKL activation, and is considered a hallmark of necroptosis pathway activation. Many of the inflammatory molecules released during necroptosis promote further necroptotic cell death and inflammation (51), creating an auto-amplification loop termed necroinflammation (52).

Necroptosis is believed to play an important role in the pathogenesis of kidney IRI (reviewed in (39) (53). Studies by Linkermann et al. (54) and Newton et al. (55) showed lower mortality of *Ripk3*-deficient mice compared to wild-type (WT) mice. In the absence of mouse-specific inhibitors of MLKL, the executioner protein of necroptosis, *in vivo* data for its role come from studies of necroptosis-deficient *Mlkl* knockout (*Mlkl*-ko) mice (55, 56). Müller et al. used a bilateral renal pedicle clamping model of IRI to demonstrate improved kidney function in *Mlkl*-ko mice compared with wild-type (WT) mice at 48 and 72 hrs post-reperfusion, but not at the earlier timepoints of 6, 12, and 24 hrs (56). Although there was a time-dependent increase in total MLKL protein expression in WT kidneys commencing at 12 hrs post-reperfusion, the authors were unable to detect pMLKL by immunostaining or Western blotting (56). This inability to reliably detect pMLKL in mouse kidney sections has been a major hindrance to understanding the dynamics of necroptosis in kidney IRI. To address this problem, we developed a reproducible method to stain pMLKL in formalin-fixed kidney tissue sections and used it to track the temporal and spatial activation of necroptosis in the kidneys of WT mice subjected to unilateral IRI. Mice were analyzed at different timepoints post-reperfusion (0, 3, 12, 24, 48, 72 hrs, and 4 weeks). The pMLKL staining pattern at each timepoint was correlated with kidney function, tubular injury, and the expression of a range of genes relevant to kidney injury, inflammation, and necroptosis. Finally, we compared *Mlkl*-ko mice with WT littermate controls at each timepoint to assess the degree and mechanism of protection from IRI afforded by deletion of MLKL.

2 Materials and methods

2.1 Animal and ethical statement

Mlkl-ko mice on a C57BL/6J background (45) and WT littermate controls were generated by heterozygous matings and screened by PCR of tail tip genomic DNA by the Walter and Eliza Hall Institute for Medical Research (WEHI) (45). Mice were housed in microisolator cages in a pathogen-free facility with a 12-hour light-dark cycle under standard conditions of temperature and humidity and fed commercial mouse chow diet with free access to drinking water. All animal experiments were conducted in compliance with the Australian Code of Practice for the Care and Use of Laboratory Animals for Scientific Purposes (Eighth edition, 2013) and the Prevention of Cruelty to Animals Act 1986, Victoria, Australia. All experiments were carried out with the approval of the Animal Ethics Committee of St. Vincent's Hospital Melbourne.

2.2 Kidney ischemia-reperfusion injury model

10–12-week-old male mice were anaesthetised by intraperitoneal injection of ketamine (100 mg/kg) and xylazine (15 mg/kg), followed by right nephrectomy prior to left renal pedicle clamping for 18 min using a microvascular clamp (Roboz, Rockville, MD). After removal of the clamp, the kidney was assessed for even reperfusion prior to abdominal wound closure. Mice received 200 µL warm normal saline (37°C) i.p. post-operatively, and core body temperature was maintained at 35.5 - 36.5°C throughout. Sham mice had a right nephrectomy but the left renal pedicle was not clamped. Separate cohorts of mice were euthanised by anesthetic overdose (ketamine/xylazine) and exsanguination immediately following injury (baseline), at 3, 12, 24, 48, 72 hours or 4 weeks after reperfusion. Blood and kidney samples were obtained to assess kidney function, kidney injury, inflammation, and necroptosis. Group sizes varied depending on availability of homozygous *Mlkl*-ko and WT littermates during experimental procedures. Specific group sizes are specified in all figure legends.

2.3 Analysis of kidney function

Serum creatinine was measured using a kinetic colorimetric assay on a COBAS Integra 400 Plus analyser (Roche, Castle Hill, NSW, Australia).

2.4 Assessment of tubular injury

Kidney tissue blocks were fixed overnight in 10% formalin and embedded in paraffin wax. 3 µm sections were cut and de-waxed prior to Periodic Acid Schiff (PAS) staining (57). Each section was divided into 12 regions. A representative area of each region was viewed under 400X magnification, with a focus on the corticomedullary junction. A score was derived by calculating the number of damaged proximal tubules as a percentage of total proximal tubules manually counted in each area (58). Markers of a damaged tubule included tubular atrophy, tubular dilatation, tubular cast formation, vacuolization, and tubular cell degeneration with loss of brush border or thickening of tubular basement membranes. An average of the 12 scores obtained per section was calculated. Scoring was performed under blinded conditions by personnel trained by an experienced veterinarian pathologist.

2.5 Immunohistochemical analysis

3 µm paraffin sections were de-waxed prior to antigen retrieval in a citrate buffer (pH 6.0) using a pressure cooker at 125°C for 90 s (pMLKL staining) or 180 s (cC3 staining), and left to cool to room temperature. Slides were then washed on a shaker prior to incubation in 10 µL 3% H_2O_2 v/v in double-distilled water for 5 min and blocked with 50 µL 10% swine serum for 1 hr at room temperature. Sections were then incubated with rabbit monoclonal anti-phospho-MLKL (pSer345) (ab196436, 1:100, Abcam, Melbourne, Australia) or rabbit monoclonal anti-human/mouse cleaved Caspase-3 (cC3) (Asp175) (IC835G, 1:200, RD Systems, Noble Park, Australia) in 2% swine serum at 4°C overnight. After incubation with DAKO anti-rabbit IgG HRP secondary antibody (Envision+ System, K4003, 1:1, Dako, Santa Clara, USA) for 1 hr, sections were developed using DAB and counterstained with hematoxylin. pMLKL- or cC3-stained sections were scanned using an Aperio ScanScope (Leica Biosystems) to generate a digitized image of the whole section. 12 representative areas of the cortex were analysed (4 upper pole, 4 mid pole and 4 lower pole) at X400 magnification. A score was manually calculated by counting the number of tubules with pMLKL or cC3 staining as a percentage of the total number of tubules in the section.

2.6 Reverse transcription-quantitative PCR

Harvested kidneys were stored in RNA Later® at 4°C for 24-48 h, followed by storage at -80°C until processing. Total RNA was extracted using the ReliaPrep ™ RNA Tissue Miniprep system (Promega Australia, Alexandria, NSW, Australia) according to manufacturer's instructions. RNA concentration and quality were measured using a Fluorostar Omega multimode microplate reader (BMG Labtech, Mornington, Australia). First-strand complementary DNA (cDNA) was generated in a reaction volume of 22 µL containing 1 µg oligo (dT), 1 µg random hexamers (Invitrogen, Carlsbad, CA), 12 µg of RNA and sterile Milli-Q H_2O. The reaction was incubated for 10 min at 70°C. Following this, a 28 µL mix comprising 2.5 µL 10 mM dNTPs, 1 µL SuperScript III recombinant reverse transcriptase, 1 µL RNaseOUT recombinant ribonuclease inhibitors, 2.5 µL 0.1 M DTT, 10 µL 5 x first strand buffer (Invitrogen, Carlsbad, USA) and 11 µL Milli-Q H_2O was added to the first reaction. Reverse transcription was performed at 42°C for 1 hr and 70°C for 10 min. The cDNA was stored at -20°C. Quantitative real-time PCR was performed using the TaqMan Universal PCR Master Mix system and TaqMan Gene Expression Assays for Kidney injury molecule 1 (*Kim1*) (Mm00506686_m1), Neutrophil gelatinase-associated lipocalin (*Ngal*) (Mm01324470_m1), Tumour necrosis factor alpha (*Tnfa*) (Mm00443258_m1), Interleukin 1 beta (*Il1b*) (Mm00434228_m1), Interleukin 33 (*Il33*) (Mm00505403_m1), Interleukin 6 (*Il6*) (Mm00446190_m1), Macrophage inflammatory protein-2 (*Mip2*) (Mm00436450_m1), Receptor interacting protein kinase 1 (*Ripk1*) (Mm00436354_m1), Receptor interacting protein kinase 3 (*Ripk3*) (Mm00444947_m1), Mixed lineage kinase domain-like protein (*Mlkl*) (Mm01244222_m1), Toll-like receptor 2 (*Tlr2*) (Mm00442346_m1), Toll-like receptor 4 (*Tlt4*) (Mm00445273_m1), and Glyceraldehyde 3-phosphate dehydrogenase (*Gapdh*) (Mm99999915_g1) (Applied Biosystems, Carlsbad, CA), using a 7400Fast Real-Time PCR System (Applied Biosystems).

2.7 Statistical analysis

Descriptive statistics were used to summarise the kinetic changes at different time points after reperfusion. Results were expressed as mean ± SEM unless otherwise indicated. A Kruskal-Wallis test and Dunn multiple comparisons test were used when comparing > 2 groups. Comparisons between 2 groups were performed using a Mann-Whitney U-test. Statistical analyses were performed using GraphPad Prism version 9.3 (GraphPad, San Diego, CA) with $p<0.05$ considered significant.

3 Results

3.1 Kinetics of kidney injury and pro-inflammatory gene expression in WT mice following IR

C57BL/6J WT mice were subjected to right nephrectomy and clamping of the left renal pedicle for 18 min, and cohorts were analyzed at 7 timepoints post-reperfusion (0, 3, 12, 24, 48, 72 hrs, and 4 weeks). Kidney injury was assessed by measuring kidney function (serum creatinine), tubular injury (semi-quantitative morphological analysis), and mRNA expression of the genes for the kidney injury markers KIM-1 and NGAL. Serum creatinine (Figure 1A) and tubular injury (Figure 1B; Supplementary Figure 2) were elevated at 3 hrs, although these increases did not reach statistical significance and there was no change in expression of *Kim1* (Figure 1C) or *Ngal* (Figure 1D) at this early timepoint. By 12 hrs, creatinine levels and tubular injury were significantly increased, and expression of both *Kim1* and *Ngal* was massively upregulated. All parameters remained elevated at 24, 48 and 72 hrs before returning to baseline by 4 weeks.

We then examined the expression of several pro-inflammatory genes relevant to necroptosis and/or kidney IRI. TNFα is the best characterized activator of necroptosis (53) and has been described as a necroptosis-associated alarmin (59). *Tnfa* expression was significantly increased at 12, 48 and 72 hrs, and remained high at 4 weeks (Figure 2A). Interleukin-6 (IL-6) is an acute inflammatory cytokine that is upregulated in necrotic cells but not in apoptotic cells (60). *Il6* expression was elevated earlier than *Tnfa* (3 hrs) and returned to baseline levels by 72 hrs (Figure 2B). IL-1β and IL-33

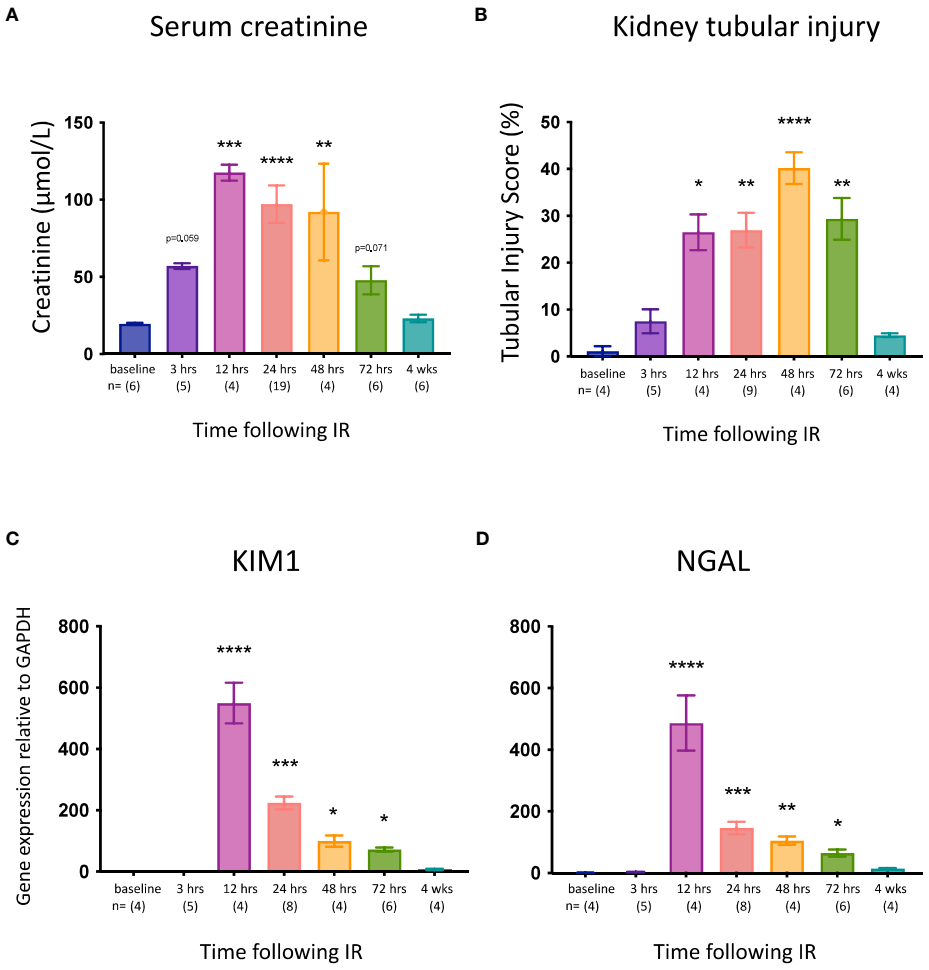

FIGURE 1
Time course of kidney injury after IR in WT mice. **(A)**: serum creatinine; **(B)**: tubular injury score; **(C)**: mRNA expression of *Kim1*; **(D)**: mRNA expression of *Ngal*. Kruskal-Wallis test with Dunn multiple comparisons test with * p<0.05, ** p<0.01, *** p<0.001, **** p<0.0001 compared to baseline control. Data presented as mean ± SEM.

10.3389/fimmu.2023.1251452

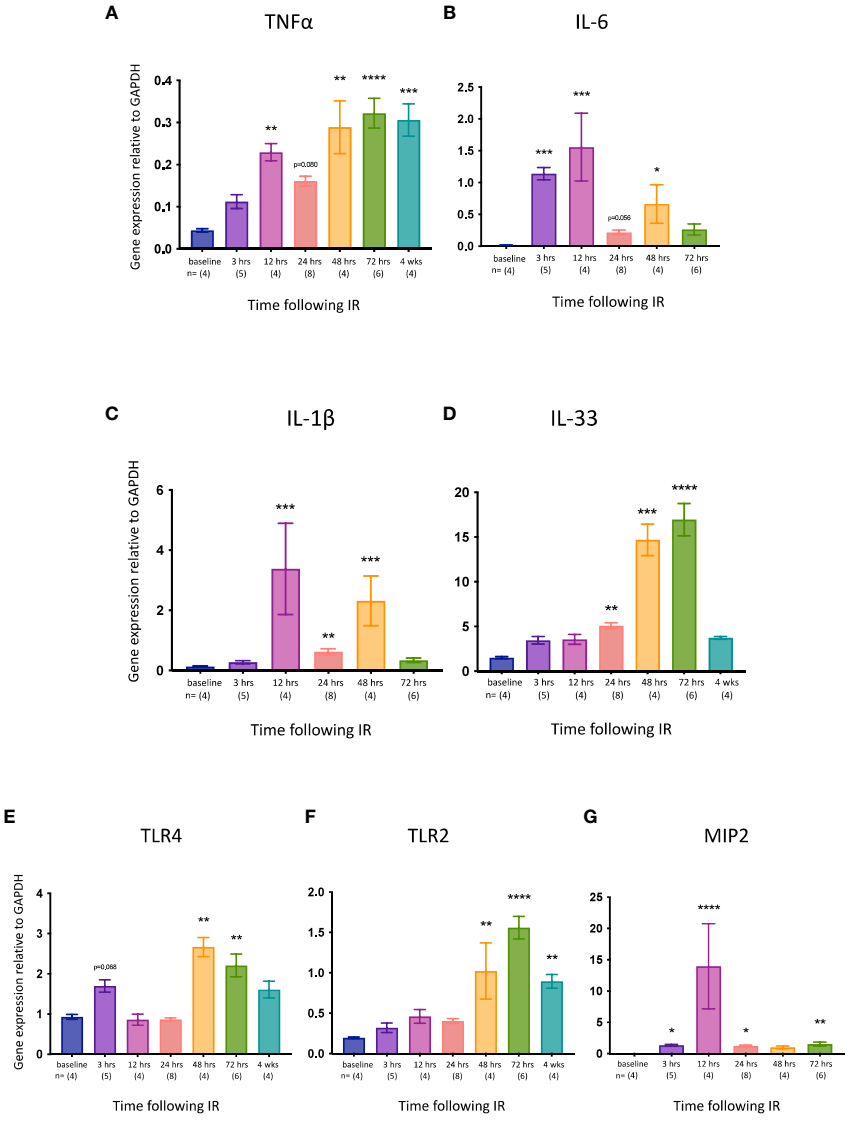

FIGURE 2
Time course of pro-inflammatory gene expression in the left kidney after IR in WT mice. **(A)**: *Tnfa*; **(B)**: *Il6*; **(C)**: *Il1b*; **(D)**: *Il33*; **(E)**: *Tlr4*; **(F)**: *Tlr2*. **(G)**: *Mip2*. Kruskal-Wallis test with Dunn multiple comparisons test with * p<0.05, ** p<0.01, *** p<0.001, **** p<0.0001 compared to baseline control. Data presented as mean ± SEM.

are released by necroptotic cells (61, 62). *Il1b* expression was upregulated at 12, 24 and 48 hrs (Figure 2C), whereas *Il33* was increased later, from 24 hrs (Figure 2D). Signalling via Toll-like receptor 4 (TLR4) can activate necroptosis, whereas TLR2 has not been shown to play a role in necroptotic cell death (53). Both *Tlr4* (Figure 2E) and *Tlr2* (Figure 2F) were upregulated relatively late (48 and 72 hrs, respectively), with *Tlr2* expression remaining high at 4 weeks. Macrophage inflammatory protein-2 (MIP-2) is a neutrophil chemoattractant/activator that is upregulated in kidney IRI (63). *Mip2* expression was significantly increased at all timepoints except 48 hrs, peaking at 12 hrs (Figure 2G).

3.2 Kinetics of necroptotic pathway gene expression in WT mice following IR

Although elevated expression of the necroptotic pathway genes *Ripk1*, *Ripk3* and *Mlkl* does not necessarily equate with increased necroptosis *in vivo* (53), it may indicate an increased propensity for this form of cell death. We therefore measured IRI-associated changes in the expression of these genes in the kidney at different times post-reperfusion. All 3 genes were significantly upregulated at most timepoints, with the highest expression observed at 48 hrs (Figure 3).

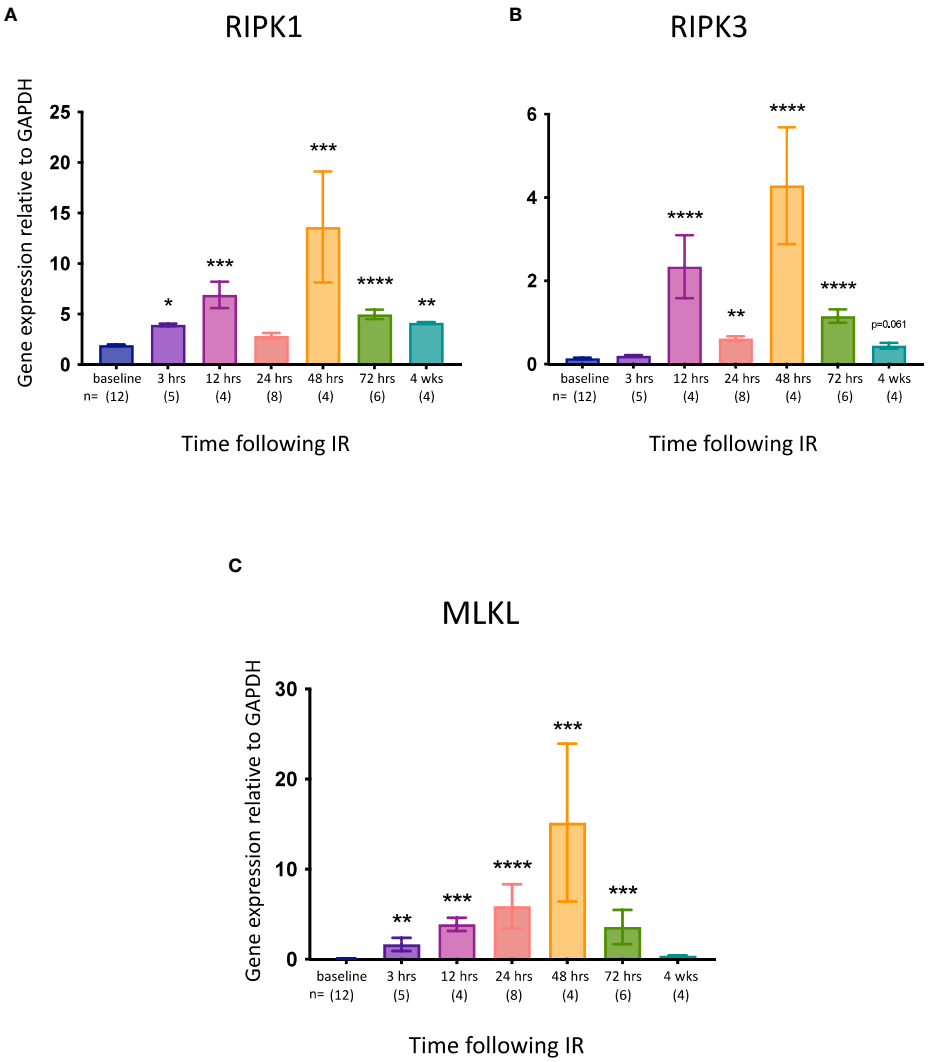

FIGURE 3
Time course of necroptotic pathway gene expression in the left kidney after IR in WT mice. **(A)**: *Ripk1*; **(B)**: *Ripk3*; **(C)**: *Mlkl*. Kruskal-Wallis test with Dunn multiple comparisons test with * p<0.05, ** p<0.01, *** p<0.001, **** p<0.0001 compared to baseline control. Data presented as mean ± SEM.

3.3 Temporal and spatial pattern of pMLKL staining in kidneys of WT mice following IR

Sections were cut from formalin-fixed left kidney tissue of WT mice from each cohort and stained for pMLKL using a rabbit monoclonal antibody [ab196436, EPR9515 (2)] This antibody has previously been used to detect pMLKL in methanol-fixed mouse dermal fibroblast cell lines (64) and in formalin-fixed mouse cecal tissue (65). Reproducible staining was achieved after optimization of the antigen retrieval step based initially on a method described by He et al., 2021 (65). *Mlkl*-ko mice subjected to IRI were used as a control to validate the antibody; *Mlkl*-ko kidneys showing substantial morphological injury were negative for pMLKL staining at each timepoint (Supplementary Figure 3). pMLKL was not detected in WT/IRI kidneys at 0 or 3 hrs post-reperfusion (Figures 4A, B). At 12 hrs, numerous tubules containing cells displaying dense punctate cytoplasmic staining were observed (Figure 4C). Interestingly, the tubules at this timepoint were either completely positive or completely negative. At 24 hrs, the pattern of staining had changed from cytoplasmic to predominantly membrane/intraluminal i.e., on the apical surface of tubular epithelial cells (Figure 4D). At 48 hrs, strong staining of proteinaceous casts within the tubules was observed, along with patchy intraluminal staining (Figure 4E). At 72 hrs (Figure 4F) and 4 weeks (Figure 4G), staining was weaker and mainly restricted to casts.

We performed a semi-quantitative analysis by counting the number of pMLKL-positive tubules as a percentage of the total number of tubules. The degree of positivity was highest at 12 hrs and remained significantly elevated at 24 and 48 hrs (Figure 4H). The data were further stratified into cytoplasmic and intraluminal staining, likely representing the activation and execution phases of necroptosis, respectively. On this basis, maximum activation of necroptosis was observed at 12 hrs, while the terminal stage of

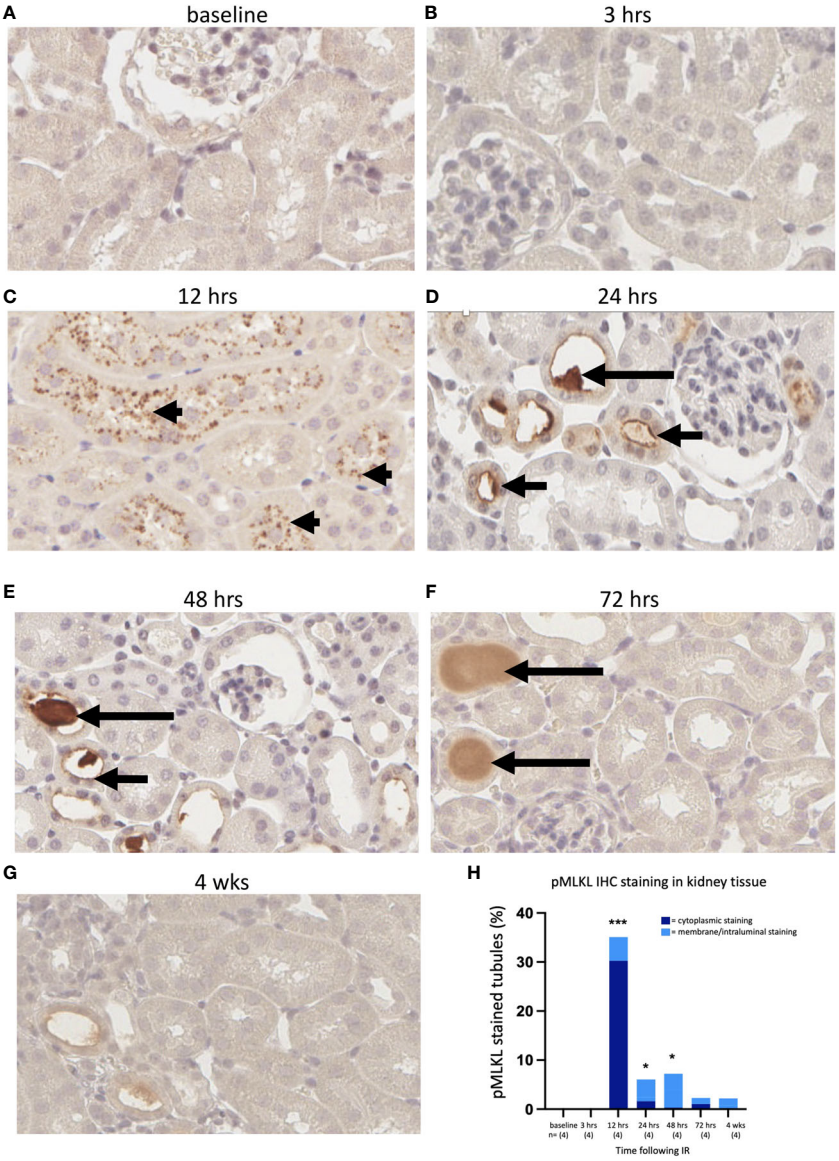

FIGURE 4
Time course of pMLKL staining in the left kidney after IR in WT mice. Representative sections from 0 hrs **(A)**, 3 hrs **(B)**, 12 hrs **(C)**, 24 hrs **(D)**, 48 hrs **(E)**, 72 hrs **(F)**, and 4 weeks **(G)** post-reperfusion. **(H)**: percentage of proximal tubules staining positive for pMLKL, stratified according to cellular location (dark blue = cytoplasmic; light blue = membrane/intraluminal). Examples of cytoplasmic, membrane and proteinaceous cast staining are indicated by arrowheads and short and long arrows, respectively. Kruskal-Wallis test with Dunn multiple comparisons test with * $p<0.05$, *** $p<0.001$ compared to baseline control. Image magnification x 400.

necroptotic cell death was relatively constant at 12, 24 and 48 hrs, and returned to close to baseline by 72 hrs (Figure 4H).

3.4 Effect of MLKL deletion on kidney IRI

Compared to WT mice, *Mlkl*-ko mice showed reduced kidney injury at 24 hrs post-reperfusion, evidenced by significant decreases in serum creatinine (Figure 5A) and tubular injury score (Figure 5B). Kidney function and injury were not significantly different at the other timepoints. Expression of *Kim1* (Figure 5C) and *Ngal* (Figure 5D) were reduced at the earlier timepoint of 12 hrs, although only the former was statistically significant. Expression of the pro-inflammatory cytokine genes *Tnfa*, *Il1b* and *Mip2* was also significantly lower at 12 hrs in *Mlkl*-ko mice compared to WT mice, whereas expression of *Il6*, *Il33*, *Tlr2* and *Tlr4*, and of the necroptosis pathway genes *Ripk1* and *Ripk3*, was generally similar in *Mlkl*-ko and WT mice at all timepoints (Supplementary Figure 1). As expected, *Mlkl* expression and pMLKL staining were undetectable in kidneys from *Mlkl*-ko mice (data not shown).

To investigate the mode of IRI-associated cell death in a necroptosis-deficient setting, kidney sections from the 24 hr timepoint were stained for cleaved Caspase-3 (cC3) as a marker of apoptosis. While WT kidneys showed a significant but modest increase in apoptotic tubules compared to sham kidneys, *Mlkl*-ko kidneys showed a major increase (Figure 6), suggesting a greater

10.3389/fimmu.2023.1251452

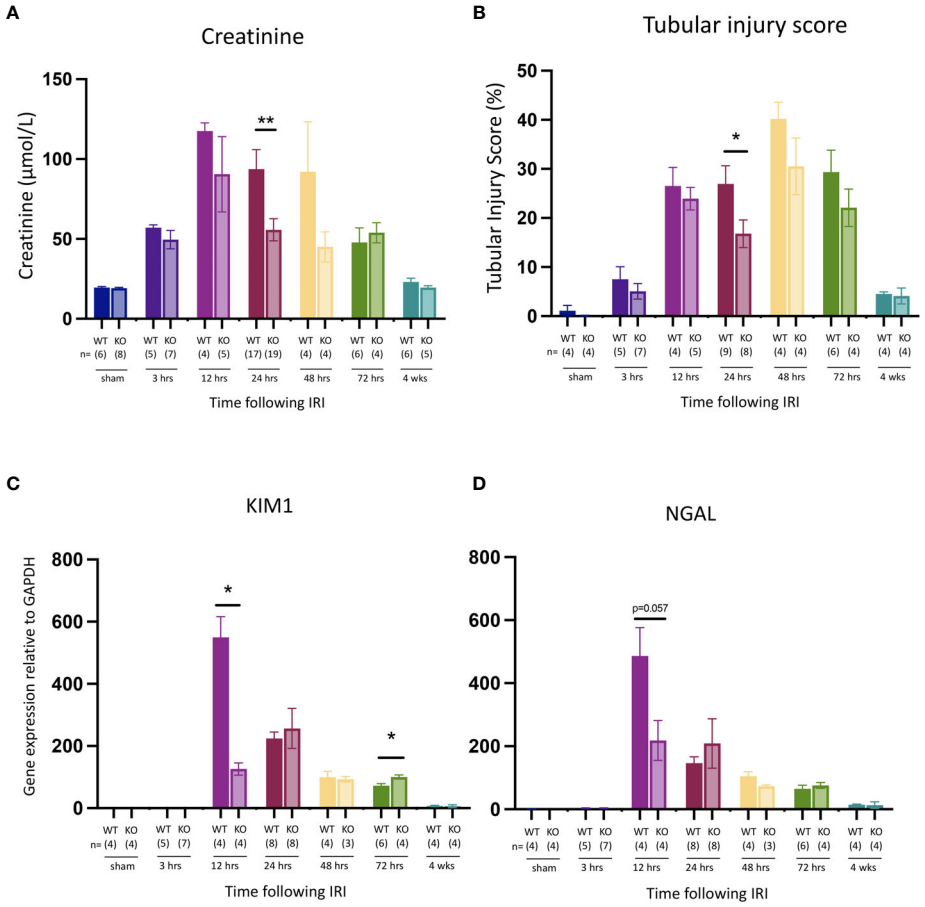

FIGURE 5
Comparison of kidney injury time course after IR in *Mlkl*-ko and WT mice. **(A)**: serum creatinine; **(B)**: tubular injury score; **(C)**: mRNA expression of *Kim1*; **(D)**: mRNA expression of *Ngal*. Mann Whitney U test comparing with *Mlkl*-ko and WT mice at each timepoint; * p<0.05, ** p<0.01. Data presented as mean ± SEM.

role for apoptosis in this model when necroptosis is inactivated. The pattern of cC3 staining in *Mlkl*-ko tubules at 24 hrs was like that of pMLKL staining in WT tubules at 12 hrs (Figure 4C) i.e., tubules were either completely positive or negative.

4 Discussion

Although several studies employing mouse models have implicated necroptosis in the pathogenesis of kidney IRI (54, 55, 66, 67), this is the first study to definitively demonstrate activation of the terminal stage of the necroptotic pathway (i.e., phosphorylation of MLKL) in this setting and to explore the dynamics of the process. We performed a time course analysis in a mouse model of unilateral warm IRI to detail the kinetics of kidney injury, inflammation and necroptosis. Our data suggest that the critical phase lies within 3-12 hrs following reperfusion. During this period, there was major activation of necroptosis as evident by strong pMLKL staining within proximal tubular cells (PTCs) at 12 hrs. Some of the PTCs exhibited pMLKL staining at the cell surface, suggesting progression to the pre-lytic/lytic phase of necroptosis. At the same time, there was upregulated expression of the necroptosis pathway genes *Ripk1*, *Ripk3* and *Mlkl* and the pro-inflammatory cytokine genes *Tnfa*, *Il6*, *Il1b* and *Mip2*. This, together with activation of the NLRP3 inflammasome by pMLKL (68), would be expected to create favourable conditions for further necroptosis and inflammation via DAMP release, driving the cycle of necroinflammation.

Of interest was the pattern of pMLKL staining. Epithelial cell injury associated with kidney IR is most apparent in the proximal tubules (1), as PTCs have low anaerobic glycolytic capacity and are located in areas with low partial pressure of oxygen such as the outer medulla and inner cortex (9). Consistent with this, we observed that tubular injury was focused in the proximal tubules in the cortico-medullary region. Necroptosis, as indicated by pMLKL staining, was also restricted to PTCs. This is in contrast to the findings of a recent single-cell analysis suggesting that necroptosis in kidney IRI occurs mainly in non-PTC cell types, with secondary effects on PTCs (69). Furthermore, injured tubules were clustered together, and necroptosis appeared to be activated in all cells within affected tubules. This suggests either a location-dependent effect, or communication between adjacent cells undergoing necroptosis resulting in the spread of necroptosis from cell to cell within affected tubules. pMLKL staining from 24 hrs appeared polarised, with staining of the apical but not basal

10.3389/fimmu.2023.1251452

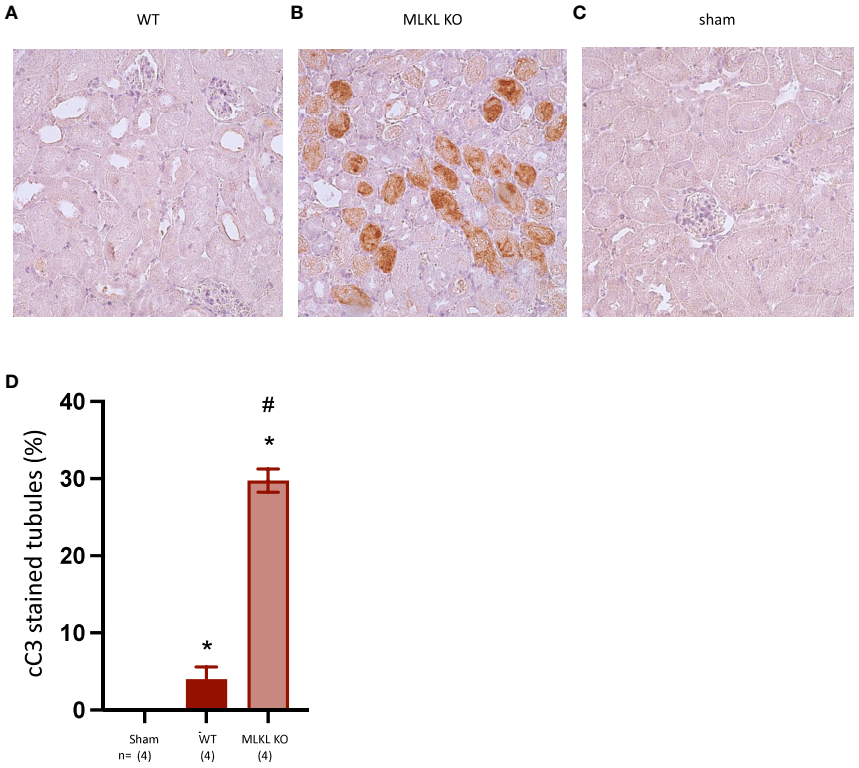

FIGURE 6
Comparison of cleaved Caspase-3 staining in WT and *Mlkl*-ko mice at 24 hrs post-reperfusion. **(A)**: WT; **(B)**: *Mlkl*-ko; **(C)**: sham; **(D)**: semi-quantitative analysis. Mann Whitney U test with * p<0.05 compared to sham procedure and # p<0.05 compared to WT mice. Data presented as mean ± SEM. Image magnification x 200.

surface of PTCs. The precise mechanism by which pMLKL clustering at the apical surface may promote cellular communication within the lumen of affected tubules remains to be further explored, with roles for pMLKL in promoting plasma membrane remodelling at intercellular junctions (50) and generation of extracellular vesicles (70, 71) previously proposed.

In the absence of necroptosis (i.e., in *Mlkl*-ko mice), early inflammation and kidney injury were reduced, providing further evidence that necroptosis and the associated inflammation play a role in kidney damage following IR. The absence of pMLKL staining at 3 hrs in WT mice indicated that the initial injury did not involve necroptosis. It is therefore unsurprising that there was no difference in serum creatinine [which is a delayed marker of kidney injury (72)] between WT and *Mlkl*-ko mice at 3 hrs. The inability of *Mlkl*-ko mice to activate necroptosis in the critical 3-12 hr phase is likely to account for the subsequent reduction in kidney inflammation at 12 hrs, and lower serum creatinine and tubular injury scores at 24 hrs. Interestingly, *Mlkl*-ko mice were protected from kidney IRI at 24 hrs but not at 48 or 72 hrs. This contrasts with an earlier study where protection was noted at 48 and 72 hrs but not at 24 hrs (56). Model differences, including the type (unilateral versus bilateral) and degree of ischemia (18 min versus 35 min), anesthesia (ketamine/xylazine versus the more IRI-protective isoflurane), and WT controls (littermates versus non-littermates), may account for this discrepancy.

While we have further defined the role of necroptosis in kidney IRI, the stimulus that triggers necroptosis in this setting remains unclear. Engagement of death receptors such as TNF receptor 1, activation of TLRs, interferon signalling, and intracellular stimuli in response to viruses, are all able to initiate necroptosis (73). A recent *in vitro* study using a genetically manipulated myeloid cell system confirmed TNF as an alarmin molecule released following necroptotic cell death to drive further inflammation (59). We suggest that TNF released by inflammatory cells triggers necroptosis during the 3-12 hours post-reperfusion, while TNF and DAMP release following necroptotic cell death stimulate subsequent waves of necroptosis. We showed upregulation of *Tnfa* gene expression in WT mice, which was reduced in *Mlkl*-ko mice, leading us to hypothesise that TNF activates necroptosis and drives ongoing necroinflammation in kidney IRI.

The concept that one regulated cell death pathway can compensate for another in acute kidney injury has previously been proposed for necroptosis and ferroptosis, although treatment of *Mlkl*-ko mice with a ferroptosis inhibitor did not provide further protection from kidney IRI (56). In our model, apoptosis appeared to become the dominant cell death pathway in the absence of necroptosis, suggesting a relationship between necroptosis and apoptosis in kidney IRI. However, a limitation of our study was that it focused on the role of necroptosis without investigating the contribution of other regulated necrosis pathways, notably ferroptosis.

Our study is the first to describe the dynamics of necroptosis and necroinflammation in a mouse model of kidney IRI. Our results suggest that treatments targeting the key necroptosis component,

MLKL, may reduce kidney injury following IR, although it should be noted that no specific inhibitors of mouse MLKL are currently available. In addition, our results suggest that such treatments may be effective even if given 3 hrs after reperfusion. This is advantageous in a clinical setting, as in many instances IRI is unpredictable and cannot be treated prophylactically. Finally, combination therapy with inhibitors of MLKL and apoptosis may provide additive protection, with the ultimate aim of preventing acute and chronic kidney disease following kidney IR.

Data availability statement

The raw data supporting the conclusions of this article will be made available by the authors, without undue reservation.

Ethics statement

The animal study was approved by St Vincent's Hospital Melbourne Animal Ethics Committee. The study was conducted in accordance with the local legislation and institutional requirements.

Author contributions

AP, JM, FI and PC designed the experimental studies. AP, AB, JM, NF, ES conducted the experimental studies. AB, JM and AP performed the IRI surgery. AP, AB, ES and JM analysed the results. AP and PC drafted the manuscript. All authors contributed to the article and approved the submitted version.

Funding

The author(s) declare financial support was received for the research, authorship, and/or publication of this article. This study was funded in part by grant number 88279 from the St Vincent's Hospital Melbourne Research Endowment Fund. AP was supported by a postgraduate scholarship and JMM by an Investigator Grant (1172929) from the National Health & Medical Research Council (NHMRC) of Australia. JMM acknowledges infrastructure support from the NHMRC (IRIISS 9000719) and the Victorian State Government Operational Infrastructure Support Scheme.

Acknowledgments

We thank Dr Andre Samson, Dr Ueli Nächbur, and Dr Anne Hempel for helpful discussion on necroptosis and provision of experimental animals; Dr Fenella Munz for advice on veterinary matters and tubular injury scoring; and staff at the Bioresources Centre, St Vincent's Hospital, Melbourne, for animal care.

Conflict of interest

Authors JMM and PC have received research funding from Anaxis Pharma Pty Ltd.

The remaining authors declare that the research was conducted in the absence of any commercial or financial relationships that could be construed as a potential conflict of interest.

Publisher's note

Supplementary material

The Supplementary Material for this article can be found online at: https://www.frontiersin.org/articles/10.3389/fimmu.2023.1251452/full#supplementary-material

SUPPLEMENTARY FIGURE 1
Comparison of pro-inflammatory and necroptotic gene expression after IR in *Mlkl*-ko and WT mice. **(A)**: *Tnfa*; **(B)**: *Il6*; **(C)**: *Il1b*; **(D)**: *Il33*; **(E)**: *Tlr4*; **(F)**: *Tlr2*; **(G)**: *Mip2*; **(H)**: *Ripk1*; **(I)**: *Ripk3*. Mann Whitney U test comparing with *Mlkl*-ko and WT mice at each timepoint; * $p<0.05$. Data presented as mean ± SEM.

SUPPLEMENTARY FIGURE 2
Representative PAS stained kidney tissue at baseline, 3 hrs, 12 hrs, 24 hrs, 48 hrs, 72 hrs and 4 weeks following IRI. Image magnification x 40.

SUPPLEMENTARY FIGURE 3
Representative pMLKL stained kidney tissue of *Mlkl*-ko mice taken at baseline, 3 hrs, 12 hrs, 24 hrs, 48 hrs, 72 hrs and 4 weeks following IRI. Image magnification x 40.

References

1. Bonventre JV, Yang L. Cellular pathophysiology of ischemic acute kidney injury. *J Clin Invest* (2011) 121(11):4210–21. doi: 10.1172/JCI45161

2. Kalogeris T, Baines CP, Krenz M, Korthuis RJ. Cell biology of ischemia/reperfusion injury. *Int Rev Cell Mol Biol* (2012) 298:229–317. doi: 10.1016/B978-0-12-394309-5.00006-7

3. Kosieradzki M, Rowinski W. Ischemia/reperfusion injury in kidney transplantation: mechanisms and prevention. *Transplant Proc* (2008) 40(10):3279–88. doi: 10.1016/j.transproceed.2008.10.004

4. Murphy E, Steenbergen C. Ion transport and energetics during cell death and protection. *Physiol (Bethesda)* (2008) 23:115–23. doi: 10.1152/physiol.00044.2007

5. Croall DE, Ersfeld K. The calpains: modular designs and functional diversity. *Genome Biol* (2007) 8(6):218. doi: 10.1186/gb-2007-8-6-218

6. Kako K, Kato M, Matsuoka T, Mustapha A. Depression of membrane-bound Na +-K+-ATPase activity induced by free radicals and by ischemia of kidney. *Americal Physiol Soc* (1988) 1988:330–7. doi: 10.1152/ajpcell.1988.254.2.C330

7. Perico N, Cattaneo D, Sayegh MH, Remuzzi G. Delayed graft function in kidney transplantation. *Lancet* (2004) 364(9447):1814–27. doi: 10.1016/S0140-6736(04)17406-0

8. Castaneda MP, Swiatecka-Urban A, Mitsnefes MM, Feuerstein D, Kaskel FJ, Tellis V, et al. Activation of mitochondrial apoptotic pathways in human renal allografts after ischemiareperfusion injury. *Transplantation* (2003) 76(1):50–4. doi: 10.1097/01.TP.0000069835.95442.9F

9. Scholz H, Boivin FJ, Schmidt-Ott KM, Bachmann S, Eckardt KU, Scholl UI, et al. Kidney physiology and susceptibility to acute kidney injury: implications for renoprotection. *Nat Rev Nephrol* (2021) 17(5):335–49. doi: 10.1038/s41581-021-00394-7

10. Brady HR, Singer GG. Acute renal failure. *Lancet* (1995) 346(8989):1533–40. doi: 10.1016/S0140-6736(95)92057-9

11. Bianchi ME, Manfredi AA. High-mobility group box 1 (HMGB1) protein at the crossroads between innate and adaptive immunity. *Immunol Rev* (2007) 220:35–46. doi: 10.1111/j.1600-065X.2007.00574.x

12. Bianchi ME. DAMPs, PAMPs and alarmins: all we need to know about danger. *J Leukoc Biol* (2007) 81(1):1–5. doi: 10.1189/jlb.0306164

13. Li L, Okusa MD. Blocking the immune response in ischemic acute kidney injury: the role of adenosine 2A agonists. *Nat Clin Pract Nephrol* (2006) 2(8):432–44. doi: 10.1038/ncpneph0238

14. Tesmer LA, Lundy SK, Sarkar S, Fox DA. Th17 cells in human disease. *Immunol Rev* (2008) 223:87–113. doi: 10.1111/j.1600-065X.2008.00628.x

15. Chadha R, Heidt S, Jones ND, Wood KJ. Th17: contributors to allograft rejection and a barrier to the induction of transplantation tolerance? *Transplantation* (2011) 91(9):939–45. doi: 10.1097/TP.0b013e3182126eeb

16. Molitoris BA, Sutton TA. Endothelial injury and dysfunction: role in the extension phase of acute renal failure. *Kidney Int* (2004) 66(2):496–9. doi: 10.1111/j.1523-1755.2004.761_5.x

17. Basile DP, Donohoe D, Roethe K, Osborn JL. Renal ischemic injury results in permanent damage to peritubular capillaries and influence long-term function. *Am J Physiol Renal Physiol* (2001) 281(5):887–99. doi: 10.1152/ajprenal.00050.2001

18. Legrand M, Mik EG, Johannes T, Payen D, Ince C. Renal hypoxia and dysoxia after reperfusion of the ischemic kidney. *Mol Med* (2008) 14(7-8):502–16. doi: 10.2119/2008-00006.Legrand

19. Basile DP, Friedrich JL, Spahic J, Knipe N, Mang H, Leonard EC, et al. Impaired endothelial proliferation and mesenchymal transition contribute to vascular rarefaction following acute kidney injury. *Am J Physiol Renal Physiol* (2011) 300(3):F721–33. doi: 10.1152/ajprenal.00546.2010

20. Norman JT, Clark IM, Garcia PL. Hypoxia promotes fibrogenesis in human renal fibroblasts. *Kidney Int* (2000) 58(6):2351–66. doi: 10.1046/j.1523-1755.2000.00419.x

21. Gueler F, Gwinner W, Schwarz A, Haller H. Long-term effects of acute ischemia and reperfusion injury. *Kidney Int* (2004) 66(2):523–7. doi: 10.1111/j.1523-1755.2004.761_11.x

22. LaFrance JP, Miller DR. Defining acute kidney injury in database studies: the effects of varying the baseline kidney function assessment period and considering CKD status. *Am J Kidney Dis* (2010) 56(4):651–60. doi: 10.1053/j.ajkd.2010.05.011

23. Hoste EA, Bagshaw SM, Bellomo R, Cely CM, Colman R, Cruz DN, et al. Epidemiology of acute kidney injury in critically ill patients: the multinational AKI-EPI study. *Intensive Care Med* (2015) 41(8):1411–23. doi: 10.1007/s00134-015-3934-7

24. See EJ, Jayasinghe K, Glassford N, Bailey M, Johnson DW, Polkinghorne KR, et al. Long-term risk of adverse outcomes after acute kidney injury: a systematic review and meta-analysis of cohort studies using consensus definitions of exposure. *Kidney Int* (2019) 95(1):160–72. doi: 10.1016/j.kint.2018.08.036

25. Yang F, Zhang L, Wu H, Zou H, Du Y. Clinical analysis of cause, treatment and prognosis in acute kidney injury patients. *PloS One* (2014) 9(2):e85214. doi: 10.1371/journal.pone.0085214

26. See EJ, Toussaint ND, Bailey M, Johnson DW, Polkinghorne KR, Robbins R, et al. Risk factors for major adverse kidney events in the first year after acute kidney injury. *Clin Kidney J* (2021) 14(2):556–63. doi: 10.1093/ckj/sfz169

27. Coca SG, Singanamala S, Parikh CR. Chronic kidney disease after acute kidney injury: a systematic review and meta-analysis. *Kidney Int* (2012) 81(5):442–8. doi: 10.1038/ki.2011.379

28. Hsu CY. Yes, AKI truly leads to CKD. *J Am Soc Nephrol* (2012) 23(6):967–9. doi: 10.1681/ASN.2012030222

29. Kovesdy CP. Epidemiology of chronic kidney disease: an update 2022. *Kidney Int Suppl* (2022) 12(1):7–11. doi: 10.1016/j.kisu.2021.11.003

30. Mortality GBDCauses of Death C. Global, regional, and national age-sex specific all-cause and cause-specific mortality for 240 causes of death, 1990-2013: a systematic analysis for the Global Burden of Disease Study 2013. *Lancet* (2015) 385(9963):117–71. doi: 10.1016/S0140-6736(14)61682-2

31. Rhee CM, Kovesdy CP. Epidemiology: Spotlight on CKD deaths-increasing mortality worldwide. *Nat Rev Nephrol* (2015) 11(4):199–200. doi: 10.1038/nrneph.2015.25

32. Degterev A, Huang Z, Boyce M, Li Y, Jagtap P, Mizushima N, et al. Chemical inhibitor of nonapoptotic cell death with therapeutic potential for ischemic brain injury. *Nat Chem Biol* (2005) 1(2):112–9. doi: 10.1038/nchembio711

33. Dixon SJ, Lemberg KM, Lamprecht MR, Skouta R, Zaitsev EM, Gleason CE, et al. Ferroptosis: an iron-dependent form of nonapoptotic cell death. *Cell* (2012) 149(5):1060–72. doi: 10.1016/j.cell.2012.03.042

34. Fink SL, Cookson BT. Caspase-1-dependent pore formation during pyroptosis leads to osmotic lysis of infected host macrophages. *Cell Microbiol* (2006) 8(11):1812–25. doi: 10.1111/j.1462-5822.2006.00751.x

35. Liu X, Zhang Z, Ruan J, Pan Y, Magupalli VG, Wu H, et al. Inflammasome-activated gasdermin D causes pyroptosis by forming membrane pores. *Nature* (2016) 535(7610):153–8. doi: 10.1038/nature18629

36. Devalaraja-Narashimha K, Diener AM, Padanilam BJ. Cyclophilin D gene ablation protects mice from ischemic renal injury. *Am J Physiol Renal Physiol* (2009) 297(3):F749–59. doi: 10.1152/ajprenal.00239.2009

37. Andrabi SA, Kim NS, Yu SW, Wang H, Koh DW, Sasaki M, et al. Poly(ADP-ribose) (PAR) polymer is a death signal. *Proc Natl Acad Sci USA* (2006) 103(48):18308–13. doi: 10.1073/pnas.0606526103

38. David KK, Andrabi SA, Dawson TM, Dawson VL. Parthanatos, a messenger of death. *Front Biosci* (2009) 14:1116–28. doi: 10.2741/3297

39. Pefanis A, Ierino FL, Murphy JM, Cowan PJ. Regulated necrosis in kidney ischemia-reperfusion injury. *Kidney Int* (2019) 96(2):291–301. doi: 10.1016/j.kint.2019.02.009

40. Horne CR, Samson AL, Murphy JM. The web of death: the expanding complexity of necroptotic signaling. *Trends Cell Biol* (2023) 33(2):162–74. doi: 10.1016/j.tcb.2022.05.008

41. Samson AL, Garnish SE, Hildebrand JM, Murphy JM. Location, location, location: A compartmentalized view of TNF-induced necroptotic signaling. *Sci Signal* (2021) 14(668):eabc6178. doi: 10.1126/scisignal.abc6178

42. Li J, McQuade T, Siemer AB, Napetschnig J, Moriwaki K, Hsiao YS, et al. The RIP1/RIP3 necrosome forms a functional amyloid signaling complex required for programmed necrosis. *Cell* (2012) 150(2):339–50. doi: 10.1016/j.cell.2012.06.019

43. Mompean M, Li W, Li J, Laage S, Siemer AB, Bozkurt G, et al. The structure of the necrosome RIPK1-RIPK3 core, a human hetero-amyloid signaling complex. *Cell* (2018) 173(5):1244–53.e10. doi: 10.1016/j.cell.2018.03.032

44. Sun L, Wang H, Wang Z, He S, Chen S, Liao D, et al. Mixed lineage kinase domain-like protein mediates necrosis signaling downstream of RIP3 kinase. *Cell* (2012) 148(1-2):213–27. doi: 10.1016/j.cell.2011.11.031

45. Murphy JM, Czabotar PE, Hildebrand JM, Lucet IS, Zhang JG, Alvarez-Diaz S, et al. The pseudokinase MLKL mediates necroptosis via a molecular switch mechanism. *Immunity* (2013) 39(3):443–53. doi: 10.1016/j.immuni.2013.06.018

46. Meng Y, Davies KA, Fitzgibbon C, Young SN, Garnish SE, Horne CR, et al. Human RIPK3 maintains MLKL in an inactive conformation prior to cell death by necroptosis. *Nat Commun* (2021) 12(1):6783. doi: 10.1038/s41467-021-27032-x

47. Petrie EJ, Sandow JJ, Jacobsen AV, Smith BJ, Griffin MDW, Lucet IS, et al. Conformational switching of the pseudokinase domain promotes human MLKL tetramerization and cell death by necroptosis. *Nat Commun* (2018) 9(1):2422. doi: 10.1038/s41467-018-04714-7

48. Petrie EJ, Birkinshaw RW, Koide A, Denbaum E, Hildebrand JM, Garnish SE, et al. Identification of MLKL membrane translocation as a checkpoint in necroptotic cell death using Monobodies. *Proc Natl Acad Sci USA* (2020) 117(15):8468–75. doi: 10.1073/pnas.1919960117

49. Garnish SE, Meng Y, Koide A, Sandow JJ, Denbaum E, Jacobsen AV, et al. Conformational interconversion of MLKL and disengagement from RIPK3 precede cell death by necroptosis. *Nat Commun* (2021) 12(1):2211. doi: 10.1038/s41467-021-22400-z

50. Samson AL, Zhang Y, Geoghegan ND, Gavin XJ, Davies KA, Mlodzianoski MJ, et al. MLKL trafficking and accumulation at the plasma membrane control the kinetics and threshold for necroptosis. *Nat Commun* (2020) 11(1):3151. doi: 10.1038/s41467-020-16887-1

51. Nakano H, Murai S, Moriwaki K. Regulation of the release of damage-associated molecular patterns from necroptotic cells. *Biochem J* (2022) 479(5):677–85. doi: 10.1042/BCJ20210604

52. Linkermann A, Stockwell BR, Krautwald S, Anders HJ. Regulated cell death and inflammation: an auto-amplification loop causes organ failure. *Nat Rev Immunol* (2014) 14(11):759–67. doi: 10.1038/nri3743

53. Kolbrink B, von Samson-Himmelstjerna FA, Murphy JM, Krautwald S. Role of necroptosis in kidney health and disease. *Nat Rev Nephrol* (2023) 19(5):300–14. doi: 10.1038/s41581-022-00658-w

54. Linkermann A, Brasen JH, Darding M, Jin MK, Sanz AB, Heller JO, et al. Two independent pathways of regulated necrosis mediate ischemia-reperfusion injury. *Proc Natl Acad Sci USA* (2013) 110(29):12024–9. doi: 10.1073/pnas.1305538110

55. Newton K, Dugger DL, Maltzman A, Greve JM, Hedehus M, Martin-McNulty B, et al. RIPK3 deficiency or catalytically inactive RIPK1 provides greater benefit than

MLKL deficiency in mouse models of inflammation and tissue injury. *Cell Death Differ* (2016) 23(9):1565–76. doi: 10.1038/cdd.2016.46

56. Muller T, Dewitz C, Schmitz J, Schroder AS, Brasen JH, Stockwell BR, et al. Necroptosis and ferroptosis are alternative cell death pathways that operate in acute kidney failure. *Cell Mol Life Sci* (2017) 74(19):3631–45. doi: 10.1007/s00018-017-2547-4

57. Crikis S, Lu B, Murray-Segal LM, Selan C, Robson SC, D'Apice AJ, et al. Transgenic overexpression of CD39 protects against renal ischemia-reperfusion and transplant vascular injury. *Am J Transplant* (2010) 10(12):2586–95. doi: 10.1111/j.1600-6143.2010.03257.x

58. McRae JL, Vikstrom IB, Bongoni AK, Salvaris EJ, Fisicaro N, Ng M, et al. Blockade of the G-CSF receptor is protective in a mouse model of renal ischemia-reperfusion injury. *J Immunol* (2020) 205(5):1433–40. doi: 10.4049/jimmunol.2000390

59. Pinci F, Gaidt MM, Jung C, Nagl D, Kuut G, Hornung V. Tumor necrosis factor is a necroptosis-associated alarmin. *Front Immunol* (2022) 13:1074440. doi: 10.3389/fimmu.2022.1074440

60. Vanden Berghe T, Kalai M, Denecker G, Meeus A, Saelens X, Vandenabeele P. Necrosis is associated with IL-6 production but apoptosis is not. *Cell Signal* (2006) 18 (3):328–35. doi: 10.1016/j.cellsig.2005.05.003

61. Li L, Shan S, Kang K, Zhang C, Kou R, Song F. The cross-talk of NLRP3 inflammasome activation and necroptotic hepatocyte death in acetaminophen-induced mice acute liver injury. *Hum Exp Toxicol* (2021) 40(4):673–84. doi: 10.1177/0960327120961158

62. Shlomovitz I, Erlich Z, Speir M, Zargarian S, Baram N, Engler M, et al. Necroptosis directly induces the release of full-length biologically active IL-33 in *vitro* and in an inflammatory disease model. *FEBS J* (2019) 286(3):507–22. doi: 10.1111/febs.14738

63. Lemay S, Rabb H, Postler G, Singh AK. Prominent and sustained up-regulation of gp130-signaling cytokines and the chemokine MIP-2 in murine renal ischemia-reperfusion injury. *Transplantation* (2000) 69(5):959–63. doi: 10.1097/00007890-200003150-00049

64. Samson AL, Fitzgibbon C, Patel KM, Hildebrand JM, Whitehead LW, Rimes JS, et al. A toolbox for imaging RIPK1, RIPK3, and MLKL in mouse and human cells. *Cell Death Differ* (2021) 28(7):2126–44. doi: 10.1038/s41418-021-00742-x

65. He P, Ai T, Yang ZH, Wu J, Han J. Detection of necroptosis by phospho-MLKL immunohistochemical labeling. *STAR Protoc* (2021) 2(1):100251. doi: 10.1016/j.xpro.2020.100251

66. Liu W, Chen B, Wang Y, Meng C, Huang H, Huang XR, et al. RGMb protects against acute kidney injury by inhibiting tubular cell necroptosis via an MLKL-dependent mechanism. *Proc Natl Acad Sci USA* (2018) 115(7):E1475–E84. doi: 10.1073/pnas.1716959115

67. Jouan-Lanhouet S, Riquet F, Duprez L, Vanden Berghe T, Takahashi N, Vandenabeele P. Necroptosis, in *vivo* detection in experimental disease models. *Semin Cell Dev Biol* (2014) 35:2–13. doi: 10.1016/j.semcdb.2014.08.010

68. Conos SA, Chen KW, De Nardo D, Hara H, Whitehead L, Nunez G, et al. Active MLKL triggers the NLRP3 inflammasome in a cell-intrinsic manner. *Proc Natl Acad Sci USA* (2017) 114(6):E961–E9. doi: 10.1073/pnas.1613305114

69. Balzer MS, Doke T, Yang YW, Aldridge DL, Hu H, Mai H, et al. Single-cell analysis highlights differences in druggable pathways underlying adaptive or fibrotic kidney regeneration. *Nat Commun* (2022) 13(1):4018. doi: 10.1038/s41467-022-31772-9

70. Yoon S, Kovalenko A, Bogdanov K, Wallach D. MLKL, the protein that mediates necroptosis, also regulates endosomal trafficking and extracellular vesicle generation. *Immunity* (2017) 47(1):51–65.e7. doi: 10.1016/j.immuni.2017.06.001

71. Gong YN, Guy C, Olauson H, Becker JU, Yang M, Fitzgerald P, et al. ESCRT-III acts downstream of MLKL to regulate necroptotic cell death and its consequences. *Cell* (2017) 169(2):286–300.e16. doi: 10.1016/j.cell.2017.03.020

72. Moran SM, Myers BD. Course of acute renal failure studied by a model of creatinine kinetics. *Kidney Int* (1985) 27(6):928–37. doi: 10.1038/ki.1985.101

73. Linkermann A, Green DR. Necroptosis. *N Engl J Med* (2014) 370(5):455–65. doi: 10.1056/NEJMra1310050

frontiers | Frontiers in Immunology

TYPE Original Research
PUBLISHED 03 November 2023
DOI 10.3389/fimmu.2023.1264447

OPEN ACCESS

EDITED BY
Wei Jing Liu,
Beijing University of Chinese Medicine, China

REVIEWED BY
John Cijiang He,
Icahn School of Medicine at Mount Sinai, United States
Adriana R. Silva,
Oswaldo Cruz Foundation (Fiocruz), Brazil
Shougang Zhuang,
Brown University, United States

*CORRESPONDENCE
Hui-Yao Lan
hylan@cuhk.edu.hk
Xueqing Yu
yuxueqing@gdph.org.cn
Xiaoqin Wang
wangxiaoqin@hbhtcm.com

RECEIVED 20 July 2023
ACCEPTED 10 October 2023
PUBLISHED 03 November 2023

CITATION
Wu W, Wang W, Liang L, Chen J, Sun S, Wei B, Zhong Y, Huang X-R, Liu J, Wang X, Yu X and Lan H-Y (2023) SARS-CoV-2 N protein induced acute kidney injury in diabetic db/db mice is associated with a Mincle-dependent M1 macrophage activation.
Front. Immunol. 14:1264447.
doi: 10.3389/fimmu.2023.1264447

SARS-CoV-2 N protein induced acute kidney injury in diabetic db/db mice is associated with a Mincle-dependent M1 macrophage activation

Wenjing Wu[1,2,3,4,5], Wenbiao Wang[1,2], Liying Liang[3,6], Junzhe Chen[3,7], Sifan Sun[3,8], Biao Wei[3], Yu Zhong[3], Xiao-Ru Huang[1,2,3], Jian Liu[9], Xiaoqin Wang[4,5]*, Xueqing Yu[2]* and Hui-Yao Lan[2,3]*

[1]Guangdong Cardiovascular Institute, Guangzhou, China, [2]Guangdong-Hong Kong Joint Laboratory for Immunological and Genetic Kidney Disease, Departments of Nephrology and Pathology, Guangdong Provincial People's Hospital (Guangdong Academy of Medical Sciences), Southern Medical University, Guangzhou, China, [3]Departments of Medicine & Therapeutics, Li Ka Shing Institute of Health Sciences, Lui Che Woo Institute of Innovative Medicine, The Chinese University of Hong Kong, Hong Kong, China, [4]The First Clinical College, Hubei University of Chinese Medicine, Wuhan, China, [5]Department of Nephrology, Hubei Provincial Hospital of Traditional Chinese Medicine, Hubei Province Academy of Traditional Chinese Medicine, Wuhan, China, [6]Department of Clinical Pharmacy, Guangzhou Eighth People's Hospital, Guangzhou Medical University, Guangzhou, China, [7]Department of Nephrology, The Third Affiliated Hospital, Southern Medical University, Guangzhou, China, [8]Department of Nephrology, Jiangsu Province Hospital of Chinese Medicine, Affiliated Hospital of Nanjing University of Chinese Medicine, Nanjing, Jiangsu, China, [9]Department of Nephrology, The Affiliated Traditional Chinese Medicine Hospital of Southwest Medical University, Luzhou, China

"Cytokine storm" is common in critically ill COVID-19 patients, however, mechanisms remain largely unknown. Here, we reported that overexpression of SARS-CoV-2 N protein in diabetic db/db mice significantly increased tubular death and the release of HMGB1, one of the damage-associated molecular patterns (DAMPs), to trigger M1 proinflammatory macrophage activation and production of IL-6, TNF-α, and MCP-1 via a Mincle-Syk/NF-κB-dependent mechanism. This was further confirmed *in vitro* that overexpression of SARS-CoV-2 N protein caused the release of HMGB1 from injured tubular cells under high AGE conditions, which resulted in M1 macrophage activation and production of proinflammatory cytokines via a Mincle-Syk/NF-κB-dependent mechanism. This was further evidenced by specifically silencing macrophage Mincle to block HMGB1-induced M1 macrophage activation and production of IL-6, TNF-α, and MCP-1 *in vitro*. Importantly, we also uncovered that treatment with quercetin largely improved SARS-CoV-2 N protein-induced AKI in db/db mice. Mechanistically, we found that quercetin treatment significantly inhibited the release of a DAMP molecule HMGB1 and inactivated M1 pro-inflammatory macrophage while promoting reparative M2 macrophage responses by

suppressing Mincle-Syk/NF-κB signaling *in vivo* and *in vitro*. In conclusion, SARS-CoV-2 N protein-induced AKI in db/db mice is associated with Mincle-dependent M1 macrophage activation. Inhibition of this pathway may be a mechanism through which quercetin inhibits COVID-19-associated AKI.

KEYWORDS

SARS-CoV-2, N protein, AKI, quercetin, Mincle, M1 macrophage

Introduction

Acute kidney injury (AKI) has been recognized as a common complication of the coronavirus disease 2019(COVID-19), which is caused by severe acute respiratory syndrome coronavirus 2 (SARS-CoV-2). AKI is common in critically ill COVID-19 patients with high mortality (1–4). Patients with older age and underlying diseases such as hypertension, diabetes, and chronic kidney disease (CKD) are at high risk for COVID-19 AKI (5, 6). However, mechanisms for COVID-19 AKI remain largely unknown.

Increasing evidence shows that cytokine storm is common in critically ill patients with AKI (7). Cytokine storm is related to excessive immune responses in patients with severe SARS-CoV-2 infection and is characterized by the production of large amounts of cytokines such as interleukin-6 (IL-6), interleukin-8 (IL-8), tumor necrosis factor-alpha (TNF-a), and monocyte chemotactic protein-1 (MCP-1) (8–13). Thus, understanding the mechanisms that lead to the cytokine storm associated with COVID-19 infection is extremely important for developing potential treatments for critically ill COVID-19 patients.

Elevated inflammatory markers such as white blood cell count, monocyte count, high levels of C-reactive protein, and proinflammatory cytokines such as IL-6, TNF-a, and MCP-1 have been demonstrated in patients with severe COVID-19 (10–15). It is also reported that the $CD68^+$ macrophages infiltrating the kidney are also associated with severe kidney injury in COVID-19 patients (16). Tubular necrosis is a pathological feature of COVID-19 patients with AKI (7). Tubular necrosis can induce renal inflammation by releasing the damage-associated molecular patterns (DAMPs) to activate immune cells through identical pattern recognition receptors (PRR) (17). Macrophage-inducible C-type lectin (Mincle) is a transmembrane pattern recognition receptor that is expressed by M1 pro-inflammatory macrophages in response DAMPs (18, 19). Mincle acts via its downstream Syk and NF-κB signaling to activate M1 pro-inflammatory macrophages and is essential for maintaining the pro-inflammatory phenotype of M1 macrophages in AKI (20). It has been reported that increased expression of DAMPs such as the high-mobility group box 1 protein (HMGB1) and S100A8/A9 is found in patients with moderate to severe COVID-19 (21, 22). Early post-mortem examination confirms that SARS-CoV-2 can directly infect human kidney tubular cells and then induce acute tubular damage by a direct cytopathic effect and CD68-positive macrophages (23). Our recent study also finds that SARS-CoV-2 N protein can activate transforming growth factor beta (TGF-β) signaling by interacting with Smad3 and thus causes tubular cell death via mechanisms associated with Smad3-dependent G1 cell cycle arrest and Ripk3/MLKL necroptosis pathways (24–26). However, Mincle-dependent M1 macrophage activation in COVID-19 AKI remains unexplored, which was investigated in the present study.

Quercetin is a widespread flavonoid found in a large variety of Chinese herbs and dietary supplements. It shows multiple pharmacological effects, including antiviral, antioxidant, and anti-inflammatory properties. Clinical trials demonstrate that treatment of COVID-19 patients with oral quercetin significantly improves the severity of COVID-19 syndromes (27, 28). Molecular docking studies predict that quercetin can bind to multiple SARS-CoV-2 proteases and thus inhibit viral infection (29, 30). Our recent studies confirmed that ultrasound-microbubble-mediated kidney-specifically overexpressing SARS-CoV-2 N protein can induce AKI in 8-week-old db/db mice by causing tubular necrosis and elevated serum levels of creatinine and blood urea nitrogen, which is further exacerbated in older age (16 weeks) of db/db mice, but is inhibited by treatment with quercetin (24). We find that quercetin can effectively block the binding of SARS-CoV-2 N protein to Smad3, therefore inhibiting SARS-CoV-2 N protein-induced tubular cell death via the Smad3-p16-dependent G1 cell cycle arrest mechanism (24). It is also reported that quercetin can inhibit proinflammatory cytokine expression in a cisplatin-induced mouse model of AKI by suppressing Mincle/Syk/NF-κB signaling (31). However, it remains unknown whether treatment with quercetin inhibits COVID-19 AKI via the Mincle-dependent mechanism, which was also investigated in the present study *in vivo* and *in vitro*.

Materials and methods

Preparation of SARS-CoV-2 N protein-expressing plasmid

Mammalian expression plasmids for pcDNA3.1(+)-Flag-N were constructed and synthesized by GenScript (Nanjing, China) and GenBank accession number is MW617760.1. The pcDNA3.1

(+)-Flag-N and pcDNA3.1(+)-Empty-Vector (EV) were purified by EndoFree Maxi Plasmid Kit (DP117, TIANGEN BIOTECH, Beijing, China). The primers used in this study were as follows:

Flag-N: Forward: GCGGATCCATGTCTGATAATGGACCCCA; Reverse: GCTCTAGATTAGGCCTGAGTTGAGTCAG.

Mouse model of AKI and treatment with quercetin

A mouse model of AKI was induced in the male db/db mice at the age of 16 weeks by ultrasound-microbubble-mediated kidney-specifically transferring SARS-CoV-2 N protein-expressing plasmid as previously described (24–26). Quercetin was dissolved in 2% DMSO and then mixed with jelly in the mouse food. Groups of 6 db/db mice at the age of 16 weeks were given oral quercetin at dosages of 150mg/kg/day from day 0 before ultrasound-microbubble-mediated SARS-CoV-2 N gene transfer until being killed on day 2 as previously described (24). In the present study, there were 5 groups of db/db mice, including untreated, EV (empty vector), NP (SARS-CoV-2 N protein), NP +QUE (NP+quercetin), and NP+DMSO (NP+DMSO-control). A group of 6 db/m mice at the age of 16 weeks was used as normal control.

Cell lines and cell cultures

The mouse tubular epithelial cells (mTEC) were a gift from Dr. Jeffrey B. Kopp (National Institutes of Health) and were transfected with SARS-CoV-2 N protein expressing plasmid as previously described (24–26). The mTEC with overexpressing SARS-CoV-2 N (or empty vector)-expressing plasmid were cultured in DMEM/F12 medium (11320082, Gibco, ThermoFisher) supplemented with 10% FBS, 1%(v/v) penicillin-streptomycin (P/S) (15070063, Gibco, ThermoFisher). Cells were stimulated with or without advanced glycation end products (AGE, 100μg/ml, ab51995, Abcam), a hyperglycemia-related products associated with the development of diabetic kidney disease for 48 hours to obtain HMGB1-rich conditional medium for the macrophage activation studies as described below.

A mouse macrophage cell line RAW264.7 was purchased from the American Type Culture Collection (ATCC) (Manassas, VA). RAW264.7 were cultured in DMEM (11965118, Gibco, ThermoFisher) supplemented with 10% FBS, 1%(v/v) P/S. To study the inhibitory effect of quercetin on M1 macrophage activation and proinflammatory cytokine production. RAW264.7 were pretreated with quercetin (32μM) or 0.05% DMSO for 24 hours prior to the addition of HMGB1-rich conditional medium. At least three independent experiments were performed in each study.

Small interfering RNA transfection

To knock down Mincle, RAW264.7 cells were transfected with small interfering RNA against mouse Mincle (sense 5'-CCUUUGAACUGGAAACAUUTT-3', antisense 5'-AAUGUUUCCAGUUCAAAGGTT-3') (designed and synthesized by Shanghai GenePharma Co., Ltd., China) by using Lipofectamine™ RNAiMAX (13778150, Invitrogen, Thermo Fisher Scientific) according to the manufacturer's instructions. A scramble sense control was used as negative control (NC). At least three independent experiments were performed in each study.

Immunohistochemistry

Immunohistochemistry was performed on paraffin-embedded tissue sections (3μm) using endogenous horseradish peroxidase blocking and microwave-based antigen retrieval technique if necessary (32). The antibodies used in this study included Ultra-LEAF purified anti-mouse F4/80 (123164, Biolegend) and p-p65 (ab97726, Abcam). After incubation with the primary antibody overnight at 4°C, sections were incubated with anti-rabbit EnVision + System-HRP Labelled Polymer (K4003, DAKO) at room temperature for 60 min. Then color was developed with a diaminobenzidine tablet (045-22833, FUJIFILM Wako Pure Chemical Corporation) and the nuclei were counterstained with Hematoxylin (H-3404, Burlingame) if necessary. The stained sections were viewed under a LEICA CRT6000 Light Microscope. The positive cells were counted in 6 random areas of kidney sections under the power field (x20) of a microscope and expected as positive rate or cells/mm^2.

Multiplex immunofluorescence

To detect the co-localization between Mincle and F4/80 expression, paraffin-embedded kidney sections (3μm) were blocked with endogenous horseradish peroxidase and then incubated with Ultra-LEAF purified anti-mouse antibody against F4/80 (123164, Biolegend) overnight, followed by adding rabbit polyclonal antibody to Mincle (BS-8541r, Bioss) as previously described (24–26). The fluorescence was developed using the Alexa Fluor ™ 488 Tyramide Reagent (B40953, Invitrogen) or Alex Fluor ™ 568 Tyramide Reagent (B40956, Invitrogen), and the nuclei were counterstained with Hoechst 33342 (H1399, Invitrogen) according to the manufacturer's protocol. All staining sections were detected and photographed by a ZEISS AXIO Microscope. The positive co-location cells were counted in 6 random areas of kidney sections under the high-power field (x40) of a microscope and expected as positive cells/mm^2.

Enzyme-linked immunosorbent assay

The serum from mouse and the supernatant from cultured mTEC were collected and the concentrations of HMGB1 were measured with a mouse HMGB1 ELISA Kit according to the manufacturer's instructions (E-EL-M0676C, Elabscience).

Flow cytometry

Total kidney tissues were digested by Liberase TM Research Grade (Roche, Indianapolis, IN) and RAW264.7 cells were digested with 0.25% trypsin–EDTA into cell suspension. All cells were fixed by IC Fixation Buffer (00-8222-49, Invitrogene) for 10 minutes. Then cells were co-stained with CD68-PE antibody (137014, Biolegend), Mincle-FITC antibody (bs-8541R-FITC, Bioss), iNOS-APC antibody (17-5920-82, eBioscience), or CD206-FITC antibody (141704, Biolegend) overnight at 4°C. After being labeled, cells were gated and analyzed by using a BD LSRFortessa flow cytometer (BD Biosciences), and the data were analyzed by FlowJo software (V10).

Western blot analysis

The total protein of mouse kidney tissues and RAW264.7 cells were extracted by RIPA lysis buffer (P0013B, Beyotime, Shanghai, China). The proteins were electrophoresed in a 10% SDS-PAGE gel and transferred to a Nitrocellulose Transfer Membrane (66485, Pall Corporation, Mexico). Then the membranes were blocked for 1 h at room temperature with 5% skim milk or BSA and incubated with primary antibodies at 4°C overnight. The next day, the membranes were incubated with mouse IgG (H&L) antibody DyLight™ 800 conjugated (610-145-002, ROCKLAND) or rabbit IgG (H&L) antibody DyLight™ 800 conjugated (611-145-002, ROCKLAND). The expression levels of protein were visualized by the Odyssey Infrared Imaging System (San Diego, CA, USA) and quantitatively analyzed by the Image J software (NIH, Bethesda, MD, USA). The antibodies used in this study included mouse antibodies against Mincle (sc-390806, Santa Cruz), TLR-4(sc-293072, Santa Cruz), β-actin (sc-69879, Santa Cruz) and rabbit antibodies against HMGB1 (ab79823, Abcam), p-Syk (#2710, Cell Signaling Technology), Syk (#13198, Cell Signaling Technology), p-p65(ab86299, Abcam), p65 (#8242, Cell Signaling Technology), iNOS (ab15323, Abcam).

Real-time PCR assay

Total RNA from mice kidneys and RAW264.7 cells were extracted with TRIzol reagent (TR118, Molecular Research Center) following the manufacturer's instructions. Real-time quantitative-PCR was measured with QuantStudio™ 6 and 7 Flex Real-time PCR systems (4489826, ThermoFisher) and SYBR Green Supermix (1725122, Bio-Rad). The primers used in this study included mouse Mincle: forward 5'-CCAAGTGCTCTC CTGGACGATA-3', reverse 5'-CTGATGCCTCACTGTAGCAG GA-3'; mouse TNF-a: forward 5'- CATCTTCTCAAAATTCGA GTGACAA-3', reverse 5'- TGGGAGTAGACAAGGTACAA CCC-3'; mouse IL-6: forward 5'- GTCCTTCCTACCC CAATTTCCA-3', reverse 5'-TAAC GCACTAGGTTTGCCGA-3'; mouse MCP-1:forward 5'-TTAAAAACCTGG ATCGG AA C CAA-3', reverse 5'-GCATTAGCTTCAGATTTACGGGT-3'; mouse IL-4:forward 5'-C C C CAGCTAGTTGTCATCCT-3', reverse 5'- TGGTGTTCTTCGTTGCTGTG-3'; mouse IL-10: forward 5'-CGGGAAGACAATAACTGCACCC-3' reverse 5'-CGGTTAG CAG TATG TTG TCCAGC-3'; mouse β-actin: forward 5'-GTGACGTTGACA T CCGTAAAGA-3', reverse 5'-GCCGGACTCATCGTACTCC-3'.

Statistical analyses

All data were presented as the mean ± SD. Statistical analysis was performed with one-way ANOVA for multiple groups from GraphPad Prism 9.0 Software (GraphPad, San Diego, CA, USA). P values less than 0.05 were considered statistically significant.

Results

Overexpression of SARS-CoV-2 N protein exacerbates renal inflammation in diabetic kidney of db/db mice, which is associated with increased HMGB1 and Mincle-expressing M1 macrophage infiltration

As inflammation is a feature of COVID-19 patients with AKI (7–17, 33). To explore the pathological link between renal inflammation and COVID-19 AKI, we first examined renal inflammation in the AKI kidney of 16-week-old db/db mice induced by overexpressing SARS-CoV-2 N protein. We found that ultrasound-microbubble-mediated overexpression of SARS-CoV-2 N protein greatly enhanced F4/80$^+$ macrophage accumulation and expression of proinflammatory cytokines such as IL-6, TNF-α and MCP-1 (Figures 1A, B). This was associated with an increase in both serum and renal tissue levels of HMGB1, one of the DAMP molecules, and upregulation of Mincle at both mRNA and protein levels (Figures 1D-F). Further studies by two-color immunofluorescence and flow cytometry clearly detected that overexpression of SARS-CoV-2 N protein largely promoted M1 proinflammatory macrophages infiltrating the kidney by co-overexpressing F4/80 and Mincle/iNOS markers, which was largely increased in the diabetic kidney of db/db mice (Figures 2, 3A, B). These observations suggest that overexpression of SARS-CoV-2 N protein may mediate severe AKI under diabetic conditions by triggering the release of DAMP molecules such as HMGB1 from the necrotic tubular cells, which then may activate M1 macrophages and stimulate the production of proinflammatory cytokines to exacerbate further AKI via a Mincle-dependent mechanism.

Overexpression of SARS-CoV-2 N protein promotes M1 pro-inflammatory macrophage activation and renal inflammation under diabetic conditions by activating Mincle-Syk-NF-κB signaling

It is well known that Mincle is a typical PRR expressed by M1 proinflammatory macrophages and can recognize the endogenous DAMPs released by necrotic cells. The binding of DAMPs to Mincle can activate Syk and NF-κB signaling

10.3389/fimmu.2023.1264447

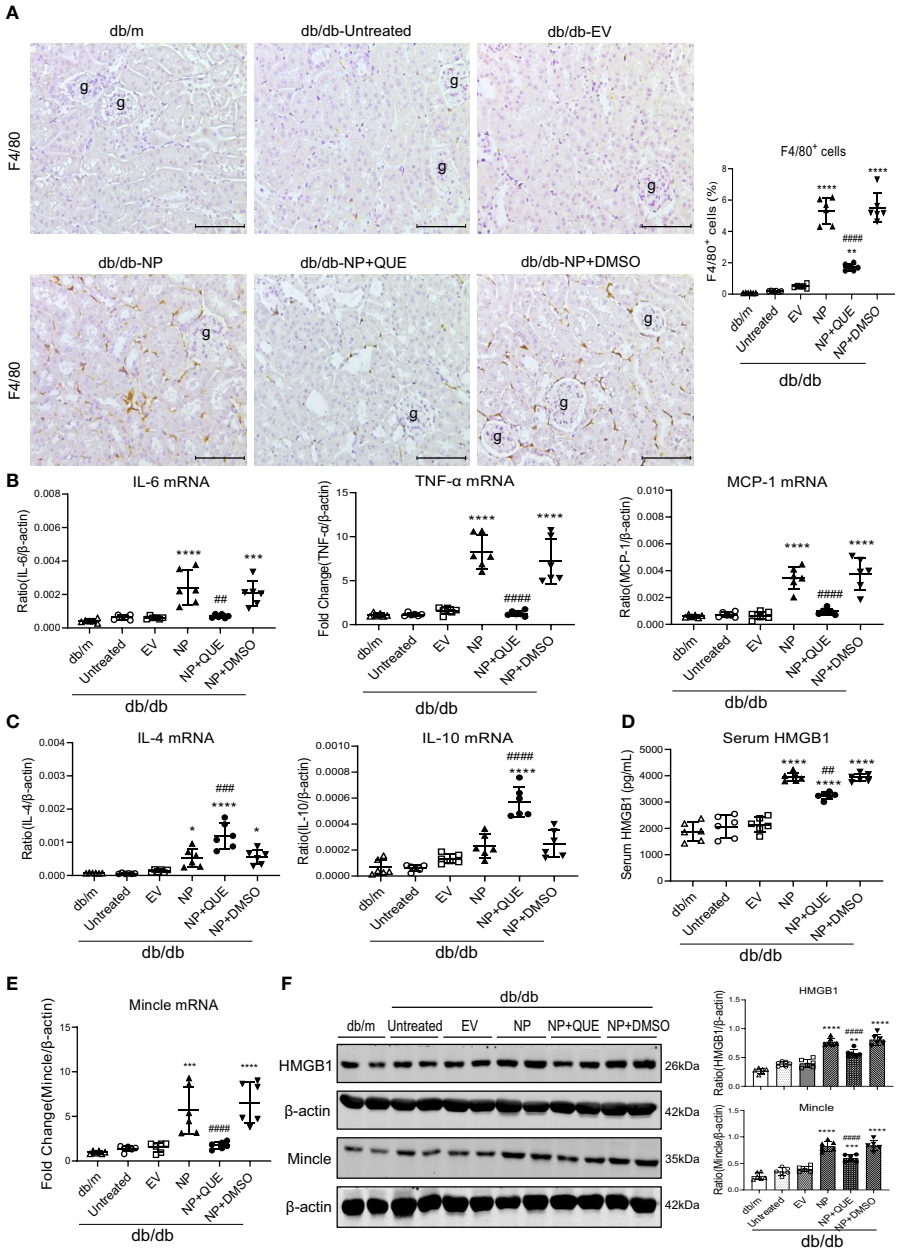

FIGURE 1
Kidney-specifically overexpressing SARS-CoV-2 N protein promotes renal inflammation in db/db mice at the age of 16 weeks by enhancing the release of HMGB1 and expression of Mincle, which is inhibited by treatment with quercetin. **(A)** Immunohistochemistry for F4/80$^+$ macrophages infiltrating the kidney of db/db mice treated with or without quercetin. **(B, C)** Real-time PCR for proinflammatory cytokines (IL-6, TNF-α and MCP-1) and anti-inflammatory cytokines (IL-4 and IL-10) mRNA expression in the diabetic kidney treated with or without quercetin. **(D)** Serum levels of HMGB1. **(E)** Real-time PCR for renal Mincle mRNA expression. **(F)** Western blot analysis for expression of HMGB1 and Mincle in the kidney of db/db mice treated with or without quercetin. Each dot represents one mouse and data are expressed as the mean ± SD for groups of 6 mice. * p<0.05, **p<0.01, ***p<0.001, **** p<0.0001 versus empty vector control group (db/db-EV); ##p<0.01, ### p<0.001, #### p<0.0001 versus DMSO-treated control group(db/db-NP+DMSO). g, glomerulus; scale bar=100μm.

byphosphorylation (19). Our previous study also demonstrated that LPS induces M1 macrophage activation in AKI via Mincle/Syk/NF-κB-dependent mechanism (34). In the present study, western blotting and immunohistochemical staining also detected that overexpressing SARS-CoV-2 N protein caused severe renal inflammation with massive M1 macrophage infiltration in the diabetic kidney of db/db mice, which was associated with upregulation of Mincle on macrophages (Figures 2, 3A, B) and activation of Syk/NF-κB signaling (Figure 4).

To further confirm the necessary role for Mincle in M1 macrophage-mediated AKI in response to SARS-CoV-2 N protein under diabetic conditions, we performed serial studies in SARS-CoV-2 N protein-overexpressing tubular cells under high AGEs conditions. We found that either SARS-CoV-2 N protein or AGEs were capable of inducing equal levels of HMGB1 released

10.3389/fimmu.2023.1264447

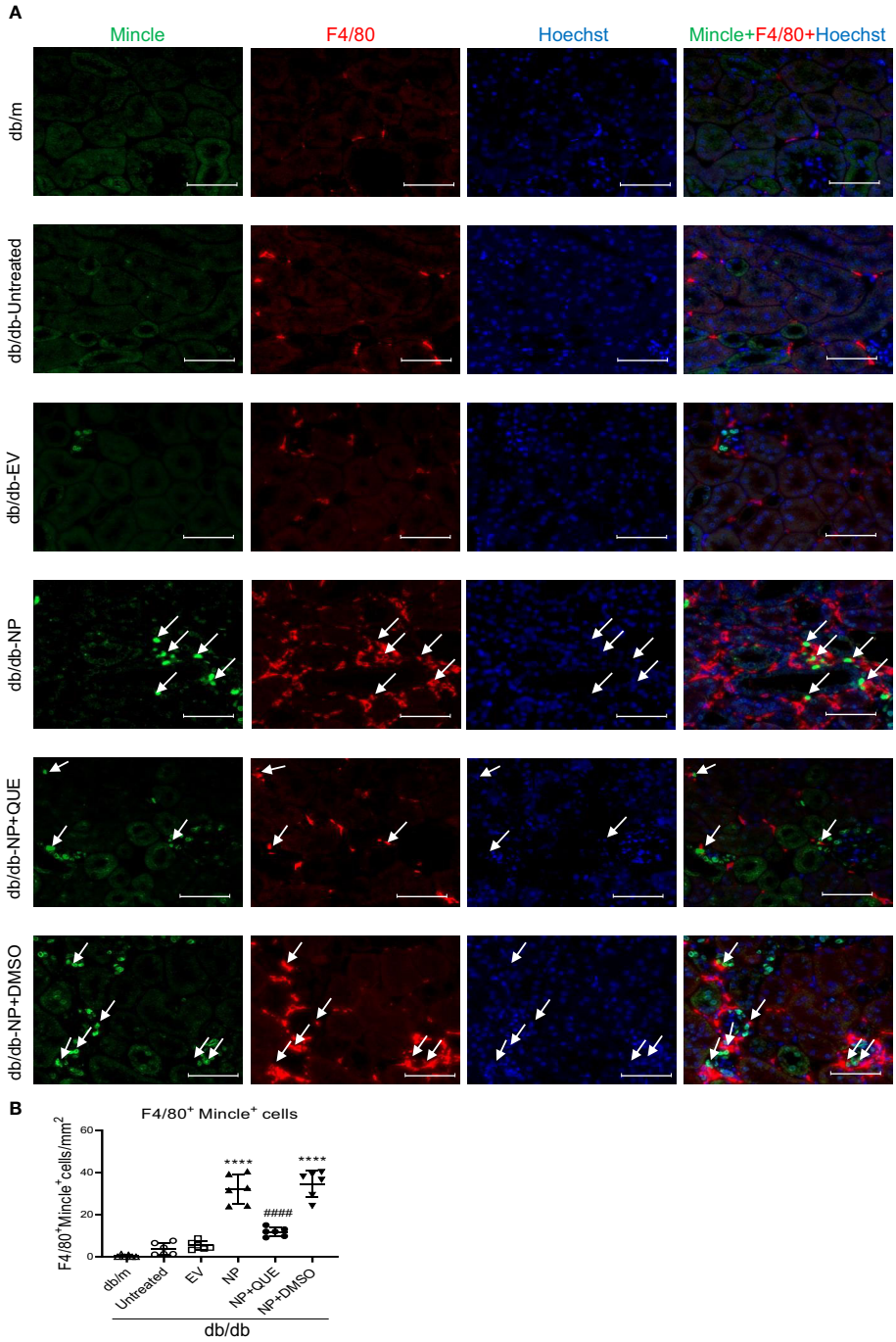

FIGURE 2
Tow-color immunofluorescence detects that overexpression of SARS-CoV-2 N protein triggers Mincle-expressing macrophages infiltrating the AKI kidney at the age of 16-week db/db mice, which is inhibited by quercetin treatment. **(A)** Two-color immunofluorescence shows the co-localization of Mincle (green) and F4/80(red) macrophages infiltrating the kidney of db/db mice treatment with or without quercetin. **(B)** Semi-quantitative analysis of Mincle-expressing macrophages ($F4/80^+Mincle^+$). Each dot represents one mouse and data are expressed as the mean ± SD for groups of 6 mice. **** p<0.0001 versus empty vector control group (db/db-EV); #### p<0.0001 versus DMSO-treated control group(db/db-NP+DMSO). Scale bar=50μm.

from injured tubular cells, indicating that either SARS-CoV-2 N protein or AGEs can induce tubular cell injury to release HMGB1. Interestingly, once SARS-CoV-2 N protein-overexpressing tubular cells were cultured with AGEs, the release of a DAMP molecule HMGB1 became double (Figure 5A), suggesting that SARS-CoV-2 N protein can potentiate HMGB1 released from injured tubular cells under diabetic conditions. To further determine whether SARS-CoV-2 N protein can activate M1 macrophages via the Mincle-dependent mechanism, we cultured macrophages (RAW264.7) with high HMGB1-contained supernatant obtained from AGEs-stimulated SARS-CoV-2 N protein-expressing tubular cells. As expected, the addition of

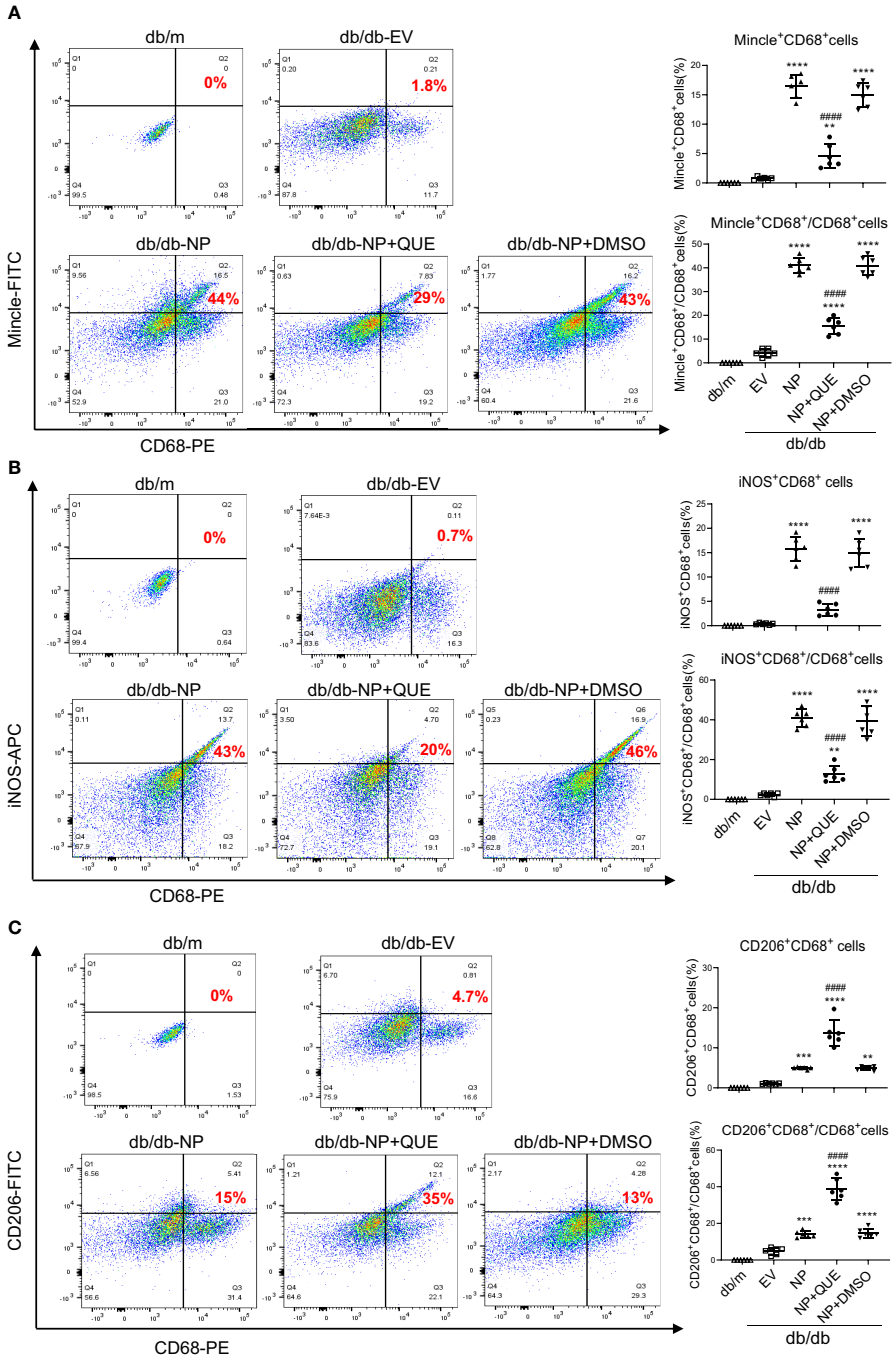

FIGURE 3
Two-color flow cytometry detects that overexpression of SARS-CoV-2 N protein largely promotes M1 macrophages infiltrating the AKI kidney at the age of 16-week db/db mice, which is inhibited by quercetin treatment. **(A)** Mincle$^+$ cluster of CD68$^+$ macrophages identified by Mincle$^+$CD68$^+$ cells in the AKI kidney of db/db mice treated with or without quercetin. **(B)** M1 macrophages identified by iNOS$^+$CD68$^+$ cells. **(C)** M2 macrophages identified by CD206$^+$CD68$^+$ cells. Note that quercetin treatment inhibits the Mincle-expressing macrophages and switches the M1 macrophages to M2 phenotype in SARS-CoV-2 N protein-induced AKI kidney of db/db mice. Each dot represents one mouse and data are expressed as the mean ± SD for groups of 6 mice. **p<0.01, ***p<0.001, **** p<0.0001 versus empty vector control group (db/db-EV); #### p<0.0001 versus DMSO-treated control group(db/db-NP+DMSO).

high HMGB1-contained supernatant largely promoted Mincle expression by macrophages, resulting in a marked activation of M1 proinflammatory macrophages by co-expressing CD68 and Mincle/iNOS and production of IL-6, TNF-α, and MCP-1 (Figures 5B-E). All these changes were blocked by specifically silencing macrophage Mincle with siRNA (Figures 5B-E), demonstrating that SARS-CoV-2 N protein may trigger M1 macrophage activation and proinflammatory response via the Mincle-dependent mechanism. This was further confirmed by western blotting that silencing macrophage Mincle suppressed

HMGB1-induced Mincle expression and activation of Syk/NF-κB signaling (Figure 5F).

Treatment with quercetin attenuates SARS-CoV-2N protein-induced AKI in diabetic db/db mice by blocking Mincle-mediated-M1 macrophage activation via a Syk-NF-κB-dependent mechanism *in vivo*

Our recent study showed that quercetin can effectively block SARS-CoV-2 N protein-induced tubular cell death by targeting the Smad3-p16-dependent G1 cell cycle arrest mechanism (24). In the present study, we further investigated whether treatment with quercetin can attenuate SARS-CoV-2 N protein-induced AKI in diabetic db/db mice by blocking M1 macrophage activation and renal inflammation in diabetic db/db mice via a Mincle-dependent mechanism. As shown in Figure 1, treatment with quercetin largely inhibited SARS-CoV-2 N protein-induced F4/80$^+$ macrophages infiltrating the diabetic kidney (Figure 1A) and greatly suppressed the mRNA expression of IL-6, TNF-α, and MCP-1 while increasing the expression of IL-4 and IL-10 mRNA levels (Figure 1B, C). This was associated with the inhibition of both serum and renal tissue levels of HMGB1 and expression of Mincle in the diabetic kidney of

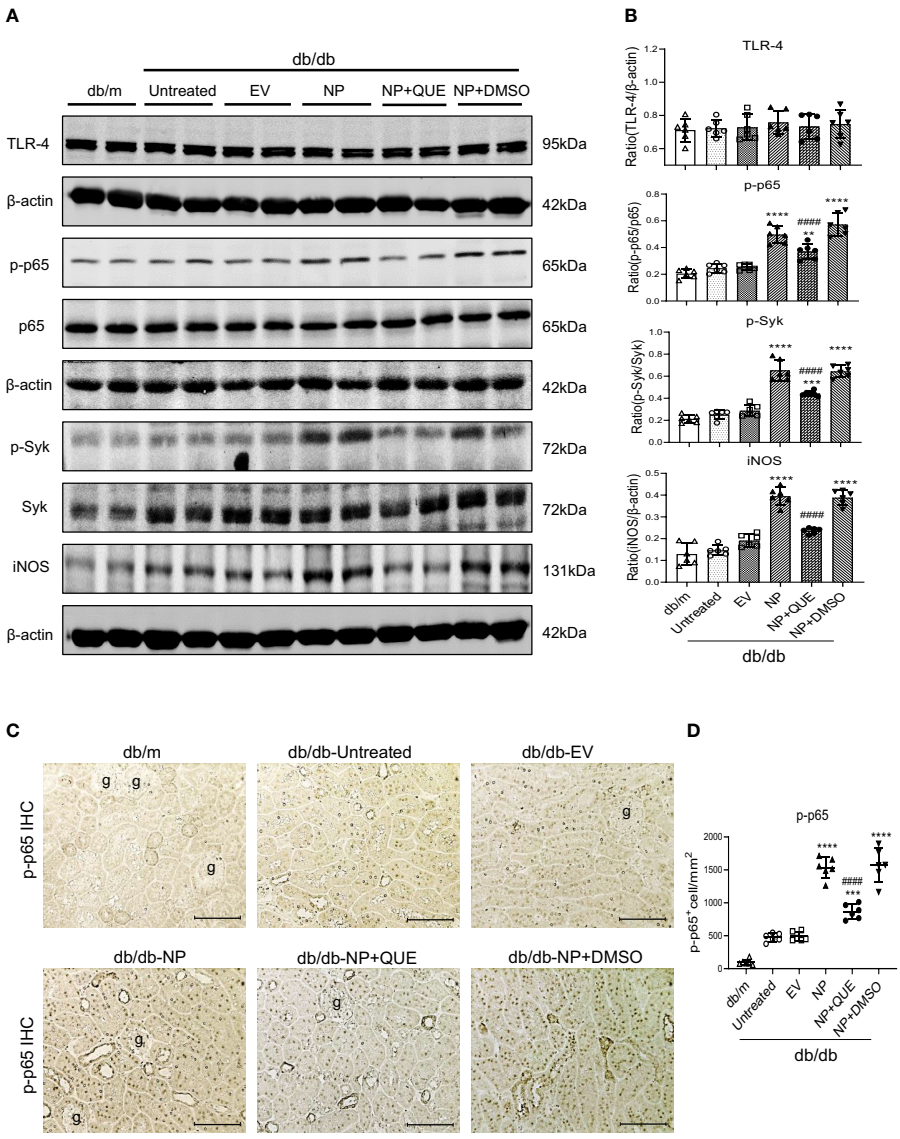

FIGURE 4
Kidney-specifically overexpressing SARS-CoV-2 N protein activates Syk/NF-κB signaling in db/db mice at the age of 16 weeks, which is inhibited by treatment with quercetin. **(A, B)** Western blot analysis of activation of Syk (p-Syk), NF-κB(p-p65) and expression of TLR-4 and iNOS in the kidney of db/db mice treated with or without quercetin. **(C, D)** Immunohistochemistry for detecting activation of NF-κB (p-p65 nuclear translocation). Note that treatment with quercetin inhibits phosphorylation of Syk and NF-κB as well p65 nucleated translocation in SARS-CoV-2 N protein-induced AKI kidney. Each dot represents one mouse and data are expressed as the mean ± SD for groups of 6 mice. ** p<0.01, *** p<0.001, **** p<0.0001 versus empty vector control group (db/db-EV); #### p<0.0001 versus DMSO-treated control group(db/db-NP+DMSO). g, glomerulus; scale bar=100μm.

db/db mice (Figures 1D-F), suggesting that treatment with quercetin may inhibit the release of DAMPs such as HMGB1 from necrotic renal tubular cells and thus suppresses M1 macrophage activation and renal inflammation. This was further demonstrated by two-color immunofluorescence, demonstrating that treatment with quercetin inhibited Mincle-expressing F4/80$^+$ macrophage infiltrating the diabetic kidney of SARS-CoV-2 N protein-induced AKI (Figure 2). Further studies by two-color flow cytometry also confirmed this notion that treatment with quercetin significantly inhibited SARS-CoV-2 N protein-induced M1 macrophages by co-expressing Mincle$^+$CD68$^+$and iNOS$^+$CD68$^+$ macrophages while increasing CD206$^+$CD68$^+$ macrophages (Figure 3). These findings suggest that quercetin may result in the switching of macrophage properties from M1 to M2 macrophage phenotype.

As Mincle is a typical PRR expressed by macrophages and can recognize endogenous DAMPs such as HMGB1 released by the necrotic cells to activate the downstream Syk/NF-κB signaling (19, 34), we further examined whether treatment with quercetin inhibits SARS-CoV-2 N protein-induced M1 macrophage activation and renal inflammation via the Mincle-Syk/NF-κB signaling pathway. Interestingly, although treatment with quercetin did not alter the expression of TLR-4 (Figures 4A, B), it did significantly suppress Mincle expression (Figure 1F) and therefore inhibited phosphorylation of Syk and NF-κB/p65 in the diabetic kidney of SARS-CoV-2 N protein-induced AKI (Figure 4).

Quercetin inhibits SARS-CoV-2 N protein-induced M1 macrophage activation while promoting M2 macrophages via Mincle-dependent Syk/NF-κB signaling in RAW264.7 cells

To further confirm the mechanism of quercetin in the inhibition of SARS-CoV-2 N protein-induced M1 macrophage activation, we treated RAW264.7 cells with HMGB1-contained medium obtained from SARS-CoV-2 N protein-overexpressing mouse tubular cells as described above. Mincle-dependent mechanism in M1 macrophage activation was confirmed by treating RAW264.7 cells with the Mincle siRNA. Results showed that, like Mincle siRNA, treatment with quercetin was capable of inhibiting HMGB1-induced M1 macrophage activation by suppressing the expression of Mincle and pro-inflammatory cytokines including IL-6, TNF-α, and MCP-1 while increasing anti-inflammatory cytokines such as IL-4 and IL-10 expression (Figure 6A). Two-color flow cytometry also revealed that the addition of quercetin resulted in the shift from M1 to M2 macrophages as demonstrated by reducing about 50% of the Mincle$^+$CD68$^+$ and iNOS$^+$CD68$^+$ M1 macrophages while increasing more than 50% of CD206$^+$CD68$^+$ macrophages (Figures 6B, C). Further study by western blot analysis also confirmed this notion that the addition of quercetin blocked the activation of Mincle-Syk-NF-κB signaling under HMGB1-rich supernatant (Figure 6D). Taken together, these findings suggest that quercetin inhibits SARS-CoV-2 N protein-induced AKI under diabetic conditions by switching M1 to M2 macrophage phenotype via the Mincle/Syk/NF-κB signaling.

Discussion

Our previous studies demonstrated that ultrasound-microbubble-mediated kidney-specifically overexpressing SARS-CoV-2 N protein is capable of inducing kidney tubular necrosis and causing AKI via Smad3-dependent G1 cell cycle arrest and necroptosis mechanisms (24–26). In the present study, we identified that SARS-CoV-2 N protein caused AKI by promoting M1 macrophage activation and renal inflammation via a Mincle-dependent mechanism, which added new information to the previous findings that SARS-CoV-2 N protein can activate NLRP3 and NF-κB to induce hyperinflammation (35, 36). We found that SARS-CoV-2 N protein-induced renal tubular cell necrosis in diabetic db/db mice resulted in the release of HMGB1, a DAMP molecule that can bind Mincle on macrophages and activate M1 macrophages via Mincle-Syk/NF-κB signaling. It is now clear that HMGB1 is an abundant non-histone nuclear protein that can be secreted into the extracellular environment and serves as an essential DAMP to activate proinflammatory signaling (37). HMGB1 can activate M1 macrophages in mouse models of ischemia-reperfusion and obstruction kidney disease and *in vitro* (38–41). In critically ill COVID-19 patients, serum HMGB1 is elevated and correlated with levels of inflammatory cytokines (7, 21, 22). The present study also found that a large amount of HMGB1 was released from injured tubular cells induced by overexpressing SARS-CoV-2 N protein under diabetic conditions *in vivo* and *in vitro*. Importantly, we also uncovered that HMGB1 could activate M1 macrophages via the Mincle-dependent mechanism, specifically silencing macrophage Mincle protected against HMGB1-induced M1 macrophage activation and production of signature cytokines such as IL-6, TNF-α, and MCP-1. It is well documented that Mincle plays an important role in renal inflammation and is a key factor for triggering and maintaining the M1 macrophage phenotype. Blockade of Mincle on macrophages can protect against cisplatin-induced AKI (34, 42). Consistent with these previous findings, we found that SARS-CoV-2 N protein-induced AKI in db/db mice was associated with a marked increase in Mincle-expressing macrophages (Mincle$^+$CD68$^+$) and iNOS$^+$CD68$^+$ M1 macrophages. It is highly possible that overexpression of SARS-CoV-2 N protein could largely promote the release of DAMPs such as HMGB1 from injured renal tubular cells in db/db mice, resulting in high levels of HMGB1 in both serum and renal tissues. After being released, HMGB1 could bind and activate Mincle on macrophages and then stimulate M1 macrophage activation and production of proinflammatory cytokines such as IL-6, TNF-α, and MCP-1 via the Syk/NF-κB pathway. This was further confirmed in RAW264.7 cells in which specifically silencing macrophage Mincle blocked HMGB1-induced activation of Mincle-Syk/NF-κB signaling and thus blocked M1 macrophage activation and proinflammatory cytokine production. It should be pointed out that HMGB1 is one of the DAMPs released from SARS-CoV-2 N protein

10.3389/fimmu.2023.1264447

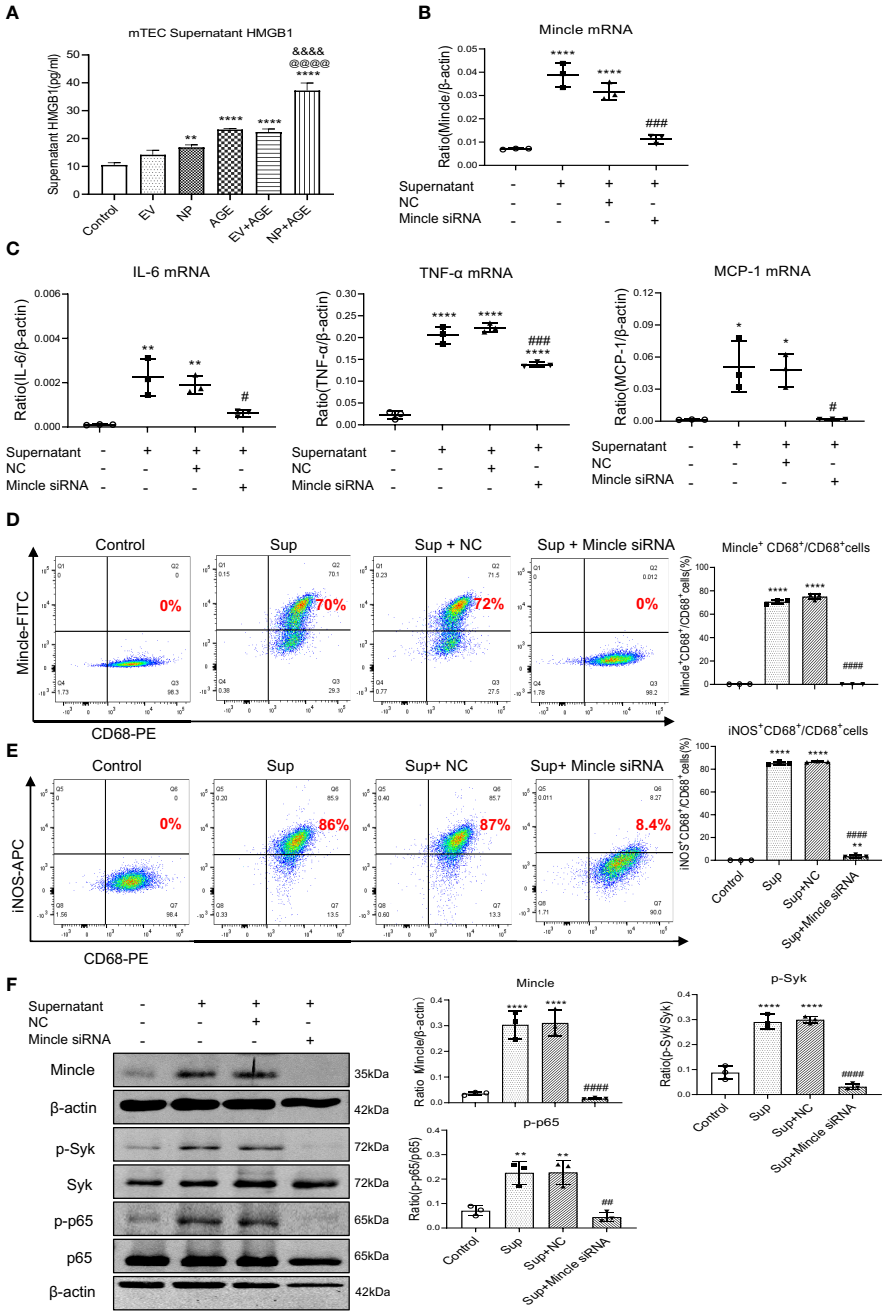

FIGURE 5
Overexpression of SARS-CoV-2 N protein in mouse tubular epithelial cells (mTEC) largely promotes the release of HMGB1 to activate M1 macrophages in RAW264.7 cells via the Mincle-dependent mechanism *in vitro*. **(A)** Concentrations of HMGB1 in the supernatant of dead mTEC induced by overexpressing SARS-CoV-2 N protein in the presence or absence of AGE (100μg/ml for 48 hours). **(B, C)** Real-time PCR shows that silencing macrophage Mincle blocks HMGB1-contained mTEC supernatant (Sup)induced upregulation of Mincle, IL-6, TNF-α, and MCP-1 mRNA expression in RAW264.7 cells. **(D, E)** Flow-cytometry analysis reveals that silencing macrophage Mincle blocks HMGB1-contained mTEC supernatant (Sup) induced M1 macrophages as determined by $Mincle^+CD68^+$ and $iNOS^+CD68^+$ populations in RAW264.7 cells. **(F)** Western blot analysis shows that silencing macrophage Mincle blocks HMGB1-contained mTEC supernatant (Sup) induced activation of Mincle-Syk/NF-κB signaling in RAW264.7 cells. Each dot represents one experiment and data are presented as mean ± SD for at least three independent experiments. *p<0.05, ** p<0.01, **** p<0.0001 versus control group; @@@@ p<0.0001 versus AGE group; &&&& p<0.0001versus Flag-empty vector with AGE group (EV+AGE); # p<0.05, ## p<0.01, ### p<0.001, #### p<0.0001 versus cells treated with supernatant from SARS-CoV-2 N protein-induced dead mTEC and negative control siRNA (Sup+NC).

overexpressing tubular cells and many other DAMP molecules released from the injured tubular cells in response to overexpression of SARS-CoV-2 N protein may also contribute to activate proinflammatory macrophages. Indeed, besides HMGB1 (7, 21, 22), other DAMP molecules such as S100A8/A9, SP-A, CIRBP, and histone may also participate in M1 proinflammatory macrophage activation in response to COVID-19 infection as previously reported (21). This novel finding may well explain the

10.3389/fimmu.2023.1264447

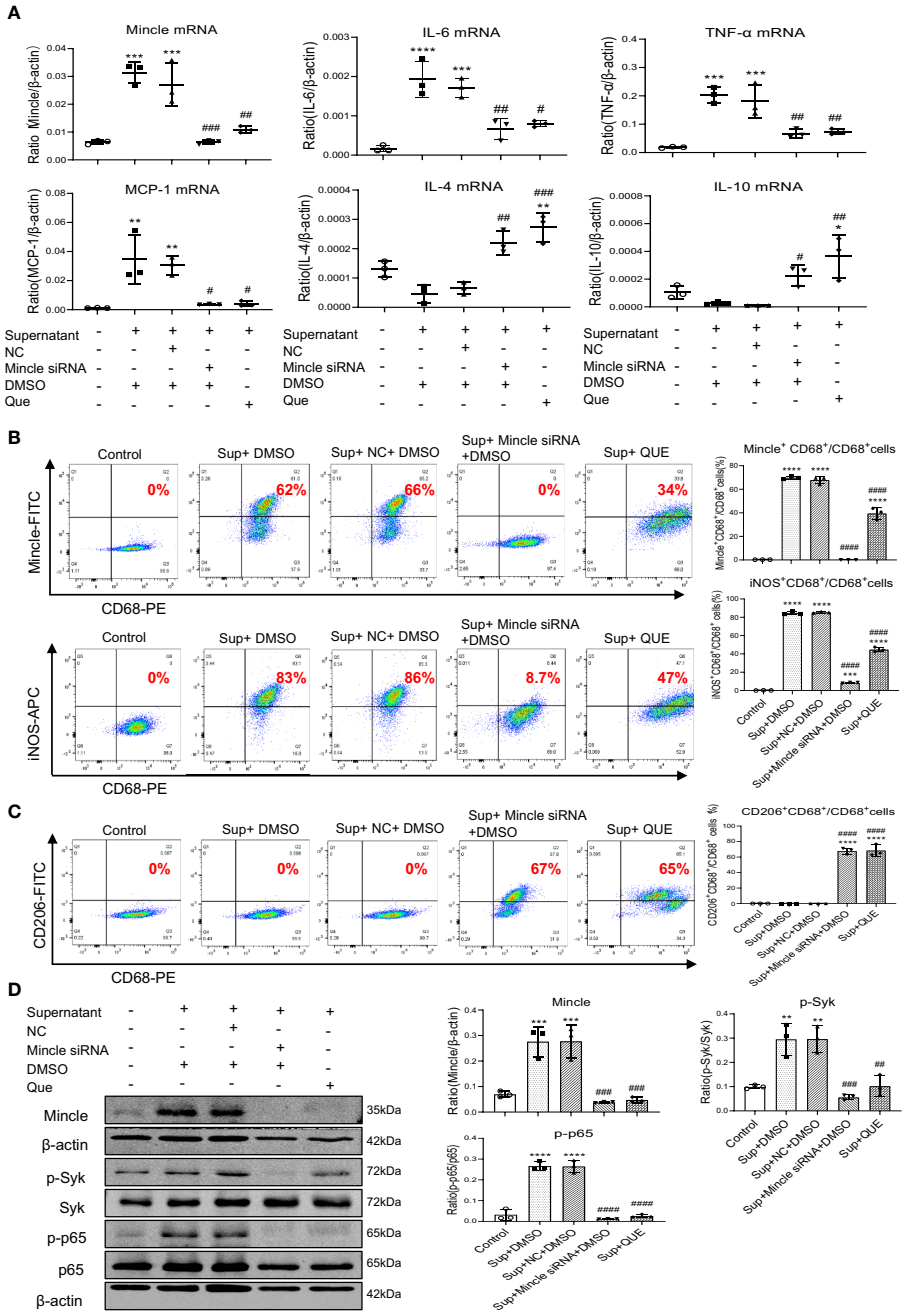

FIGURE 6
Quercetin inhibits HMGB1-contained mTEC supernatant-induced M1 macrophages while promoting M2 populations by targeting Mincle-Syk/NF-κB signaling in RAW264.7 cells. **(A)** Real-time PCR detects that like a Mincle siRNA, pre-treatment of RAW264.7 cells with quercetin (32μM) for 24 hour is able to inhibit Mincle, IL-6, TNF-α, MCP-1, while increasing IL-4 and IL-10 mRNA expression induced by the HMGB1-contained supernatant (Sup) from SARS-CoV-2 N protein-expressing mTEC. **(B, C)** Two-color flow-cytometry analysis reveals that like specifically silencing macrophage Mincle, pre-treatment with quercetin (32μM) for 24 hour inhibits M1 ($Mincle^+CD68^+$ and $iNOS^+CD68^+$) while increasing M2 ($CD206^+CD68^+$) macrophage populations induced by the HMGB1-contained supernatant (Sup) from SARS-CoV-2 N protein-expressing mTEC. **(D)** Western blot analysis shows that like treatment with Mincle siRNA, pre-treatment with quercetin blocks Mincle-Syk/NF-κB signaling in RAW264.7 cells in response to the HMGB1-contained supernatant (Sup) from SARS-CoV-2 N protein-expressing mTEC. Each dot represents one experiment and data are presented as mean ± SD for at least three independent experiments. * p<0.05, ** p<0.01, *** p<0.001, **** p<0.0001 versus control group; # p<0.05, ## p<0.01, ### p<0.001, #### p<0.0001 versus cells treated with supernatant from SARS-CoV-2 N protein-induced dead mTEC and negative control siRNA and DMSO group (Sup+NC+DMSO).

clinical notions that DAMPs can cause the "cytokine storm" and lead to organ damage in critically ill COVID-19 patients (17). Thus, SARS-CoV-2 N protein is pathogenic in COVID-19 AKI. It can induce tubular cell death via the Smad3-dependent G1 cell cycle arrest and necroptosis mechanisms as previously reported (24–26). It may also cause severe AKI under diabetic conditions by activating M1 macrophages and promoting massive renal inflammation via the Mincle-dependent mechanism. However, it should be pointed

out that systemic inflammatory responses such as "cytokine storm" after COVID-19 infection may also contribute to the M1 macrophage activation. It has been well documented that there are excessive immune responses with massive production of proinflammatory cytokines such as IL-6, IL-1β, TNF-a, and MCP-1 in patients with severe SARS-CoV-2 infection (8–13). These proinflammatory cytokines can activate M1 macrophages systemically and then promote their migration into the diseased kidney where they become further activated and maintain the M1 proinflammatory phenotype via Mincle-dependent mechanism as previously reported (34). Nevertheless, in the present study, macrophages may be primarily activated locally within the kidney via the Mincle-dependent mechanism as AKI was induced by overexpressing SARS-CoV-2 N protein locally in the diabetic kidney.

In the present study, we also uncovered that quercetin functions as a Mincle inhibitor to block Mincle/Syk/NF-κB signaling, thereby inhibiting M1 while promoting M2 macrophage activation in SARS-CoV-2 N protein-induced AKI in db/db mice. Quercetin is a natural flavonoid compound, which is widely found in various heat-clearing and detoxifying herbs and food. Quercetin has antiviral, anti-inflammatory, antioxidant, and other biological activities (43). Many studies suggest that quercetin is effective for the treatment of patients with COVID-19. Both experimental and clinical trials showed that quercetin has a therapeutic effect on COVID-19-associated AKI (27–30, 44). *In vitro*, quercetin can inhibit LPS-induced M1 macrophages while promoting M2 macrophage differentiation (45), indicating that quercetin ameliorates renal injury in AKI by regulating macrophage polarization. Our previous study also showed that quercetin inhibits M1 while upregulating M2 macrophages by blocking Mincle/Syk/NF-κB signaling in cisplatin-induced AKI mouse models and in LPS-induced bone marrow-derived macrophages (31). Interestingly, the present study found that treatment with quercetin inhibited SARS-CoV-2 N protein-induced Mincle but not TLR4 expression in db/db mice with AKI. This suggested that Mincle but not TLR4 may be involved in the M1 macrophage activation during the development of SARS-CoV-2 N protein-induced AKI. We have previously reported that treatment with quercetin can inhibit SARS-CoV-2 N protein-induced tubular cell death via the Smad3-p16-dependent G1 cell cycle arrest mechanism (24). This may also inhibit the release of DAPMs such as HMGB1 from the injured tubular cells and inactivate M1 proinflammatory macrophages by suppressing the binding of HMGB1 to Mincle. Thus, quercetin treatment inhibited macrophage activation and progressive renal inflammation in SARS-CoV-2 N protein-induced AKI via a Mincle-dependent mechanism. This was further confirmed in cultured macrophages in which the addition of quercetin was capable of inhibiting HMGB1-induced Mincle expression and activation of Syk/NF-κB signaling, thereby blocking M1 while promoting M2 macrophage activation. Thus, consistent with previous findings clinically (27, 28), quercetin may be an effective therapeutic agent for COVID-19 AKI (27, 28). Furthermore, results from this study also revealed that blockade of Mincle-Syk/NF-κB-mediated M1 macrophage activation may be a novel molecular mechanism through which quercetin treatment improves the severity of COVID-19 patients clinically.

In summary, SARS-CoV-2 N protein is pathogenic for AKI and may mediate AKI by activating M1 macrophages via a Mincle-Syk/NF-κB-dependent mechanism. Quercetin is a therapeutic agent for SARS-CoV-2 N protein-induced AKI in db/db mice and may inhibit AKI by switching M1 to M2 macrophage activation, which may be associated with inactivation of Mincle signaling.

Data availability statement

The original contributions presented in the study are included in the article/supplementary material. Further inquiries can be directed to the corresponding authors.

Ethics statement

The animal study was approved by Animal Experimentation Ethics Committee at the Chinese University of Hong Kong. The study was conducted in accordance with the local legislation and institutional requirements.

Author contributions

HL: Writing – review & editing. WWu: Writing – original draft. WWa: Investigation, Writing – original draft. LL: Writing – original draft. JC: Writing – original draft. SS: Writing – original draft. BW: Writing – original draft. YZ: Software, Writing – original draft. JL: Writing-review & editing. XH: Writing – review & editing. XW: Writing – review & editing. XY: Writing – review & editing.

Funding

The author(s) declare financial support was received for the research, authorship, and/or publication of this article. This study was supported by grants from the Research Grants Council of Hong Kong (GRF 14104019, 14101121, and R4012-18); the High-Level Hospital Construction Project from Guangdong Provincial People's Hospital, Guangdong Academy of Medical Science(KJ012019108), the Guangdong-Hong Kong-Macao-Joint Labs Program from Guangdong Science and Technology Department (2019B121205005), the Sichuan Science and Technology Program (2022YFH0118), and Health and Medical Research Fund of Hong Kong (HMRF 06173986), and the Lui Che Woo Institute of Innovative Medicine (CARE program).

Conflict of interest

The authors declare that the research was conducted in the absence of any commercial or financial relationships that could be construed as a potential conflict of interest.

Publisher's note

References

1. Zheng X, Zhao Y, Yang L. Acute kidney injury in COVID-19: the chinese experience. *Semin Nephrol* (2020) 40(5):430–42. doi: 10.1016/j.semnephrol.2020.09.001

2. Chan L, Chaudhary K, Saha A, Chauhan K, Vaid A, Zhao S, et al. AKI in hospitalized patients with COVID-19. *J Am Soc Nephrol* (2021) 32(1):151–60. doi: 10.1681/ASN.2020050615

3. Cummings MJ, Baldwin MR, Abrams D, Jacobson SD, Meyer BJ, Balough EM, et al. Epidemiology, clinical course, and outcomes of critically ill adults with COVID-19 in New York City: a prospective cohort study. *Lancet* (2020) 395(10239):1763–70. doi: 10.1016/S0140-6736(20)31189-2

4. Cheng Y, Luo R, Wang K, Zhang M, Wang Z, Dong L, et al. Kidney disease is associated with in-hospital death of patients with COVID-19. *Kidney Int* (2020) 97 (5):829–38. doi: 10.1016/j.kint.2020.03.005

5. Gao YD, Ding M, Dong X, Zhang JJ, Kursat Azkur A, Azkur D, et al. Risk factors for severe and critically ill COVID-19 patients: A review. *Allergy* (2021) 76(2):428–55. doi: 10.1111/all.14657

6. Gupta S, Coca SG, Chan L, Melamed ML, Brenner SK, Hayek SS, et al. AKI treated with renal replacement therapy in critically ill patients with COVID-19. *J Am Soc Nephrol* (2021) 32(1):161–76. doi: 10.1681/ASN.2020060897

7. Fukao Y, Nagasawa H, Nihei Y, Hiki M, Naito T, Kihara M, et al. COVID-19-induced acute renal tubular injury associated with elevation of serum inflammatory cytokine. *Clin Exp Nephrol* (2021) 25(11):1240–6. doi: 10.1007/s10157-021-02101-z

8. Yang L, Xie X, Tu Z, Fu J, Xu D, Zhou Y. The signal pathways and treatment of cytokine storm in COVID-19. *Signal Transduct Target Ther* (2021) 6(1):255. doi: 10.1038/s41392-021-00679-0

9. Legrand M, Bell S, Forni L, Joannidis M, Koyner JL, Liu K, et al. Pathophysiology of COVID-19-associated acute kidney injury. *Nat Rev Nephrol* (2021) 17(11):751–64. doi: 10.1038/s41581-021-00452-0

10. Mehta P, McAuley DF, Brown M, Sanchez E, Tattersall RS, Manson JJ, et al. COVID- 19: consider cytokine storm syndromes and immunosuppression. *Lancet* (2020) 395(10229):1033–4. doi: 10.1016/S0140-6736(20)30628-0

11. Liu J, Li S, Liu J, Liang B, Wang X, Wang H, et al. Longitudinal characteristics of lymphocyte responses and cytokine profiles in the peripheral blood of SARS-CoV-2 infected patients. *EBioMedicine* (2020) 55:102763. doi: 10.1016/j.ebiom.2020.102763

12. Gradin A, Andersson H, Luther T, Anderberg SB, Rubertsson S, Lipcsey M, et al. Urinary cytokines correlate with acute kidney injury in critically ill COVID-19 patients. *Cytokine* (2021) 146:155589. doi: 10.1016/j.cyto.2021.155589

13. Wang J, Yang X, Li Y, Huang JA, Jiang J, Su N. Specific cytokines in the inflammatory cytokine storm of patients with COVID-19-associated acute respiratory distress syndrome and extrapulmonary multiple-organ dysfunction. *Virol J* (2021) 18 (1):117. doi: 10.1186/s12985-021-01588-y

14. Li XQ, Liu H, Meng Y, Yin HY, Gao WY, Yang X, et al. Critical roles of cytokine storm and secondary bacterial infection in acute kidney injury development in COVID-19: A multi- center retrospective cohort study. *J Med Virol* (2021) 93(12):6641–52. doi: 10.1002/jmv.27234

15. Gabarre P, Dumas G, Dupont T, Darmon M, Azoulay E, Zafrani L. Acute kidney injury in critically ill patients with COVID-19. *Intensive Care Med* (2020) 46(7):1339–48. doi: 10.1007/s00134-020-06153-9

16. Diao B, Wang C, Wang R, Feng Z, Zhang J, Yang H, et al. Human kidney is a target for novel severe acute respiratory syndrome coronavirus 2 infection. *Nat Commun* (2021) 12(1):2506. doi: 10.1038/s41467-021-22781-1

17. Paludan SR, Mogensen TH. Innate immunological pathways in COVID-19 pathogenesis. *Sci Immunol* (2022) 7(67):eabm5505. doi: 10.1126/sciimmunol.abm5505

18. Tang PM, Nikolic-Paterson DJ, Lan HY. Macrophages: versatile players in renal inflammation and fibrosis. *Nat Rev Nephrol* (2019) 15(3):144–58. doi: 10.1038/s41581-019-0110-2

19. Brown GD. Sensing necrosis with mincle. *Nat Immunol* (2008) 9(10):1099–100. doi: 10.1038/ni1008-1099

20. Kingeter LM, Lin X. C-type lectin receptor-induced NF-κB activation in innate immune and inflammatory responses. *Cell Mol Immunol* (2012) 9(2):105–12. doi: 10.1038/cmi.2011.58

21. Parthasarathy U, Martinelli R, Vollmann EH, Best K, Therien AG. The impact of DAMP-mediated inflammation in severe COVID-19 and related disorders. *Biochem Pharmacol* (2022) 195:114847. doi: 10.1016/j.bcp.2021.114847

22. Chen R, Huang Y, Quan J, Liu J, Wang H, Billiar TR, et al. HMGB1 as a potential biomarker and therapeutic target for severe COVID-19. *Heliyon* (2020) 6(12):e05672. doi: 10.1016/j.heliyon.2020.e05672

23. Izzedine H, Jhaveri KD. Acute kidney injury in patients with COVID-19: an update on the pathophysiology. *Nephrol Dial Transplant* (2021) 36(2):224–6. doi: 10.1093/ndt/gfaa184

24. Wu W, Wang W, Liang L, Chen J, Wei B, Huang XR, et al. Treatment with quercetin inhibits SARS-CoV-2 N protein-induced acute kidney injury by blocking Smad3-dependent G1 cell-cycle arrest. *Mol Ther* (2023) 31(2):344–61. doi: 10.1016/j.ymthe.2022.12.002

25. Wang W, Chen J, Hu D, Pan P, Liang L, Wu W, et al. SARS-coV-2 N protein induces acute kidney injury via smad3-dependent G1 cell cycle arrest mechanism. *Adv Sci (Weinh)* (2022) 9(3):e2103248. doi: 10.1002/advs.202103248

26. Liang L, Wang W, Chen J, Wu W, Huang XR, Wei B, et al. SARS-CoV-2 N protein induces acute kidney injury in diabetic mice via the Smad3-Ripk3/MLKL necroptosis pathway. *Signal Transduct Target Ther* (2023) 8(1):147. doi: 10.1038/s41392-023-01410-x

27. Di Pierro F, Iqtadar S, Khan A, Ullah Mumtaz S, Masud Chaudhry M, Bertuccioli A, et al. Potential clinical benefits of quercetin in the early stage of COVID-19: results of a second, pilot, randomized, controlled and open-label clinical trial. *Int J Gen Med* (2021) 14:2807–2816. doi: 10.2147/IJGM.S318949

28. Di Pierro F, Derosa G, Maffioli P, Bertuccioli A, Togni S, Riva A, et al. Possible therapeutic effects of adjuvant quercetin supplementation against early-stage COVID-19 infection: A prospective, randomized, controlled, and open-label study. *Int J Gen Med* (2021) 14:2359–2366. doi: 10.2147/IJGM.S318720

29. Gu YY, Zhang M, Cen H, Wu YF, Lu Z, Lu F, et al. Quercetin as a potential treatment for COVID-19-induced acute kidney injury: Based on network pharmacology and molecular docking study. *PloS One* (2021) 16(1):e0245209. doi: 10.1371/journal.pone.0245209

30. Munafo F, Donati E, Brindani N, Ottonello G, Armirotti A, De Vivo M. Quercetin and luteolin are single-digit micromolar inhibitors of the SARS-CoV-2 RNA-dependent RNA polymerase. *Sci Rep* (2022) 12(1):10571. doi: 10.1038/s41598-022-14664-2

31. Tan RZ, Wang C, Deng C, Zhong X, Yan Y, Luo Y, et al. Quercetin protects against cisplatin-induced acute kidney injury by inhibiting Mincle/Syk/NF-κB signaling maintained macrophage inflammation. *Phytother Res* (2020) 34(1):139–52. doi: 10.1002/ptr.6507

32. Lan HY, Mu W, Nikolic-Paterson DJ, Atkins RC. A novel, simple, reliable, and sensitive method for multiple immunoenzyme staining: use of microwave oven heating to block antibody crossreactivity and retrieve antigens. *J Histochem Cytochem* (1995) 43 (1):97–102. doi: 10.1177/43.1.7822770

33. Ahmadian E, Hosseiniyan Khatibi SM, Razi Soofiyani S, Abediazar S, Shoja MM, Ardalan M, et al. Covid-19 and kidney injury: Pathophysiology and molecular mechanisms. *Rev Med Virol* (2021) 31(3):e2176. doi: 10.1002/rmv.2176

34. Lv LL, Tang PM, Li CJ, You YK, Li J, Huang XR, et al. The pattern recognition receptor, Mincle, is essential for maintaining the M1 macrophage phenotype in acute renal inflammation. *Kidney Int* (2017) 91(3):587–602. doi: 10.1016/j.kint.2016.10.020

35. Pan P, Shen M, Yu Z, Ge W, Chen K, Tian M, et al. SARS-CoV-2 N protein promotes NLRP3 inflammasome activation to induce hyperinflammation. *Nat Commun* (2021) 12(1):4664. doi: 10.1038/s41467-021-25015-6

36. Wu Y, Ma L, Cai S, Zhuang Z, Zhao Z, Jin S, et al. RNA-induced liquid phase separation of SARS-CoV-2 nucleocapsid protein facilitates NF-κB hyper-activation and inflammation. *Signal Transduct Target Ther* (2021) 6(1):167. doi: 10.1038/s41392-021-00575-7

37. Yanai H, Ban T, Taniguchi T. High-mobility group box family of proteins: ligand and sensor for innate immunity. *Trends Immunol* (2012) 33(12):633–40. doi: 10.1016/j.it.2012.10.005

38. Wu H, Ma J, Wang P, Corpuz TM, Panchapakesan U, Wyburn KR, et al. HMGB1 contributes to kidney ischemia reperfusion injury. *J Am Soc Nephrol* (2010) 21 (11):1878–90. doi: 10.1681/ASN.2009101048

39. Li J, Gong Q, Zhong S, Wang L, Guo H, Xiang Y, et al. Neutralization of the extracellular HMGB1 released by ischaemic damaged renal cells protects against renal ischaemia- reperfusion injury. *Nephrol Dial Transplant* (2011) 26(2):469–78. doi: 10.1093/ndt/gfq466

40. Tian S, Zhang L, Tang J, Guo X, Dong K, Chen SY. HMGB1 exacerbates renal tubulointerstitial fibrosis through facilitating M1 macrophage phenotype at the early stage of obstructive injury. *Am J Physiol Renal Physiol* (2015) 308(1):F69–75. doi: 10.1152/ajprenal.00484.2014

41. Jiang Y, Chen R, Shao X, Ji X, Lu H, Zhou S, et al. HMGB1 silencing in macrophages prevented their functional skewing and ameliorated EAM development: Nuclear HMGB1 may be a checkpoint molecule of macrophage reprogramming. *Int Immunopharmacol* (2018) 56:277–84. doi: 10.1016/j.intimp.2018.01.013

42. Inoue T. M1 macrophage triggered by Mincle leads to a deterioration of acute kidney injury. *Kidney Int* (2017) 91(3):526–9. doi: 10.1016/j.kint.2016.11.026

43. Bernini R, Velotti F. Natural polyphenols as immunomodulators to rescue immune response homeostasis: quercetin as a research model against severe COVID-19. *Molecules* (2021) 26(19):5803. doi: 10.3390/molecules 26195803

44. Diniz LRL, Souza MTS, Duarte ABS, Sousa DP. Mechanistic aspects and therapeutic potential of quercetin against COVID-19-associated acute kidney injury. *Molecules* (2020) 25(23):5772. doi: 10.3390/molecules25235772

45. Lu H, Wu L, Liu L, Ruan Q, Zhang X, Hong W, et al. Quercetin ameliorates kidney injury and fibrosis by modulating M1/M2 macrophage polarization. *Biochem Pharmacol* (2018) 154:203–12. doi: 10.1016/j.bcp.2018.05.007

frontiers | Frontiers in Immunology

TYPE Original Research
PUBLISHED 16 November 2023
DOI 10.3389/fimmu.2023.1259434

OPEN ACCESS

EDITED BY
Xu-jie Zhou,
Peking University, China

REVIEWED BY
Zhen Wang,
Huazhong University of Science and Technology, China
Zhichao Fan,
UCONN Health, United States

*CORRESPONDENCE
Qiuhua Yang
qiyang@augusta.edu
Qingqing Wei
qwei@augusta.edu

RECEIVED 15 July 2023
ACCEPTED 27 October 2023
PUBLISHED 16 November 2023

CITATION
Yang Q, Huo E, Cai Y, Zhang Z, Dong C, Asara JM, Shi H and Wei Q (2023) Myeloid PFKFB3-mediated glycolysis promotes kidney fibrosis. *Front. Immunol.* 14:1259434. doi: 10.3389/fimmu.2023.1259434

Myeloid PFKFB3-mediated glycolysis promotes kidney fibrosis

Qiuhua Yang[1*], Emily Huo[1,2], Yongfeng Cai[1], Zhidan Zhang[1], Charles Dong[3], John M. Asara[4], Huidong Shi[5,6] and Qingqing Wei[1*]

[1]Department of Cellular Biology and Anatomy, Medical College of Georgia, Augusta University, Augusta, GA, United States, [2]Augusta Preparatory Day School, Martinez, GA, United States, [3]Dental College of Georgia, Augusta University, Augusta, GA, United States, [4]Division of Signal Transduction, Beth Israel Deaconess Medical Center and Department of Medicine, Harvard Medical School, Boston, MA, United States, [5]Department of Biochemistry and Molecular Biology, Medical College of Georgia, Augusta University, Augusta, GA, United States, [6]Georgia Cancer Center, Medical College of Georgia, Augusta University, Augusta, GA, United States

Excessive renal fibrosis is a common pathology in progressive chronic kidney diseases. Inflammatory injury and aberrant repair processes contribute to the development of kidney fibrosis. Myeloid cells, particularly monocytes/macrophages, play a crucial role in kidney fibrosis by releasing their proinflammatory cytokines and extracellular matrix components such as collagen and fibronectin into the microenvironment of the injured kidney. Numerous signaling pathways have been identified in relation to these activities. However, the involvement of metabolic pathways in myeloid cell functions during the development of renal fibrosis remains understudied. In our study, we initially reanalyzed single-cell RNA sequencing data of renal myeloid cells from Dr. Denby's group and observed an increased gene expression in glycolytic pathway in myeloid cells that are critical for renal inflammation and fibrosis. To investigate the role of myeloid glycolysis in renal fibrosis, we utilized a model of unilateral ureteral obstruction in mice deficient of *Pfkfb3*, an activator of glycolysis, in myeloid cells (*Pfkfb3*$^{\Delta M\phi}$) and their wild type littermates (*Pfkfb3*^{WT}). We observed a significant reduction in fibrosis in the obstructive kidneys of *Pfkfb3*$^{\Delta M\phi}$ mice compared to *Pfkfb3*^{WT} mice. This was accompanied by a substantial decrease in macrophage infiltration, as well as a decrease of M1 and M2 macrophages and a suppression of macrophage to obtain myofibroblast phenotype in the obstructive kidneys of *Pfkfb3*$^{\Delta M\phi}$ mice. Mechanistic studies indicate that glycolytic metabolites stabilize HIF1α, leading to alterations in macrophage phenotype that contribute to renal fibrosis. In conclusion, our study implicates that targeting myeloid glycolysis represents a novel approach to inhibit renal fibrosis.

KEYWORDS

macrophage, glycolysis, renal fibrosis, PFKFB3, inflammation

Introduction

Fibrosis is a pathological condition commonly observed in advanced stages of organ disease, such as chronic kidney disease (CKD) (1). The progression of renal fibrosis relies heavily on the activation of myofibroblasts, a specialized type of fibroblast characterized by the expression of alpha-smooth muscle actin (α-SMA). These myofibroblasts play a pivotal role in renal fibrosis by producing and secreting excessive extracellular matrix proteins such as fibronectin and collagens (2) and other components to affect renal function (3). Various cell types have been identified as potential sources of myofibroblasts involved in the development of renal fibrosis including resident fibroblasts, hematopoietic cells, and pericytes (4–11).

Extensive research has elucidated the significant involvement of myeloid cells, particularly monocytes/macrophages, in the development of renal fibrosis (12–17). During the early stage of renal injury, upon the stimulation of various inflammatory cytokines (18, 19), circulating monocytes are recruited to the injured kidney and undergo differentiation into M1 macrophages. These M1 macrophages not only proliferate locally but also have the ability to differentiate to be M2 macrophages in response to the changes in the microenvironment (20). Additionally, a subset of M2 macrophages can further undergo a phenotype change, acquiring some characteristics of myofibroblasts, which has been described as macrophage-myofibroblast transition (MMT) in some recent studies (11, 14, 21–23). Inhibition of monocyte infiltration into the kidney (24–26), attenuation of renal injury caused by M1 macrophages (27) (28), as well as modulation of fibrotic activity associated with M2 and MMT processes (14, 29), have all been shown to inhibit the progression of renal fibrosis effectively.

Metabolic reprogramming, particularly the shift toward glycolysis, plays a critical role in various pathological cellular procedures such as tumor cell growth and metastasis (30, 31), drug resistant epilepsy (32), and the function and polarization of myeloid cells (33). One important enzyme involved in this process is 6-phosphofructo-2-kinase/fructose-2,6-bisphosphatase 3 (PFKFB3), which catalyzes the synthesis of fructose-2, 6-bisphosphate (F-2,6-P2). F-2,6-P2 serves as a potent allosteric activator of 6-phosphofructo-1-kinase (PFK-1), one of key rate-limiting enzymes in glycolysis (34). Previous studies utilizing mice deficient in myeloid Pfkfb3 have demonstrated its role in suppressing ocular angiogenesis (35, 36), pulmonary hypertension (37), and atherosclerosis (38). Metabolic shifting to glycolysis has been noted in renal repair and fibrosis development with renal acidosis developed after the accumulation of lactate (39, 40). In studies from our lab and other research groups, glycolysis has emerged as a notable contributor to renal fibrosis with divergent effect on different renal cells, and glycolysis inhibitors can reduce the macrophage infiltration in renal fibrosis (41–43). However, the effect of glycolysis on macrophage differentiation and the significance of myeloid PFKFB3-mediated glycolysis in the development of renal fibrosis has yet to be fully elucidated. In this study, we employed a combination of *in vitro* and *in vivo* approaches to investigate the role of myeloid PFKFB3 in myeloid cell infiltration to kidney, renal inflammation, M2 macrophage differentiation, and ultimately the development of renal fibrosis in the unilateral ureteral obstruction (UUO) model.

Method

Mouse generation

All animal care and experimental procedures were conducted in compliance with the National Institutes of Health Guide for the Care and Use of Laboratory Animals. The protocol (Animal protocol # 2011-0401 and # 2018-0971) followed was approved by the Institutional Animal Care and Use Committee at Augusta University. Prior to, during, and after the experiment, welfare assessments, measurements, and interventions were performed. The mice were housed under controlled environmental conditions, including a temperature range of 21-25 °C, humidity between 40-60%, and a 12-hour light/dark cycle. All animals had ad libitum access to food (Teklad global 18% protein rodent diet; 2918-060622M, Envigo, Madison, WI, USA) and water. Floxed *Pfkfb3* (*Pfkfb3*$^{flox/flox}$) mice were generated by Xenogen Biosciences Corporation (Cranbury, NJ, USA) (44). To achieve cell-specific deficiency of *Pfkfb3* in macrophages, *Pfkfb3*$^{flox/flox}$ mice were crossbred with Lysm-Cre transgenic mice (The Jackson Laboratory, stock no. 004781, Bar Harbor, ME, USA) to generate *Pfkfb3*$^{flox/flox}$ Lysm-Cre (*Pfkfb3*$^{\Delta M\varphi}$) mice, with *Pfkfb3*$^{WT/WT}$ Lysm-Cre (*Pfkfb3*^{WT}) mice used as wild type control. All mice were genotyped by PCR amplification of tail-clip samples (Supplementary Table 1).

Unilateral ureteral obstruction mouse model

As described previously (41), Adult male mice weighing between 20-25 grams were used for this study. Under anesthesia induced by i.p. injection of ketamine (100 mg/kg) and xylazine (10 mg/kg), a midline abdominal incision was made to expose the left ureter. A double-ligature technique was utilized to create a complete obstruction by tying a suture around the left ureter at two distinct points, with a 1-mm interval between the ligatures. The ureter was then gently compressed between the ligatures and carefully examined to ensure complete occlusion. The mice were allowed to recover under controlled temperature and humidity conditions. At designated time points, the mice were euthanized using i.p. injection of ketamine (100 mg/kg) and xylazine (10 mg/kg) to collect kidney samples for analysis. The kidneys were carefully dissected and processed for histological examination and gene expression studies. The contralateral kidneys without ligation were used as control.

Culture of bone marrow-derived macrophages

After euthanizing the mice, femurs and tibias were collected and transected. The bone marrow cells were flushed out from the femurs and tibias. These cells were then passed through a 70 μm cell

strainer and centrifuged at 1000 x g for 3 minutes to obtain a single-cell suspension. The collected cells were plated onto a 10 cm^2 dish and allowed to incubate for 6-8 hours to discard the attached cells. The remaining suspension cells were collected and reseeded into a 6-well plate at a density of 2 x 10^6 cells/mL. Cells were cultured in RPMI 1640 medium (SH30027.01, Cytiva, Marlborough, MA, USA) supplemented with 10% FBS (F4135, Sigma-Aldrich, St. Louis, MO, USA), 10 ng/mL MCSF (315-02, PeproTech, Cranbury, NJ, USA) and 1% Antibiotic-Antimycotic (15240062, Thermo Scientific, Grand Island, NY, USA) in a humidified incubator with 5% CO2 at 37°C for 7 days to induce macrophage differentiation as described before (45). After 7 days, the differentiated cells were cultured in RPMI 1640 medium supplemented with 1% FBS, 1% Antibiotic-Antimycotic, and 10 ng/mL MCSF. Subsequently, the cells were treated with or without 10 ng/mL mouse TGFβ1 (7666-MB-005, R&D SYSTEMS, Minneapolis, MN, USA) to induce macrophage differentiation for 5 days.

Real-time PCR

To extract total RNA from cells or tissues, the Trizol Reagent (15596018, Invitrogen, Grand Island, NY) was employed following the manufacturer's protocol, as previously described (46). For cDNA synthesis, the iScriptTM cDNA synthesis kit (1708891, Bio-Rad Hercules, CA, USA) was utilized. RT-qPCR was performed on a StepOne Plus System (Applied Biosystems, Grand Island, NY) using the Power SYBR Green Master Mix (1725122, Bio-Rad Hercules). The relative gene expression was quantified using the efficiency-corrected $2^{-\triangle\triangle CT}$ method, with 18S ribosomal RNA serving as the internal control. The obtained data are presented as fold change relative to the control groups. Supplementary Table 2 includes the list of gene-specific primers employed in our study.

Western blot analysis

Protein extracts were obtained from kidney tissues and cells by lysing them in RIPA buffer supplemented with protease inhibitor cocktails (05892970001, Roche, SC, USA). The kidney tissues were ground and then lysed to prepare the tissue lysates. The extracts were centrifuged at 12,000 rpm for 10 minutes, and the resulting supernatant was collected. The protein concentration in the supernatant was determined using the BCA assay. Subsequently, the samples were subjected to SDS-PAGE and transferred onto nitrocellulose membrane. After blocking with 5% skim milk for one hour, the blots were probed with the following primary antibodies: PFKFB3 (diluted 1:1000, ab181861, abcam), ACTA2 (diluted 1:1000, sc-56499, Santa Cruz), Vimentin (diluted 1:1000, CST5741, Cell Signaling Technology), Collagen I (diluted 1:1000, NB600-408, NOVUS), Collagen IV (diluted 1:1000, ab6586, abcam), Fibronectin (diluted 1:1000, ab2413, abcam), Cyclophilin B (diluted 1:1000, CST43603, Cell Signaling Technology), HIF1A (diluted 1:500, AF1935-SP, R&D systems). Anti-β-actin (diluted 1:1000, sc47776, Santa Cruz) and GAPDH (diluted 1:1000, 2118, CST) were used as loading controls. The antibodies used are provided in Supplementary Table 3. The western blots were quantified with a method described previously (47).

Immunofluorescence

Cells were cultured in 8-Chambered Cell Culture Slides (08-774-26, Fisher Scientific). Frozen or paraffin blocks were sectioned at 7 μm thickness using a Microm cryostat or paraffin microtome. For cells or frozen sections, a PBS wash was performed, followed by fixation with 4% paraformaldehyde for 15 minutes. Subsequently, permeabilization was achieved by treating the cells or slides with 0.5% Triton X-100 for 20 minutes at room temperature. In the case of paraffin sections, slides were subjected to deparaffinization and rehydration before permeabilization. For antigen retrieval, slides were heated in citrate acid buffer (10 mM, pH 6.0) by microwaving at 98°C for 10 minutes. Following these steps, cells or sections were blocked with 10% normal goat serum (50062Z, Thermo Scientific) for 1 hour at room temperature. Primary antibodies against PFKFB3, ACTA2, F4/80, Arg1, IL1β, or COL1 were then added and incubated overnight at 4°C in a humidified chamber. After washing, samples were incubated with Alexa Fluor 488, 594, or 647-conjugated secondary antibodies for 1 hour at room temperature. Nuclei were counterstained with DAPI for 10 minutes at room temperature. The imaging process was carried out using an inverted confocal microscope (Zeiss 780, Carl Zeiss). The images were quantified with a method described previously (35). Four images/section/kidney were used for statistic purpose. The primary antibodies used in our study can be found in Supplementary Table 3.

Immunohistochemistry

Paraffin-embedded kidneys were sectioned and underwent deparaffinization using xylene, followed by rehydration with a gradient of ethanol and water solutions. The activity of endogenous peroxidase in the tissue was eliminated by a treatment with methanol containing 30% H_2O_2 for 30 minutes at room temperature. Antigen retrieval was performed by exposing the sections to 10 mM sodium citrate buffer (pH 6.0) at 98°C for 10 minutes, followed by blocking with avidin blocking solution for 1 hour at room temperature. The antibodies were mixed with biotin blocking solution as per the manufacturer's instructions and applied to the slides, which were then incubated overnight at 4°C. Subsequently, the tissue sections were treated with a biotinylated secondary antibody for 1 hour at room temperature, followed by incubation with ABC solution (PK-6100, Vector Laboratories) for 30 minutes at room temperature. The antibody was visualized using the peroxidase substrate 3, 3'-diaminobenzidine (3468, Dako, Santa Clara, CA, USA). Hematoxylin I (GHS116, Sigma) was used for counterstaining of the kidney sections. Finally, the slides were dehydrated and mounted using a xylene-based mounting medium (8312-4, Richard-Allan Scientific). The image data was quantified with the method described previously (48), using Image J Software

(National Institutes of Health, USA, http://imagej.nih.gov/ij). Four images/section/kidney were used for statistic purpose. The primary antibodies used in our study can be found in Supplementary Table 3.

Histological staining

We performed H & E staining on 7 μm sections of kidney with hematoxylin (22050111, Thermo Scientific) and eosin (220501110, Thermo Scientific) following the manufacturer's standard protocol. Collagen deposition was visualized using Masson's Trichrome staining kit (25088-1, Polysciences, PA, USA) and Sirius Red staining kit (ab150681, Abcam, CA, USA) according to the manufacturer's instructions. Four images of were randomly taken in cortex/outer medulla region per section for each kidney, captured with a Keyence Microscope BZ-X800, and the percentage of collagen deposition area was quantified with Image J Software (National Institutes of Health, USA, http://imagej.nih.gov/ij).

Metabolomics assay

In the experiment, biological triplicate 10 cm^2 dishes were utilized to cultivate BMDMs in the presence of complete cell medium. Following the specific treatment, metabolites were extracted using 1 mL of ice-cold 80% methanol on dry ice. Subsequently, the samples underwent centrifugation at 14000 rpm for a duration of 5 minutes. To ensure thorough extraction, the cell pellet was subjected to an additional step involving the use of 0.5 mL of 80% methanol. For accurate protein quantitation, the cell pellet was dissolved in an 8 M urea solution. To facilitate convenient shipment or storage, the supernatant obtained from the metabolite extraction was desiccated into a pellet using a SpeedVac from Eppendorf (Hamburg, Germany), employing a heat-free technique. When it was time for analysis, the dried pellets were re-suspended in 20 μL of HPLC grade water in preparation for mass spectrometry as described before (49). A volume of 5-7 μL of the resulting resuspension was injected and subjected to analysis using a cutting-edge hybrid 6500 QTRAP triple quadrupole mass spectrometer from AB/SCIEX (MA, USA), which was coupled to a Prominence UFLC HPLC system from Shimadzu (Kyoto, Japan). The analysis was carried out through selected reaction monitoring (SRM), targeting a comprehensive set of 298 endogenous water-soluble metabolites, enabling a thorough examination of the steady-state characteristics of the samples. The original data has been uploaded to MetaboLights (MTBLS8278) for public data sharing.

Measurement of cytokines

The levels of mouse cytokines TNFα and IL1β were measured with ELISA kits (MTA00B and MLB00C, R&D, Minneapolis, MN, USA) according to the manufacturer's instructions.

Statistical analysis

Statistical analysis was conducted using GraphPad Prism Software (Version 9.0, RRID: SCR_000306). The significance of differences between two groups was evaluated using the unpaired Student's t-test or unpaired two-tailed Student's t-test with Welch's correction (with unequal variances). Multiple comparisons were performed through one-way ANOVA followed by Bonferroni *post hoc* test. All results are presented as mean ± SEM. A significance level of $P < 0.05$ was considered statistically significant. To calculate the Z-score, we used the formula below: $Z\text{-score} = (x - \mu)/\sigma$, x is the value of the data point, μ is the mean of the sample or data set, σ is the standard deviation. Each biological experiment was repeated a minimum of three times, utilizing independent cell cultures or individual animals as biological replications.

Results

Increased glycolytic gene expression in myeloid cells infiltrating in the UUO kidney

In a study by Conway et al., myeloid populations crucial for renal fibrosis in the UUO kidney were characterized using single-cell RNA sequencing (scRNAseq) (50). Among these myeloid populations, the significance of $Ly6c2^+$ and $Arg1^+$ myeloid cells in renal fibrosis were observed (50). To gain further insights of the early events in kidney obstruction, we conducted a reanalysis of the inflammation, TGFβ signaling, and glycolysis related mRNA expression in these myeloid cells and compared them to resident macrophages in UUO 2-day condition. Our findings revealed substantially higher levels of mRNA expression in inflammation, TGFβ signaling, and glycolysis pathways in $Ly6c^+$ and $Arg1^+$ myeloid cells than those of resident macrophages (Figure 1A, Supplementary Figure 1). Consistent with these altered pathways, the corresponding genes involved in these pathways were upregulated in $Ly6C^+$ and $Arg1^+$ myeloid cells compared to resident macrophages. Notably, these genes included Il1, Tgfb1, and Hif1 (Figure 1B, Supplementary Figure 2). Intriguingly, $Ly6C^+$ and $Arg1^+$ myeloid cells also exhibited elevated levels of Fn1 and Vim in comparison to resident macrophages (Figure 1B), suggesting a potential role of myeloid glycolysis in renal fibrosis initiation.

Decreased renal fibrosis in myeloid-specific *Pfkfb3*-deficient mice following UUO

To investigate the role of myeloid PFKFB3 in renal fibrosis, we generated myeloid-specific *Pfkfb3*-deficient mice ($Pfkfb3^{\Delta M\phi}$) and their controls ($Pfkfb3^{WT}$) by breeding floxed *Pfkfb3* mice with Lysm-Cre mice (Supplementary Figures 3A, B). Deletion of *Pfkfb3* in myeloid cells was confirmed through Real time PCR, Western blot analysis and immunostaining of PFKFB3 in Bone marrow derived macrophages (Supplementary Figures 3C-E). We conducted unilateral ureter

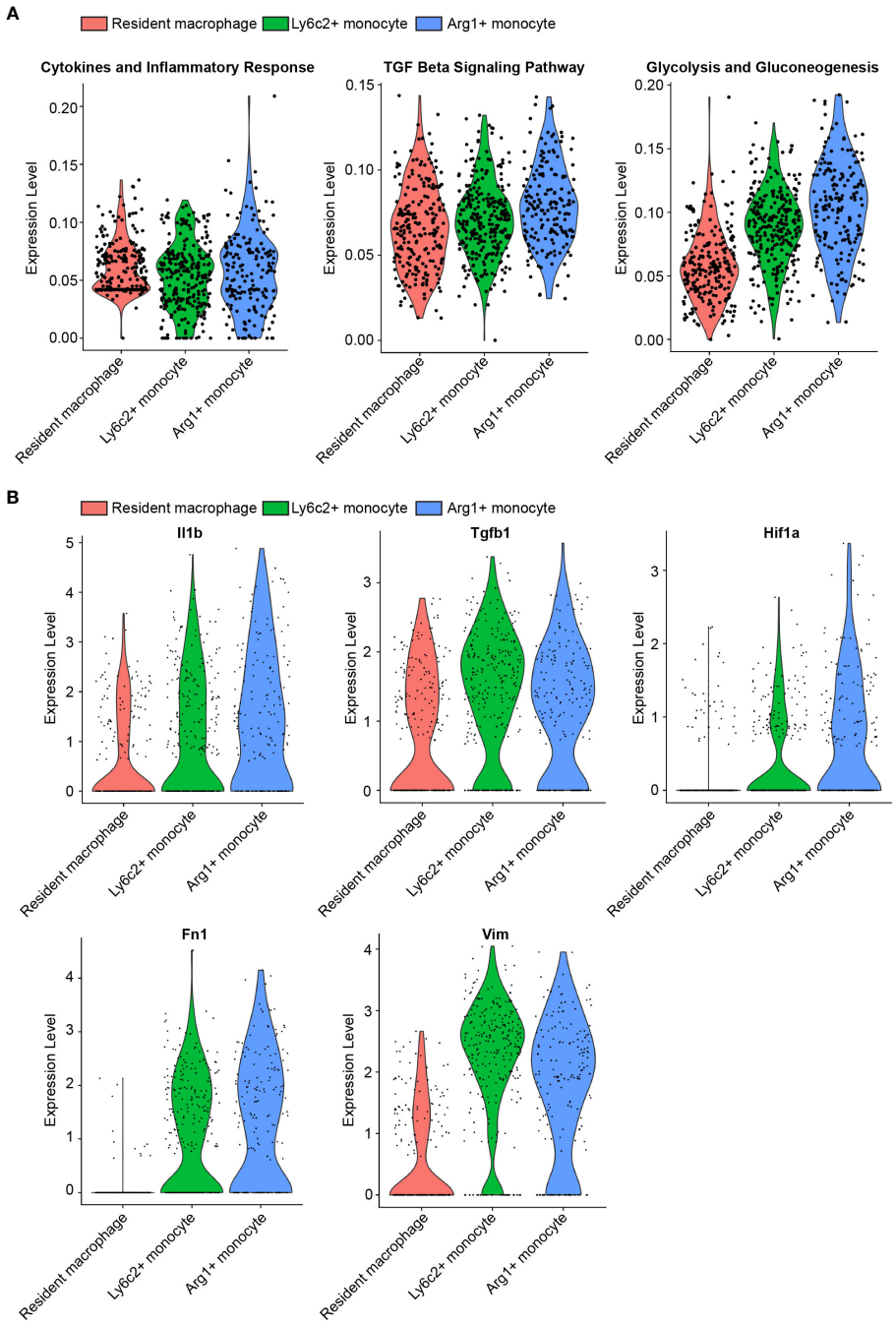

FIGURE 1
scRNAseq reveals upregulated glycolysis in myeloid cells infiltrating in the UUO kidney. **(A)** Violin plots of inflammation, TGFβ signaling, and glycolysis pathways in resident macrophage, Ly6c2+ macrophage and Arg1+ monocyte clusters. **(B)** Violin plots of indicated genes in resident macrophage, Ly6c2+ macrophage and Arg1+ monocyte clusters.

obstruction (UUO) surgery in these mice (Figure 2A). The change in mouse body weight following the UUO procedure did not show a significant difference between the two groups (Figure 2B). After 14 days, the weight of obstructive kidneys was significantly reduced compared to that of control kidneys, indicating obvious kidney atrophy (Figures 2C, D, Supplementary Figure 4). And hydronephrosis was observed at kidney harvesting, indicating the success of ureter obstruction. Meanwhile, there was no significant difference of kidney weight between groups of *Pfkfb3*$^{\Delta M\phi}$ and *Pfkfb3*^{WT} mice (Figures 2C, D). The co-staining of PFKFB3 and F4/80 confirmed the induction of PFKFB3 in *Pfkfb3*^{WT} macrophages and the depletion of *Pfkfb3* in *Pfkfb3*$^{\Delta M\phi}$ macrophages in kidneys after UUO injury (Supplementary Figure 5). Using qRT-PCR, we examined the mRNA levels of multiple fibrotic factors. The expression of *Acta2*, *Col*1 and 3, *Mmp*2 and 9, and *Tgfb* were significantly increased in UUO kidneys compared to control kidneys (Figure 3A). Notably, the upregulation of these fibrotic factors in UUO kidneys of *Pfkfb3*$^{\Delta M\phi}$ mice was markedly reduced compared to *Pfkfb3*^{WT} mice (Figure 3A). We also assessed the protein levels of a few

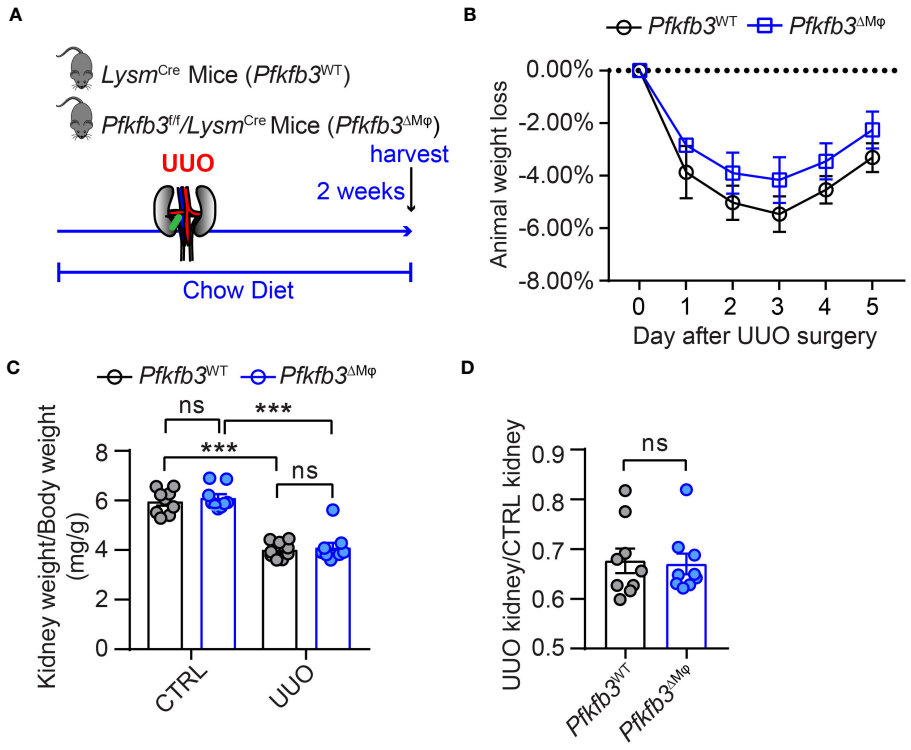

FIGURE 2
The myeloid *Pfkfb3* deficiency does not show significant impact on body weight and kidney weight loss after ureter obstruction. **(A)** Schematic illustration of Unilateral ureteral obstruction (UUO) in myeloid *Pfkfb3* deficient mice. **(B)** The daily body weight loss percentage for *Pfkfb3*$^{\Delta M\varphi}$ and *Pfkfb3*^{WT} mice subjected to UUO surgery for 5 days. **(C)** The ratio of kidney weight to body weight from *Pfkfb3*$^{\Delta M\varphi}$ and *Pfkfb3*^{WT} mice subjected to UUO surgery for 14 days. **(D)** The ratio of fibrotic kidney weight to control from *Pfkfb3*$^{\Delta M\varphi}$ and *Pfkfb3*^{WT} mice subjected to UUO surgery for 14 days. n = 9 mice per group. Data are means ± SEM. ns, no significance; ***p < 0.001 for indicated comparisons. Statistical significance was determined by one-way ANOVA followed by the Bonferroni test **(C)** or by Student's *t* test **(D)**.

fibrotic factors through Western blot analysis (Figure 3B). The levels of α-smooth muscle actin (ACTA2), vimentin (VIM), collagen (COL) I and IV and fibronectin (FN) were significantly elevated in UUO kidneys compared to control kidneys. However, the increased levels of these fibrotic factors in UUO kidneys of *Pfkfb3*$^{\Delta M\varphi}$ mice were significantly reduced compared to *Pfkfb3*^{WT} mice (Figure 3B).

Furthermore, we verified the interstitial renal fibrosis by staining renal sections of UUO and control kidneys with Sirius Red and Masson's trichrome. In the UUO kidneys from *Pfkfb3*^{WT} mice, characterized by pronounced tubular dilation and thinning on hematoxylin and eosin (HE) stained sections, there was evident collagen deposition with Masson's trichrome and Sirius Red staining, indicating a significant interstitial renal fibrosis (Figures 4A, B, Supplementary Figure 4). In contrast, there were fewer tubular destruction and less collagen deposition shown by Masson's trichrome and Sirius Red staining in the sections of UUO kidneys from *Pfkfb3*$^{\Delta M\varphi}$ mice compared to *Pfkfb3*^{WT} mice (Figures 4A, B).

We also performed immunostaining to examine the presence of specific myofibroblast marker and components of extracellular matrix. As shown in Figure 4C, the levels of ACTA2, Collagen I and IV, which were low but detectable in the control kidneys from both groups of mice, were remarkably elevated in the UUO kidneys of *Pfkfb3*^{WT} mice. However, these increased levels of myofibroblast marker and extracellular matrix proteins were significantly reduced in the UUO kidneys from *Pfkfb3*$^{\Delta M\varphi}$ mice (Figure 4C).

Declined number of renal macrophages in myeloid-specific *Pfkfb3*-deficient mice following UUO

We investigated the infiltration of macrophages in the UUO kidney of *Pfkfb3*$^{\Delta M\varphi}$ mice by performing immunostaining on renal sections using the F4/80 antibody. The presence of F4/80 positive cells was not noticeable in control kidneys from both *Pfkfb3*^{WT} and *Pfkfb3*$^{\Delta M\varphi}$ mice (Figures 5A, B). However, an obvious increase of F4/80-positive cells was observed in the UUO *Pfkfb3*^{WT} kidneys (Figures 5A, B). Remarkably, the F4/80 positive area was significantly reduced in the UUO *Pfkfb3*$^{\Delta M\varphi}$ kidney sections compared to the UUO *Pfkfb3*^{WT} kidney (Figures 5A, B). These findings strongly suggest that myeloid *Pfkfb3* deficiency markedly inhibits the infiltration of macrophages into the UUO kidneys.

Reduced markers of M1 and M2 macrophages and related cytokines in myeloid-specific *Pfkfb3*-deficient mice following UUO

To assess the impact of myeloid *Pfkfb3* deficiency on the infiltration of M1 and M2 macrophages in the UUO kidneys, we

10.3389/fimmu.2023.1259434

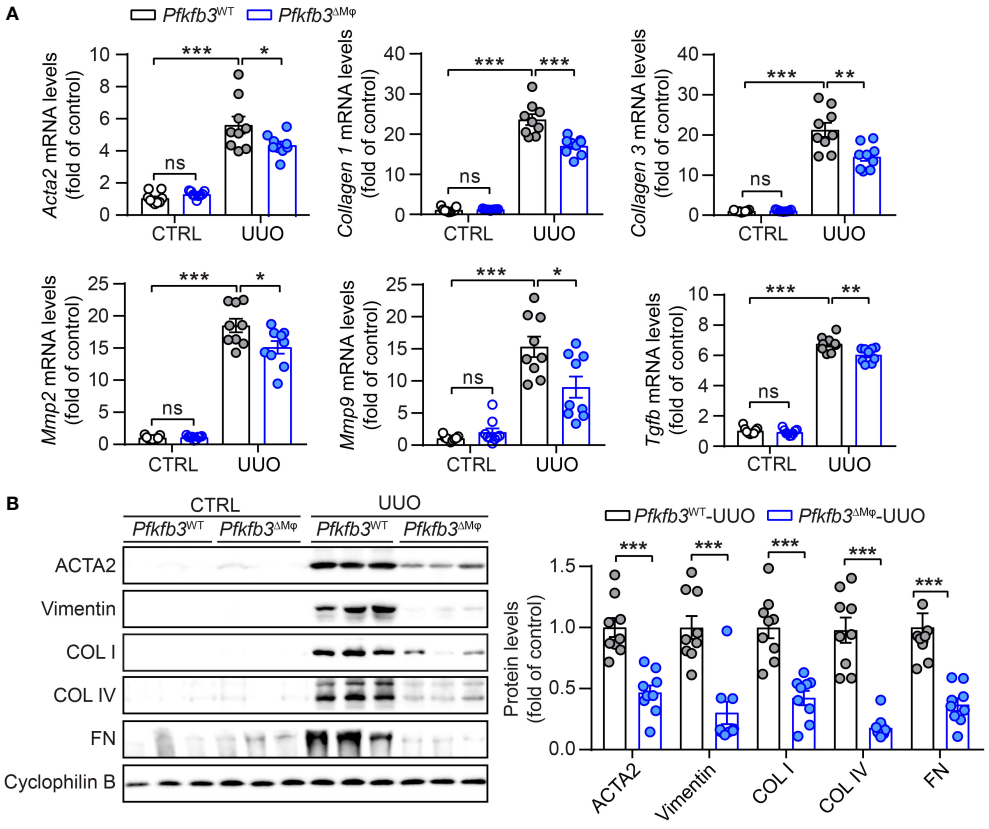

FIGURE 3
The myeloid *Pfkfb3* deficiency suppresses renal fibrosis in UUO mouse model. **(A)** qRT-PCR analysis of the mRNA expression of *Acta2*, *Col1*, *Col3*, *Mmp2*, *Mmp9* and *Tgfb* in kidney collected from *Pfkfb3*$^{\Delta M\varphi}$ and *Pfkfb3*^{WT} mice at day 14 post UUO surgery. **(B)** Representative Western Blots and their quantification showing ACTA2, Vimentin, COL I, COL IV, FN protein expression in kidney collected from *Pfkfb3*$^{\Delta M\varphi}$ and *Pfkfb3*^{WT} mice at day 14 post UUO surgery. n = 9 mice per group. Data are means ± SEM. ns, no significance; *p < 0.05; **p < 0.01; ***p < 0.001 for indicated comparisons. Statistical significance was determined by one-way ANOVA followed by the Bonferroni test **(A)** or by Student's *t* test **(B)**.

examined the mRNA and protein levels of M1/M2 markers and cytokines associated with M1/M2 macrophages. As shown in Figure 6A, the expression levels of M2 markers *Arg1*, *Cd206*, and M1 markers *Cd80* were detectable but similar in the control kidneys of both groups of mice. However, in the UUO *Pfkfb3*^{WT} kidney, there was a substantial upregulation of both M2 and M1 markers (Figure 6A). In contrast, these markers were significantly reduced in the UUO *Pfkfb3*$^{\Delta M\varphi}$ kidney compared to the UUO *Pfkfb3*^{WT} kidney (Figure 6A). Consistent with the levels of M1/M2 markers, the levels of cytokines, including Il10, Mgl2, Retnla, Il6, Mcp1, Tnfa, Il1b, Nos2, and Cxcl10, were significantly lower in the UUO *Pfkfb3*$^{\Delta M\varphi}$ kidney compared to the UUO *Pfkfb3*^{WT} kidney (Figure 6A). To validate the expression of some genes at protein levels, we examined the expression of Arg1 and Il1β on F4/80 positive cells by immunostaining in renal sections with their specific antibodies. The staining intensity of Arg1 and Il1β on F4/80-positive cells were much lower in sections of the UUO *Pfkfb3*$^{\Delta M\varphi}$ kidney compared to the UUO *Pfkfb3*^{WT} kidney (Figure 6B). These findings indicate that *Pfkfb3* deficiency leads to a significant reduction in the number of M1 and M2 macrophages, as well as the levels of cytokines associated with these macrophage phenotypes in UUO kidneys.

Lowered macrophage differentiation in myeloid-specific *Pfkfb3*-deficient obstructive kidneys

To investigate whether myeloid *Pfkfb3* deficiency affected macrophage differentiation to obtain myofibroblast phenotype in the UUO kidney, we quantified the number of macrophages expressing ACTA2 through co-immunostaining of the renal sections. In the control kidneys, the presence of ACTA2 and F4/80 positive cells was rare (Figures 7A, B). Conversely, the UUO *Pfkfb3*^{WT} kidneys exhibited a significant induction of F4/80 positive cells, with about 6% of them co-stained with ACTA2 (Figures 7A, B), suggesting their transition to myofibroblasts. Remarkably, the UUO *Pfkfb3*$^{\Delta M\varphi}$ kidneys showed a substantial reduction of F4/80 positive area as well as the double-positive area of F4/80 and ACTA2 compared to the UUO *Pfkfb3*^{WT} kidney (Figures 7A, B). Further analysis on the lineage of myofibroblasts revealed that, in the UUO Pfkfb3WT kidneys, about 32% of myofibroblasts (ACTA2 positive) expressed F4/80. This percentage dropped to approximately 15% in the UUO Pfkfb3ΔMϕ kidneys (Figure 7B). These findings indicate that myeloid-specific *Pfkfb3* deficiency leads

10.3389/fimmu.2023.1259434

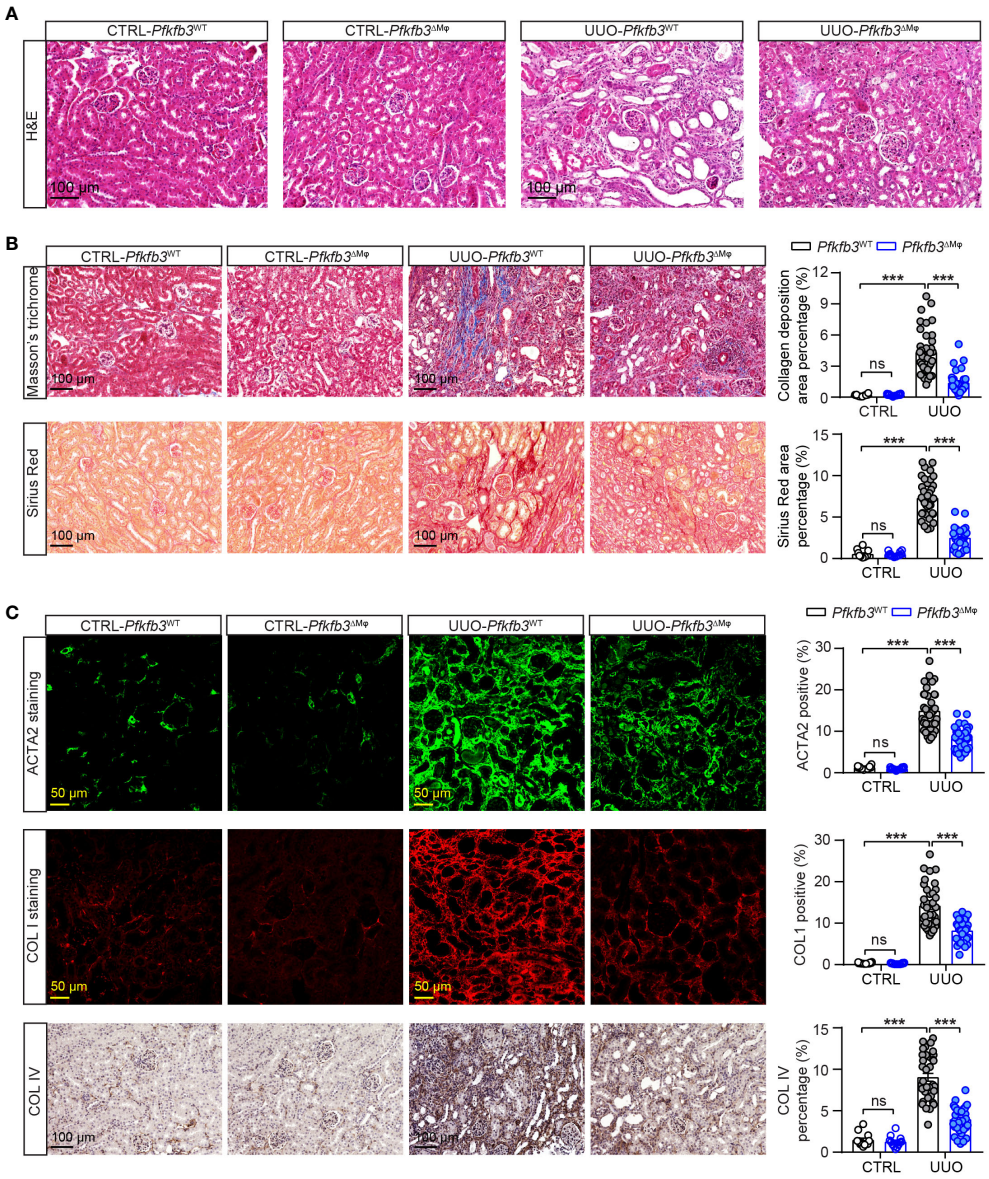

FIGURE 4
The myeloid *Pfkfb3* deficiency suppresses renal fibrosis in obstructive kidney. *Pfkfb3*$^{\Delta M\varphi}$ and *Pfkfb3*^{WT} mice were subject to UUO for 14 days, kidneys were collected and fixed for paraffin-embedded sections. **(A)** Representative image of hematoxylin and eosin (H&E) staining. n = 9 mice/group. **(B)** Representative image and quantification data of Masson's trichrome staining and Sirius red staining. **(C)** Representative image and quantification data of ACTA2, COL1 and COL IV staining. Scale bar = 100 μm or 50 μm. n = 3 mice/control group and n = 9 mice/UUO group, 4 areas/section were quantified. Data are means ± SEM. ns, no significance; ***p < 0.001 for indicated comparisons. Statistical significance was determined by one-way ANOVA followed by the Bonferroni test.

to a decrease of differentiated macrophage with myofibroblast characteristics in the UUO kidney.

Decreased TGFβ1-induced M1 and M2 markers, cytokines and macrophage differentiation with *Pfkfb3* deficiency

After observing the phenotypic changes of M1 and M2 markers, cytokines, and myofibroblast maker in the UUO *Pfkfb3*$^{\Delta M\phi}$ kidney, we further examined whether *Pfkfb3* deficiency could induce similar changes in macrophages *in vitro*. We first isolated bone marrow cells from *Pfkfb3*^{WT} and *Pfkfb3*$^{\Delta M\phi}$ mice and cultured bone marrow-derived macrophages (BMDMs). Upon TGFβ1 treatment, the expression of Pfkfb3 at both mRNA and protein levels was enhanced in BMDMs from *Pfkfb3*^{WT} mice (Figures 8A, B). Subsequently, TGFβ1 incubation significantly upregulated the mRNA levels of M1 and M2 markers and associated cytokines, such as *Tnfa* and *Arg1* (Figure 8C). In contrast, *Pfkfb3* deficient BMDMs exhibited significantly lower levels of these mRNAs compared to WT BMDMs with TGFβ1 (Figure 8C). Furthermore, TGFβ1 treatment resulted in the differentiation of BMDMs, as evidenced by the expression of Acta2 at both mRNA and protein levels in the TGFβ1-treated group but not in the vehicle-treated group, and it

10.3389/fimmu.2023.1259434

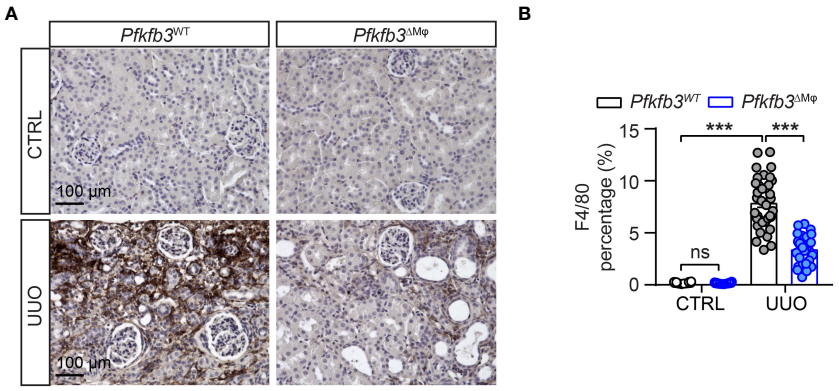

FIGURE 5
Declined number of macrophages in myeloid-specific *Pfkfb3*-deficient mice following UUO. *Pfkfb3*$^{\Delta M\varphi}$ and *Pfkfb3*^{WT} mice were subject to UUO for 14 days, kidneys were collected and fixed for paraffin-embedded sections. **(A)** Representative image of F4/80 staining. Scale bar = 100 μm. **(B)** Quantification data of F4/80 staining. n = 3 mice/control group and n = 9 mice/UUO group, 4 areas/section/kidney were quantified. The percentage of F4/80 staining was determined by calculating the ratio of the F4/80-positive area to the total area, observed under a 20X microscope objective. Data are means ± SEM. ns, no significance; ***p < 0.001 for indicated comparisons. Statistical significance was determined by one-way ANOVA followed by the Bonferroni test.

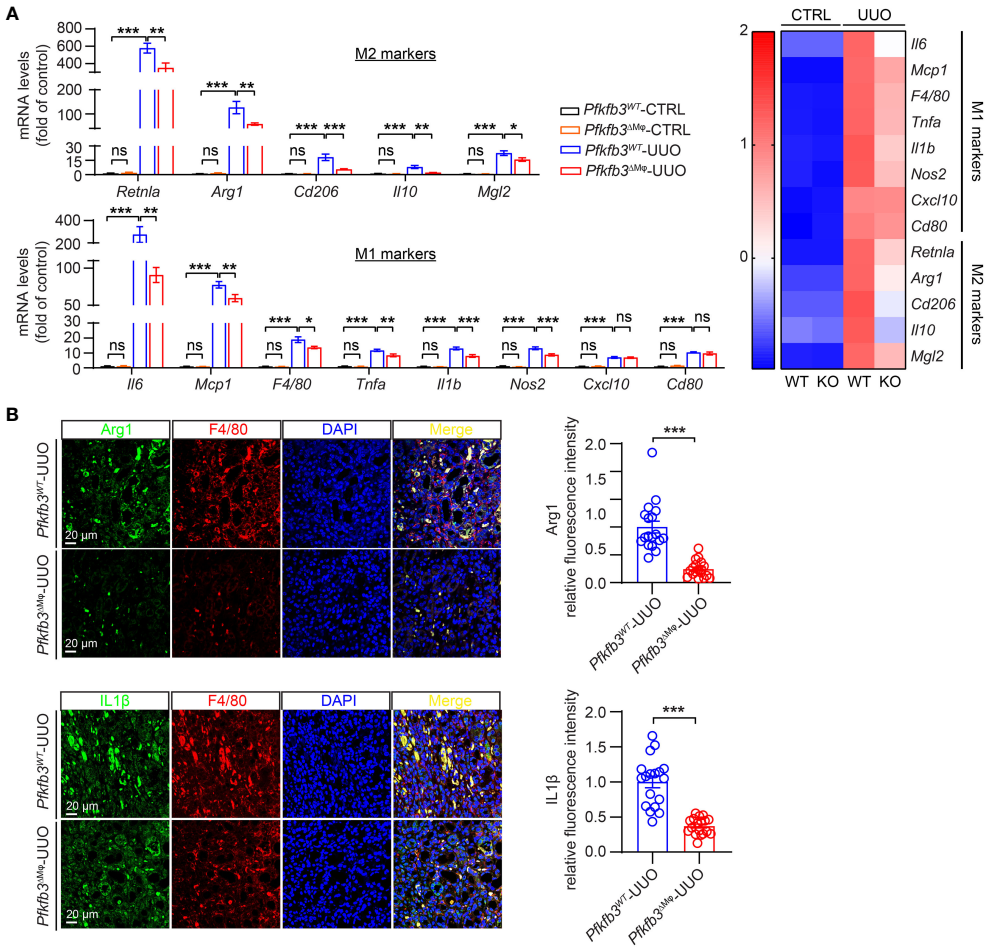

FIGURE 6
Reduced markers of M1 and M2 macrophages and related cytokines in myeloid-specific *Pfkfb3*-deficient mice following UUO. **(A)** qRT-PCR analysis of the mRNA expression of indicated genes in kidney collected from *Pfkfb3*$^{\Delta M\varphi}$ and *Pfkfb3*^{WT} mice at day 14 post UUO. n = 9 mice/group. In the heatmap, Z-scores were calculated for each gene. **(B)** Representative images and the relative intensity quantification of Arg1 and IL1β staining in kidney collected from *Pfkfb3*$^{\Delta M\varphi}$ and *Pfkfb3*^{WT} mice at day 14 post UUO surgery. Nuclei were counterstained with DAPI (blue). n = 9 mice/group. Scale bar = 100 μm. Data are means ± SEM. ns, no significance; *p < 0.05; **p < 0.01; ***p < 0.001 for indicated comparisons. Statistical significance was determined by one-way ANOVA followed by the Bonferroni test.

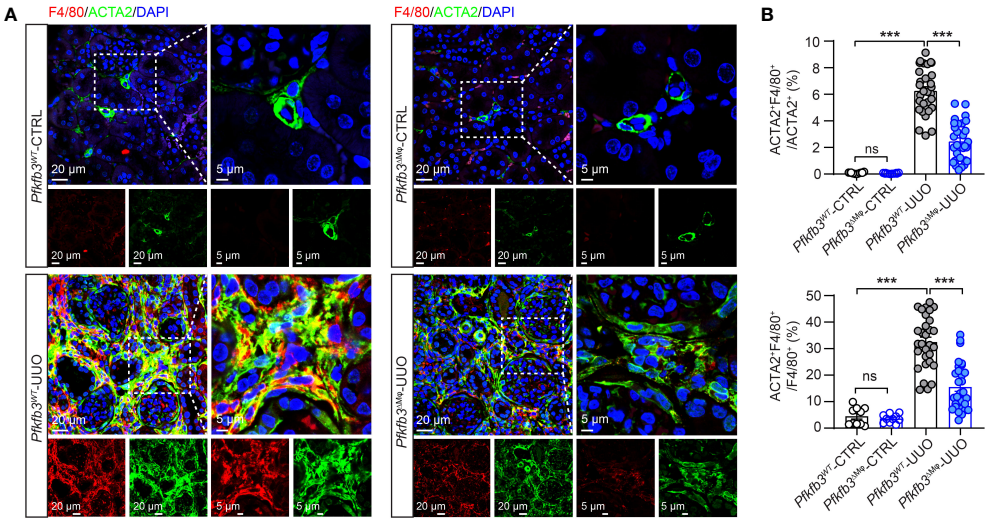

FIGURE 7
Reduced macrophage to myofibroblast cell transition (MMT) in myeloid-specific *Pfkfb3*-deficient mice following UUO. *Pfkfb3*$^{\Delta M\varphi}$ and *Pfkfb3*^{WT} mice were subject to UUO for 14 days, kidneys were collected and fixed for paraffin-embedded sections. **(A)** Representative image of ACTA2 and F4/80 staining. Nuclei were counterstained with DAPI (blue). Scale bar = 20 μm and 5 μm. **(B)** Quantification of the percentages of ACTA2 and F4/80 co-stained cells in myofibroblasts (ACTA2+) or macrophage (F4/80+). n = 3 mice/sham group and n = 9 mice/UUO group, 4 areas/section/kidney were quantified. Data are means ± SEM. ns, no significance; ***p < 0.001 for indicated comparisons. Statistical significance was determined by one-way ANOVA followed by the Bonferroni test.

was associated with *Col1a1* mRNA change (Figures 8D-G). Remarkably, TGFβ1-induced Acta2 expression was nearly abolished in *Pfkfb3* deficient BMDMs (Figures 8D-G). We subsequently analyzed the release of pro-inflammatory cytokines, TNFα and IL1β, by the BMDMs into the culture medium. As depicted in Figure 8H, TGFβ1 triggered a substantial release of these cytokines, which was markedly attenuated by the PFKFB3 knockout.

Involvement of HIF1α in PFKFB3-regulated macrophage phenotypic change

We assessed glucose metabolism in cultured WT and *Pfkfb3*-deficient BMDMs using liquid chromatography-tandem mass spectrometry (LC-MS/MS). *Pfkfb3*-deficient BMDMs displayed a modest decrease in the levels of some glycolytic metabolites compared with vehicle-treated WT BMDMs (Figure 9A). Upon TGFβ1 treatment, WT BMDMs exhibited a substantial increase in glycolytic metabolites, whereas *Pfkfb3*-deficient BMDMs failed to show similar increases (Figure 9A). Most importantly, the increase of the glycolysis end-product lactate relied on PFKFB3 induction (Figure 9A). Additionally, we observed the PFKFB3-dependent glycolysis level change after TGFβ1 by Seahorse analysis of ECAR (data not shown).

Since glycolytic metabolites are known to stabilize HIFs and modulate the phenotypic change of vascular cells (51), we investigated the protein level of HIF1α in our cultured BMDMs. The level of HIF1α was comparable between vehicle treated WT and *Pfkfb3*-deficient BMDMs (Figure 9B). However, TGFβ1 treatment significantly elevated the level of HIF1α in WT BMDMs (Figure 9B), while this upregulation was compromised in *Pfkfb3*-deficient BMDMs (Figure 9B). To determine whether this decreased HIF1α in TGFβ1-treated *Pfkfb3*-deficient BMDMs is responsible for the decreased expression of M1 and M2 markers, cytokines and Acta2, we transduced *Pfkfb3*-deficient BMDMs with an adenovirus-packaged non-degradable mutant HIF1α, aiming to restore the HIF1α level in these cells (Figure 9C). We measured mRNA levels of M1, M2 macrophage markers, Acta2, and cytokines with qPCR and observed that the decreased expression of these molecules in *Pfkfb3*-deficient BMDMs was enhanced following HIF1α overexpression (Figure 9D). Furthermore, it correlated with the cytokine release changes in the culture medium (Figure 9E). The ECAR measurement also indicated that HIF1α restoration in *Pkffb3*-deficent BMDMs partially reversed the glycolysis level (data not shown). These findings indicate that HIF1α, at least partially, participates in PFKFB3-mediated macrophage phenotypic change.

Discussion

Our study has revealed the crucial involvement of PFKFB3-mediated glycolysis in myeloid cells in the progression of renal fibrosis. The impact of myeloid glycolysis on the development of renal fibrosis encompasses multiple mechanisms, including both the modulation of monocyte recruitment and the differentiation of M1 and M2 macrophages (Figure 10).

Monocyte recruitment to the injured kidney is significantly impaired in mice lacking myeloid *Pfkfb3*. The accumulation of monocytes in the kidney is a prominent feature of both acute and chronic kidney disease. This accumulation occurs through the

10.3389/fimmu.2023.1259434

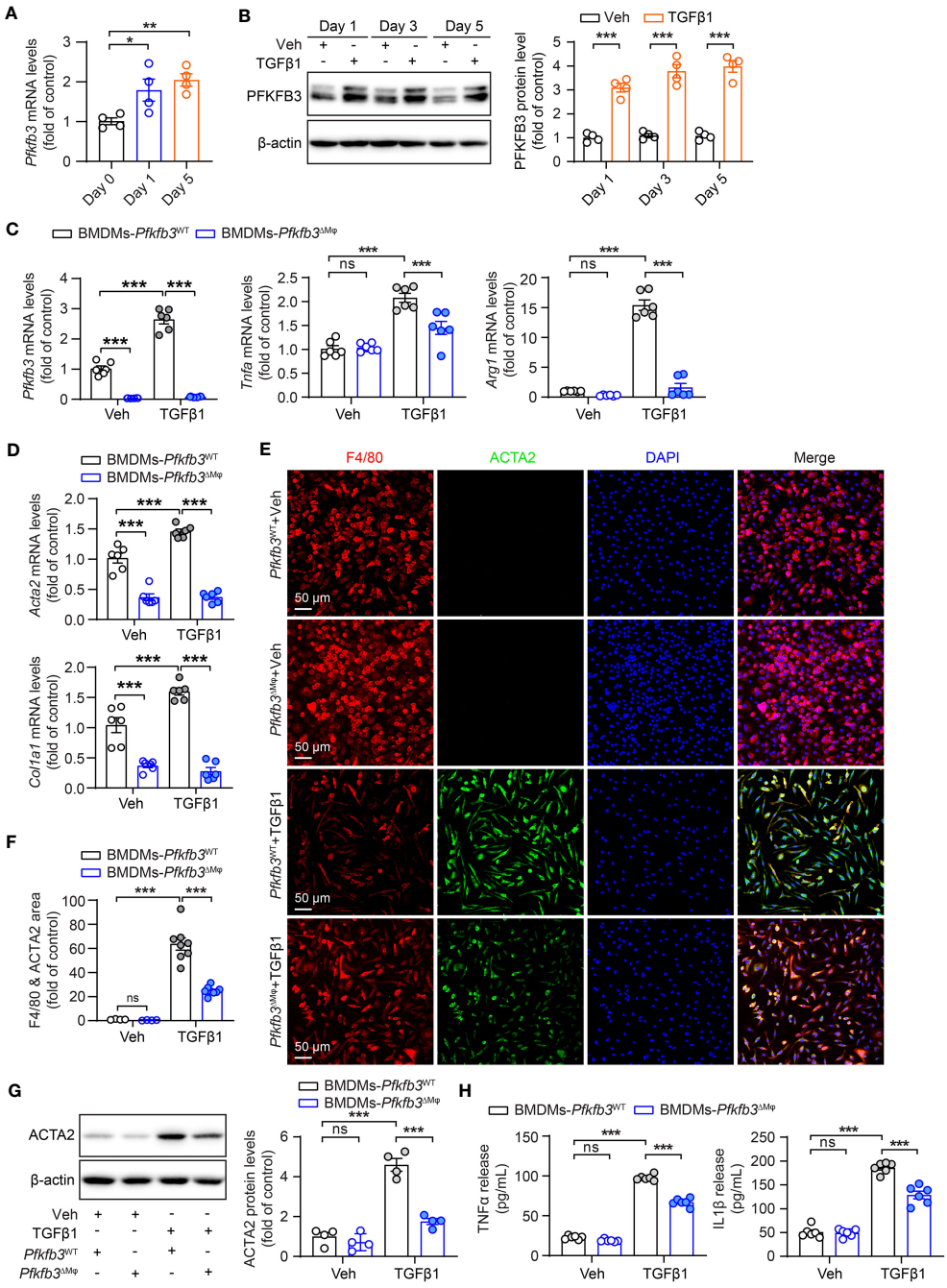

FIGURE 8
Decreased TGFβ1-induced cytokine production and MMT of *Pfkfb3* deficient macrophages. **(A)** qRT-PCR analysis of the mRNA expression of *Pfkfb3* in BMDMs cultured from *Pfkfb3*^{WT} mice and treated with TGFβ1 or vehicle for 1 day and 5 days. n = 4. **(B)** Representative Western Blots and their quantification showing PFKFB3 protein levels in BMDMs cultured from *Pfkfb3*^{WT} mice and treated with TGFβ1 or vehicle for 1 day, 3 days and 5 days. n = 4. **(C)** qRT-PCR analysis of the mRNA expression of *Pfkfb3*, *Tnfa* and *Arg1* in BMDMs cultured from *Pfkfb3*^{WT} or *Pfkfb3*$^{\Delta M\varphi}$ mice and treated with TGFβ1 for 5 days. n = 6. **(D)** qRT-PCR analysis of the mRNA expression of *Acta2* and *Col1* in BMDMs cultured from *Pfkfb3*^{WT} or *Pfkfb3*$^{\Delta M\varphi}$ mice and treated with TGFβ1 for 5 days. n = 6. **(E, F)** Representative image and quantification data of ACTA2 and F4/80 staining area percentage of BMDMs cultured from *Pfkfb3*^{WT} or *Pfkfb3*$^{\Delta M\varphi}$ mice and treated with TGFβ1 for 5 days. **(G)** Representative immunoblots and densitometry quantification of ACTA2 in BMDMs cultured from *Pfkfb3*^{WT} or *Pfkfb3*$^{\Delta M\varphi}$ mice and treated with TGFβ1 for 5 days. n = 4. **(H)** Measurement of TNFα and IL1β in BMDMs culture medium by ELISA. n = 6. Data are means ± SEM. ns, no significance; *p < 0.05; **p < 0.01; ***p < 0.001 for indicated comparisons. Statistical significance was determined by one-way ANOVA followed by the Bonferroni test **(A, C, D, F-H)** or by Student's *t* test **(B)**.

recruitment of circulating monocytes to the kidney, followed by their subsequent proliferation of these recruited monocytes (52, 53). In mice, there are two major subsets of monocytes, named Ly-6C^{hi} and Ly-6C^{lo} (54). Ly-6C^{hi} monocytes are known as inflammatory cells that are actively recruited to the injured kidney (55). The chemokine monocyte chemoattractant protein-1 (MCP-1)/CC-chemokine ligand 2 and its receptor C-C chemokine receptor 2 (CCR2) plays a critical role in monocyte recruitment. Blocking this

10.3389/fimmu.2023.1259434

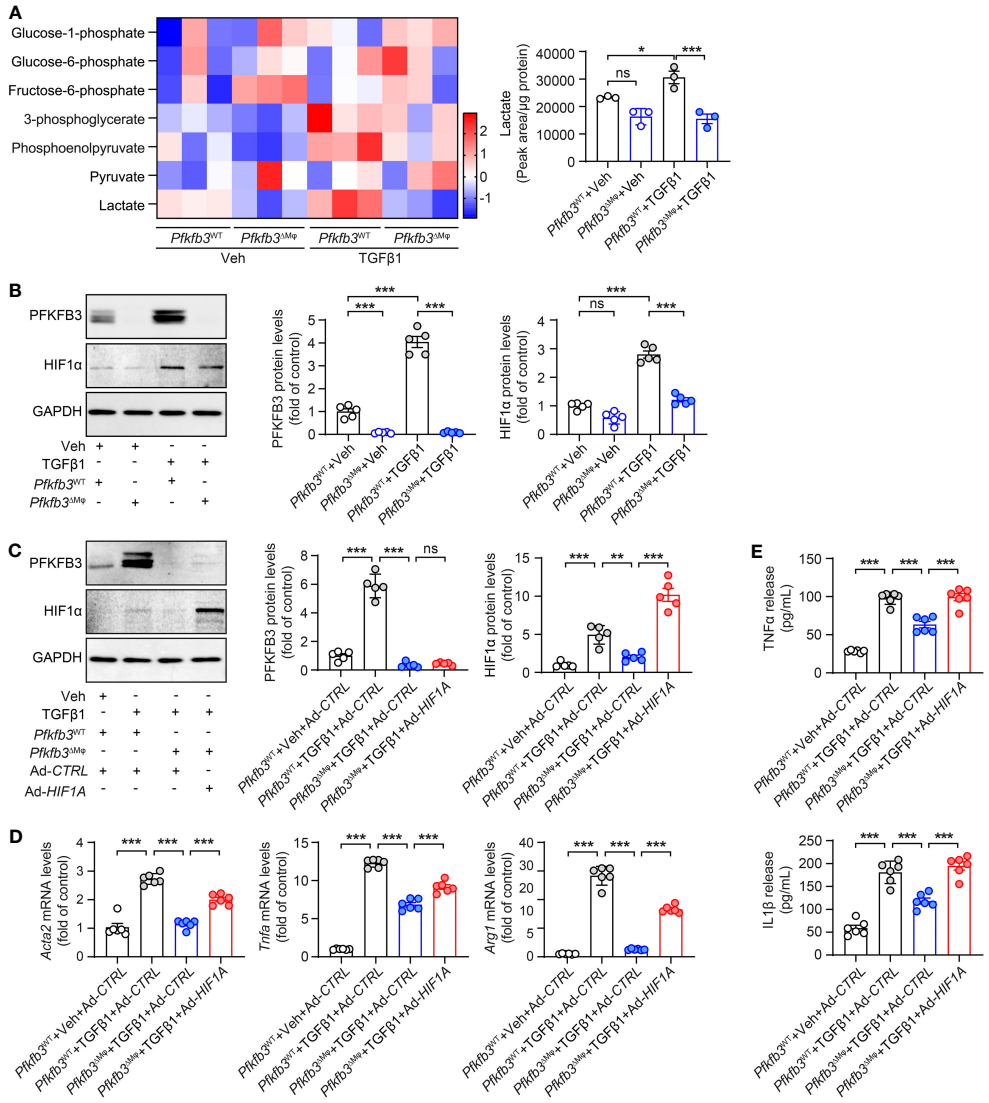

FIGURE 9
Pfkfb3 regulated the expression of pro-inflammatory cytokines through Hif1a. **(A)** Heat map showing the metabolites in the glycolysis pathway and quantification data of lactate level in BMDMs cultured from *Pfkfb3*^{WT} or *Pfkfb3*$^{\Delta M\varphi}$ mice and treated with TGFβ1 for 24 h. n = 3. **(B)** Representative Western Blots and their quantification showing PFKFB3 and HIF1α protein levels in BMDMs cultured from *Pfkfb3*^{WT} or *Pfkfb3*$^{\Delta M\varphi}$ mice and treated with TGFβ1 for 5 days. n = 5. **(C)** Representative Western Blots and their quantification showing PFKFB3 and HIF1α protein levels in BMDMs cultured from *Pfkfb3*^{WT} or *Pfkfb3*$^{\Delta M\varphi}$ mice transfected with Ad-*CTRL* or Ad- *HIF1α* adenovirus and treated with TGFβ1 for 5 days. n = 5. **(D)** qRT-PCR analysis of the mRNA expression of *Acta2, Tnfa* and *Arg1* in BMDMs cultured from *Pfkfb3*^{WT} or *Pfkfb3*$^{\Delta M\varphi}$ mice transfected with Ad-*CTRL* or Ad- *HIF1α* adenovirus and treated with TGFβ1 for 5 days. n = 6. **(E)** Measurement of TNFα and IL1β in culture medium by ELISA. n = 6. Data are means ± SEM. ns, no significance; *p < 0.05; **p < 0.01; ***p < 0.001 for indicated comparisons. Statistical significance was determined by one-way ANOVA followed by the Bonferroni test.

pathway, either through the deletion of Mcp-1 or using a CCR2 antagonist, suppresses renal injury and the associated renal fibrosis (25, 56, 57). Once infiltrated into the kidney, monocytes differentiate to M1 macrophages and proliferate locally via MCSF/cfms pathway. Inhibiting macrophage proliferation using antibodies against MCSF and c-fms also hinders renal injury and kidney fibrosis (58–62). PFKFB3 is predominantly expressed in Ly-6C^{hi} myeloid cells and provides energy for cell motility (38). Loss of *Pfkfb3* impaired myeloid cell infiltration into the vessel wall and lung (37, 38). Using a similar mechanism, myeloid cells may also have a compromised ability to recruit to the injury kidney. Furthermore, PFKFB3-mediated glycolysis supplies metabolic intermediates for biomass generation, which is essential for myeloid proliferation (38). In the absence of *Pfkfb3*, local infiltrated macrophages may experience impaired proliferation. This may explain why the number of macrophages in the UUO kidney was dramatically reduced (Figure 5).

Deficiency of *Pfkfb3* suppresses both M1 and M2 macrophages in the UUO kidney. Both M1 and M2 macrophages play significant roles in the development of renal fibrosis (12). M1 macrophages are typically present in early stage of kidney injury (27, 63, 64), and their detrimental impact on kidney injury and fibrosis have been demonstrated in studies where accelerated renal injury occurred upon infusion of M1 macrophages in mice (65), whereas reduced

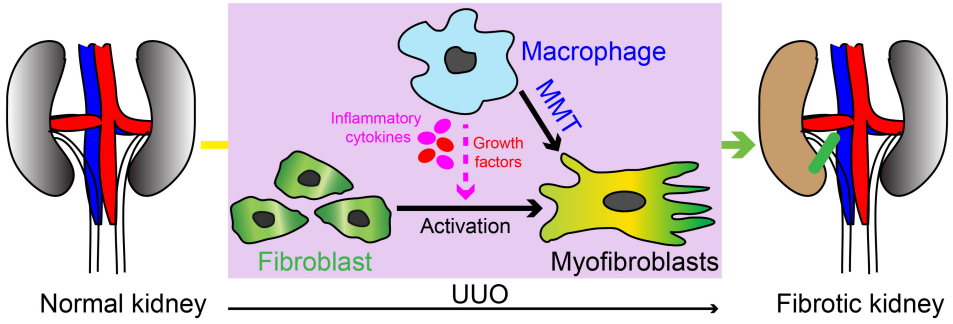

FIGURE 10
Schematic illustration of the myeloid cell contribution in UUO induced kidney fibrosis. Our study has revealed the crucial involvement of PFKFB3-mediated glycolysis in myeloid cells in the progression of renal fibrosis. The impact of myeloid glycolysis on the development of renal fibrosis encompasses multiple mechanisms, including the modulation of monocyte recruitment, differentiation of M1 and M1 macrophages, and macrophage with myofibroblast phenotype differentiation (also called MMT).

renal injury was observed in mice with depletion of M1 macrophages (66, 67). M1 macrophages exacerbate renal inflammation through the release of proinflammatory cytokines (12, 68) and contribute to renal injury through the release of matrix metalloproteinases (MMPs) (69, 70). In addition to M1 macrophages, M2 macrophages also plays a crucial role in renal fibrosis (12). M2 macrophages expressing CD206 and/or CD163 have been closely associated with kidney fibrosis in human kidney diseases (71, 72) as well as animal kidney diseases (73–76). Depletion of M2 macrophages in experimental setups has been shown to protect rodents from fibrosis, while adoptive transfusion of M2 macrophages to rodents with renal injury has accelerated kidney fibrosis (29, 77), thus demonstrating the causal role of M2 macrophages in the development of kidney fibrosis. In our study, both *in vivo* renal samples and *in vitro* experiments using cultured BMDMs consistently showed decreased levels of both M1 and M2 macrophages, indicating a dual role of PFKFB3-mediated glycolysis in regulating M1 and M2 macrophage phenotypes. The role of PFKFB3-mediated glycolysis in myeloid cells in renal fibrosis aligns with its role in myeloid cells in pathological angiogenesis (36). In hypoxic angiogenesis, *Pfkfb3* deficiency in myeloid cells reduces both M1 and M2 markers, as well as related cytokines/growth factors (36).

The induction of macrophage phenotype differentiation in the kidneys of mice with UUO is significantly hindered in mice lacking myeloid *Pfkfb3*. A notable portion of fibroblasts in fibrotic kidneys in both humans and animals exhibit markers associated with bone marrow cells and/or CD68 (4, 22, 78). This population of cells may arise from a further differentiation of M2, as evidenced by the expression of M2 markers including CD206 (22). Over the past few years, several studies conducted by different research groups have reported the presence of MMT and its critical role in kidney fibrosis (14, 22, 23, 79, 80). However, recent single-cell sequencing data does not provide substantial evidence supporting a significant contribution of myofibroblasts originating from macrophages (10). And the myofibroblast population is characterized by their production of extracellular matrix (10). It is important to note that this macrophage phenotypic change is also accompanied by a notable alteration in cytokine production (Figure 8), suggesting an important regulatory function of these cells in renal fibrosis, despite their direct involvement in extracellular matrix production.

Notably, macrophage is not the only source of myofibroblasts in UUO kidneys. Other cells such as resident renal fibroblast and pericytes also contribute to the myofibroblasts activation (7, 9). Concurrently, decreased macrophage infiltration leads to less pro-inflammatory cytokines release which can regulate all renal myofibroblast activation. Overall, macrophages influence renal fibrosis through both their differentiation into myofibroblasts and their role in inflammatory regulation (19). In our study, we observed the decrease of macrophage-originated myofibroblasts and reduced pro-inflammatory cytokines release in PFKFB3 deficient kidney after UUO injury. However, we do not have conclusive evidence indicating which of these mechanisms is predominant.

Our study also implicates that PFKFB3 may act as a bridge to mediate the crosstalk of TGF-β1 and HIF-1α signaling pathways in renal fibrosis (Figures 8, 9). The regulatory role of PFKFB3-mediated glycolysis in fibrotic activity of TGFβ has been demonstrated in pulmonary fibroblast (81). In line with previous study with fibroblasts (81), the TGFβ-induced expression of αSMA and extracellular matrix, such as collagen, is significantly suppressed in myeloid cells both in mouse kidney and *in vitro* cultured BMDMs in the absence of *Pfkfb3*(Figure 8). This suggests a similarity in the regulatory role of PFKFB3 in TGFβ-mediated pathways in different cell types. In myeloid cells, several pathways have been identified as being regulated by glycolytic metabolites (33). For instance, the deficiency of *Pfkfb3* in macrophages resulted in decreased levels of Acetyl-CoA, leading to reduced histone acetylation and subsequently suppressing the transcription of growth factors and proinflammatory cytokines (36). Additionally, a decline in the protein level of phosphor-NF-kB p65 was observed in *Pfkfb3*-deficient BMDMs (35). Glycolytic metabolites have also been shown to stabilize HIFs in vascular cells and macrophages (82, 83). Our study indicates that HIF1α plays a significant role in the effect of PFKFB3-medaited glycolysis on phenotypic alterations observed in macrophages in renal fibrosis. Under fibrotic conditions, PFKFB3-mediated glycolysis can likewise stabilize HIF1α. The mediatory role of HIF1α in PFKFB3-regulated

myeloid phenotypic change was demonstrated through the gain-of-function of HIF1α in *Pfkfb3*-deficient BMDMs (Figure 9).

Collectively, this study highlights the critical role of PFKFB3-medicated glycolysis in myeloid cells for the progression of kidney fibrosis (Figure 10). The activity of PFKFB3 can be effectively suppressed through knockdown using siRNA or inhibition using small molecules (84). Recent advancements have described the development of tool specifically designed to target macrophages (85). Consequently, the inhibition of myeloid PFKFB3-mediated glycolysis holds great promise as a potential therapeutic strategy for treating kidney fibrosis.

Data availability statement

The original contributions presented in the study are included in the article/Supplementary Material. Further inquiries can be directed to the corresponding authors.

Ethics statement

The animal study was approved by Institutional Animal Care and Use Committee at Augusta University. The study was conducted in accordance with the local legislation and institutional requirements.

Author contributions

QY: Conceptualization, Data curation, Formal Analysis, Funding acquisition, Investigation, Methodology, Project administration, Supervision, Validation, Writing – original draft, Writing – review & editing. EH: Conceptualization, Data curation, Formal Analysis, Investigation, Methodology, Writing – review & editing. YC: Data curation, Formal Analysis, Investigation, Methodology, Writing – review & editing. ZZ: Data curation, Formal Analysis, Investigation, Methodology, Writing – review & editing. CD: Data curation, Formal Analysis, Investigation, Methodology, Writing – review & editing. JA: Investigation, Methodology, Supervision, Writing – review & editing. HS: Data curation, Investigation, Methodology, Supervision, Writing – review & editing. QW: Conceptualization, Data curation, Formal Analysis, Funding acquisition, Investigation, Methodology, Project administration, Supervision, Validation, Writing – original draft, Writing – review & editing.

Funding

The author(s) declare financial support was received for the research, authorship, and/or publication of this article. QY was supported by AHA Postdoc Fellowship Award (834582) and National Eye Institute K99 award (1K99EY034577-01A1). QW was supported by a grant from NIH/NIDDK (1 RO1 DK126763-01).

Conflict of interest

The authors declare that the research was conducted in the absence of any commercial or financial relationships that could be construed as a potential conflict of interest.

Publisher's note

Supplementary material

The Supplementary Material for this article can be found online at: https://www.frontiersin.org/articles/10.3389/fimmu.2023.1259434/full#supplementary-material

References

1. Rockey DC, Bell PD, Hill JA. Fibrosis–a common pathway to organ injury and failure. *New Engl J Med* (2015) 372(12):1138–49. doi: 10.1056/NEJMra1300575

2. LeBleu VS, Taduri G, O'Connell J, Teng Y, Cooke VG, Woda C, et al. Origin and function of myofibroblasts in kidney fibrosis. *Nat Med* (2013) 19(8):1047–53. doi: 10.1038/nm.3218

3. Miyauchi K, Nakai T, Saito S, Yamamoto T, Sato K, Kato K, et al. Renal interstitial fibroblasts coproduce erythropoietin and renin under anaemic conditions. *EBioMedicine.* (2021) 64:103209. doi: 10.1016/j.ebiom.2021.103209

4. Broekema M, Harmsen MC, van Luyn MJ, Koerts JA, Petersen AH, van Kooten TG, et al. Bone marrow-derived myofibroblasts contribute to the renal interstitial myofibroblast population and produce procollagen I after ischemia/reperfusion in rats. *J Am Soc Nephrol.* (2007) 18(1):165–75. doi: 10.1681/ASN.2005070730

5. Li J, Deane JA, Campanale NV, Bertram JF, Ricardo SD. The contribution of bone marrow-derived cells to the development of renal interstitial fibrosis. *Stem Cells* (2007) 25(3):697–706. doi: 10.1634/stemcells.2006-0133

6. Jang HS, Kim JI, Han SJ, Park KM. Recruitment and subsequent proliferation of bone marrow-derived cells in the postischemic kidney are important to the progression of fibrosis. *Am J Physiol Renal Physiol* (2014) 306(12):F1451–61. doi: 10.1152/ajprenal.00017.2014

7. Mack M, Yanagita M. Origin of myofibroblasts and cellular events triggering fibrosis. *Kidney Int* (2015) 87(2):297–307. doi: 10.1038/ki.2014.287

8. Zeisberg EM, Tarnavski O, Zeisberg M, Dorfman AL, McMullen JR, Gustafsson E, et al. Endothelial-to-mesenchymal transition contributes to cardiac fibrosis. *Nat Med* (2007) 13(8):952–61. doi: 10.1038/nm1613

9. Humphreys BD, Lin SL, Kobayashi A, Hudson TE, Nowlin BT, Bonventre JV, et al. Fate tracing reveals the pericyte and not epithelial origin of myofibroblasts in kidney fibrosis. *Am J Pathol* (2010) 176(1):85–97. doi: 10.2353/ajpath.2010.090517

10. Kuppe C, Ibrahim MM, Kranz J, Zhang X, Ziegler S, Perales-Paton J, et al. Decoding myofibroblast origins in human kidney fibrosis. *Nature.* (2021) 589 (7841):281–6. doi: 10.1038/s41586-020-2941-1

11. Wei J, Xu Z, Yan X. The role of the macrophage-to-myofibroblast transition in renal fibrosis. *Front Immunol* (2022) 13:934377. doi: 10.3389/fimmu.2022.934377

12. Tang PM, Nikolic-Paterson DJ, Lan HY. Macrophages: versatile players in renal inflammation and fibrosis. *Nat Rev Nephrol.* (2019) 15(3):144–58. doi: 10.1038/s41581-019-0110-2

13. He Y, Deng B, Liu S, Luo S, Ning Y, Pan X, et al. Myeloid piezo1 deletion protects renal fibrosis by restraining macrophage infiltration and activation. *Hypertension.* (2022) 79(5):918–31. doi: 10.1161/HYPERTENSIONAHA.121.18750

14. Wang YY, Jiang H, Pan J, Huang XR, Wang YC, Huang HF, et al. Macrophage-to-myofibroblast transition contributes to interstitial fibrosis in chronic renal allograft injury. *J Am Soc Nephrol.* (2017) 28(7):2053–67. doi: 10.1681/ASN.2016050573

15. Bhatia D, Chung KP, Nakahira K, Patino E, Rice MC, Torres LK, et al. Mitophagy-dependent macrophage reprogramming protects against kidney fibrosis. *JCI Insight* (2019) 4(23). doi: 10.1172/jci.insight.132826

16. Wen Y, Lu X, Ren J, Privratsky JR, Yang B, Rudemiller NP, et al. KLF4 in macrophages attenuates TNFalpha-mediated kidney injury and fibrosis. *J Am Soc Nephrol.* (2019) 30(10):1925–38. doi: 10.1681/ASN.2019020111

17. Sasaki K, Terker AS, Pan Y, Li Z, Cao S, Wang Y, et al. Deletion of Myeloid Interferon Regulatory Factor 4 (Irf4) in Mouse Model Protects against Kidney Fibrosis after Ischemic Injury by Decreased Macrophage Recruitment and Activation. *J Am Soc Nephrol.* (2021) 32(5):1037–52. doi: 10.1681/ASN.2020071010

18. Xu S, Yang X, Chen Q, Liu Z, Chen Y, Yao X, et al. Leukemia inhibitory factor is a therapeutic target for renal interstitial fibrosis. *EBioMedicine.* (2022) 86:104312. doi: 10.1016/j.ebiom.2022.104312

19. Cao Q, Harris DC, Wang Y. Macrophages in kidney injury, inflammation, and fibrosis. *Physiol (Bethesda).* (2015) 30(3):183–94. doi: 10.1152/physiol.00046.2014

20. Gordon S, Plüddemann A. Tissue macrophages: heterogeneity and functions. *BMC Biol* (2017) 15(1):53. doi: 10.1186/s12915-017-0392-4

21. Nikolic-Paterson DJ, Wang S, Lan HY. Macrophages promote renal fibrosis through direct and indirect mechanisms. *Kidney Int Suppl (2011).* (2014) 4(1):34–8. doi: 10.1038/kisup.2014.7

22. Meng XM, Wang S, Huang XR, Yang C, Xiao J, Zhang Y, et al. Inflammatory macrophages can transdifferentiate into myofibroblasts during renal fibrosis. *Cell Death Dis* (2016) 7(12):e2495. doi: 10.1038/cddis.2016.402

23. Tang PM, Zhang YY, Xiao J, Tang PC, Chung JY, Li J, et al. Neural transcription factor Pou4f1 promotes renal fibrosis via macrophage-myofibroblast transition. *Proc Natl Acad Sci U S A.* (2020) 117(34):20741–52. doi: 10.1073/pnas.1917663117

24. Wada T, Furuichi K, Sakai N, Iwata Y, Kitagawa K, Ishida Y, et al. Gene therapy via blockade of monocyte chemoattractant protein-1 for renal fibrosis. *J Am Soc Nephrol.* (2004) 15(4):940–8. doi: 10.1097/01.ASN.0000120371.09769.80

25. Chow FY, Nikolic-Paterson DJ, Ozols E, Atkins RC, Rollin BJ, Tesch GH. Monocyte chemoattractant protein-1 promotes the development of diabetic renal injury in streptozotocin-treated mice. *Kidney Int* (2006) 69(1):73–80. doi: 10.1038/sj.ki.5000014

26. Schneider A, Panzer U, Zahner G, Wenzel U, Wolf G, Thaiss F, et al. Monocyte chemoattractant protein-1 mediates collagen deposition in experimental glomerulonephritis by transforming growth factor-beta. *Kidney Int* (1999) 56 (1):135–44. doi: 10.1046/j.1523-1755.1999.00543.x

27. Huen SC, Cantley LG. Macrophage-mediated injury and repair after ischemic kidney injury. *Pediatr Nephrol.* (2015) 30(2):199–209. doi: 10.1007/s00467-013-2726-y

28. Ko GJ, Boo CS, Jo SK, Cho WY, Kim HK. Macrophages contribute to the development of renal fibrosis following ischaemia/reperfusion-induced acute kidney injury. *Nephrol Dial Transplant.* (2008) 23(3):842–52. doi: 10.1093/ndt/gfm694.

29. Kim MG, Kim SC, Ko YS, Lee HY, Jo SK, Cho W. The role of M2 macrophages in the progression of chronic kidney disease following acute kidney injury. *PloS One* (2015) 10(12):e0143961. doi: 10.1371/journal.pone.0143961

30. Xu JQ, Fu YL, Zhang J, Zhang KY, Ma J, Tang JY, et al. Targeting glycolysis in non-small cell lung cancer: Promises and challenges. *Front Pharmacol* (2022) 13:1037341. doi: 10.3389/fphar.2022.1037341

31. Zhou D, Duan Z, Li Z, Ge F, Wei R, Kong L. The significance of glycolysis in tumor progression and its relationship with the tumor microenvironment. *Front Pharmacol* (2022) 13:1091779. doi: 10.3389/fphar.2022.1091779

32. Zhang M, Qin Q, Zhang S, Liu W, Meng H, Xu M, et al. Aerobic glycolysis imaging of epileptic foci during the inter-ictal period. *EBioMedicine.* (2022) 79:104004. doi: 10.1016/j.ebiom.2022.104004

33. Langston PK, Shibata M, Horng T. Metabolism supports macrophage activation. *Front Immunol* (2017) 8:61. doi: 10.3389/fimmu.2017.00061

34. Van Schaftingen E, Lederer B, Bartrons R, Hers HG. A kinetic study of pyrophosphate: fructose-6-phosphate phosphotransferase from potato tubers. Application to a microassay of fructose 2,6-bisphosphate. *Eur J Biochem* (1982) 129 (1):191–5 doi: 10.1111/j.1432-1033.1982.tb07039.x.

35. Liu Z, Mao X, Yang Q, Zhang X, Xu J, Ma Q, et al. Suppression of myeloid PFKFB3-driven glycolysis protects mice from choroidal neovascularization. *Br J Pharmacol* (2022) 179(22):5109–31. doi: 10.1111/bph.15925

36. Liu Z, Xu J, Ma Q, Zhang X, Yang Q, Wang L, et al. Glycolysis links reciprocal activation of myeloid cells and endothelial cells in the retinal angiogenic niche. *Sci Transl Med* (2020) 12(555). doi: 10.1126/scitranslmed.aay1371

37. Wang L, Zhang X, Cao Y, Ma Q, Mao X, Xu J, et al. Mice with a specific deficiency of Pfkfb3 in myeloid cells are protected from hypoxia-induced pulmonary hypertension. *Br J Pharmacol* (2021) 178(5):1055–72. doi: 10.1111/bph.15339

38. Guo S, Li A, Fu X, Li Z, Cao K, Song M, et al. Gene-dosage effect of Pfkfb3 on monocyte/macrophage biology in atherosclerosis. *Br J Pharmacol* (2022) 179(21):4974–91. doi: 10.1111/bph.15926

39. Zhu X, Jiang L, Long M, Wei X, Hou Y, Du Y. Metabolic reprogramming and renal fibrosis. *Front Med (Lausanne).* (2021) 8:746920. doi: 10.3389/fmed.2021.746920

40. Wen L, Li Y, Li S, Hu X, Wei Q, Dong Z. Glucose metabolism in acute kidney injury and kidney repair. *Front Med (Lausanne).* (2021) 8:744122. doi: 10.3389/fmed.2021.744122

41. Wei Q, Su J, Dong G, Zhang M, Huo Y, Dong Z. Glycolysis inhibitors suppress renal interstitial fibrosis via divergent effects on fibroblasts and tubular cells. *Am J Physiol Renal Physiol* (2019) 316(6):F1162–F72. doi: 10.1152/ajprenal.00422.2018

42. Ding H, Jiang L, Xu J, Bai F, Zhou Y, Yuan Q, et al. Inhibiting aerobic glycolysis suppresses renal interstitial fibroblast activation and renal fibrosis. *Am J Physiol Renal Physiol* (2017) 313(3):F561–F75. doi: 10.1152/ajprenal.00036.2017

43. Yang Q, Huo E, Cai Y, Zhang Z, Dong C, Asara JM, et al. PFKFB3-mediated glycolysis boosts fibroblast activation and subsequent kidney fibrosis. *Cells.* (2023) 12 (16). doi: 10.3390/cells12162081

44. Xu Y, An X, Guo X, Habtetsion TG, Wang Y, Xu X, et al. Endothelial PFKFB3 plays a critical role in angiogenesis. *Arteriosclerosis thrombosis Vasc Biol* (2014) 34 (6):1231–9. doi: 10.1161/ATVBAHA.113.303041

45. Yang Q, Ma Q, Xu J, Liu Z, Zou J, Shen J, et al. Prkaa1 metabolically regulates monocyte/macrophage recruitment and viability in diet-induced murine metabolic disorders. *Front Cell Dev Biol* (2020) 8:611354. doi: 10.3389/fcell.2020.611354

46. Yang Q, Ma Q, Xu J, Liu Z, Mao X, Zhou Y, et al. Endothelial AMPKα1/PRKAA1 exacerbates inflammation in HFD-fed mice. *Br J Pharmacol* (2022) 179 (8):1661–78. doi: 10.1111/bph.15742

47. Yang Q, Xu J, Ma Q, Liu Z, Zhou Y, Cai Y, et al. Disruption of endothelial Pfkfb3 ameliorates diet-induced murine insulin resistance. *J Endocrinol* (2021) 250(3):93–104. doi: 10.1530/JOE-20-0524

48. Yang Q, Xu J, Ma Q, Liu Z, Sudhahar V, Cao Y, et al. PRKAA1/AMPKα1-driven glycolysis in endothelial cells exposed to disturbed flow protects against atherosclerosis. *Nat Commun* (2018) 9(1):4667 doi: 10.1038/s41467-018-07132-x.

49. Ma Q, Yang Q, Xu J, Zhang X, Kim D, Liu Z, et al. ATIC-associated *de novo* purine synthesis is critically involved in proliferative arterial disease. *Circulation.* (2022) 146(19):1444–60. doi: 10.1161/CIRCULATIONAHA.121.058901

50. Conway BR, O'Sullivan ED, Cairns C, O'Sullivan J, Simpson DJ, Salzano A, et al. Kidney single-cell atlas reveals myeloid heterogeneity in progression and regression of kidney disease. *J Am Soc Nephrol.* (2020) 31(12):2833–54. doi: 10.1681/ASN.2020060806

51. Cao Y, Zhang X, Wang L, Yang Q, Ma Q, Xu J, et al. PFKFB3-mediated endothelial glycolysis promotes pulmonary hypertension. *Proc Nat Acad Sci* (2019) 116 (27):13394–403. doi: 10.1073/pnas.1821401116

52. Yang N, Isbel NM, Nikolic-Paterson DJ, Li Y, Ye R, Atkins RC, et al. Local macrophage proliferation in human glomerulonephritis. *Kidney Int* (1998) 54(1):143–51. doi: 10.1046/j.1523-1755.1998.00978.x

53. Isbel NM, Nikolic-Paterson DJ, Hill PA, Dowling J, Atkins RC. Local macrophage proliferation correlates with increased renal M-CSF expression in human glomerulonephritis. *Nephrol Dial Transplant.* (2001) 16(8):1638–47. doi: 10.1093/ndt/16.8.1638

54. Geissmann F, Jung S, Littman DR. Blood monocytes consist of two principal subsets with distinct migratory properties. *Immunity.* (2003) 19(1):71–82. doi: 10.1016/S1074-7613(03)00174-2

55. Lin SL, Castaño AP, Nowlin BT, Lupher ML Jr., Duffield JS. Bone marrow Ly6Chigh monocytes are selectively recruited to injured kidney and differentiate into functionally distinct populations. *J Immunol (Baltimore Md 1950).* (2009) 183 (10):6733–43. doi: 10.4049/jimmunol.0901473

56. Tesch GH. MCP-1/CCL2: a new diagnostic marker and therapeutic target for progressive renal injury in diabetic nephropathy. *Am J Physiol Renal Physiol* (2008) 294 (4):F697–701. doi: 10.1152/ajprenal.00016.2008

57. Kang YS, Lee MH, Song HK, Ko GJ, Kwon OS, Lim TK, et al. CCR2 antagonism improves insulin resistance, lipid metabolism, and diabetic nephropathy in type 2 diabetic mice. *Kidney Int* (2010) 78(9):883–94. doi: 10.1038/ki.2010.263

58. Lan HY, Nikolic-Paterson DJ, Mu W, Atkins RC. Local macrophage proliferation in the progression of glomerular and tubulointerstitial injury in rat anti-GBM glomerulonephritis. *Kidney Int* (1995) 48(3):753–60. doi: 10.1038/ki.1995.347

59. Isbel NM, Hill PA, Foti R, Mu W, Hurst LA, Stambe C, et al. Tubules are the major site of M-CSF production in experimental kidney disease: correlation with local macrophage proliferation. *Kidney Int* (2001) 60(2):614–25. doi: 10.1046/j.1523-1755.2001.060002614.x

60. Le Meur Y, Tesch GH, Hill PA, Mu W, Foti R, Nikolic-Paterson DJ, et al. Macrophage accumulation at a site of renal inflammation is dependent on the M-CSF/c-fms pathway. *J Leukoc Biol* (2002) 72(3):530–7. doi: 10.1189/jlb.72.3.530

61. Jose MD, Le Meur Y, Atkins RC, Chadban SJ. Blockade of macrophage colony-stimulating factor reduces macrophage proliferation and accumulation in renal

allograft rejection. *Am J Transplant.* (2003) 3(3):294–300. doi: 10.1034/j.1600-6143.2003.00068.x

62. Lim AK, Ma FY, Nikolic-Paterson DJ, Thomas MC, Hurst LA, Tesch GH. Antibody blockade of c-fms suppresses the progression of inflammation and injury in early diabetic nephropathy in obese db/db mice. *Diabetologia.* (2009) 52(8):1669–79. doi: 10.1007/s00125-009-1399-3

63. Kashem A, Endoh M, Yano N, Yamauchi F, Nomoto Y, Sakai H. Expression of inducible-NOS in human glomerulonephritis: the possible source is infiltrating monocytes/macrophages. *Kidney Int* (1996) 50(2):392–9. doi: 10.1038/ki.1996.328

64. Noronha IL, Krüger C, Andrassy K, Ritz E, Waldherr R. *In situ* production of TNF-alpha, IL-1 beta and IL-2R in ANCA-positive glomerulonephritis. *Kidney Int* (1993) 43(3):682–92. doi: 10.1038/ki.1993.98

65. Ikezumi Y, Atkins RC, Nikolic-Paterson DJ. Interferon-gamma augments acute macrophage-mediated renal injury via a glucocorticoid-sensitive mechanism. *J Am Soc Nephrol.* (2003) 14(4):888–98. doi: 10.1097/01.ASN.0000056604.13964.62

66. Duffield JS, Tipping PG, Kipari T, Cailhier JF, Clay S, Lang R, et al. Conditional ablation of macrophages halts progression of crescentic glomerulonephritis. *Am J pathology.* (2005) 167(5):1207–19. doi: 10.1016/S0002-9440(10)61209-6

67. Ferenbach DA, Sheldrake TA, Dhaliwal K, Kipari TM, Marson LP, Kluth DC, et al. Macrophage/monocyte depletion by clodronate, but not diphtheria toxin, improves renal ischemia/reperfusion injury in mice. *Kidney Int* (2012) 82(8):928–33. doi: 10.1038/ki.2012.207

68. Inoue T. M1 macrophage triggered by Mincle leads to a deterioration of acute kidney injury. *Kidney Int* (2017) 91(3):526–9. doi: 10.1016/j.kint.2016.11.026

69. Kunugi S, Shimizu A, Kuwahara N, Du X, Takahashi M, Terasaki Y, et al. Inhibition of matrix metalloproteinases reduces ischemia-reperfusion acute kidney injury. *Lab Invest.* (2011) 91(2):170–80. doi: 10.1038/labinvest.2010.174

70. Huang WC, Sala-Newby GB, Susana A, Johnson JL, Newby AC. Classical macrophage activation up-regulates several matrix metalloproteinases through mitogen activated protein kinases and nuclear factor-κB. *PloS One* (2012) 7(8): e42507. doi: 10.1371/journal.pone.0042507

71. Klessens CQF, Zandbergen M, Wolterbeek R, Bruijn JA, Rabelink TJ, Bajema IM, et al. Macrophages in diabetic nephropathy in patients with type 2 diabetes. *Nephrol Dial Transplant.* (2017) 32(8):1322–9. doi: 10.1093/ndt/gfw260

72. Ikezumi Y, Suzuki T, Karasawa T, Hasegawa H, Yamada T, Imai N, et al. Identification of alternatively activated macrophages in new-onset paediatric and adult immunoglobulin A nephropathy: potential role in mesangial matrix expansion. *Histopathology.* (2011) 58(2):198–210. doi: 10.1111/j.1365-2559.2011.03742.x

73. Han Y, Ma FY, Tesch GH, Manthey CL, Nikolic-Paterson DJ. Role of macrophages in the fibrotic phase of rat crescentic glomerulonephritis. *Am J Physiol Renal Physiol* (2013) 304(8):F1043–53. doi: 10.1152/ajprenal.00389.2012

74. Braga TT, Correa-Costa M, Guise YF, Castoldi A, de Oliveira CD, Hyane MI, et al. MyD88 signaling pathway is involved in renal fibrosis by favoring a TH2 immune response and activating alternative M2 macrophages. *Mol Med* (2012) 18(1):1231–9. doi: 10.2119/molmed.2012.00131

75. Kushiyama T, Oda T, Yamada M, Higashi K, Yamamoto K, Sakurai Y, et al. Alteration in the phenotype of macrophages in the repair of renal interstitial fibrosis in mice. *Nephrol (Carlton).* (2011) 16(5):522–35. doi: 10.1111/j.1440-1797.2010.01439.x

76. Yamate J, Sato K, Ide M, Nakanishi M, Kuwamura M, Sakuma S, et al. Participation of different macrophage populations and myofibroblastic cells in chronically developed renal interstitial fibrosis after cisplatin-induced renal injury in rats. *Vet Pathol* (2002) 39(3):322–33. doi: 10.1354/vp.39-3-322

77. Shen B, Liu X, Fan Y, Qiu J. Macrophages regulate renal fibrosis through modulating TGFβ superfamily signaling. *Inflammation.* (2014) 37(6):2076–84. doi: 10.1007/s10753-014-9941-y

78. Haudek SB, Xia Y, Huebener P, Lee JM, Carlson S, Crawford JR, et al. Bone marrow-derived fibroblast precursors mediate ischemic cardiomyopathy in mice. *Proc Natl Acad Sci United States America.* (2006) 103(48):18284–9. doi: 10.1073/pnas.0608799103

79. Feng Y, Guo F, Xia Z, Liu J, Mai H, Liang Y, et al. Inhibition of fatty acid-binding protein 4 attenuated kidney fibrosis by mediating macrophage-to-myofibroblast transition. *Front Immunol* (2020) 11:566535. doi: 10.3389/fimmu.2020.566535

80. Liang H, Liu B, Gao Y, Nie J, Feng S, Yu W, et al. Jmjd3/IRF4 axis aggravates myeloid fibroblast activation and m2 macrophage to myofibroblast transition in renal fibrosis. *Front Immunol* (2022) 13:978262. doi: 10.3389/fimmu.2022.978262

81. Xie N, Tan Z, Banerjee S, Cui H, Ge J, Liu RM, et al. Glycolytic reprogramming in myofibroblast differentiation and lung fibrosis. *Am J Respir Crit Care Med* (2015) 192 (12):1462–74. doi: 10.1164/rccm.201504-0780OC

82. Lu H, Dalgard CL, Mohyeldin A, McFate T, Tait AS, Verma A. Reversible inactivation of HIF-1 prolyl hydroxylases allows cell metabolism to control basal HIF-1. *J Biol Chem* (2005) 280(51):41928–39. doi: 10.1074/jbc.M508718200

83. Lu H, Forbes RA, Verma A. Hypoxia-inducible factor 1 activation by aerobic glycolysis implicates the Warburg effect in carcinogenesis. *J Biol Chem* (2002) 277 (26):23111–5. doi: 10.1074/jbc.M202487200

84. Boyd S, Brookfield JL, Critchlow SE, Cumming IA, Curtis NJ, Debreczeni J, et al. Structure-based design of potent and selective inhibitors of the metabolic kinase PFKFB3. *J medicinal Chem* (2015) 58(8):3611–25. doi: 10.1021/acs.jmedchem.5b00352

85. Tao W, Yurdagul A Jr., Kong N, Li W, Wang X, Doran AC, et al. siRNA nanoparticles targeting CaMKIIγ in lesional macrophages improve atherosclerotic plaque stability in mice. *Sci Transl Med* (2020) 12(553). doi: 10.1126/scitranslmed.aay1063

frontiers | Frontiers in Immunology

TYPE Original Research
PUBLISHED 03 January 2024
DOI 10.3389/fimmu.2023.1269261

OPEN ACCESS

EDITED BY
Xu-jie Zhou,
Peking University, China

REVIEWED BY
Leandro Pires Araujo,
Federal University Rural Semi-Arid, Brazil
Hee-Seong Jang,
Johns Hopkins University, United States

*CORRESPONDENCE
John D. Imig
john.imig@frontiersin.org

RECEIVED 29 July 2023
ACCEPTED 12 December 2023
PUBLISHED 03 January 2024

CITATION
Khan MAH, Nolan B, Stavniichuk A, Merk D and Imig JD (2024) Dual soluble epoxide hydrolase inhibitor – farnesoid X receptor agonist interventional treatment attenuates renal inflammation and fibrosis.
Front. Immunol. 14:1269261.
doi: 10.3389/fimmu.2023.1269261

Dual soluble epoxide hydrolase inhibitor – farnesoid X receptor agonist interventional treatment attenuates renal inflammation and fibrosis

Md. Abdul Hye Khan [1], Benjamin Nolan [1], Anna Stavniichuk [1,2], Daniel Merk [3] and John D. Imig [1,4]

[1]Drug Discovery Center, Medical College of Wisconsin, Milwaukee, WI, United States, [2]Department of Integrative Biology and Pharmacology, The University of Texas Health Science Center at Houston, Houston, TX, United States, [3]Department of Pharmacy, Ludwig-Maximilians Universität München, Munich, Germany, [4]Department of Pharmaceutical Sciences, University of Arkansas for Medical Sciences, Little Rock, AR, United States

Introduction: Renal fibrosis associated with inflammation is a critical pathophysiological event in chronic kidney disease (CKD). We have developed DM509 which acts concurrently as a farnesoid X receptor agonist and a soluble epoxide hydrolase inhibitor and investigated DM509 efficacy as an interventional treatment using the unilateral ureteral obstruction (UUO) mouse model.

Methods: Male mice went through either UUO or sham surgery. Interventional DM509 treatment (10mg/kg/d) was started three days after UUO induction and continued for 7 days. Plasma and kidney tissue were collected at the end of the experimental protocol.

Results: UUO mice demonstrated marked renal fibrosis with higher kidney hydroxyproline content and collagen positive area. Interventional DM509 treatment reduced hydroxyproline content by 41% and collagen positive area by 65%. Renal inflammation was evident in UUO mice with elevated MCP-1, CD45-positive immune cell positive infiltration, and profibrotic inflammatory gene expression. DM509 treatment reduced renal inflammation in UUO mice. Renal fibrosis in UUO was associated with epithelial-to-mesenchymal transition (EMT) and DM509 treatment reduced EMT. UUO mice also had tubular epithelial barrier injury with increased renal KIM-1, NGAL expression. DM509 reduced tubular injury markers by 25-50% and maintained tubular epithelial integrity in UUO mice. Vascular inflammation was evident in UUO mice with 9 to 20-fold higher ICAM and VCAM gene expression which was reduced by 40-50% with DM509 treatment. Peritubular vascular density was reduced by 35% in UUO mice and DM509 prevented vascular loss.

Discussion: Interventional treatment with DM509 reduced renal fibrosis and inflammation in UUO mice demonstrating that DM509 is a promising drug that combats renal epithelial and vascular pathological events associated with progression of CKD.

KEYWORDS

dual acting molecule, farnesoid X receptor agonist, soluble epoxide hydrolase, inflammation kidney, fibrosis, chronic kidney disease

Introduction

Renal fibrosis associated with inflammation is considered as the final common pathway by which chronic kidney disease (CKD) leads to end stage renal disease (ESRD) (1, 2). Occurrence of CKD and ESRD are very common in patients with inflammatory diseases such as cardiometabolic syndrome, diabetes, and hypertension (2–4). These are the most common chronic diseases of the modern world that cause CKD and high mortality (3, 4). The high mortality and morbidity associated with CKD often linked to the lack of an effective anti-fibrotic and anti-inflammatory agents that could target renal fibrosis (4).

There is an unmet need of novel combined anti-inflammatory and anti-fibrotic agents, particularly as an effective therapeutic approach for CKD and its progression to ESRD (5–7). Angiotensin-converting enzyme inhibitors and angiotensin II receptor blockers are the current therapeutic choices for the clinical management and treatment of CKD (8). However, these mainstay treatment options have limited efficacy to prevent or treat renal fibrosis, the major pathological event that leads to the progression of CKD to ESRD (5, 6). More recently, finerenone, a nonsteroidal selective mineralocorticoid receptor antagonist, has been demonstrated to decrease albuminuria and risk of CKD progression in chronic heart failure and diabetes (9, 10). Other novel approaches that have been attempted include the nuclear factor E2-related factor 2 inducer bardoxolone and the endothelin receptor blocker avosentan which proved largely ineffective in treating inflammation and associated renal fibrosis (11, 12). Findings from these studies clearly underscore a critical need for agent that can effectively treat renal fibrosis, the final common pathophysiological event in the progression of CKD to ESRD.

Potential targets for combating inflammation and renal fibrosis in CKD are the nuclear farnesoid X receptor (FXR) and the soluble epoxide hydrolase (sEH) enzyme (13, 14). FXR expression is decreased in the human and rodent models of kidney disease and this decrease correlated with the level of inflammation and fibrosis in the kidney (13, 15). Activation of FXR demonstrated kidney protective actions in animal models by decreasing kidney inflammation, oxidative stress, and fibrosis (16, 17). FXR is expressed on immune cells and FXR activation has anti-inflammatory actions (17, 18). These findings indicated an important role for FXR in kidney disease. Similar to FXR activation, inhibition of sEH that metabolizes and inactivates kidney protective epoxyeicosatrienoic acids (EETs) can combat inflammation and kidney disease (14, 19, 20). Experimental studies demonstrated beneficial kidney actions of EETs and sEH genetic deletion or inhibition in animal models of renal fibrosis and CKD (19, 20). Interestingly, it has also been demonstrated that FXR activation can induce the expression of EET producing cytochrome P450 enzymes and several polyunsaturated fatty acids including arachidonic acid act as FXR ligands (21, 22). Intriguingly, our research group has developed a dual acting FXR agonist and sEH inhibitor, DM509 which could decrease renal inflammation and fibrosis that occurs in CKD (23, 24).

Previous studies have demonstrated in mice that DM509 protected against liver and kidney fibrosis (23, 25, 26). Our previous kidney study demonstrated that DM509 administered one day prior to unilateral ureteral obstruction (UUO) prevented development of renal fibrosis (26). Unfortunately, the clinical treatment of CKD occurs after significant renal inflammation and fibrosis are evident. Thus, in the present study DM509 was tested in a clinically relevant manner.

In the current study we investigated interventional treatment with DM509 to reduce renal inflammation and fibrosis to halt the progression of CKD. Our findings demonstrate the therapeutic potential for the dual acting agent DM509 to combat renal inflammation and fibrosis associated with CKD progression.

Materials and methods

Animal experiments

All animal experiments carried out in this study were approved and conducted according to guidelines of the Medical College of Wisconsin Institutional Animal Care and Use Committee guidelines. All mice were housed in the Biomedical Resource Center at the Medical College of Wisconsin with free access to water and food under a 12/12h light-dark cycle. Male C57Bl/6J mice (8-10 weeks) were purchased from Jackson Laboratories, Bar

Harbor, ME. Mice were randomized in three groups (n=6 mice/group) and were subjected to Sham or UUO surgery to induce kidney disease. Prior to and during the surgical procedure, mice were administered 2.0% isoflurane to induce anesthesia. The UUO surgery was carried out by obstructing the left ureter proximal to the renal pelvis using a 6-0 silk tie (20, 26). Sham surgery was carried out in a set of mice using same procedure as the UUO mice except that the ureter was not ligated. In the present study we started DM509 interventional treatment 3 days after UUO as previous studies demonstrated robust renal inflammation and fibrosis on day 3 after UUO surgery (20). Mice were kept in separate cages to accurately measure fluid intake. Vehicle (hydroxypropyl methylcellulose (HPMC) and 0.01% Tween 80) and DM509 were administrated in drinking water and the correct daily dose was maintained by monitoring daily fluid intake. At the end of the 7-day treatment protocol, the mice were euthanized, and blood and kidney samples were obtained. The experimental protocol used in this study is shown in Figure 1A. Kidney samples for histological and immunohistological studies were fixed in 10% buffered formalin and stored at room temperature. Kidney tissue samples for biochemical and gene expression analysis were snap-frozen in liquid nitrogen and stored at -80°C until used.

Biochemical analysis

Kidney hydroxyproline tissue levels were determined in tissue homogenates using a colorimetric assay kit (Catalog # MAK008, Sigma-Aldrich, USA). Protein content of the tissue homogenates was measured using Pierce™ BCA Protein Assay Kit (Catalog # 23225, Thermo Fisher Scientific, USA). Monocyte chemoattractant protein-1 (MCP-1) levels in kidney tissues were measured using ELISA (Catalog # BMS6005, Thermo Fisher Scientific, USA). Blood urea nitrogen (BUN) was measured using a colorimetric assay kit (Catalog # EIABUN, Thermo Fisher Scientific, USA).

RNA isolation and real-time PCR analysis

Renal mRNA was isolated from kidney homogenates of each individual sample by RNeasy Mini Kit (QIAGEN, CA, USA) according to the manufacturer's protocol. The purity and amount of mRNA in samples was quantified spectrophotometrically. For each sample, 1μg of total RNA was reverse transcribed to cDNA using iScript™ Select cDNA Synthesis Kit (Bio-Rad, Hercules, CA, USA). Real-Time (RT) PCR analysis was carried out using cDNAs to determine renal mRNA expression of the markers of fibrogenesis [fibronectin, α-smooth muscle actin (α-SMA), fibroblast specific protein-1 (FSP-1)], tubular injury [neutrophil gelatinase-associated lipocalin (NGAL), kidney injury molecule-1 (KIM-1), Claudin-1,-3 and -4], inflammation [tumor necrosis factor-α (TNF-α), interleukin-1β (IL-1β), and interleukin-6 (IL-6)], and vascular injury [intercellular adhesion molecule-1 (ICAM-1), vascular cell adhesion molecule-1 (VCAM-1), Claudin-5, and VE-Cadherin]. Gene expression was quantified by iScript One-Step RT-PCR Kit with SYBR green using the MyiQ™ Single Color RT-PCR Detection

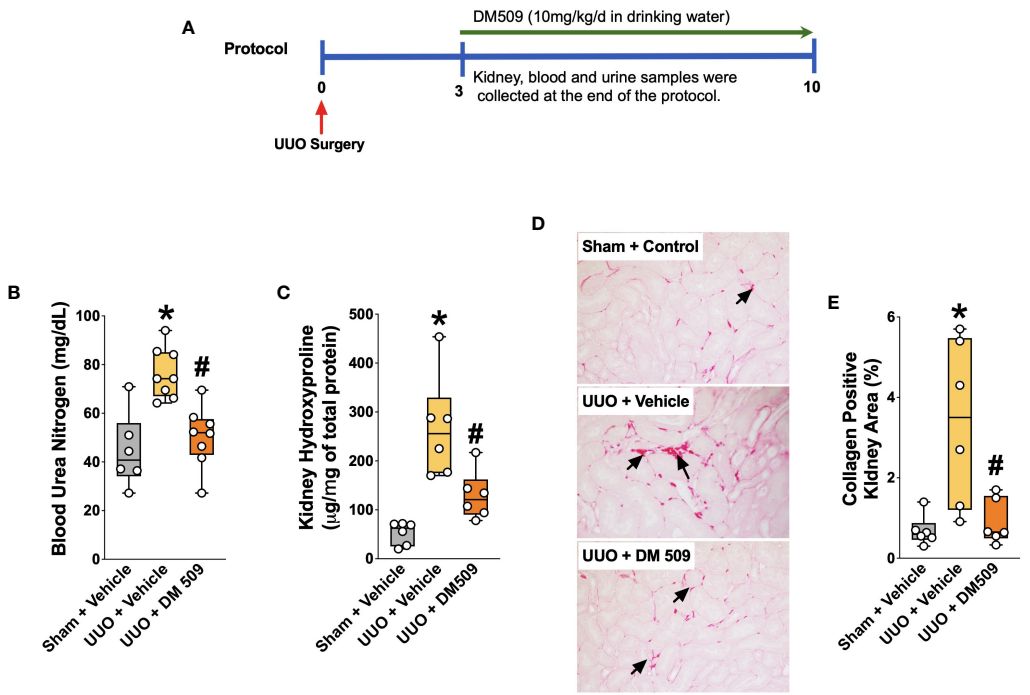

FIGURE 1
Experimental Protocol and DM509 Interventional Treatment on Renal Fibrosis in UUO Mice. Experimental protocol **(A)**; Blood urea nitrogen levels in experimental groups **(B)**; Kidney hydroxyproline levels in experimental groups **(C)**; Representative photomicrographs **(D)** depicting renal interstitial collagen (black arrows) and quantitative measurements of tubular interstitial collagen in experimental groups **(E)**. Data are reported as box and whisker plots with median and minimum to maximum, n=6. p<0.05, * UUO + Vehicle vs. Sham + Vehicle; # UUO + DM509 vs. UUO + Vehicle.

System (Bio-Rad Laboratories, Hercules, CA, USA). Dissociation curve analysis was done with iQ5 Optical System Software, Version 2.1 (Bio-Rad Laboratories, Hercules, CA, USA. During RT-PCR, denaturation was done at 95°C for 2 min followed by 40 cycles at 95°C for 10s and 30s at 60°C. Each sample was run in triplicate and fold change in gene expression compared to controls was calculated using the comparative threshold cycle (C_t) method. The expression levels of the gene of interest were determined by normalizing C_t values to three housekeeping genes. All statistical analyses were carried out using 6 samples from each experimental group.

Histopathology

Formalin-fixed kidney samples from each animal were paraffin embedded. Kidney samples were sectioned (5µm thickness), mounted on slides, and stained with Picrosirius Red (PSR) (Alfa Aesar, Tewksbury, MA). The stained slides were examined for interstitial fibrosis (PSR-collagen positive area) in the kidney at 200x magnification using NIS Elements AR version 3.0 imaging software (Nikon instruments Inc., Melville, NY, USA). Collagen-positive renal fibrotic area is presented as a percentage area-fraction relative to the total area. Histological analysis and the scoring of collagen-positive kidney area were performed by two observers in a blinded fashion.

Immunohistopathological analysis of the kidney sections

Kidney histological slides prepared from the paraffin-embedded kidney tissue samples were deparaffinized and re-hydrated followed by overnight incubation with antibodies against α-SMA (1:100, Santa Cruz Biotechnology, USA), FSP-1 (1:50, Cell Signaling Technology, USA) and Epithelial-Cadherin (E-Cadherin, 1:100, Cell Signaling Technology, USA). Using similar experimental steps, kidney slides were incubated with antibodies against CD45 (1:100, Cell Signaling Technology) and CD31(1:50, Cell Signaling Technology). On the second day, slides were washed and incubated with biotinylated secondary antibody (1:200-1:300) for 45-60 minutes at room temperature. The presence of the target proteins in the kidney sections were determined from avidin-biotinylated HRP complex (Vectastain ABC Elite kit, Vector Laboratories, USA) followed by counterstaining with hematoxylin. Stained kidney slides were examined at 200x magnification with a light microscope and analyzed using Nikon NIS Elements Software (Nikon Instruments Inc., Melville, NY, USA). The renal area positive for a specific target protein was calculated by Nikon NIS Elements Software and expressed as the percentage area relative to total area examined. The analysis and scoring process was carried out in blinded fashion by two observers.

Statistical analysis

GraphPad Prism® Version 4.0 software was utilized to carry out one-way ANOVA followed by Tukey's *post-hoc* test in order to establish statistical significance between groups (GraphPad Software Inc, La Jolla, CA, USA). All data are reported as box and whisker plots with median and minimum to maximum. A p value smaller or equal to 0.05 was considered significant.

Results

Interventional DM509 treatment attenuates renal fibrosis progression

Ten days following surgery, UUO mice exhibited renal injury with elevated BUN compared to the sham group. DM509 administered from day 3 to 10 reduced BUN by 40%. Mice with UUO developed marked renal fibrosis and demonstrated 5 times higher kidney level of hydroxyproline and 3 times higher collagen positive renal fibrotic area compared to sham mice. Dual FXR agonism-sEH inhibition with DM509 demonstrated marked anti-fibrotic effects and reduced kidney hydroxyproline content in UUO mice by 50% compared to UUO mice treated with vehicle. DM509 also reduced collagen positive fibrotic area in the kidney of UUO mice with levels like that in Sham mice (Figures 1B–E). Anti-fibrotic actions of DM509 were further assessed by evaluating renal mRNA protein expression of prominent fibrotic markers fibronectin, α-SMA and FSP-1 in UUO mice. We observed 3 to 19-fold higher mRNA expression of these fibrotic markers in the kidney of UUO compared to sham mice. In UUO mice, DM509 interventional treatment reduced renal mRNA expression of these markers by 40-50% compared to vehicle (Figures 2A–C). Renal expression of fibrotic markers was also determined at the protein level. UUO mice kidneys had nearly 90% higher expression of α-SMA and FSP-1 compared to sham mice. DM509 interventional treatment resulted in a robust 60-70% reduction of the renal expression of these markers in UUO mice compared to vehicle which further demonstrates a marked anti-fibrotic action (Figures 2E, F). An important mechanism of the fibrogenesis process is epithelial-to-mesenchymal transition (EMT). We observed higher renal expression of several mesenchymal markers including α-SMA and FSP-1 at both the mRNA and protein level in UUO mice. Renal expression of an important epithelial marker, epithelial-cadherin (E-Cadherin) demonstrated a robust 90% reduction in UUO compared to Sham mice. Interestingly, our findings demonstrate that DM509 interventional treatment reduced the loss of kidney E-cadherin levels in UUO mice kidney (Figure 2D). Overall, we demonstrate marked renal fibrosis and a fibrogenic process that involves EMT in UUO mice. We further demonstrated that interventional DM509 treatment has anti-fibrotic actions that are linked to a reduction in renal EMT in UUO mice.

10.3389/fimmu.2023.1269261

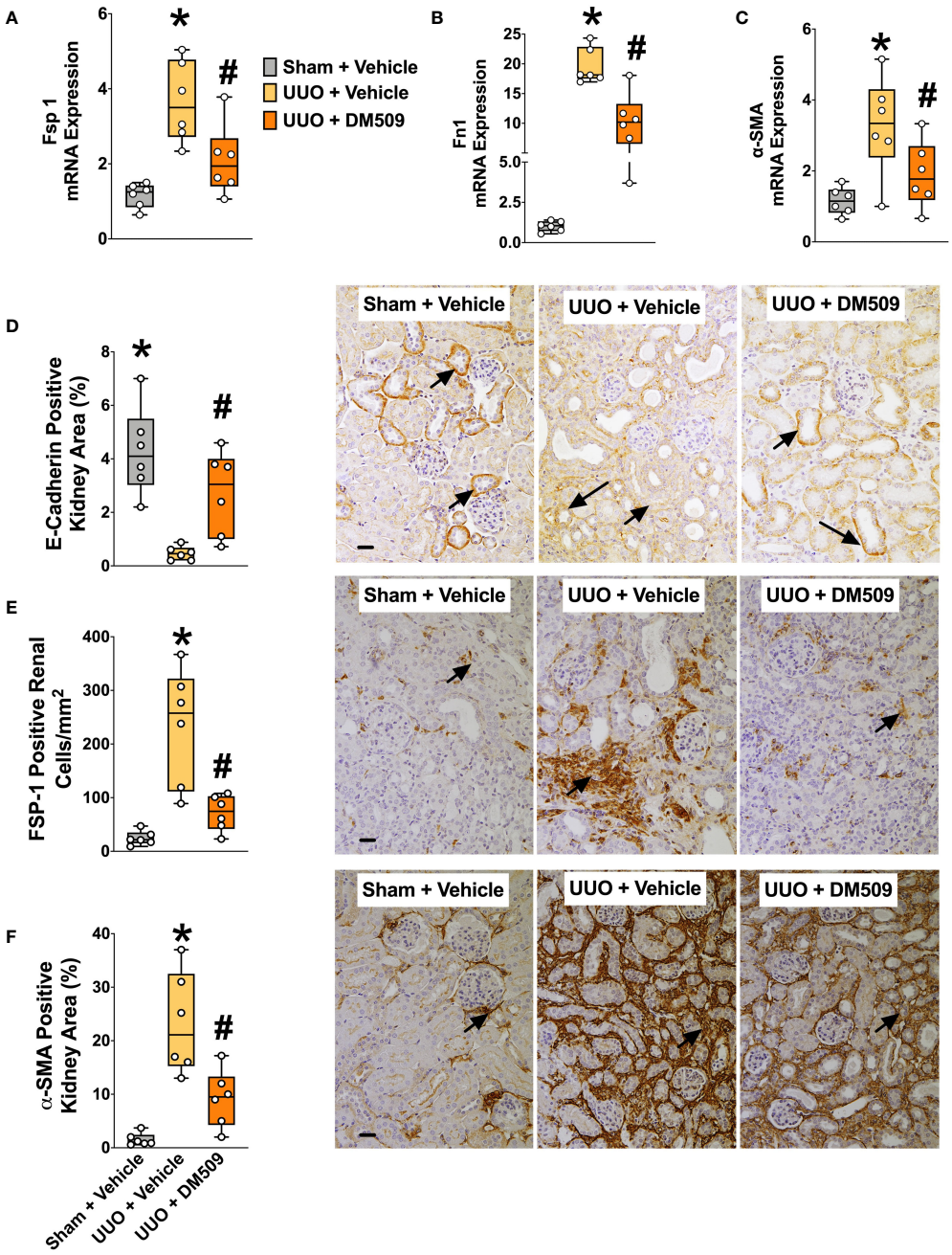

FIGURE 2
Attenuation of Renal Fibrosis Markers in UUO Mice by DM509 Interventional Treatment. Renal mRNA expression of fibrotic markers in experimental groups **(A–C)**; Quantitative measurement and representative photomicrographs for renal expression of FSP-1 **(E)** and α-SMA **(F)** in experimental groups; Quantitative measurement and representative photomicrographs showing renal expression of E-Cadherin **(D)** in experimental groups. Data are reported as box and whisker plots with median and minimum to maximum, n=6. $p<0.05$, * UUO + Vehicle vs. Sham + Vehicle; # UUO + DM509 vs. UUO + Vehicle.

Renal inflammation is attenuated by DM509 interventional treatment in UUO mice

In the present study, we demonstrate that UUO mice developed marked renal inflammation. Kidney content of an important chemokine, MCP-1 was 90% higher in the UUO mice compared to sham mice. DM509 interventional treatment reduced kidney MCP-1 levels by 35% in UUO mice (Figure 3A). UUO mice also demonstrated marked renal infiltration of CD45 positive immune cells as indicated by 80% higher kidney area that were positive for CD45 in UUO compared to sham mice. Interestingly, DM509 treatment markedly reduced renal infiltration of immune cells by 50% in UUO mice (Figures 3B, C). Considering a positive effect of DM509 on renal chemotaxis in UUO mice, we investigated renal mRNA expressions of several pro-fibrotic cytokines. We

10.3389/fimmu.2023.1269261

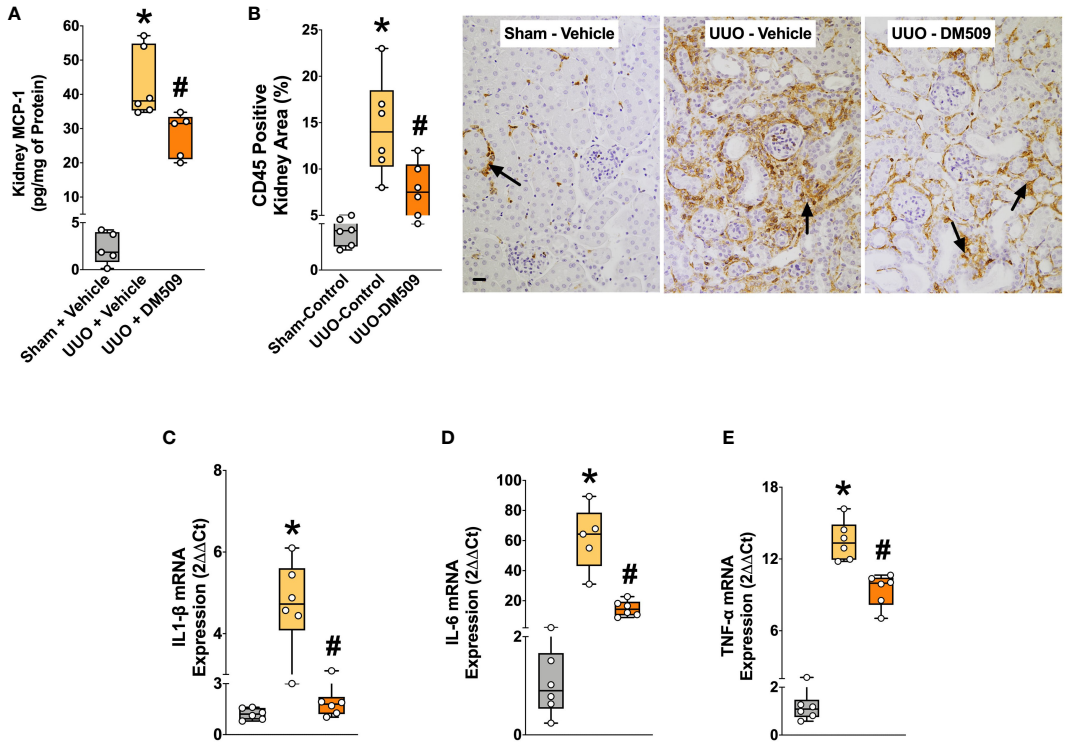

FIGURE 3
DM509 Interventional Treatment Reduced Renal Inflammation in UUO Mice. Kidney MCP-1 level in experimental groups **(A)**; Quantitative measurement of CD45 immunopositive kidney area **(B)** and representative photomicrographs showing CD45+ kidney area in experimental groups **(C)**; Renal mRNA expression of profibrotic cytokines in experimental groups **(D-E)**. Data are reported as box and whisker plots with median and minimum to maximum, n=6. $p<0.05$, * UUO + Vehicle vs. Sham + Vehicle; # UUO + DM509 vs. UUO + Vehicle.

demonstrated a 5-60-fold higher renal expression of TNF-α, IL-6, and IL-1β mRNA in UUO compared sham mice. Interventional DM509 treatment reduced renal mRNA expression of these cytokines by 30-70% in UUO mice (Figures 3D–E). In summary, we demonstrated marked chemotaxis and higher levels of pro-fibrotic cytokines at mRNA level in the kidney of fibrotic UUO mice. Our findings also demonstrated that interventional DM509 treatment has anti-inflammatory actions on chemotaxis and profibrotic cytokine mRNA expression in the kidney of UUO mice.

DM509 interventional treatment reduced renal tubular injury in UUO mice

In renal fibrosis, tubular injury is a critical pathophysiological event and contributes to extracellular matrix formation. We demonstrated marked renal tubular injury in UUO mice with 100 to 150-fold higher mRNA expressions of KIM-1 and NGAL, two important tubular injury markers. Interventional DM509 treatment attenuated renal tubular injury and reduced mRNA expression of KIM-1 and NGAL by 40 to 50% in UUO mice (Figures 4A, B). Tubular injury was further assessed from the renal mRNA expressions of claudin-1, -3, and -4, tight junction proteins that are important for epithelial integrity. We demonstrated that renal mRNA expression of claudin-1, -3, and -4 was decreased by 50-75% in UUO mice compared to sham mice. Interestingly, Interventional DM509 treatment restored expression of claudins and brought renal mRNA expression levels in UUO mice to that in sham mice (Figures 4C–E). Overall, we demonstrated marked renal tubular injury in UUO mice which attenuated by interventional DM509 treatment.

Renal vascular loss is attenuated by interventional DM509 treatment in UUO mice

In the present study, we demonstrated that UUO mice have marked 10-20-fold higher renal mRNA expression of vascular adhesion molecules ICAM and VCAM compared to sham mice. In UUO mice, interventional DM509 treatment reduced renal mRNA expression of these vascular adhesion molecules by 50-60% (Figures 5A, B). Renal mRNA expression of tight junction proteins VE-Cadherin and Claudin-5 that are important for endothelial integrity were significantly reduced by 60-70% in the kidney of UUO compared to Sham mice. Interestingly, DM509 treatment markedly attenuated the renal decrease of VE-Cadherin and Claudin-5 mRNA in UUO mice and the expression of these genes was restored to levels similar to sham mice (Figures 5C, D). Most importantly, we observed a marked 80% decrease in the renal vasculature as assessed by CD31 immunopositive area in the UUO mice kidneys. We further demonstrated that DM509 interventional treatment reduced renal vascular loss in UUO mice by restoring renal vasculature to a level similar to sham mice and CD31 positive

10.3389/fimmu.2023.1269261

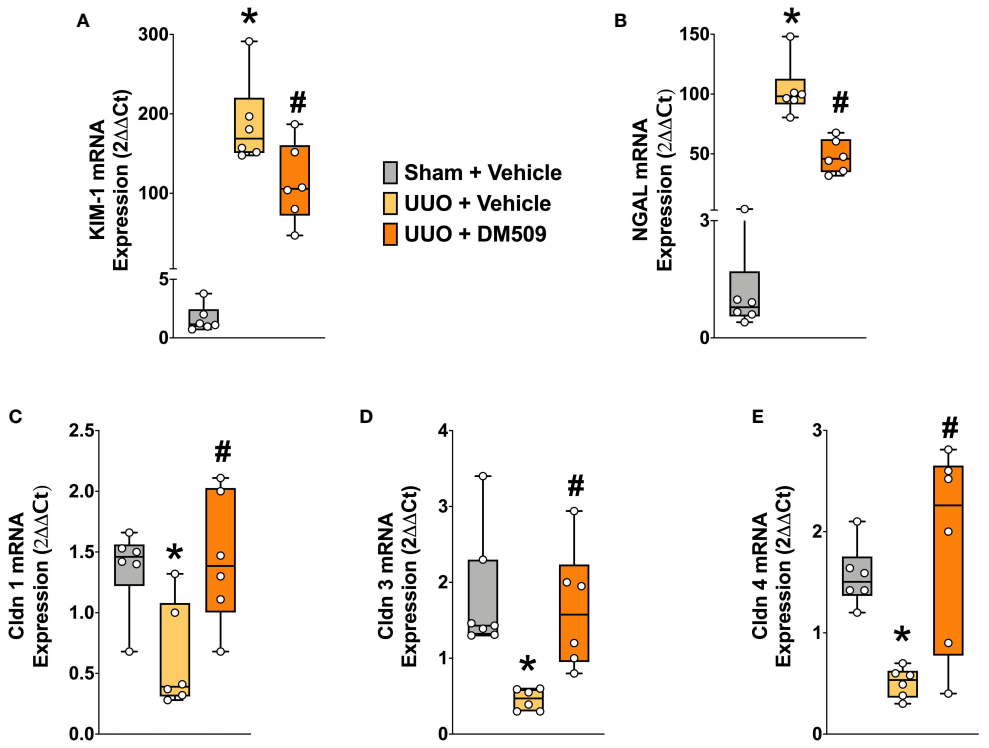

FIGURE 4
Renal Tubular Injury was Attenuated in UUO Mice by DM509 Interventional Treatment. Renal mRNA expression of tubular injury markers KIM-1 **(A)** and NGAL **(B)** in experimental groups; Renal mRNA expression of claudin 1,3 and 4 in experimental groups **(C–E)**. Data are reported as box and whisker plots with median and minimum to maximum, n=6. $p<0.05$, * UUO + Vehicle vs. Sham + Vehicle; # UUO + DM509 vs. UUO + Vehicle.

kidney area of DM509 treated animals was 75% higher than vehicle treated UUO mice (Figure 5E). In summary, UUO mice exhibited marked renal vascular loss along with elevated expression of vascular adhesin molecules and reduced expression endothelial tight junction protein. Interventional DM509 treatment markedly reduced vascular loss in the kidney of UUO mice.

Discussion

Fibrosis, a characteristic of all chronic kidney diseases (CKD), is recognized to be an independent predictor of disease progression (1, 3, 27). CKD and ESRD are major public health problems with increasing prevalence worldwide and in the US almost 15% (37 million) people are suffering from CKD (28, 29). Unfortunately, at present, there are no effective therapies to prevent or slow the progression of renal inflammation and fibrosis, and the treatment options for patients with ESRD are limited to dialysis and renal transplant (4–6). The lack of novel drugs targeting the pathological events of renal inflammation and fibrosis often give mixed results with unwanted side effects (5, 6). The shortcomings of these experimental therapies are likely due to the fact that the pathogenesis of fibrosis is complex. Renal fibrosis is linked to expansion of the interstitium with activated myofibroblasts, elevated inflammation, tubular atrophy, and microvascular injury (2, 30). In previous study our laboratory demonstrated that DM509 administered in a preventive manner reduced renal fibrosis in UUO mice (26). A major shortcoming of the previous study is that the clinical treatment CKD takes place after renal damage is evident. The current study administered DM509 to UUO mice at three days where renal inflammation and fibrosis is established (19, 20). DM509 is a dual acting FXR agonist and sEH inhibitor that possesses low nanomolar dual potency (31). Previous studies have demonstrated that following a single 10 mg/kg dose of DM509 to mice results in a robust increase in the EET/DHET (sEH substrate product) ratio and modulation of FXR regulated gene expression in the liver (31). In the present study we have demonstrate the unique ability of DM509 given in an interventional mode to reduce renal inflammation and slow progression of renal fibrosis in the mouse UUO model. Our findings demonstrate promising anti-inflammatory and anti-fibrotic effects of interventional DM509 treatment in regard to its ability to affect all renal fibrotic pathological events.

During renal fibrosis there is marked accumulation of myofibroblasts in the tubular interstitial space and these are the primary cells to synthesize and deposit pathological components of fibrillar matrix namely collagen and fibronectin (30, 32). Accumulation of fibrotic matrix progressively destroys the normal kidney tissue architecture by contraction and increased stiffness, resulting in disrupted blood flow supply and nephron function, as well as by increasing the space between vascular and tubular structures (30, 32). In the present study, we have used an established UUO mouse model that demonstrates marked renal fibrosis with accumulation of activated myofibroblast and collagen

10.3389/fimmu.2023.1269261

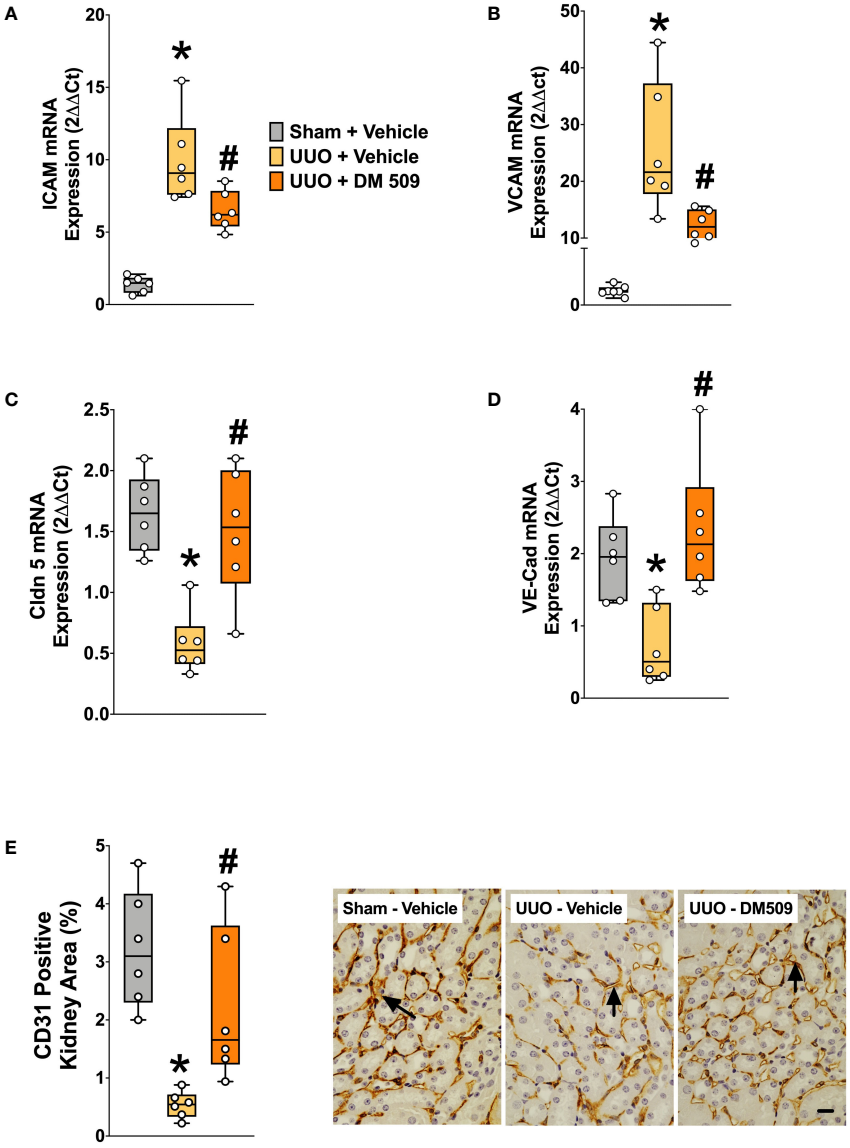

FIGURE 5
DM509 Interventional Treatment Reduced Renal Vascular Inflammation and Vascular Loss in UUO Mice. Renal mRNA expression of adhesion molecules ICAM **(A)** and VCAM **(B)** in experimental groups Renal mRNA expression of VE-Cadherin **(C)** and claudin 5 **(D)** in experimental groups; Quantitative measurement and representative photomicrographs showing renal expression for CD31+ kidney area in experimental groups **(E)**. Data are reported as box and whisker plots with median and minimum to maximum, n=6. $p<0.05$, * UUO + Vehicle vs. Sham + Vehicle; # UUO + DM509 vs. UUO + Vehicle.

formation. These critical fibrotic events are evident from elevated renal collagen level and high expression of activated myofibroblast markers α-SMA and FSP-1. Interventional treatment with the dual FXR agonist and sEH inhibitor, DM509 attenuated collagen and myofibroblast formation and demonstrated a robust anti-fibrotic effect in the UUO kidney. The observed anti-fibrotic ability of DM509 can be attributed to the biological actions of both FXR agonist and sEH inhibitor pharmacophores.

Several earlier studies reported marked anti-fibrotic actions of sEHi in animal models of CKD and renal fibrosis, including the mouse UUO model (19, 20, 33). Indeed, genetic or pharmacological sEH inhibition markedly reduced renal fibrosis and extracellular matrix protein formation in UUO mice by acting on multiple fibrotic pathophysiological events (19, 20). The other pharmacophore of DM509, FXR is highly expressed within the kidney, and studies have demonstrated that FXR activation can mitigate renal injury (13, 16). FXR levels were inversely correlated with CKD progression in mice and the degree of interstitial fibrosis in humans (34). FXR activation using obeticholic acid also decreased kidney inflammation and fibrosis in an ischemic reperfusion model of renal injury (34). It has been demonstrated that the renal expression of FXR is decreased in UUO mice (35). In the same study, it was also demonstrated that a novel FXR agonist EDP-305 reduced renal fibrosis (35). Consistent with these findings, we suggest that the anti-fibrotic actions of interventional DM509 treatment is due to both FXR agonism and sEH inhibition.

Renal fibrosis is complex process consisting of several mechanisms that ultimately leads to myofibroblast formation and extracellular matrix synthesis (36–38). Initial cell injury in response to UUO results in cell stress and necrosis which leads to release of damage-associated molecular patterns (DAMPs) leading to inflammation (36, 37). Several mechanisms including cellular activation, cellular proliferation, immune cell infiltration, EMT, mesothelial-to-mesenchymal transition (MMT), and endothelial-to-mesenchymal transition (EndoMT) are responsible for increasing the net pool of myofibroblast (37, 38). The current study evaluated the ability for interventional DM509 treatment to reduce EMT, inflammation and EndoMT in UUO mice.

EMT is one of several contributors to renal fibrosis in UUO mice (39, 40). Consistent with these findings, in the present study the renal fibrosis in UUO kidney was accompanied by EMT with a markedly reduced expression of epithelial marker E-cadherin and higher expression of mesenchymal markers α-SMA and FSP-1. UUO mice also demonstrated marked renal fibrosis with collagen formation and myofibroblast formation. It has been reported that the anti-fibrotic effect of the FXR agonist, EDP-305 could be associated with its ability to reduce mesenchymal expression and restoration of epithelial expression within the renal tubules (35). The ability of DM509 to also act as an sEH inhibitor to maintain and elevate epoxyeicosatrienoic acids (EETs) levels could contribute to the reduction in EMT and anti-fibrotic actions. EETs have strong cardiovascular and renal actions and are kidney protective with potent anti-fibrotic actions (14, 33). Interestingly, FXR agonist have the ability to affect the production of EETs from arachidonic acid by inducing CYP P450 (CYP) epoxygenases (21, 22). Indeed, it has been reported that in a liver fibrosis model FXR activation reprogrammed arachidonic acid metabolism by inducing CYP epoxygenase expression and EET production (21). The current study demonstrated that the anti-fibrotic actions of DM509 in UUO model is associated with a reduction in EMT. The anti-fibrotic action of DM509 was associated with its ability to reduce renal tubular EMT. Our findings suggest that the reduction in EMT induced by DM509 is due to FXR agonism, sEH inhibition and the important interactive relationship of these two DM509 pharmacophore activities.

During renal fibrosis, inflammation plays a key role in the activation of fibroblast and extracellular matrix formation in the kidney (2, 30, 41). Upon activation by profibrotic cytokines, resident interstitial fibroblasts progressively gain the myofibroblast phenotype, which was consistently seen in various CKD models including the UUO model (39, 42). Indeed, it was found that the monocytes/macrophages are the most abundant immune cells in most CKD models, and the presence of macrophages in human CKD biopsies is associated with tubular interstitial fibrosis and poor renal survival (43). In the present study, we demonstrated marked renal inflammation with elevated kidney MCP-1 levels and renal infiltration of immune cells in the UUO kidney. Elevated kidney chemokine levels and presence of immune cells in the UUO kidney were accompanied by elevated renal expression of key profibrotic cytokines. These findings are consistent with our earlier findings in the UUO renal fibrosis model (19, 20, 39). The dual acting molecule DM509 administered as an interventional treatment markedly reduced renal inflammation by reducing MCP-1 levels, infiltration of immune cells, and cytokine expression in UUO mice. The anti-inflammatory action of DM509 can be attributed to the biological actions of both FXR agonism and sEH inhibition activities. Anti-inflammatory actions of sEH inhibition in reducing kidney injury are well established in CKD animal models (19, 20, 44). Inhibition of sEH is known to reduce chemotaxis by reducing chemokines, renal infiltration of immune cells, and cytokine production in CKD (14, 20, 33). The sEH inhibitory anti-inflammatory actions in reducing renal fibrosis are also well established (14, 20). It has been reported that sEH inhibition either by genetic manipulation or by a pharmacological inhibition provides robust anti-inflammatory actions and attenuates renal fibrosis progression in UUO mice (19, 20). In UUO mice, sEH inhibition resulted in a marked decrease in renal infiltration of different types of immune cells and reduced profibrotic cytokine production which are linked to renal fibrotic pathophysiology (19, 20). The increase in EET levels in response to sEH inhibition could have direct actions on immune cells. A recent study provided evidence that renal EETs may act locally to regulate the ENaC activity in circulating monocytes entering the kidney to reduce inflammation in salt-sensitive hypertension (45). FXR activation has also been shown to suppress the inflammatory response by affecting several critical aspects of inflammatory processes (13, 17). FXR activation inhibited inflammation in various organ systems including liver, lung, and kidney (17). In several studies using rodent models of type I diabetes, high-fat diet-induced cardiometabolic syndrome, and type 2 diabetes mellitus, FXR expression and its target genes were down regulated in the kidney (46–48). Interestingly, such changes in the renal expression of FXR and its target genes in these models with renal pathology correlated with elevated inflammation and fibrosis in the kidney (46–48). A role of FXR was also reported in the UUO renal fibrosis model where it was demonstrated that FXR activation reduced renal inflammation and fibrosis by decreasing renal immune cell infiltration and expression of profibrotic cytokines (35). Like sEH inhibition and increased EET levels, FXR could act directly on immune cells. Indeed, previous studies have demonstrated that FXR agonists inhibit gastrointestinal inflammation through direct actions on immune cells to preserve the intestinal barrier during inflammatory bowel disease (49). A link to sEH inhibition could also exists as the FXR mediated anti-inflammatory actions require active CYP epoxygenases (21). Overall, the well-known anti-inflammatory actions of sEH inhibition and FXR agonism indicate that the robust anti-inflammatory actions of the novel dual acting DM509 are associated with the biological consequences of both molecular activities.

Renal inflammation caused by elevated chemokines, infiltrating immune cells and cytokine productions cause tubular injury and this tubular injury is considered an important event in renal fibrosis and CKD progression (3, 30, 42). Indeed, tubular degeneration evokes a vivid peritubular environment, and the injured tubular cells initiate a local inflammation, that finally leads to the removal of all tubular remnants and the formation of fibrosis (30, 42). An interesting finding from a recent reversal UUO study found an important contribution for F4/80 positive macrophages but not

CD3+ T-cells in salt-sensitive hypertension (44). Our research group has previously demonstrated that DM509 treatment to non-alcoholic steatohepatitis mice decreased liver CXCR3, CXCL9, CXCL10, TNFα, IL-1β, and TGF-β expression (23). In the current study we demonstrate a similar DM509 anti-inflammatory action in UUO. Kidney MCP- levels, CD45 positive immune cells, and TNFα, IL-1β, and IL-6 IL gene expression were decreased by DM509 treatment. Previous studies with sEH inhibitors or genetic deletion have demonstrated decreased transforming growth factor beta (TGF-β) in UUO mice (19, 20, 50). Likewise, FXR has been demonstrated to have anti-fibrotic actions in UUO mice via regulating TGFβ-Smad3 pathway (16, 34). FXR expression can be found on macrophages, tissue resident macrophages, and dendritic cells (18, 51). Future studies are necessary to evaluate the actions of interventional DM509 treatment on TGF-β and specific immune cells. Nevertheless, TGF-β is a critical regulator that is likely inhibited by DM509 to decrease myofibroblast activation, renal fibrosis, and tubular injury.

In the present study, we demonstrated tubular injury with elevated renal KIM-1 and NGAL expression. These findings are consistent with findings of a recent study with the UUO renal fibrosis model (26). The current study also demonstrated reduced expression of claudins in the UUO mice. Claudins exhibit a specific expression pattern in the kidney and are considered to be essential in tight junction formation to establish close connections between epithelial cells, thereby maintaining cell polarity and tubular integrity (52, 53). Loss of tubular integrity and polarity of the tubular epithelial cells are associated with tubular epithelial injury and renal fibrosis (53, 54). Interventional treatment with dual acting FXR agonist and sEH inhibitor, DM509 reduced renal tubular injury and restored tubular epithelial integrity in UUO mice. We suggest that this DM509 action is a consequence of both FXR agonism as well as sEH inhibition. Several studies have demonstrated that sEH inhibition can reduce renal tubular injury (14, 19, 20). A similar renal tubular protective effect of sEH inhibition has also been reported in ob/ob mice with diabetic nephropathy and renal fibrosis (55). These findings indicate that sEH inhibitory activity byDM509 protects renal tubules. FXR agonism has also demonstrated to be renal tubule protective in several studies (34, 56). Obeticholic acid, a FXR agonist provided renal protection with reduced renal inflammation, tubular injury, and fibrosis in a lipopolysaccharide-induced acute kidney injury model (56). The FXR agonist obeticholic acid demonstrated a similar renal tubular protective and anti-fibrotic effect in a rodent model of renal ischemia injury (34). The findings of the current study demonstrate that interventional treatment with the dual FXR agonists and sEH inhibitor, DM509 acts through combined reduction in inflammation, attenuation of EMT, and decreased tubulointerstitial fibrosis significantly decreased renal injury in UUO mice.

Similar to renal tubular injury, another important pathophysiological event in CKD progression is vascular injury followed by vascular loss (56, 57). Intact microvasculature is a prerequisite for normal tubular structure and functions and peritubular vascular injury is associated with CKD progression (56–58). Indeed, a decrease in CD34+ tubulointerstitial capillaries has been observed together with tubular interstitial fibrosis in the UUO model (59). In a recent study, we demonstrated marked renal vascular loss in the UUO kidney with a decrease in CD31+ renal vasculature (50). Consistent with these previous findings, the current study demonstrated marked renal vascular loss in UUO mice with reduced renal CD31+ vascular levels. UUO mice also demonstrated kidney vascular inflammation with elevated expression of adhesion molecules ICAM and VCAM and a leaky endothelial barrier with elevation in claudin-5 and VE-cadherin. Claudin-5 and VE-Cadherin are specifically expressed in endothelial cells to maintain vascular barrier functions and regulate endothelial permeability (60, 61). In the UUO model reduction of renal Claudin-5 and VE-Cadherin was demonstrated to be associated with renal fibrosis progression (62). Interestingly, in the present study the dual acting molecule DM509 reduced CD31+ renal vascular loss in UUO mice. DM509 interventional treatment also reduced renal vascular inflammation and endothelial permeability in the UUO kidney by reducing ICAM and VCAM expression and also by attenuating the loss of claudin-5 and VE-Cadherin.

It is important to note that in the UUO kidney, we demonstrated markedly higher expressions of mesenchymal markers α-SMA and FSP-1 and reduced expression of endothelial markers VE-cadherin and CD31. This difference in the expressions of endothelial and mesenchymal markers indicate a possible endothelial-to-mesenchymal transition (EndoMT) in the UUO kidney. The EndoMT is a complex process by which certain endothelial cell subsets lose endothelial characteristics and transform into mesenchymal or smooth muscle cells (63, 64). EndoMT is often linked to the development of fibrosis in animal models, including the UUO model (65). We suggest that the effects of DM509 on the renal vasculature in UUO mice is caused by both its FXR agonistic property and ability to inhibit sEH. FXR activation by obeticholic acid, a synthetic FXR agonist, attenuated vascular remodeling of pulmonary vasculature in a rat model of pulmonary hypertension (66). This study suggested that FXR activation mediated anti-inflammatory actions to reduce EndoMT (66). Likewise, sEH inhibition has been demonstrated to stabilize EET levels, inhibit vascular inflammation, and promote vascular repair through neovascularization (14, 67, 68). An increase in EET levels induced by treatment with the sEH inhibitor 12-(3-adamantan-1-yl-ureido)-dodecanoic acid (AUDA) promoted vascular repair in human coronary arterial endothelial cells (68). Pharmacological sEH inhibition also reduced coronary artery inflammation in a mouse model of heart disease associated with coronary artery aneurysms and myocardial infarction (68). Similar to AUDA, another sEH inhibitor t-AUCB dose dependently increased the expression of the angiogenic factor vascular endothelial growth factor (VEGF) (67, 69). Overall, we demonstrated that the novel dual acting molecule DM509 given as an interventional treatment reduced vascular loss during renal fibrosis by reducing vascular inflammation, restoring renal vasculature, and restoring vascular endothelial integrity. Our data also indicated a possible role of DM509 on EndoMT to reduce renal vascular injury in UUO mice.

Conclusion

We demonstrated renal anti-fibrotic actions of a novel first-in-class dual acting molecule DM509 that simultaneously act as a FXR agonist and sEH inhibitor. Interventional treatment with DM509 reduced renal fibrosis in UUO mice by acting on several critical inflammatory mediated pathophysiological events. Our data demonstrated that DM509 uniquely reduced extracellular matrix formation and renal tubular and vascular injury in UUO mice. Our data also suggest that DM509 anti-inflammatory and anti-fibrotic actions are associated with its ability to reduce renal EMT and EndoMT. Overall, these data reveal that DM509 given in a clinically relevant manner is a promising dual acting anti-fibrotic and anti-inflammatory therapeutic that attenuates renal epithelial and vascular pathological events associated with progression of CKD to ESRD.

Data availability statement

The raw data supporting the conclusions of this article will be made available by the authors, without undue reservation.

Ethics statement

The animal study was approved by Medical College of Wisconsin Institutional Animal Care and Use Committee. The study was conducted in accordance with the local legislation and institutional requirements.

Author contributions

MK: Conceptualization, Data curation, Formal analysis, Investigation, Methodology, Validation, Writing – original draft, Writing – review & editing. BN: Data curation, Formal analysis, Investigation, Methodology, Writing – review & editing. AS: Data curation, Formal analysis, Investigation, Methodology, Writing – review & editing. DM: Conceptualization, Data curation, Formal analysis, Funding acquisition, Investigation, Resources, Writing – review & editing. JI: Conceptualization, Funding acquisition, Resources, Supervision, Writing – original draft, Writing – review & editing.

Funding

The author(s) declare financial support was received for the research, authorship, and/or publication of this article. National Institute of Health (NIH) grant DK126452 and Arkansas Research Alliance to JI and ETH Zürich Fellowship (Grant 16-2 FEL-07) to DM supported this study.

Conflict of interest

The authors declare that the research was conducted in the absence of any commercial or financial relationships that could be construed as a potential conflict of interest.

The author(s) declared that they were an editorial board member of Frontiers, at the time of submission. This had no impact on the peer review process and the final decision.

Publisher's note

References

1. Campanholle G, Ligresti G, Gharib SA, Duffield JS. Cellular mechanisms of tissue fibrosis. 3. Novel mechanisms of kidney fibrosis. *Am J Physiol Cell Physiol* (2013) 304(7): C591–603. doi: 10.1152/ajpcell.00414.2012

2. Kadatane SP, Satariano M, Massey M, Mongan K, Raina R. The role of inflammation in CKD. *Cells* (2023) 12(12):1581. doi: 10.3390/cells12121581

3. Liu Y. Renal fibrosis: new insights into the pathogenesis and therapeutics. *Kidney Int* (2006) 69(2):213–7. doi: 10.1038/sj.ki.5000054

4. Collins AJ, Foley RN, Gilbertson DT, Chen SC. The state of chronic kidney disease, ESRD, and morbidity and mortality in the first year of dialysis. *Clin J Am Soc Nephrol* (2009) 4 Suppl 1:S5–11. doi: 10.2215/CJN.05980809

5. Huang R, Fu P, Ma L. Kidney fibrosis: from mechanisms to therapeutic medicines. *Signal Transduct Target Ther* (2023) 8(1):129. doi: 10.1038/s41392-023-01379-7

6. Xu X, Zhang B, Wang Y, Shi S, Lv J, Fu Z, et al. Renal fibrosis in type 2 cardiorenal syndrome: An update on mechanisms and therapeutic opportunities. *BioMed Pharmacother* (2023) 164:114901. doi: 10.1016/j.biopha.2023.114901

7. Zhong J, Yang HC, Fogo AB. A perspective on chronic kidney disease progression. *Am J Physiol Renal Physiol* (2017) 312(3):F375–84. doi: 10.1152/ajprenal.00266.2016

8. Fried LF, Emanuele N, Zhang JH, Brophy M, Conner TA, Duckworth W, et al. Combined angiotensin inhibition for the treatment of diabetic nephropathy. *N Engl J Med* (2013) 369(20):1892–903. doi: 10.1056/NEJMoa1303154

9. González-Juanatey JR, Górriz JL, Ortiz A, Valle A, Soler MJ, Facila L. Cardiorenal benefits of finerenone: protecting kidney and heart. *Ann Med* (2023) 55(1):502–13. doi: 10.1080/07853890.2023.2171110

10. Lv R, Xu L, Che L, Liu S, Wang Y, Dong B. Cardiovascular-renal protective effect and molecular mechanism of finerenone in type 2 diabetic mellitus. *Front Endocrinol (Lausanne)* (2023) 14:1125693. doi: 10.3389/fendo.2023.1125693

11. de Zeeuw D, Akizawa T, Audhya P, Bakris GL, Chin M, Christ-Schmidt H, et al. Bardoxolone methyl in type 2 diabetes and stage 4 chronic kidney disease. *N Engl J Med* (2013) 369(26):2492–503. doi: 10.1056/NEJMoa1306033

12. Mann JF, Green D, Jamerson K, Ruilope LM, Kuranoff SJ, Littke T, et al. Avosentan for overt diabetic nephropathy. *J Am Soc Nephrol* (2010) 21(3):527–35. doi: 10.1681/ASN.2009060593

13. Guo Y, Xie G, Zhang X. Role of FXR in renal physiology and kidney diseases. *Int J Mol Sci* (2023) 24(3):2408. doi: 10.3390/ijms24032408

14. Imig JD. Prospective for cytochrome P450 epoxygenase cardiovascular and renal therapeutics. *Pharmacol Ther* (2018) 192:1–19. doi: 10.1016/j.pharmthera.2018.06.015

15. Kim DH, Park JS, Choi HI, Kim CS, Bae EH, Ma SK, et al. The role of the farnesoid X receptor in kidney health and disease: a potential therapeutic target in kidney diseases. *Exp Mol Med* (2023) 55(2):304–12. doi: 10.1038/s12276-023-00932-2

16. Zhao K, He J, Zhang Y, Xu Z, Xiong H, Gong R, et al. Activation of FXR protects against renal fibrosis via suppressing Smad3 expression. *Sci Rep* (2016) 6:37234. doi: 10.1038/srep37234

17. Herman-Edelstein M, Weinstein T, Levi M. Bile acid receptors and the kidney. *Curr Opin Nephrol Hypertens* (2018) 27(1):56–62. doi: 10.1097/MNH.0000000000000374

18. Shaik FB, Prasad DV, Narala VR. Role of farnesoid X receptor in inflammation and resolution. *Inflammation Res* (2015) 64(1):9–20. doi: 10.1007/s00011-014-0780-y

19. Kim J, Imig JD, Yang J, Hammock BD, Padanilam BJ. Inhibition of soluble epoxide hydrolase prevents renal interstitial fibrosis and inflammation. *Am J Physiol Renal Physiol* (2014) 307(8):F971–80. doi: 10.1152/ajprenal.00256.2014

20. Kim J, Yoon SP, Toews ML, Imig JD, Hwang SH, Hammock BD, et al. Pharmacological inhibition of soluble epoxide hydrolase prevents renal interstitial fibrogenesis in obstructive nephropathy. *Am J Physiol Renal Physiol* (2015) 308(2):F131–9. doi: 10.1152/ajprenal.00531.2014

21. Gai Z, Visentin M, Gui T, Zhao L, Thasler WE, Häusler S, et al. Effects of farnesoid X receptor activation on arachidonic acid metabolism, NF-kB signaling, and hepatic inflammation. *Mol Pharmacol* (2018) 94(2):802–11. doi: 10.1124/mol.117.111047

22. Zhao A, Yu J, Lew JL, Huang L, Wright SD, Cui J. Polyunsaturated fatty acids are FXR ligands and differentially regulate expression of FXR targets. *DNA Cell Biol* (2004) 23(8):519–26. doi: 10.1089/1044549041562267

23. Hye Khan MA, Schmidt J, Stavniichuk A, Imig JD, Merk D. A dual farnesoid X receptor/soluble epoxide hydrolase modulator treats non-alcoholic steatohepatitis in mice. *Biochem Pharmacol* (2019) 166:212–21. doi: 10.1016/j.bcp.2019.05.023

24. Imig JD, Merk D, Proschak E. Multi-target drugs for kidney diseases. *Kidney360* (2021) 2(10):1645–53. doi: 10.34067/KID.0003582021

25. Helmstädter M, Schmidt J, Kaiser A, Weizel L, Proschak E, Merk D. Differential therapeutic effects of FXR activation, sEH inhibition, and dual FXR/sEH modulation in NASH in diet-induced obese mice. *ACS Pharmacol Transl Sci* (2021) 4(2):966–79. doi: 10.1021/acsptsci.1c00041

26. Stavniichuk A, Savchuk O, Khan AH, Jankiewicz WK, Imig JD, Merk D. The effect of compound DM509 on kidney fibrosis in the conditions of the experimental model. *Visnyk Kyivskoho Natsionalnoho Universytetu Imeni Tarasa Shevchenka Biolohiia* (2020) 80(1):10–5. doi: 10.17721/1728_2748.2020.80.10-15

27. Nicholson ML, McCulloch TA, Harper SJ, Wheatley TJ, Edwards CM, Feehally J, et al. Early measurement of interstitial fibrosis predicts long-term renal function and graft survival in renal transplantation. *Br J Surg* (1996) 83(8):1082–5. doi: 10.1002/bjs.1800830813

28. Kovesdy CP. Epidemiology of chronic kidney disease: an update 2022. *Kidney Int Suppl* (2022) 12(1):7–11. doi: 10.1016/j.kisu.2021.11.003

29. Hsu RK, Powe NR. Recent trends in the prevalence of chronic kidney disease: not the same old song. *Curr Opin Nephrol Hypertens* (2017) 26(3):187–96. doi: 10.1097/MNH.0000000000000315

30. Leaf IA, Duffield JS. What can target kidney fibrosis? *Nephrol Dial Transplant* (2017) 32(suppl_1):i89–97. doi: 10.1093/ndt/gfw388

31. Schmidt J, Rotter M, Weiser T, Wittmann S, Weizel L, Kaiser A, et al. A dual modulator of farnesoid X receptor and soluble epoxide hydrolase to counter nonalcoholic steatohepatitis. *J Med Chem* (2017) 60(18):7703–24. doi: 10.1021/acs.jmedchem.7b00398

32. Miguel V, Kramann R. Metabolic reprogramming heterogeneity in chronic kidney disease. *FEBS Open Bio* (2023) 13(7):1154–63. doi: 10.1002/2211-5463.13568

33. Imig JD. Epoxide hydrolase and epoxygenase metabolites as therapeutic targets for renal diseases. *Am J Physiol Renal Physiol* (2005) 289(3):F496–503. doi: 10.1152/ajprenal.00350.2004

34. Gai Z, Chu L, Xu Z, Song X, Sun D, Kullak-Ublick GA. Farnesoid X receptor activation protects the kidney from ischemia-reperfusion damage. *Sci Rep* (2017) 7(1):9815. doi: 10.1038/s41598-017-10168-6

35. Li S, Ghoshal S, Sojoodi M, Arora G, Masia R, Erstad DJ, et al. The farnesoid X receptor agonist EDP-305 reduces interstitial renal fibrosis in a mouse model of unilateral ureteral obstruction. *FASEB J* (2019) 33(6):7103–12. doi: 10.1096/fj.201801699R

36. Wyczanska M, Lange-Sperandio B. DAMPs in unilateral ureteral obstruction. *Front Immunol* (2020) 11:581300. doi: 10.3389/fimmu.2020.581300

37. Ruiz-Ortega M, Rayego-Mateos S, Lamas S, Ortiz A, Rodrigues-Diez RR. Targeting the progression of chronic kidney disease. *Nat Rev Nephrol* (2020) 16(5):269–88. doi: 10.1038/s41581-019-0248-y

38. Weiskirchen R, Weiskirchen S, Tacke F. Organ and tissue fibrosis: Molecular signals, cellular mechanisms and translational implications. *Mol Aspects Med* (2019) 65:2–15. doi: 10.1016/j.mam.2018.06.003

39. Skibba M, Hye Khan MA, Kolb LL, Yeboah MM, Falck JR, Amaradhi R, et al. Epoxyeicosatrienoic acid analog decreases renal fibrosis by reducing epithelial-to-mesenchymal transition. *Front Pharmacol* (2017) 8:406. doi: 10.3389/fphar.2017.00406

40. Zeisberg EM, Potenta SE, Sugimoto H, Zeisberg M, Kalluri R. Fibroblasts in kidney fibrosis emerge via endothelial-to-mesenchymal transition. *J Am Soc Nephrol* (2008) 19(12):2282–7. doi: 10.1681/ASN.2008050513

41. Huang G, Zhang Y, Zhang Y, Ma Y. Chronic kidney disease and NLRP3 inflammasome: Pathogenesis, development and targeted therapeutic strategies. *Biochem Biophys Rep* (2022) 33:101417. doi: 10.1016/j.bbrep.2022.101417

42. Kaissling B, Lehir M, Kriz W. Renal epithelial injury and fibrosis. *Biochim Biophys Acta* (2013) 1832(7):931–9. doi: 10.1016/j.bbadis.2013.02.010

43. Eardley KS, Kubal C, Zehnder D, Quinkler M, Lepenies J, Savage CO, et al. The role of capillary density, macrophage infiltration and interstitial scarring in the pathogenesis of human chronic kidney disease. *Kidney Int* (2008) 74(4):495–504. doi: 10.1038/ki.2008.183

44. Imig JD, Khan MAH, Stavniichuk A, Jankiewicz WK, Goorani S, Yeboah MM, et al. Salt-sensitive hypertension after reversal of unilateral ureteral obstruction. *Biochem Pharmacol* (2023) 210:115438. doi: 10.1016/j.bcp.2023.115438

45. Ertuglu LA, Pitzer Mutchler A, Jamison S, Laffer CL, Elijovich F, Saleem M, et al. Eicosanoid-regulated myeloid ENaC and isolevuglandin formation in human salt-sensitive hypertension. *Hypertension* (2023). doi: 10.1161/HYPERTENSIONAHA.123.21285

46. Wang XX, Luo Y, Wang D, Adorini L, Pruzanski M, Dobrinskikh E, et al. A dual agonist of farnesoid X receptor (FXR) and the G protein-coupled receptor TGR5, INT-767, reverses age- related kidney disease in mice. *J Biol Chem* (2017) 292(29):12018–24. doi: 10.1074/jbc.C117.794982

47. Proctor G, Jiang T, Iwahashi M, Wang Z, Li J, Levi M. Regulation of renal fatty acid and cholesterol metabolism, inflammation, and fibrosis in Akita and OVE26 mice with type 1 diabetes. *Diabetes* (2006) 55(9):2502–9. doi: 10.2337/db05-0603

48. Wang XX, Jiang T, Shen Y, Adorini L, Pruzanski M, Gonzalez FJ, et al. The farnesoid X receptor modulates renal lipid metabolism and diet-induced renal inflammation, fibrosis, and proteinuria. *Am J Physiol Renal Physiol* (2009) 297(6):F1587–96. doi: 10.1152/ajprenal.00404.2009

49. Gadaleta RM, van Erpecum KJ, Oldenburg B, Willemsen EC, Renooij W, Murzilli S, et al. Farnesoid X receptor activation inhibits inflammation and preserves the intestinal barrier in inflammatory bowel disease. *Gut* (2011) 60(4):463–72. doi: 10.1136/gut.2010.212159

50. Stavniichuk A, Hye Khan MA, Yeboah MM, Chesnik MA, Jankiewicz WK, Hartmann M, et al. Dual soluble epoxide hydrolase inhibitor/PPAR-γ agonist attenuates renal fibrosis. *Prostaglandins Other Lipid Mediat* (2020) 150:106472. doi: 10.1016/j.prostaglandins.2020.106472

51. Yan N, Yan T, Xia Y, Hao H, Wang G, Gonzalez FJ. The pathophysiological function of non-gastrointestinal farnesoid X receptor. *Pharmacol Ther* (2021) 226:107867. doi: 10.1016/j.pharmthera.2021.107867

52. Balkovetz DF. Tight junction claudins and the kidney in sickness and in health. *Biochim Biophys Acta* (2009) 1788(4):858–63. doi: 10.1016/j.bbamem.2008.07.004

53. Yu AS. Claudins and the kidney. *J Am Soc Nephrol* (2015) 26(1):11–9. doi: 10.1681/ASN.2014030284

54. Kiuchi-Saishin Y, Gotoh S, Furuse M, Takasuga A, Tano Y, Tsukita S. Differential expression patterns of claudins, tight junction membrane proteins, in mouse nephron segments. *J Am Soc Nephrol* (2002) 13(4):875–86. doi: 10.1681/ASN.V134875

55. Jiang XS, Xiang XY, Chen XM, He JL, Liu T, Gan H, et al. Inhibition of soluble epoxide hydrolase attenuates renal tubular mitochondrial dysfunction and ER stress by restoring autophagic flux in diabetic nephropathy. *Cell Death Dis* (2020) 11(5):385. doi: 10.1038/s41419-020-2594-x

56. Zhu JB, Xu S, Li J, Song J, Luo B, Song YP, et al. Farnesoid X receptor agonist obeticholic acid inhibits renal inflammation and oxidative stress during lipopolysaccharide-induced acute kidney injury. *Eur J Pharmacol* (2018) 838:60–8. doi: 10.1016/j.ejphar.2018.09.009

57. Basile DP. Rarefaction of peritubular capillaries following ischemic acute renal failure: a potential factor predisposing to progressive nephropathy. *Curr Opin Nephrol Hypertens* (2004) 13(1):1–7. doi: 10.1097/00041552-200401000-00001

58. Humphreys BD. Mechanisms of renal fibrosis. *Annu Rev Physiol* (2018) 80:309–26. doi: 10.1146/annurev-physiol-022516-034227

59. Masum MA, Ichii O, Elewa YHA, Nakamura T, Kon Y. Local CD34-positive capillaries decrease in mouse models of kidney disease associating with the severity of glomerular and tubulointerstitial lesions. *BMC Nephrol* (2017) 18(1):280. doi: 10.1186/s12882-017-0694-3

60. Corada M, Zanetta L, Orsenigo F, Breviario F, Lampugnani MG, Bernasconi S, et al. A monoclonal antibody to vascular endothelial-cadherin inhibits tumor angiogenesis without side effects on endothelial permeability. *Blood* (2002) 100(3):905–11. doi: 10.1182/blood.v100.3.905

61. Morita K, Sasaki H, Furuse M, Tsukita S. Endothelial claudin: claudin-5/TMVCF constitutes tight junction strands in endothelial cells. *J Cell Biol* (1999) 147(1):185–94. doi: 10.1083/jcb.147.1.185

62. Pulskens WP, Butter LM, Teske GJ, Claessen N, Dessing MC, Flavell RA, et al. Nlrp3 prevents early renal interstitial edema and vascular permeability in unilateral ureteral obstruction. *PloS One* (2014) 9(1):e85775. doi: 10.1371/journal.pone.0085775

63. He J, Xu Y, Koya D, Kanasaki K. Role of the endothelial-to-mesenchymal transition in renal fibrosis of chronic kidney disease. *Clin Exp Nephrol* (2013) 17 (4):488–97. doi: 10.1007/s10157-013-0781-0

64. Goligorsky MS. Pathogenesis of endothelial cell dysfunction in chronic kidney disease: a retrospective and what the future may hold. *Kidney Res Clin Pract* (2015) 34 (2):76–82. doi: 10.1016/j.krcp.2015.05.003

65. Hung TW, Chu CY, Yu CL, Lee CC, Hsu LS, Chen YS, et al. Endothelial cell-specific molecule 1 promotes endothelial to mesenchymal transition in renal fibrosis. *Toxins (Basel)* (2020) 12(8):506. doi: 10.3390/toxins12080506

66. Vignozzi L, Morelli A, Cellai I, Filippi S, Comeglio P, Sarchielli E, et al. Cardiopulmonary protective effects of the selective FXR agonist obeticholic acid in the rat model of monocrotaline-induced pulmonary hypertension. *J Steroid Biochem Mol Biol* (2017) 165(Pt B):277–92. doi: 10.1016/j.jsbmb.2016.07.004

67. Sander AL, Jakob H, Sommer K, Sadler C, Fleming I, Marzi I, et al. Cytochrome P450-derived epoxyeicosatrienoic acids accelerate wound epithelialization and neovascularization in the hairless mouse ear wound model. *Langenbecks Arch Surg* (2011) 396(8):1245–53. doi: 10.1007/s00423-011-0838-z

68. Dai N, Zhao C, Kong Q, Li D, Cai Z, Wang M. Vascular repair and anti-inflammatory effects of soluble epoxide hydrolase inhibitor. *Exp Ther Med* (2019) 17 (5):3580–8. doi: 10.3892/etm.2019.7396

69. Xu DY, Davis BB, Wang ZH, Zhao SP, Wasti B, Liu ZL, et al. A potent soluble epoxide hydrolase inhibitor, t-AUCB, acts through PPARγ to modulate the function of endothelial progenitor cells from patients with acute myocardial infarction. *Int J Cardiol* (2013) 167(4):1298–304. doi: 10.1016/j.ijcard.2012.03.167

frontiers | Frontiers in Immunology

TYPE Review
PUBLISHED 04 January 2024
DOI 10.3389/fimmu.2023.1303076

OPEN ACCESS

EDITED BY
Xu-jie Zhou,
Peking University, China

REVIEWED BY
Ana Cristina Simões E Silva,
Federal University of Minas Gerais, Brazil
Hossein Khorramdelazad,
Rafsanjan University of Medical Sciences, Iran

*CORRESPONDENCE
Yan Bai
1447003128@qq.com
Shuju Li
lsj20051029@126.com

†These authors share first authorship

RECEIVED 27 September 2023
ACCEPTED 12 December 2023
PUBLISHED 04 January 2024

CITATION
Liu Y, Xu K, Xiang Y, Ma B, Li H, Li Y, Shi Y, Li S and Bai Y (2024) Role of MCP-1 as an inflammatory biomarker in nephropathy. *Front. Immunol.* 14:1303076. doi: 10.3389/fimmu.2023.1303076

Role of MCP-1 as an inflammatory biomarker in nephropathy

Yanlong Liu[1†], Ke Xu[2†], Yuhua Xiang[3], Boyan Ma[2], Hailong Li[3], Yuan Li[4], Yue Shi[2], Shuju Li[3*] and Yan Bai[3*]

[1]Heilongjiang Provincial Health Commission, Harbin, China, [2]Heilongjiang University of Chinese Medicine, The Second Clinical Medical College, Harbin, China, [3]Heilongjiang Academy of Traditional Chinese Medicine, Harbin, China, [4]The First Affiliated Hospital of Harbin Medical University, Harbin, China

The Monocyte chemoattractant protein-1 (MCP-1), also referred to as chemokine ligand 2 (CCL2), belongs to the extensive chemokine family and serves as a crucial mediator of innate immunity and tissue inflammation. It has a notable impact on inflammatory conditions affecting the kidneys. Upon binding to its receptor, MCP-1 can induce lymphocytes and NK cells' homing, migration, activation, differentiation, and development while promoting monocytes' and macrophages' infiltration, thereby facilitating kidney disease-related inflammation. As a biomarker for kidney disease, MCP-1 has made notable advancements in primary kidney diseases such as crescentic glomerulonephritis, chronic glomerulonephritis, primary glomerulopathy, idiopathic proteinuria glomerulopathy, acute kidney injury; secondary kidney diseases like diabetic nephropathy and lupus nephritis; hereditary kidney diseases including autosomal dominant polycystic kidney disease and sickle cell kidney disease. MCP-1 not only predicts the occurrence, progression, prognosis of the disease but is also closely associated with the severity and stage of nephropathy. When renal tissue is stimulated or experiences significant damage, the expression of MCP-1 increases, demonstrating a direct correlation with the severity of renal injury.

KEYWORDS

MCP-1, inflammatory markers, primary nephropathy, secondary nephropathy, hereditary nephropathy

1 Introduction

The immune system plays a crucial role in the pathogenesis of kidney disease. Dysfunction of the immune system in patients with kidney disease leads to injury to renal parenchymal cells, subsequently triggering an inflammatory response. Deposition of immune complexes within the kidneys disrupts normal renal function, resulting in manifestations such as proteinuria and fibrosis (1).

Chemokines are a class of small cytokines or signaling proteins secreted by cells that possess the ability to induce directional chemotaxis of nearby responsive cells. They play a crucial role in the migration of innate and adaptive immune cells and are closely associated with the initiation and maintenance of inflammatory response (2). Chemokines can be classified into four primary subfamilies, namely CXC, CC, CX3C, and XC. Monocyte chemoattractant protein-1 (MCP-1), also referred to as chemokine ligand 2 (CCL2), belongs to the CC subfamily of cytokines (3). The main producers of MCP-1 are monocytes and macrophages, although it is also expressed by various other cell types such as endothelial cells, fibroblasts, epithelial cells, smooth muscle cells, mesangial cells, astrocytes, and microglia (4, 5). Upon binding to its receptor, MCP-1 can induce homing, migration, activation, differentiation,and development of lymphocytes and NK cells; facilitate infiltration of monocytes and macrophages; promote inflammation occurrence; stimulate angiogenesis; as well as exert fibrotic effects (6). Studies have demonstrated that MCP-1 plays a significant role in fibrosis affecting multiple organs (7). When the renal tissue is stimulated, there is a notable rise in the expression level of MCP-1, which exhibits a strong positive correlation with the extent of renal injury. The primary mechanism involves MCP-1 activating monocytes through chemotaxis thereby promoting their secretion offibrogenic cytokines such as TGF-B,resulting in extracellular matrix accumulation within glomeruliand renal tubules leading to renal interstitial fibrosis,promoting glomerulosclerosis,and ultimately causing renal failure (8). Research has shown that the release of MCP-1 is controlled by both cytokines with pro-inflammatory properties and those with anti-inflammatory properties. Inflammatory cytokines, including IL-1, TNF-α, and IL-6, have the potential to augment MCP-1 secretion from renal tubular epithelial cells. On the other hand, anti-inflammatory cytokines like retinoic acid and glucocorticoids can inhibit MCP-1 secretion. Moreover, various cytokines or growth factors including IL-4, macrophage colony-stimulating factor, platelet-derived growth factor, TGF-β, lipopolysaccharide, reactive oxygen species, and immune complexes are also capable of inducing MCP-1 production and participating in the reparative processes following kidney injury (9).

Conventional clinical indicators, such as proteinuria levels, hypertension status, and decreased glomerular filtration rate (GFR), fail to effectively detect patients with substantial tubulointerstitial involvement or individuals at higher risk of accelerated disease progression (10, 11). The evaluation of interstitial fibrosis and tubular atrophy (IFTA) necessitates invasive and delayed renal biopsy, which hampers the ability to continuously monitor disease progression (12, 13). Blood urea nitrogen, GFR estimation formula, serum creatinine, and albuminuria are currently utilized to evaluate the presence and progression of diabetic nephropathy (DN). However, they lack precision and sensitivity towards minor changes in renal function (14, 15). The most dependable indicator for renal function in patients with autosomal dominant polycystic kidney disease (ADPKD) is the height corrected total kidney volume (htTKV). Nevertheless, it is relatively expensive and exhibits limited sensitivity (16, 17). Therefore, there is an urgent need to discover novel biomarkers that possess high sensitivity, specificity, and ease of operation. The role of MCP-1 as a non-invasive biomarker has garnered significant attention in research. In this context, the utilization of MCP-1 as an inflammation marker in nephropathy is summarized below.

2 MCP-1/CCR2 signaling axis and functional architecture

The MCP-1 gene is located on human chromosome 17q11.2-q21.1 (18), with a size of approximately 13 kilodaltons and consisting of 76 amino acid residues (19). Within its primary structure, there are two crucial regions for biological activity: amino acids 10 to 13 and amino acids 34 to 35 (3). Alterations in the former region result in reduced biological activity, while mutations in the latter region lead to a complete loss of MCP-1's activity. Four conserved cysteine residues can be found at positions 11, 12, 36, and 52 within the MCP-1 protein molecule (20). These cysteine residues form disulfide bonds between them, specifically Cys11-Cys36 and Cys12-Cys52 which create a left-handed helix structure. The presence of these disulfide bonds may be essential for maintaining MCP-1's biological function. In terms of secondary structure, MCP-1 consists of a four-stranded β-sheet along with an unstructured N-terminal loop and a C-terminal α-helix positioned above the Greek bond formed by β-folding process (21). The N-terminal segment plays a significant role in activating receptors associated with MCP-1 signaling pathway activation. Additionally, any missing residues at the N-terminal region would result in loss or reduction of its activity (21). Figure 1 illustrates the mechanism of MCP-1 as an inflammatory marker in nephropathy.

CCR2, the major receptor of MCP-1, belongs to the G protein-coupled receptor superfamily and consists of an amino-terminal extracellular domain and seven A-helix transmembrane structures rich in hydrophobic amino acids (22). CCR2 is widely expressed in immature dendritic cells, plasmacytoid dendritic cells, basophils, helper T cells 1, helper T cells 2, natural killer cells and helper T cells 17, etc (23). CCR2, as the main receptor of MCP-1, is an important chemokine in renal fibrosis. When MCP-1 binds to CCR2, the MCP-1/CCR2 axis is activated (24). Activation of the MCP-1/CCR2 axis induces chemotaxis and activation of inflammatory cells and initiates a series of signaling cascades in renal fibrosis (25). It mediates and promotes renal fibrosis by recruiting monocytes and promotes the activation and transdifferentiation of macrophages (26). The rationale for targeting MCP-1/CCR2 to treat human related diseases is to use drugs to block MCP-1 or CCR2 and inhibit the activation and conduction of the MCP-1/CCR2 axis, thereby reducing inflammatory cells and proinflammatory cytokines. Thus, the MCP-1/CCR2 axis is also a very important player in chemokine signaling in renal fibrosis (27).

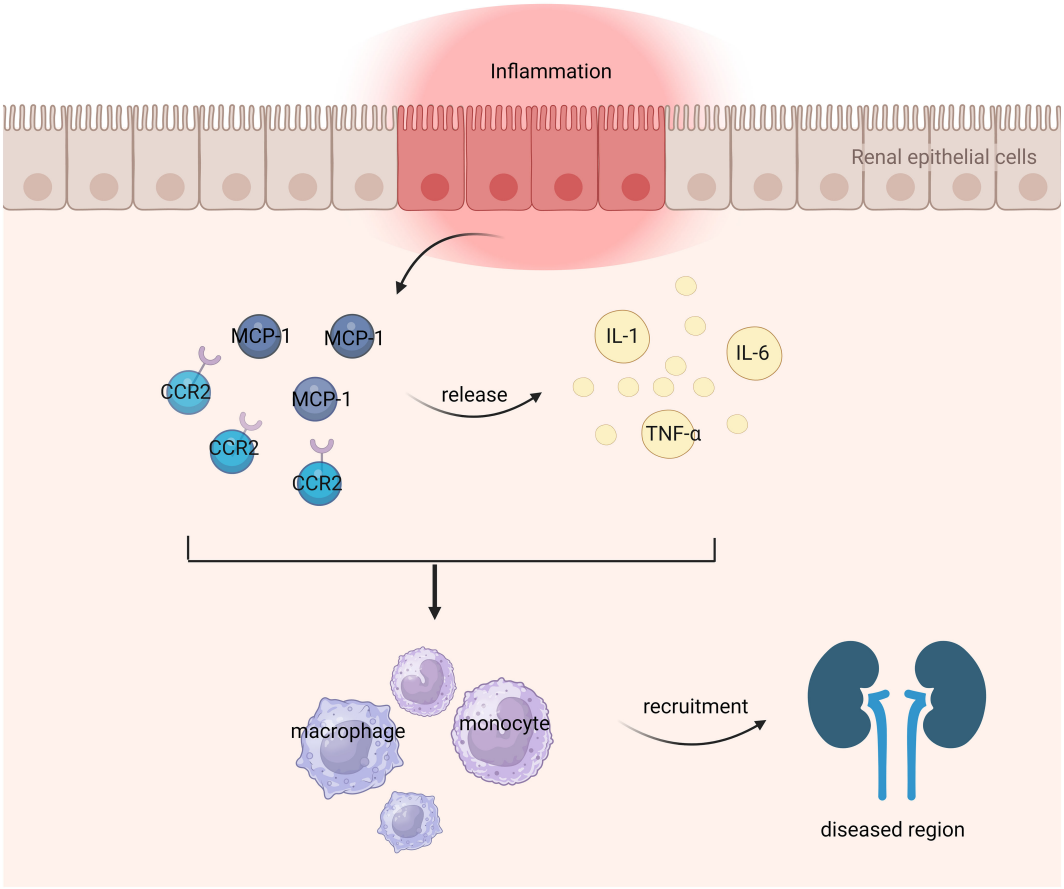

FIGURE 1
Role of MCP-1 as an inflammatory marker in nephropathy.

3 MCP-1 as a biomarker

3.1 Primary nephropathy

3.1.1 Crescentic glomerulonephritis

In a prospective cohort study, 82 patients with pathologically confirmed crescentic glomerulonephritis (CrGN) were followed up for 5 years to investigate the role of urinary chemokines and cytokines as prognostic biomarkers in CrGN patients. This study supports the clinical significance of baseline GFR and IFTA score, while previous research has demonstrated that urinary MCP-1 (uMCP-1) can be utilized as a predictive biomarker for assessing renal prognosis in patients with CrGN (28). MCP-1 is essential for attracting macrophages, which stimulates tissue factor expression and fibrin deposition, leading to glomerular crescent formation and subsequent promotion of chronic fibrosis phase in CrGN (29). Macrophage depletion can reduce kidney injury and glomerular crescents, whereas adoptive transfer of macrophages can exacerbate crescentic glomerulonephritis in mice (30). The reduction of MCP-1 levels can result in a decrease in crescent formation, deposition of type I collagen, and renal damage in a mouse model of glomerulonephritis (31). uMCP-1 shows potential as a predictor for favorable prognosis in CrGN; however, further studies are warranted.

3.1.2 Chronic glomerulonephritis

The progression of renal damage in individuals with chronic glomerulonephritis is significantly associated with the activation of the renin-angiotensin system (RAS). By evaluating the expression level of angiotensinogen (AGT) in glomerulonephritis and urinary AGT (uAGT), it becomes feasible to evaluate the extent of RAS activation within the renal region and determine the pathological state of chronic glomerulonephritis (32, 33). Hattori observed the levels of uAGT and uMCP-1 in a group of 48 children diagnosed with chronic glomerulonephritis prior to any treatment. Furthermore, they conducted an immunohistochemical analysis on AGT and CD68, while also investigating the impact of angiotensin II (Ang II) on MCP-1 expression in a separate group of 27 children who had undergone RAS blockade and received immunosuppressive agents for two years. The findings revealed a positive correlation between urinary protein level, mesangial cell proliferation score, crescent formation rate, as well as AGT and

CD68 expression in renal tissue with both uAGT and uMCP-1 levels (P<0.05). In addition, the levels of uAGT and uMCP-1 showed a significant reduction after the administration of RAS blockade and immunosuppressive therapy (p<0.01). Cultured human mesangial cells (MCs) exhibited elevated MCP-1 mRNA and protein levels after Ang II treatment (p<0.01). Therefore, both uMCP-1 and uAGT can serve as valuable biomarkers for assessing the extent of glomerular injury during RAS blockade and immunosuppressive therapy among children diagnosed with chronic glomerulonephritis (34).

3.1.3 Primary glomerulopathy

In a research investigation, urine specimens were obtained from individuals diagnosed with primary glomerulopathy (including IgA nephropathy, focal and segmental glomerulosclerosis, minimal change disease, membranous nephropathy) during the biopsy procedure. The value of MCP-1, EGF, and the EGF/MCP-1 ratio in predicting moderate to severe IFTA in primary glomerulonephritis was assessed using the enzyme-linked immunosorbent assay (ELISA). Univariate analysis identified connections between glomerular filtration rate, levels of EGF, the ratio of EGF to MCP-1, and IFTA. However, upon conducting multivariate analysis, it was determined that only the independent correlation between the EGF/MCP-1 ratio and IFTA remained significant. The sensitivity of the EGF/MCP-1 ratio in detecting IFTA was found to be 88%, while its specificity stood at 74% (35). Another study also came to a similar conclusion when investigating urinary biomarkers (EGF, MCP-1) and their ratio as predictors for achieving complete response in patients with biopsy-proven glomerulonephritis. The investigation also analyzed the association between these biomarkers and renal function following a period of 24 months. Complete remission (CR) was determined as the presence of urine protein levels equal to or less than 0.3 g/gCr. Out of 74 patients included in this study, 38 (51.4%) achieved CR status. The CR group exhibited significantly elevated baseline urinary levels of both EGF and the ratio of EGF/MCP-1 in comparison to the non-CR group. However, uMCP-1 did not exhibit a strong prognostic effect relative to EGF/MCP-1 (36).

3.1.4 Idiopathic proteinuria glomerulopathy

A cohort of 165 individuals, including 150 females, diagnosed with idiopathic albuminuric glomerulopathy and presenting a serum concentration below 68μmol/L at the time of diagnosis, were enrolled in this study. The uMCP-1 concentrations of these patients were measured using ELISA on the day of renal biopsy, followed by subsequent follow-up. The rate of progression in end-stage renal disease (ESKD) was assessed through the application of Kaplan-Meier survival analysis. The level of uMCP-1 excretion in patients with proliferative glomerulonephritis was significantly higher compared to those with non-proliferative glomerulonephritis (p<0.001). The percentage of patients exhibiting significantly worse renal function was 0.1% in the high uMCP-1 excretion group and 9.1% in the low uMCP-1 excretion group. However, after adjusting for confounding variables such as GFR and proteinuria, there was no significant association between uMCP-1 concentration and the progression of ESKD (HR = 1.75, 95%CI = 0.64-4.75, p = 0.27). Contrary to expectations, uMCP-1 could not be considered an independent predictor for long-term outcomes in patients with idiopathic glomerulonephritis (37). Nevertheless, it should be noted that this study's limitation lies in measuring uMCP-1 only once; thus it cannot differentiate between patients experiencing rapid remission or recurrent seizures. Further studies are warranted to repeat measurements of uMCP-1 levels throughout the course of the disease for analyzing its predictive ability regarding prognosis.

3.1.5 Acute kidney injury

The baseline estimated glomerular filtration rate (eGFR) of 2,351 participants in the SPRINT study was below 60 ml/min/1.73m^2. Exploratory factor analysis (EFA) was employed to capture distinct tubular pathophysiological processes, while a linear mixed-effect model was utilized to evaluate the association between each factor and longitudinal changes in eGFR. Cox proportional hazard regression analysis was conducted to assess the relationship between tubular factor scores and acute kidney injury (AKI). Among the 10 biomarkers examined, EFA revealed a reflection of tubular injury/fibrosis through KIM-1 and MCP-1, which were independently associated with an increased risk of AKI (HR 1.23 [1.02, 1.48]) (38). The longitudinal examination of AKI suggests that damage and inflammation may persist long after the initial insult. In a prospective cohort study involving 656 hospitalized subjects with AKI, multiple assessments of biomarkers were performed from diagnosis up to 7 months post-AKI. Cox proportional risk regression analysis was used to determine their association with a composite outcome comprising both incidence and progression of chronic kidney disease (CKD). After a follow-up period of 4.3 years, CKD and CKD progression were observed in 106 and 52 subjects respectively. Each increase in uMCP-1 levels by one standard deviation from baseline to one month was found to be significantly associated with a two- to three-fold increase in the risk of developing CKD (39). Other studies have controlled urinary concentrations for detecting biomarkers related to renal disease progression following AKI by using urinary creatinine (UCr) or urine osmolarity (UOsm) as covariates or calculating ratios such as biomarker-to-UCr ratio or biomarker-to-UOsm ratio for better prediction of outcomes. These studies have demonstrated that adjusting for UCr or UOsm strengthens the association and predictive ability for CKD when considering MCP-1 (40). The studies on MCP-1 in primary nephropathy are summarized in Table 1.

3.2 Secondary nephropathy

3.2.1 Diabetic nephropathy

The presence of macroalbuminuria serves as a crucial indicator for the progression of DN (41), with most studies focusing on renal function decline or the development of ESRD in DN patients. The predictive value of uMCP-1 in determining the risk of requiring dialysis, experiencing a doubling of serum creatinine levels, or facing mortality (referred to as the primary outcome, PO) was assessed in a cohort of 56 patients with DN and type 2 diabetes mellitus (T2DM),

TABLE 1 MCP-1 as a marker of inflammation in primary nephropathy.

Research	Disease	Research Methods	Subjects	Sample Size	Source	Result
(28)	crescentic glomerulonephritis	prospective cohort study	human	36	urine and serum	urinary MCP-1, IL-10 and fractalkine are favorable prognostic markers
(34)	chronic glomerulonephritis	Clinical Research	human	48	urine	uMCP-1 and uAGT are available biomarkers
(35)	primary glomerulopathy	controlled trial	human	76	urine	EGF/MCP-1 ratio is independently associated IFTA severity
(35)	primary glomerulopathy	prospective cohort study	human	74	urine	In contrast to EGF/MCP-1, uMCP-1 did not show a strong prognostic effect
(37)	idiopathic proteinuria glomerulopathy	Long-Term Follow-Up Study	human	165	urine	Progression to ESRD in patients with idiopathic glomerulopathy was not associated with urinary MCP-1 concentration at diagnosis
(38)	acute kidney injury	Observational cohort nested in a clinical trial	human	2351	urine and serum	MCP-1 is associated with future risk for AKI
(39)	acute kidney injury	prospective cohort study	human	656	urine	Each SD increase in the change of uMCP-1 from baseline to 12 months was associated with 2- to 3-fold increased risk for CKD
(40)	acute kidney injury	prospective cohort study	human	1583	urine	The associations and predictions with CKD were significantly strengthened after indexing or adjusting for UCr or UOsm for urine kidney injury MCP-1 in patients with AKI

who also had macroalbuminuria. This analysis was conducted over a follow-up period lasting approximately 30.7 ± 10 months. In Cox regression analysis, uMCP-1 levels were positively associated with the risk of PO. After adjusting for baseline albuminuria, blood pressure, and baseline creatinine, uMCP-1 (OR 11.0; 95% CI 1.6-76.4, p=0.02 for log MCP-1) remained a significant independent predictor of PO. The study concluded that uMCP-1 is independently associated with the risk of CKD progression in DN patients with macroalbuminuria. However, further investigation is needed to determine whether these biomarkers also play a role in DN patients with normoalbuminuria and microalbuminuria (42). The urinary albumin is initially filtered through the glomerulus and subsequently reabsorbed by renal tubular cells via the pathway mediated by giant protein-cubes (43). A study conducted in 2020 arrived at a similar conclusion by evaluating levels of urinary markers, such as MCP-1, in individuals with DN and analyzing their associations with eGFR and albuminuria. Urinary markers like MCP-1 exhibited significant associations with eGFR (MCP-1/Cr, p=0.023) and albuminuria (MCP-1/Cr, p<0.001). This study suggests that there is a widespread increase in urinary markers during advanced stages of DN (the extremely high risk/macroalbuminuria group), indicating their greater prominence during progressive glomerular and tubular structural abnormalities and dysfunction. Even after accounting for risk factors related to DN, the association between MCP-1/Cr and both eGFR and albuminuria remained statistically significant (44). Diabetes is recognized as the leading cause of ESKD. By examining the correlation between biomarkers indicative of tubular damage or repair, such as uMCP-1, renal function decline, and mortality rates; it was found that individuals within the highest quartile of MCP-1 had a 2.18-fold increased risk of experiencing renal function decline compared to those within the lowest quartile when considering fully adjusted models. Furthermore, for every twofold increase in baseline levels of urinary markers like MCP-1, there was an associated 10% to 40% higher risk of death (45).

The relationship between early normoalbuminuria and microalbuminuria in DN and biomarkers has been insufficiently investigated. The study included seventy-five type 2 diabetic patients with normoalbuminuria (n=25), microalbuminuria (n=25), or macroalbuminuria (n=25), as well as twenty-five healthy controls. The level of uMCP-1 was measured using ELISA. Significantly elevated levels of uMCP-1 were observed in DN patients with macroalbuminuria and microalbuminuria compared to those with normoalbuminuria and the healthy controls. Receiver operating characteristic (ROC) curve analysis was conducted to determine the optimal threshold of uMCP-1 for early diagnosis and detection of DN. The identified cut-off value was 110 pg/mg, demonstrating a sensitivity of 92% and specificity of 100%. The findings suggest that uMCP-1 holds potential as a promising novel diagnostic biomarker for the early detection of DN (46). A composite panel consisting of six biomarkers, namely osteopontin, soluble human tumor necrosis factor receptor-1, tenascin-C, vascular endothelial growth factor-a, and kidney injury molecule-1 (KIM-1), was developed using LASSO technique in a cohort of 346 normoalbuminic T2DM patients. The research findings demonstrated that a novel panel comprising six urinary biomarkers including MCP-1 effectively predicted the onset of microalbuminuria in T2DM patients with normal albuminuria (47).

The level of MCP-1 is also associated with gender, and RASS may have a significantly greater impact on interstitial lesions compared to glomerular lesions in detecting the effect of uMCP-1 on early DN (48). In this research, women exhibited a

comparatively elevated initial level of uMCP-1, which displayed a more pronounced association with renal interstitial dilatation. This underscores the significance of gender as a potential risk factor for DN. Early detection of elevated uMCP-1 levels in women with T1DM may suggest a potential link between inflammatory processes and the development of renal interstitial changes during the initial stages of DN (49).

Most of the studies investigating MCP-1 and human kidney disease have primarily focused on urine, with limited research conducted on plasma or serum MCP-1 levels. uMCP-1 has been associated with unfavorable outcomes such as graft failure (50), heart disease (51), increased mortality in kidney transplant recipients (52), and impaired renal function in individuals with preserved renal function who have T2DM (53). However, there was no significant association found between serum MCP-1 concentration and decreased eGFR in T2DM patients with relatively preserved renal function (54). This study observed an elevated risk of DN progression with higher plasma MCP-1 concentrations, but only among individuals with baseline eGFR less than 45 ml/min per 1.73 m2. It is noteworthy that this study presents innovative findings regarding the association between plasma MCP-1 levels and the progression of DN in patients with moderate to severe CKD (55). Extracellular vesicles (EVs), which encompass exosomes and microvesicles, play a vital role in facilitating intercellular communication by transporting biomolecules like mRNA (56). The investigation focused on MCP-1 mRNA expression within blood EVs of patients with DN to determine its accuracy in predicting the early stages of DN. Quantitative analysis of the mRNA profile within blood EVs was conducted using qRT-PCR, while the diagnostic effectiveness of mRNA was evaluated through ROC curve analysis. A total of 196 subjects were enrolled, including 35 patients with overt DN, 53 patients with newly diagnosed DN, 62 patients with DM, and 46 healthy subjects. The predictive accuracy of MCP-1 mRNA for overt DN was determined to be at a level of 0.66 (95%CI:0.55–0.77), whereas its accuracy for predicting early-stage DN stood at a level of 0.61 (95%CI:0.51–0.71) (57).

3.2.2 Lupus nephritis

A study was conducted on 20 patients with LN episodes to evaluate the association between uMCP-1 and LN severity, as well as its role as a prognostic predictor. The concentrations of uMCP-1 exhibited a significant rise in cases of acute LN (2.74 ± 0.95 ng/mg creatinine), moderate LN (1.43 ± 0.46 ng/mg creatinine), and mild LN (0.76 ± 0.57 ng/mg). There was a notable association observed between the severity of LN and the level of uMCP-1 ($P<0.0358$), suggesting that uMCP-1 could potentially serve as a noninvasive indicator for evaluating the grade and onset of LN. Throughout the follow-up period, 15 patients achieved either complete or partial response, resulting in a significant reduction in average uMCP-1 levels by week 8 ($P<0.0001$). However, for the five participants who did not respond to treatment, there was no significant alteration in average uMCP-1 levels by week 8 ($P<0.4858$), indicating that a lack of reduction in uMCP-1 levels at this point may indicate an unfavorable prognosis (58). The correlation coefficients and area under curve (AUC) between renal damage and uMCP-1 and tumor necrosis factor-like weak inducer of apoptosis (uTWEAK) were found to be significantly higher. The combined model of uMCP-1 and uTWEAK demonstrated an AUC of 0.887 for distinguishing active LN, with a sensitivity of 86.67% and specificity of 80.00%. For distinguishing poor prognosis LN, the AUC was 0.778, with a sensitivity of 75.00% and specificity of 81.82%. These results indicate that the combination of both biomarkers outperforms their individual use (59). Another study evaluated uMCP-1 and uTWEAK separately, revealing sensitivities for detecting active LN as follows: uTWEAK - 80.43% and 100%, while specificities were recorded at 50% and 100%, respectively; for uMCP-1 - sensitivities were observed at 82.6% and 100%, with specificities also at values of 50% and 100%, respectively (60). Furthermore, Moloi's study concluded that during the active phase, levels of uMCP-1 are elevated but decrease after CR (61). Additionally, MCP-1 has shown potential in predicting tubulointerstitial lesions in early stages compared to traditional markers when investigating patients diagnosed with active DN through pathological biopsy analysis involving a cohort consisting of 109 LN patients along with a control group comprising 50 individuals without any kidney abnormalities. "The levels of uMCP-1 showed a marked elevation in patients diagnosed with active LN compared to those diagnosed with inactive LN ($P<0.001$) or individuals from the normal control group ($P<<0.001$) (62). Additionally, heightened levels of uMCP-l correlated positively with intensified infiltration of inflammatory cells within the interstitium, as well as increased interstitial fibrosis and tubular atrophy.

In the clinical evaluation process, quantification of proteinuria is crucial as it serves as one of the determinants for renal prognosis. The 24-hour urinary protein excretion test has traditionally been considered the "gold standard" for measuring proteinuria. However, due to its inconvenience and potential inaccuracies, many kidney disease guidelines now recommend using urinary protein/creatinine ratio (uPCR) and urinary albumin/creatinine ratio (uACR) instead (63). Relevant research has been conducted on MCP-1 as a promising candidate for biomarker identification in LN. Spearman correlation analysis was utilized to investigate the association between uMCP-1 and conventional clinical indicators. The diagnostic efficacy of uMCP-1 and uACR in assessing proteinuria levels was evaluated through ROC curve analysis. Patients with biopsy-proven LN exhibited higher levels of uMCP-1 compared to those without LN. In addition, elevated levels of both uMCP-1 and uTWEAK were observed in patients with active renal involvement (rSLEDAI ≥4). Significantly, a strong association was observed between uMCP-1 levels and the rSLEDAI score, 24-hour urinary protein excretion, and anti-double-stranded DNA antibodies in the patient cohort. Furthermore, there was a positive correlation observed between the severity of LN damage and the levels of both uMCP-1 and uTWEAK; thus suggesting that their combined use could potentially serve as a predictor for LN-associated proteinuria (64).

In relation to different pathological categories, the assessment of MCP-1 levels in various forms of LN demonstrated notably elevated urine and serum MCP-1 levels in the proliferative group compared to the non-proliferative group. The urine and serum MCP-1 levels observed in the proliferation group were 1240.65 ± 876.38 pg/ml

creatinine and 354.49 ± 598.60 pg/ml creatinine, respectively. Conversely, the urine and serum MCP-1 levels noted in the non-proliferative group were 544.47 ± 430.63 pg/ml creatinine and 200.40 ± 171.83 pg/mL creatinine, correspondingly (65). The non-selective immunosuppressive drugs utilized in the clinical management of proliferative LN are associated with significant adverse effects (66). In an attempt to identify a more targeted therapeutic agent with comparable efficacy but reduced side effects, one study focused on inhibiting MCP-1 and the homeostatic chemokine stromal cell-derived factor-1 (SDF-1/CXCL12). L-enantiomeric RNA Spiegelmer® chemokine antagonists, specifically MCP-1-specific mN 0X-E36 and CXCL12-specific N 0X-A12, will be administered to female MRL/lpr mice aged between 12 and 20 weeks. Research has demonstrated that simultaneous blockade of MCP-1 and CXCL12 can effectively impede the progression of proliferative LN similar to cyclophosphamide, a non-selective immunosuppressant (67).

In terms of gene prediction, a study utilizing data from gene network and GO analysis was conducted to identify candidate genes associated with LN in macrophages, revealing MCP-1's localization in the core of the network. Further investigations have provided insights into the gene expression pattern of macrophages and revealed that macrophages derived from LN patients exhibit an upregulation of MCP-1. The Rat Genome Database (RGD) disease portal database has also indicated the association between MCP-1 and the development as well as progression of LN (68). A study conducted in Egypt aimed to investigate the potential of MCP-1 gene polymorphism as an early indicator for the development of nephropathy in patients with systemic lupus erythematosus (SLE). The findings revealed that individuals with a genotype of A/A were more prevalent among healthy controls compared to SLE patients. On the other hand, genotypes A/G ($P < 0.000$) and G/G ($P < 0.000$) were found to be more common among SLE patients than in the control group. It was observed that carriers of the G allele at MCP-1-2518 polymorphism had a significantly higher risk, over seven times, for developing nephropathy within the SLE patient population. Furthermore, patients with A/G and G/G genotypes exhibited notably elevated levels of MCP-1 when compared to those with an A/A genotype. Both MCP-1A (−2518) G gene polymorphism and increased levels of MCP-1 are believed to play crucial roles in the occurrence and progression specifically of SLE-associated nephropathy within Egypt (69). In a meta-analysis conducted in 2017 assessing the association between MCP-1 -2518A/G polymorphism and LN risk, a total sample size consisting of 1867 LN cases from 961 published case-control studies along with 10 control groups were included. The findings indicated a higher susceptibility to LN in individuals with the MCP-1 -2518A/G polymorphism. However, when stratified by ethnicity, no significant association was observed within European or Asian populations but rather predominantly found within US population due to potential genetic background variations as well as environmental exposures (70).

For comparison between urine and blood, Gupta measured serum MCP-1 and uMCP-1 in patients with ELISA. Urinary creatinine excretion values were standardized. Baseline uMCP-1 was significantly higher in active nephritis (AN) compared with active disease without nephritis (ANR), inactive disease (ID), healthy subjects (HC), and rheumatoid arthritis (RA) ($p<0.001$), but did not differ from DN and showed a good correlation with rSLEDAI and SLEDAI ($r = 0.52$ and 0.47, $p<0.001$), but not correlated with serum MCP-1 levels. uMCP-1 performed better than serum MCP-1, anti-dsdna antibody, C3, and C4 in ROC analysis to distinguish active nephritis from active disease without nephritis. uMCP-1 but not serum MCP-1 decreased significantly ($p<0.001$) (71). The 2022 study marks the initial exploration into the durability of emerging urinary biomarkers for LN, with a specific focus on assessing the renal activity index for lupus (RAIL). This comprehensive index incorporates MCP-1, KIM-1, ceruloplasmin, adiponectin, neutrophil gelatinase-associated lipocalin (NGAL), and blood phosphate. The findings demonstrate that urine biomarkers stored at -80°C for a duration of 3 months or at either 4 or 25°C for a period of 48 hours followed by storage at -80°C exhibit comparable results to freshly collected urine samples. Regardless of the conditions examined, there was no degradation in signal quality observed when exposed to dry or wet ice, or when subjected to two freeze-thaw cycles. The Spearman correlation coefficients indicated a high level of concordance. These findings suggest that RAIL biomarkers exhibit consistent stability even following brief storage under conditions relevant to clinical settings, and are capable of enduring transportation, extended storage periods, as well as multiple freeze-thaw cycles prior to bulk measurements. Table 2 summarizes the studies of MCP-1 in secondary nephropathy.

3.3 Hereditary nephropathy

3.3.1 Autosomal dominant polycystic kidney disease

The urinary biomarkers uMCP-1, KIM-1, immunoglobulin G, 24-hour urinary albumin, β2-microglobulin (β2MG), heart-type fatty acid binding protein, and NGAL were evaluated at the beginning of the study. The changes in eGFR for each participant over time were calculated using mixed-model analysis. After accounting for age, gender, and initial htTKV levels, all indicators of urinary impairment and inflammation demonstrated correlations with baseline eGFR. Subsequent backward analysis identified uMCP-1 and β2MG as the most strongly associated factors with accelerated disease progression. When the participants were divided into three groups based on levels of uMCP-1 and β2MG, the urine biomarker score showed a stronger predictive value compared to Mayo htTKV classification (area under the curve [AUC] 0.73 [0.64-0.82] vs. 0.61 [0.51-0.71], $p = 0.04$). Similar to the PROPKD score (AUC 0.73 [0.64-0.82] vs.65

TABLE 2 MCP-1 as a marker of inflammation in secondary nephropathy.

Research	Disease	Research Methods	Subjects	Sample Size	Source	Result
(42)	Diabetic nephropathy	double-blind placebo-controlled randomized clinical trial	human	56	urine	Urinary MCP-1 and RBP are independently related to the risk of CKD progression in patients with macroalbuminuric DN
(44)	Diabetic nephropathy	cohort study	human	185	urine	The level of MCP-1 increased with the severity of diabetic nephropathy
(45)	Diabetic nephropathy	double-blinded, randomized, controlled trial	human	712	urine	Higher baseline levels of MCP-1 (per 2-fold higher) were independently associated with 10–40% higher risk of mortality
(46)	Diabetic nephropathy	rosssectional study	human	100	urine	uMCP-1was 110 pg/mg with 92% sensitivity and 100% specificity
(47)	Diabetic nephropathy	cohort study	human	346	urine	The panel consisting of six novel urinary biomarkers effectively predicted incident microalbuminuria in people with type 2 diabetes
(49)	Diabetic nephropathy	multicenter clinical trial	human	224	urine	Elevated uMCP-1 concentration measured before clinical findings of DN in women with T1D was associated with changes in kidney interstitial volume
(53)	Diabetic nephropathy	nested case-control design	human	190	urine	Urinary monocyte chemotactic protein-1-to-creatinine ratio concentrations were strongly associated with sustained renal decline in patients with T2DM with preserved renal function
(55)	Diabetic nephropathy	cohort study	human	894	plasma	Higher plasma levels of MCP-1 was associated with increased risk of progression of DN
(57)	Diabetic nephropathy	controlled trial	human	196	blood EVs	MCP-1 mRNAs expression in blood EVs could serve as diagnostic biomarkers for early-stage DN
(58)	Lupus nephritis	controlled trial	human	40	urine	uMCP-1 could be used as a non-invasive marker for the judgement of lupus flare and lupus nephritis class
(59)	Lupus nephritis	controlled trial	human	90	urine	The combined model of uMCP-1 and uTWEAK was superior to any marker used alone
(60)	Lupus nephritis	controlled trial	human	114	urine	uMCP-1 and uTWEAK have high sensitivity and specificity in detecting active LN
(61)	Lupus nephritis	prospective observational study	human	20	urine	uMCP-1 and uTWEAK are biomarkers for active LN
(62)	Lupus nephritis	controlled trial	human	159	urine	uMCP-1 level in patients with LN is correlated with renal injury indicators
(64)	Lupus nephritis	controlled trial	human	69	urine	uMCP-1 can be used as a potential predictor of proteinuria in LN
(65)	Lupus nephritis	controlled trial	human	178	urine and serum	MCP-1 may be associated with different pathological types of LN
(67)	Lupus nephritis	controlled trial	human	120	serum	Dual blockade of CCL 2 and CXCL12 can inhibit the progression of proliferative LN
(69)	Lupus nephritis	controlled trial	human	220	urine and serum	carriers of G allele of the MCP-1 2518 polymorphism had more than 7 fold increased risk to develop glomerulo-nephropathy in patients with SLE
(71)	Lupus nephritis	controlled trial	human	121	urine and serum	uMCP-1 correlates well with LN disease activity and helps differentiate between AN and ANR patients. Its levels fall with treatment and may have a potential to predict poor response and relapse of LN

[.55-.75], p =0.18), these findings suggest that proximal tubules and inflammation contribute to the pathophysiology of ADPKD. Furthermore, this urine marker is more user-friendly than traditional markers (72). Another study enrolled 130 patients with ADPKD, 55 patients with renal vascular sclerosis, and 40 patients with non-ischemic CKD. The study revealed a significant upregulation of uMCP-1 under ischemic conditions. In univariate analysis, htTKV emerged as the most reliable predictor of eGFR slope variability. However, a multivariate model incorporating uMCP-1, VEGF, and β2MG levels demonstrated an enhanced ability to predict decreased eGFR in ADPKD patients compared to htTKV alone. Urinary levels of molecules associated with renal ischemia (VEGF and MCP-1) or tubular injury (β2MG) were correlated with deteriorating renal function in ADPKD patients, thus suggesting their potential as biomarkers for monitoring disease progression (73). Additionally, another study identified associations between uMCP-1 and β2MG levels and annual changes in eGFR even after adjusting for traditional risk markers (standardized β = -0.35, P = 0.001; standardized β = -0.29,P = 0.009). Incorporating uMCP-1 and β2MG into the model containing traditional risk markers significantly improved its performance (final R2 = 0.152 vs. 0.292, P = 0.001). Therefore, uMCP-1 and β2MG levels are independently linked to decreased GFR in ADPKD patients and offer greater predictive value than conventional risk indicators (74). Furthermore, several studies have assessed the urinary concentrations of 28 biomarkers in ADPKD patients while gene expression analysis has been conducted on kidneys from DBA/2FG-pcy mice alongside urine samples from these mice to evaluate the efficacy of biomarkers.The findings indicated that out of the prospective urinary biomarkers examined, twelve exhibited statistical significance with high specificity observed for uMCP-1.Moreover,the content of uMCP-1 was significantly elevated in urine samples from DBA/2FG-pcy mice compared to wild-type mice,suggesting its potential utility as a urinary biomarker for ADPKD (75).

MCP-1 may facilitate the expansion of renal cysts in ADPKD patients with PKD1 or PKD2 mutations by promoting macrophage-mediated processes. The abnormal accumulation of macrophages around the cysts promotes their growth (76). In order to explore the potential contribution of MCP-1 and macrophages in facilitating cyst expansion, a study was conducted where Pkd1 knockout alone (single knockout) or both Pkd1 and MCP-1 were knocked out in mouse renal tubules. Upregulation of MCP-1 preceded the infiltration of macrophages in single-gene knockout mice. Initially, macrophages induce a proinflammatory response and cause damage to renal tubular cells, leading to oxidative DNA damage, morphological flattening, and proliferation-dependent cystic expansion within 0-2 weeks after induction. At 2-6 weeks after induction, macrophages switch to an alternative activation phenotype that further promotes cyst growth by increasing the rate of renal tubular cell proliferation threefold more than before. In double knockout mice, reduced expression of MCP-1 and fewer numbers of macrophages resulted in less initial tubular cell damage, slower cyst growth, and improved renal function. The upregulation of MCP-1 following Pkd1 knockdown promotes the accumulation of macrophages and subsequent cyst growth through a mechanism dependent on cellular proliferation (77). The objective of this research was to examine how the absence of MCP-1 affects the concentration of macrophages in the kidneys and the progression of disease in a mouse model with congenital polycystic kidney (Cpk). To achieve this, a genetic knockout of MCP-1 was generated. The results revealed that Cpk mice exhibited rapid enlargement of renal cysts, leading to decreased renal function and mortality by postnatal day 21. However, the genetic knockdown of MCP-1 extended the survival rate, with some mice living for more than 3 months. Notably, the MCP-1 genetic knockout effectively prevented the development of pulmonary edema observed in Cpk mice and also facilitated a decrease in resting heart rate along with an increase in heart rate variability in both Cpk and non-cystic mice. These findings suggest that besides its role as a macrophage chemoattractant (78), MCP-1 plays a significant role in altering cardiac and lung function while promoting mortality in this mouse model of ADPKD.

3.3.2 Sickle cell kidney disease

In a cross-sectional study of 213 children with sickle cell disease (SCD), the researchers discovered that the presence of glomerular damage was associated with elevated levels of inflammatory biomarkers, such as uMCP-1. Additionally, a short-term prospective observational cohort study involving 89 children was conducted to assess the predictive value of changes in urinary inflammatory biomarkers like MCP-1 over time for the development of glomerular proteinuria. The findings suggest that inflammatory molecules may play a crucial role in both the progression and onset of kidney disease in pediatric patients with SCD. Patients exhibiting albuminuria had significantly higher levels of inflammatory biomarkers, including MCP-1, compared to those without albuminuria. Correlation analysis revealed a significant positive association between the albumin/creatinine ratio and inflammatory biomarkers like MCP-1. These findings have important implications for understanding inflammation's involvement in kidney disease among children with SCD and identifying potential therapeutic targets (79). Furthermore, MCP-1, which is potentially indicative of kidney damage in sickle cell patients, has also been linked to oxidative stress status. This study assessed blood and urine samples to evaluate MCP-1 levels and their correlation with malondialdehyde, a product resulting from lipid peroxidation. The results demonstrated significantly elevated levels of MCP-1 in SCD patients along with a positive correlation between MCP-1 and malondialdehyde levels, suggesting its

potential as a biomarker for kidney damage associated with SCD as well as reflecting oxidative stress-induced harm present within this condition. Consequently, this research provides valuable insights into diagnosing and treating kidney damage related to SCD (80, 81). Table 3 summarizes the studies of MCP-1 in hereditary nephropathy.

4 Conclusion

The investigation of MCP-1 as a biomarker in primary nephropathy is limited, primarily encompassing certain glomerular diseases; however, it has demonstrated significant value in crescentic glomerulonephritis,chronic glomerulonephritis and AKI. Based on current research findings, MCP-1 exhibits potential utility in primary nephropathy; nevertheless, its specificity and sensitivity are relatively low, rendering it unsuitable for independent prediction.

In terms of secondary nephropathy, the research on MCP-1 primarily focuses on DN and LN. MCP-1 has been extensively investigated in various stages of DN, including early stage, progression, and ESKD. Nevertheless, early prediction remains understudied and the majority of research has centered on uMCP-1 as opposed to blood MCP-1. Additionally, gender correlation has been observed in DN. Regarding LN, MCP-1 has been well-studied and shows significant correlation with disease severity and prognosis. It exhibits increased levels during active stages and decreased levels during remission stages. Moreover, increased MCP-1 levels are linked to the infiltration of inflammatory cells in the interstitial space, fibrosis in the interstitium, and atrophy of tubules. Notably, compared to traditional markers for prediction purposes in this context. uMCP-1 can serve as a promising predictor of proteinuria in LN, with higher levels observed in proliferative LN. In terms of the genetic aspect, MCP-1-2518A/G is closely associated with the pathogenesis of LN. Additionally, uMCP-1 exhibits excellent storage stability and holds great potential as a biomarker.

In the context of hereditary kidney diseases, the level of uMCP-1 is associated with a decline in GFR among patients with ADPKD, and it exhibits superior predictive value compared to traditional risk indicators while also being more operationally convenient. Within the realm of ADPKD, MCP-1 facilitates macrophage accumulation and cyst growth through a proliferation-dependent mechanism, thereby contributing to cardiac lesions, pulmonary edema, and mortality. Patients with SCD often have glomerular and tubular dysfunction, and the emergence of some new non-invasive urine biomarkers, such as MCP-1, provides hope for early diagnosis and treatment strategies. Biomarkers expand the methods and indicators for the assessment of renal function in SCD, and provide a new way for early diagnosis and treatment. The practical significance is that it provides a non-invasive, simple, and reproducible method for renal function assessment, which helps to improve the clinical management and treatment outcomes of patients with SCD.

TABLE 3 MCP-1 as a marker of inflammation in hereditary nephropathy.

Research	Disease	Research Methods	Subjects	Sample Size	Source	Result
(72)	Autosomal dominant polycystic kidney disease	prospective randomized controlled trial	human	302	urine	uMCP-1 can screen ADPKD patients with rapid disease progression
(73)	Autosomal dominant polycystic kidney disease	controlled trial	human	225	urine	uMCP-1 is associated with deterioration of renal function in patients with ADPKD
(74)	Autosomal dominant polycystic kidney disease	controlled trial	human	104	urine	uMCP-1 excretion were both associated with GFR decline in ADPKD
(75)	Autosomal dominant polycystic kidney disease	gene expression analysis	human and mice	huaman(29), mice(2)	urine	uMCP-1 can be a potential common biomarker for human and murine ADPKD
(77)	Autosomal dominant polycystic kidney disease	Animal experiments	mice	Not explicitly mentioned	gene	MCP-1 was upregulated after Pkd1 knockdown
(78)	Autosomal dominant polycystic kidney disease	Animal experiments	mice	Not explicitly mentioned	gene	MCP-1 altered cardiac/pulmonary function
(79)	Sickle cell kidney disease	prospective cohort study	human	213	urine	Albumin/creatinine ratio was significantly positively correlated with MCP-1
(80)	Sickle cell kidney disease	prospective cohort study	human	50	urine	MCP-1 can also reflect damage caused by oxidative stress present in SCD.

Author contributions

YaL: Writing – original draft. KX: Writing – original draft. YX: Investigation, Writing – review & editing. BM: Investigation, Writing – review & editing. HL: Supervision, Writing – review & editing. YuL: Data curation, Writing – review & editing. YS: Data curation, Writing – review & editing. SL: Writing – review & editing, Writing – original draft. YB: Writing – review & editing, Writing – original draft.

Funding

The author(s) declare that no financial support was received for the research, authorship, and/or publication of this article.

Conflict of interest

The authors declare that the research was conducted in the absence of any commercial or financial relationships that could be construed as a potential conflict of interest.

Publisher's note

References

1. He S, Yao L, Li J. Role of MCP-1/CCR2 axis in renal fibrosis: Mechanisms and therapeutic targeting. *Med (Baltimore)* (2023) 102(42):e35613. doi: 10.1097/md.0000000000035613

2. Hughes CE, Nibbs RJB. A guide to chemokines and their receptors. *FEBS J* (2018) 285(16):2944–71. doi: 10.1111/febs.14466

3. Singh S, Anshita D, Ravichandiran V. MCP-1: Function, regulation, and involvement in disease. *Int Immunopharmacol* (2021) 101(Pt B):107598. doi: 10.1016/j.intimp.2021.107598

4. Chen Y, Liu S, Wu L, Liu Y, Du J, Luo Z, et al. Epigenetic regulation of chemokine (CC-motif) ligand 2 in inflammatory diseases. *Cell Prolif* (2023) 56(7):e13428. doi: 10.1111/cpr.13428

5. Galipeau J. Macrophages at the nexus of mesenchymal stromal cell potency: The emerging role of chemokine cooperativity. *Stem Cells* (2021) 39(9):1145–54. doi: 10.1002/stem.3380

6. Cianci R, Simeoni M, Cianci E, De Marco O, Pisani A, Ferri C, et al. Stem cells in kidney ischemia: from inflammation and fibrosis to renal tissue regeneration. *Int J Mol Sci* (2023) 24(5):4631. doi: 10.3390/ijms24054631

7. Lv W, Booz GW, Wang Y, Fan F, Roman RJ. Inflammation and renal fibrosis: Recent developments on key signaling molecules as potential therapeutic targets. *Eur J Pharmacol* (2018) 820:65–76. doi: 10.1016/j.ejphar.2017.12.016

8. Sandokji I, Greenberg JH. Plasma and urine biomarkers of CKD: A review of findings in the CKiD study. *Semin Nephrol* (2021) 41(5):416–26. doi: 10.1016/j.semnephrol.2021.09.003

9. Haller H, Bertram A, Nadrowitz F, Menne J. Monocyte chemoattractant protein-1 and the kidney. *Curr Opin Nephrol Hypertens* (2016) 25(1):42–9. doi: 10.1097/mnh.0000000000000186

10. Greenberg JH, Abraham AG, Xu Y, Schelling JR, Feldman HI, Sabbisetti VS, et al. Urine biomarkers of kidney tubule health, injury, and inflammation are associated with progression of CKD in children. *J Am Soc Nephrol* (2021) 32(10):2664–77. doi: 10.1681/asn.2021010094

11. Tam FWK, Ong ACM. Renal monocyte chemoattractant protein-1: an emerging universal biomarker and therapeutic target for kidney diseases? *Nephrol Dial Transplant* (2020) 35(2):198–203. doi: 10.1093/ndt/gfz082

12. Islamoglu MS, Gulcicek S, Seyahi N. Kidney tissue elastography and interstitial fibrosis observed in kidney biopsy. *Ren Fail* (2022) 44(1):314–9. doi: 10.1080/0886022x.2022.2035763

13. Ix JH, Shlipak MG. The promise of tubule biomarkers in kidney disease: A review. *Am J Kidney Dis* (2021) 78(5):719–27. doi: 10.1053/j.ajkd.2021.03.026

14. Pérez-López L, Boronat M, Melián C, Brito-Casillas Y, Wägner AM. Animal models and renal biomarkers of diabetic nephropathy. *Adv Exp Med Biol* (2021) 1307:521–51. doi: 10.1007/5584_2020_527

15. Jung CY, Yoo TH. Pathophysiologic mechanisms and potential biomarkers in diabetic kidney disease. *Diabetes Metab J* (2022) 46(2):181–97. doi: 10.4093/dmj.2021.0329

16. Shukoor SS, Vaughan LE, Edwards ME, Lavu S, Kline TL, Senum SR, et al. Characteristics of patients with end-stage kidney disease in ADPKD. *Kidney Int Rep* (2021) 6(3):755–67. doi: 10.1016/j.ekir.2020.12.016

17. Kim K, Trott JF, Gao G, Chapman A, Weiss RH. Plasma metabolites and lipids associate with kidney function and kidney volume in hypertensive ADPKD patients early in the disease course. *BMC Nephrol* (2019) 20(1):66. doi: 10.1186/s12882-019-1249-6

18. Wang L, Lan J, Tang J, Luo N. MCP-1 targeting: Shutting off an engine for tumor development. *Oncol Lett* (2022) 23(1):26. doi: 10.3892/ol.2021.13144

19. Zhang H, Yang K, Chen F, Liu Q, Ni J, Cao W, et al. Role of the CCL2-CCR2 axis in cardiovascular disease: Pathogenesis and clinical implications. *Front Immunol* (2022) 13:975367. doi: 10.3389/fimmu.2022.975367

20. Miller MC, Mayo KH. Chemokines from a structural perspective. *Int J Mol Sci* (2017) 18(10):2088. doi: 10.3390/ijms18102088

21. Joshi N, Nagar N, Gulati K, Gangele K, Mishra A, Kumar D, et al. Dissecting the differential structural and dynamics features of CCL2 chemokine orthologs. *Int J Biol Macromol* (2020) 156:239–51. doi: 10.1016/j.ijbiomac.2020.04.067

22. Deng S, Zhou F, Wang F, Jiang Y, Tang J, Hu X, et al. C5a enhances Vδ1 T cells recruitment via the CCL2-CCR2 axis in IgA nephropathy. *Int Immunopharmacol* (2023) 125(Pt A):111065. doi: 10.1016/j.intimp.2023.111065

23. Gong X, Duan Y, Zheng J, Ye Z, Hei TK. Tetramethylpyrazine prevents contrast-induced nephropathy via modulating tubular cell mitophagy and suppressing mitochondrial fragmentation, CCL2/CCR2-mediated inflammation, and intestinal injury. *Oxid Med Cell Longev* (2019) 2019:7096912. doi: 10.1155/2019/7096912

24. Wu Q, Sun S, Wei L, Liu M, Liu H, Liu T, et al. Twist1 regulates macrophage plasticity to promote renal fibrosis through galectin-3. *Cell Mol Life Sci* (2022) 79(3):137. doi: 10.1007/s00018-022-04137-0

25. Kashyap S, Warner GM, Hartono SP, Boyilla R, Knudsen BE, Zubair AS, et al. Blockade of CCR2 reduces macrophage influx and development of chronic renal damage in murine renovascular hypertension. *Am J Physiol Renal Physiol* (2016) 310(5):F372–84. doi: 10.1152/ajprenal.00131.2015

26. Zhou H, Mu L, Yang Z, Shi Y. Identification of a novel immune landscape signature as effective diagnostic markers related to immune cell infiltration in diabetic nephropathy. *Front Immunol* (2023) 14:1113212. doi: 10.3389/fimmu.2023.1113212

27. Chen A, Lee K, He JC. Treating crescentic glomerulonephritis by targeting macrophages. *Kidney Int* (2022) 102(6):1212–4. doi: 10.1016/j.kint.2022.09.004

28. Jeon J, Park J, Boo HJ, Yang KE, Lee CJ, Lee JE, et al. Clinical value of urinary cytokines/chemokines as prognostic markers in patients with crescentic glomerulonephritis. *Sci Rep* (2022) 12(1):10221. doi: 10.1038/s41598-022-13261-7

29. Cantero-Navarro E, Rayego-Mateos S, Orejudo M, Tejedor-Santamaria L, Tejera-Muñoz A, Sanz AB, et al. Role of macrophages and related cytokines in kidney disease. *Front Med (Lausanne)* (2021) 8:688060. doi: 10.3389/fmed.2021.688060

30. Trimarchi H. Crescents in primary glomerulonephritis: a pattern of injury with dissimilar actors. *A Pathophysiol Perspective Pediatr Nephrol* (2022) 37(6):1205–14. doi: 10.1007/s00467-021-05199-1

31. Urushihara M, Kondo S, Kinoshita Y, Ozaki N, Jamba A, Nagai T, et al. (Pro) renin receptor promotes crescent formation via the ERK1/2 and Wnt/β-catenin pathways in glomerulonephritis. *Am J Physiol Renal Physiol* (2020) 319(4):F571–f578. doi: 10.1152/ajprenal.00250.2020

32. Urushihara M, Kagami S. Role of the intrarenal renin-angiotensin system in the progression of renal disease. *Pediatr Nephrol* (2017) 32(9):1471–9. doi: 10.1007/s00467-016-3449-7

33. Jang HR, Jeon J, Park JH, Lee JE, Huh W, Oh HY, et al. Clinical relevance of urinary angiotensinogen and renin as potential biomarkers in patients with overt proteinuria. *Transl Res* (2014) 164(5):400–10. doi: 10.1016/j.trsl.2014.05.009

34. Hattori T, Fujioka K, Nagai T, Kondo S, Kagami S, Hirayama M, et al. Intrarenal renin-angiotensin system activation and macrophage infiltrations in pediatric chronic glomerulonephritis. *Pediatr Nephrol* (2023) 38(11):3711–9. doi: 10.1007/s00467-023-06026-5

35. Worawichawong S, Worawichawong S, Radinahamed P, Muntham D, Sathirapongsasuti N, Nongnuch A, et al. Urine epidermal growth factor, monocyte chemoattractant protein-1 or their ratio as biomarkers for interstitial fibrosis and tubular atrophy in primary glomerulonephritis. *Kidney Blood Press Res* (2016) 41 (6):997–1007. doi: 10.1159/000452595

36. Chanrat E, Worawichawong S, Radinahamed P, Sathirapongsasuti N, Nongnuch A, Assanatham M, et al. Urine epidermal growth factor, monocyte chemoattractant protein-1 or their ratio as predictors of complete remission in primary glomerulonephritis. *Cytokine* (2018) 104:1–7. doi: 10.1016/j.cyto.2018.01.015

37. Tofik R, Ohlsson S, Bakoush O. Urinary concentration of monocyte chemoattractant protein-1 in idiopathic glomerulonephritis: a long-term follow-up study. *PloS One* (2014) 9(1):e87857. doi: 10.1371/journal.pone.0087857

38. Bullen AL, Katz R, Jotwani V, Garimella PS, Lee AK, Estrella MM, et al. Biomarkers of kidney tubule health, CKD progression, and acute kidney injury in SPRINT (Systolic blood pressure intervention trial) participants. *Am J Kidney Dis* (2021) 78(3):361–368.e1. doi: 10.1053/j.ajkd.2021.01.021

39. Wen Y, Xu L, Melchinger I, Thiessen-Philbrook H, Moledina DG, Coca SG, et al. Longitudinal biomarkers and kidney disease progression after acute kidney injury. *JCI Insight* (2023) 8(9):e167731. doi: 10.1172/jci.insight.167731

40. Wen Y, Thiessen-Philbrook H, Moledina DG, Kaufman JS, Reeves WB, Ghahramani N, et al. Considerations in controlling for urine concentration for biomarkers of kidney disease progression after acute kidney injury. *Kidney Int Rep* (2022) 7(7):1502–13. doi: 10.1016/j.ekir.2022.03.026

41. Tagaya M, Kume S, Yasuda-Yamahara M, Kuwagata S, Yamahara K, Takeda N, et al. Inhibition of mitochondrial fission protects podocytes from albumin-induced cell damage in diabetic kidney disease. *Biochim Biophys Acta Mol Basis Dis* (2022) 1868 (5):166368. doi: 10.1016/j.bbadis.2022.166368

42. Titan SM, Vieira JM Jr., Dominguez WV, Moreira SR, Pereira AB, Barros RT, et al. Urinary MCP-1 and RBP: independent predictors of renal outcome in macroalbuminuric diabetic nephropathy. *J Diabetes Complications* (2012) 26(6):546–53. doi: 10.1016/j.jdiacomp.2012.06.006

43. Liu D, Lv LL. New understanding on the role of proteinuria in progression of chronic kidney disease. *Adv Exp Med Biol* (2019) 1165:487–500. doi: 10.1007/978-981-13-8871-2_24

44. Siddiqui K, Joy SS, George TP, Mujammami M, Alfadda AA. Potential role and excretion level of urinary transferrin, KIM-1, RBP, MCP-1 and NGAL markers in diabetic nephropathy. *Diabetes Metab Syndr Obes* (2020) 13:5103–11. doi: 10.2147/dmso.S282166

45. Chen TK, Coca SG, Thiessen-Philbrook HR, Heerspink HJL, Obeid W, Ix JH, et al. Urinary biomarkers of tubular health and risk for kidney function decline or mortality in diabetes. *Am J Nephrol* (2022) 53(11-12):775–85. doi: 10.1159/000528918

46. Shoukry A, Bdeer Sel A, El-Sokkary RH. Urinary monocyte chemoattractant protein-1 and vitamin D-binding protein as biomarkers for early detection of diabetic nephropathy in type 2 diabetes mellitus. *Mol Cell Biochem* (2015) 408(1-2):25–35. doi: 10.1007/s11010-015-2479-y

47. Yamashita S, Shinozaki T, Murata H, Matsuyama Y, Babazono T. Panel of novel urine biomarkers for incident microalbuminuria in people with type 2 diabetes mellitus. *Diabetes Med* (2020) 37(11):1910–8. doi: 10.1111/dme.14280

48. Ning J, Xiang Z, Xiong C, Zhou Q, Wang X, Zou H. Alpha1-antitrypsin in urinary extracellular vesicles: A potential biomarker of diabetic kidney disease prior to microalbuminuria. *Diabetes Metab Syndr Obes* (2020) 13:2037–48. doi: 10.2147/dmso.S250347

49. Fufaa GD, Weil EJ, Nelson RG, Hanson RL, Knowler WC, Rovin BH, et al. Urinary monocyte chemoattractant protein-1 and hepcidin and early diabetic nephropathy lesions in type 1 diabetes mellitus. *Nephrol Dial Transplant* (2015) 30 (4):599–606. doi: 10.1093/ndt/gfv012

50. Lai Y, Wang Y, Fan X, Zhao Y. Allograft inflammatory factor-1 stimulates inflammatory properties of peripheral blood leukocytes and increases cell viability via enhancing mitochondrial function in Ctenopharyngodon idellus. *Fish Shellfish Immunol* (2022) 127:412–8. doi: 10.1016/j.fsi.2022.06.051

51. Bernardino JI, Alejos B, Rodriguez-Centeno J, Esteban-Cantos A, Mora-Rojas B, Montejano R, et al. Monocyte activation and ageing biomarkers in the development of cardiovascular ischaemic events or diabetes in people with HIV. *Microorganisms* (2023) 11(7):1818. doi: 10.3390/microorganisms11071818

52. Gniewkiewicz M, Gozdowska J, Deborska-Materkowska D, Czerwinska K, Perkowska-Ptasinska A, Burban A, et al. Potential utility of urinary chemokine CCL2 to creatinine ratio in prognosis of 5-year graft failure and mortality post 1-year protocol biopsy in kidney transplant recipients. *Immun Inflammation Dis* (2023) 11(6):e901. doi: 10.1002/iid3.901

53. Nadkarni GN, Rao V, Ismail-Beigi F, Fonseca VA, Shah SV, Simonson MS, et al. Association of urinary biomarkers of inflammation, injury, and fibrosis with renal function decline: the ACCORD trial. *Clin J Am Soc Nephrol* (2016) 11(8):1343–52. doi: 10.2215/cjn.12051115

54. Pena MJ, Heinzel A, Heinze G, Alkhalaf A, Bakker SJ, Nguyen TQ, et al. A panel of novel biomarkers representing different disease pathways improves prediction of renal function decline in type 2 diabetes. *PloS One* (2015) 10(5):e0120995. doi: 10.1371/journal.pone.0120995

55. Schrauben SJ, Shou H, Zhang X, Anderson AH, Bonventre JV, Chen J, et al. Association of multiple plasma biomarker concentrations with progression of prevalent diabetic kidney disease: findings from the chronic renal insufficiency cohort (CRIC) study. *J Am Soc Nephrol* (2021) 32(1):115–26. doi: 10.1681/asn.2020040487

56. Das K, Paul S, Mukherjee T, Ghosh A, Sharma A, Shankar P, et al. Beyond macromolecules: extracellular vesicles as regulators of inflammatory diseases. *Cells* (2023) 12(15):1963. doi: 10.3390/cells12151963

57. Dehghanbanadaki H, Forouzanfar K, Kakaei A, Zeidi S, Salehi N, Arjmand B, et al. The role of CDH2 and MCP-1 mRNAs of blood extracellular vesicles in predicting early-stage diabetic nephropathy. *PloS One* (2022) 17(4):e0265619. doi: 10.1371/journal.pone.0265619

58. Singh RG, Usha, Rathore SS, Behura SK, Singh NK. Urinary MCP-1 as diagnostic and prognostic marker in patients with lupus nephritis flare. *Lupus* (2012) 21(11):1214–8. doi: 10.1177/0961203312452622

59. Dong XW, Zheng ZH, Ding J, Luo X, Li ZQ, Li Y, et al. Combined detection of uMCP-1 and uTWEAK for rapid discrimination of severe lupus nephritis. *Lupus* (2018) 27(6):971–81. doi: 10.1177/0961203318758507

60. Elsaid DS, Abdel Noor RA, Shalaby KA, Haroun RA. Urinary tumor necrosis factor-like weak inducer of apoptosis (uTWEAK) and urinary monocyte chemoattractant protein-1 (uMCP-1): promising biomarkers of lupus nephritis activity? *Saudi J Kidney Dis Transpl* (2021) 32(1):19–29. doi: 10.4103/1319-2442.318522

61. Moloi MW, Rusch JA, Omar F, Ekrikpo U, Dandara C, Bello AK, et al. Urinary MCP-1 and TWEAK as non-invasive markers of disease activity and treatment response in patients with lupus nephritis in South Africa. *Int Urol Nephrol* (2021) 53 (9):1865–73. doi: 10.1007/s11255-020-02780-9

62. Ding Y, Nie LM, Pang Y, Wu WJ, Tan Y, Yu F, et al. Composite urinary biomarkers to predict pathological tubulointerstitial lesions in lupus nephritis. *Lupus* (2018) 27(11):1778–89. doi: 10.1177/0961203318788167

63. Jensen MB, Viken I, Høgh F, Jacobsen KK. Quantification of urinary albumin and -creatinine: A comparison study of two analytical methods and their impact on albumin to creatinine ratio. *Clin Biochem* (2022) 108:5–9. doi: 10.1016/j.clinbiochem.2022.06.014

64. Dong X, Zheng Z, Luo X, Ding J, Li Y, Li Z, et al. Combined utilization of untimed single urine of MCP-1 and TWEAK as a potential indicator for proteinuria in lupus nephritis: A case-control study. *Med (Baltimore)* (2018) 97(16):e0343. doi: 10.1097/md.0000000000010343

65. Lan L, Han F, Lang X, Chen J. Monocyte chemotactic protein-1, fractalkine, and receptor for advanced glycation end products in different pathological types of lupus nephritis and their value in different treatment prognoses. *PloS One* (2016) 11(7): e0159964. doi: 10.1371/journal.pone.0159964

66. Thakare SB, So PN, Rodriguez S, Hassanein M, Lerma E, Wiegley N. Novel therapeutics for management of lupus nephritis: what is next? *Kidney Med* (2023) 5 (8):100688. doi: 10.1016/j.xkme.2023.100688

67. Devarapu SK, Kumar Vr S, Rupanagudi KV, Kulkarni OP, Eulberg D, Klussmann S, et al. Dual blockade of the pro-inflammatory chemokine CCL2 and the homeostatic chemokine CXCL12 is as effective as high dose cyclophosphamide in murine proliferative lupus nephritis. *Clin Immunol* (2016) 169:139–47. doi: 10.1016/j.clim.2016.07.003

68. Shu B, Fang Y, He W, Yang J, Dai C. Identification of macrophage-related candidate genes in lupus nephritis using bioinformatics analysis. *Cell Signal* (2018) 46:43–51. doi: 10.1016/j.cellsig.2018.02.006

69. Mohammad LA, Atef DM, Abul-Saoud AM. Association of monocyte chemoattractant protein 1 (MCP-1) gene polymorphism with lupus nephritis in Egyptian patients. *Hum Immunol* (2015) 76(10):724–8. doi: 10.1016/j.humimm.2015.09.027

70. Sang GY, Meng CR, Hao YF, Dai JH. Monocyte chemoattractant protein-1 (MCP-1)-2518 A/G polymorphism and lupus nephritis risk: A PRISMA-compliant meta-analysis. *Med (Baltimore)* (2017) 96(51):e9401. doi: 10.1097/md.0000000000009401

71. Gupta R, Yadav A, Aggarwal A. Longitudinal assessment of monocyte chemoattractant protein-1 in lupus nephritis as a biomarker of disease activity. *Clin Rheumatol* (2016) 35(11):2707–14. doi: 10.1007/s10067-016-3404-9

72. Messchendorp AL, Meijer E, Visser FW, Engels GE, Kappert P, Losekoot M, et al. Rapid progression of autosomal dominant polycystic kidney disease: urinary biomarkers as predictors. *Am J Nephrol* (2019) 50(5):375–85. doi: 10.1159/000502999

73. Segarra-Medrano A, Martin M, Agraz I, Vilaprinyó M, Chamoun B, Jatem E, et al. Association between urinary biomarkers and disease progression in adults with autosomal dominant polycystic kidney disease. *Clin Kidney J* (2020) 13(4):607–12. doi: 10.1093/ckj/sfz105

74. Messchendorp AL, Meijer E, Boertien WE, Engels GE, Casteleijn NF, Spithoven EM, et al. Urinary biomarkers to identify autosomal dominant polycystic kidney disease patients with a high likelihood of disease progression. *Kidney Int Rep* (2018) 3 (2):291–301. doi: 10.1016/j.ekir.2017.10.004

75. Kawano H, Muto S, Ohmoto Y, Iwata F, Fujiki H, Mori T, et al. Exploring urinary biomarkers in autosomal dominant polycystic kidney disease. *Clin Exp Nephrol* (2015) 19(5):968–73. doi: 10.1007/s10157-014-1078-7

76. Hosseinpour M, Ardalani F, Mohseni M, Beheshtian M, Arzhangi S, Ossareh S, et al. Targeted next generation sequencing revealed novel variants in the PKD1 and PKD2 genes of Iranian patients with autosomal dominant polycystic kidney disease. *Arch Iran Med* (2022) 25(9):600–8. doi: 10.34172/aim.2022.95

77. Cassini MF, Kakade VR, Kurtz E, Sulkowski P, Glazer P, Torres R, et al. Mcp1 promotes macrophage-dependent cyst expansion in autosomal dominant polycystic kidney disease. *J Am Soc Nephrol* (2018) 29(10):2471–81. doi: 10.1681/asn.2018050518

78. Salah SM, Meisenheimer JD, Rao R, Peda JD, Wallace DP, Foster D, et al. MCP-1 promotes detrimental cardiac physiology, pulmonary edema, and death in the cpk model of polycystic kidney disease. *Am J Physiol Renal Physiol* (2019) 317(2):F343–60. doi: 10.1152/ajprenal.00240.2018

79. Belisário AR, Vieira É LM, de Almeida JA, Mendes FG, Miranda AS, Rezende PV, et al. Evidence for interactions between inflammatory markers and renin-angiotensin system molecules in the occurrence of albuminuria in children with sickle cell anemia. *Cytokine* (2020) 125:154800. doi: 10.1016/j.cyto.2019.154800

80. dos Santos TE, Gonçalves RP, Barbosa MC, da Silva GB Jr., Daher Ede F. Monocyte chemoatractant protein-1: a potential biomarker of renal lesion and its relation with oxidative status in sickle cell disease. *Blood Cells Mol Dis* (2015) 54(3):297–301. doi: 10.1016/j.bcmd.2014.11.019

81. Cody EM, Rose JE, Huang B, Qiu T, Brunner HI, Devarajan P. Stability of novel urinary biomarkers used for lupus nephritis. *Front Pediatr* (2022) 10:974049. doi: 10.3389/fped.2022.974049

frontiers | Frontiers in Immunology

TYPE Review
PUBLISHED 15 January 2024
DOI 10.3389/fimmu.2023.1335936

OPEN ACCESS

EDITED BY
Xu-jie Zhou,
Peking University, China

REVIEWED BY
Giuseppe Remuzzi,
Istituto di Ricerche Farmacologiche Mario Negri IRCCS, Italy
Tongtong Liu,
China Academy of Chinese Medical Sciences, China

*CORRESPONDENCE
Hong Jiang
jangh-yt@163.com
Xuefei Tian
xuefei.tian@yale.edu

†These authors have contributed equally to this work and share first authorship

RECEIVED 09 November 2023
ACCEPTED 29 December 2023
PUBLISHED 15 January 2024

CITATION
Jiang H, Shen Z, Zhuang J, Lu C, Qu Y, Xu C, Yang S and Tian X (2024) Understanding the podocyte immune responses in proteinuric kidney diseases: from pathogenesis to therapy.
Front. Immunol. 14:1335936.
doi: 10.3389/fimmu.2023.1335936

Understanding the podocyte immune responses in proteinuric kidney diseases: from pathogenesis to therapy

Hong Jiang[1*†], Zhirang Shen[1†], Jing Zhuang[1], Chen Lu[2], Yue Qu[1], Chengren Xu[1], Shufen Yang[1] and Xuefei Tian[3*]

[1]Division of Nephrology, Department of Internal Medicine, People's Hospital of Xinjiang Uygur Autonomous Region, Urumqi, China, [2]Division of Nephrology, Department of Internal Medicine, The First Affiliated Hospital of Xinjiang Medical University, Urumqi, China, [3]Section of Nephrology, Department of Internal Medicine, Yale University School of Medicine, New Haven, CT, United States

The glomerular filtration barrier, comprising the inner layer of capillary fenestrated endothelial cells, outermost podocytes, and the glomerular basement membrane between them, plays a pivotal role in kidney function. Podocytes, terminally differentiated epithelial cells, are challenging to regenerate once injured. They are essential for maintaining the integrity of the glomerular filtration barrier. Damage to podocytes, resulting from intrinsic or extrinsic factors, leads to proteinuria in the early stages and eventually progresses to chronic kidney disease (CKD). Immune-mediated podocyte injury is a primary pathogenic mechanism in proteinuric glomerular diseases, including minimal change disease, focal segmental glomerulosclerosis, membranous nephropathy, and lupus nephritis with podocyte involvement. An extensive body of evidence indicates that podocytes not only contribute significantly to the maintenance of the glomerular filtration barrier and serve as targets of immune responses but also exhibit immune cell-like characteristics, participating in both innate and adaptive immunity. They play a pivotal role in mediating glomerular injury and represent potential therapeutic targets for CKD. This review aims to systematically elucidate the mechanisms of podocyte immune injury in various podocyte lesions and provide an overview of recent advances in podocyte immunotherapy. It offers valuable insights for a deeper understanding of the role of podocytes in proteinuric glomerular diseases, and the identification of new therapeutic targets, and has significant implications for the future clinical diagnosis and treatment of podocyte-related disorders.

KEYWORDS

podocyte, immunity response, pathogenesis, proteinuria, treatment

1 Introduction

The glomerulus, a specialized unit within the kidney, serves as a crucial filtration system that eliminates waste products from the blood. Maintaining internal stability by clearing external and internally produced waste is its primary function. Its filtration structure relies on the intricate network of glomerular capillaries, comprising glomerular endothelial cells, the glomerular basement membrane (GBM), and glomerular podocytes, collectively forming the unique filtration barrier of the glomerulus (1). Any impairment in this barrier may result in protein loss. Notably, proteinuric kidney disease originating from glomerular dysfunction accounts for 80% of individuals who eventually progress to end-stage kidney disease (ESKD), necessitating kidney replacement therapy (2).

Podocytes, the largest cells in the glomerulus, attach to the outer layer of the GBM. They consist of a cell body housing a nucleus, several prominent primary processes branching out from the cell, and secondary processes that further branch to form interdigitating foot processes (tertiary processes) on the GBM (3). The podocyte cytoskeleton plays a vital role in stabilizing its morphology and maintaining its biological function. It contributes to the integrity of the glomerular filtration barrier through interactions with cell-cell junctions and cell-matrix proteins (4). Podocytes can be categorized into three distinct membrane domains: the basal domain, the apical domain, and the intercellular/slit diaphragm domain. The slit diaphragm, a complex structure comprising multiple protein molecules, plays a pivotal role in regulating glomerular permeability, in coordination with the glomerular basement membrane and the glomerular endothelial cells. Key protein molecules within the slit diaphragm of podocytes include nephrin, neph1, neph2, CD2-associated protein(CD2AP), and podocin, among others (5). Furthermore, emerging evidence suggests that podocytes possess diverse functions beyond their mechanical supportive role, contributing to the innate and adaptive immune system to maintain glomerular health homeostasis (6). The immune malfunction of podocytes is considered to be associated with the pathogenesis of several common proteinuric glomerular diseases. Immune complexes, complement factors, various immune cells, and even the immune attributes of podocytes might contribute to the development of these proteinuric glomerular diseases. However, the intricate mechanisms of immune responses leading to podocyte injury remain incompletely understood. This review aims to consolidate current insights into the pathogenic mechanisms of immune responses triggering podocyte injury and the latest therapeutic strategies targeting the immune system.

2 Immunological mechanisms in podocyte

2.1 Innate immune responses in podocytes

An expanding body of evidence underscores the significant role of podocytes in the glomerular filtration barrier and their involvement in innate immune responses. Podocytes have been found to express various pattern recognition receptors (PRRs), including Toll-like Receptors (TLRs), enabling them to actively participate in innate immune responses by recognizing and eliminating foreign pathogens or endogenous danger signals (7). Notably, Toll-like Receptor 4 (TLR4) is a specific subtype capable of recognizing bacterial lipopolysaccharide (LPS) (8). Furthermore, exposure to a high-glucose milieu has been demonstrated to directly enhance the activation of TLR4. This activation is posited to contribute to the pathogenesis of podocyte damage and the subsequent progression of interstitial fibrosis (9). TLRs are present on the cell surface or intracellularly and are expressed by a range of cell types, including dendritic cells, macrophages, fibroblasts, B cells, T cells, as well as endothelial and epithelial cells (10). They play a pivotal role in recognizing pathogen-associated biomarkers (11). For instance, cell surface TLRs mainly recognize microbial membrane components like LPS, lipids, and proteins, while intracellular TLRs primarily detect bacterial and viral nucleic acids (12). However, it's worth noting that some studies have reported that stimuli like puromycin aminonucleoside (PAN) can induce glomerular podocyte injury, increase Toll-like Receptor 9 (TLR9) expression, activate Nuclear factor kappa-B (NF-κB) and p38,mitogen-activated protein kinase (MAPK) signaling pathways, and potentially use endogenous mitochondrial DNA as a ligand. This results in damage to glomerular podocytes and leads to apoptosis, suggesting that TLRs can have a dual effect on podocytes—both protecting the integrity of the glomerular filtration barrier and potentially promoting glomerulosclerosis (13). Moreover, Masum and colleagues utilized BXSB/MpJ-Yaa (Yaa) mice to demonstrate that overexpression of TLR9 correlated with podocyte injury and the development of typical membranoproliferative glomerulonephritis (MPGN) lesions. In contrast, BXSB control mice, with weak TLR9 expression, showed no MPGN lesions. These findings suggest a potential role of TLR9 in podocyte injury and MPGN development (14).

In addition to TLRs, podocytes also express other critical PRRs that actively participate in processes related to inflammation, cell death, and proteinuria (15). For example, Nod-like receptors (NLRs) have been implicated in podocyte injury, with abnormal activation of the NOD-like receptor thermal protein domain associated protein 3 (NLRP3) inflammasome leading to podocyte damage (16). The activation of the NLRP3 inflammasome contributes to aldosterone-induced podocyte injury, yet studies indicate that its targeted silencing can substantially reduce the severity of such damage. This finding underscores the potential therapeutic role of NLRP3 inhibition in conditions characterized by aldosterone-mediated damage to podocytes (17). More recently, researchers have uncovered the significance of the Cyclic GMP-AMP synthase (cGAS) - Stimulator of interferon genes (STING) axis in podocyte innate immunity (18). cGAS serves as a PRR and is a key sensor of cytosolic Deoxyribonucleic acid (DNA) (19). It can catalyze the production of the second messenger 2'3'-cyclic GMP-AMP (cGAMP), which binds to STING, activates TANK binding kinase 1 (TBK1) and interferon regulatory factor 3 (IRF3), ultimately leading to the production of type I interferons (20).

Upon activation, the cGAS-STING pathway triggers apoptosis or autophagy-mediated death in podocytes. This event initiates proteinuria and expedites the loss of podocytes (21). Consequently, these chain reactions contribute significantly to the acceleration of the development and the progression of glomerular diseases. The cGAS-STING pathway is a critical innate immune pathway that senses cytosolic DNA, contributing to antiviral immunity and inflammatory responses. High-mobility group box 1 (HMGB1), a nuclear protein that is overexpressed in podocytes, becomes actively secreted or passively released into the extracellular milieu following cellular damage (22). Upon its release, HMGB1 interacts with various receptors, notably the Receptor for Advanced Glycation End products (RAGE) and TLR4, which subsequently triggers podocyte apoptosis and promotes epithelial-mesenchymal transition (EMT)—processes that compromise podocyte integrity and function (23, 24). Therapeutic strategies that interrupt the HMGB1-receptor signaling axis have demonstrated potential in ameliorating podocyte injury, consequently enhancing the integrity of the glomerular filtration barrier (25). This avenue represents a promising therapeutic target for ameliorating the progression of CKD (Figure 1).

2.2 Adaptive immune responses in podocytes

In addition to their role in innate immunity, podocytes also participate in adaptive immune responses (26). Podocytes have the capacity to express major histocompatibility complex (MHC) class I and II antigens, which can respectively activate $CD8^+$ and $CD4^+$ T cells (27, 28). $CD4^+$ T cells are involved in activating innate immune cells, B-lymphocytes, cytotoxic T cells, as well as nonimmune cells by secreting cytokines (29). On the other hand, $CD8^+$ T cells exert specific cytotoxic effects, aiding in the body's defense against pathogens and tumor cells (30). The activation of T cells relies on a two-signal process: the first signal involves the binding of MHC antigens to the T cell receptor (TCR), and the second signal entails the interaction between a co-stimulatory molecule and its ligand. Remarkably, podocytes can express B7-1 (CD80), which is a T cell co-stimulatory molecule that binds to CD28 on T cells, resulting in the generation of a positive synergistic stimulation signal. B7-1/CD80 is associated with B cells and antigen-presenting cells (APCs), and it can augment T cell responses to antigens presented by MHC class I/II (31). In contrast, B7-2 (CD86) is another co-stimulatory

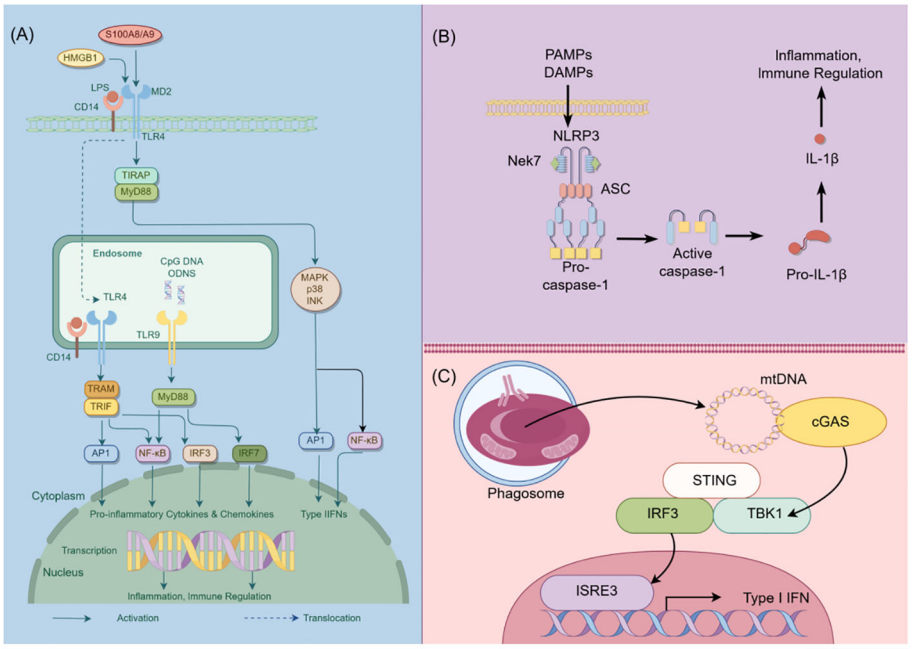

FIGURE 1
Schematic diagram of innate immunity in podocytes. This figure illustrates the role of TLR, NLRP3, and cGAS-STING signaling pathways in podocyte innate immunity. **(A)** Intracellular TLR signaling pathway: TLR, a pattern recognition receptor, can identify pathogen-related molecular patterns (PAMPs) and damage-related molecular patterns (DAMPs) within and outside cells, such as lipopolysaccharides (LPS). Upon TLR activation, downstream signaling molecules, including IRF3, IRF7, NF-κB, among others, are stimulated through various adapter proteins like MyD88, TRIF, etc., leading to the expression of antiviral and inflammatory genes. **(B)** NLRP3 Inflammasome activation: NLRP3, a member of the NOD-like receptor (NLR) family, is capable of recognizing intracellular PAMPs and DAMPS. Following NLRP3 activation, it assembles an inflammasome complex with ASC and Caspase-1, thereby triggering Caspase-1 activity and facilitating the maturation and secretion of IL-1β. **(C)** CGAS-STING signal pathway: CGAS, a cyclic GMP-AMP synthase, can detect DNA within cells. Upon eGAS binding to DNA, it synthesizes cyclic GMP-AMP (cGAMP) as a second messenger, which activates the STING protein. The STING protein subsequently triggers downstream signaling molecules like TBK1 and IRF3, leading to the expression of antiviral and inflammatory genes. HMGB1, High mobility group box-1 protein; LPS, Lipopolysaccharide; TIRAP, Toll-interleukin Receptor domain-containing adaptor protein; MyD88, Myeloid Differentiation Factor 88; MAPK, mitogen-activated protein kinases; AP1, activator protein-1; NF-κB, Nuclear factor kappa-B; IRF3, Interferon regulatory Factor 3; IRF7, Interferon regulatory Factor 7; PAMPs, pathogen-associated molecular patterns; DAMPs, damage-associated molecular patterns; NLRP3, NOD-like receptor thermal protein domain associated protein 3; Nek7, never in mitosis gene a-related kinase 7; ASC, apoptosis-associated speck-like protein containing a CARD domain; CGAS, cyclic guanosine monophosphate-adenosine monophosphate synthase; TBK1, TANK-binding kinase 1; STING, Stimulator of interferon genes; By Figdraw (www.figdraw.com).

molecule found on B cells and APCs, which can also bind to CD28 (32) (Figure 2). These findings underscore the specific role of podocytes in adaptive immune regulation, which may have a significant impact on renal inflammation and injury. The complement system, an important integral component of innate and adaptive immune responses, has gained increasing attention in understanding the underlying pathogenesis of glomerular diseases. With a better understanding of the complement system and its role in glomerular diseases, treatments targeting complement activation are being explored for various glomerular conditions. Abnormal activation of the complement system is implicated in causing podocyte injury through multiple pathways. This involvement includes the production of reactive oxygen species (ROS), stimulation of cytokine release, and induction of endoplasmic reticulum stress. Collectively, these biochemical events compromise cytoskeletal stability, leading to podocyte detachment from the GBM and initiating the development of proteinuria (33). Studies investigating primary membranous nephropathy have demonstrated the critical involvement of the C3a/C3aR pathway in podocyte injury, noting that increased levels of plasma C3a and glomerular C3aR are associated with disease progression and serve as predictive indicators for patient prognosis (34). Podocytes serve a dual role in the narrative of complement-mediated damage: they are not only a target but also a source of complement system activation (35). Podocytes employ multiple defense mechanisms, including the expression of regulatory proteins like complement factor H and surface regulators such as CD46, CD55, and CD59, as well as processes like autophagy and actin-mediated endocytosis, to protect against and maintain homeostasis in the face of complement-induced damage (36). The interplay between the complement system and podocyte damage is intricate and comprises multiple dimensions. Elucidating the nuances of this relationship is pivotal for the innovation of therapeutic approaches aimed at treating conditions linked to podocyte damage (Table 1) (Figure 3).

3 Crosstalk between podocytes and other cells in the glomerulus

Cellular crosstalk is a fundamental process of intercellular signaling and interaction that exerts a significant influence on the behavior and function of various cells. This dynamic communication can occur between identical cell types or across different cell types (45). The interaction between other cells in the glomerulus and podocytes is critical in the development of glomerular diseases.Research has demonstrated a correlation between mitochondrial oxidative stress in glomerular endothelial cells and an increased expression of Endothelin-1 (Edn1) along with its receptor, Endothelin-1 receptor A (Ednra) (46). Targeted attenuation of mitochondrial oxidative stress or the disruption of the Edn1/Ednra signaling cascade has been shown to effectively ameliorate damage to glomerular endothelial cells, reduce the depletion of podocytes, decrease proteinuria levels, and attenuate the progression of glomerulosclerosis in D2 mice (47).

Vascular endothelial growth factor A (VEGF-A) and angiopoietin 1 (Ang-1) secreted by podocytes serve as protective factors that uphold the integrity and stability of endothelial cells by binding to receptors on the endothelial cells (48–50), Nevertheless, both the overexpression and deficiency of VEGF-A can lead to endothelial cell injury and proteinuria (51). Angiopoietin 2 (Ang2),

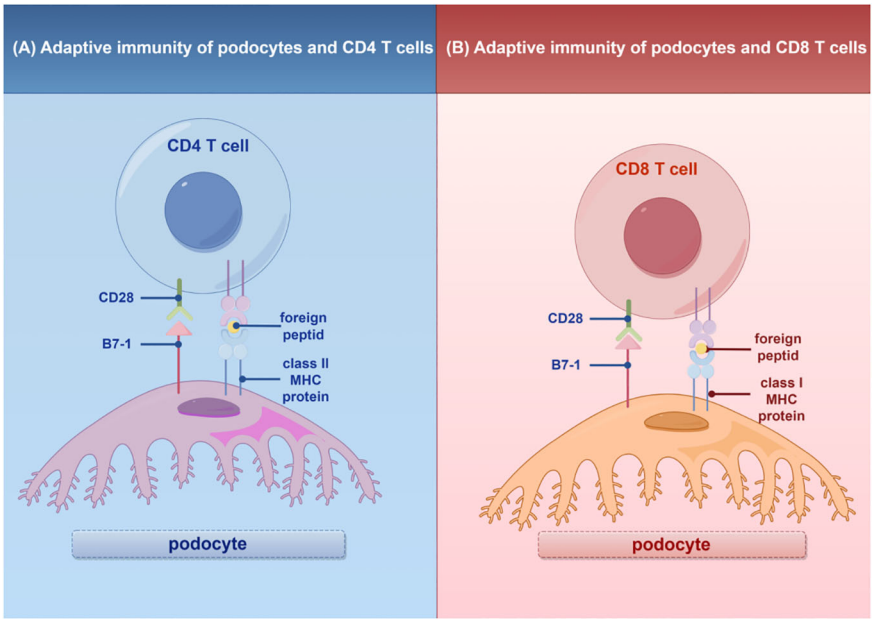

FIGURE 2
Adaptive immunity of T cells in podocytes. **(A)** Interaction of podocytes with CD4 T Cells: Podocytes express B7-1 and MHC II molecules, facilitating interactions with CD4 T cells and promoting glomerular inflammatory responses. **(B)** Interaction of podocytes with CD8 T Cells: Podocytes express B7-1 and MHC I molecules, enabling interactions with CD8 T cells and promoting glomerular inflammatory responses. MHC, major histocompatibility (www.figdraw.com). complex; By Figdraw.

TABLE 1 The role of immunity in podocyte injury.

Immunization route	Mechanism of action on podocytes	Reference
TLRs	TLRs recognize and eliminate foreign pathogens or endogenous danger signals. They can also induce glomerular podocyte injury, increase TLR9 expression, activate NF-κB and MAPK signaling pathways, and potentially use endogenous mitochondrial DNA as a ligand, leading to podocyte damage and apoptosis	(11, 13, 14, 37)
NLRs	Abnormal activation of the NLRP3 inflammasome leads to podocyte damage. NLRs actively participate in processes related to inflammation, cell death, and proteinuria	(38–41)
cGAS-STING	Upon activation, the cGAS-STING pathway triggers apoptosis or autophagy-mediated death in podocytes, initiating proteinuria and expediting the loss of podocytes	(18, 42)
HMGB1	HMGB1 interacts with various receptors, notably the Receptor for Advanced Glycation End products (RAGE) and TLR4, which subsequently triggers podocyte apoptosis and promotes epithelial-mesenchymal transition (EMT), compromising podocyte integrity and function	(24, 43, 44)
MHC class I and II antigens	MHC class I and II antigens can respectively activate CD8+ and CD4+ T cells, which are involved in activating innate immune cells, B-lymphocytes, cytotoxic T cells, as well as nonimmune cells by secreting cytokines	(27–29)
Complement system	The complement system is implicated in causing podocyte injury via multiple pathways, including the production of reactive oxygen species (ROS), stimulation of cytokine release, and induction of endoplasmic reticulum stress. This compromises the cytoskeletal stability, precipitating podocyte detachment from the GBM, and initiates the development of proteinuria	(33, 36)

primarily produced by glomerular endothelial cells, exhibits an antagonistic effect. It competitively inhibits the activation of the Tie2 receptor by Ang1, thereby increasing endothelial cell apoptosis and permeability (47). Additionally, vascular endothelial growth factor B (VEGF-B) secreted by podocytes acts as a pathogenic factor, fostering lipid accumulation and lipotoxicity, damaging the endothelial cell surface, and inducing proteinuria by binding to receptors on the endothelial cells (52).

Glomerular endothelial cells secrete endothelin-1 (ET-1), a vasoconstrictive peptide with multifaceted effects. ET-1 exerts diverse physiological and pathophysiological roles by binding to ETAR or ETBR on the surface of endothelial cells, mesangial cells, or surrounding cells (53). While ETAR primarily mediates vasoconstriction, cell proliferation, fibrosis, podocyte injury, and inflammatory response (54), ETBR predominantly mediates vasodilation, anti-proliferation, and anti-fibrosis, thereby exerting a protective effect (55). These crosstalk mechanisms significantly contribute to the regulatory processes involved in glomerular injury and repair.

Furthermore, the transforming growth factor β (TGF-β) released by podocytes activates various downstream signals within the Smad signaling pathway by binding to distinct receptors. This activation promotes mesangial cell proliferation, differentiation, and matrix deposition, influencing the phenotype and function of endothelial cells, mesangial cells, and podocytes themselves, ultimately leading to glomerular fibrosis (56). Exosomes, small extracellular vesicles, possess the capability to transport numerous molecular components, including proteins, lipids, DNA, miRNA, and lncRNA (57). Recent evidence has shed light on the role of exosomes in compromising the structural integrity of glomeruli, renal tubules, and renal interstitium. Under hyperglycemic conditions, mesangial cell-derived exosomes can potentially alter the functionality of podocytes through the delivery of TGF-β1, thereby contributing to the pathogenesis of diabetic nephropathy (58, 59).

Cytokines, such as TNF-α and TGF-β, secreted by mesangial cells, are known to reduce the expression of podocyte-associated proteins, including nephrin and podocin. This reduction weakens or disrupts junctions within the slit diaphragm, subsequently increasing the permeability of the glomerular filtration membrane. Consequently, proteinuria and impaired renal function ensue (60). This mechanism may partially elucidate the pathogenesis of FSGS.

The interplay between podocytes and other cells in glomeruli, as well as among podocytes themselves, plays a critical role in the pathogenesis of various kidney diseases, including glomerulonephritis, FSGS, and LN. This intricate process involves the complex interaction and regulation of various cytokines and receptors, ultimately contributing to the progression of glomerular damage and dysfunction. Understanding the molecular mechanisms underlying these crosstalks is instrumental in deciphering the pathogenesis of kidney diseases and serves as a foundation for the development of novel therapeutic strategies aimed at preserving glomerular function and ameliorating the progression of proteinuric glomerular diseases.

4 Common proteinuric glomerular diseases associated with immune responses in podocytes

4.1 Minimal change disease

MCD is the predominant type of nephrotic syndrome in children and adolescents. However, in adults, MCD accounts for a smaller proportion, approximately 10% to 16% of nephrotic

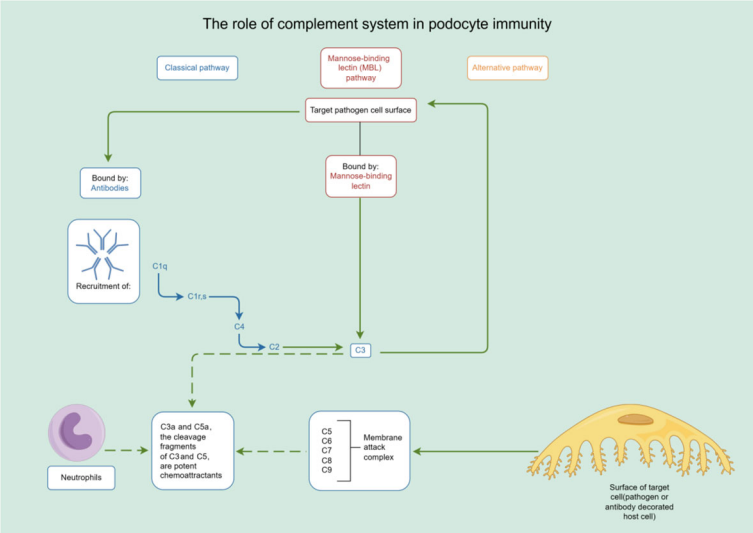

FIGURE 3
The role of complement system in podocyte immunity. Diagrammatic representation of complement system pathways and their involvement in podocyte immunity, highlighting the classical, lectin, and alternative pathways leading to pathogen lysis and immune cell recruitment. By Figdraw (www.figdraw.com).

syndrome cases (61). Clinically, MCD is characterized by massive proteinuria, hypoalbuminemia, edema, and dyslipidemia. Kidney biopsy typically reveals predominantly normal glomeruli under light microscopy, with the only notable finding being the diffuse disappearance of podocyte foot processes observed under transmission electron microscopy (62). Although the precise pathogenesis of MCD remains elusive, numerous research findings suggest its association with immune system dysregulation.

Traditionally, it has been postulated that MCD is mediated by certain unidentified circulating factors, possibly released by T cells, which target podocytes directly, leading to their dysfunction and consequent proteinuria (63). Evidence indicates that the circulating factors responsible for MCD may include specific cytokines, primarily belonging to the T helper 2 cell (Th2) subgroup, such as interleukin-13 (IL-13), interleukin-8 (IL-8), interleukin-4 (IL-4), among others (64–67). On one hand, T cell effector factors serve as the source of the aforementioned pro-inflammatory cytokines and others, which can directly or indirectly impair podocytes, resulting in proteinuria. On the other hand, regulatory T cells (Treg cells) maintain immune balance by binding to CD80 on antigen-presenting cells (APCs) through the expression of Cytotoxic T lymphocyte associate protein-4 (CTLA-4) (68). The reduced number and function of Treg cells in MCD patients may lead to immune dysregulation and an inflammatory response (69). Additionally, MCD has been associated with certain Treg cell-related genetic or acquired immune deficiency syndromes (70).

While much of the research on MCD has traditionally focused on T cell-related cytokines, recent studies have shed light on the involvement of B cells and specific autoantibodies, such as those targeting nephrin, a critical podocyte protein (71). The role of B cells in MCD pathogenesis has gained increased attention in recent years, particularly following the use of rituximab (RTX), a monoclonal antibody targeting the pan-B-cell marker CD20, which has shown efficacy in reducing recurrence rates (72, 73). In the process of antibody synthesis, B cells are capable of exerting a direct impact on the structural integrity and functional capacities of podocytes through the release of particular cytokines. Additionally, B cells can modulate T cell responses, thereby contributing to the pathogenesis of diseases. This dual capacity underscores the complex and integral participation of B cells in disease pathology, extending their influence beyond the classical role of antibody generation (74). Some studies suggest that B cells may contribute to MCD development by promoting T cell responses or producing autoantibodies. For instance, elevated levels of B cell-activating factor in the serum of MCD patients have been observed, which may drive T cell activation in MCD (75). Research has also revealed increased levels of T cells bearing immunoglobulin M (IgM) on their surface in patients with idiopathic nephrotic syndrome (INS) who exhibit poor treatment responses. *In vitro* experiments have demonstrated that these T cells can induce rearrangement of the podocyte cytoskeleton, indicating that the interplay between B cells and T cells may play a crucial role in MCD pathogenesis (76). Furthermore, IgM can trigger the classical complement activation pathway in the glomeruli of INS patients (77). These studies suggest that B cells may contribute to MCD through various mechanisms, but further research is required to elucidate their exact roles. In addition, certain autoantibodies have been considered mediators of MCD. Studies have shown that around 50% of children with relapsing hormone-sensitive nephrotic syndrome have elevated plasma anti-UCHL1 (ubiquitin C-terminal hydrolase-L1) antibody levels. However, in adult MCD patients, no elevation of anti-UCHL1 antibody levels was observed (78). This suggests the existence of different immune mechanisms in children and adults with MCD.

In summary, the pathogenesis of MCD involves complex interactions among the immune system, glomerular cells, and

genetics, with multiple potential pathogenic factors and mechanisms at play. MCD is not a straightforward immune or podocyte disease. Heterogeneity and the absence of reliable animal models pose challenges to our understanding of MCD. Therefore, future research should focus on developing new experimental models, screening for new autoantibodies, and improving our understanding of cell-cell interactions in this disease.

4.2 Focal segmental glomerulosclerosis

FSGS is a group of glomerular lesions that were once considered to have a low incidence but have shown a gradual increase in global prevalence in recent decades. Reports suggest that the annual incidence of FSGS ranges from 0.2 to 1.8 cases per 100,000 people (79). Histopathologically, FSGS is characterized by partial sclerosis of some glomeruli, with each affected glomerulus showing only segmental involvement. Clinically, FSGS commonly presents as proteinuria, nephrotic syndrome, with or without kidney function impairment (80). While the precise mechanisms underlying the development of FSGS remain incompletely understood, emerging evidence suggests significant involvement of the immune system in the pathogenesis, with podocyte injury considered to be at the core of the disease.

FSGS has been linked to various immune-related factors, including infections, tumors, drugs, and genetic mutations, which can impact the structure and function of podocytes, leading to proteinuria and a decline in kidney function (81–85). T cells, a crucial component of the adaptive immune system, secrete various cytokines that regulate glomerular permeability and inflammatory responses. As early as 1974, Shalhoub proposed the hypothesis that FSGS is a T-cell-mediated disease (86). Subsequent research has identified abnormalities in different subtypes and functional states of T cells in FSGS patients. Some studies have reported a progressive decrease in the relative numbers of CD4 and CD8 T cells with disease progression (87). Reports have also demonstrated an increase in Th17 cells and a decrease in Treg cells among CD4 T cells in some adult patients with INS (88). Furthermore, various observations have associated the levels of certain cytokines secreted by T cells with glomerulosclerosis in FSGS patients. For example, interleukin-17 (IL-17), produced by the Th17 subgroup, has been linked to glomerulosclerosis in FSGS patients (89). Other studies have revealed that FSGS is related to the activation of the tumor necrosis factor-α (TNF-α) pathway in podocytes (90, 91). These cytokines may induce morphological changes, dedifferentiation, and apoptosis in podocytes by directly or indirectly affecting them. Podocytes express various TLRs involved in innate immunity, capable of activating signaling pathways that lead to morphological changes in podocytes and induce the expression of chemokines (92, 93). Moreover, TLR signaling can enhance the expression of CD80 on podocytes, a molecule that stimulates T cells (93, 94). Therefore, TLRs may also modulate the interaction between podocytes and T cells.

B cells are another crucial component of the adaptive immune system, primarily responsible for mediating humoral immune responses through the production of antibodies. Additionally, they perform various other immune functions. B cells function as efficient APCs, processing and presenting antigens to T cells, thereby activating T cell responses to antigens. Moreover, B cells secrete various cytokines, including both pro-inflammatory and anti-inflammatory factors, to regulate the balance of immune responses (95). While FSGS is not typically considered a typical immune complex-mediated disease, increasing evidence suggests that B cells also play a significant role in FSGS. Several potential autoantigens and antibodies associated with B cells have been identified in FSGS. For instance, annexin A2, a protein involved in apoptosis and signal transduction, has been identified as a potential autoantigen through mass spectrometry analysis (96). Another study found that 29% of INS patients had anti-nephrin immunoglobulin G (IgG) antibodies in their plasma, which decreased with treatment and disappeared in patients with complete remission (97). A recent report by Dr. Hattori and colleagues showed that circulating anti-nephrin autoantibodies detected in plasma samples from a recurrent FSGS patient after kidney transplantation results in the tyrosine phosphorylation of nephrin, leading to alterations in nephrin distribution and podocyte foot process effacement. It was indicated that circulating anti-nephrin autoantibodies could be a possible pathogenic candidate for circulating factors in the posttransplant recurrence of primary FSGS (97). Furthermore, there is evidence indicating a higher frequency of the human leukocyte antigen (HLA)-A30 antigen in primary FSGS patients, with HLA-A30 being associated with FSGS recurrence (98).

The Src homology 3 domain-binding protein 2 (SH3BP2) is an adaptor protein ubiquitously expressed in immune cells, governing signaling pathways within the cell (99). Kidney biopsy samples from patients with these conditions consistently exhibit upregulation of the SH3BP2 signaling complex, suggesting its potential involvement in immune activation—a prominent feature of these podocytopathies (100). Research led by Tarak Srivastava and colleagues, using murine models, has further underscored the significance of SH3BP2 in podocyte injury. Transgenic mice with induced mutations in the SH3BP2 gene displayed features indicative of podocyte dysfunction, including elevated urinary albumin levels, a decrease in serum albumin, and an increase in mesangial cell proliferation (100). Collectively, these findings position SH3BP2 and its associated proteins at the forefront of immunological processes that contribute to podocyte injury.

Despite the unclear pathogenesis of FSGS, comprehensively studying the structure and function of proteins related to podocytes, as well as the mechanisms underlying podocyte injury in FSGS, offers essential insights for deciphering its pathophysiology. These investigations could reveal novel avenues for clinical treatment, potentially resulting in the effective reduction or deceleration of the glomerulosclerosis process and postponing the onset of end-stage kidney failure.

4.3 Primary membranous nephropathy

Membranous nephropathy (MN) is a common kidney disease affecting individuals across different age groups, particularly adults.

Pathologically, it involves the deposition of immune complexes on the outer side of the GBM located beneath the podocyte, accompanied by diffuse GBM thickening. Approximately 20% to 30% of MN cases are associated with secondary factors such as systemic autoimmune diseases, infections, drugs, malignancy, or hematopoietic stem cell transplantation, known as secondary MN. In cases where no clear causal relationship or recognizable systemic disease, infection, or drug exposure is identified, the condition is termed primary membranous nephropathy (pMN), often perceived as a kidney-specific autoimmune disease (101, 102). pMN is the most common cause of primary nephrotic syndrome in non-diabetic patients, accounting for approximately 30% of adult non-diabetic nephrotic syndrome cases. It is characterized by massive proteinuria, hypoalbuminemia, dyslipidemia, and edema, while a small number of patients present with asymptomatic proteinuria (103). The typical microscopic pathological features of pMN include GBM thickening, podocyte foot process effacement, and spike-like electron-dense deposits under the glomerular podocytes. Immunofluorescence analysis typically shows granular deposits of IgG and C3 along the capillary wall, with IgG4 being the dominant IgG subtype in pMN (104).

The pathogenesis of pMN is not yet fully elucidated. According to the classical theory, antigens on the podocytes bind to specific antibodies, forming *in situ* immune complexes that deposit at the GBM. This deposition activates complement and creates membrane attack complexes, leading to damage to the glomerular filtration barrier and subsequent proteinuria (105). Recent progress in understanding the pathogenesis of pMN has been driven by the discovery of two key podocyte antigens: phospholipase A2 receptor (PLA2R) and thrombospondin type-1 domain-containing 7A (THSD7A), which serve as antibody markers in 70% and 2-3% of pMN patients, respectively (106). Animal models have validated the pathogenicity of human PLA2R and THSD7A antibodies. Both PLA2R and THSD7A are transmembrane proteins expressed by podocytes that can bind to circulating IgG4 subtype autoantibodies, forming subepithelial immune complexes (107, 108). Tomas NM and colleagues engineered a transgenic mouse model that specifically expresses human phospholipase A2 receptor 1 (hPLA2R1) in podocytes. These mice spontaneously generate antibodies against hPLA2R1, resulting in the development of nephrotic syndrome and demonstrating classical histological features of MN (109). This rodent model faithfully recapitulates key aspects of human MN, providing a valuable tool for probing the pathophysiological underpinnings of the disease and for the assessment of targeted therapeutic interventions. Additionally, several other podocyte-intrinsic antigens, such as high-temperature requirement A1 (HTRA1), netrin G1 (NTNG1), contactin-1 (CNTN1), and Semaphorin 3B (SEMA3B), have been identified, although the pathogenicity of these antigens in MN remains to be confirmed (110–113).

Furthermore, some potential antigens that are not expressed by podocytes have been associated with pMN. Studies have shown that certain pMN cases are linked to the accumulation of exostosin glycosyltransferase 1 (EXT1) and exostosin glycosyltransferase 2 (EXT2). In a study of 48 PLA2R-negative pMN cases, EXT1 and EXT2 were detected in 21 of them but not in PLA2R-related pMN cases or control cases (114). Additionally, a mass spectrometry study conducted on 126 PLA2R-negative MN cases revealed that 29 cases were positive for neural epidermal growth factor-like 1 protein (NELL-1) (115). The clinical and kidney biopsy results of NELL-1-positive MN exhibited characteristics of pMN. In 5.7% of PLA2R-negative pMN cases, a unique protein called protocadherin 7 (PCDH7) was detected, and notably, all other antigens were negative in these cases (116). PCDH7-associated pMN appears to be a distinct, previously unidentified type of MN. Additionally, researchers have identified a novel antigen, neural cell adhesion molecule 1 (NCAM1), in rare pMN cases, with a prevalence of 2.0% in pMN cases (117). These antigens may be neo- or allo-antigens that deposit in the subepithelial space and bind to IgG1 or IgG3 subtype autoantibodies. The mechanism of action of these antigens in MN is unclear, and their potential associations with other diseases remain uncertain (102).

The pathogenesis of pMN is highly complex and results from the interaction of multiple factors. As our understanding of the molecular structure and gene loci of target antigens continues to grow, different target antigens and gene loci may provide new insights for the diagnosis and treatment of this disease. Further exploration of the mechanism of podocyte immunity in MN and the discovery of more effective and safe therapeutic targets are crucial directions for future pMN research.

4.4 Lupus nephritis with podocyte injury

Systemic lupus erythematosus (SLE) is a complex autoimmune disease that affects multiple systems and organs throughout the body. It's estimated that up to 40% of SLE patients will develop lupus nephritis (LN) (118). LN is a common and serious complication of SLE, significantly impacting the long-term prognosis of patients. The hallmark histopathological feature of LN is the deposition of immune complexes and inflammatory reactions in the kidneys. This ultimately leads to the destruction of kidney parenchyma and a clinical decline in kidney function (119). The most internationally recognized pathological classification of LN is the 2003 classification of lupus nephritis by the International Society of Nephrology (ISN) and the Renal Pathology Society (RPS), which divides LN into types I-VI (120). However, this classification system does not encompass all types of LN pathology. Some LN patients may have kidney biopsy results that do not align with their clinical manifestations, such as having massive proteinuria with relatively normal glomeruli or only mild glomerular mesangial proliferation. These patients may have a unique subtype of LN known as LN with podocyte lesions (119).

The pathogenesis of LN is not completely understood, but the prevailing view is that LN is characterized by the deposition of immune complexes (IC) formed by various autoantibodies, such as anti-double-stranded DNA (ds-DNA) antibodies and antigens. Infiltration of inflammatory cells occurs, with podocytes being one of the primary targets of IC attacks (121). Anti-dsDNA antibodies can recognize various DNA structures and also cross-react with various non-DNA molecules present in the renal matrix or on the surfaces of endogenous renal cells, such as α-actinin,

annexin II, collagen III/IV, and others (122–124). Additionally, the degree of glycosylation of anti-dsDNA antibodies can affect their pathogenicity, with α-2,6-sialylation attenuating their effects and fructosylation exacerbating their nephritogenic activity (125). The deposition of IC can activate the complement system, leading to the production of various complement components, such as C3, C4, C5a, and more. These complement components can attract and activate inflammatory cells like neutrophils, monocytes, and macrophages, which in turn release podocyte-toxic substances, resulting in direct damage or apoptosis of podocytes (126). An alternative hypothesis posits that the interplay of podocytes and TLRs could be a contributing factor in the pathogenesis of LN. The overexpression of TLR8 and TLR9 plays a key role in stimulating the NF-κB pathway, which results in the generation of specific inflammatory cytokines, namely IL1b, IL6, IFN-g, and TNF-α (127). This, in turn, intensifies the inflammatory response and contributes to glomerular damage. Significantly, an increase in TLR9 expression has been robustly associated with podocyte impairment. This is evident in the decline in podocyte numbers, loss of foot processes, and emergence of microvillous protrusions, along with the thickening and subsequent wrinkling of the basal membrane (14).

Recent research has revealed that, in addition to the involvement of relevant aberrant autoantibodies in antigen-antibody reactions contributing to the pathogenesis of LN, renal cells actively participate in the inflammation and immune response of LN. Kidneys harbor tertiary lymphoid structures (TLSs), resembling lymph node-like structures housing immune cells such as T cells, B cells, dendritic cells, macrophages, and more. TLSs serve as local immunity structures that promote adaptive immunity; their unencapsulated structure enables direct exposure to diverse stimuli from an inflamed environment, including CKD. These immune cells proliferate, differentiate, activate, and form memory within TLSs, actively engaging in the production of autoantibodies and pro-inflammatory factors, ultimately causing kidney tissue damage. Functional characterization of TLSs in CKD and the development of interventions to regulate kidney TLSs potentially lead to promising therapeutic avenues (128, 129). Notably, the preferential expression of TCR Vβ gene expression in intrarenal T cells, driven by antigen stimulation compared to peripheral blood lymphocytes, and the high expression of IL-4 and IL-10 on intrarenal T cells from LN patients, suggest that intrarenal T cells potentially play a critical role in the pathogenesis of LN (130). Furthermore, $CD8^+$ T cells can induce podocyte injury, directly or indirectly, leading to crescent formation (131). Macrophages play a pivotal role in the pathogenesis of LN by mediating impaired kidney repair mechanisms in lupus-susceptible mice. Studies have revealed that these aberrant macrophages facilitate suboptimal kidney repair, precipitating the onset of LN in such mice (132). Similarly, dendritic cells, renowned as the most powerful APCs, are integral to bridging innate and adaptive immunity. Their role in engulfing apoptotic blebs followed by the promotion of Th17 cell differentiation is pivotal, leading to the maladaptive immune responses and the breakdown of self-tolerance that are hallmarks of SLE (133). Furthermore, podocytes are not only structural components of the glomerulus but also actively contribute to immune responses. These cells have been increasingly recognized for their significant role in the pathogenic mechanisms underlying LN. Dysregulated autophagy in podocytes is posited to be a contributory factor in the pathogenesis of SLE (134). Observations indicate that LN stimulates Cyclooxygenase-2(COX-2) in the endoplasmic reticulum stress pathway and activates Activating Transcription Factor 4(ATF4) in podocytes, while inhibition of COX-2 reduces LN-induced autophagy in these cells, highlighting COX-2 as a viable therapeutic target for LN (135). TLR9 has been identified as playing a significant role in the pathophysiology of LN, evidenced by its substantial up-regulation within glomerular structures (136). The interaction between TLR9 and IgG originating from patients is a critical aspect of the disease mechanism. These IgG molecules infiltrate podocytes, eliciting an enhanced expression of calcium/calmodulin-dependent protein kinase IV (CaMK4) (32). This increase in CaMK4 expression subsequently leads to the up-regulation of genes involved in podocyte damage and T-cell activation (137). Moreover, there is a discernible expression and activation of Nod-like receptor protein 3 (NLRP3) inflammasomes within the podocytes in instances of LN, as observed in lupus-susceptible murine models (38). Importantly, the pharmacological inhibition of the NLRP3 inflammasome has been shown to mitigate proteinuria and diminish both the histological deterioration of kidney tissue and the effacement of podocyte foot processes (138). These findings suggest that the activation of NLRP3 plays a crucial role in the advancement of podocyte injury and the ensuing proteinuria, comprising a significant aspect of the pathogenesis of LN.

In recent years, significant progress has been made in understanding the pathogenesis, diagnosis, and treatment of podocyte immune injury in LN. However, there is still a significant research agenda focused on exploring various pathogenic mechanisms and identifying biomarkers associated with this condition. Current research aims to uncover new diagnostic methods and biomarkers to gain a deeper understanding of the underlying processes causing podocyte immune injury in LN. Moreover, identifying potential therapeutic targets is crucial for the development of more effective treatments for this severe complication of SLE.

5 Therapeutic strategies targeting immunity in podocyte injury

5.1 Current standard therapies for podocyte-related proteinuric glomerular diseases

The clinical manifestations of podocyte-related kidney diseases often present as proteinuria. Most of the diseases are widely acknowledged as immune-mediated kidney disorders. As a result, the standard approach to treating proteinuric glomerular kidney diseases associated with podocyte injury primarily revolves around reducing proteinuria and moderating hyperactive immune responses through the application of immunosuppressive therapy (139). Aside from the commonly used drugs like renin-angiotensin-

aldosterone inhibitors, sodium-glucose cotransporter-1 inhibitors, glucagon-like peptide-1 agonists, and mineralocorticoid receptor antagonists, which reduce proteinuria and protect kidney functions through non-immunological mechanisms of action (140), we will focus on the immune-related drugs for podocyte-related proteinuric kidney diseases below.

5.1.1 Immunosuppressive drugs

Glucocorticoids (GCs) have been the mainstay in the treatment of podocyte-related proteinuric kidney diseases for several decades (141). These agents primarily exert their effects by binding to the glucocorticoid receptor (GR) in podocytes, thereby modulating gene expression and influencing the structure and function of these cells (142). For instance, GCs are capable of suppressing the secretion of various pro-inflammatory cytokines, such as interleukins (IL), TGF-β, and tumor necrosis factor (TNF), thereby attenuating the inflammatory response in the glomerulus (143). Furthermore, GCs activate the gene promoter of nephrin, a critical protein in the kidney's slit diaphragm, thereby facilitating its proper glycosylation and phosphorylation, and reinforcing its connection with the actin cytoskeleton, ultimately maintaining the integrity and stability of the slit diaphragm (144–147). The KDIGO (Kidney Disease: Improving Global Outcomes) 2012 guidelines classified nephrotic syndrome into different types based on the response to glucocorticoid therapy, namely, glucocorticoid-sensitive and glucocorticoid-resistant nephrotic syndrome (148). It has been observed that oral glucocorticoid therapy in children with nephrotic syndrome may encounter issues of resistance, with approximately 50% of affected children eventually progressing to end-stage kidney disease if unresponsive after five years of treatment (149). Consequently, the implementation of specific immunosuppressive therapies, including drugs such as cyclophosphamide, has become necessary (150). The combination of alkylating agents with steroids has demonstrated high efficacy in managing high-risk podocyte-associated proteinuric kidney diseases such as MN (151). Studies have indicated the effectiveness of the combination of cyclophosphamide with prednisone for various high-risk MN patients (152). Research indicates that high-dose cyclophosphamide suppresses $CD103^+$ dendritic cells in a rat model, resulting in changes in their frequency, surface molecule expression, and antigen-capturing ability. This alteration enhances $CD4^+$ T cell activation, modulates the TLR/MyD88/MAPK pathway, and results in increased Treg levels while reducing Th1/Th2 differentiation and Th17 generation (153). In a ten-year multicenter retrospective study involving 752 pMN patients, cyclophosphamide demonstrated superior performance compared to calcineurin inhibitors. Cyclophosphamide showed statistically significant improvements in treatment response, kidney function preservation, and a lower recurrence rate (154). Despite the fact that calcineurin inhibitors are less effective compared to cyclophosphamide in the management of PMN, they maintain a crucial role in the treatment of podocyte immunological injury.

Calcineurin inhibitors, such as cyclosporine A, tacrolimus, and voclosporin, belong to a class of immunosuppressants that inhibit T cell activation and regulate the Th17 immune response, thereby modulating the occurrence and development of podocyte-related proteinuric kidney diseases (155, 156). Cyclosporine A is of vital importance for the stabilization and protection of podocytes. Evidence has shown that it directly stabilizes the actin cytoskeleton in podocytes, thus helping to maintain the integrity of the glomerular filtration barrier, which is essential for proper podocyte functioning (157). Moreover, research has revealed that Cyclosporine A indirectly safeguards podocytes by regulating the phosphorylation of proteins implicated in the control of actin dynamics, such as WAVE1 (158), and by stabilizing the expression of cofilin-1 (159). Furthermore, Cyclosporine A has proven to be efficacious in addressing specific genetic podocyte damage (160). Tacrolimus is a substance that has been conclusively shown to offer protection to podocytes via mechanisms that include cytoskeleton stabilization, cell apoptosis inhibition, and damage repair (161). Various rodent models of kidney injury have highlighted the ability of Tacrolimus to rejuvenate impaired podocytes and maintain the expression level of Calcineurin Binding Protein 1 (Cabin1) (162, 163). In the context of diabetic nephropathy, Tacrolimus confers protection to podocytes from apoptotic death through downregulating Transient Receptor Potential Channel 6 (TRPC6) (164). Moreover, Tacrolimus aids in mitigating podocytic injury by reinstating FK506 Binding Protein 12 (FKBP12) on the actin cytoskeleton (165). Despite the rapid reduction in proteinuria in pMN upon treatment with calcineurin inhibitors, their long-term effects tend to be unstable, leading to relapses upon discontinuation, and are associated with certain toxic side effects (166). Therefore, the KDIGO 2021 guidelines suggest the use of calcineurin inhibitors in patients with normal kidney function and a moderate risk of disease progression to shorten the duration of proteinuria (139). Voclosporin, a newly developed calcineurin inhibitor, has been licensed in a multitude of countries for the management of lupus nephritis (167). Besides its recognized T-cell immunosuppressive capabilities, Voclosporin serves a dual role in the stabilization of podocytes and exhibiting anti-proteinuric traits. Empirical evidence suggests its superior efficacy in proteinuria reduction, outpacing both cyclosporine A and Tacrolimus (168).

While mycophenolate mofetil (MMF) is well-established as an immunosuppressant for renal immune diseases, the intricacies of its mechanistic effect on podocytes remain to be fully elucidated. Nevertheless, several lines of research provide intriguing insights into potential modes of action. It has been suggested that one facet of MMF's protective effect against podocyte injury could be attributed to its role in restoring the integrity of the cytoskeletal axis of actin filaments (169, 170). Furthermore, experiments utilizing diabetic mouse models treated with MMF showed a notable reduction in the number of infiltrated CD4 and CD8 T cells within the kidneys. More interestingly, the previous downward trajectory of nephrin and WT1 expression in the glomeruli appeared to be successfully arrested and reversed (171).

While immunosuppressive drugs primarily target immune-mediated glomerular diseases, their use may lead to serious side effects, especially after prolonged use, such as infections, osteoporosis, and hypertension. Moreover, these drugs may not be effective or have limited efficacy in some non-immune

proteinuric glomerular diseases, including genetic or metabolic glomerular diseases. Consequently, the development of novel drugs to manage various types of podocyte immune injury is urgently needed.

5.1.2 Biological agents

In recent years, our understanding of the molecular mechanisms and immune targets involved in podocyte injury has advanced, leading to the continuous exploration and development of novel immune-targeted therapeutic strategies (Table 2). Biologic agents have emerged as a pivotal treatment option for immune-related diseases and hold significant promise for addressing podocyte-related conditions. RTX, a human-mouse chimeric CD20 monoclonal antibody, disrupts the interaction between B cells and T cells by specifically binding to CD20, inducing $CD20^+$ B cell depletion through antibody-dependent and complement-dependent cytotoxic effects (186, 187). In podocytes, RTX also plays a protective role by preserving the actin cytoskeleton, preventing the downregulation of SMPDL-3b, and inhibiting actin cytoskeleton remodeling, ultimately reducing proteinuria (188). A combined treatment approach involving RTX, initial short-term low-dose oral cyclophosphamide, and a rapid tapering of prednisone has shown encouraging results. After a follow-up period of 25 to 62 months for 60 patients with pMN receiving this combined treatment, the study by Zonozi et al. reported that 100% of patients achieved partial remission, with 90% achieving lasting complete remission, while maintaining an acceptable safety profile (189). Ofatumumab (OFA), a new generation of anti-CD20 IgG1κ human monoclonal antibodies, offers an excellent alternative for patients resistant to or sensitized against RTX. OFA is a well-tolerated and safe treatment with longer intervals between doses, which can effectively replace RTX (190). Some studies even suggest that low-dose OFA can induce remission of proteinuria in children with long-term treatment-resistant INS (191). RTX can also be used in combination with calcineurin inhibitors to enhance therapeutic efficacy (192).

Abatacept, categorized as an immunomodulatory drug, is formed by fusing cytotoxic T-lymphocyte-associated antigen 4 (CTLA-4), a surface protein, with the Fc segment of human immunoglobulin. External factors like viral infections and Treg function can impact the expression of B7-1 (CD80) on podocytes, potentially causing podocyte cytoskeletal disarray and severe proteinuria (193). CTLA-4, a critical co-factor expressed on podocytes and Tregs, binds to B7-1 (CD80), inhibits T cell activation, and reinstates SS1 integrin activation, thereby alleviating podocyte injury and proteinuria (194). Contrary to conventional wisdom, recent research challenges the notion of increased B7-1 expression within the podocytes of individuals with proteinuria. Studies investigating minimal change disease (MCD) and focal segmental glomerulosclerosis (FSGS) utilizing multiple antibodies and assays found no significant upregulation of podocyte B7-1 in these conditions, casting doubt on the efficacy of B7-1 inhibitory treatment (195). Moreover, B7-1 is not induced in podocytes of patients with diabetic nephropathy (DN) or in BTBR ob/ob mice, a type 2 diabetes model (196). A recent study exploring abatacept's efficacy in post-kidney transplant FSGS patients who

TABLE 2 Commonly used immunotherapy drugs for podocyte-related proteinuric kidney disease.

Immunosuppressive drugs	Effect on podocytes	References
Glucocorticoids	Inducing downregulation of pro-inflammatory genes by binding to specific cytoplasmic glucocorticoid receptors (GR); Blocking the TRPC6 signaling pathway and upregulating CD80; Regulating gene expression by binding to glucocorticoid responsive elements (GRE) on DNA; Reducing cell apoptosis by downregulating p53 and increasing miR-30s and Bcl-2	(142, 172–174)
cyclophosphamide	Causing cross-linking of DNA and RNA and inhibiting protein synthesis through cytotoxic effects.	(150)
calcineurin inhibitor	Inhibiting the activation of T cells by targeting the Calcineurin Enzyme while also exerting a direct protective effect on podocytes.	(156, 157)
Calmodulin inhibitors	Preserving the phosphorylation-dependent synaptopodin-14-3-3β interaction; Resulting in upregulation of TRPC6 and ANGPTL4; Reduces cell apoptosis	(175–177)
Mycophenolate mofetil	Reduce uPAR mRNA and protein expression levels; Regulating ATP depletion and stabilizing actin cytoskeleton	(178, 179)
Adrenocorticotropic hormone	Inhibiting cell apoptosis and stabilizing the cytoskeleton	(180)
Rituximab	Binding to CD20 on B cells stabilizes the podocyte cytoskeleton by preventing downregulation of sphingomyelin phosphodiesterase acid-like 3b (SMLPD-3b) and acid sphingomyelinase (ASMase)	(181)
Abatacept	Blocking of B7-1 signal transduction and recovery of SS1 integrin activation	(182)
Eculizumab	Block C5 complement protein and prevent the generation of C5a and C5b	(183)
Avacopan	Inhibits the C5a receptor, preventing the activation	(184)

(Continued)

TABLE 2 Continued

Immunosuppressive drugs	Effect on podocytes	References
	of the complement system and the subsequent inflammation and cell damage	
Narsolimab	Inhibits the MASP-2, thus preventing the activation of the complement system	(185)

developed FSGS after transplantation and failed conventional therapy revealed that responders to abatacept were B7-1 positive. This suggests that podocyte B7-1 staining in kidney transplant biopsies might identify patients benefiting from abatacept (197). Researchers propose that the mechanism behind the anti-proteinuric effects of B7-1 inhibitors may involve the suppression of immune cell activation rather than direct effects on podocytes (195). Furthermore, some evidence suggests a direct podocyte protective role of abatacept (198). Consequently, further research is crucial to elucidate the association between B7-1 and podocyte damage in different kidney conditions.

Immunotherapy, which leverages the immune system to intervene in podocyte damage, is a promising approach known for its high specificity, minimal side effects, and durable benefits. It can be applied to treat various types of podocyte damage. Future research should prioritize a deeper understanding of the mechanisms involved and the optimization of parameters for immunotherapy to improve its clinical applicability and effectiveness.

5.2 Novel therapeutic approaches

In recent years, as our understanding of the immune mechanisms underlying podocyte injury in proteinuric kidney diseases has deepened, new prospects for immunotherapy in managing podocyte diseases have emerged. The involvement of the complement system in the pathogenesis of podocyte injury has been highlighted (199). C5b is known to induce osmotic lysis of podocytes, leading to alterations in the actin cytoskeleton and the podocyte slit diaphragm, as well as limiting the proliferation of podocytes (200). Therefore, the utilization of the complement inhibitor Eculizumab to impede the activation of the complement cascade and the subsequent generation of C5b constitutes an effective strategy for intervention (183). Avacopan, as a selective inhibitor of the C5a receptor, orchestrates a blockade against C5a activity (201). By attenuating the complement system's activation and thereby abating subsequent inflammatory responses and cellular damage, this inhibition facilitates an indirect protective effect on podocytes through the modulation of the inflammatory environment (184). Narsolimab, or OMS721, is a fully human monoclonal antibody that specifically targets and inhibits mannan-binding lectin-associated serine protease-2 (MASP-2) (202). MASP-2 serves as the effector enzyme within the lectin pathway of the complement system, which is regarded as one of the principal routes of complement activation (203). By effectively inhibiting MASP-2, narsolimab disrupts the activation of the lectin pathway, thereby mitigating complement-mediated inflammation and minimizing endothelial damage (204). In a recent study, the administration of narsolimab demonstrated clinically significant reductions in proteinuria and sustained stability in estimated glomerular filtration rates (185).

In the case of patients with MCD, podocytes express angiopoietin-like 4 (Angptl4), with one of its forms being hyposialylated Angptl4, which binds to the glomerular basement membrane and endothelial cells, leading to proteinuria (205). Utilizing N-acetyl-D-mannosamine has shown promise in converting hyposialylated Angptl4 to its sialylated form, which can be taken up and stored by podocytes, thereby reducing the production of proteinuria (206). Although this appears to be a potential treatment option, relevant clinical data remains limited.

The field of immunotherapy for podocyte preservation is in a state of constant advancement, highlighted by the emergence of various natural compounds and small-molecule inhibitors known for their podocyte-protective properties. For example, curcumin, derived from turmeric, has been recognized for effectively reducing reactive oxygen species (ROS) and RIPK3 expression, thereby establishing itself as a potential therapeutic agent for combating diabetic nephropathy (207). Additionally, luteolin exerts a protective effect against glucose-induced podocyte stress by inhibiting the NLRP3 inflammasome, a critical component of the immune system and inflammatory response (208). Expanding the scope, Astragaloside IV is acknowledged for its comprehensive protective capabilities, which include mitigating endoplasmic reticulum stress, promoting autophagy, and improving mitochondrial function (209). This multitargeted approach involves interaction with several signaling pathways such as SERCA2, AMPKα, and Nrf2-ARE/TFAM, highlighting the molecule's potential in supporting podocyte integrity (210, 211). In a similar vein, hyperoside presents a protective strategy by modulating mitochondrial dynamics. It specifically inhibits mitochondrial fission, which has been observed to diminish albuminuria and renal damage in experimental models, further emphasizing its therapeutic potential (212).

Within the realm of metabolic regulation, the Rho-associated coiled-coil-containing protein kinase 2 (ROCK2) signaling pathway has been identified as a crucial regulator with significant implications for podocyte health. The ROCK2 signaling pathway plays an instrumental role in numerous metabolic functions critical to podocyte health, notably the initiation of apoptosis (213). Additionally, it disrupts fatty acid oxidation through the downregulation of peroxisome proliferator-activated receptor alpha (PPARα), thus underlining the pathway's fundamental influence on cellular metabolism and the podocyte's adaptability to metabolic stress (214). Additionally, in the intricate web of intracellular signaling, the mechanistic target of the rapamycin (mTOR) pathway stands out, particularly through its two distinct complexes, mTORC1, and mTORC2, as a vital target for immunotherapeutic intervention (215). Inhibiting these complexes has been shown to offer reprieve to stressed podocytes, principally by counteracting the adverse effects of hyperglycemia (216). These effects extend to safeguarding cell viability, reducing apoptosis, and maintaining the stability of structural proteins,

which are fundamental to podocyte function. Moreover, contemporary research has shed light on the utility of angiotensin II inhibition in podocyte protection and the retardation of glomerulosclerosis progression (217). The benefits of this inhibition extend beyond the direct antagonism of angiotensin II type 1 (AT1) receptors on the podocytes themselves (218). Emerging evidence suggests additional protective mechanisms that may involve crosstalk with other cellular entities or alternative molecular pathways, presenting potential avenues for therapeutic interventions (Table 3).

Collectively, these diverse strategies underscore the rapid advancement in the realm of podocyte immunotherapy, paving the way for novel, tailored treatment options aimed at reducing the burden of podocyte injury and related kidney diseases. Each compound or pathway presents its mechanism of action, which when considered in conjunction, could offer a comprehensive, multi-targeted approach to combat renal pathologies associated with podocyte damage.

6 Conclusion remarks

Podocytes play a crucial role in both renal physiology and pathology, providing valuable insights into kidney function. While prior research has highlighted tubulointerstitial fibrosis as a key pathological mechanism in the progression and kidney failure of CKD, recent studies have also underscored the connection between the dysfunction and death of podocytes and the advancement of CKD. The immune response of podocytes serves as a pivotal factor in the development and progression of various proteinuric kidney diseases and presents itself as a promising therapeutic target. Despite advancements, numerous aspects of the mechanisms governing podocyte immune responses remain uncharted, emphasizing the need for further exploration. Subsequent research endeavors should aim to identify novel podocyte-related antigens and antibodies, unravel the intricacies of the regulatory mechanisms governing the interaction between podocytes and other immune cells, and develop innovative therapeutic strategies that specifically target podocyte immune responses. These efforts are essential for enhancing the prognosis and overall quality of life for patients affected by kidney disease and for addressing the current unmet medical needs in this area.

TABLE 3 Some natural medications with immunotherapeutic effects on podocyte injury.

Nature medicine	Effect on podocytes	References
Curcumin	Attenuates Angiotensin II-induced podocyte injury and apoptosis by inhibiting endoplasmic reticulum stress; Reduce the expression of ROS and RIPK3	(207, 219)
Luteolin	Attenuates high glucose-induced podocyte injury via suppressing NLRP3 inflammasome pathway	(208)
Astragaloside IV	Collaborate with SERCA2 and AMPK α Multiple signaling pathways such as Nrf2-ARE/TFAM protect podocytes	(210, 211)
Hyperoside	Reduces albuminuria in diabetic nephropathy at the early stage through ameliorating renal damage and podocyte injury	(220)

Author contributions

HJ: Conceptualization, Supervision, Writing – review & editing. ZS: Investigation, Writing – original draft. JZ: Investigation, Writing – review & editing. CL: Funding acquisition, Writing – review & editing. YQ: Writing – review & editing. CX: Software, Writing – review & editing. SY: Writing – review & editing. XT: Conceptualization, Supervision, Writing – review & editing.

Funding

The author(s) declare financial support was received for the research, authorship, and/or publication of this article. This work was supported by a grant from the Central government guide local science and technology development special fund project: Xinjiang kidney disease big data smart medical innovation research and application base construction (grant number ZYYD2022C18) to CL. It was also supported by the Tianshan Talents - High-level Leading Talents Project (Department of Science and Technology of Xinjiang Uygur Autonomous Region): Construction and expansion of precision diagnosis and treatment system of chronic kidney disease based on clinical pathway and DRG (grant number 2022TSYCLJ0022) to CL.

Acknowledgments

We thank the Clinical Research Center of Kidney Disease of Xinjiang Uygur Autonomous Region for providing technical support. We also thank the Figdraw (www.figdraw.com) for their support in drawing the figures.

Conflict of interest

The authors declare that the research was conducted in the absence of any commercial or financial relationships that could be construed as a potential conflict of interest.

The author(s) declared that they were an editorial board member of Frontiers, at the time of submission. This had no impact on the peer review process and the final decision.

Publisher's note

References

1. Hausmann R, Grepl M, Knecht V, Moeller MJ. The glomerular filtration barrier function. *Curr Opin Nephrol Hypertension* (2012) 21:441–9. doi: 10.1097/MNH.0b013e328354a28e

2. Medina Rangel PX, Priyadarshini A, Tian X. New insights into the immunity and podocyte in glomerular health and disease: from pathogenesis to therapy in proteinuric kidney disease. *Integr Med Nephrol Androl* (2021) 8:5. doi: 10.4103/imna.imna_26_21

3. Garg P. A review of podocyte biology. *Am J Nephrol* (2018) 47:3–13. doi: 10.1159/000481633

4. Schell C, Huber TB. The evolving complexity of the podocyte cytoskeleton. *J Am Soc Nephrol* (2017) 28:3166–74. doi: 10.1681/asn.2017020143

5. Kocylowski MK, Aypek H, Bildl W, Helmstädter M, Trachte P, Dumoulin B, et al. A slit-diaphragm-associated protein network for dynamic control of renal filtration. *Nat Commun* (2022) 13:6446. doi: 10.1038/s41467-022-33748-1

6. Bhargava R, Tsokos GC. The immune podocyte. *Curr Opin Rheumatol* (2019) 31:167–74. doi: 10.1097/bor.0000000000000578

7. Banas MC, Banas B, Hudkins KL, Wietecha TA, Iyoda M, Bock E, et al. TLR4 links podocytes with the innate immune system to mediate glomerular injury. *J Am Soc Nephrol* (2008) 19:704–13. doi: 10.1681/asn.2007040395

8. Mazgaeen L, Gurung P. Recent advances in lipopolysaccharide recognition systems. *Int J Mol Sci* (2020) 21:379. doi: 10.3390/ijms21020379

9. Ma J, Chadban SJ, Zhao CY, Chen X, Kwan T, Panchapakesan U, et al. TLR4 activation promotes podocyte injury and interstitial fibrosis in diabetic nephropathy. *PloS One* (2014) 9:e97985. doi: 10.1371/journal.pone.0097985

10. Behzadi P, García-Perdomo HA, Karpiński TM, Niedźwiedzka-Rystwej P. Toll-like receptors: general molecular and structural biology. *J Immunol Res* (2021) 2021:1–21. doi: 10.1155/2021/9914854

11. Janssens S, Beyaert R. Role of toll-like receptors in pathogen recognition. *Clin Microbiol Rev* (2003) 16:637–46. doi: 10.1128/cmr.16.4.637-646.2003

12. Kawasaki T, Kawai T. Toll-like receptor signaling pathways. *Front Immunol* (2014) 300:461. doi: 10.3389/fimmu.2014.00461

13. Bao W, Xia H, Liang Y, Ye Y, Lu Y, Xu X, et al. Toll-like receptor 9 can be activated by endogenous mitochondrial DNA to induce podocyte apoptosis. *Sci Rep* (2016) 6:22579. doi: 10.1038/srep22579

14. Masum MA, Ichii O, Hosny Ali Elewa Y, Nakamura T, Otani Y, Hosotani M, et al. Overexpression of toll-like receptor 9 correlates with podocyte injury in a murine model of autoimmune membranoproliferative glomerulonephritis. *Autoimmunity* (2018) 51:386–98. doi: 10.1080/08916934.2018.1549234

15. Burke GW, Mitrofanova A, Fontanella A, Ciancio G, Roth D, Ruiz P, et al. The podocyte: glomerular sentinel at the crossroads of innate and adaptive immunity. *Front Immunol* (2023) 14:1201619. doi: 10.3389/fimmu.2023.1201619

16. Komada T, Muruve DA. The role of inflammasomes in kidney disease. *Nat Rev Nephrol* (2019) 15:501–20. doi: 10.1038/s41581-019-0158-z

17. Bai M, Chen Y, Zhao M, Zhang Y, He JC, Huang S, et al. NLRP3 inflammasome activation contributes to aldosterone-induced podocyte injury. *Am J Physiol Renal Physiol* (2017) 312:F556–F64. doi: 10.1152/ajprenal.00332.2016

18. Zang N, Cui C, Guo X, Song J, Hu H, Yang M, et al. cGAS-STING activation contributes to podocyte injury in diabetic kidney disease. *iScience* (2022) 25:105145. doi: 10.1016/j.isci.2022.105145

19. Ge Z, Ding S. Regulation of cGAS/STING signaling and corresponding immune escape strategies of viruses. *Front Cell Infect Microbiol* (2022) 12:954581. doi: 10.3389/fcimb.2022.954581

20. Guey B, Ablasser A. Emerging dimensions of cellular cGAS-STING signaling. *Curr Opin Immunol* (2022) 74:164–71. doi: 10.1016/j.coi.2022.01.004

21. Mitrofanova A, Fontanella A, Tolerico M, Mallela S, Molina David J, Zuo Y, et al. Activation of stimulator of interferon genes (STING) causes proteinuria and contributes to glomerular diseases. *J Am Soc NEPHROL* (2022) 33:2153–73. doi: 10.1681/ASN.2021101286

22. Gao Z, Lu L, Chen X, Dobrzyn A. Release of HMGB1 in podocytes exacerbates lipopolysaccharide-induced acute kidney injury. *Mediators Inflamm* (2021) 2021:1–10. doi: 10.1155/2021/5220226

23. Tesch G, Sourris KC, Summers SA, McCarthy D, Ward MS, Borg DJ, et al. Deletion of bone-marrow-derived receptor for AGEs (RAGE) improves renal function in an experimental mouse model of diabetes. *Diabetologia* (2014) 57:1977–85. doi: 10.1007/s00125-014-3291-z

24. Jin J, Gong J, Zhao L, Zhang H, He Q, Jiang X. Inhibition of high mobility group box 1 (HMGB1) attenuates podocyte apoptosis and epithelial-mesenchymal transition by regulating autophagy flux. *J Diab* (2019) 11:826–36. doi: 10.1111/1753-0407.12914

25. Liu T, Li Q, Jin Q, Yang L, Mao H, Qu P, et al. Targeting HMGB1: A potential therapeutic strategy for chronic kidney disease. *Int J Biol Sci* (2023) 19:5020–35. doi: 10.7150/ijbs.87964

26. Reggiani F, Ponticelli C. Focal segmental glomerular sclerosis: do not overlook the role of immune response. *J Nephrol* (2016) 29:525–34. doi: 10.1007/s40620-016-0272-y

27. Goldwich A, Burkard M, Ölke M, Daniel C, Amann K, Hugo C, et al. Podocytes are nonhematopoietic professional antigen-presenting cells. *J Am Soc Nephrol* (2013) 24:906–16. doi: 10.1681/asn.2012020133

28. Li S, Liu Y, He Y, Rong W, Zhang M, Li L, et al. Podocytes present antigen to activate specific T cell immune responses in inflammatory renal disease. *J Pathol* (2020) 252:165–77. doi: 10.1002/path.5508

29. Luckheeram RV, Zhou R, Verma AD, Xia B. CD4+T cells: differentiation and functions. *Clin Dev Immunol* (2012) 2012:1–12. doi: 10.1155/2012/925135

30. Ruszkowski J, Lisowska KA, Pindel M, Heleniak Z, Dębska-Ślizień A, Witkowski JM. T cells in IgA nephropathy: role in pathogenesis, clinical significance and potential therapeutic target. *Clin Exp Nephrol* (2018) 23:291–303. doi: 10.1007/s10157-018-1665-0

31. Novelli R, Benigni A, Remuzzi G. The role of B7-1 in proteinuria of glomerular origin. *Nat Rev Nephrol* (2018) 14:589–96. doi: 10.1038/s41581-018-0037-z

32. Liu R, Wen X, Peng X, Zhao M, Mi L, Lei J, et al. Immune podocytes in the immune microenvironment of lupus nephritis (Review). *Mol Med Rep* (2023) 28:204. doi: 10.3892/mmr.2023.13091

33. Nagata M. Podocyte injury and its consequences. *Kidney Int* (2016) 89:1221–30. doi: 10.1016/j.kint.2016.01.012

34. Gao S, Cui Z, Zhao M-h. Complement C3a and C3a receptor activation mediates podocyte injuries in the mechanism of primary membranous nephropathy. *J Am Soc Nephrol* (2022) 33:1742–56. doi: 10.1681/asn.2021101384

35. Li X, Ding F, Zhang X, Li B, Ding J. The expression profile of complement components in podocytes. *Int J Mol Sci* (2016) 17:471. doi: 10.3390/ijms17040471

36. Bruno V, Mühlig AK, Oh J, Licht C. New insights into the immune functions of podocytes: the role of complement. *Mol Cell Pedia* (2023) 10:3. doi: 10.1186/s40348-023-00157-3

37. Gomes MT, Campos PC, Pereira Gde S, Bartholomeu DC, Splitter G, Oliveira SC. TLR9 is required for MAPK/NF-kappaB activation but does not cooperate with TLR2 or TLR6 to induce host resistance to Brucella abortus. *J Leukoc Biol* (2016) 99:771–80. doi: 10.1189/jlb.4A0815-346R

38. Fu R, Guo C, Wang S, Huang Y, Jin O, Hu H, et al. Podocyte activation of NLRP3 inflammasomes contributes to the development of proteinuria in lupus nephritis. *Arthritis Rheumatol* (2017) 69:1636–46. doi: 10.1002/art.40155

39. Xiang H, Zhu F, Xu Z, Xiong J. Role of inflammasomes in kidney diseases *via* both canonical and non-canonical pathways. *Front Cell Dev Biol* (2020) 8:106. doi: 10.3389/fcell.2020.00106

40. Wang Z, Zhang S, Xiao Y, Zhang W, Wu S, Qin T, et al. NLRP3 inflammasome and inflammatory diseases. *Oxid Med Cell Longev* (2020) 2020:4063562. doi: 10.1155/2020/4063562

41. Wu M, Yang Z, Zhang C, Shi Y, Han W, Song S, et al. Inhibition of NLRP3 inflammasome ameliorates podocyte damage by suppressing lipid accumulation in diabetic nephropathy. *Metabolism* (2021) 118:154748. doi: 10.1016/j.metabol.2021.154748

42. Mitrofanova A, Fontanella A, Tolerico M, Mallela S, Molina David J, Zuo Y, et al. Activation of stimulator of IFN genes (STING) causes proteinuria and contributes to glomerular diseases. *J Am Soc NEPHROL* (2022) 33:2153–73. doi: 10.1681/ASN.2021101286

43. Yang H, Wang H, Andersson U. Targeting inflammation driven by HMGB1. *Front Immunol* (2020) 11:484. doi: 10.3389/fimmu.2020.00484

44. Zhong H, Li X, Zhou S, Jiang P, Liu X, Ouyang M, et al. Interplay between RAGE and TLR4 regulates HMGB1-induced inflammation by promoting cell surface expression of RAGE and TLR4. *J Immunol* (2020) 205:767–75. doi: 10.4049/jimmunol.1900860

45. Zhang H, Deng Z, Wang Y. Molecular insight in intrarenal inflammation affecting four main types of cells in nephrons in IgA nephropathy. *Front Med* (2023) 10:1128393. doi: 10.3389/fmed.2023.1128393

46. Daehn I, Casalena G, Zhang T, Shi S, Fenninger F, Barasch N, et al. Endothelial mitochondrial oxidative stress determines podocyte depletion in segmental glomerulosclerosis. *J Clin Invest* (2014) 124:1608–21. doi: 10.1172/jci71195

47. Qi H, Casalena G, Shi S, Yu L, Ebefors K, Sun Y, et al. Glomerular endothelial mitochondrial dysfunction is essential and characteristic of diabetic kidney disease susceptibility. *Diabetes* (2017) 66:763–78. doi: 10.2337/db16-0695

48. Tufro A, Veron D. VEGF and podocytes in diabetic nephropathy. *Semin Nephrol* (2012) 32:385–93. doi: 10.1016/j.semnephrol.2012.06.010

49. Gnudi L. Angiopoietins and diabetic nephropathy. *Diabetologia* (2016) 59:1616–20. doi: 10.1007/s00125-016-3995-3

50. Thurston G, Rudge JS, Ioffe E, Zhou H, Ross L, Croll SD, et al. Angiopoietin-1 protects the adult vasculature against plasma leakage. *Nat Med* (2000) 6:460–3. doi: 10.1038/74725

51. Suyama M, Miyazaki Y, Matsusaka T, Sugano N, Ueda H, Kawamura T, et al. Forced expression of vascular endothelial growth factor-A in podocytes decreases mesangial cell numbers and attenuates endothelial cell differentiation in the mouse glomerulus. *Clin Exp Nephrol* (2017) 22:266–74. doi: 10.1007/s10157-017-1450-5

52. Karpanen T, Bry M, Ollila HM, Seppänen-Laakso T, Liimatta E, Leskinen H, et al. Overexpression of vascular endothelial growth factor-B in mouse heart alters cardiac lipid metabolism and induces myocardial hypertrophy. *Circ Res* (2008) 103:1018–26. doi: 10.1161/circresaha.108.178459

53. Zanatta CM, Veronese FV, Loreto M, Sortica DA, Carpio VN, Eldeweiss MIA, et al. Endothelin-1 and endothelin A receptor immunoreactivity is increased in patients with diabetic nephropathy. *Renal Fail* (2012) 34:308–15. doi: 10.3109/0886022x.2011.647301

54. Ebefors K, Wiener RJ, Yu L, Azeloglu EU, Yi Z, Jia F, et al. Endothelin receptor-A mediates degradation of the glomerular endothelial surface layer *via* pathologic crosstalk between activated podocytes and glomerular endothelial cells. *Kidney Int* (2019) 96:957–70. doi: 10.1016/j.kint.2019.05.007

55. Ferland-McCollough D, Slater S, Richard J, Reni C, Mangialardi G. Pericytes, an overlooked player in vascular pathobiology. *Pharmacol Ther* (2017) 171:30–42. doi: 10.1016/j.pharmthera.2016.11.008

56. Lodyga M, Hinz B. TGF-β1 – A truly transforming growth factor in fibrosis and immunity. *Semin Cell Dev Biol* (2020) 101:123–39. doi: 10.1016/j.semcdb.2019.12.010

57. Kalluri R, LeBleu VS. The biology, function, and biomedical applications of exosomes. *Science* (2020) 367:eaau6977. doi: 10.1126/science.aau6977

58. Wu X-m, Gao Y-b, Cui F-q, Zhang N. Exosomes from high glucose-treated glomerular endothelial cells activate mesangial cells to promote renal fibrosis. *Biol Open* (2016) 5:484–91. doi: 10.1242/bio.015990

59. Wu X, Gao Y, Xu L, Dang W, Yan H, Zou D, et al. Exosomes from high glucose-treated glomerular endothelial cells trigger the epithelial-mesenchymal transition and dysfunction of podocytes. *Sci Rep* (2017) 7:9371. doi: 10.1038/s41598-017-09907-6

60. Ghayur A, Margetts PJ. Transforming growth factor-beta and the glomerular filtration barrier. *Kidney Res Clin Pract* (2013) 32:3–10. doi: 10.1016/j.krcp.2013.01.003

61. Purohit S, Piani F, Ordoñez FA, de Lucas-Collantes C, Bauer C, Cara-Fuentes G. Molecular mechanisms of proteinuria in minimal change disease. *Front Med* (2021) 8:761600. doi: 10.3389/fmed.2021.761600

62. Kopp JB, Anders H-J, Susztak K, Podestà MA, Remuzzi G, Hildebrandt F, et al. Podocytopathies. *Nat Rev Dis Prime* (2020) 31:167–74. doi: 10.1038/s41572-020-0196-7

63. Vivarelli M, Massella L, Ruggiero B, Emma F. Minimal change disease. *Clin J Am Soc Nephrol* (2017) 12:332–45. doi: 10.2215/cjn.05000516

64. Araya CE, Wasserfall CH, Brusko TM, Mu W, Segal MS, Johnson RJ, et al. A case of unfulfilled expectations. Cytokines in idiopathic minimal lesion nephrotic syndrome. *Pediatr Nephrol* (2006) 21:603–10. doi: 10.1007/s00467-006-0026-5

65. Lai K-W, Wei C-L, Tan L-K, Tan P-H, Chiang GSC, Lee CGL, et al. Overexpression of interleukin-13 induces minimal-change–like nephropathy in rats. *J Am Soc Nephrol* (2007) 18:1476–85. doi: 10.1681/asn.2006070710

66. Garin E, West L, Zheng W. Effect of interleukin-8 on glomerular sulfated compounds and albuminuria. *Pediatr NEPHROL* (1997) 11:274–9. doi: 10.1007/s004670050276

67. Kim AHJ, Chung J-J, Akilesh S, Koziell A, Jain S, Hodgin JB, et al. B cell–derived IL-4 acts on podocytes to induce proteinuria and foot process effacement. *JCI Insight* (2017) 2:e81836. doi: 10.1172/jci.insight.81836

68. Cara-Fuentes G, Wasserfall CH, Wang H, Johnson RJ, Garin EH. Minimal change disease: a dysregulation of the podocyte CD80–CTLA-4 axis? *Pediatr Nephrol* (2014) 29:2333–40. doi: 10.1007/s00467-014-2874-8

69. Bertelli R, Bonanni A, Caridi G, Canepa A, Ghiggeri GM. Molecular and cellular mechanisms for proteinuria in minimal change disease. *Front Med* (2018) 5:170. doi: 10.3389/fmed.2018.00170

70. Hashimura Y, Nozu K, Kanegane H, Miyawaki T, Hayakawa A, Yoshikawa N, et al. Minimal change nephrotic syndrome associated with immune dysregulation, polyendocrinopathy, enteropathy, X-linked syndrome. *Pediatr Nephrol* (2009) 24:1181–6. doi: 10.1007/s00467-009-1119-8

71. Watts AJB, Keller KH, Lerner G, Rosales I, Collins AB, Sekulic M, et al. Discovery of autoantibodies targeting nephrin in minimal change disease supports a novel autoimmune etiology. *J Am Soc Nephrol* (2022) 33:238–52. doi: 10.1681/asn.2021060794

72. Ruggenenti P, Ruggiero B, Cravedi P, Vivarelli M, Massella L, Marasà M, et al. Rituximab in steroid-dependent or frequently relapsing idiopathic nephrotic syndrome. *J Am Soc Nephrol* (2014) 25:850–63. doi: 10.1681/asn.2013030251

73. Zhuang J, Zhao Z, Zhang C, Song X, Lu C, Tian X, et al. Case report: Successful outcome of treatment using rituximab in an adult patient with refractory minimal change disease and β-thalassemia complicating autoimmune hemolytic anemia. *Front Med* (2022) 9:1059740. doi: 10.3389/fmed.2022.1059740

74. Colucci M, Oniszczuk J, Vivarelli M, Audard V. B-cell dysregulation in idiopathic nephrotic syndrome: what we know and what we need to discover. *Front Immunol* (2022) 13:823204. doi: 10.3389/fimmu.2022.823204

75. Oniszczuk J, Beldi-Ferchiou A, Audureau E, Azzaoui I, Molinier-Frenkel V, Frontera V, et al. Circulating plasmablasts and high level of BAFF are hallmarks of minimal change nephrotic syndrome in adults. *Nephrol Dialysis Transplant* (2021) 36:609–17. doi: 10.1093/ndt/gfaa279

76. Colucci M, Carsetti R, Rosado MM, Cascioli S, Bruschi M, Candiano G, et al. Atypical IgM on T cells predict relapse and steroid dependence in idiopathic nephrotic syndrome. *Kidney Int* (2019) 96:971–82. doi: 10.1016/j.kint.2019.04.006

77. Trachtman H, Laskowski J, Lee C, Renner B, Feemster A, Parikh S, et al. Natural antibody and complement activation characterize patients with idiopathic nephrotic syndrome. *Am J Physiology-Renal Physiol* (2021) 321:F505–F16. doi: 10.1152/ajprenal.00041.2021

78. Jamin A, Berthelot L, Couderc A, Chemouny JM, Boedec E, Dehoux L, et al. Autoantibodies against podocytic UCHL1 are associated with idiopathic nephrotic syndrome relapses and induce proteinuria in mice. *J Autoimmun* (2018) 89:149–61. doi: 10.1016/j.jaut.2017.12.014

79. McGrogan A, Franssen CFM, de Vries CS. The incidence of primary glomerulonephritis worldwide: a systematic review of the literature. *Nephrol Dialysis Transplant* (2010) 26:414–30. doi: 10.1093/ndt/gfq665

80. Rosenberg AZ, Kopp JB. Focal segmental glomerulosclerosis. *Clin J Am Soc Nephrol* (2017) 12:502–17. doi: 10.2215/cjn.05960616

81. Zhang H, Wang Z, Dong L, Guo Y, Wu J, Zhai S. New insight into the pathogenesis of minimal change nephrotic syndrome: Role of the persistence of respiratory tract virus in immune disorders. *Autoimmun Rev* (2016) 15:632–7. doi: 10.1016/j.autrev.2016.02.007

82. Morel A, Meuleman M-S, Moktefi A, Audard V. Renal diseases associated with hematologic Malignancies and thymoma in the absence of renal monoclonal immunoglobulin deposits. *Diagnostics* (2021) 11:710. doi: 10.3390/diagnostics11040710

83. Bakhriansyah M, Souverein PC, van den Hoogen MWF, de Boer A, Klungel OH. Risk of nephrotic syndrome for non-steroidal anti-inflammatory drug users. *Clin J Am Soc Nephrol* (2019) 14:1355–62. doi: 10.2215/cjn.14331218

84. Davis J, Desmond M, Berk M. Lithium and nephrotoxicity: Unravelling the complex pathophysiological threads of the lightest metal. *Nephrology* (2018) 23:897–903. doi: 10.1111/nep.13263

85. De Vriese AS, Sethi S, Nath KA, Glassock RJ, Fervenza FC. Differentiating primary, genetic, and secondary FSGS in adults: A clinicopathologic approach. *J Am Soc Nephrol* (2018) 29:759–74. doi: 10.1681/asn.2017090958

86. Shalhoub R. Pathogenesis of lipoid nephrosis: a disorder of T-cell function. *LANCET* (1974) 2:556–60. doi: 10.1016/s0140-6736(74)91880-7

87. Kemper MJ, Zepf K, Klaassen I, Link A, Müller-Wiefel DE. Changes of lymphocyte populations in pediatric steroid-sensitive nephrotic syndrome are more pronounced in remission than in relapse. *Am J Nephrol* (2005) 25:132–7. doi: 10.1159/000085357

88. Ye Q, Zhou C, Li S, Wang J, Liu F, Liu Z, et al. The immune cell landscape of peripheral blood mononuclear cells from PNS patients. *Sci Rep* (2021) 11:13083. doi: 10.1038/s41598-021-92573-6

89. Zhai S, Sun B, Zhang Y, Zhao L, Zhang L. IL–17 aggravates renal injury by promoting podocyte injury in children with primary nephrotic syndrome. *Exp Ther Med* (2020) 20:409–17. doi: 10.3892/etm.2020.8698

90. Dryer SE, Otalora L, Chavez E, Watford D, Tueros L, Correa M, et al. Identification of glomerular and podocyte-specific genes and pathways activated by sera of patients with focal segmental glomerulosclerosis. *PloS One* (2019) 14:e0222948. doi: 10.1371/journal.pone.0222948

91. Dryer SE, Chung C-F, Kitzler T, Kachurina N, Pessina K, Babayeva S, et al. Intrinsic tumor necrosis factor-α pathway is activated in a subset of patients with focal segmental glomerulosclerosis. *PloS One* (2019) 14:e0216426. doi: 10.1371/journal.pone.0216426

92. Shimada M, Ishimoto T, Lee PY, Lanaspa MA, Rivard CJ, Roncal-Jimenez CA, et al. Toll-like receptor 3 ligands induce CD80 expression in human podocytes *via* an NF- B-dependent pathway. *Nephrol Dialysis Transplant* (2011) 27:81–9. doi: 10.1093/ndt/gfr271

93. Ishimoto T, Shimada M, Gabriela G, Kosugi T, Sato W, Lee PY, et al. Toll-like receptor 3 ligand, polyIC, induces proteinuria and glomerular CD80, and increases urinary CD80 in mice. *Nephrol Dialysis Transplant* (2012) 28:1439–46. doi: 10.1093/ndt/gfs543

94. Reiser J, von Gersdorff G, Loos M, Oh J, Asanuma K, Giardino L, et al. Induction of B7-1 in podocytes is associated with nephrotic syndrome. *J Clin Invest* (2004) 113:1390–7. doi: 10.1172/jci20402

95. Hoffman W, Lakkis FG, Chalasani G. B cells, antibodies, and more. *Clin J Am Soc Nephrol* (2016) 11:137–54. doi: 10.2215/cjn.09430915

96. Ye Q, Zhang Y, Zhuang J, Bi Y, Xu H, Shen Q, et al. The important roles and molecular mechanisms of annexin A2 autoantibody in children with nephrotic syndrome. *Ann Trans Med* (2021) 9:1452–. doi: 10.21037/atm-21-3988

97. Hattori M, Shirai Y, Kanda S, Ishizuka K, Kaneko N, Ando T, et al. Circulating nephrin autoantibodies and posttransplant recurrence of primary focal segmental glomerulosclerosis. *Am J Transplant* (2022) 22:2478–80. doi: 10.1111/ajt.17077

98. Batal I, Khairallah P, Weins A, Andeen NK, Stokes MB. The role of HLA antigens in recurrent primary focal segmental glomerulosclerosis. *Front Immunol* (2023) 14:1124249. doi: 10.3389/fimmu.2023.1124249

99. Kawahara K, Mukai T, Iseki M, Nagasu A, Nagasu H, Akagi T, et al. SH3BP2 deficiency ameliorates murine systemic lupus erythematosus. *Int J Mol Sci* (2021) 22:4169. doi: 10.3390/ijms22084169

100. Srivastava T, Garola RE, Zhou J, Boinpelly VC, Rezaiekhaligh MH, Joshi T, et al. Scaffold protein SH3BP2 signalosome is pivotal for immune activation in nephrotic syndrome. *JCI Insight* (2023) e170055. doi: 10.1172/jci.insight.170055

101. Cattran DC, Brenchley PE. Membranous nephropathy: integrating basic science into improved clinical management. *Kidney Int* (2017) 91:566–74. doi: 10.1016/j.kint.2016.09.048

102. Sethi S, Beck LH, Glassock RJ, Haas M, De Vriese AS, Caza TN, et al. Mayo Clinic consensus report on membranous nephropathy: proposal for a novel classification. *Kidney Int* (2023) 104:1092–102. doi: 10.1016/j.kint.2023.06.032

103. Bally S, Debiec H, Ponard D, Dijoud F, Rendu J, Fauré J, et al. Phospholipase A2 receptor–related membranous nephropathy and mannan-binding lectin deficiency. *J Am Soc Nephrol* (2016) 27:3539–44. doi: 10.1681/asn.2015101155

104. Couser WG. Primary membranous nephropathy. *Clin J Am Soc Nephrol* (2017) 12:983–97. doi: 10.2215/cjn.11761116

105. Hoxha E, Reinhard L, Stahl RAK. Membranous nephropathy: new pathogenic mechanisms and their clinical implications. *Nat Rev Nephrol* (2022) 18:466–78. doi: 10.1038/s41581-022-00564-1

106. Ronco P, Debiec H. Membranous nephropathy: current understanding of various causes in light of new target antigens. *Curr Opin Nephrol Hypertension* (2021) 30:287–93. doi: 10.1097/mnh.0000000000000697

107. Beck L, Bonegio R, Lambeau G, Beck D, Powell D, Cummins T, et al. M-type phospholipase A2 receptor as target antigen in idiopathic membranous nephropathy. *N Engl J Med* (2009) 361:11–21. doi: 10.1056/NEJMoa0810457

108. Tomas NM, Beck LH, Meyer-Schwesinger C, Seitz-Polski B, Ma H, Zahner G, et al. Thrombospondin type-1 domain-containing 7A in idiopathic membranous nephropathy. *New Engl J Med* (2014) 371:2277–87. doi: 10.1056/NEJMoa1409354

109. Tomas NM, Dehde S, Meyer-Schwesinger C, Huang M, Hermans-Borgmeyer I, Maybaum J, et al. Podocyte expression of human phospholipase A2 receptor 1 causes immune-mediated membranous nephropathy in mice. *Kidney Int* (2023) 103:297–303. doi: 10.1016/j.kint.2022.09.008

110. Al-Rabadi LF, Caza T, Trivin-Avillach C, Rodan AR, Andeen N, Hayashi N, et al. Serine protease HTRA1 as a novel target antigen in primary membranous nephropathy. *J Am Soc Nephrol* (2021) 32:1666–81. doi: 10.1681/asn.2020101395

111. Reinhard L, Machalitza M, Wiech T, Gröne H, Lassé M, Rinschen M, et al. Netrin G1 is a novel target antigen in primary membranous nephropathy. *J Am Soc NEPHROL* (2022) 33:1823–31. doi: 10.1681/ASN.2022050608

112. Le Quintrec M, Teisseyre M, Bec N, Delmont E, Szwarc I, Perrochia H, et al. Contactin-1 is a novel target antigen in membranous nephropathy associated with chronic inflammatory demyelinating polyneuropathy. *Kidney Int* (2021) 100:1240–9. doi: 10.1016/j.kint.2021.08.014

113. Sethi S, Debiec H, Madden B, Vivarelli M, Charlesworth MC, Ravindran A, et al. Semaphorin 3B–associated membranous nephropathy is a distinct type of disease predominantly present in pediatric patients. *Kidney Int* (2020) 98:1253–64. doi: 10.1016/j.kint.2020.05.030

114. Sethi S, Madden BJ, Debiec H, Charlesworth MC, Gross L, Ravindran A, et al. Exostosin 1/exostosin 2–associated membranous nephropathy. *J Am Soc Nephrol* (2019) 30:1123–36. doi: 10.1681/asn.2018080852

115. Sethi S, Debiec H, Madden B, Charlesworth MC, Morelle J, Gross L, et al. Neural epidermal growth factor-like 1 protein (NELL-1) associated membranous nephropathy. *Kidney Int* (2020) 97:163–74. doi: 10.1016/j.kint.2019.09.014

116. Sethi S, Madden B, Debiec H, Morelle J, Charlesworth MC, Gross L, et al. Protocadherin 7–associated membranous nephropathy. *J Am Soc Nephrol* (2021) 32:1249–61. doi: 10.1681/asn.2020081165

117. Caza TN, Hassen SI, Kuperman M, Sharma SG, Dvanajscak Z, Arthur J, et al. Neural cell adhesion molecule 1 is a novel autoantigen in membranous lupus nephritis. *Kidney Int* (2021) 100:171–81. doi: 10.1016/j.kint.2020.09.016

118. Fanouriakis A, Kostopoulou M, Cheema K, Anders H-J, Aringer M, Bajema I, et al. 2019 Update of the Joint European League Against Rheumatism and European Renal Association–European Dialysis and Transplant Association (EULAR/ERA–EDTA) recommendations for the management of lupus nephritis. *Ann Rheum Dis* (2020) 79:713–23. doi: 10.1136/annrheumdis-2020-216924

119. Sakhi H, Moktefi A, Bouachi K, Audard V, Hénique C, Remy P, et al. Podocyte injury in lupus nephritis. *J Clin Med* (2019) 8:1340. doi: 10.3390/jcm8091340

120. Oliva-Damaso N, Payan J, Oliva-Damaso E, Pereda T, Bomback AS. Lupus podocytopathy: an overview. *Adv Chronic Kidney Disease* (2019) 26:369–75. doi: 10.1053/j.ackd.2019.08.011

121. Tsai C-Y, Li K-J, Shen C-Y, Lu C-H, Lee H-T, Wu T-H, et al. Decipher the immunopathological mechanisms and set up potential therapeutic strategies for patients with lupus nephritis. *Int J Mol Sci* (2023) 24:10066. doi: 10.3390/ijms241210066

122. Zou X, Cheng H, Zhang Y, Fang C, Xia Y. The antigen-binding fragment of anti-double-stranded DNA IgG enhances F-actin formation in mesangial cells by binding to alpha-actinin-4. *Exp Biol Med* (2012) 237:1023–31. doi: 10.1258/ebm.2012.012033

123. Yung S, Cheung KF, Zhang Q, Chan TM. Anti-dsDNA antibodies bind to mesangial annexin II in lupus nephritis. *J Am Soc Nephrol* (2010) 21:1912–27. doi: 10.1681/asn.2009080805

124. Deocharan B, Qing X, Lichauco J, Putterman C. α-actinin is a cross-reactive renal target for pathogenic anti-DNA antibodies. *J Immunol* (2002) 168:3072–8. doi: 10.4049/jimmunol.168.6.3072

125. Crispin J, Liou L-b, Huang C-c. Sialyltransferase and neuraminidase levels/ratios and sialic acid levels in peripheral blood B cells correlate with measures of disease activity in patients with systemic lupus erythematosus and rheumatoid arthritis: A pilot study. *PloS One* (2016) 11:e0151669. doi: 10.1371/journal.pone.0151669

126. Yung S, Chan TM. Mechanisms of kidney injury in lupus nephritis – the role of anti-dsDNA antibodies. *Front Immunol* (2015) 6:475. doi: 10.3389/fimmu.2015.00475

127. Kawai T, Akira S. The role of pattern-recognition receptors in innate immunity: update on Toll-like receptors. *Nat Immunol* (2010) 11:373–84. doi: 10.1038/ni.1863

128. Sato Y, Tamura M, Yanagita M. Tertiary lymphoid tissues: a regional hub for kidney inflammation. *Nephrol Dialysis Transplant* (2023) 38:26–33. doi: 10.1093/ndt/gfab212

129. Sato Y, Silina K, van den Broek M, Hirahara K, Yanagita M. The roles of tertiary lymphoid structures in chronic diseases. *Nat Rev Nephrol* (2023) 19:525–37. doi: 10.1038/s41581-023-00706-z

130. Murata H, Matsumura R, Koyama A, Sugiyama T, Sueishi M, Shibuya K, et al. T cell receptor repertoire of T cells in the kidneys of patients with lupus nephritis. *Arthritis Rheum* (2002) 46:2141–7. doi: 10.1002/art.10432

131. Kitching AR, Alikhan MA. CD8+ cells and glomerular crescent formation: outside-in as well as inside-out. *J Clin Invest* (2018) 128:3231–3. doi: 10.1172/jci122045

132. Iwata Y, Boström EA, Menke J, Rabacal WA, Morel L, Wada T, et al. Aberrant macrophages mediate defective kidney repair that triggers nephritis in lupus-susceptible mice. *J Immunol* (2012) 188:4568–80. doi: 10.4049/jimmunol.1102154

133. Klarquist J, Zhou Z, Shen N, Janssen EM. Dendritic cells in systemic lupus erythematosus: from pathogenic players to therapeutic tools. *Mediators Inflamm* (2016) 2016:1–12. doi: 10.1155/2016/5045248

134. Zhou X-J, Klionsky DJ, Zhang H. Podocytes and autophagy: a potential therapeutic target in lupus nephritis. *Autophagy* (2019) 15:908–12. doi: 10.1080/15548627.2019.1580512

135. Jin J, Zhao L, Zou W, Shen W, Zhang H, He Q. Activation of cyclooxygenase-2 by ATF4 during endoplasmic reticulum stress regulates kidney podocyte autophagy induced by lupus nephritis. *Cell Physiol Biochem* (2018) 48:753–64. doi: 10.1159/000491904

136. Papadimitraki ED, Tzardi MB G, Sotsiou E, Boumpas DT. Glomerular expression of toll-like receptor-9 in lupus nephritis but not in normal kidneys: implications for the amplification of the inflammatory response. *LUPUS* (2009) 18:831–5. doi: 10.1177/0961203309103054

137. Kwok S-K, Tsokos GC. New insights into the role of renal resident cells in the pathogenesis of lupus nephritis. *Korean J Internal Med* (2018) 33:284–9. doi: 10.3904/kjim.2017.383

138. Lv F, He Y, Xu H, Li Y, Han L, Yan L, et al. CD36 aggravates podocyte injury by activating NLRP3 inflammasome and inhibiting autophagy in lupus nephritis. *Cell Death Disease* (2022) 13:729. doi: 10.1038/s41419-022-05179-9

139. Teisseyre M, Cremoni M, Boyer-Suavet S, Ruetsch C, Graça D, Esnault VLM, et al. Advances in the management of primary membranous nephropathy and rituximab-refractory membranous nephropathy. *Front Immunol* (2022) 13:859419. doi: 10.3389/fimmu.2022.859419

140. Xu C, Ha X, Yang S, Tian X, Jiang H. Advances in understanding and treating diabetic kidney disease: focus on tubulointerstitial inflammation mechanisms. *Front Endocrinol* (2023) 14:1232790. doi: 10.3389/fendo.2023.1232790

141. Müller-Deile J, Schenk H, Schiffer M. Minimal-change-Glomerulonephritis und fokal-segmentale Glomerulosklerose. *Der Internist* (2019) 60:450–7. doi: 10.1007/s00108-019-0590-y

142. Cruz-Topete D, Cidlowski JA. One hormone, two actions: anti- and pro-inflammatory effects of glucocorticoids. *Neuroimmunomodulation* (2015) 22:20–32. doi: 10.1159/000362724

143. Ponticelli C, Locatelli F. Glucocorticoids in the treatment of glomerular diseases. *Clin J Am Soc Nephrol* (2018) 13:815–22. doi: 10.2215/cjn.12991117

144. Broek M, Smeets B, Schreuder MF, Jansen J. The podocyte as a direct target of glucocorticoids in nephrotic syndrome. *Nephrol Dialysis Transplant* (2022) 37:1808–15. doi: 10.1093/ndt/gfab016

145. Li X, Chuang PY, D'Agati VD, Dai Y, Yacoub R, Fu J, et al. Nephrin preserves podocyte viability and glomerular structure and function in adult kidneys. *J Am Soc Nephrol* (2015) 26:2361–77. doi: 10.1681/asn.2014040405

146. Agrawal S, Chanley MA, Westbrook D, Nie X, Kitao T, Guess AJ, et al. Pioglitazone enhances the beneficial effects of glucocorticoids in experimental nephrotic syndrome. *Sci Rep* (2016) 6:24392. doi: 10.1038/srep24392

147. Zhao X, Khurana S, Charkraborty S, Tian Y, Sedor JR, Bruggman LA, et al. α Actinin 4 (ACTN4) regulates glucocorticoid receptor-mediated transactivation and transrepression in podocytes. *J Biol Chem* (2017) 292:1637–47. doi: 10.1074/jbc.M116.755546

148. Lombel RM, Gipson DS, Hodson EM. Treatment of steroid-sensitive nephrotic syndrome: new guidelines from KDIGO. *Pediatr Nephrol* (2012) 28:415–26. doi: 10.1007/s00467-012-2310-x

149. Liu Y, Yang R, Yang C, Dong S, Zhu Y, Zhao M, et al. Cyclophosphamide versus cyclosporine A therapy in steroid-resistant nephrotic syndrome: a retrospective study with a mean 5-year follow-up. *J Int Med Res* (2018) 46:4506–17. doi: 10.1177/0300060518782017

150. Grenda R, Obrycki Ł. Second and third generational advances in therapies of the immune-mediated kidney diseases in children and adolescents. *Children* (2022) 9:536. doi: 10.3390/children9040536

151. Hackl A, Zed SEDA, Diefenhardt P, Binz-Lotter J, Ehren R, Weber LT. The role of the immune system in idiopathic nephrotic syndrome. *Mol Cell Pedia* (2021) 8:18. doi: 10.1186/s40348-021-00128-6

152. Zhang M, Lv Y, Liu H. The efficacy of cyclophosphamide combined with prednisone in membranous nephropathy patients with different cytochrome P450 2B6 gene polymorphisms and analysis of factors influencing the efficacy. *Drug Design Dev Ther* (2022) 16:3655–62. doi: 10.2147/dddt.S373487

153. Bao L, Hao C, Wang J, Wang D, Zhao Y, Li Y, et al. High-dose cyclophosphamide administration orchestrates phenotypic and functional alterations of immature dendritic cells and regulates th cell polarization. *Front Pharmacol* (2020) 11:775. doi: 10.3389/fphar.2020.00775

154. Stangou M, Marinaki S, Papachristou E, Kolovou K, Sambani E, Zerbala S, et al. Immunosuppressive regimens based on Cyclophospamide or Calcineurin inhibitors: Comparison of their effect in the long term outcome of Primary Membranous Nephropathy. *PloS One* (2019) 14:e0217116. doi: 10.1371/journal.pone.0217116

155. Gallon L, Traitanon O, Yu Y, Shi B, Leventhal JR, Miller J, et al. Differential effects of calcineurin and mammalian target of rapamycin inhibitors on alloreactive th1, th17, and regulatory T cells. *Transplantation* (2015) 99:1774–84. doi: 10.1097/tp.0000000000000717

156. Li Y, Guptill JT, Russo MA, Massey JM, Juel VC, Hobson-Webb LD, et al. Tacrolimus inhibits Th1 and Th17 responses in MuSK-antibody positive myasthenia gravis patients. *Exp Neurol* (2019) 312:43–50. doi: 10.1016/j.expneurol.2018.11.006

157. Niazi M, Shirpoor A, Taghizadeh Afshari A, Naderi R, Bagheri M, Pourjabali M, et al. Cyclosporine A induces kidney dysfunction by the alteration of molecular mediators involved in slit diaphragm regulation and matrix metalloproteins: the mitigating effect of curcumin. *Expert Opin Drug Metab Toxicol* (2020) 16:1223–31. doi: 10.1080/17425255.2020.1822323

158. Li X, Ding F, Wang S, Li B, Ding J. Cyclosporine A protects podocytes by regulating WAVE1 phosphorylation. *Sci Rep* (2015) 5:17694. doi: 10.1038/srep17694

159. Li X, Zhang X, Li X, Wang X, Wang S, Ding J. Cyclosporine A protects podocytes *via* stabilization of cofilin-1 expression in the unphosphorylated state. *Exp Biol Med* (2014) 239:922–36. doi: 10.1177/1535370214530365

160. Chiba Y, Inoue CN. Once-daily low-dose cyclosporine A treatment with angiotensin blockade for long-term remission of nephropathy in frasier syndrome. *Tohoku J Exp Med* (2019) 247:35–40. doi: 10.1620/tjem.247.35

161. Bobé P, Liao R, Liu Q, Zheng Z, Fan J, Peng W, et al. Tacrolimus protects podocytes from injury in lupus nephritis partly by stabilizing the cytoskeleton and inhibiting podocyte apoptosis. *PloS One* (2015) 10:e0132724. doi: 10.1371/journal.pone.0132724

162. Peng T, Chang X, Wang J, Zhen J, Yang X, Hu Z. Protective effects of tacrolimus on podocytes in early diabetic nephropathy in rats. *Mol Med Rep* (2017) 15:3172–8. doi: 10.3892/mmr.2017.6354

163. Wen Y, Liu L, Zhou P, Li H, Wang Z, Zhang Y, et al. Tacrolimus restores podocyte injury and stabilizes the expression of Cabin1 in 5/6 nephrectomized rats. *Renal Fail* (2016) 38:564–70. doi: 10.3109/0886022x.2016.1148936

164. Ma R, Wang Y, Xu Y, Wang R, Wang X, Yu N, et al. Tacrolimus protects podocytes from apoptosis *via* downregulation of TRPC6 in diabetic nephropathy. *J Diabetes Res* (2021) 2021:1–11. doi: 10.1155/2021/8832114

165. Yasuda H, Fukusumi Y, Ivanov V, Zhang Y, Kawachi H. Tacrolimus ameliorates podocyte injury by restoring FK506 binding protein 12 (FKBP12) at actin cytoskeleton. *FASEB J* (2021) 35:e21983. doi: 10.1096/fj.202101052R

166. Fervenza FC, Appel GB, Barbour SJ, Rovin BH, Lafayette RA, Aslam N, et al. Rituximab or cyclosporine in the treatment of membranous nephropathy. *New Engl J Med* (2019) 381:36–46. doi: 10.1056/NEJMoa1814427

167. Rovin BH, Teng YKO, Ginzler EM, Arriens C, Caster DJ, Romero-Diaz J, et al. Efficacy and safety of voclosporin versus placebo for lupus nephritis (AURORA 1): a double-blind, randomised, multicentre, placebo-controlled, phase 3 trial. *Lancet* (2021) 397:2070–80. doi: 10.1016/s0140-6736(21)00578-x

168. Abdel-Kahaar E, Keller F. Clinical pharmacokinetics and pharmacodynamics of voclosporin. *Clin Pharmacokinetics* (2023) 62:693–703. doi: 10.1007/s40262-023-01246-2

169. Abo Zed SED, Hackl A, Bohl K, Ebert L, Kieckhöfer E, Müller C, et al. Mycophenolic acid directly protects podocytes by preserving the actin cytoskeleton and increasing cell survival. *Sci Rep* (2023) 13:4281. doi: 10.1038/s41598-023-31326-z

170. Hackl A, Nüsken E, Voggel J, Abo Zed SED, Binz-Lotter J, Unnersjö-Jess D, et al. The effect of mycophenolate mofetil on podocytes in nephrotoxic serum nephritis. *Sci Rep* (2023) 13:14167. doi: 10.1038/s41598-023-41222-1

171. Seo J-W, Kim YG, Lee SH, Lee A, Kim D-J, Jeong K-H, et al. Mycophenolate mofetil ameliorates diabetic nephropathy in db/db mice. *BioMed Res Int* (2015) 2015:1–11. doi: 10.1155/2015/301627

172. Lin D-W, Chang C-C, Hsu Y-C, Lin C-L. New insights into the treatment of glomerular diseases: when mechanisms become vivid. *Int J Mol Sci* (2022) 23:3525. doi: 10.3390/ijms23073525

173. Sun K, Verhoog N, Allie-Reid F, Vanden Berghe W, Smith C, Haegeman G, et al. Inhibition of corticosteroid-binding globulin gene expression by glucocorticoids involves C/EBPβ. *PloS One* (2014) 9:e110702. doi: 10.1371/journal.pone.0110702

174. Achuthan A, Aslam ASM, Nguyen Q, Lam P-Y, Fleetwood AJ, Frye AT, et al. Glucocorticoids promote apoptosis of proinflammatory monocytes by inhibiting ERK activity. *Cell Death Disease* (2018) 9:267. doi: 10.1038/s41419-018-0332-4

175. Faul C, Donnelly M, Merscher-Gomez S, Chang YH, Franz S, Delfgaauw J, et al. The actin cytoskeleton of kidney podocytes is a direct target of the antiproteinuric effect of cyclosporine A. *Nat Med* (2008) 14:931–8. doi: 10.1038/nm.1857

176. Schlöndorff J, del Camino D, Carrasquillo R, Lacey V, Pollak MR. TRPC6 mutations associated with focal segmental glomerulosclerosis cause constitutive activation of NFAT-dependent transcription. *Am J Physiology-Cell Physiol* (2009) 296:C558–C69. doi: 10.1152/ajpcell.00077.2008

177. Léger C, Pitard I, Sadi M, Carvalho N, Brier S, Mechaly A, et al. Dynamics and structural changes of calmodulin upon interaction with the antagonist calmidazolium. *BMC Biol* (2022) 20:176. doi: 10.1186/s12915-022-01381-5

178. Wei C, Möller CC, Altintas MM, Li J, Schwarz K, Zacchigna S, et al. Modification of kidney barrier function by the urokinase receptor. *Nat Med* (2007) 14:55–63. doi: 10.1038/nm1696

179. Lee HW, Khan SQ, Faridi MH, Wei C, Tardi NJ, Altintas MM, et al. A podocyte-based automated screening assay identifies protective small molecules. *J Am Soc Nephrol* (2015) 26:2741–52. doi: 10.1681/asn.2014090859

180. Gong R. The renaissance of corticotropin therapy in proteinuric nephropathies. *Nat Rev Nephrol* (2011) 8:122–8. doi: 10.1038/nrneph.2011.190

181. Fornoni A, Sageshima J, Wei C, Merscher-Gomez S, Aguillon-Prada R, Jauregui AN, et al. Rituximab targets podocytes in recurrent focal segmental glomerulosclerosis. *Sci Trans Med* (2011) 3:85ra46. doi: 10.1126/scitranslmed.3002231

182. Lattermann C, Gomoll AH, Cole BJ. Arthroscopic partial meniscectomy for degenerative meniscal tear. *New Engl J Med* (2014) 370:1259–61. doi: 10.1056/NEJMc1401128

183. Walsh PR, Johnson S. Eculizumab in the treatment of Shiga toxin haemolytic uraemic syndrome. *Pediatr Nephrol* (2018) 34:1485–92. doi: 10.1007/s00467-018-4025-0

184. Bruchfeld A, Magin H, Nachman P, Parikh S, Lafayette R, Potarca A, et al. C5a receptor inhibitor avacopan in immunoglobulin A nephropathy—an open-label pilot study. *Clin Kidney J* (2022) 15:922–8. doi: 10.1093/ckj/sfab294

185. Lafayette RA, Rovin BH, Reich HN, Tumlin JA, Floege J, Barratt J. Safety, tolerability and efficacy of narsoplimab, a novel MASP-2 inhibitor for the treatment of igA nephropathy. *Kidney Int Rep* (2020) 5:2032–41. doi: 10.1016/j.ekir.2020.08.003

186. Kaegi C, Wuest B, Schreiner J, Steiner UC, Vultaggio A, Matucci A, et al. Systematic review of safety and efficacy of rituximab in treating immune-mediated disorders. *Front Immunol* (2019) 10:1990. doi: 10.3389/fimmu.2019.01990

187. Seitz-Polski B, Dahan K, Debiec H, Rousseau A, Andreani M, Zaghrini C, et al. High-dose rituximab and early remission in PLA2R1-related membranous nephropathy. *Clin J Am Soc Nephrol* (2019) 14:1173–82. doi: 10.2215/cjn.11791018

188. Trachtman H. Busy bs. *J Am Soc Nephrol* (2016) 27:1584–6. doi: 10.1681/asn.2015101171

189. Zonozi R, Laliberte K, Huizenga NR, Rosenthal JK, Jeyabalan A, Collins AB, et al. Combination of rituximab, low-dose cyclophosphamide, and prednisone for primary membranous nephropathy: A case series with extended follow up. *Am J Kidney Diseases* (2021) 78:793–803. doi: 10.1053/j.ajkd.2021.04.014

190. Masoud S, McAdoo SP, Bedi R, Cairns TD, Lightstone L. Ofatumumab for B cell depletion in patients with systemic lupus erythematosus who are allergic to rituximab. *Rheumatology* (2018) 57:1156–61. doi: 10.1093/rheumatology/key042

191. Bonanni A, Rossi R, Murtas C, Ghiggeri GM. Low-dose ofatumumab for rituximab-resistant nephrotic syndrome. *BMJ Case Rep* (2015) 2015:bcr2015210208. doi: 10.1136/bcr-2015-210208

192. Ramachandran R, Kumar V, Bharati J, Rovin B, Nada R, Kumar V, et al. Long-term follow-up of cyclical cyclophosphamide and steroids versus tacrolimus and steroids in primary membranous nephropathy. *Kidney Int Rep* (2021) 6:2653–60. doi: 10.1016/j.ekir.2021.07.028

193. Ishimoto T, Shimada M, Araya CE, Huskey J, Garin EH, Johnson RJ. Minimal change disease: A CD80 podocytopathy? *Semin Nephrol* (2011) 31:320–5. doi: 10.1016/j.semnephrol.2011.06.002

194. Teh YM, Lim SK, Jusoh N, Osman K, Mualif SA, Abu Shahin N. CD80 insights as therapeutic target in the current and future treatment options of frequent-relapse minimal change disease. *BioMed Res Int* (2021) 2021:1–17. doi: 10.1155/2021/6671552

195. Novelli R, Gagliardini E, Ruggiero B, Benigni A, Remuzzi G. Any value of podocyte B7-1 as a biomarker in human MCD and FSGS? *Am J Physiology-Renal Physiol* (2016) 310:F335–F41. doi: 10.1152/ajprenal.00510.2015

196. Gagliardini E, Novelli R, Corna D, Zoja C, Ruggiero B, Benigni A, et al. B7–1 is not induced in podocytes of human and experimental diabetic nephropathy. *J Am Soc Nephrol* (2016) 27:999–1005. doi: 10.1681/asn.2015030266

197. Burke GW, Chandar J, Sageshima J, Ortigosa-Goggins M, Amarapurkar P, Mitrofanova A, et al. Benefit of B7-1 staining and abatacept for treatment-resistant post-transplant focal segmental glomerulosclerosis in a predominantly pediatric cohort: time for a reappraisal. *Pediatr Nephrol* (2022) 38:145–59. doi: 10.1007/s00467-022-05549-7

198. Herrera M, Söderberg M, Sabirsh A, Valastro B, Mölne J, Santamaria B, et al. Inhibition of T-cell activation by the CTLA4-Fc Abatacept is sufficient to ameliorate proteinuric kidney disease. *Am J Physiology-Renal Physiol* (2017) 312:F748–F59. doi: 10.1152/ajprenal.00179.2016

199. Mühlig AK, Keir LS, Abt JC, Heidelbach HS, Horton R, Welsh GI, et al. Podocytes produce and secrete functional complement C3 and complement factor H. *Front Immunol* (2020) 11:1833. doi: 10.3389/fimmu.2020.01833

200. Nangaku M, Shankland SJ, Couser WG. Cellular response to injury in membranous nephropathy. *J Am Soc Nephrol* (2005) 16:1195–204. doi: 10.1681/asn.2004121098

201. Harigai M, Takada H. Avacopan, a selective C5a receptor antagonist, for anti-neutrophil cytoplasmic antibody-associated vasculitis. *MOD Rheumatol* (2022) 32:475–83. doi: 10.1093/mr/roab104/6497529

202. Khaled SK, Claes K, Goh YT, Kwong YL, Leung N, Mendrek W, et al. Narsoplimab, a mannan-binding lectin-associated serine protease-2 inhibitor, for the treatment of adult hematopoietic stem-cell transplantation–associated thrombotic microangiopathy. *J Clin Oncol* (2022) 40:2447–57. doi: 10.1200/jco.21.02389

203. Freeman J, Cummings J, Chuidian M, Dudler T. Development of pharmacodynamic assays to assess ex vivo masp-2 inhibition and their use to characterize the pharmacodynamics of narsoplimab (OMS721) in humans and monkeys. *Blood* (2020) 136:26–7. doi: 10.1182/blood-2020-142208

204. Elhadad S, Redmond D, Huang J, Tan A, Laurence J. MASP2 inhibition by narsoplimab suppresses endotheliopathies characteristic of transplant-associated thrombotic microangiopathy:*in vitro*andex vivoevidence. *Clin Exp Immunol* (2023) 213:252–64. doi: 10.1093/cei/uxad055

205. Clement LC, Avila-Casado C, Macé C, Soria E, Bakker WW, Kersten S, et al. Podocyte-secreted angiopoietin-like-4 mediates proteinuria in glucocorticoid-sensitive nephrotic syndrome. *Nat Med* (2010) 17:117–22. doi: 10.1038/nm.2261

206. Macé C, Chugh SS. Nephrotic syndrome. *J Am Soc Nephrol* (2014) 25:2393–8. doi: 10.1681/asn.2014030267

207. Chung H, Lee S-W, Hyun M, Kim SY, Cho HG, Lee ES, et al. Curcumin blocks high glucose-induced podocyte injury *via* RIPK3-dependent pathway. *Front Cell Dev Biol* (2022) 10:800574. doi: 10.3389/fcell.2022.800574

208. Yu Q, Zhang M, Qian L, Wen D, Wu G. Luteolin attenuates high glucose-induced podocyte injury *via* suppressing NLRP3 inflammasome pathway. *Life Sci* (2019) 225:1–7. doi: 10.1016/j.lfs.2019.03.073

209. Zhang J, Wu C, Gao L, Du G, Qin X. Astragaloside IV derived from Astragalus membranaceus: A research review on the pharmacological effects. *Adv Pharmacol* (2020) 87:89–112. doi: 10.1016/bs.apha.2019.08.002

210. Shen Q, Fang J, Guo H, Su X, Zhu B, Yao X, et al. Astragaloside IV attenuates podocyte apoptosis through ameliorating mitochondrial dysfunction by up-regulated Nrf2-ARE/TFAM signaling in diabetic kidney disease. *Free Radic Biol Med* (2023) 203:45–57. doi: 10.1016/j.freeradbiomed.2023.03.022

211. Guo H, Wang Y, Zhang X, Zang Y, Zhang Y, Wang L, et al. Astragaloside IV protects against podocyte injury *via* SERCA2-dependent ER stress reduction and AMPKalpha-regulated autophagy induction in streptozotocin-induced diabetic nephropathy. *Sci Rep* (2017) 7:6852. doi: 10.1038/s41598-017-07061-7

212. Chen Z, An X, Liu X, Qi J, Ding D, Zhao M, et al. Hyperoside alleviates adriamycin-induced podocyte injury *via* inhibiting mitochondrial fission. *Oncotarget* (2017) 8:88792–803. doi: 10.18632/oncotarget.21287

213. Matoba K, Kawanami D, Nagai Y, Takeda Y, Akamine T, Ishizawa S, et al. Rho-kinase blockade attenuates podocyte apoptosis by inhibiting the notch signaling pathway in diabetic nephropathy. *Int J Mol Sci* (2017) 18:1795. doi: 10.3390/ijms18081795

214. Matoba K, Takeda Y, Nagai Y, Sekiguchi K, Ukichi R, Takahashi H, et al. ROCK2-induced metabolic rewiring in diabetic podocytopathy. *Commun Biol* (2022) 5:341. doi: 10.1038/s42003-022-03300-4

215. Linke M, Fritsch SD, Sukhbaatar N, Hengstschlager M, Weichhart T. mTORC1 and mTORC2 as regulators of cell metabolism in immunity. *FEBS Lett* (2017) 591:3089–103. doi: 10.1002/1873-3468.12711

216. Li Q, Zeng Y, Jiang Q, Wu C, Zhou J. Role of mTOR signaling in the regulation of high glucose-induced podocyte injury. *Exp Ther Med* (2019) 17:2495–502. doi: 10.3892/etm.2019.7236

217. Yang HC, Fogo AB. Mechanisms of disease reversal in focal and segmental glomerulosclerosis. *Adv Chronic Kidney Dis* (2014) 21:442–7. doi: 10.1053/j.ackd.2014.04.001

218. Matsusaka T, Asano T, Niimura F, Kinomura M, Shimizu A, Shintani A, et al. Angiotensin receptor blocker protection against podocyte-induced sclerosis is podocyte angiotensin II type 1 receptor-independent. *Hypertension* (2010) 55:967–73. doi: 10.1161/HYPERTENSIONAHA.109.141994

219. Yu N, Yang L, Ling L, Liu Y, Yu Y, Wu Q, et al. Curcumin attenuates angiotensin II-induced podocyte injury and apoptosis by inhibiting endoplasmic reticulum stress. *FEBS Open Bio* (2020) 10:1957–66. doi: 10.1002/2211-5463.12946

220. Zhang J, Fu H, Xu Y, Niu Y, An X. Hyperoside reduces albuminuria in diabetic nephropathy at the early stage through ameliorating renal damage and podocyte injury. *J Nat Med* (2016) 70:740–8. doi: 10.1007/s11418-016-1007-z

frontiers | Frontiers in Immunology

TYPE Review
PUBLISHED 19 January 2024
DOI 10.3389/fimmu.2024.1333429

OPEN ACCESS

EDITED BY
Xu-jie Zhou,
Peking University, China

REVIEWED BY
Lea Dib,
University of Oxford, United Kingdom
Carolina Susana Cerrudo,
Universidad Nacional de Quilmes (UNQ), Argentina
Belisario Enrique Fernandez,
University Institute of Health Sciences, Argentina

*CORRESPONDENCE
Zhenjie Chen
ruoshui8000@126.com
Jingwei Zhou
13910634708@163.com

RECEIVED 05 November 2023
ACCEPTED 08 January 2024
PUBLISHED 19 January 2024

CITATION
Liang Y, Chen Q, Chang Y, Han J, Yan J, Chen Z and Zhou J (2024) Critical role of FGF21 in diabetic kidney disease: from energy metabolism to innate immunity.
Front. Immunol. 15:1333429.
doi: 10.3389/fimmu.2024.1333429

Critical role of FGF21 in diabetic kidney disease: from energy metabolism to innate immunity

Yingnan Liang, Qi Chen, Yue Chang, Junsong Han, Jiaxin Yan, Zhenjie Chen* and Jingwei Zhou*

Department of Nephrology, Dongzhimen Hospital, Beijing University of Chinese Medicine, Beijing, China

Diabetic kidney disease (DKD) stands as the predominant cause of chronic kidney disease (CKD) on a global scale, with its incidence witnessing a consistent annual rise, thereby imposing a substantial burden on public health. The pathogenesis of DKD is primarily rooted in metabolic disorders and inflammation. Recent years have seen a surge in studies highlighting the regulatory impact of energy metabolism on innate immunity, forging a significant area of research interest. Within this context, fibroblast growth factor 21 (FGF21), recognized as an energy metabolism regulator, assumes a pivotal role. Beyond its role in maintaining glucose and lipid metabolism homeostasis, FGF21 exerts regulatory influence on innate immunity, concurrently inhibiting inflammation and fibrosis. Serving as a nexus between energy metabolism and innate immunity, FGF21 has evolved into a therapeutic target for diabetes, nonalcoholic steatohepatitis, and cardiovascular diseases. While the relationship between FGF21 and DKD has garnered increased attention in recent studies, a comprehensive exploration of this association has yet to be systematically addressed. This paper seeks to fill this gap by summarizing the mechanisms through which FGF21 operates in DKD, encompassing facets of energy metabolism and innate immunity. Additionally, we aim to assess the diagnostic and prognostic value of FGF21 in DKD and explore its potential role as a treatment modality for the condition.

KEYWORDS

diabetic kidney disease, energy metabolism, fibroblast growth factor 21, innate immunity, inflammation

1 Introduction

Diabetic kidney disease (DKD) stands as a prevalent complication of diabetes mellitus (DM), estimated to affect 50% patients with DM globally (1). The prevalence of DM among adults aged 20 to 79 over the world is anticipated to reach 12.2% (783.2 million) by 2045 (2). Concurrently, as the prevalence of DM continues to rise, DKD has emerged as the predominant cause of chronic kidney disease on a global scale, imposing a substantial economic burden. The natural progression of DKD encompasses glomerular

hyperfiltration, progressive albuminuria, a gradual decline in the estimated glomerular filtration rate (eGFR), ultimately culminating in end-stage renal disease. It is imperative to elucidate the pathogenesis of DKD and institute preventive measures at an early stage (3). DKD is usually a clinical diagnosis made based on the presence of albuminuria and/or reduced eGFR in the absence of signs or symptoms of other primary causes of kidney damage (4). Under comprehensive and multifactorial interventions, the clinical manifestations of DKD have shown an increasingly complex heterogeneity, which can be characterized by both a clinical phenotype with no proteinuria or with the appearance of proteinuric remission, and a clinical phenotype with a rapid decline in eGFR (5). Notably, studies have revealed that even in DM patients exhibiting normal urinary protein levels, there exists a greater than 50% probability of grade IIa or more severe glomerulopathy (6). Therefore, more sensitive biomarkers are needed for early diagnosis and prediction of DKD. In recent years, the completion of several phase 3 clinical trials has ushered in a transformative era in the management of DKD, prompting the expeditious revision of clinical guidelines (7, 8). However, a residual risk of DKD progression persists, underscoring the need for novel treatments (9).

Fibroblast growth factor 21 (FGF21) emerges as a stress-inducible hormone, operating in concert with FGF receptor 1 (FGFR1) and β-klotho as a heterodimeric receptor complexz. Its regulatory prowess extends to energy balance, glucose, and lipid homeostasis, yielding significant benefits such as the reduction of fat mass and mitigation of hyperglycemia, insulin resistance, dyslipidemia, cardiovascular disease, and non-alcoholic steatohepatitis (10). Energy metabolism plays a key role in innate immune regulation. Lipid metabolism and the signaling pathways defining macrophage functions are intertwined, enabling coordinated regulation of macrophage biology (11). Immune system cells that are activated, split, and differentiated during an immune response depend on the metabolic reprogramming of both catabolic and anabolic pathways to produce metabolites that play crucial roles in regulating the response in addition to producing energy in the form of ATP (12). FGF21, beyond its role as a metabolic regulator, assumes the mantle of an innate immunity regulator, exerting anti-inflammatory effects (13).

DKD is instigated by disruptions in glucose metabolism associated with DM. These disruptions subsequently activate various metabolic, hemodynamic, inflammatory, and fibrotic processes that collectively contribute to the progression of the disease. The intertwining of energy metabolism and innate immunity plays a crucial role in the advancement of DKD (14). Serving as a focal point bridging energy metabolism and compromised innate immunity, FGF21 holds promise as a potential target for the diagnosis and treatment of DKD.As research interest burgeons around the multifaceted functions and pharmacological potential of FGF21, it has become a focal point in recent years (15). However, despite the increasing attention, a systematic exploration of the relationship between FGF21 and DKD remains lacking. To address this gap, we conducted a comprehensive review of relevant studies, elucidating the mechanisms and application value of FGF21 in the context of DKD.

2 Energy metabolism and innate immunity in DKD

Disturbed energy metabolism is one of the main pathogenic mechanisms of DKD (Figure 1A). DM is associated with the dysregulation of various metabolites, such as glucose, insulin, and lipids, contributing to the progression of DKD (16). DKD usually develops in genetically susceptible individuals due to poor metabolic (blood sugar) control. Hyperglycemia alters endothelial and podocyte metabolism, overburdening proximal tubular cells, which are a major source of cellular stress in the kidney. Lipid metabolites may also predict DKD progression (17). DM inflicts direct injury upon renal tubules, resulting in mitochondrial dysfunction. This dysfunction encompasses reduced bioenergetics,

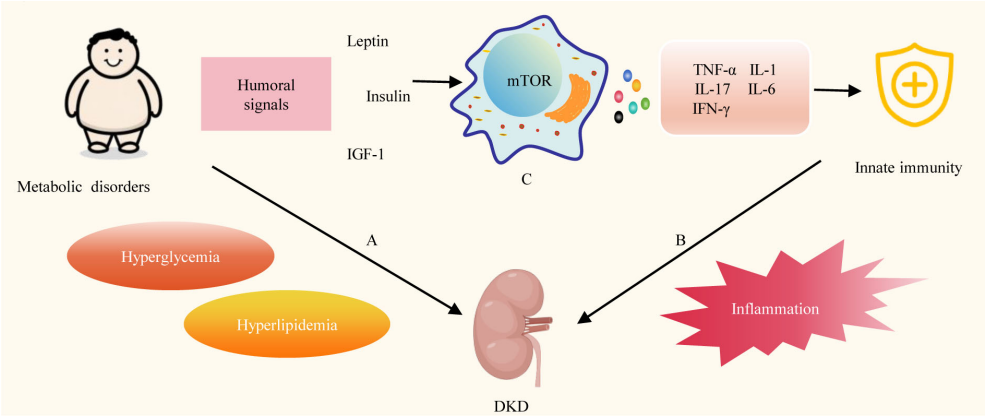

FIGURE 1
Energy metabolism and Innate immunity in DKD. **(A)** Disturbed energy metabolism is one of the main pathogenic mechanisms of DKD. **(B)** Innate immunity plays a key role in the progression of DKD. **(C)** Metabolic disorders can affect innate immune cell metabolism, signaling and the release of various cytokines. TGF-1, Insulin-like growth factor-1; mTOR, mechanistic target of rapamycin; TNF-α, tumor necrosis factor-alpha; IL-1, interleukin-1; IL-6, interleukin-6; IL-17, interleukin-17; IFN-Y, interferon-gamma.

an accumulation of mitochondrial reactive oxygen species (mtROSs), impaired mitophagy, and dynamic abnormalities. These dysfunctions, in turn, initiate a cascade of abnormalities related to metabolism (18).

Concurrently, innate immunity plays a pivotal role in the progression of DKD. (Figure 1B) Multiple innate immune cells, molecules, and signaling pathways are involved in the pathogenesis of DKD (19). Innate immune malfunction in DKD patients leads to inflammation. Inflammation is triggered in reaction to damaging circumstances to preserve tissue integrity and homeostasis. Nevertheless, persistent stimulation of the inflammatory response results in unintended harmful consequences (20). Toll-like receptors (TLRs) emerge as a dynamic receptor family adept at recognizing both pathogen-associated molecular patterns and damage-associated molecular patterns in the context of DM. This recognition process facilitates the activation of leukocytes and intrinsic renal cells in DKD, thereby initiating the proinflammatory cascade during DKD (21). A variety of proinflammatory molecules, chemotactic factors, and adhesion molecules, through multiple inflammatory pathways involving mitogen-activated protein kinases (MAPK), signal transducer and activator of transcription (STAT), and protein kinase C (PKC), induce interactions among intrinsic renal cells and various innate immune cells (macrophages, dendritic cells). These interactions contribute to the progression of DKD (22). Additionally, the complement system, as a crucial component of the innate immune system, swiftly generates a substantial quantity of protein fragments upon activation. These fragments serve as effective mediators for inflammation, vascular activity, and metabolic responses. They also contribute to the progression of DKD (23). Insights from preclinical studies suggest that targeting these innate immune pathways holds promise for developing novel therapies for DKD (24).

Energy metabolism plays a key role in the regulation of innate immunity (Figure 1C) Changes in cell metabolism affect the activity of immune cells, and the function of immune cells in turn determines the metabolic state of cells. Immune cells require a lot of energy to activate. Different methods are used by immune cells to produce this energy. Energy is produced by boosting glycolysis in pro-inflammatory cells like M1 macrophages, and by enhancing mitochondrial activity and beta-oxidation in regulatory cells such as M2 macrophages (25). Overnutrition is linked to low-grade, chronic inflammation that raises the risk of metabolic and cardiovascular disease, promotes autoreactivity, and compromises protective immunity, while undernutrition is linked to immunosuppression, which increases susceptibility to infection and protection against various types of autoimmune disease (26). DM is a chronic metabolic disorder, and insufficient insulin secretion and insufficient insulin action are the two main reasons for the development of DM (27). Metabolic disorders induce the expression of nutritionally and metabolically related growth factors, such as leptin, insulin, and insulin-like growth factor 1 (IGF-1), which activate mechanistic target of rapamycin (mTOR) signaling in immune cells, thereby affecting systemic and intracellular immune metabolism, and consequently inflammation. Further promotes the production of inflammatory cytokines such as interleukin-1 (IL-1), tumor necrosis factor-alpha (TNF-α), interleukin-6 (IL-6), interleukin-17 (IL-17), and interferon-gamma (28). Proinflammatory cytokine production and low-grade inflammation both locally and systemically are linked to the onset and advancement of DKD (29).

3 FGF21 is a bridge between energy metabolism and innate immunity

3.1 FGF21 regulates energy metabolism in DM patients

FGF21, a peptide hormone synthesized by various organs, plays a crucial role in regulating energy homeostasis. It functions as an autocrine, paracrine, and endocrine factor, exerting diverse metabolic effects on several target organs (30). The molecular mechanism of FGF21 signaling is complex and involves several FGF receptors (FGFRs), FGF21 binds to FGFR with very low affinity, and effective binding and signaling requires interaction with the co-receptor β-klotho (31). FGF21 production is influenced by factors such as diet, exercise, and environmental temperature (32) (Figure 2A). In a study employing a whole-room indirect calorimeter, researchers assessed alterations in plasma FGF21 concentrations in 64 healthy individuals with well-regulated glucose levels after a 24-hour period of exposure to seven food treatments with varying macronutrient contents. Notably, it was only after the consumption of two low-protein (3%) overfeeding diets—one rich in carbohydrates (75%) and the other in fat (46%)—that plasma FGF21 concentrations consistently surged by threefold. Larger increments in FGF21 were positively correlated with greater enhancements in 24-hour energy expenditure. These findings underscore that diets characterized by high carbohydrate content but low protein content substantially elevate circulating FGF21 levels (33). The impact of exercise on FGF21 is contingent upon the type of exercise performed. Short-term strenuous muscular exercise has been associated with an elevation in serum FGF21 levels, primarily attributed to the stimulation of skeletal muscle production. In contrast, long-term aerobic exercise has been shown to significantly decrease serum FGF21 concentrations (34). A separate clinical investigation has revealed that exposure to mild cold results in elevated levels of circulating FGF21, thereby anticipating heightened lipolysis and cold-induced thermogenesis. Subtle reductions in ambient temperature have proven effective in regulating FGF21 circadian rhythms in humans, potentially acting as a mediator for cold-induced metabolic alterations analogous to those observed in animals (35). Elevated levels of circulating FGF21 are observed in various metabolic disorders, including DM, obesity, and cardiovascular disease. This seemingly paradoxical occurrence is commonly characterized as a state of "FGF21 resistance" or viewed as a compensatory protective response to metabolic stress (36, 37). A clinical investigation assessed circulating FGF21 levels in 2066 hospitalized patients with DM, revealing that individuals in the low urinary glucose excretion group exhibited higher body mass index (BMI) and serum FGF21 levels. Additionally, lower urinary glucose excretion was found to be associated with increased insulin resistance in patients with type 2 DM (T2DM) (38).

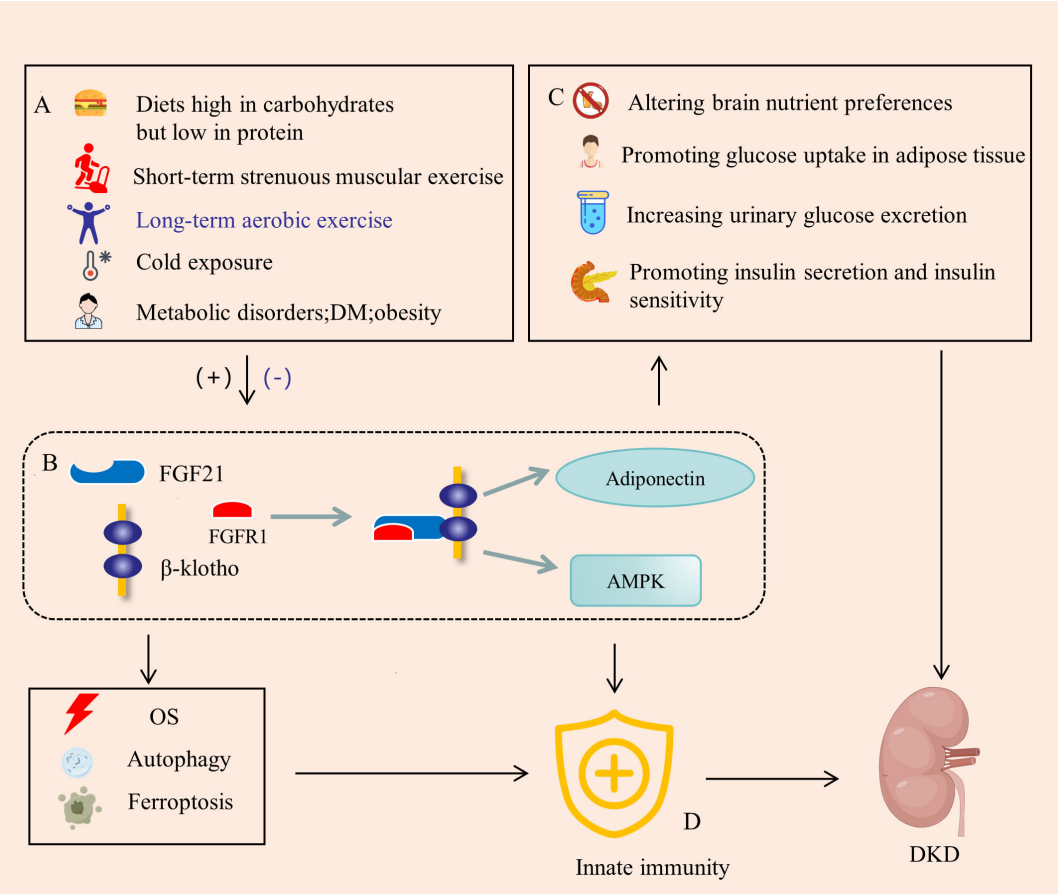

FIGURE 2
FGF21 is a bridge between energy metabolism and innate immunity. **(A)** FGF21 is induced by diet, exercise, cold, and metabolic disorders, significantly up-regulated in DM environments. **(B)** FGF21 binds to FGFR1 and β-klotho to form a complex that activates AMPK signaling in target tissues and promotes adiponectin expression. **(C)** FGF21 regulates metabolism by altering brain nutrient preferences, promoting glucose uptake in adipose tissue, increasing urinary glucose excretion, and promoting insulin secretion and insulin sensitivity. **(D)** FGF21 can also directly regulate innate immune signals and pathways, or indirectly regulate innate immunity through OS, autophagy and ferroptosis. DM, diabites mellitus; AMPK, AMP-activated protein kinase; OS, oxidative stress. (+), Upregulation; (-), Downregulation.

FGF21 exerts its influence through various downstream factors (Figure 2B). Mouse experiments have illustrated that FGF21 treatment enhances both the expression and secretion of adiponectin in adipocytes, consequently elevating serum adiponectin levels in mice. Notably, the therapeutic benefits of FGF21 are compromised in Adiponectin Knockout (KO) mice, highlighting the integral role of adiponectin in mediating the multiple therapeutic effects of FGF21. Consequently, FGF21 actions within local adipocytes are intricately linked to the liver and skeletal muscle through adiponectin, thereby facilitating the systemic effects of FGF21 on insulin sensitivity and energy metabolism (39). However, in obese animals and human subjects, there is a paradoxical scenario where circulating FGF21 levels are elevated, while plasma adiponectin concentrations are diminished, potentially attributed to FGF21 resistance (40). Additionally, the AMP-activated protein kinase (AMPK), a crucial player in preserving tissue integrity and energy balance, is implicated in this process. Endocrine FGF21 signaling has been demonstrated to stimulate the AMPK system, either directly through FGFR1/β-klotho signaling or indirectly by promoting the release of corticosteroids and adiponectin. These released factors, in turn, activate AMPK signaling in the target tissues, contributing to the intricate regulatory network of FGF21 in energy metabolism (41).

In the DM, the up-regulation of FGF21 orchestrates the regulation of blood glucose and metabolism through a comprehensive fourfold action (Figure 2C). Firstly, FGF21 exerts its influence on the brain to homeostatically modify macronutrient preference. Notably, exogenous FGF21 therapy induces a reduction in the consumption of alcohol and sweets, concomitant with an augmentation in protein intake (42). Secondly, FGF21 is locally released from adipose tissue following activation of the β-adrenergic receptor, subsequently enhancing glucose uptake in adipocytes (43). The application of a half-life extended form of FGF21 (FGF21-PEG) has been demonstrated to normalize plasma glucose levels in streptozotocin-treated mice, a model of type 1 diabetes mellitus (T1DM), without reinstating pancreatic β-cell function. This study underscores that insulin-independent glucose uptake in adipocytes persists even in the presence of insulin receptor antagonists (44). Thirdly, administration of FGF21 to mice with both T2DM and T1DM led to a dose-dependent

decrease in the kidney's glucose transport maximum, accompanied by an increase in urine glucose excretion. Experimental findings in mice indicate that FGF21 mitigates hyperglycemia, in part, by reducing renal glucose reabsorption through the peroxisome proliferator-activated receptor-δ (PPARδ)-mediated sodium-glucose cotransporter 2 (SGLT2) pathway (45). Fourthly, the absence of FGF21 (FGF21 KO) exacerbated palmitate-induced islet β-cell failure and suppression of glucose-stimulated insulin secretion (GSIS). In db/db mice, overexpression of pancreatic FGF21 markedly improved islet morphology, elevated GSIS, decreased β-cell apoptosis, and increased insulin expression. Pancreatic FGF21 in T2DM mice induced phosphatidylinositol 3-kinase (PI3K)/Akt signaling-dependent insulin expression and secretion (46). FGF21 demonstrates protective effects against lipotoxicity-induced β-cell dysfunction and apoptosis by down-regulating islet cell lipid accumulation and reducing cell death under lipotoxic conditions, likely through the activation of AMPK-acetyl-CoA carboxylase (ACC) and PPARδ/γ signaling (47). Moreover, experiments have indicated that FGF21 represses mammalian target of rapamycin complex 1 (mTORC1), thereby improving insulin sensitivity and glycogen storage in a hepatocyte-autonomous manner (48). Therapeutic administration of FGF-21 to both ob/ob and db/db mice brought their plasma glucose and triglyceride levels close to normal, with effects persisting for a minimum of twenty-four hours after cessation of FGF-21 treatment. Notably, FGF-21 did not induce hypoglycemia or weight gain (49). The FGF21-mediated regulation of blood glucose and metabolism has been demonstrated to contribute to the delay in the progression of DKD (50).

3.2 FGF21 regulates innate immunity in DM patients

An expanding body of research substantiates the involvement of FGF21 in the regulation of innate immunity(Figure 2D). Endothelial dysfunction, a precursor to proteinuria, glomerular sclerosis, and interstitial fibrosis, contributes to the progression of DKD (51). FGF21 plays a pivotal role in enhancing endothelial cell function through the modulation of innate immunity and the inhibition of inflammatory pathways. In a cellular experiment utilizing varying concentrations of recombinant FGF21 to treat human umbilical vascular endothelial cells (HUVECs), a notable improvement in glycolysis, increased nitric oxide release, and cellular protection against oxidative damage induced by H_2O_2 were observed at an optimal FGF21 concentration of 400 pg/mL. Subsequent to FGF21 treatment, the majority of upregulated genes were enriched in metabolic pathways, while downregulated genes were associated with signaling pathways linked to apoptosis and inflammation (52). Another cellular experiment suggested that FGF21 may mitigate uric acid (UA)-induced endoplasmic reticulum (ER) stress, inflammation, and vascular endothelial cell dysfunction by activating sirtuin 1 (Sirt1) (53). By targeting PPARγ, miR-27b was found to trigger the nuclear factor-κB (NF-κB) signaling pathway and the expression of inflammatory factors, including IL-1β, IL-6, and TNF-α. FGF21 alleviated hypoxia-induced dysfunction and inflammation in human pulmonary arterial endothelial cells by inhibiting miR-27b expression and consequently promoting PPARγ expression (54). Moreover, studies indicated that the deletion of FGF21 in mice exacerbated deoxycorticosterone acetate (DOCA)-salt-induced nephropathy. Supplementation with recombinant human FGF21 (RhFGF21) restored renal damage caused by DOCA and salt. Mechanistically, RhFGF21 activated AMPK, which suppressed NF-κB-regulated inflammation and nuclear factor erythroid 2-related factor 2 (NRF2)-mediated oxidative stress (OS) (55). FGF21 combined with insulin promotes the conversion of M1 macrophages to M2 macrophages to reduce inflammation in DN mice (56). Transcriptome analysis consequently demonstrated that, in FGF21 KO mice but not in WT mice, inflammation-related pathways were markedly enriched and elevated (57). In a mouse model of lipotoxicity and diabetes, FGF21 partially prevented renal injury induced by free fatty acids and diabetes by reducing renal lipid accumulation and inhibiting inflammation, oxidative stress (OS), and fibrosis (58).

Beyond its direct role in regulating innate immunity to suppress inflammation, FGF21 also indirectly influences innate immunity through oxidative stress (OS), autophagy, and ferroptosis, thereby contributing to the delayed progression of DKD. Prolonged OS has the potential to activate innate immunity through multiple transcription factors (59). FGF21, with its associations with genes such as NRF2, thioredoxin binding protein-2 (TBP-2), uncoupling protein 3 (UCP3), superoxide dismutase-2 (SOD2), extracellular signal-regulated kinase (ERK), and p38, and the identification of a crucial response element for activating transcription factor 4 (ATF4) involved in OS regulation, assumes a critical role as a regulator of the cellular response to OS (60). A cross-sectional study including 382 CKD patients showed an independent positive correlation between serum FGF21 and OS levels (61). FGF21 has demonstrated its capacity to inhibit vascular calcification, partially by restoring the antioxidant superoxide dismutase (SOD) levels and reducing vascular OS (62). The peroxisome proliferator-activated receptor alpha (PPARα) agonist, fenofibrate (FF), known for its efficacy in DKD, has been shown to prevent DKD development by mediating NRF2 pathway activation through FGF21 (63). Autophagy, a protective mechanism against various forms of renal inflammatory injury, is also under the regulation of FGF21. Through receptor for activated C kinase 1 (RACK1)-mediated AMPK activation and interaction with autophagy-related 5 (Atg5), FGF21 induces autophagy to enhance cholesterol efflux and minimize cholesterol accumulation in foam cells (64, 65). Epigenetically upregulating global autophagy-network genes, including transcription factor EB, Atg7, Atgl, and FGF21, Jumonji-D3 (JMJD3) demethylates histone H3K27-me3 in response to FGF21 stimulation, leading to autophagy-mediated lipid breakdown (66). FF has been shown to prevent type 1 diabetes-induced pathological and functional abnormalities of the heart by increasing FGF21, which may up-regulate Sirt1-mediated autophagy (67). Ferroptosis is a form of regulated necrosis, wherein excessive or deficient ferroptotic cell death is associated with a dysregulated immune response (68). FGF21 serves as a novel

suppressor of ferroptosis. Both the administration of recombinant FGF21 and the overexpression of FGF21 have demonstrated significant protection against iron overload-induced damage to hepatocyte mitochondria, liver injury, and fibrosis by inhibiting ferroptosis. Conversely, the absence of FGF21 has been shown to exacerbate iron overload-induced ferroptosis (69).

4 FGF21 is a potential marker for the diagnosis and prognosis of DKD

FGF21 undergoes upregulation in the diabetic environment, exerting both metabolic regulation and immunomodulatory effects. Consequently, it holds potential as a valuable marker for the early diagnosis and prognosis of DKD (Figure 3A). A cohort study in China, encompassing 312 patients with T2DM who had their baseline FGF21 levels measured and were subsequently followed for 6 months, defined renal endpoint events as a 30% decrease in eGFR or worsening categories of albuminuria. The findings revealed a correlation between FGF-21 levels and the risks of renal events in a broad-spectrum of Chinese T2DM subjects (70). In a prospective observational study examining the association of soluble tumor necrosis factor receptor type 1 (sTNFR1), FGF-21, endocan, N-terminal pro-brain natriuretic peptide (NT-pro-BNP), and renal outcomes in patients with or without clinical signs of DKD, both sTNFR1 and FGF-21 levels in patients with T2DM were linked to renal outcomes. The combination of these markers demonstrated improved predictability (71). A meta-analysis involving 28 studies with 19,348 participants indicated that a high serum FGF21 level may predict the incidence of chronic kidney disease (CKD) and renal outcomes in patients with T2DM (72). A study involving 1136 Chinese T2DM patients revealed that serum FGF21 levels increased progressively with eGFR category. In a subset comprising 559 individuals with normoalbuminuria and baseline eGFR ≥ 60 mL/min/1.73 m^2, serum FGF21 continued to be a reliable indicator of eGFR decline. Elevated serum FGF21 levels were proposed as a useful biomarker for predicting the progression of renal disease, particularly in the early stages of DKD (73). Another cross-sectional study with 130 individuals demonstrated that serum FGF21 was independently associated with microalbuminuria in patients with T2DM (74). An intriguing prospective cohort study in Singapore, involving 1700 Asian people with T2DM and a mean follow-up of 6.3 years, found that in women with T2DM, plasma FGF21 levels independently predicted the risk of progression to end-stage renal disease. Further research is needed to comprehend the pathophysiological connections between FGF21, sex, and renal progression (75).

5 FGF21 is a potential target for DKD therapy

FGF21 plays a crucial role in regulating both energy metabolism and innate immunity, making it a potential target for therapeutic interventions in DKD (Figure 3B). Based on the kidney disease: improving global outcomes (KDIGO) 2022 clinical practice guideline for diabetes management in chronic kidney disease, the treatment of DKD involves both life management and medication (76). Diet and exercise management, and multiple guideline-recommended hypoglycemic agents are associated with FGF21.An experimental study revealed that fasting-induced FGF21 signaling activates hepatic autophagy and lipid degradation through the JMJD3 histone demethylase (66). In humans, circulating FGF21 levels experienced a significant surge after 28 days on a low-protein (LP) diet, establishing FGF21 as an endocrine signal for protein restriction, coordinating metabolism and growth during reduced protein intake (77). Fasting, protein restriction, and specific reductions in essential amino acid levels impact FGF21 activity, promoting healthy longevity (78). Muscle exercise stimulates

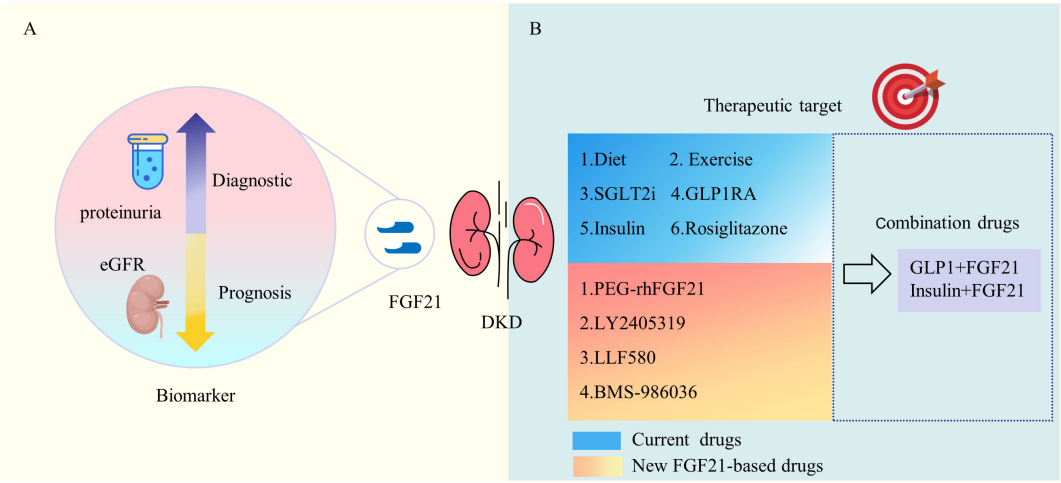

FIGURE 3
Clinical Use of FGF21 in DKD. **(A)** FGF21 is associated with DKD proteinuria and eGFR and is a marker for DKD diagnosis and prognosis. **(B)** Multiple current DKD treatments and medications including diet and exercise are associated with FGF21. A variety of new FGF21-based drugs show favorable metabolic modulation effects. eGFR, estimated glomerular filtration rate; SGLT2i, sodium-glucose cotransporter 2 inhibitor; GLP-IRA, glucagon-like peptide 1 receptor agonist; PEG-rhFGF21, PEGylated recombinant human FGF21.

FGF21 production in muscles, subsequently secreted into circulation to induce lipophagy in the liver through an AMPK-dependent pathway (79). Through PPARγ-mediated transcriptional activation, exercise induces adipose expression of FGFR1 and β-klotho, sensitizing FGF21 actions in adipose tissues to send humoral signals for multi-organ crosstalk, thereby maintaining metabolic homeostasis (80). A systematic review, involving 376 participants from 10 studies, demonstrated a significant increase in FGF-21 levels after exercise compared to no exercise (81). Long-term aerobic exercise has been observed to lower human FGF21 levels and is associated with an improvement in FGF21 resistance (34).

SGLT2 inhibitors (SGLT2i) have emerged as the primary choice for DKD with cardiorenal protective effects. Studies indicate that the SGLT2 inhibitor canagliflozin induces transcriptional reprogramming, activating catabolic pathways, increasing fatty acid oxidation, reducing hepatic steatosis and diacylglycerol content, and elevating hepatic and plasma FGF21 levels (82). Furthermore, empagliflozin shifts energy metabolism towards fat utilization, increases phosphorylation levels of AMP-activated protein kinase and acetyl-CoA carboxylase in skeletal muscle, and enhances liver and plasma FGF21 levels (83). The mechanism behind SGLT2 inhibitors preserving renal function in T2DM while promoting ketogenesis may be attributed to the activation of SIRT1/PGC-1α/FGF21 (84). A sub-study of the DAPA-VO2 investigation revealed that, within the cohort of patients experiencing stable heart failure with reduced ejection fraction (HFrEF), dapagliflozin initiated a temporary elevation in klotho levels. The author speculates that the observed increase in klotho may potentially signify an improvement in proximal tubular function mediated through the reduction of oxidative stress and inflammation within the renal tubules. This improvement might lead to a decreased resistance to FGF-23 (85). Another class of hypoglycemic agents with weight-loss effects, glucagon-like peptide 1 (GLP-1) receptor agonist, is also strongly associated with FGF21. Experimental studies have demonstrated that hepatic FGF21 is essential for liraglutide to effectively reduce body weight and enhance hepatic lipid homeostasis (86). In a clinical study, it was shown that exenatide could aid patients in improving glycemic levels, inflammatory biomarkers, and urine albumin concentration. The effects of exenatide may be partially mediated by FGF21 (87). The traditional glucose-lowering drug, metformin, remains the first-line agent for treating DKD. A clinical study suggests that metformin suppresses circulating fibroblast activation protein activity, upregulates the expression of FGFR1c and β-klotho, thereby increasing FGF21 signaling in adipose tissue and improving peripheral FGF21 sensitivity (88). Additionally, insulin also stimulates FGF21 expression; insulin-induced expression of muscle FGF21 is strongly correlated with an increase in serum FGF21, and this response appears to be intact in T2DM (89). The action of the peroxisome proliferator-activated receptor gamma (PPARγ) agonist rosiglitazone is also reliant on FGF21. FGF21-KO mice do not respond to both the beneficial insulin-sensitizing effects and the adverse side effects of weight gain and edema associated with rosiglitazone (90).

In addition to existing medications, several novel FGF21-based drugs and therapies have demonstrated therapeutic potential for diabetic kidney disease (DKD). The natural form of FGF21 poses challenges for biopharmaceutical applications due to its short half-life, tendency to aggregate in soluble preparations, and susceptibility to protein hydrolysis. As a result, biopharmaceutical technology has undergone significant advancements to extend the duration of action of FGF21 (91). Preclinical studies showed that PEGylated recombinant human FGF21(PEG-rhFGF21) significantly lowered lipid levels in the kidney, decreased urine albumin/creatinine ratio (ACR) and improved mesangial expansion in db/db and DIO mice (92). A randomized, placebo-controlled, double-blind proof-of-concept trial conducted in patients with obesity and T2DM revealed that LY2405319 (LY), an investigational FGF21 variant deemed suitable for early-phase clinical development, demonstrated significant improvements in dyslipidemia. Positive outcomes were observed in terms of increased adiponectin levels, reduced fasting insulin, and decreased body weight. However, it should be noted that only a trend toward glucose lowering was observed (93). LLF580 represents a novel genetically engineered variant of human FGF21, distinguished by its stabilization through the introduction of a disulfide bond and fusion at its N-terminus to the human IgG (subclass IgG1) Fc domain. Generally considered safe, LLF580 exhibits favorable effects on biomarkers associated with lipids, liver fat, and liver injury. In comparison to a placebo, insulin levels, C-peptide levels, and insulin resistance measured by the homeostatic model were all lower, while adiponectin levels were higher during LLF580 treatment. However, it is noteworthy that fasting glucose and glycated hemoglobin remained unchanged (94). The results of a phase II clinical trial indicate that Pegbelfermin (BMS-986036), a PEGylated FGF21 analog, did not exert an impact on HbA1c concentrations. However, weekly (QW) and higher daily doses demonstrated an association with improved metabolic parameters and fibrosis biomarkers in patients with obesity and T2DM who were predisposed to fatty liver (95).

Although the aforementioned FGF21-based new drugs have shown a trend towards improving metabolism, they did not impact HbA1c concentrations in clinical studies. Considering the elevated serum FGF21 levels in metabolic disorders such as T2DM and obesity, and the potential association with FGF21 resistance, artificially increasing the levels of FGF21 (or FGF21 analogs) may not necessarily enhance their actual biological effects in such states of metabolic disruption. The formulation of FGF21 may offer enhanced benefits when combined with other drugs targeting glycemic control and weight loss. In db/db mice, the combined administration of subtherapeutic doses of FGF21 and insulin maintains blood glucose levels for at least 24 hours, inhibits weight gain, and significantly improves lipid parameters. These results indicate that insulin renders FGF21 more sensitive in regulating glucose and lipid metabolism (96). The combined treatment of FGF21 with insulin further improves various parameters, including blood glucose, HbA1c, oral glucose tolerance tests (OGTT), renal function, liver function, blood lipid levels, histopathological alterations, oxidative stress (OS), and advanced glycation end-products (AGEs) in mice with diabetic kidney disease (DKD), compared to insulin or FGF21 administered alone (56). A novel biological agent, which fuses GLP-1 to FGF21 using an elastin-like polypeptide linker acting as a sustained release

module with zero-order drug release, has been developed. Administering this dual agonist once a week to diabetic mice results in significant weight loss and improved glycemic control, effects not observed when either agonist is used alone. Moreover, the dual-agonist formulation surpasses the efficacy of a GLP-1/FGF21 combination, underscoring the value of integrating two structurally different peptides into a single, multipurpose molecule (97). Additionally, a novel GLP-1/FGF21 dual agonist has demonstrated superior weight loss effects compared to GLP-1 or FGF21 administered individually (98).

6 Summary and prospect

DKD is highly prevalent and poses significant harm, with ongoing opportunities for advancements in its diagnosis and treatment. The progression of DKD is associated with a variety of metabolic dysregulations, and glucose and lipid metabolites in the DM setting can directly damage the kidneys while further exacerbating metabolic disturbances. Innate immunity plays an important role in DKD and microinflammation can persistently exacerbate kidney damage. At the same time, metabolic disorders can affect innate immune cell metabolism, signaling and the release of various cytokines. Crosstalk between energy metabolism and innate immunity is one of the main targets of DKD. FGF21, induced by factors such as diet, exercise, cold exposure, and metabolic disorders, is significantly upregulated in diabetic environments. FGF21 forms a complex with FGFR1 and β-klotho, activating AMPK signaling in target tissues and promoting adiponectin expression. The multifaceted roles of FGF21 include the regulation of metabolism by altering brain nutrient preferences, enhancing glucose uptake in adipose tissue, increasing urinary glucose excretion, and promoting insulin secretion and sensitivity. Moreover, FGF21 directly regulates innate immune signals and pathways, while also indirectly influencing innate immunity through mechanisms such as OS, autophagy, and ferroptosis. This dual action enables FGF21 to safeguard renal endothelial cells and impede the progression of DKD. Functioning as a bridge between energy metabolism and innate immunity, FGF21 emerges as a potential marker for both the diagnosis and prognosis of DKD, presenting itself as a promising therapeutic target. Several clinical studies have demonstrated associations between FGF21, DKD proteinuria, and eGFR. Additionally, various current treatments for DKD, including dietary interventions and exercise, exhibit connections with FGF21. The promising metabolic modulation effects of numerous novel FGF21-based drugs further underscore the potential of FGF21 as a pivotal player in DKD management and therapy.

Despite the significant potential of FGF21 in DKD, several challenges persist that warrant attention. Firstly, there is an insufficient body of basic research on the interactions between FGF21 and DKD. While FGF21 is known for its clear metabolic regulation and innate immunomodulatory effects, the specific mechanisms underlying its actions in the context of DKD remain unclear and warrant further investigation. Secondly, many clinical studies examining FGF21 and DKD are characterized by single-center designs and small sample sizes. Consequently, the value of FGF21 in the diagnosis and prognosis of DKD needs to be validated through larger, multi-center studies with diverse patient populations. Robust and comprehensive clinical evidence is essential to establish FGF21 as a reliable biomarker for DKD. Finally, several new drugs developed based on FGF21 have demonstrated metabolic benefits, but their impact on glycemic improvement and innate immunity modulation remains unclear. These drugs have not been extensively studied in clinical trials specifically focused on DKD. The potential of combining novel hypoglycemic agents with FGF21 for enhanced therapeutic effects is promising, but further research is essential to understand the comprehensive impact of these interventions in the context of DKD. Addressing these research gaps will contribute to a more thorough understanding of FGF21's role in DKD and may pave the way for more effective therapeutic strategies.

Author contributions

YL: Writing – original draft. QC: Writing – original draft. YC: Writing – original draft. JH: Writing – original draft. JY: Writing – original draft. ZC: Writing – review & editing. JZ: Writing – review & editing.

Funding

The author(s) declare that no financial support was received for the research, authorship, and/or publication of this article.

Acknowledgments

We would like to acknowledge all the authors.

Conflict of interest

The authors declare that the research was conducted in the absence of any commercial or financial relationships that could be construed as a potential conflict of interest.

Publisher's note

References

1. Thomas MC, Cooper ME, Zimmet P. Changing epidemiology of type 2 diabetes mellitus and associated chronic kidney disease. *Nat Rev Nephrol* (2016) 12(2):73–81. doi: 10.1038/nrneph.2015.173

2. Sun H, Saeedi P, Karuranga S, Pinkepank M, Ogurtsova K, Duncan BB, et al. IDF Diabetes Atlas: Global, regional and country-level diabetes prevalence estimates for 2021 and projections for 2045. *Diabetes Res Clin Pract* (2022) 183:109119. doi: 10.1016/j.diabres.2021.109119

3. Alicic RZ, Rooney MT, Tuttle KR. Diabetic kidney disease: challenges, progress, and possibilities. *Clin J Am Soc Nephrol* (2017) 12(12):2032–45. doi: 10.2215/CJN.11491116

4. ElSayed NA, Aleppo G, Aroda VR, Bannuru RR, Brown FM, Bruemmer D, et al. 11. Chronic kidney disease and risk management: standards of care in diabetes-2023. *Diabetes Care* (2023) 46(Suppl 1):S191–191S202. doi: 10.2337/dc23-S011

5. Oshima M, Shimizu M, Yamanouchi M, Toyama T, Hara A, Furuichi K, et al. Trajectories of kidney function in diabetes: a clinicopathological update. *Nat Rev Nephrol* (2021) 17(11):740–50. doi: 10.1038/s41581-021-00462-y

6. Sasaki T, Nakagawa K, Hata J, Hirakawa Y, Shibata M, Nakano T, et al. Pathologic diabetic nephropathy in autopsied diabetic cases with normoalbuminuria from a Japanese community-based study. *Kidney Int Rep* (2021) 6(12):3035–44. doi: 10.1016/j.ekir.2021.09.007

7. Jongs N, Greene T, Chertow GM, McMurray J, Langkilde AM, Correa-Rotter R, et al. Effect of dapagliflozin on urinary albumin excretion in patients with chronic kidney disease with and without type 2 diabetes: a prespecified analysis from the DAPA-CKD trial. *Lancet Diabetes Endocrinol* (2021) 9(11):755–66. doi: 10.1016/S2213-8587(21)00243-6

8. Bakris GL, Agarwal R, Anker SD, Pitt B, Ruilope LM, Rossing P, et al. Effect of finerenone on chronic kidney disease outcomes in type 2 diabetes. *N Engl J Med* (2020) 383(23):2219–29. doi: 10.1056/NEJMoa2025845

9. Rayego-Mateos S, Rodrigues-Diez RR, Fernandez-Fernandez B, Mora-Fernández C, Marchant V, Donate-Correa J, et al. Targeting inflammation to treat diabetic kidney disease: the road to 2030. *Kidney Int* (2023) 103(2):282–96. doi: 10.1016/j.kint.2022.10.030

10. Geng L, Lam K, Xu A. The therapeutic potential of FGF21 in metabolic diseases: from bench to clinic. *Nat Rev Endocrinol* (2020) 16(11):654–67. doi: 10.1038/s41574-020-0386-0

11. Yan J, Horng T. Lipid metabolism in regulation of macrophage functions. *Trends Cell Biol* (2020) 30(12):979–89. doi: 10.1016/j.tcb.2020.09.006

12. Cardoso D, Perucha E. Cholesterol metabolism: a new molecular switch to control inflammation. *Clin Sci (Lond)* (2021) 135(11):1389–408. doi: 10.1042/CS20201394

13. Ren Y, Zhao H, Yin C, Lan X, Wu L, Du X, et al. Adipokines, hepatokines and myokines: focus on their role and molecular mechanisms in adipose tissue inflammation. *Front Endocrinol (Lausanne)* (2022) 13:873699. doi: 10.3389/fendo.2022.873699

14. Tuttle KR, Agarwal R, Alpers CE, Bakris GL, Brosius FC, Kolkhof P, et al. Molecular mechanisms and therapeutic targets for diabetic kidney disease. *Kidney Int* (2022) 102(2):248–60. doi: 10.1016/j.kint.2022.05.012

15. She QY, Li LJ, Liu MH, Tan RY, Zhong YW, Bao JF, et al. Bibliometric analysis of fibroblast growth factor 21 research over the period 2000 to 2021. *Front Pharmacol* (2022) 13:1011008. doi: 10.3389/fphar.2022.1011008

16. Audzeyenka I, Bierżyńska A, Lay AC. Podocyte bioenergetics in the development of diabetic nephropathy: the role of mitochondria. *Endocrinology* (2022) 163(1):bqab234. doi: 10.1210/endocr/bqab234

17. Mohandes S, Doke T, Hu H, Mukhi D, Dhillon P, Susztak K. Molecular pathways that drive diabetic kidney disease. *J Clin Invest* (2023) 133(4):e165654. doi: 10.1172/JCI165654

18. Yao L, Liang X, Qiao Y, Chen B, Wang P, Liu Z. Mitochondrial dysfunction in diabetic tubulopathy. *Metabolism* (2022) 131:155195. doi: 10.1016/j.metabol.2022.155195

19. Chen J, Liu Q, He J, Li Y. Immune responses in diabetic nephropathy: Pathogenic mechanisms and therapeutic target. *Front Immunol* (2022) 13:958790. doi: 10.3389/fimmu.2022.958790

20. Rayego-Mateos S, Morgado-Pascual JL, Opazo-Ríos L, Guerrero-Hue M, García-Caballero C, Vázquez-Carballo C, et al. Pathogenic pathways and therapeutic approaches targeting inflammation in diabetic nephropathy. *Int J Mol Sci* (2020) 21(11):3798. doi: 10.3390/ijms21113798

21. Lin M, Tang SC. Toll-like receptors: sensing and reacting to diabetic injury in the kidney. *Nephrol Dial Transplant* (2014) 29(4):746–54. doi: 10.1093/ndt/gft446

22. Wada J, Makino H. Inflammation and the pathogenesis of diabetic nephropathy. *Clin Sci (Lond)* (2013) 124(3):139–52. doi: 10.1042/CS20120198

23. Petr V, Thurman JM. The role of complement in kidney disease. *Nat Rev Nephrol* (2023) 19(12):771–87. doi: 10.1038/s41581-023-00766-1

24. Tang S, Yiu WH. Innate immunity in diabetic kidney disease. *Nat Rev Nephrol* (2020) 16(4):206–22. doi: 10.1038/s41581-019-0234-4

25. Faas MM, de Vos P. Mitochondrial function in immune cells in health and disease. *Biochim Biophys Acta Mol Basis Dis* (2020) 1866(10):165845. doi: 10.1016/j.bbadis.2020.165845

26. Alwarawrah Y, Kiernan K, MacIver NJ. Changes in nutritional status impact immune cell metabolism and function. *Front Immunol* (2018) 9:1055. doi: 10.3389/fimmu.2018.01055

27. Oza MJ, Laddha AP, Gaikwad AB, Mulay SR, Kulkarni YA. Role of dietary modifications in the management of type 2 diabetic complications. *Pharmacol Res* (2021) 168:105602. doi: 10.1016/j.phrs.2021.105602

28. Matarese G. The link between obesity and autoimmunity. *Science* (2023) 379(6639):1298–300. doi: 10.1126/science.ade0113

29. Wada J, Makino H. Innate immunity in diabetes and diabetic nephropathy. *Nat Rev Nephrol* (2016) 12(1):13–26. doi: 10.1038/nrneph.2015.175

30. Fisher FM, Maratos-Flier E. Understanding the physiology of FGF21. *Annu Rev Physiol* (2016) 78:223–41. doi: 10.1146/annurev-physiol-021115-105339

31. Kuro-O M. The Klotho proteins in health and disease. *Nat Rev Nephrol* (2019) 15(1):27–44. doi: 10.1038/s41581-018-0078-3

32. Hollstein T, Heinitz S, Ando T, Rodzevik TL, Basolo A, Walter M, et al. Metabolic responses to 24-hour fasting and mild cold exposure in overweight individuals are correlated and accompanied by changes in FGF21 concentration. *Diabetes* (2020) 69(7):1382–8. doi: 10.2337/db20-0153

33. Vinales KL, Begaye B, Bogardus C, Walter M, Krakoff J, Piaggi P. FGF21 is a hormonal mediator of the human "Thrifty" metabolic phenotype. *Diabetes* (2019) 68(2):318–23. doi: 10.2337/db18-0696

34. Stine JG, Welles JE, Keating S, Hussaini Z, Soriano C, Heinle JW, et al. Serum fibroblast growth factor 21 is markedly decreased following exercise training in patients with biopsy-proven nonalcoholic steatohepatitis. *Nutrients* (2023) 15(6):1481. doi: 10.3390/nu15061481

35. Lee P, Brychta RJ, Linderman J, Smith S, Chen KY, Celi FS. Mild cold exposure modulates fibroblast growth factor 21 (FGF21) diurnal rhythm in humans: relationship between FGF21 levels, lipolysis, and cold-induced thermogenesis. *J Clin Endocrinol Metab* (2013) 98(1):E98–102. doi: 10.1210/jc.2012-3107

36. Yang M, Liu C, Jiang N, Liu Y, Luo S, Li C, et al. Fibroblast growth factor 21 in metabolic syndrome. *Front Endocrinol (Lausanne)* (2023) 14:1220426. doi: 10.3389/fendo.2023.1220426

37. Keipert S, Ost M. Stress-induced FGF21 and GDF15 in obesity and obesity resistance. *Trends Endocrinol Metab* (2021) 32(11):904–15. doi: 10.1016/j.tem.2021.08.008

38. Zhang R, Cai X, Du Y, Liu L, Han X, Liu W, et al. Association of serum fibroblast growth factor 21 and urinary glucose excretion in hospitalized patients with type 2 diabetes. *J Diabetes Complications* (2021) 35(1):107750. doi: 10.1016/j.jdiacomp.2020.107750

39. Lin Z, Tian H, Lam KS, Lin S, Hoo RC, Konishi M, et al. Adiponectin mediates the metabolic effects of FGF21 on glucose homeostasis and insulin sensitivity in mice. *Cell Metab* (2013) 17(5):779–89. doi: 10.1016/j.cmet.2013.04.005

40. Hui X, Feng T, Liu Q, Gao Y, Xu A. The FGF21-adiponectin axis in controlling energy and vascular homeostasis. *J Mol Cell Biol* (2016) 8(2):110–9. doi: 10.1093/jmcb/mjw013

41. Salminen A, Kauppinen A, Kaarniranta K. FGF21 activates AMPK signaling: impact on metabolic regulation and the aging process. *J Mol Med (Berl)* (2017) 95(2):123–31. doi: 10.1007/s00109-016-1477-1

42. Hill CM, Qualls-Creekmore E, Berthoud HR, Soto P, Yu S, McDougal DH, et al. FGF21 and the physiological regulation of macronutrient preference. *Endocrinology* (2020) 161(3):bqaa019. doi: 10.1210/endocr/bqaa019

43. Justesen S, Haugegaard KV, Hansen JB, Hansen HS, Andersen B. The autocrine role of FGF21 in cultured adipocytes. *Biochem J* (2020) 477(13):2477–87. doi: 10.1042/BCJ20200220

44. Diener JL, Mowbray S, Huang WJ, Yowe D, Xu J, Caplan S, et al. FGF21 normalizes plasma glucose in mouse models of type 1 diabetes and insulin receptor dysfunction. *Endocrinology* (2021) 162(9):bqab092. doi: 10.1210/endocr/bqab092

45. Li S, Wang N, Guo X, Li J, Zhang T, Ren G, et al. Fibroblast growth factor 21 regulates glucose metabolism in part by reducing renal glucose reabsorption. *BioMed Pharmacother* (2018) 108:355–66. doi: 10.1016/j.biopha.2018.09.078

46. Pan Y, Wang B, Zheng J, Xiong R, Fan Z, Ye Y, et al. Pancreatic fibroblast growth factor 21 protects against type 2 diabetes in mice by promoting insulin expression and secretion in a PI3K/Akt signaling-dependent manner. *J Cell Mol Med* (2019) 23(2):1059–71. doi: 10.1111/jcmm.14007

47. Xie T, So WY, Li XY, Leung PS. Fibroblast growth factor 21 protects against lipotoxicity-induced pancreatic β-cell dysfunction via regulation of AMPK signaling and lipid metabolism. *Clin Sci (Lond)* (2019) 133(19):2029–44. doi: 10.1042/CS20190093

48. Gong Q, Hu Z, Zhang F, Cui A, Chen X, Jiang H, et al. Fibroblast growth factor 21 improves hepatic insulin sensitivity by inhibiting mammalian target of rapamycin complex 1 in mice. *Hepatology* (2016) 64(2):425–38. doi: 10.1002/hep.28523

49. Kharitonenkov A, Shiyanova TL, Koester A, Ford AM, Micanovic R, Galbreath EJ, et al. FGF-21 as a novel metabolic regulator. *J Clin Invest* (2005) 115(6):1627–35. doi: 10.1172/JCI23606

50. Kitada M, Ogura Y, Suzuki T, Monno I, Kanasaki K, Watanabe A, et al. A low-protein diet exerts a beneficial effect on diabetic status and prevents diabetic nephropathy in Wistar fatty rats, an animal model of type 2 diabetes and obesity. *Nutr Metab (Lond)* (2018) 15:20. doi: 10.1186/s12986-018-0255-1

51. Dumas SJ, Meta E, Borri M, Luo Y, Li X, Rabelink TJ, et al. Phenotypic diversity and metabolic specialization of renal endothelial cells. *Nat Rev Nephrol* (2021) 17 (7):441–64. doi: 10.1038/s41581-021-00411-9

52. Yang N, Zhang Y, Huang Y, Yan J, Qian Z, Li H, et al. FGF21 at physiological concentrations regulates vascular endothelial cell function through multiple pathways. *Biochim Biophys Acta Mol Basis Dis* (2022) 1868(12):166558. doi: 10.1016/j.bbadis.2022.166558

53. Ouyang R, Zhao X, Zhang R, Yang J, Li S, Deng D. FGF21 attenuates high uric acid–induced endoplasmic reticulum stress, inflammation and vascular endothelial cell dysfunction by activating Sirt1. *Mol Med Rep* (2022) 25(1):35. doi: 10.3892/mmr.2021.12551

54. Yao D, He Q, Sun J, Cai L, Wei J, Cai G, et al. FGF21 attenuates hypoxia–induced dysfunction and inflammation in HPAECs via the microRNA–27b–mediated PPARγ pathway. *Int J Mol Med* (2021) 47(6):116. doi: 10.3892/ijmm.2021.4949

55. Weng HC, Lu XY, Xu YP, Wang YH, Wang D, Feng YL, et al. Fibroblast growth factor 21 attenuates salt-sensitive hypertension-induced nephropathy through anti-inflammation and anti-oxidation mechanism. *Mol Med* (2021) 27(1):147. doi: 10.1186/s10020-021-00408-x

56. Meng F, Cao Y, Khoso MH, Kang K, Ren G, Xiao W, et al. Therapeutic effect and mechanism of combined use of FGF21 and insulin on diabetic nephropathy. *Arch Biochem Biophys* (2021) 713:109063. doi: 10.1016/j.abb.2021.109063

57. Fang H, Ghosh S, Sims LC, Stone KP, Hill CM, Spires D, et al. FGF21 prevents low-protein diet-induced renal inflammation in aged mice. *Am J Physiol Renal Physiol* (2021) 321(3):F356–356F368. doi: 10.1152/ajprenal.00107.2021

58. Zhang C, Shao M, Yang H, Chen L, Yu L, Cong W, et al. Attenuation of hyperlipidemia- and diabetes-induced early-stage apoptosis and late-stage renal dysfunction via administration of fibroblast growth factor-21 is associated with suppression of renal inflammation. *PloS One* (2013) 8(12):e82275. doi: 10.1371/journal.pone.0082275

59. Reuter S, Gupta SC, Chaturvedi MM, Aggarwal BB. Oxidative stress, inflammation, and cancer: how are they linked. *Free Radic Biol Med* (2010) 49 (11):1603–16. doi: 10.1016/j.freeradbiomed.2010.09.006

60. Gómez-Sámano MÁ, Grajales-Gómez M, Zuarth-Vázquez JM, Navarro-Flores MF, Martínez-Saavedra M, Juárez-León ÓA, et al. Fibroblast growth factor 21 and its novel association with oxidative stress. *Redox Biol* (2017) 11:335–41. doi: 10.1016/j.redox.2016.12.024

61. Gómez-Sámano MÁ, Vargas-Abonce VP, Martínez-Sánchez FD, Palacios-Báez L, Vera-Zertuche JM, Navarro-Flores MF, et al. Fibroblast growth factor 21 is associated with increased serum total antioxidant capacity and oxidized lipoproteins in humans with different stages of chronic kidney disease. *Ther Adv Endocrinol Metab* (2021) 12. doi: 10.1177/20420188211001160

62. Li Y, He S, Wang C, Jian W, Shen X, Shi Y, et al. Fibroblast growth factor 21 inhibits vascular calcification by ameliorating oxidative stress of vascular smooth muscle cells. *Biochem Biophys Res Commun* (2023) 650:39–46. doi: 10.1016/j.bbrc.2023.01.054

63. Cheng Y, Zhang J, Guo W, Li F, Sun W, Chen J, et al. Up-regulation of Nrf2 is involved in FGF21-mediated fenofibrate protection against type 1 diabetic nephropathy. *Free Radic Biol Med* (2016) 93:94–109. doi: 10.1016/j.freeradbiomed.2016.02.002

64. Kimura T, Isaka Y, Yoshimori T. Autophagy and kidney inflammation. *Autophagy* (2017) 13(6):997–1003. doi: 10.1080/15548627.2017.1309485

65. Xiaolong L, Dongmin G, Liu M, Zuo W, Huijun H, Qiufen T, et al. FGF21 induces autophagy-mediated cholesterol efflux to inhibit atherogenesis via RACK1 up-regulation. *J Cell Mol Med* (2020) 24(9):4992–5006. doi: 10.1111/jcmm.15118

66. Byun S, Seok S, Kim YC, Zhang Y, Yau P, Iwamori N, et al. Fasting-induced FGF21 signaling activates hepatic autophagy and lipid degradation via JMJD3 histone demethylase. *Nat Commun* (2020) 11(1):807. doi: 10.1038/s41467-020-14384-z

67. Zhang J, Cheng Y, Gu J, Wang S, Zhou S, Wang Y, et al. Fenofibrate increases cardiac autophagy via FGF21/SIRT1 and prevents fibrosis and inflammation in the hearts of Type 1 diabetic mice. *Clin Sci (Lond)* (2016) 130(8):625–41. doi: 10.1042/CS20150623

68. Chen X, Kang R, Kroemer G, Tang D. Ferroptosis in infection, inflammation, and immunity. *J Exp Med* (2021) 218(6):e20210518. doi: 10.1084/jem.20210518

69. Wu A, Feng B, Yu J, Yan L, Che L, Zhuo Y, et al. Fibroblast growth factor 21 attenuates iron overload-induced liver injury and fibrosis by inhibiting ferroptosis. *Redox Biol* (2021) 46:102131. doi: 10.1016/j.redox.2021.102131

70. Chang LH, Chu CH, Huang CC, Lin LY. Fibroblast growth factor 21 levels exhibit the association with renal outcomes in subjects with type 2 diabetes mellitus. *Front Endocrinol (Lausanne)* (2022) 13:846018. doi: 10.3389/fendo.2022.846018

71. Chang LH, Hwu CM, Chu CH, Lin YC, Huang CC, You JY, et al. The combination of soluble tumor necrosis factor receptor type 1 and fibroblast growth factor 21 exhibits better prediction of renal outcomes in patients with type 2 diabetes mellitus. *J Endocrinol Invest* (2021) 44(12):2609–19. doi: 10.1007/s40618-021-01568-7

72. Yong G, Li L, Hu S. Fibroblast growth factor 21 may be a strong biomarker for renal outcomes: a meta-analysis. *Ren Fail* (2023) 45(1):2179336. doi: 10.1080/0886022X.2023.2179336

73. Lee CH, Hui EY, Woo YC, Yeung CY, Chow WS, Yuen MM, et al. Circulating fibroblast growth factor 21 levels predict progressive kidney disease in subjects with type 2 diabetes and normoalbuminuria. *J Clin Endocrinol Metab* (2015) 100(4):1368–75. doi: 10.1210/jc.2014-3465

74. Esteghamati A, Khandan A, Momeni A, Behdadnia A, Ghajar A, Nikdad MS, et al. Circulating levels of fibroblast growth factor 21 in early-stage diabetic kidney disease. *Ir J Med Sci* (2017) 186(3):785–94. doi: 10.1007/s11845-017-1554-7

75. Liu JJ, Liu S, Choo R, Wee SL, Xu A, Lim SC. Sex modulates the association of fibroblast growth factor 21 with end-stage renal disease in Asian people with Type 2 diabetes: a 6.3-year prospective cohort study. *Diabetes Med* (2018) 35(7):880–6. doi: 10.1111/dme.13641

76. Rossing P, Caramori ML, Chan J, Heerspink H, Hurst C, Khunti K, et al. Executive summary of the KDIGO 2022 Clinical Practice Guideline for Diabetes Management in Chronic Kidney Disease: an update based on rapidly emerging new evidence. *Kidney Int* (2022) 102(5):990–9. doi: 10.1016/j.kint.2022.06.013

77. Laeger T, Henagan TM, Albarado DC, Redman LM, Bray GA, Noland RC, et al. FGF21 is an endocrine signal of protein restriction. *J Clin Invest* (2014) 124(9):3913–22. doi: 10.1172/JCI74915

78. Green CL, Lamming DW, Fontana L. Molecular mechanisms of dietary restriction promoting health and longevity. *Nat Rev Mol Cell Biol* (2022) 23(1):56–73. doi: 10.1038/s41580-021-00411-4

79. Gao Y, Zhang W, Zeng LQ, Bai H, Li J, Zhou J, et al. Exercise and dietary intervention ameliorate high-fat diet-induced NAFLD and liver aging by inducing lipophagy. *Redox Biol* (2020) 36:101635. doi: 10.1016/j.redox.2020.101635

80. Geng L, Liao B, Jin L, Huang Z, Triggle CR, Ding H, et al. Exercise alleviates obesity-induced metabolic dysfunction via enhancing FGF21 sensitivity in adipose tissues. *Cell Rep* (2019) 26(10):2738–52.e4. doi: 10.1016/j.celrep.2019.02.014

81. Kim H, Jung J, Park S, Joo Y, Lee S, Sim J, et al. Exercise-induced fibroblast growth factor-21: A systematic review and meta-analysis. *Int J Mol Sci* (2023) 24 (8):7284. doi: 10.3390/ijms24087284

82. Osataphan S, Macchi C, Singhal G, Chimene-Weiss J, Sales V, Kozuka C, et al. SGLT2 inhibition reprograms systemic metabolism *via* FGF21-dependent and -independent mechanisms. *JCI Insight* (2019) 4(5):e123130. doi: 10.1172/jci.insight.123130

83. Xu L, Nagata N, Nagashimada M, Zhuge F, Ni Y, Chen G, et al. SGLT2 inhibition by empagliflozin promotes fat utilization and browning and attenuates inflammation and insulin resistance by polarizing M2 macrophages in diet-induced obese mice. *EBioMedicine* (2017) 20:137–49. doi: 10.1016/j.ebiom.2017.05.028

84. Packer M. Role of ketogenic starvation sensors in mediating the renal protective effects of SGLT2 inhibitors in type 2 diabetes. *J Diabetes Complications* (2020) 34 (9):107647. doi: 10.1016/j.jdiacomp.2020.107647

85. Mora-Fernández C, Pérez A, Mollar A, Palau P, Amiguet M, de la Espriella R, et al. Short-term changes in klotho and FGF23 in heart failure with reduced ejection fraction-a substudy of the DAPA-VO(2) study. *Front Cardiovasc Med* (2023) 10:1242108. doi: 10.3389/fcvm.2023.1242108

86. Liu D, Pang J, Shao W, Gu J, Zeng Y, He HH, et al. Hepatic fibroblast growth factor 21 is involved in mediating functions of liraglutide in mice with dietary challenge. *Hepatology* (2021) 74(4):2154–69. doi: 10.1002/hep.31856

87. Kang C, Qiao Q, Tong Q, Bai Q, Huang C, Fan R, et al. Effects of exenatide on urinary albumin in overweight/obese patients with T2DM: a randomized clinical trial. *Sci Rep* (2021) 11(1):20062. doi: 10.1038/s41598-021-99527-y

88. Nissen Pedersen AK, Gormsen LC, Nielsen S, Jessen N, Bjerre M. Metformin improves the prerequisites for FGF21 signaling in patients with type 2 diabetes. *J Clin Endocrinol Metab* (2023), dgad583. doi: 10.1210/clinem/dgad583

89. Kruse R, Vienberg SG, Vind BF, Andersen B, Højlund K. Effects of insulin and exercise training on FGF21, its receptors and target genes in obesity and type 2 diabetes. *Diabetologia* (2017) 60(10):2042–51. doi: 10.1007/s00125-017-4373-5

90. Dutchak PA, Katafuchi T, Bookout AL, Choi JH, Yu RT, Mangelsdorf DJ, et al. Fibroblast growth factor-21 regulates PPARγ activity and the antidiabetic actions of thiazolidinediones. *Cell* (2012) 148(3):556–67. doi: 10.1016/j.cell.2011.11.062

91. Yang R, Xu A, Kharitonenkov A. Another kid on the block: long-acting FGF21 analogue to treat dyslipidemia and fatty liver. *J Clin Endocrinol Metab* (2022) 107(1): e417–417e419. doi: 10.1210/clinem/dgab686

92. Zhao L, Wang H, Xie J, Chen Z, Li X, Niu J. Potent long-acting rhFGF21 analog for treatment of diabetic nephropathy in db/db and DIO mice. *BMC Biotechnol* (2017) 17(1):58. doi: 10.1186/s12896-017-0368-z

93. Gaich G, Chien JY, Fu H, Glass LC, Deeg MA, Holland WL, et al. The effects of LY2405319, an FGF21 analog, in obese human subjects with type 2 diabetes. *Cell Metab* (2013) 18(3):333–40. doi: 10.1016/j.cmet.2013.08.005

94. Rader DJ, Maratos-Flier E, Nguyen A, Hom D, Ferriere M, Li Y, et al. LLF580, an FGF21 analog, reduces triglycerides and hepatic fat in obese adults with modest hypertriglyceridemia. *J Clin Endocrinol Metab* (2022) 107(1):e57–57e70. doi: 10.1210/clinem/dgab624

95. Charles ED, Neuschwander-Tetri BA, Pablo Frias J, Kundu S, Luo Y, Tirucherai GS, et al. Pegbelfermin (BMS-986036), PEGylated FGF21, in patients with obesity and type 2 diabetes: results from a randomized phase 2 study. *Obes (Silver Spring)* (2019) 27 (1):41–9. doi: 10.1002/oby.22344

96. Yu D, Ye X, Wu Q, Li S, Yang Y, He J, et al. Insulin sensitizes FGF21 in glucose and lipid metabolisms via activating common AKT pathway. *Endocrine* (2016) 52 (3):527–40. doi: 10.1007/s12020-015-0801-9

97. Gilroy CA, Capozzi ME, Varanko AK, Tong J, D'Alessio DA, Campbell JE, et al. Sustained release of a GLP-1 and FGF21 dual agonist from an injectable depot protects mice from obesity and hyperglycemia. *Sci Adv* (2020) 6(35):eaaz9890. doi: 10.1126/sciadv.aaz9890

98. Pan Q, Lin S, Li Y, Liu L, Li X, Gao X, et al. A novel GLP-1 and FGF21 dual agonist has therapeutic potential for diabetes and non-alcoholic steatohepatitis. *EBioMedicine* (2021) 63:103202. doi: 10.1016/j.ebiom.2020.103202

frontiers | Frontiers in Immunology

TYPE Review
PUBLISHED 16 February 2024
DOI 10.3389/fimmu.2024.1294807

OPEN ACCESS

EDITED BY
Xu-jie Zhou,
Peking University, China

REVIEWED BY
Lionel Franz Poulin,
INSERM U1003 Laboratoire de Physiologie Cellulaire, France
Latha P. Ganesan,
The Ohio State University, United States

*CORRESPONDENCE
Denglu Zhang
dlzhang01@163.com
Weipin Niu
niuweipin0708@sina.com
Yi Li
liyi1991_sdu@126.com

RECEIVED 15 September 2023
ACCEPTED 05 February 2024
PUBLISHED 16 February 2024

CITATION
Lv D, Jiang H, Yang X, Li Y, Niu W and Zhang D (2024) Advances in understanding of dendritic cell in the pathogenesis of acute kidney injury.
Front. Immunol. 15:1294807.
doi: 10.3389/fimmu.2024.1294807

Advances in understanding of dendritic cell in the pathogenesis of acute kidney injury

Dongfang Lv[1], Huihui Jiang[2], Xianzhen Yang[3], Yi Li[4,5]*, Weipin Niu[6,7]* and Denglu Zhang[6,7]*

[1]College of First Clinical Medicine, Shandong University of Traditional Chinese Medicine, Jinan, China, [2]Clinical Laboratory, Affiliated Hospital of Shandong University of Traditional Chinese Medicine, Jinan, China, [3]Department of Urology, Afliated Hospital of Shandong University of Traditional Chinese Medicine, Jinan, China, [4]Department of Central Laboratory, Shandong Provincial Hospital Affiliated to Shandong First Medical University, Jinan, China, [5]Engineering Laboratory of Urinary Organ and Functional Reconstruction of Shandong Province, Shandong Provincial Hospital Affiliated to Shandong First Medical University, Jinan, China, [6]Central Laboratory, Affiliated Hospital of Shandong University of Traditional Chinese Medicine, Jinan, China, [7]Shandong Key Laboratory of Dominant Diseases of traditional Chinese Medicine, Affiliated Hospital of Shandong University of Traditional Chinese Medicine, Jinan, China

Acute kidney injury (AKI) is characterized by a rapid decline in renal function and is associated with a high morbidity and mortality rate. At present, the underlying mechanisms of AKI remain incompletely understood. Immune disorder is a prominent feature of AKI, and dendritic cells (DCs) play a pivotal role in orchestrating both innate and adaptive immune responses, including the induction of protective proinflammatory and tolerogenic immune reactions. Emerging evidence suggests that DCs play a critical role in the initiation and development of AKI. This paper aimed to conduct a comprehensive review and analysis of the role of DCs in the progression of AKI and elucidate the underlying molecular mechanism. The ultimate objective was to offer valuable insights and guidance for the treatment of AKI.

KEYWORDS

dendritic cells, acute kidney injury, protective proinflammatory, tolerogenic immune reactions, tolerogenic dendritic cells

1 Introduction

Acute kidney injury (AKI) is defined as a sudden decrease in the glomerular filtration rate, as evidenced by a 50% increase in serum creatinine (SCr) within 7 days, a 0.3 mg/dL increase in SCr within 2 days, or oliguria (1). In recent years, the incidence of AKI due to chronic kidney disease has been increasing due to the ageing of the population and the increasing prevalence of underlying conditions such as diabetes mellitus and hypertension (2). Furthermore, in conjunction with the continued emergence of novel pharmaceuticals and the use of interventional therapies, drug-induced AKI is increasingly contributing to the aetiology of this condition (3). A global meta-analysis of AKI prevalence showed that

the incidence of AKI was 21.6% among adults and 33.7% among children, and AKI-related mortality rates were 23.9% among adults and 13.8% among children (4). Due to the increased rates of morbidity and the high rate of mortality, AKI has become a significant public health concern in contemporary society, and it represents a challenging and prominent area of current research.

The aetiology of AKI is multifactorial and includes renal ischaemia, nephrotoxin exposure, and sepsis, each with distinct pathophysiological mechanisms (5). During the progression of AKI, the inflammatory response plays a crucial role, and the innate and adaptive immune systems participate in the inflammatory process. Throughout the progression of AKI, various factors contribute to the activation and recruitment of immune cells to the injured kidney, including damage-associated molecular patterns (DAMPs), hypoxia-inducible factors (HIFs), renal vascular endothelial dysfunction, adhesion molecules, chemokines, cytokines, and Toll-like receptors (6). Dendritic cells (DCs), neutrophils, macrophages, and lymphocytes are immune cells that are implicated in the pathophysiology of AKI, and some of their subsets are involved in healing processes (7).

In terms of innate and adaptive immune responses, DCs are specialized antigen-presenting cells (APCs). DCs constantly sense pathogen- or inflammation-associated signals and keep peripheral T cells in a resting state in the absence of DAMPs or inflammation (8). Once DAMPs or inflammation-related signals are recognized by pattern recognition receptors (PRRs) on DCs, DCs become activated or mature and migrate toward the injured tissue (9). Mature DCs can efficiently ingest antigens, process them into proteolytic peptides, and load these peptides onto major histocompatibility complex (MHC) class I and class II molecules to form MHC-peptide complexes (10). DCs then migrate from the site of antigen uptake to secondary lymphoid organs and can present antigens to $CD8^+$ T cells and $CD4^+$ T cells, inducing effector T cell differentiation and regulatory T (Treg) cell tolerance, thereby initiating an antigen-specific immune response or immune tolerance (11, 12). DCs also secrete cytokines and growth factors enhance or regulate the immune response. Because immune cells are recruited to the site of injury after the onset of AKI and DCs are efficient APCs, in this paper, we examined the role of DCs during the onset of AKI and the recent research advances in this area of study.

2 Subsets and ontogeny of DCs

DCs can be categorized into different subsets, and different subsets have significant phenotypic heterogeneity and functional plasticity. The terminology used to describe these different subsets has changed in recent years. More recently, consistency in assigning subsets has been adopted by many groups based on origin, associated regulatory transcription factors, surface markers, and biological function (13, 14). We briefly summarize the basic characteristics of different subsets of DCs, including conventional DCs (cDCs), plasmacytoid DCs (pDCs), monocyte-derived DCs (mo-DCs), and newly discovered DC3s as shown in Table 1; Figure 1. The mechanism of DC-induced helper T cell polarization for different subsets of DCs is shown in Figure 2.

2.1 cDCs

cDCs are distributed in almost all lymphoid and nonlymphoid tissues and are divided into two subgroups, cDC1s and cDC2s. cDCs serve as the principal APCs in the immune system and can detect tissue damage and effectively capture and process environmentally associated and cell-associated antigens. Subsequently, cDCs transport these antigens to the draining lymph nodes for presentation to T cells (43).

cDC1s specialize in the antigenic cross-presentation to $CD8^+$ T cells, the activation of T helper type 1 (Th1) $CD4^+$ T cells, and the generation of type III interferons (IFN-III) (44). Murine cDC1s are typically characterized as $CLEC9A^+$, $XCR1^+$, $CD103^+$, $CD26^+$, and $CD8^+$ (15). Human cDC1s are characterized as $CD141^+$, $CD14^-$, $CLEC9A^+$, $XCR1^+$, $FLT3^+$, and $CD103^+$ (19). Almost all human and mouse cDC1s express $XCR1^+$, $Clec9A^+$, and $CD103^+$. Developmentally, cDC1s depend on transcription factors Batf3, Irf8, Id2, and Nfil3 (16–18).

TABLE 1 Key transcription factors, markers and cytokines ofDC subsets.

Subsets	Key transcription factors	Key markers		Cytokines	Refs
		Mouse	Human		
cDC1s	Batf3, Irf8, Id2, Nfil3	$CLEC9A^+$, $XCR1^+$, $CD103^+$, $CD26^+$, $CD8^+$	$CD141^+$, $CD14^-$, $CLEC9A^+$, $XCR1^+$, $FLT3^+$, $CD103^+$	IL-12, IFN-III	(15–18)
cDC2s	Relb, Rbpj, Irf4	, $CD26^+$, $CX3CR1^+$, $CD11b^+$, $F4/80^-$	$CD1c^+$, $CD5^+$, $CD14^-$, $CD163^-$	IL-6, IL-23	(19, 20)
DC3s	IRF8, Klf4	$CD172a^+$, $Lyz2^+$, $CD16/32^+$	CD5-, CD163+, CD14+	/	(21–24)
pDCs	E2-2, Tcf4, Irf8, Irf7, Stat3, Stat5	$CD11c^-$, MHC II^-, $CD11b^-$, $B220^+$, $CD123^+$, $Ly6C^+$, $BST2^+$, $SiglecH^+$	$BDCA2^+$, $CD11c^-$, $CD4^+$, $BDCA4^+$, $CD123^+$	IFN-α	(25–27)
moDCs	PU.1, IRF4, NR4A3, NCOR2, Etv3, Etv6	, $CX3CR1^+$, $CD11b^+$, $F4/80^+$, $Ly6C^+$	$CD86^+$, $CD40^+$, $CD80^+$, $CD83^+$, $CCR7^+$, $CD14^-$, $CD209^+$	TNF-α, IL-1, IL-12, IL-23, iNOS	(28–33)
tolDCs	Nrf2, Baff	$CD40^-$, $CD80^-$, $CD86^-$, MHC-II^-, PD-$L1^+$	$CD163^+$, $CD141^+$, $CD16^+$, $CD14^+$	IL-10, TGF-β, IFN-γ	(34–38)

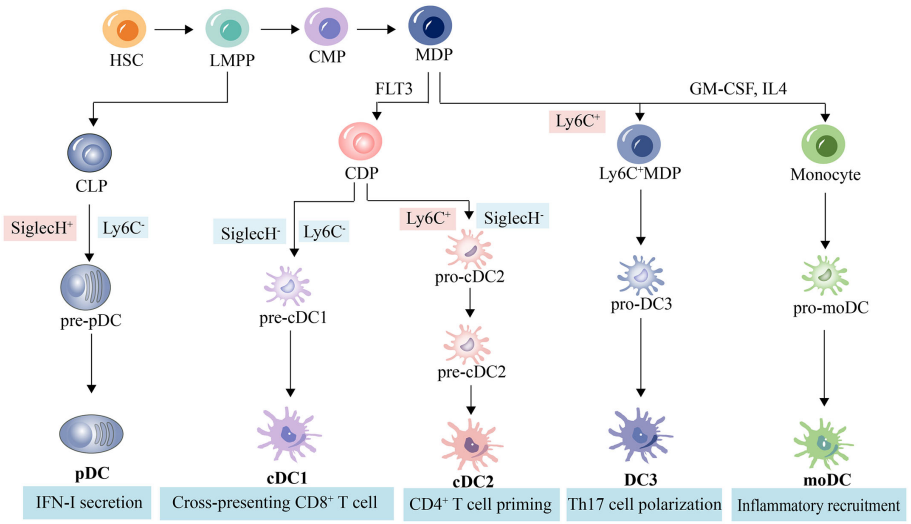

FIGURE 1
DC subpopulations and related lineages in mice. Hematopoietic stem cells differentiate into pluripotent progenitors (LMPP), which further differentiate into common myeloid progenitors (CPM) and common lymphoid progenitor (CLP). CLP then differentiate into pDC precursors and ultimately pDC. CPM differentiate into macrophage dendritic progenitors (MDP), which in turn differentiate into common DC progenitors (CDP), Ly6C$^+$MDP, and monocytes. cDP give rise to cDC precursors, which are induced by FLT3 and ultimately give rise to cDC or pDC (39, 40). Monocytes produce moDC from granulocyte-macrophage colony-stimulating factor (GM-CSF)- and interleukin-4 (IL-4)-stimulated myeloid stem cells (41, 42). Ly6C$^+$MDP produce pro-DC3s and eventually DC3s (23).

cDC2s primarily facilitate the differentiation of T helper type 2 and type 17 (Th2 and Th17) CD4$^+$ T cells and the secretion of interleukin-6 (IL-6) and interleukin-23 (IL-23) (45, 46). The development of cDC2s is largely dependent on Relb, Rbpj, Irf4 (19, 20). Murine cDC2s are typically characterized as CD26$^+$, CX3CR1$^+$, CD11b$^+$, F4/80$^-$, and in human as CD1c$^+$, CD5$^+$, CD14$^-$, CD163$^-$ (45). In addition, the expression of SiglecH and Ly6C distinguishes precursor cells that will become cDC1s (SiglecH$^-$; Ly6C$^-$), cDC2s (SiglecH$^-$; Ly6C$^+$) and pDCs (SiglecH$^+$; Ly6C$^-$) (47). Notably, Irf8 deficiency induces the transcriptional, functional, and epigenetic reprogramming of cDC1s to cDC2s (48).

2.2 pDCs

pDCs are a unique sentinel cell type with a plasma cell-like capacity for rapid and high production of interferon type I (IFN-I) in response to viruses, as well as the ability to differentiate into cDCs

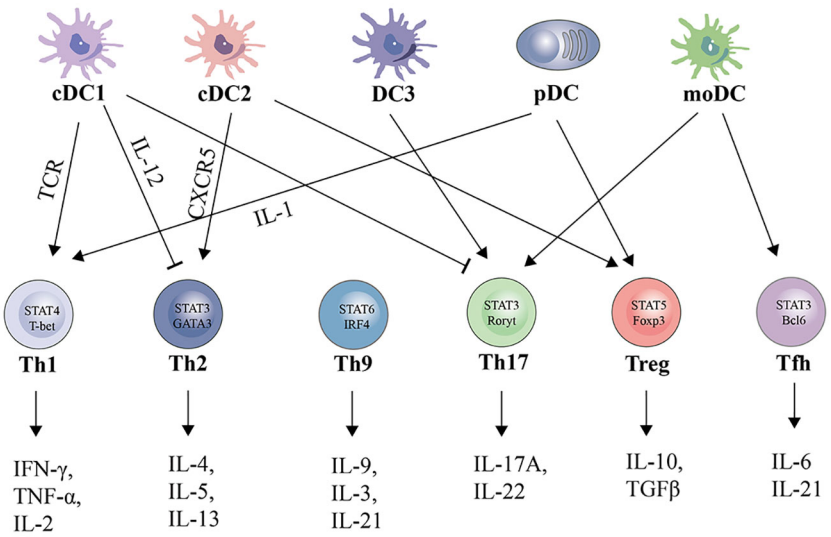

FIGURE 2
Subsets, polarizing cytokines, and effector cytokines of DCs-regulated CD4$^+$ cell polarization.

(49). Upon activation of human plasma cell-like predendritic cells (pDCs) by a single microbial or cytokine stimulus, the cells differentiated into three stable subpopulations (P1-P3), and notably the pDCs differentiated into subpopulations after SARS-CoV-2 infection and rapidly produced IFN-I and IFN-III upon viral exposure (50, 51). Murine cDC1s are typically characterized as $CD11c^{-}$, MHC II^{-}, $CD11b^{-}$, $B220_{+}$, and $CD123^{+}$ (52). Human cDC1s are characterized as $BDCA2^{+}$, $BDCA4^{+}$, $CD11c^{-}$, $CD4^{+}$, and $CD123^{+}$ (53). pDCs develop primarily through an Flt3-driven pathway shared with cDCs, and the transcription factor PU.1 controls Flt3, while subsequent specialization of pDCs requires the helix-loop-helix transcription factor (E protein) E2-2/Tcf4 (25, 26). E2-2/Tcf2-deficient pDCs are converted to cDCs *in vitro*. E2-2 deficiency is associated with aberrant expression profiles and impaired IFN responses in pDCs, and E2-2 directly activates transcription factors (SpiB, Irf8) and functional factors (Irf7) involved in pDC development (54). Furthermore, Stat3 is required for DC progenitor cell expansion, whereas Stat5 inhibits the transcriptional network of pDCs in Irf8 and lineage-negative, Flt3+ progenitor cells to control pDC production (27).

2.3 moDCs

moDCs is a subset of DCs formed by monocytes during inflammation.Monocyte-derived cells exhibit high plasticity to the environment and show high susceptibility to inflammatory stimuli in an inflammatory microenvironment, including increased levels of CCL2 and IL-8, which promote monocyte recruitment (55). Monocytes are stimulated by GM-CSF and IL-4 to form immature moDCs, which differentiate into mature moDCs when stimulated by inflammatory cytokines or PAMPs (56). Fully differentiated moDCs acquire DC morphology and localize to T-cell regions via L-selectin and CCR7 (57). Increased production of inflammatory factors and chemokines, such as TNF-α, IL-1, IL-12, IL-23 and CXCL10, was observed in LPS-stimulated GM-CSF-induced bone marrow-derived moDCs (28, 29). In contrast to the increased antigen-presentation and migratory capacity of cDCs, moDCs mainly coordinate the secretion of inflammatory factors and chemokines for local immune responses. The transcriptional factors PU.1, IRF4, NR4A3, NCOR2, Etv3 and Etv6 control the differentiation of human monocytes into moDCs, and the production of moDCs can be inhibited by targeted modulation of these transcription factors, which provides a new perspective on inflammatory diseases (30–33).

2.4 DC3s

DC3s are becoming better known as a new subset of DCs, and a developmental atlas of DC3s has been established (21). Human DC3s were identified as $CD5^{-}CD163^{+}CD14^{+}$ cells (22). Murine DC3s were identified as $CD172a^{+}Lyz2^{+}CD16/32^{+}$ cells derived from $Ly6C^{+}$ monocyte-dendritic cell precursors (23). Irf8 is a key transcription factor that regulates the development and maintenance of DC3s, and patients with low Irf8 expression show reduced cDC and pDC, while DC3 is maintained or amplified (24). In addition, the transcription factor Klf4 is also involved in regulating DC3s development, and Klf4 deficiency affects the transition of Ly6C+ MDPs to pro-DC3s (23). Functionally, DC3s have the ability to induce the transformation of T cells into IL-17A-producing T helper-17 (Th17) cells, which makes DC3s important players in inflammatory diseases and immune regulation (22).

3 Kidney DCs (kDCs) in homeostasis

In a state of renal health, kDCs act as sentinels, using their dendrites to continuously monitor the kidney milieu (58–60). kDCs sample autoantigens from the tubules and glomeruli and subsequently migrate to the renal lymph nodes (61, 62). Within these lymph nodes, kDCs maintain immune self-tolerance, immune system functionality, and tissue equilibrium by inducing the activation of Treg cells, restraining T-cell activation, proliferation, and effector capacities, and accommodating autoreactive T cells in the presence of T helper cells (13, 63). Furthermore, kDCs play a crucial role in fostering immune tolerance toward harmless antigens present in the circulation. Specifically, low molecular weight antigens are concentrated and sieved within the kidney, subsequently reaching the kidney lymph nodes through lymphatic drainage. Within these lymph nodes, kDCs can capture these antigens and induce apoptosis in cytotoxic T cells by means of PD-L1 expression (62, 64). In a state of homeostasis, the movement of DCs into lymph nodes to execute these functions is regulated by the expression of CCR7 (65). The passage of low molecular weight antigens through this tolerance mechanism plays a significant role in the prevention of undesired immune responses, and kDCs play a role in maintaining peripheral immune tolerance to these harmless antigens. Notably, this tolerance mechanism is disrupted in diseases characterized by proteinuria. In these diseases, the glomerular filters become permeable, leading to increased recognition and acceptance of filtered proteins by kDCs, including high molecular weight proteins. Consequently, this stimulates potentially harmful T cells, providing an additional mechanism through which proteinuria can cause damage (60). The characteristics and functions of monocyte-derived tolerant DCs and mature DCs are shown in Table 2.

4 kDC maturation and migration in AKI

As specialized APCs, DCs migrate to the kidney, which is critical for initiating protective proinflammatory and tolerogenic immune responses in AKI. The transport of different DC subpopulations in the kidney and renal lymph nodes is essential for DC-dependent activation and modulation of inflammation and immunity. DC chemotaxis and migration are triggered by interactions between chemokines and their receptors (68). After the onset of AKI, renal DCs are activated, increase in number and activity and have an enhanced ability to present antigens to T cells in renal draining lymph nodes (69). Previous studies have shown that CCR and CC chemokine expression is closely associated with FLT3 ligand-induced migration of renal DCs, including CCR1,

TABLE 2 The induction factors, secretion factors, phenotypes and functions of tolerogenic DCs and mature DCs.

	Induction factors	Phenotypes	Cytokines	Functions	Refs
Tolerogenic DCs	IL-10, TGFβ, VIP, IFN-γ, Galectin-1, Vitamine D3, Ra	$CD40^-$, $CD80^-$, $CD86^-$, MHC-II^-, $PD\text{-}L1^+$	IL-10, TGFβ	Treg cell activation	(66)
Mature DCs	LPS, TNF, IL-1β, PGE2, IL-6	CD80+, CD83+, CD86+, CD40+, MHC-II+	TGF- α, IL-1β, IL-6, IL-12	Induction of effector/ cytotoxic T cell respons	(67)

CCR2, CCR5, CX3CR1, CCR7, CCL19, and CCL21 (59, 61). cDCs, which are the major DC type, mature in response to stimulation with DAMPs or inflammatory signals and express high levels of CCR7, which interacts with its ligands CCL19 and CCL21 to direct mature cDCs transport to the lymph nodes via afferent lymphatic vessels to regulate T-cell immunity (70–72). After ischaemic kidney injury, dilated renal lymphatic vessels express high levels of CCL21, which stimulates the recruitment of more $CCR7^+$ DCs to renal draining lymph nodes, worsening renal inflammation and fibrosis, and inhibiting CCR7 expression (blocking the binding of VEGF-C/D to VEGFR3) or renal lymphangiogenesis reduces the migration of $CCR7^+$ DCs (73). Furthermore, CCR7 and its ligand SLC/CCL21 are constitutively expressed in glomeruli in adjacent cell types in the human kidney and play a role in glomerular homeostasis and regenerative processes (74, 75).

Under normal physiological conditions, pDCs are mainly located in the peripheral blood and T-cell-rich lymphoid tissues. Under pathological conditions, pDCs migrate from the peripheral blood into inflamed tissues and lymph nodes to initiate an immune response (76). Multiple chemokine receptors are highly expressed on the surface of pDCs, and the chemotaxis of pDCs is promoted by the binding of corresponding ligands; for example, when CCR2, CCR9, and CXCR3 receptors are expressed on the surface of pDCs, the transfer of pDCs from the peripheral blood to inflammatory tissues is promoted, and when CCR2, CCR7, and CXCR3 receptors are expressed on the surface of pDCs, the direct transfer of pDCs from the peripheral blood to the lymph nodes is promoted (68). While the chemokines responsible for regulating the recruitment and migration of pDCs in various tissues, such as the small intestine (77), have been confirmed, the precise factors governing pDC recruitment in AKI remain unclear. The regulatory mechanisms by which DCs are activated and mature and their migration to the site of renal injury and renal lymphatics are shown in Figure 3.

5 Mechanisms of the kDC-mediated immune response in AKI

5.1 Renal ischaemia–reperfusion injury (RIRI)

RIRI is defined as a pathophysiological phenomenon in which there is a temporary loss of renal blood flow and tissue perfusion, followed by regaining of blood supply and increased tissue damage. RIRI is the leading cause of acute renal failure and transplant renal insufficiency. Early after ischemic injury, inflammatory mediators, including tumor necrosis factor-α (TNF-α), are produced, and previous studies have shown that TNF secretion is usually attributed to infiltrating monocytes, resident or infiltrating macrophages, and DCs (78). Subsequent studies have revealed that renal resident F4/80+ CD11c+ DCs have been shown to be the primary producers of TNF-α, and despite significant phenotypic overlap with resident macrophages, these cells migrate from the injured kidney to the draining lymph nodes within 24 to 48 hours of acute injury-a typical feature of DC function (79). After RIRI, DCs are activated and recruited to the kidneys, which mediates efficient induction and activation of adaptive immunity, antigen presentation to T cells and activation of T cells (mainly naïve antigen-specific $CD8^+$ cells) (69). Hypoxia is an important marker of RIRI and regulates the innate immune response during this process (6). Previous studies have shown that DC activation in RIRI is accompanied by an increase in HIF-1α protein levels, and knockdown of HIF-1α significantly inhibits DC maturation and impairs the stimulation of allogeneic T cells (80, 81). In contrast, a recent study showed that HIF-2α deficiency in DCs upregulated CD36 expression in DCs, leading to cellular lipid accumulation, causing the overactivation of natural killer T (NKT) cells the production of IFN-γ and IL4, and ultimately exacerbating RIRI in mice (82). This finding suggests that hypoxia plays a crucial role in DC activation, and targeting and regulating HIF-1α or HIF-2α expression could be a potential therapeutic strategy for RIRI. The expression of miR-21 in hypoxia/reoxygenation-treated BMDCs significantly increased the proportion of mature DCs ($CD11c^+$/MHC-II^+/$CD80^+$), and miR-21 overexpression could reduce the expression of HIF1α in RIRI and inhibit the maturation of DCs to protect epithelial cells from ischaemia reperfusion injury (83). Another study showed that miR-21 could target and regulate the CCR7 receptor on the surface of mature BMDCs and reduce the maturation of DCs and that RIRI-induced proinflammatory cytokine production could be attenuated by transferring miR-21-overexpressing BMDCs (84). During the transition from normal renal repair to maladaptive fibrosis in RIRI, persistent GM-CSF expression in renal tubular cells significantly increases monocyte chemoattractant protein-1 (MCP-1) expression in macrophages, which activates DCs and induces the secretion of the proinflammatory factors TNF-α and IL-1β by T cells. By inhibiting the expression of CCR2, which is a receptor for CCL2, the accumulation and persistence of macrophages, DCs, and T cells in the kidneys can be

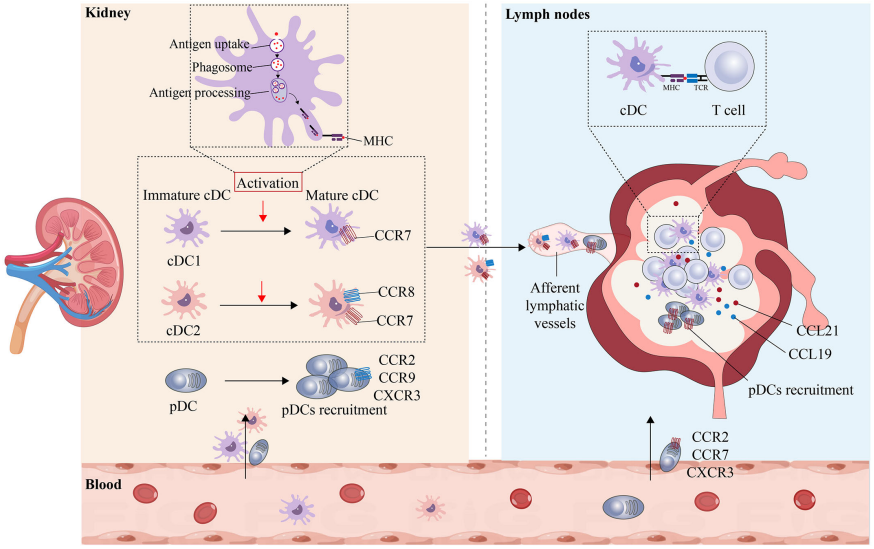

FIGURE 3
Maturation and migration of kDCs in AKI. The ability of DCs in the peripheral blood to migrate to the kidneys plays an important role in maintaining health and mediating disease. In the healthy state, DCs that enter the kidney are in an immature state and maintain renal immune tolerance to innocuous antigens. In AKI, immature cDCs are activated and undergo maturation, resulting in the upregulation of MHC and costimulatory molecules, the uptake and processing of antigens, and an increase in CCR7 expression. Mature cDCs can then migrate toward the lumen of lymphatic vessels containing CCL19 and CCL21, where they bind to T cells and present antigens to T cells. In the inflammatory state, pDCs express CCR2, CCR9, and CXCR3, are recruited from the peripheral blood to the site of injury and can directly enter the lymphatic lumen by expressing CCR2, CCR7, and CXCR3.

reduced, and therapeutic inhibition of CCL2/CCR2 signaling attenuates fibrosis and inflammation after RIRI (85). The regulatory mechanism by which kDCs affects RIRI is shown in Figure 4A.

5.2 Cis-platinum induced tubular injury

Renal tubular epithelial cells are particularly susceptible to pharmacotoxic injury and undergo necrotic apoptosis. In a prior investigation, it was demonstrated that in a cisplatin-induced acute tubular injury model, mice with DC depletion through the use of diphtheria toxin experienced increased renal dysfunction, tubular injury, neutrophil infiltration, and mortality compared to mice without DC depletion. Additionally, the authors provided evidence that the increase in renal injury could be attributed to the depletion of haematopoietic cells expressing CD11c (86). These studies show that renal DCs play a role in reducing cisplatin-induced kidney damage and the resulting inflammation. This protective mechanism is believed to be linked to the secretion of IL-10 by renal DCs immediately following cisplatin treatment (87, 88). However, it remains unknown whether activated DCs stimulate IL-10 secretion by Treg cells to protect against cisplatin-induced kidney injury. In

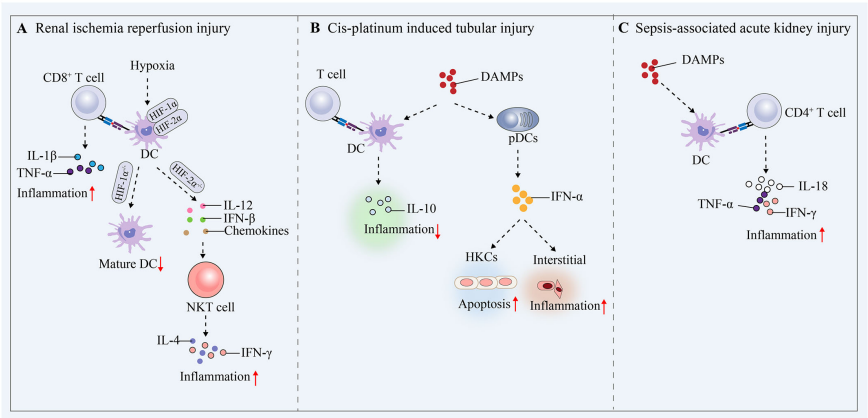

FIGURE 4
Mechanisms by which DCs mediate protective proinflammatory and tolerogenic immune responses in AKI. **(A)** Renal ischaemia–reperfusion injury. **(B)** Cis-platinum induced tubular injury. **(C)** Sepsis-induced AKI.

contrast, pDCs express low levels of CD11c and are not targeted in these mouse models (89). Another study showed that renal tubular epithelial cells produce chemokines in response to IFN-α stimulation, and these chemokines initiate the recruitment and activation of pDCs, increasing the local production of IFN-α and leading to the development of renal interstitial inflammation and apoptosis in renal tubular epithelial cells (90). The regulatory mechanism by which kDCs affect cis-platinum-induced tubular injury is shown in Figure 4B.

5.3 Sepsis-associated AKI (SA-AKI)

AKI is a common form of tissue damage and organ dysfunction that occurs during sepsis (91). SA-AKI occurs mainly due to the release of PAMPs (e.g., LPS) and DAMPs from damaged cells and tissues, which dysregulate the immune system and lead to systemic and renal inflammation, complement activation, mitochondrial dysfunction, and metabolic reprogramming (92). In the presence of systemic inflammation or renal inflammation, kDCs receive inflammatory stimuli and increase their transfer and antigen-presenting capacity in the renal lymph nodes. In LPS-induced AKI, DCs in the renal interstitium were shown to migrate into the renal lymph nodes and stimulate local activation of $CD4^+$ T cells and the production of IL-18, IFN-γ and TNF-α (93, 94). These studies confirm that under septic conditions, kDCs are subjected to inflammatory stimuli, become activated and migrate, thereby mediating immune responses and exacerbating renal injury (Figure 4C). Deficiency of kDCs inhibits LPS-induced tubular and interstitial injury in the acute phase of AKI but delays tissue repair in the recovery phase, suggesting that kDCs influence SA-AKI progression and renal repair (94). kDCs are involved in the development of SA-AKI, and it is crucial to clarify the exact mechanisms of renal injury and repair mediated by kDCs, including the signaling pathways involved, the effects on T-cell activation, and the secretion of relevant cytokines.

Numerous molecules and signaling pathways play important roles in DCs and are involved in the development and progression of SA-AKI. The induction of proinflammatory factors in DCs requires the involvement of TLR2 and TLR4, and specific intercellular adhesion molecule-3-grabbing non-integrin (SIGN) on DCs captures nonintegrin 1, which interacts with TLR4 to regulate the inflammatory response of renal tubular epithelial cells and is involved in the pathogenesis of AKI (95, 96). The IL-18 receptor signaling pathway plays an important role in DC- and $CD4^+$ T-cell-mediated inflammatory responses, and inhibiting IL-18Rα in LPS-induced AKI reduces the mRNA expression of IL-18, IFN-γ, TNF, and IL-6 in the kidney (97). The spleen tyrosine kinase (Syk) signaling pathway has an important role in DCs and neutrophils in SA-AKI, and the inflammatory cascade during SA-AKI can be limited by inhibiting the Syk signaling pathway (98). Furthermore, Bruton's tyrosine kinase (BTK) was activated in DCs, neutrophils, and B cells during the onset of SA-AKI, and renal function after AKI could be ameliorated by inhibiting the BTK signaling pathway (99).

5.4 COVID-19-associated AKI

AKI is a common complication of COVID-19, reported in more than a quarter of COVID-19 patients, and the mortality rate of COVID-19-associated AKI is higher in hospitalized patients than in those without renal involvement (100). The lack of renal recovery in COVID-19-associated AKI survivors compared to patients with other forms of AKI is of particular concern (101, 102). Both innate and adaptive immune responses play critical roles in the recognition and elimination of foreign pathogens. However, an excessive immune response during SARS-CoV-2 infection can lead to disease severity and associated complications in COVID-19 (103). Patients with poor COVID-19 progression develop dysregulation of cytokines and chemokines such as IL-2, IL-6, GM-CSF, CXCL10, CCL2, CCL7, CCL3 and TNF (104, 105). Decreased absolute numbers, activation, and function of $CD4^+$ and $CD8^+$ T cells were observed in patients with severe COVID-19, as evidenced by significantly lower levels of TCR expression, T-cell migration stimulator (DDP4), TCR signaling kinase, and MHC II molecules (106). Notably, depletion of pDCs (the main source of IFN-α) was observed in patients with COVID-19, which may have led to the inability of a subset of patients to effectively clear the virus from renal cells (107). Despite the insights into immune infiltration and activation of the innate and adaptive immune system in COVID-19-associated AKI, further studies are needed on the exact molecular mechanisms mediated by DCs in which they are involved, which may represent promising future specific therapeutic approaches for COVID-19-associated AKI.

6 DCs–targeted therapies in AKI: a promising therapeutic strategy

6.1 Induction of tolerogenic DCs (tolDCs)

tolDCs are a class of DCs with immature phenotypes and tolerance-inducing properties that do not induce antigen-specific immune responses but rather mediate immune tolerance (34). tolDCs express low levels of MHC and costimulatory molecules and can disrupt effector T-cell responses and induce regulatory T-cell proliferation and the production of immunosuppressive factors (e.g., IL-10), thereby inducing immune tolerance (108, 109). The plasticity of DCs allows for phenotypic modulation through tolerogenic transcriptional program modulation or proinflammatory transcription factor inhibition, and these modified DCs can induce therapeutic immunosuppression *in vivo* through direct interactions with T cells (110). The induction of tolDCs for the treatment of AKI has become a promising therapeutic strategy and is being actively promoted.

In Table 3, we summarize the available strategies and mechanisms for treating AKI by inducing tolDCs. DCs and NKT cells play a key role in the initiation of the immune response to RIRI in mice, and blocking DC-mediated NKT cell activation could be a novel therapeutic strategy for the prevention of AKI. Li et al. protected the kidney from RIRI by using the A2AR activator

ATL313 to induce the production of tolDCs, which targeted and blocked DC-NKT interactions, inhibited NKT cell activation and reduced IFN-γ production (111). This study provides proof-of-principle for the use of pharmacologic approaches to induce the production of tolDCs to treat AKI. Sphingosine 1-phosphate (S1P), an important intracellular and extracellular signaling molecule, is a natural ligand of five G-protein-coupled receptors (S1P1, S1P2, S1P3, S1P4, and S1P5) that regulate cellular functions and modulate the immune system. S1P1 receptor agonist (FTY720) attenuated RIRI in mice, and *in vitro* studies showed that FTY720-treated DCs were rich in mitochondria, and further transplantation of FTY720-DCs observed that transfer of mitochondria-rich DCs protected the kidneys from RIRI because the transferred DCs donated their mitochondria to recipient splenocytes (i.e., macrophages), increased the activation of $CD4FoxP3^+$ Tregs, and inhibited TNF-α production (112). In addition, in S1P3-deficient RIRI DCs exhibited reduced expression of costimulatory molecules, MHC II, and proinflammatory cytokines and chemokines and promoted Th2/IL-4 responses (113). This finding suggests that antagonizing S1P3 expression may result in the formation of tolDCs and could be used as a treatment for RIRI, but there are currently no studies of the use of S1P3 inhibitors to induce tolDCs. An mTOR inhibitor (rapamycin) reduced the immunogenicity and immunostimulatory phenotype of DCs after LPS stimulation, induced resistance to phenotypic maturation induced by proinflammatory stimuli, and modulated mitochondrial dynamics in DCs by increasing mitochondrial numbers, decreasing TNF-α and IL-6 secretion, and increasing IL-10 secretion, synergistically protecting the kidney from ischaemic injury (114, 115). Notably, in a recent study of vitamin D3/IL-10-conditioned tolDCs, treated cells exhibited high PD-L1 and CD86 expression, elevated IL-10 levels, decreased IL-12 p70 secretion, and suppressed transcriptome inflammatory profiles, which successfully abrogated renal injury without altering the infiltrating inflammatory cell population during systemic infusion (116). Current evidence from transplant-tolerant phase I/II clinical trials suggests that tolDCs are safe, and multiple regimens have been used to induce tolDC production, providing the basis for the clinical use of tolDC therapy in AKI. Further exploration of the role of tolDCs in AKI and postinjury repair is necessary in the future.

6.2 Targeting cytokine production and co–stimulation

After maturation, DCs secrete cytokines to stimulate and activate T cells or act directly on damaged tissues, including pro-inflammatory factors such as IL-1, IL-6, IL-12, TNF, and IFN-α. miR-21 is a key inhibitory factor in the maturation of DCs, which can inhibit the maturation of DCs and decrease the secretion of IL-12, IL-6, and TNF-α, and attenuate the local inflammation (83). At the onset of AKI, pDCs rapidly infiltrated the kidneys and promoted renal injury through the production of IFN-α, whereas pDCs knockdown reduced the release of IFN-α, decreasing further renal injury (90). Upon binding of DCs surface antigenic peptide MHC complexes to T-cell surface TCRs, co-stimulatory substance molecules can provide positive signals that increase T-cell stimulation. DCs surface co-stimulatory molecules include CD80 (B7-1), CD86(B7-2) and CD40 (117). The deletion of Rictor in DCs was observed in the AKI model to cause an increase in CD80 and CD86 on the surface of DCs, causing enhanced migration to the damaged kidney and greater tissue damage (118). Targeted modulation of Rictor expression in DCs in can attenuate further damage in AKI, but there are no studies of Rictor agonists in AKI. By targeting and regulating DCs maturation, secretory factor release and co-stimulatory molecules provides a new direction for the treatment of AKI.

7 Conclusions and perspectives

Immunoinflammatory mechanisms mediate the development of AKI, and the protective and injurious effects of DCs and their regulatory factors on AKI are receiving increasing attention. This paper provides a comprehensive review of the various subpopulations of DCs and their respective functions, as well as the molecular mechanisms involved in maintaining homeostasis and facilitating injury and repair in AKI. Additionally, the research progress on the use of tolDCs as a potential therapeutic strategy for AKI was discussed. The migration of immature DCs plays a crucial role in maintaining homeostasis and inducing peripheral tolerance. Conversely, the migration of activated and mature DCs to renal

TABLE 3 Induction strategy and characterization of tolDCs for the treatment of AKI.

Induction strategy	Phenotype	Intervention	Model	Mechanism	Refs
Adenosine-2A receptor agonist (ATL313)	$CD40^{low}$; $OX40L^{low}$; $B7\text{-}DC^{high}$	ATL313 (1 ng/kg, i.v.)	RIRI mouse	$IFN\text{-}\gamma^+$ NKT cell↓	(111)
Sphingosine-1-phosphate agonist (FTY720)	$CD80^{low}$; $CD86^{low}$; $MHCII^{low}$; $IL\text{-}10^{high}$	1 μM FTY720 processing BMDC (0.5×10^6, i.v.)	RIRI mouse	CD4FoxP3 Tregs↑, mitochondria↑, TNF-α↓	(112, 113)
mTOR inhibitor (Rapamycin)	$CD80^{low}$; $CD86^{low}$; $CD40^{low}$; $MHCII^{low}$; $IL10^{low}$	10 ng/mL rapamycin processing BMDC (0.5×10^6, i.v.)	RIRI mouse	TNF-α↓; IL-6↓, IL-10↑, mitochondria↑	(114, 115)
Vitamin-D3 and IL-10	$CD86^{low}$; $CD40^{low}$; $MHCII^{low}$; $PDL1^{high}$	20 nM VitD3 and 10 ng/ml IL-10 processing DC (1×10^6, i.p.)	RIRI mouse	PDLl: CD 86↑, lymphocyte↓, IL-10↑ , IL-12 p70↓	(116)

"↑" indicates increased expression and "↓" indicates decreased expression.

lymphoid organs in AKI is a significant characteristic of DC-mediated immunity. Therefore, targeting DC chemokines to modulate their migratory capacity has the potential to treat AKI. Additionally, therapeutic strategies to induce tolDCs by inhibiting proinflammatory cytokine release and costimulatory molecules are currently being developed. Promisingly, findings derived from animal studies indicate the efficacy of tolDCs in the treatment of AKI, and evidence from phase I/II clinical trials suggests a positive safety profile for tolDCs (119). Consequently, it is imperative to pursue additional research elucidating the intricate molecular mechanisms involved in the interaction between DCs, tolDCs, and other renal cells. These investigations can enhance our understanding of the underlying mechanisms driving immune inflammation-induced AKI and pave the way for novel therapeutic interventions.

Author contributions

DL: Writing – original draft. HJ: Writing – review & editing. XY: Writing – review & editing. YL: Conceptualization, Writing – review & editing. WN: Conceptualization, Writing – review & editing. DZ: Conceptualization, Supervision, Writing – review & editing.

Funding

The author(s) declare financial support was received for the research, authorship, and/or publication of this article. This research was funded by the National Natural Science Foundation of China (grant numbers 82074171, 82003611 and 81700592).

Conflict of interest

The authors declare that the research was conducted in the absence of any commercial or financial relationships that could be construed as a potential conflict of interest.

Publisher's note

References

1. Levey AS, Levin A, Kellum JA. Definition and classification of kidney diseases. *Am J Kidney Dis*. (2013) 61:686–8. doi: 10.1053/j.ajkd.2013.03.003

2. Rewa O, Bagshaw SM. Acute kidney injury-epidemiology, outcomes and economics. *Nat Rev Nephrol*. (2014) 10:193–207. doi: 10.1038/nrneph.2013.282

3. Cox ZL, McCoy AB, Matheny ME, Bhave G, Peterson NB, Siew ED, et al. Adverse drug events during aki and its recovery. *Clin J Am Soc Nephrol*. (2013) 8:1070–8. doi: 10.2215/CJN.11921112

4. Susantitaphong P, Cruz DN, Cerda J, Abulfaraj M, Alqahtani F, Koulouridis I, et al. World incidence of aki: A meta-analysis. *Clin J Am Soc Nephrol*. (2013) 8:1482–93. doi: 10.2215/CJN.00710113

5. Scholz H, Boivin FJ, Schmidt-Ott KM, Bachmann S, Eckardt KU, Scholl UI, et al. Kidney physiology and susceptibility to acute kidney injury: implications for renoprotection. *Nat Rev Nephrol*. (2021) 17:335–49. doi: 10.1038/s41581-021-00394-7

6. Jang HR, Rabb H. Immune cells in experimental acute kidney injury. *Nat Rev Nephrol*. (2015) 11:88–101. doi: 10.1038/nrneph.2014.180

7. Zheng L, Gao W, Hu C, Yang C, Rong R. Immune cells in ischemic acute kidney injury. *Curr Protein Pept Sci*. (2019) 20:770–6. doi: 10.2174/1389203720666190507102529

8. Rogers NM, Matthews TJ, Kausman JY, Kitching AR, Coates PT. Review article: kidney dendritic cells: their role in homeostasis, inflammation and transplantation. *Nephrol (Carlton)*. (2009) 14:625–35. doi: 10.1111/j.1440-1797.2009.01200.x

9. Nutt SL, Chopin M. Transcriptional networks driving dendritic cell differentiation and function. *Immunity*. (2020) 52:942–56. doi: 10.1016/j.immuni.2020.05.005

10. Guermonprez P, Valladeau J, Zitvogel L, Thery C, Amigorena S. Antigen presentation and T cell stimulation by dendritic cells. *Annu Rev Immunol*. (2002) 20:621–67. doi: 10.1146/annurev.immunol.20.100301.064828

11. Tiberio L, Del Prete A, Schioppa T, Sozio F, Bosisio D, Sozzani S. Chemokine and chemotactic signals in dendritic cell migration. *Cell Mol Immunol*. (2018) 15:346–52. doi: 10.1038/s41423-018-0005-3

12. Yin X, Chen S, Eisenbarth SC. Dendritic cell regulation of T helper cells. *Annu Rev Immunol*. (2021) 39:759–90. doi: 10.1146/annurev-immunol-101819-025146

13. Kurts C, Ginhoux F, Panzer U. Kidney dendritic cells: fundamental biology and functional roles in health and disease. *Nat Rev Nephrol*. (2020) 16:391–407. doi: 10.1038/s41581-020-0272-y

14. Murphy TL, Grajales-Reyes GE, Wu X, Tussiwand R, Briseno CG, Iwata A, et al. Transcriptional control of dendritic cell development. *Annu Rev Immunol*. (2016) 34:93–119. doi: 10.1146/annurev-immunol-032713-120204

15. Brahler S, Zinselmeyer BH, Raju S, Nitschke M, Suleiman H, Saunders BT, et al. Opposing roles of dendritic cell subsets in experimental gn. *J Am Soc Nephrol*. (2018) 29:138–54. doi: 10.1681/ASN.2017030270

16. Hildner K, Edelson BT, Purtha WE, Diamond M, Matsushita H, Kohyama M, et al. Batf3 deficiency reveals a critical role for cd8alpha+ Dendritic cells in cytotoxic T cell immunity. *Science*. (2008) 322:1097–100. doi: 10.1126/science.1164206

17. Li N, Steiger S, Fei L, Li C, Shi C, Salei N, et al. Irf8-dependent type I conventional dendritic cells (Cdc1s) control post-ischemic inflammation and mildly protect against post-ischemic acute kidney injury and disease. *Front Immunol*. (2021) 12:685559. doi: 10.3389/fimmu.2021.685559

18. Bagadia P, Huang X, Liu TT, Durai V, Grajales-Reyes GE, Nitschke M, et al. An nfil3-zeb2-id2 pathway imposes irf8 enhancer switching during cdc1 development. *Nat Immunol*. (2019) 20:1174–85. doi: 10.1038/s41590-019-0449-3

19. Collin M, Bigley V. Human dendritic cell subsets: an update. *Immunology*. (2018) 154:3–20. doi: 10.1111/imm.12888

20. Guilliams M, Ginhoux F, Jakubzick C, Naik SH, Onai N, Schraml BU, et al. Dendritic cells, monocytes and macrophages: A unified nomenclature based on ontogeny. *Nat Rev Immunol*. (2014) 14:571–8. doi: 10.1038/nri3712

21. Villar J, Segura E. The more, the merrier: dc3s join the human dendritic cell family. *Immunity*. (2020) 53:233–5. doi: 10.1016/j.immuni.2020.07.014

22. Dutertre CA, Becht E, Irac SE, Khalilnezhad A, Narang V, Khalilnezhad S, et al. Single-cell analysis of human mononuclear phagocytes reveals subset-defining markers and identifies circulating inflammatory dendritic cells. *Immunity*. (2019) 51:573–89 e8. doi: 10.1016/j.immuni.2019.08.008

23. Liu Z, Wang H, Li Z, Dress RJ, Zhu Y, Zhang S, et al. Dendritic cell type 3 arises from ly6c(+) monocyte-dendritic cell progenitors. *Immunity*. (2023) 56:1761–77 e6. doi: 10.1016/j.immuni.2023.07.001

24. Cytlak U, Resteu A, Pagan S, Green K, Milne P, Maisuria S, et al. Differential irf8 transcription factor requirement defines two pathways of dendritic cell development in humans. *Immunity*. (2020) 53:353–70 e8. doi: 10.1016/j.immuni.2020.07.003

25. Carotta S, Dakic A, D'Amico A, Pang SH, Greig KT, Nutt SL, et al. The transcription factor pu.1 controls dendritic cell development and flt3 cytokine receptor expression in a dose-dependent manner. *Immunity*. (2010) 32:628–41. doi: 10.1016/j.immuni.2010.05.005

26. Cisse B, Caton ML, Lehner M, Maeda T, Scheu S, Locksley R, et al. Transcription factor E2-2 is an essential and specific regulator of plasmacytoid dendritic cell development. *Cell*. (2008) 135:37–48. doi: 10.1016/j.cell.2008.09.016

27. Esashi E, Wang YH, Perng O, Qin XF, Liu YJ, Watowich SS. The signal transducer stat5 inhibits plasmacytoid dendritic cell development by suppressing transcription factor irf8. *Immunity*. (2008) 28:509–20. doi: 10.1016/j.immuni.2008.02.013

28. Guilliams M, van de Laar L. A hitchhiker's guide to myeloid cell subsets: practical implementation of a novel mononuclear phagocyte classification system. *Front Immunol*. (2015) 6:406. doi: 10.3389/fimmu.2015.00406

29. Wu CJ, Sheu JR, Chen HH, Liao HF, Yang YC, Yang S, et al. Renal ischemia/reperfusion injury inhibits differentiation of dendritic cells derived from bone marrow monocytes in rats. *Life Sci*. (2006) 78:1121–8. doi: 10.1016/j.lfs.2005.06.043

30. Villar J, Cros A, De Juan A, Alaoui L, Bonte PE, Lau CM, et al. Etv3 and etv6 enable monocyte differentiation into dendritic cells by repressing macrophage fate commitment. *Nat Immunol*. (2023) 24:84–95. doi: 10.1038/s41590-022-01374-0

31. Boulet S, Daudelin JF, Odagiu L, Pelletier AN, Yun TJ, Lesage S, et al. The orphan nuclear receptor nr4a3 controls the differentiation of monocyte-derived dendritic cells following microbial stimulation. *Proc Natl Acad Sci U.S.A*. (2019) 116:15150–9. doi: 10.1073/pnas.1821296116

32. Lehtonen A, Veckman V, Nikula T, Lahesmaa R, Kinnunen L, Matikainen S, et al. Differential expression of ifn regulatory factor 4 gene in human monocyte-derived dendritic cells and macrophages. *J Immunol*. (2005) 175:6570–9. doi: 10.4049/jimmunol.175.10.6570

33. Briseno CG, Haldar M, Kretzer NM, Wu X, Theisen DJ, Kc W, et al. Distinct transcriptional programs control cross-priming in classical and monocyte-derived dendritic cells. *Cell Rep*. (2016) 15:2462–74. doi: 10.1016/j.celrep.2016.05.025

34. Morante-Palacios O, Fondelli F, Ballestar E, Martinez-Caceres EM. Tolerogenic dendritic cells in autoimmunity and inflammatory diseases. *Trends Immunol*. (2021) 42:59–75. doi: 10.1016/j.it.2020.11.001

35. Comi M, Avancini D, Santoni de Sio F, Villa M, Uyeda MJ, Floris M, et al. Coexpression of cd163 and cd141 identifies human circulating il-10-producing dendritic cells (Dc-10). *Cell Mol Immunol*. (2020) 17:95–107. doi: 10.1038/s41423-019-0218-0

36. Nikolic T, Roep BO. Regulatory multitasking of tolerogenic dendritic cells - lessons taken from vitamin D3-treated tolerogenic dendritic cells. *Front Immunol*. (2013) 4:113. doi: 10.3389/fimmu.2013.00113

37. Wei HJ, Gupta A, Kao WM, Almudallal O, Letterio JJ, Pareek TK. Nrf2-mediated metabolic reprogramming of tolerogenic dendritic cells is protective against aplastic anemia. *J Autoimmun*. (2018) 94:33–44. doi: 10.1016/j.jaut.2018.07.005

38. Zhao Y, Sun X, Yang X, Zhang B, Li S, Han P, et al. Tolerogenic dendritic cells generated by baff silencing ameliorate collagen-induced arthritis by modulating the th17/regulatory T cell balance. *J Immunol*. (2020) 204:518–30. doi: 10.4049/jimmunol.1900552

39. Naik SH, Proietto AI, Wilson NS, Dakic A, Schnorrer P, Fuchsberger M, et al. Cutting edge: generation of splenic cd8+ and cd8- dendritic cell equivalents in fms-like tyrosine kinase 3 ligand bone marrow cultures. *J Immunol*. (2005) 174:6592–7. doi: 10.4049/jimmunol.174.11.6592

40. Naik SH, Sathe P, Park HY, Metcalf D, Proietto AI, Dakic A, et al. Development of plasmacytoid and conventional dendritic cell subtypes from single precursor cells derived *in vitro* and *in vivo*. *Nat Immunol*. (2007) 8:1217–26. doi: 10.1038/ni1522

41. Helft J, Bottcher J, Chakravarty P, Zelenay S, Huotari J, Schraml BU, et al. Gm-csf mouse bone marrow cultures comprise a heterogeneous population of cd11c(+) Mhcii(+) macrophages and dendritic cells. *Immunity*. (2015) 42:1197–211. doi: 10.1016/j.immuni.2015.05.018

42. Boyette LB, Macedo C, Hadi K, Elinoff BD, Walters JT, Ramaswami B, et al. Phenotype, function, and differentiation potential of human monocyte subsets. *PloS One*. (2017) 12:e0176460. doi: 10.1371/journal.pone.0176460

43. Chrisikos TT, Zhou Y, Slone N, Babcock R, Watowich SS, Li HS. Molecular regulation of dendritic cell development and function in homeostasis, inflammation, and cancer. *Mol Immunol*. (2019) 110:24–39. doi: 10.1016/j.molimm.2018.01.014

44. Cytlak U, Resteu A, Bogaert D, Kuehn HS, Altmann T, Gennery A, et al. Ikaros family zinc finger 1 regulates dendritic cell development and function in humans. *Nat Commun*. (2018) 9:1239. doi: 10.1038/s41467-018-02977-8

45. Brown CC, Gudjonson H, Pritykin Y, Deep D, Lavallee VP, Mendoza A, et al. Transcriptional basis of mouse and human dendritic cell heterogeneity. *Cell*. (2019) 179:846–63 e24. doi: 10.1016/j.cell.2019.09.035

46. Chrun T, Lacote S, Urien C, Jouneau L, Barc C, Bouguyon E, et al. A rift valley fever virus gn ectodomain-based DNA vaccine induces a partial protection not improved by apc targeting. *NPJ Vaccines*. (2018) 3:14. doi: 10.1038/s41541-018-0052-x

47. Schlitzer A, Sivakamasundari V, Chen J, Sumatoh HR, Schreuder J, Lum J, et al. Identification of cdc1- and cdc2-committed dc progenitors reveals early lineage priming at the common dc progenitor stage in the bone marrow. *Nat Immunol*. (2015) 16:718–28. doi: 10.1038/ni.3200

48. Lanca T, Ungerback J, Da Silva C, Joeris T, Ahmadi F, Vandamme J, et al. Irf8 deficiency induces the transcriptional, functional, and epigenetic reprogramming of cdc1 into the cdc2 lineage. *Immunity*. (2022) 55:1431–47 e11. doi: 10.1016/j.immuni.2022.06.006

49. Leylek R, Idoyaga J. The versatile plasmacytoid dendritic cell: function, heterogeneity, and plasticity. *Int Rev Cell Mol Biol*. (2019) 349:177–211. doi: 10.1016/bs.ircmb.2019.10.002

50. Onodi F, Bonnet-Madin L, Meertens L, Karpf L, Poirot J, Zhang SY, et al. Sars-cov-2 induces human plasmacytoid predendritic cell diversification via unc93b and irak4. *J Exp Med*. (2021) 218(4):e20201387. doi: 10.1084/jem.20201387

51. Alculumbre SG, Saint-Andre V, Di Domizio J, Vargas P, Sirven P, Bost P, et al. Diversification of human plasmacytoid predendritic cells in response to a single stimulus. *Nat Immunol*. (2018) 19:63–75. doi: 10.1038/s41590-017-0012-z

52. Anderson DA 3rd, Dutertre CA, Ginhoux F, Murphy KM. Genetic models of human and mouse dendritic cell development and function. *Nat Rev Immunol*. (2021) 21:101–15. doi: 10.1038/s41577-020-00413-x

53. Liu YJ. Ipc: professional type 1 interferon-producing cells and plasmacytoid dendritic cell precursors. *Annu Rev Immunol*. (2005) 23:275–306. doi: 10.1146/annurev.immunol.23.021704.115633

54. Barchet W, Cella M, Colonna M. Plasmacytoid dendritic cells–virus experts of innate immunity. *Semin Immunol*. (2005) 17:253–61. doi: 10.1016/j.smim.2005.05.008

55. Chauvin C, Alvarez-Simon D, Radulovic K, Boulard O, Laine W, Delacre M, et al. Nod2 in monocytes negatively regulates macrophage development through tnfalpha. *Front Immunol*. (2023) 14:1181823. doi: 10.3389/fimmu.2023.1181823

56. Luhr JJ, Alex N, Amon L, Krater M, Kubankova M, Sezgin E, et al. Maturation of monocyte-derived dcs leads to increased cellular stiffness, higher membrane fluidity, and changed lipid composition. *Front Immunol*. (2020) 11:590121. doi: 10.3389/fimmu.2020.590121

57. Cheong C, Matos I, Choi JH, Dandamudi DB, Shrestha E, Longhi MP, et al. Microbial stimulation fully differentiates monocytes to dc-sign/cd209(+) dendritic cells for immune T cell areas. *Cell*. (2010) 143:416–29. doi: 10.1016/j.cell.2010.09.039

58. Woltman AM, de Fijter JW, Zuidwijk K, Vlug AG, Bajema IM, van der Kooij SW, et al. Quantification of dendritic cell subsets in human renal tissue under normal and pathological conditions. *Kidney Int*. (2007) 71:1001–8. doi: 10.1038/sj.ki.5002187

59. Teteris SA, Engel DR, Kurts C. Homeostatic and pathogenic role of renal dendritic cells. *Kidney Int*. (2011) 80:139–45. doi: 10.1038/ki.2011.129

60. Weisheit CK, Engel DR, Kurts C. Dendritic cells and macrophages: sentinels in the kidney. *Clin J Am Soc Nephrol*. (2015) 10:1841–51. doi: 10.2215/CJN.07100714

61. Coates PT, Colvin BL, Ranganathan A, Duncan FJ, Lan YY, Shufesky WJ, et al. Ccr and cc chemokine expression in relation to flt3 ligand-induced renal dendritic cell mobilization. *Kidney Int*. (2004) 66:1907–17. doi: 10.1111/j.1523-1755.2004.00965.x

62. Lukacs-Kornek V, Burgdorf S, Diehl L, Specht S, Kornek M, Kurts C. The kidney-renal lymph node-system contributes to cross-tolerance against innocuous circulating antigen. *J Immunol*. (2008) 180:706–15. doi: 10.4049/jimmunol.180.2.706

63. Mikami N, Sakaguchi S. Regulatory T cells in autoimmune kidney diseases and transplantation. *Nat Rev Nephrol*. (2023) 19:544–57. doi: 10.1038/s41581-023-00733-w

64. Gottschalk C, Damuzzo V, Gotot J, Kroczek RA, Yagita H, Murphy KM, et al. Batf3-dependent dendritic cells in the renal lymph node induce tolerance against circulating antigens. *J Am Soc Nephrol*. (2013) 24:543–9. doi: 10.1681/ASN.2012101022

65. MartIn-Fontecha A, Sebastiani S, Hopken UE, Uguccioni M, Lipp M, Lanzavecchia A, et al. Regulation of dendritic cell migration to the draining lymph node: impact on T lymphocyte traffic and priming. *J Exp Med*. (2003) 198:615–21. doi: 10.1084/jem.20030448

66. Svajger U, Rozman P. Induction of tolerogenic dendritic cells by endogenous biomolecules: an update. *Front Immunol*. (2018) 9:2482. doi: 10.3389/fimmu.2018.02482

67. Sozzani S, Del Prete A, Bosisio D. Dendritic cell recruitment and activation in autoimmunity. *J Autoimmun*. (2017) 85:126–40. doi: 10.1016/j.jaut.2017.07.012

68. Liu J, Zhang X, Cheng Y, Cao X. Dendritic cell migration in inflammation and immunity. *Cell Mol Immunol*. (2021) 18:2461–71. doi: 10.1038/s41423-021-00726-4

69. Snelgrove SL, Lo C, Hall P, Lo CY, Alikhan MA, Coates PT, et al. Activated renal dendritic cells cross present intrarenal antigens after ischemia-reperfusion injury. *Transplantation*. (2017) 101:1013–24. doi: 10.1097/TP.0000000000001427

70. Forster R, Schubel A, Breitfeld D, Kremmer E, Renner-Muller I, Wolf E, et al. Ccr7 coordinates the primary immune response by establishing functional microenvironments in secondary lymphoid organs. *Cell*. (1999) 99:23–33. doi: 10.1016/s0092-8674(00)80059-8

71. Gunn MD, Kyuwa S, Tam C, Kakiuchi T, Matsuzawa A, Williams LT, et al. Mice lacking expression of secondary lymphoid organ chemokine have defects in lymphocyte homing and dendritic cell localization. *J Exp Med*. (1999) 189:451–60. doi: 10.1084/jem.189.3.451

72. Summers KM, Bush SJ, Hume DA. Network analysis of transcriptomic diversity amongst resident tissue macrophages and dendritic cells in the mouse mononuclear phagocyte system. *PloS Biol*. (2020) 18:e3000859. doi: 10.1371/journal.pbio.3000859

73. Pei G, Yao Y, Yang Q, Wang M, Wang Y, Wu J, et al. Lymphangiogenesis in kidney and lymph node mediates renal inflammation and fibrosis. *Sci Adv*. (2019) 5:eaaw5075. doi: 10.1126/sciadv.aaw5075

74. Banas B, Wornle M, Berger T, Nelson PJ, Cohen CD, Kretzler M, et al. Roles of slc/ccl21 and ccr7 in human kidney for mesangial proliferation, migration, apoptosis, and tissue homeostasis. *J Immunol*. (2002) 168:4301–7. doi: 10.4049/jimmunol.168.9.4301

75. Wurm S, Steege A, Rom-Jurek EM, van Roeyen CR, Kurtz A, Banas B, et al. Ccr7 is important for mesangial cell physiology and repair. *J Histochem Cytochem*. (2018) 66:7–22. doi: 10.1369/0022155417737975

76. Worbs T, Hammerschmidt SI, Forster R. Dendritic cell migration in health and disease. *Nat Rev Immunol*. (2017) 17:30–48. doi: 10.1038/nri.2016.116

77. Rivera CA, Randrian V, Richer W, Gerber-Ferder Y, Delgado MG, Chikina AS, et al. Epithelial colonization by gut dendritic cells promotes their functional diversification. *Immunity*. (2022) 55:129–44 e8. doi: 10.1016/j.immuni.2021.11.008

78. Friedewald JJ, Rabb H. Inflammatory cells in ischemic acute renal failure. *Kidney Int*. (2004) 66:486–91. doi: 10.1111/j.1523-1755.2004.761_3.x

79. Dong X, Swaminathan S, Bachman LA, Croatt AJ, Nath KA, Griffin MD. Resident dendritic cells are the predominant tnf-secreting cell in early renal ischemia-reperfusion injury. *Kidney Int*. (2007) 71:619–28. doi: 10.1038/sj.ki.5002132

80. Jantsch J, Chakravortty D, Turza N, Prechtel AT, Buchholz B, Gerlach RG, et al. Hypoxia and hypoxia-inducible factor-1 alpha modulate lipopolysaccharide-induced dendritic cell activation and function. *J Immunol*. (2008) 180:4697–705. doi: 10.4049/jimmunol.180.7.4697

81. Rama I, Bruene B, Torras J, Koehl R, Cruzado JM, Bestard O, et al. Hypoxia stimulus: an adaptive immune response during dendritic cell maturation. *Kidney Int*. (2008) 73:816–25. doi: 10.1038/sj.ki.5002792

82. Qu J, Li D, Jin J, Sun N, Wu J, Yang C, et al. Hypoxia-inducible factor 2alpha attenuates renal ischemia-reperfusion injury by suppressing cd36-mediated lipid accumulation in dendritic cells in a mouse model. *J Am Soc Nephrol*. (2023) 34:73–87. doi: 10.1681/ASN.0000000000000027

83. Song N, Zhang T, Xu X, Lu Z, Yu X, Fang Y, et al. Mir-21 protects against ischemia/reperfusion-induced acute kidney injury by preventing epithelial cell apoptosis and inhibiting dendritic cell maturation. *Front Physiol*. (2018) 9:790. doi: 10.3389/fphys.2018.00790

84. Jia P, Pan T, Xu S, Fang Y, Song N, Guo M, et al. Depletion of mir-21 in dendritic cells aggravates renal ischemia-reperfusion injury. *FASEB J*. (2020) 34:11729–40. doi: 10.1096/fj.201903222RR

85. Xu L, Sharkey D, Cantley LG. Tubular gm-csf promotes late mcp-1/ccr2-mediated fibrosis and inflammation after ischemia/reperfusion injury. *J Am Soc Nephrol*. (2019) 30:1825–40. doi: 10.1681/ASN.2019010068

86. Tadagavadi RK, Reeves WB. Renal dendritic cells ameliorate nephrotoxic acute kidney injury. *J Am Soc Nephrol*. (2010) 21:53–63. doi: 10.1681/ASN.2009040407

87. Tadagavadi RK, Reeves WB. Endogenous il-10 attenuates cisplatin nephrotoxicity: role of dendritic cells. *J Immunol*. (2010) 185:4904–11. doi: 10.4049/jimmunol.1000383

88. Wang WW, Wang Y, Li K, Tadagavadi R, Friedrichs WE, Budatha M, et al. Il-10 from Dendritic Cells but Not from T Regulatory Cells Protects against Cisplatin-Induced Nephrotoxicity. *PloS One*. (2020) 15:e0238816. doi: 10.1371/journal.pone.0238816

89. Sapoznikov A, Fischer JA, Zaft T, Krauthgamer R, Dzionek A, Jung S. Organ-dependent *in vivo* priming of naive cd4+, but not cd8+, T cells by plasmacytoid dendritic cells. *J Exp Med*. (2007) 204:1923–33. doi: 10.1084/jem.20062373

90. Deng B, Lin Y, Chen Y, Ma S, Cai Q, Wang W, et al. Plasmacytoid dendritic cells promote acute kidney injury by producing interferon-alpha. *Cell Mol Immunol*. (2021) 18:219–29. doi: 10.1038/s41423-019-0343-9

91. Venet F, Monneret G. Advances in the understanding and treatment of sepsis-induced immunosuppression. *Nat Rev Nephrol*. (2018) 14:121–37. doi: 10.1038/nrneph.2017.165

92. Zarbock A, Nadim MK, Pickkers P, Gomez H, Bell S, Joannidis M, et al. Sepsis-associated acute kidney injury: consensus report of the 28th acute disease quality initiative workgroup. *Nat Rev Nephrol*. (2023) 19:401–17. doi: 10.1038/s41581-023-00683-3

93. Dong X, Swaminathan S, Bachman LA, Croatt AJ, Nath KA, Griffin MD. Antigen presentation by dendritic cells in renal lymph nodes is linked to systemic and local injury to the kidney. *Kidney Int*. (2005) 68:1096–108. doi: 10.1111/j.1523-1755.2005.00502.x

94. Li J, Nozaki Y, Akazawa H, Kishimoto K, Kinoshita K, Matsumura I. Deletion of antigen-presenting cells in lipopolysaccharide-induced acute kidney injury (Aki) affects the exacerbation and repair in aki. *Curr Issues Mol Biol*. (2022) 44:5655–65. doi: 10.3390/cimb44110383

95. Allam R, Scherbaum CR, Darisipudi MN, Mulay SR, Hagele H, Lichtnekert J, et al. Histones from dying renal cells aggravate kidney injury via tlr2 and tlr4. *J Am Soc Nephrol*. (2012) 23:1375–88. doi: 10.1681/ASN.2011111077

96. Feng D, Wang Y, Liu Y, Wu L, Li X, Chen Y, et al. Dc-sign reacts with tlr-4 and regulates inflammatory cytokine expression via nf-kappab activation in renal tubular epithelial cells during acute renal injury. *Clin Exp Immunol*. (2018) 191:107–15. doi: 10.1111/cei.13048

97. Nozaki Y, Hino S, Ri J, Sakai K, Nagare Y, Kawanishi M, et al. Lipopolysaccharide-induced acute kidney injury is dependent on an il-18 receptor signaling pathway. *Int J Mol Sci*. (2017) 18(12):2777. doi: 10.3390/ijms18122777

98. Al-Harbi NO, Nadeem A, Ahmad SF, Alanazi MM, Aldossari AA, Alasmari F. Amelioration of sepsis-induced acute kidney injury through inhibition of inflammatory cytokines and oxidative stress in dendritic cells and neutrophils respectively in mice: role of spleen tyrosine kinase signaling. *Biochimie*. (2019) 158:102–10. doi: 10.1016/j.biochi.2018.12.014

99. Nadeem A, Ahmad SF, Al-Harbi NO, Ibrahim KE, Alqahtani F, Alanazi WA, et al. Bruton's tyrosine kinase inhibition attenuates oxidative stress in systemic immune cells and renal compartment during sepsis-induced acute kidney injury in mice. *Int Immunopharmacol*. (2021) 90:107123. doi: 10.1016/j.intimp.2020.107123

100. Ng JH, Hirsch JS, Hazzan A, Wanchoo R, Shah HH, Malieckal DA, et al. Outcomes among patients hospitalized with covid-19 and acute kidney injury. *Am J Kidney Dis*. (2021) 77:204–15 e1. doi: 10.1053/j.ajkd.2020.09.002

101. Cummings MJ, Baldwin MR, Abrams D, Jacobson SD, Meyer BJ, Balough EM, et al. Epidemiology, clinical course, and outcomes of critically ill adults with covid-19 in new york city: A prospective cohort study. *Lancet*. (2020) 395:1763–70. doi: 10.1016/S0140-6736(20)31189-2

102. Gupta S, Coca SG, Chan L, Melamed ML, Brenner SK, Hayek SS, et al. Aki treated with renal replacement therapy in critically ill patients with covid-19. *J Am Soc Nephrol*. (2021) 32:161–76. doi: 10.1681/ASN.2020060897

103. Perico L, Benigni A, Casiraghi F, Ng LFP, Renia L, Remuzzi G. Immunity, endothelial injury and complement-induced coagulopathy in covid-19. *Nat Rev Nephrol*. (2021) 17:46–64. doi: 10.1038/s41581-020-00357-4

104. Mehta P, McAuley DF, Brown M, Sanchez E, Tattersall RS, Manson JJ, et al. Covid-19: consider cytokine storm syndromes and immunosuppression. *Lancet*. (2020) 395:1033–4. doi: 10.1016/S0140-6736(20)30628-0

105. Yang Y, Shen C, Li J, Yuan J, Wei J, Huang F, et al. Plasma ip-10 and mcp-3 levels are highly associated with disease severity and predict the progression of covid-19. *J Allergy Clin Immunol*. (2020) 146:119–27 e4. doi: 10.1016/j.jaci.2020.04.027

106. Chen G, Wu D, Guo W, Cao Y, Huang D, Wang H, et al. Clinical and immunological features of severe and moderate coronavirus disease 2019. *J Clin Invest*. (2020) 130:2620–9. doi: 10.1172/JCI137244

107. Laing AG, Lorenc A, Del Molino Del Barrio I, Das A, Fish M, Monin L, et al. A dynamic covid-19 immune signature includes associations with poor prognosis. *Nat Med*. (2020) 26:1623–35. doi: 10.1038/s41591-020-1038-6

108. Zahorchak AF, Macedo C, Hamm DE, Butterfield LH, Metes DM, Thomson AW. High pd-L1/cd86 mfi ratio and il-10 secretion characterize human regulatory dendritic cells generated for clinical testing in organ transplantation. *Cell Immunol*. (2018) 323:9–18. doi: 10.1016/j.cellimm.2017.08.008

109. Morelli AE, Thomson AW. Tolerogenic dendritic cells and the quest for transplant tolerance. *Nat Rev Immunol*. (2007) 7:610–21. doi: 10.1038/nri2132

110. Ness S, Lin S, Gordon JR. Regulatory dendritic cells, T cell tolerance, and dendritic cell therapy for immunologic disease. *Front Immunol*. (2021) 12:633436. doi: 10.3389/fimmu.2021.633436

111. Li L, Huang L, Ye H, Song SP, Bajwa A, Lee SJ, et al. Dendritic cells tolerized with adenosine a(2)Ar agonist attenuate acute kidney injury. *J Clin Invest*. (2012) 122:3931–42. doi: 10.1172/JCI63170

112. Rousselle TV, Kuscu C, Kuscu C, Schlegel K, Huang L, Namwanje M, et al. Fty720 regulates mitochondria biogenesis in dendritic cells to prevent kidney ischemic reperfusion injury. *Front Immunol*. (2020) 11:1278. doi: 10.3389/fimmu.2020.01278

113. Bajwa A, Huang L, Ye H, Dondeti K, Song S, Rosin DL, et al. Dendritic cell sphingosine 1-phosphate receptor-3 regulates th1-th2 polarity in kidney ischemia-reperfusion injury. *J Immunol*. (2012) 189:2584–96. doi: 10.4049/jimmunol.1200999

114. Namwanje M, Bisunke B, Rousselle TV, Lamanilao GG, Sunder VS, Patterson EC, et al. Rapamycin alternatively modifies mitochondrial dynamics in dendritic cells to reduce kidney ischemic reperfusion injury. *Int J Mol Sci*. (2021) 22(10):5386. doi: 10.3390/ijms22105386

115. Macedo C, Turquist H, Metes D, Thomson AW. Immunoregulatory properties of rapamycin-conditioned monocyte-derived dendritic cells and their role in transplantation. *Transplant Res*. (2012) 1:16. doi: 10.1186/2047-1440-1-16

116. Li JSY, Robertson H, Trinh K, Raghubar AM, Nguyen Q, Matigian N, et al. Tolerogenic dendritic cells protect against acute kidney injury. *Kidney Int*. (2023) 104:492–507. doi: 10.1016/j.kint.2023.05.008

117. Zhao Y, Caron C, Chan YY, Lee CK, Xu X, Zhang J, et al. Cis-B7:Cd28 interactions at invaginated synaptic membranes provide cd28 co-stimulation and promote cd8(+) T cell function and anti-tumor immunity. *Immunity*. (2023) 56:1187–203 e12. doi: 10.1016/j.immuni.2023.04.005

118. Dai H, Watson AR, Fantus D, Peng L, Thomson AW, Rogers NM. Rictor deficiency in dendritic cells exacerbates acute kidney injury. *Kidney Int*. (2018) 94:951–63. doi: 10.1016/j.kint.2018.06.010

119. Moreau A, Kervella D, Bouchet-Delbos L, Braudeau C, Saiagh S, Guerif P, et al. A phase I/iia study of autologous tolerogenic dendritic cells immunotherapy in kidney transplant recipients. *Kidney Int*. (2023) 103:627–37. doi: 10.1016/j.kint.2022.08.037

frontiers | Frontiers in Immunology

TYPE Original Research
PUBLISHED 28 February 2024
DOI 10.3389/fimmu.2024.1334109

OPEN ACCESS

EDITED BY
Xu-jie Zhou,
Peking University, China

REVIEWED BY
Dong Zhou,
University of Connecticut, United States
Adil Bhat,
University of California, Los Angeles, United States

*CORRESPONDENCE
Liang Peng
pengliang8028@163.com
Yongli Zhan
zhanyongli88@sina.com
Ping Li
lp8675@163.com

RECEIVED 06 November 2023
ACCEPTED 15 February 2024
PUBLISHED 28 February 2024

CITATION
Liu T, Zhao H, Wang Y, Qu P, Wang Y, Wu X, Zhao T, Yang L, Mao H, Peng L, Zhan Y and Li P (2024) Serum high mobility group box 1 as a potential biomarker for the progression of kidney disease in patients with type 2 diabetes.
Front. Immunol. 15:1334109.
doi: 10.3389/fimmu.2024.1334109

Serum high mobility group box 1 as a potential biomarker for the progression of kidney disease in patients with type 2 diabetes

Tongtong Liu[1], Hailing Zhao[2], Ying Wang[3], Peng Qu[2], Yanmei Wang[2], Xiai Wu[2], Tingting Zhao[2], Liping Yang[1], Huimin Mao[1], Liang Peng[2*], Yongli Zhan[1*] and Ping Li[2*]

[1]Guang'anmen Hospital, China Academy of Chinese Medical Sciences, Beijing, China, [2]China-Japan Friendship Hospital, Institute of Medical Science, Beijing, China, [3]Dongzhimen Hospital, Beijing University of Chinese Medicine, Beijing, China

Background: As a damage-associated molecular pattern protein, high mobility group box 1 (HMGB1) is associated with kidney and systemic inflammation. The predictive and therapeutic value of HMGB1 as a biomarker has been confirmed in various diseases. However, its value in diabetic kidney disease (DKD) remains unclear. Therefore, this study aimed to investigate the correlation between serum and urine HMGB1 levels and DKD progression.

Methods: We recruited 196 patients with type 2 diabetes mellitus (T2DM), including 109 with DKD and 87 T2DM patients without DKD. Additionally, 60 healthy participants without T2DM were also recruited as controls. Serum and urine samples were collected for HMGB1 analysis. Simultaneously, tumor necrosis factor receptor superfamily member 1A (TNFR-1) in serum and kidney injury molecule (KIM-1) in urine samples were evaluated for comparison.

Results: Serum and urine HMGB1 levels were significantly higher in patients with DKD than in patients with T2DM and healthy controls. Additionally, serum HMGB1 levels significantly and positively correlated with serum TNFR-1 (R^2 = 0.567, p<0.001) and urine KIM-1 levels (R^2 = 0.440, p<0.001), and urine HMGB1 has a similar correlation. In the population with T2DM, the risk of DKD progression increased with an increase in serum HMGB1 levels. Multivariate logistic regression analysis showed that elevated serum HMGB1 level was an independent risk factor for renal function progression in patients with DKD, and regression analysis did not change in the model corrected for multiple variables. The restricted cubic spline depicted a nonlinear relationship between serum HMGB1 and renal function progression in patients with DKD (p-nonlinear=0.007, p<0.001), and this positive effect remained consistent across subgroups.

10.3389/fimmu.2024.1334109

Conclusion: Serum HMGB1 was significantly correlated with DKD and disease severity. When the HMGB1 level was ≥27 ng/ml, the risk of renal progression increased sharply, indicating that serum HMGB1 can be used as a potential biomarker for the diagnosis of DKD progression.

KEYWORDS

HMGB1, biomarker, diabetic kidney disease, progression, T2DM

1 Introduction

Diabetes mellitus is a major cause of chronic kidney disease (CKD) worldwide and is a strong risk factor for the progression of CKD to end-stage renal disease (ESRD) (1, 2). Diabetic kidney disease (DKD) affects up to 40% of patients with diabetes and is associated with a substantial incidence and mortality of ESRD and cardiovascular events (3, 4). The mortality risk associated with early-stage DKD is much higher than that associated with CKD or diabetes without DKD (5). The estimated glomerular filtration rate (eGFR) and albuminuria are established markers for assessing renal function progression (6, 7). However, there is a significant difference between albuminuria and renal impairment in diabetic neuropathy, and DKD can occur without increased albuminuria and subsequent progression to ESKD (8, 9). On the other hand, owing to the regulation of complex environmental and genetic factors, there is heterogeneity in the progression rate of CKD in patients with diabetes, which is manifested by the rapid decrease in the eGFR in some populations with DKD. Conversely, others experience a more indolent course (10, 11). Therefore, it is necessary to identify new biomarkers that can reliably predict the development and progression of DKD.

Over the past decade, many new biomarkers have been evaluated and provided insight into the pathophysiology of kidney disease progression in the context of diabetes. Inflammation is of particular importance (12, 13). Inflammation plays a crucial role in the development and progression of DKD. Persistent inflammation leads to glomerulosclerosis and renal fibrosis, which in turn lead to proteinuria and decreased glomerular filtration rate (14). Numerous inflammation-related molecules, as biomarkers, have been found to be strongly correlated with the progression and prognosis of DKD (13). For example, kidney risk inflammatory signature, composed of 17 proteins including the tumor necrosis factor, is associated with a 10-year risk of ESRD by promoting the inflammatory process of diabetes (15). A study of 2553 participants with normoalbuminuria at a median follow-up of 6.1 years found that TNFR-1 (hazard ratio [HR]=4.2) and TNFR-2 (HR=2.3) were associated with renal outcomes in patients with type 2 diabetes and normoalbuminuria, whereas KIM-1 did not find an association with renal outcomes (16). Similarly, another study reported that TNFR-1 is associated with the risk of kidney failure with replacement therapy in adults with diabetes (HR=1.91) (12). High mobility group box 1 (HMGB1), as an important pro-inflammatory factor, has been found to be elevated in many metabolic and immune diseases, including sepsis (17), rheumatoid arthritis (18), and Alzheimer's disease (19), and significantly correlated with their progression and prognosis. We recently noticed that HMGB1 activation in kidney disease promotes multiple key events in CKD progression by activating downstream signals, including kidney inflammation, development of persistent fibrosis, kidney aging, acute kidney injury to CKD transition, and important cardiovascular complications (20). Several clinical studies have also shown that elevation of the HMGB1 level is significantly correlated with kidney disease progression (21–23). Furthermore, on the basis of the Nephroseq database, we found an increase of HMGB1 expression in CKD and a significant correlation with eGFR and proteinuria (Figure 1). However, the potential role of HMGB1 as a biomarker for the occurrence and progression of DKD has not yet been investigated.

Therefore, in this study, we attempted to investigate the relationship between serum and urine HMGB1 levels and the occurrence and progression of DKD. To verify this, serum tumor necrosis factor receptor superfamily member 1A (TNFR-1) and urine kidney injury molecule (KIM-1), previously reported biomarkers

Abbreviations: CKD, chronic kidney disease; ESRD, end-stage renal disease; DKD, diabetic kidney disease; eGFR, estimated glomerular filtration rate; HMGB1, high mobility group box 1; TNFR-1, tumor necrosis factor receptor superfamily member 1A; KIM-1, urine kidney injury molecule; T2DM, type 2 diabetes mellitus; ADA, American Diabetes Association; NKF-KDOQI, National Kidney Foundation's Quality Initiative for Renal Disease Outcomes; ROC, receiver-operator characteristic; AUC, area under the curve; RCS, restricted cubic spline; AIC, akaike information criterion; BMI, body-mass index; HGB, hemoglobin; HbA1c, glycated haemoglobin A1c; ALT, alanine transaminase; AST, aspartate aminotransferase; ALB, albumin; Scr, serum creatinine; eGFR, estimated glomerular filtration rate; UA, uric acid; TC, total cholesterol; TG, triglycerides; HDL-C, high density lipoprotein cholesterol; LDL-C, low density lipoprotein; hs-CRP, high-sensitivity C-reactive protein; UACR, Urinary albumin/creatinine ratio; UTP, urinary total protein; HMGB1, high mobility group box protein 1; CVD, cardiovascular diseases; DAMPs, damage-associated molecular pattern; RAGE, receptor of advanced glycation endproducts.

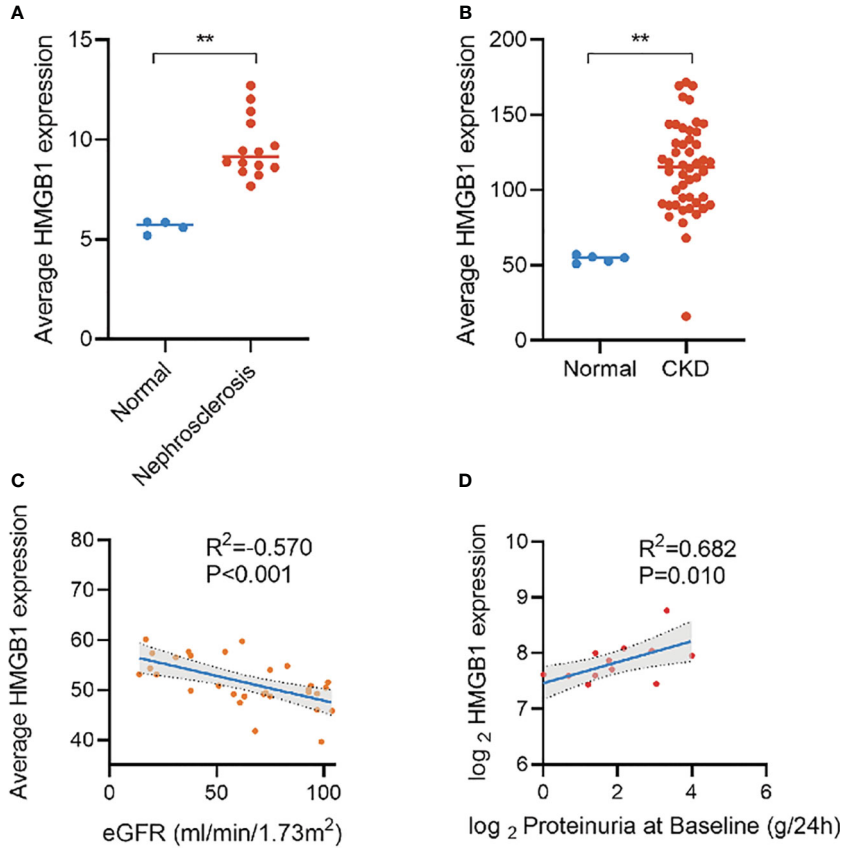

FIGURE 1
Expression of HMGB1 in different kidney diseases and its correlation with eGFR and proteinuria based on Nephroseq database. **(A)** expression of HMGB1 in nephrosclerosis, **(B)** expression of HMGB1 in CKD, **(C)** correlation between average HMGB1 expression and eGFR, **(D)** correlation between average HMGB1 expression and proteinuria. **P < 0.01, n.s. = no significance.

significantly associated with the prognosis of DKD, were also evaluated for comparison.

2 Methods

2.1 Study design and population

In this cross-sectional study, we recruited 256 participants as the study set from Guang'anmen Hospital of the Chinese Academy of Traditional Chinese Medicine and China-Japan Friendship Hospital from May 2016 to December 2022, including 87 type 2 diabetes mellitus (T2DM) patients without CKD, 109 with DKD, and 60 healthy control participants, and another 42 participants from Dongzhimen Hospital Affiliated to Beijing University of Chinese Medicine (including 15 T2DM patients without CKD, 22 with DKD, and 5 healthy control participants) were included in this study as the validation set. We performed power analysis based on G*Power (Version 3.1.9.7) software to ensure the sample size of each subgroup is sufficient. The inclusion and exclusion criteria of the validation set were the same as those of the study set. The diagnosis of T2DM is based on the guidelines of the American Diabetes Association (ADA) (glycosylated hemoglobin level of 6.5%, fasting blood glucose level of 126 mg/dl, and/or random blood glucose level of 200 mg/dl) (24). The diagnostic criteria of DKD were based on the guidelines of the National Kidney Foundation's Quality Initiative for Renal Disease Outcomes (NKF-KDOQI) (25), i.e., urinary albumin excretion rate of ≥30 mg/24 hours or abnormal eGFR of <60 mL/min/1.73 m^2. Individuals with type 1 diabetes, autoimmunity, infection, liver dysfunction, cancer, kidney replacement therapy, or cardiovascular diseases with serious complications were excluded. We also excluded patients with non-DKD, according to previously described (26). Including: 1) diabetes duration less than 5 years; 2) rapid decline of eGFR; 3) rapid increase of urinary albumin or nephrotic syndrome; 4) active urinary sediment (red blood cell, white blood cell or cell tube type); 5) intractable hypertension; 6) combined with other systemic diseases. This study was approved by the Ethics Committee of Guang'anmen Hospital of the Chinese Academy of Traditional Chinese Medicine, Dongzhimen Hospital Affiliated to Beijing University of Chinese Medicine and China-Japan Friendship Hospital respectively, and all participants gave informed consent.

2.2 Data collection

All participants were instructed to complete a questionnaire that included their demographic characteristics (age, sex, height, and weight), living habits (smoking and drinking), medical history (duration of type 2 diabetes, hypertension, cardiovascular disease, hyperlipidemia, and fatty liver disease), and standard laboratory functional test results (values of hemoglobin, urinary microalbumin, and 24-hour urine protein quantification). eGFR was evaluated according to the 2009 Chronic Kidney Disease Epidemiology Collaboration formula (27). Blood and urine samples were obtained from all participants. Blood samples were centrifuged at 3000 rpm for 10 minutes, and the supernatant was kept at -80 °C. Urine samples were centrifuged at 1500 rpm for 10 minutes, and the supernatant was kept at -80 °C.

2.3 Laboratory tests of HMGB1

Both serum and urine HMGB1 levels were detected using the human high-mobility group protein B1 (HMGB1) enzyme-linked immunosorbent assay (ELISA) kit (E-EL-H1554c, Elabscience), and ELISA was performed according to the manufacturer's instructions. The coefficient of inter-assay and intra-assay variation was <10%. All measurements were repeated thrice horizontally, and the average of these values was used to prevent measurement bias. Additionally, urine HMGB1 levels were corrected for urinary creatinine levels.

2.4 Measurement of TNFR-1 and KIM-1 levels

According to the manufacturer's instructions, the human tumor necrosis factor receptor superfamily member 1A (TNFRSF1A) ELISA kit (E-EL-H0217c, Elabscience) and the human kidney injury molecule 1 (KIM-1) ELISA kit (E-EL-H6029, Elabscience) were used to quantify the contents of TNFR-1 in the serum samples and KIM-1 in the urine samples, respectively. The coefficient of inter-assay and intra-assay variation was <10%. All samples were measured thrice horizontally, and the average of these values was used to prevent measurement bias. Moreover, urinary KIM-1 levels were corrected for urinary creatinine levels.

2.5 Statistical analysis

Descriptive statistics were used to determine the baseline characteristics of the study population. The results are reported using descriptive statistical methods, where the continuous variables are continuously presented as variables with normal or non-normal distribution through means and standard deviations (SD) or medians and interquartile ranges (IQRs), and categorical variables are presented as quantities and percentages. We used t-tests, one-way analysis of variance, and Kruskal–Wallis tests to analyze the relationship between continuous variables for comparison between different groups; the chi-square test was used to analyze the relationship between categorical variables. Correlations between different indicators were tested using the Spearman correlation test. The relationship between serum HMGB1 and CKD stage was tested using ordinal logistic regression. While, some potential confounders were corrected in the multivariate regression models. Receiver-operator characteristic (ROC) curves were drawn, and the performance of serum and urine HMGB1 were evaluated by the area under the curve (AUC). Considering the possible non-monotonic effects between serum HMGB1 and renal function progression in DKD, we also used restricted cubic spline (RCS) fitting univariate and multivariate regression models to flexibly model and visualize the nonlinear relationship between serum HMGB1 levels and the risk of DKD progression (28). To get the best fitting effect, we fitted the model with the number of knots between 3-7 separately, and selected the knots corresponding to the lowest value for the akaike information criterion (AIC) as the number of knots. We set the median of the first quartile of serum HMGB1 as the reference. To test for potential nonlinearity, a likelihood ratio test was used to compare the RCS model with a model containing only linear terms. A two-tailed p-value of <0.05 was considered significant. All statistical analyses were performed using SPSS statistics 25.0 (SPSS, Inc., Chicago, IL, USA) and R software, version 4.2.2, along with MSTATA software (www.mstata.com).

3 Results

3.1 Basic characteristics of the study population

The demographic characteristics of the participants are presented in Table 1. Among the 256 participants, 109 had DKD, 87 had T2DM, and 60 were healthy control, and there were 130 males (50.78%) with an average age of 57.71 ± 9.69 years and a body mass index (BMI) of 24.70 ± 3.36 kg/m^2. Less than a quarter of the participants reported smoking (20.31%) or drinking (21.48%).

Compared with T2DM patients without CKD and healthy controls, patients with DKD were older and there was significant predominance in male sex, duration of diabetes, hypertension, cardiovascular disease, smoking, and alcohol consumption. Among the population with DKD, while there was no statistically significant difference in LDL-C and hs-CRP between T2DM patients without CKD and healthy controls.

3.2 Elevation of the HMGB1 level in the population with DKD

The serum HMGB1 levels in the population with DKD was significantly higher than that in the population with long-term diabetes but without CKD or in healthy control people without diabetes (52.03 ± 28.45 *v.s.* 19.87 ± 12.82 and 19.81 ± 10.01)

TABLE 1 Baseline demographic and clinical characteristics of the study population.

Characteristics	Total (n=256)	Healthy control (n=60)	T2DM (n=87)	DKD (n=109)	*p*-value
Age (years)	57.71 ± 9.69	55.43 ± 10.00	55.51 ± 10.18	60.72 ± 8.28	<0.001
Male (%)	130 (50.78)	22 (36.67)	41 (47.13)	67 (61.47)	0.006
BMI (kg/m^2)	24.70 ± 3.36	22.99 ± 2.71	24.99 ± 3.55	25.42 ± 3.24	<0.001
Duration of diabetes (years)	12.30 ± 8.06	/	9.31 ± 8.43	13.77 ± 7.61	<0.001
Hypertension (%)	143 (55.86)	3 (5.00)	46 (52.87)	94 (86.24)	<0.001
CVD (%)	86 (33.59)	9 (15.00)	31 (35.63)	46 (42.20)	0.001
Hyperlipidemia (%)	122 (46.48)	6 (10.00)	50 (57.47)	66 (60.55)	<0.001
Smokers (%)	52 (20.31)	3 (5.00)	19 (21.84)	30 (27.52)	0.002
Drinkers (%)	55 (21.48)	5 (8.33)	24 (27.59)	26 (23.85)	0.015
HGB (g/L)	132.09 ± 20.44	139.28 ± 14.23	135.79 ± 18.87	125.17 ± 22.46	<0.001
HbA1c (%)	7.47 ± 1.91	6.18 ± 1.18	7.96 ± 1.97	7.78 ± 1.87	<0.001
ALT (U/L)	18.00 (14.00,27.00)	18.00 (13.00,29.00)	20.00 (15.00,28.70)	17.80 (13.40,24.00)	0.104
AST (U/L)	19.00 (15.93,23.45)	20.00 (17.00,25.00)	18.90 (15.20,24.00)	18.20 (14.00,23.00)	0.116
ALB (g/L)	41.26 ± 5.71	44.37 ± 3.22	43.38 ± 2.98	37.84 ± 6.59	<0.001
Scr (μmol/L)	98.57 ± 87.03	58.55 ± 11.15	63.59 ± 17.04	148.53 ± 114.85	<0.001
eGFR (ml/min/1.73m^2)	82.93 ± 30.66	102.06 ± 9.06	98.35 ± 14.09	60.10 ± 33.10	<0.001
Urea (mmol/L)	8.07 ± 6.56	4.95 ± 1.17	5.91 ± 2.26	11.50 ± 8.70	<0.001
UA (μmol/L)	344.98 ± 87.87	307.46 ± 70.92	343.53 ± 88.17	366.79 ± 89.60	<0.001
TC (mmol/L)	4.95 ± 1.49	4.91 ± 1.33	4.77 ± 1.45	5.11 ± 1.59	0.594
TG (mmol/L)	1.78 ± 1.01	1.34 ± 0.65	1.88 ± 1.17	1.94 ± 0.97	<0.001
LDL-C (mmol/L)	2.97 ± 1.02	2.90 ± 0.93	3.01 ± 1.03	2.97 ± 1.07	0.742
HDL-C (mmol/L)	1.28 ± 0.42	1.37 ± 0.33	1.22 ± 0.31	1.28 ± 0.52	0.011
hs-CRP (mg/L)	1.32 (0.65,2.30)	1.02 (0.82,2.60)	1.36 (0.66,2.23)	1.37 (0.50,2.15)	0.937
UACR (mg/g)	20.00 (4.08,355.48)	5.74 (2.96,15.04)	3.73 (0.80,9.21)	539.70 (77.44,959.61)	<0.001
24h-UTP (mg/24h)	110.24 (60.05,1660.00)	49.31 (25.35,82.28)	82.09 (60.00,110.00)	2250.00 (475.00,4645.00)	<0.001
Serum HMGB1 (ng/ml)	33.55 ± 25.99	19.81 ± 10.01	19.87 ± 12.82	52.03 ± 28.45	<0.001
Urine HMGB1/Cr (pg/ug)	3.77 (2.19,7.93)	2.30 (1.25,4.91)	2.96 (2.01,4.56)	7.72 (3.8,12.13)	<0.001
KIM-1/Cr (pg/ug)	0.45 (0.24,0.90)	0.32 (0.16,0.48)	0.30 (0.18,0.49)	0.94 (0.51,1.66)	<0.001
TNFR-1 (ng/ml)	2.45 ± 0.76	2.10 ± 0.41	2.21 ± 0.34	2.84 ± 0.95	<0.001

BMI, body-mass index; HGB, hemoglobin; HbA1c, glycated haemoglobin A1c; ALT, alanine transaminase; AST, aspartate aminotransferase; ALB, albumin; Scr, serum creatinine; eGFR, estimated glomerular filtration rate; UA, uric acid; TC, total cholesterol; TG, triglycerides; HDL-C, high density lipoprotein cholesterol; LDL-C, low density lipoprotein cholesterol; hs-CRP, high-sensitivity C-reactive protein; UACR, Urinary albumin/creatinine ratio; UTP, urinary total protein; HMGB1, high mobility group box protein 1; TNFR-1, tumor necrosis factor receptor superfamily member 1A; KIM-1, kidney injury molecule-1; CVD, cardiovascular diseases; DKD, diabetic kidney disease.

(Figure 2A). Urine HMGB1 levels corrected by urinary creatinine levels showed results similar to serum HMGB1 levels (Figure 2B). Notably, we found a significant positive correlation between serum and urine HMGB1 levels in this population (R^2 = 0.477, p<0.001) (Figure 2C).

Urine KIM-1 is a known and confirmed marker of renal tubular injury. Consistent with previous reports (29), we found that KIM-1 levels corrected for urinary creatinine levels were significantly elevated in the population with DKD (Figure 2D), and there was a significant correlation between serum HMGB1 and urine KIM-1 levels (R^2 = 0.440, p<0.001) (Figure 2E). Similarly, creatinine-corrected urinary HMGB1 levels were significantly correlated with KIM-1 levels (R^2 = 0.604, p<0.001) (Figure 2F).

More importantly, recent study reported that TNFR-1 expression is strongly correlated with the prognosis of DKD. Every unit of TNFR-1 increased the risk of DKD renal function decline by 117% (30). We also found that serum TNFR-1 levels were significantly elevated in the population with DKD (2.84 ± 0.95 *v.s.* 2.21 ± 0.34 and 2.10 ± 0.41) (Figure 2G), and there was a significant correlation between serum

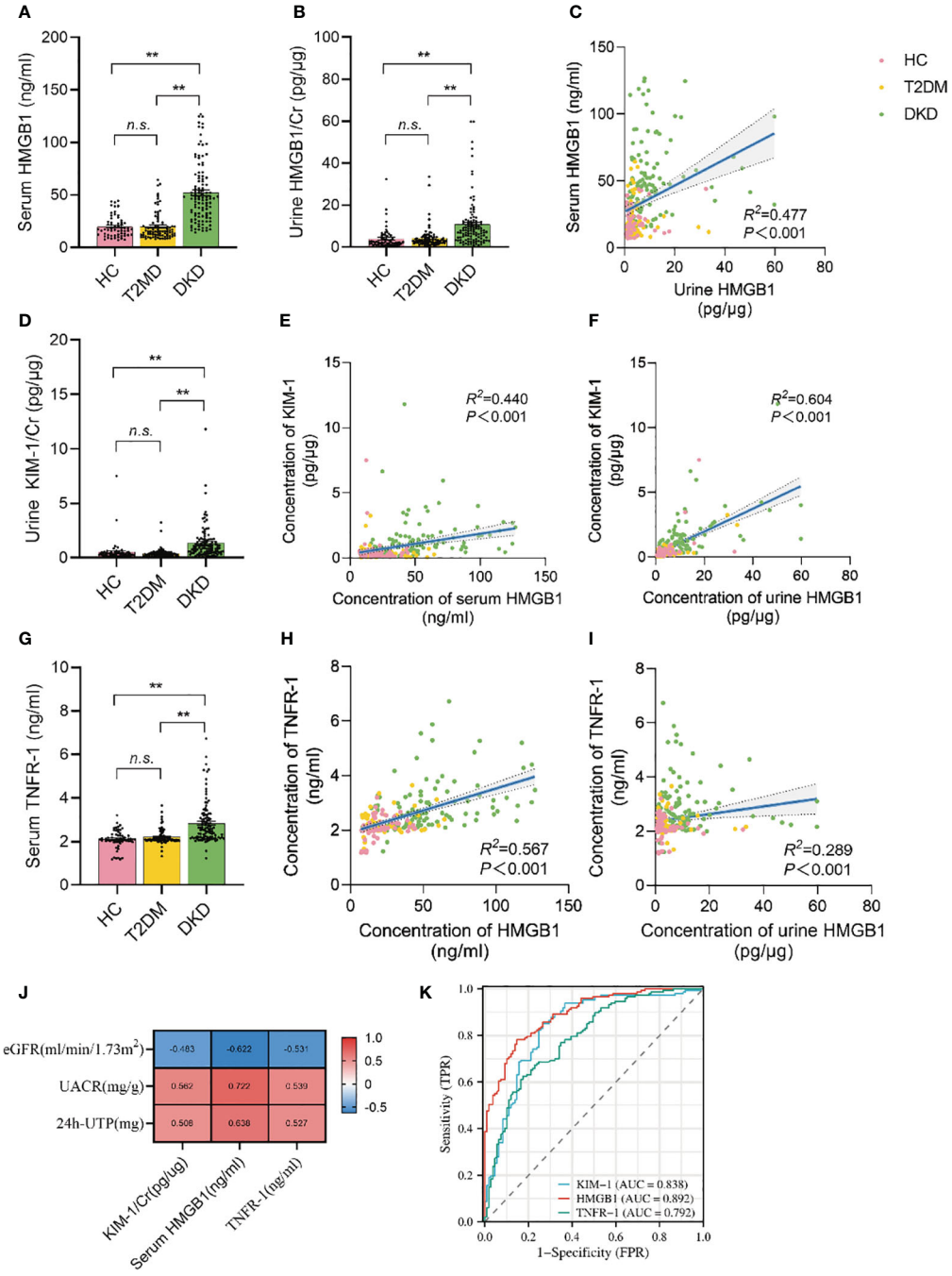

FIGURE 2
Serum and urine HMGB1 were significantly elevated in DKD population and correlated with TNFR-1 and KIM-1. **(A)** serum HMGB1 levels in the study population, **(B)** urine HMGB1 levels in the study population, **(C)** correlation between serum and urine HMGB1, **(D)** urine KIM-1/Cr levels in the study population, **(E)** correlation between serum HMGB1 and urine KIM-1/Cr, **(F)** correlation between urine HMGB1 and KIM-1/Cr, **(G)** serum TNFR-1 levels in the study population, **(H)** correlation between serum HMGB1 and TNFR-1, **(I)** correlation between urine HMGB1 and serumTNFR-1, **(J)** correlation between serum HMGB1, urine KIM-1 and serum TNFR-1 and proteinuria and renal function progression, **(K)** the performance of serum HMGB1, urine KIM-1 and serum TNFR-1 to identify DKD based on the ROC curve. n.s. = no significance.

HMGB1 and serum TNFR-1 levels (R^2 = 0.567, p<0.001) (Figure 2H). Moreover, there was a significant correlation between creatinine-corrected urine HMGB1 levels and serum TNFR-1 levels (Figure 2I). (R^2 = 0.289, p<0.001). More importantly, we found that serum HMGB1 showed a higher correlation with proteinuria and renal function progression compared to urine KIM-1 and serum TNFR-1 (Figure 2J), and its efficacy in predicting DKD occurrence was better (Figure 2K).

TABLE 2 Association of serum HMGB1 with various patient characteristics.

Variables		Serum HMGB1		Urine HMGB1	
		Mean± SD or R correlation factor	*p*-value	Mean± SD or R correlation factor	*p*-value
Age (years)		0.258	<0.001	0.450	<0.001
Sex	Male (n=130)	42.39 ± 28.30	<0.001	3.82 (2.07,7.98)	0.914
	Female (n=126)	24.42 ± 19.66		3.67 (2.14,7.72)	
BMI (kg/m^2)		0.150	0.016	-0.003	0.965
Duration of diabetes (years)		0.392	<0.001	0.333	<0.001
Hypertension	Yes (n=143)	43.86 ± 29.44	<0.001	5.62 (3.03,10.13)	<0.001
	No (n=113)	20.49 ± 11.48		2.56 (1.66,5.31)	
CVD	Yes (n=86)	39.02 ± 28.50	0.023	5.52 (3.03,8.97)	0.003
	No (n=170)	30.77 ± 24.25		3.23 (1.96,6.87)	
Hyperlipidemia	Yes (n=122)	35.06 ± 26.51	0.375	4.51 (2.37,8.91)	0.109
	No (n=134)	32.17 ± 25.54		3.37 (2.07,6.76)	
Smokers	Yes (n=52)	45.40 ± 28.63	<0.001	3.82 (2.20,8.91)	0.533
	No (n=204)	30.52 ± 24.45		3.68 (2.14,7.56)	
Drinkers	Yes (n=55)	36.55 ± 21.69	0.335	3.50 (2.15,6.49)	0.293
	No (n=201)	32.72 ± 27.04		4.09 (2.19,8.08)	
ALB (g/L)		-0.406	<0.001	-0.408	<0.001
Scr (μmol/L)		0.711	<0.001	0.349	<0.001
eGFR (ml/min/1.73m^2)		-0.622	<0.001	-0.483	<0.001
Urea (mmol/L)		0.600	<0.001	0.413	<0.001
UA (μmol/L)		0.287	<0.001	0.106	0.091
TC (mmol/L)		-0.014	0.819	-0.041	0.516
TG (mmol/L)		0.072	0.252	0.036	0.568
hs-CRP (mg/L)		0.051	0.412	-0.048	0.448
UACR (mg/g)		0.722	<0.001	0.532	<0.001
24h-UTP (mg)		0.638	<0.001	0.405	<0.001
CKD stage	G1 (n=153) (eGFR≥ 90)	21.18 ± 11.92	<0.001	2.83 (1.70,5.37)	<0.001
	G2 (n=50) (60≤eGFR < 90)	32.24 ± 18.97		4.59 (2.68,6.78)	
	G3 (n=27) (30≤eGFR < 60)	62.46 ± 21.96		9.96 (5.26,12.81)	
	G4 (n=17) (15≤eGFR < 30)	73.08 ± 28.40		8.97 (7.72,16.68)	
	G5 (n=9) (eGFR <15)	89.61 ± 28.92		9.53 (7.98,22.53)	
Serum HMGB1 (ng/ml)		1	/	0.477	<0.001
Urine HMGB1 (pg/ug)		0.477	<0.001	1	/
KIM-1/Cr (pg/ug)		0.440	<0.001	0.604	<0.001
TNFR-1 (ng/ml)		0.567	<0.001	0.289	<0.001

BMI, body-mass index; ALB, albumin; Scr, serum creatinine; eGFR, estimated glomerular filtration rate; UA, uric acid; TC, total cholesterol; TG, triglycerides; HDL-C, high density lipoprotein cholesterol; LDL-C, low density lipoprotein cholesterol; hs-CRP, high-sensitivity C-reactive protein; UACR, urinary albumin/creatinine ratio; UTP, urinary total protein; HMGB1, high mobility group box protein 1; TNFR-1, tumor necrosis factor receptor superfamily member 1A; KIM-1, kidney injury molecule-1; CVD, cardiovascular diseases; CKD, chronic kidney disease.

3.3 Association of the HMGB1 levels with DKD-related traits

Next, we found that the levels of HMGB1 in serum and urine are related to age, duration of diabetes, the proportion of hypertension and CVD (Table 2, Figure 2A). In addition, serum HMGB1 is also related to sex and smoking status (Table 2). We further found that serum and urine HMGB1 levels were significantly correlated with clinical indicators related to DKD (Table 2, Figure 3A), and the diagnostic efficacy of serum HMGB1 for the occurrence of DKD was better than that of corrected urine HMGB1 (AUC=0.892 *v.s.* AUC=0.792) (Figure 3B). Therefore, serum HMGB1 levels were selected for further analyses.

3.4 Correlations between serum HMGB1 and other variables

To determine the relationship between serum HMGB1 levels and DKD progression-related variables, we divided the included population into four groups according to the quartiles of serum HMGB1 levels, and the baseline characteristics of the included participants are shown in Table 3. Age, male proportion, duration of diabetes, hypertension proportion, CVD proportion, smokers' proportion, and serum TNFR-1 levels increased with increasing serum HMGB1 levels (all p values < 0.05). Additionally, HGB levels decreased in the highest quartile of serum HMGB1 levels. The differences in blood lipid levels were not statistically significant (all p values > 0.05). Importantly, we found that an increase in the quartile of serum HMGB1 levels was associated with an increased incidence of renal function decline and an increased number of patients with higher CKD stages compared with the lowest quartile (Table 3) (all p values < 0.05). This indicates that there is a dose-response relationship between serum HMGB1 levels and the renal progression of DKD.

3.5 Dose-response relationships of serum HMGB1 with the risk of kidney function decline in DKD

Based on univariate and multivariate logistic regression, we found that higher HMGB1 levels significantly increased the risk of renal function decline compared with the first quartile (Table 4, Figure 4), and we constructed three additional multivariate logistic regression models to adjust for confounding variables. As Table 4 shows, elevated serum HMGB1 levels remained an independent risk factor for renal function decline in DKD.

Next, we constructed an RCS model to flexibly visualize the relationship between serum HMGB1 levels and DKD progression on a continuous scale with or without correction for covariates. We observed an inverted J-shaped nonlinear relationship between serum HMGB1 levels and eGFR (p-nonlinear=0.007, p<0.001, knots=6, AIC=2137.97), after excluding the confounding factors of age, sex, hypertension, smokers, and duration of diabetes. When the concentration of HMGB1 was <27 ng/ml, the risk of renal function decline in DKD was stable (OR per SD=0.82, p=0.017). In contrast,

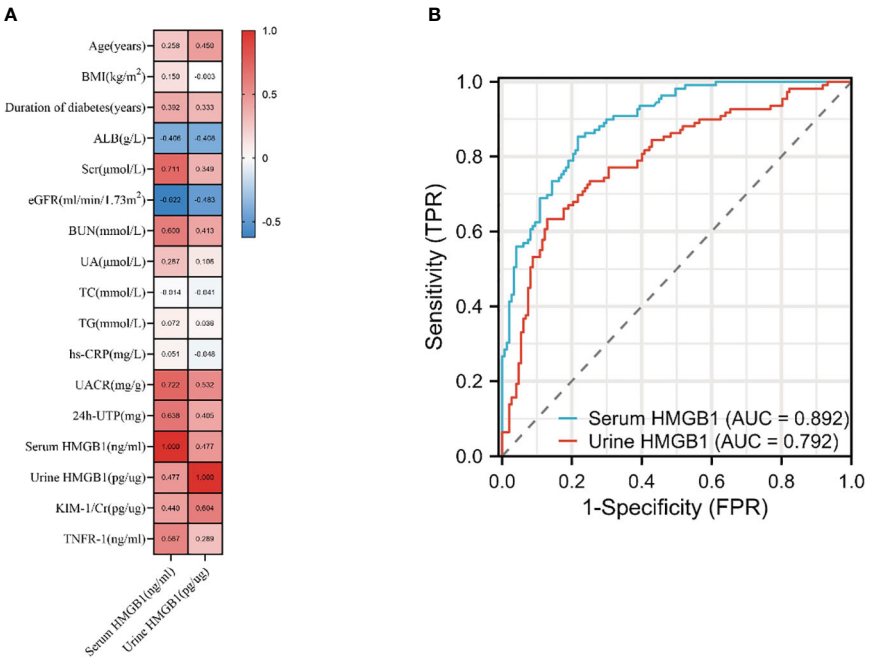

FIGURE 3
Association of the HMGB1 levels with DKD-related traits. **(A)** correlation of serum and urine HMGB1 and DKD related variables based on Spearman correlation test, **(B)** the performance of serum and urine HMGB1 to identify DKD based on the ROC curve.

when the concentration of serum HMGB1 was ≥27 ng/ml, the risk of renal function decline rapidly increases (OR per SD=0.53, $p<0.001$) (Table 5, Figure 5A). When adjusting for confounders, we found no nonlinear relationship between serum HMGB1 and UACR (p-nonlinear=0.071, $p<0.001$, knots=5, AIC=3500.54, Table 5, Figure 5B. Additionally, a similar relationship was observed between serum HMGB1 and UTP (p-nonlinear=0.011, $p<0.001$, knots=7, AIC=4417.18). Serum HMGB1 and UTP also showed a J-shaped relationship, after excluding the confounding factors of age, sex, hypertension, smokers, and duration of diabetes (Table 5, Figure 5C).

TABLE 3 Clinical and biochemical parameters for participants, according to quartile of Serum HMGB1 levels.

Characteristics	Total	Q1 (<15.20)	Q2 (15.20-23.62)	Q3 (23.62-46.12)	Q4 (>46.12)	*p*-value
N	256	64	64	64	64	/
Age (years)	57.71 ± 9.69	54.86 ± 9.41	57.34 ± 9.33	57.84 ± 10.23	60.80 ± 9.05	0.006
Male (%)	130 (50.78)	13 (20.31)	28 (43.75)	44 (68.75)	45 (70.31)	<0.001
BMI (kg/m^2)	24.70 ± 3.36	24.45 ± 3.12	23.90 ± 3.45	24.92 ± 3.64	25.53 ± 3.08	0.042
Duration of diabetes (years)	11.78 ± 8.27	7.94 ± 7.62	10.90 ± 9.03	11.15 ± 7.73	15.32 ± 7.25	<0.001
Hypertension (%)	143 (55.86)	20 (31.25)	27 (42.19)	36 (56.25)	60 (93.75)	<0.001
CVD (%)	86 (33.59)	17 (26.56)	17 (26.56)	22 (34.38)	30 (46.88)	0.015
Hyperlipidemia (%)	122 (47.66)	33 (51.56)	24 (37.50)	28 (43.75)	37 (57.81)	0.134
Smokers (%)	52 (20.31)	4 (6.25)	12 (18.75)	13 (20.31)	23 (35.94)	0.001
Drinkers (%)	55 (21.48)	9 (14.06)	11 (17.19)	19 (29.69)	16 (25.00)	0.121
HGB (g/L)	132.09 ± 20.44	132.98 ± 18.46	137.02 ± 13.92	140.19 ± 18.02	118.17 ± 23.30	<0.001
HbA1c (%)	7.47 ± 1.91	7.49 ± 1.92	7.46 ± 2.26	7.53 ± 2.00	7.39 ± 1.41	0.978
ALT (U/L)	18.00 (14.00,27.00)	17.00 (14.00,27.00)	18.00 (16.00,25.60)	21.00 (14.10,31.00)	15.50 (13.00,22.80)	0.05
AST (U/L)	19.00 (15.93,23.45)	18.00 (15.00,22.00)	19.00 (16.00,24.00)	19.30 (16.00,25.00)	18.20 (15.00,22.00)	0.304
ALB (g/L)	41.26 ± 5.71	43.32 ± 2.85	43.28 ± 3.94	42.37 ± 4.91	36.06 ± 6.86	<0.001
Scr (μmol/L)	98.57 ± 87.03	56.38 ± 11.67	63.10 ± 14.89	82.35 ± 39.19	192.46 ± 128.28	<0.001
eGFR (ml/min/1.73m^2)	82.93 ± 30.66	101.95 ± 11.54	97.37 ± 11.97	86.49 ± 24.78	45.92 ± 30.50	<0.001
Urea (mmol/L)	8.07 ± 6.56	5.17 ± 1.87	5.63 ± 1.43	7.21 ± 4.39	14.26 ± 9.76	<0.001
UA (μmol/L)	344.98 ± 87.87	320.61 ± 77.96	334.31 ± 89.53	349.97 ± 102.59	375.02 ± 70.53	0.003
TC (mmol/L)	4.95 ± 1.49	4.93 ± 1.52	4.91 ± 1.32	4.72 ± 1.32	5.22 ± 1.75	0.314
TG (mmol/L)	1.78 ± 1.01	1.92 ± 1.25	1.54 ± 0.84	1.79 ± 1.05	1.86 ± 0.78	0.157
LDL-C (mmol/L)	2.97 ± 1.02	3.16 ± 1.09	2.93 ± 0.92	2.79 ± 0.91	2.98 ± 1.13	0.225
HDL-C (mmol/L)	1.28 ± 0.42	1.24 ± 0.27	1.38 ± 0.37	1.25 ± 0.37	1.27 ± 0.58	0.211
hs-CRP (mg/L)	1.32 (0.65,2.30)	1.31 (0.68,2.21)	1.04 (0.59,1.86)	1.42 (0.79,2.54)	1.59 (0.50,2.32)	0.352
UACR (mg/g)	20.00 (4.08,355.48)	3.33 (0.69,9.40)	13.22 (3.95,24.53)	51.48 (5.84,207.18)	734.85 (358.72,1107.01)	<0.001
24h-UTP (mg)	110.24 (60.05,1660.00)	72.81 (60.05,95.26)	87.55 (50.00,143.48)	195.00 (43.53,1082.5)	3680.00 (2255.00,5445.00)	<0.001
CKD stage						
G1 (%) (eGFR≥90)	153 (59.77)	55 (85.94)	51 (79.69)	39 (60.94)	8 (12.50)	<0.001
G2 (%) (60≤eGFR<90)	50 (19.53)	9 (14.06)	13 (20.31)	17 (26.56)	11 (17.19)	0.323
G3 (%) (30≤eGFR <60)	27 (10.55)	0 (0.00)	0 (0.00)	6 (9.38)	21 (32.81)	<0.001
G4 (%) (15≤eGFR<30)	17 (6.64)	0 (0.00)	0 (0.00)	2 (3.12)	15 (23.44)	<0.001

(Continued)

TABLE 3 Continued

Characteristics	Total	Q1 (<15.20)	Q2 (15.20-23.62)	Q3 (23.62-46.12)	Q4 (>46.12)	*p*-value
CKD stage						
G5 (%) (eGFR<15)	9 (3.51)	0 (0.00)	0 (0.00)	0 (0.00)	9 (14.06)	<0.001
Serum HMGB1 (ng/ml)	33.55 ± 25.99	11.19 ± 2.15	18.59 ± 2.35	34.13 ± 6.79	70.27 ± 23.95	<0.001
Urine HMGB1 (pg/ug)	3.77 (2.19,7.93)	2.42 (1.30,4.05)	2.89 (2.07,6.04)	4.92 (2.25,9.63)	7.96 (4.82,12.70)	<0.001
KIM-1/Cr (pg/ug)	0.45 (0.24,0.90)	0.33 (0.22,0.54)	0.33 (0.18,0.50)	0.41 (0.19,1.02)	1.10 (0.66,1.72)	<0.001
TNFR-1 (ng/ml)	2.45 ± 0.76	2.05 ± 0.36	2.25 ± 0.40	2.40 ± 0.52	3.12 ± 1.04	<0.001

BMI, body-mass index; HGB, hemoglobin; HbA1c, glycated haemoglobin A1c; ALT, alanine transaminase; AST, aspartate aminotransferase; ALB, albumin; Scr, serum creatinine; eGFR, estimated glomerular filtration rate; UA, uric acid; TC, total cholesterol; TG, triglycerides; HDL-C, high density lipoprotein cholesterol; LDL-C, low density lipoprotein cholesterol; hs-CRP, high-sensitivity C-reactive protein; UACR, urinary albumin/creatinine ratio; UTP, urinary total protein; HMGB1, high mobility group box protein 1; TNFR-1, tumor necrosis factor receptor superfamily member 1A; KIM-1, kidney injury molecule-1; CVD, cardiovascular diseases; CKD, chronic kidney disease.

3.6 Subgroup and sensitivity analyses

Subgroup analysis showed that the association between HMGB1 and the risk of DKD progression was not significantly affected in the data stratified by age, sex, and BMI. The sensitivity analysis did not reveal substantial changes in the results after excluding participants with CVD, hypertension, and smokers, respectively, indicating that our results are robust.

3.7 Validation set

To validate the role of serum HMGB1, we analyzed the data of 42 participants recruited independently in another center. As shown in Table 6, the study set and validation set had similar baseline characteristics. The median levels of baseline serum HMGB1 were similar in both sets. Similar findings were observed in the validation set: serum HMGB1 levels were also higher in patients with DKD compared with patients with long-term diabetes but without CKD nephropathy or in healthy control people without diabetes (Figure 6A). The calibration plot showed that there was a good fit between the observed and predicted probabilities, and no statistical difference from the perfect fit was found for the study (p=0.202) and the validation set (p=0.825) (Figure 6B). At the same time, according to the above threshold, we also grouped the population whether the serum HMGB1 ≥27 ng/ml. We found that the proportion of DKD was significantly increased (Figure 6C), the level of 24h-UTP and ACR were significantly increased (Figures 6D, E), and the level of GFR was significantly decreased (Figure 6F) in the population with serum HMGB1 ≥27 ng/ml.

4 Discussion

Liquid biopsy is increasingly used for early diagnosis and precision medicine (31), especially for cancer (32). More importantly, advances in omics techniques and computational analysis have increased the sensitivity, specificity, and accuracy of liquid biopsies (33, 34). In kidney disease, the use of this noninvasive fluid biopsy compensates for the risk of bleeding, pain, infection, and renal vein thrombosis associated with invasive kidney biopsy and the limitation of not being able to perform repeat kidney biopsies to monitor disease progression (35). However, for DKD, the number of biomarkers for identifying renal disease progression and poor prognosis remains limited. Therefore, the identification of specific and sensitive biomarkers is essential for

TABLE 4 OR and 95% CI for kidney function decline in each quartile based on univariate and multivariate logistic regression.

Serum HMGB1, ng/ml	Crude		Model 1		Model 2		Model 3	
	OR (95% CI)	*p*-value	OR (95% CI)	*p*-value	OR (95% CI)	*p*-value	OR (95% CI)	*p*-value
Serum HMGB1	1.071 (1.058,1.085)	<0.001	1.070 (1.054,1.086)	<0.001	1.067 (1.050,1.083)	<0.001	1.043 (1.024,1.061)	<0.001
Q1-Q2(<23.62)	1.080 (0.970,1.204)	0.161	1.127 (0.958,1325)	0.150	1.059 (0.886,1.265)	0.532	1.030 (0.848,1.250)	0.769
Q3-Q4(>23.62)	1.062 (1.045,1.080)	<0.001	1.066 (1.046,1.087)	<0.001	1.066 (1.046,1.088)	<0.001	1.047 (1.024,1.069)	<0.001
p for trend	<0.001		<0.001		<0.001		<0.001	

Model 1: adjusted for age, sex, BMI and duration of diabetes.
Model 2: further adjusted for hypertension, hyperlipidemia, CVD and smokers.
Model 3: further adjusted for ALB, UA, KIM-1/Cr, TNFR-1.
BMI, body-mass index; ALB, albumin; UA, uric acid; HMGB1, high mobility group box protein 1; TNFR-1, tumor necrosis factor receptor superfamily member 1A; KIM-1, kidney injury molecule-1; CVD, cardiovascular diseases; DKD, diabetic kidney disease; OR, odds ratio; CI, confidence interval.

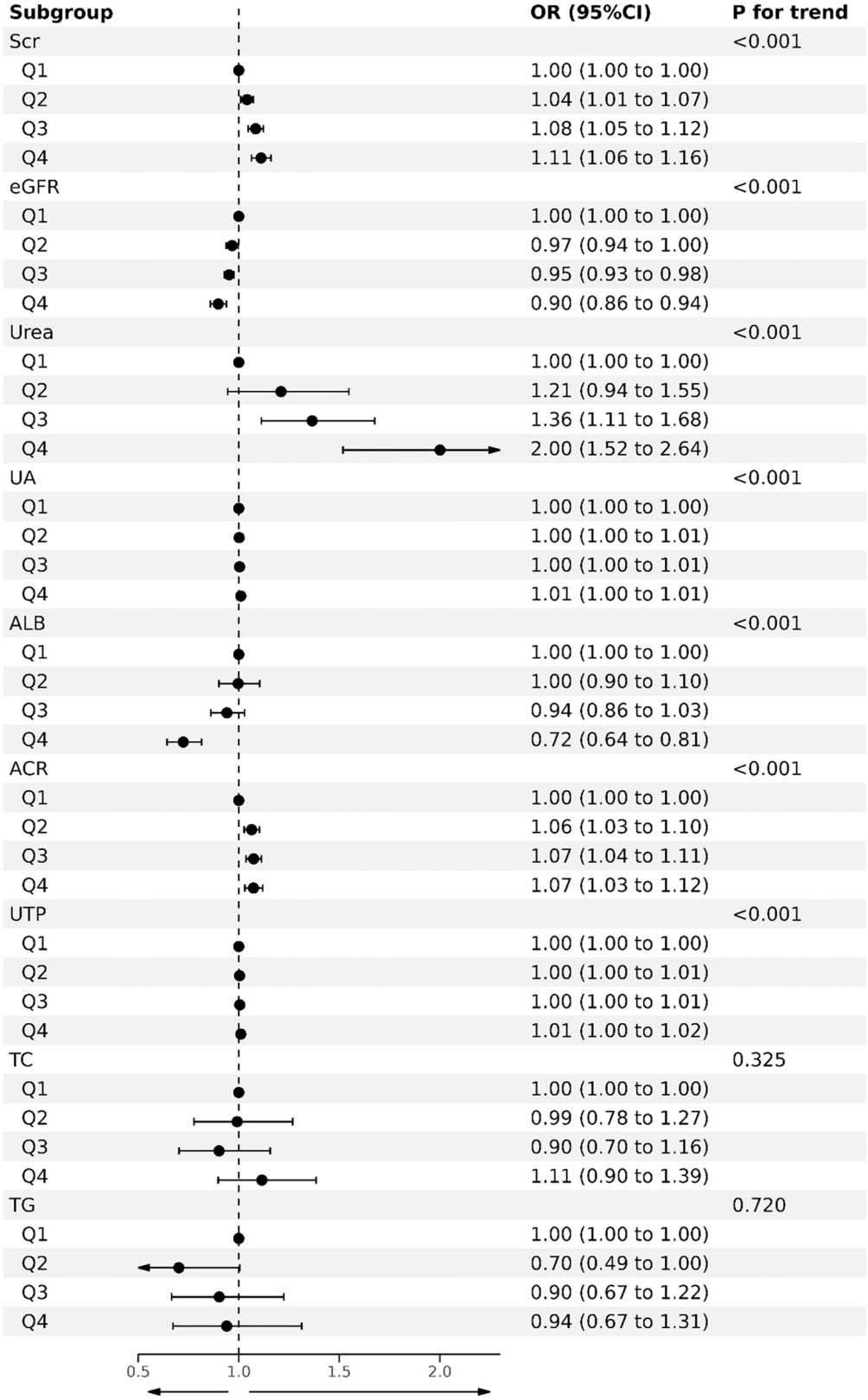

FIGURE 4
Forest plot of quartile of serum HMGB1 levels and DKD-related variables based on logistic regression.

TABLE 5 Effect of standardized serum HMGB1 level on eGFR adjusted coefficients from segmented linear regression analysis.

Characteristic	Serum HMGB1, ng/ml	OR per SD	95% CI	*p*-value
eGFR	< 27	0.82	0.69,0.96	0.017
	≥ 27	0.53	0.46,0.62	<0.001
UACR	< 27	1.51	1.30,1.75	<0.001
	≥ 27	1.62	1.38,1.90	<0.001
UTP	< 27	1.36	1.17,1.57	<0.001
	≥ 27	1.49	1.23,1.80	<0.001

eGFR, estimated glomerular filtration rate; UACR, urinary albumin/creatinine ratio; UTP, urinary total protein; HMGB1, high mobility group box protein 1; OR, odds ratio; CI, confidence interval.
OR were adjusted for sex, hypertension, smokers, duration of diabetes, and age.

early diagnosis and disease management. For example, a urine proteomics-based study found that urinary CKD273, composed of 273 peptides, has great potential for predicting kidney outcomes in diabetes (36, 37). Another study, based on the SOMAscan proteomics platform, screened three proteins (Delta-like 1, endothelial cell adhesion molecule, and mitogen-activated protein kinase 11) as candidate biomarkers for predicting the risk of DKD progression to renal failure (38). Several biomarkers have been reported to increase over time before the onset of albuminuria (39). Therefore, the discovery and identification of additional biomarkers to reliably predict renal function progression in patients with DKD are essential.

In this study, we demonstrated, for the first time, that serum and urine HMGB1 levels were significantly higher in patients with DKD than in T2DM patients without DKD and healthy controls. Serum and urine HMGB1 levels were significantly associated with known markers of renal progression. Serum HMGB1 levels were more effective than urine HMGB1 levels in predicting the occurrence of DKD. Interestingly, on the basis of RCS, we found a nonlinear relationship between serum HMGB1 levels and the progression of renal function in DKD. When the serum HMGB1 was <27 ng/ml, the risk of DKD progression was almost stable and weak. However, when the HMGB1 level was ≥27 ng/ml, the risk of DKD progression increased sharply.

In our study, both age and sex were associated with elevated serum HMGB1 levels. A preclinical study, which supports our findings, reported that HMGB1 expression varied between the sexes in kidney injury and increased more in male rats with kidney injury than in female rats (40). We also found that the expression of serum HMGB1 was associated with smoking. A recent study confirmed our finding that nicotine promoted the release and secretion of HMGB1 by enhancing cathepsin B-dependent NLRP3 inflammasome activation, which led to the disruption of endothelial permeability (41). Additionally, an interesting finding of our study was that the positive correlation between serum HMGB1 and the duration of diabetes may indicate that serum HMGB1 plays a significant role in the underlying mechanisms of diabetes-induced renal disease. As previously discussed, HMGB1 may play a more indispensable role in chronic diseases than in acute lesions (20), although extracellular HMGB1 levels can change at the moment of injury. A preclinical study also found that in the early stage after unilateral ureteral obstruction, renal tubular HMGB1 deletion had no obvious effect on renal injury, but it can significantly reduce renal interstitial fibrosis in the late/subacute stage (42). As described in our study and the literature, serum HMGB1 plays an important role in DKD, emphasizing the importance of serum HMGB1 as a biomarker for the occurrence and progression of DKD.

HMGB1 is a member of the family of high-mobility proteins with secretory and intracellular activities (43). As a DNA chaperone, autophagy regulator, and damage-associated molecular pattern (DAMPs), HMGB1 is ubiquitously expressed in almost all cell types and plays an important role in DNA repair, telomere maintenance, autophagy homeostasis, and immune regulation (44, 45). HMGB1, as a biomarker and drug target, is related to the progression of many diseases (46, 47). In kidney disease, serum HMGB1 levels are significantly elevated and show differences in different pathologies. Elevated serum HMGB1 levels are associated with renal function progression and risks of inflammation, malnutrition, and cardiovascular disease in patients with CKD (48, 49). Similarly, serum and urine HMGB1 levels have been found to be associated with disease activity and renal involvement in patients with systemic lupus erythematosus (50, 51). Interestingly, serum HMGB1 levels have also been found to be independently associated with coronary artery disease and carotid plaque susceptibility in diabetic populations (52, 53). On the basis of

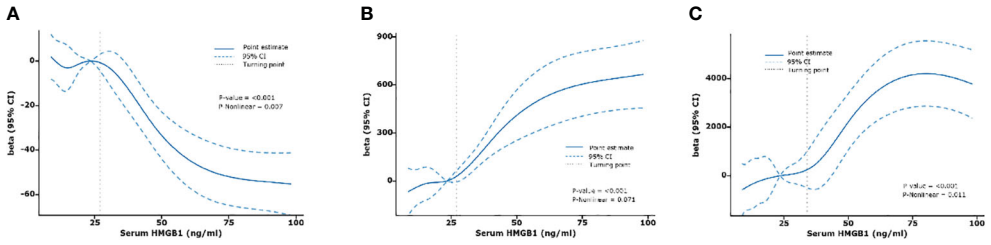

FIGURE 5
Relationships between serum HMGB1 and renal function fitted with restricted cubic spline (RCS) models. The solid lines indicate multivariate-adjusted Betas, and dotted lines indicate the 95% CIs derived from restricted cubic spline regression. Adjusted for age, sex, hypertension, smokers, and duration of diabetes. **(A)** serum HMGB1 and eGFR, **(B)** serum HMGB1 and UACR, **(C)** serum HMGB1 and UTP.

TABLE 6 Baseline characteristics of participants included in the validation set compared to the study set.

Characteristics	Study set (n=256)	Validation set (n=42)	*p*-value
DKD (%)	109 (42.58)	22 (52.38)	0.235
Age (years)	57.71 ± 9.69	59.05 ± 8.45	0.400
Male (%)	130 (50.78)	25 (59.52)	0.293
BMI (kg/m^2)	24.70 ± 3.36	24.96 ± 3.96	0.657
Duration of diabetes (years)	12.30 ± 8.06	11.20 ± 8.90	0.454
Hypertension (%)	143 (55.86)	30 (71.42)	0.058
CVD (%)	86 (33.59)	10 (23.81)	0.209
Hyperlipidemia (%)	122 (46.48)	28 (83.33)	0.022
Smokers (%)	52 (20.31)	10 (23.81)	0.605
Drinkers (%)	55 (21.48)	6 (15.00)	0.346
HGB (g/L)	132.09 ± 20.44	133.62 ± 17.80	0.648
HbA1c (%)	7.47 ± 1.91	7.63 ± 1.77	0.627
ALT (U/L)	18.00 (14.00,27.00)	18.00 (13.00,22.00)	0.787
AST (U/L)	19.00 (15.93,23.45)	17.00 (13.60,20.00)	0.076
ALB (g/L)	41.26 ± 5.71	40.37 ± 6.30	0.360
Scr (μmol/L)	98.57 ± 87.03	107.15 ± 89.78	0.556
eGFR (ml/min/1.73m^2)	82.93 ± 30.66	77.81 ± 26.62	0.319
Urea (mmol/L)	8.07 ± 6.56	8.30 ± 4.42	0.824
UA (μmol/L)	344.98 ± 87.87	364.61 ± 83.74	0.178
TC (mmol/L)	4.95 ± 1.49	4.70 ± 1.05	0.313
TG (mmol/L)	1.78 ± 1.01	1.72 ± 0.82	0.735
LDL-C (mmol/L)	2.97 ± 1.02	2.97 ± 0.97	0.984
HDL-C (mmol/L)	1.28 ± 0.42	1.34 ± 0.40	0.426
UACR (mg/g)	20.00 (4.08,355.48)	25.00 (3.61,428.32)	0.761
24h-UTP (mg/24h)	110.24 (60.05,1660.00)	350.00 (30.00,1720.00)	0.216
Serum HMGB1 (ng/ml)	33.55 ± 25.99	30.72 ± 23.21	0.513
KIM-1/Cr (pg/ug)	0.45 (0.24,0.90)	0.50 (0.28,0.89)	0.509
TNFR-1 (ng/ml)	2.45 ± 0.76	2.26 ± 0.49	0.108

this evidence, we explored the association between HMGB1 and DKD in a population with diabetes. This study found, for the first time, that the serum and urine levels of HMGB1 in patients with DKD were significantly higher than those in the non-DKD diabetic and healthy control populations (2.5–10 times), and with the aggravation of DKD, serum HMGB1 levels increased significantly and was positively correlated with the serum TNFR-1 level. In summary, serum HMGB1 may reflect the regulatory response of the inflammatory state during DKD pathogenesis, and can be used as a potential marker for the prediction of DKD, which is helpful for the diagnosis and targeted treatment of DKD.

Based on the above evidence, we hypothesized several main reasons why serum HMGB1 could be used as a biomarker of DKD progression. First, HMGB1 promotes renal inflammation by recruiting immune cells and activating the nuclear factor-kB pathway, which in turn mediates the apoptosis of glomerular cells and deposition of the mesangial matrix, thereby aggravating proteinuria and glomerulosclerosis. On the other hand, circulating HMGB1 exacerbates renal fibrosis by promoting renal epithelial cell and macrophage trans-differentiation, thereby promoting renal disease progression. Hence, we hypothesized that elevated serum HMGB1 levels may reflect a persistent chronic inflammatory state in DKD. However, the detailed origin of circulating HMGB1 in DKD cannot be determined. Studies have shown that renal tubular cells and podocytes are the main sources of HMGB1 secretion in the kidneys (54). There is evidence that receptor of advanced glycation endproducts (RAGE) is the primary receptor for HMGB1, and deletion of bone marrow-derived RAGE was shown to improve renal function in a DKD mouse model (55). On the other hand, studies have shown that splenectomy can transiently reduce circulating HMGB1 levels, which in turn improves CKD (56). The current results do not explain the origin of HMGB1 in DKD in detail. This is critical for targeted therapy of DKD, and further research should be conducted to investigate this issue.

Notably, HMGB1 can be neutralized or inhibited by polypeptides, natural products, or small molecules, and exhibits potential benefits in the treatment of various diseases (57–59). Additionally, studies have shown that serum HMGB1 levels are associated with disease treatment outcomes and that high levels of HMGB1 may indicate greater sensitivity to drugs (60). Interestingly, despite increased renal tissue expression and serum HMGB1 levels in lupus nephritis, HMGB1 expression in the serum and tissues did not decrease after immunosuppressive therapy (61). These studies' findings suggest that HMGB1 plays a complex role in the treatment of different diseases; however, the changes in HMGB1 during DKD treatment and their correlation with treatment effects remain unknown. Here, although we observed elevated levels of HMGB1 in the serum and urine of patients with DKD, we lacked follow-up information on patients after treatment. Therefore, we could not confirm a causal relationship between HMGB1 and DKD or the exact mechanism by which HMGB1 affects DKD. Therefore, future studies should focus on changes in HMGB1 levels before and after treatment, which will help in the treatment and management of DKD.

This was a preliminary study showing a correlation between elevated serum HMGB1 levels and DKD progression. However, this study has some limitations that must be addressed. First, this was a

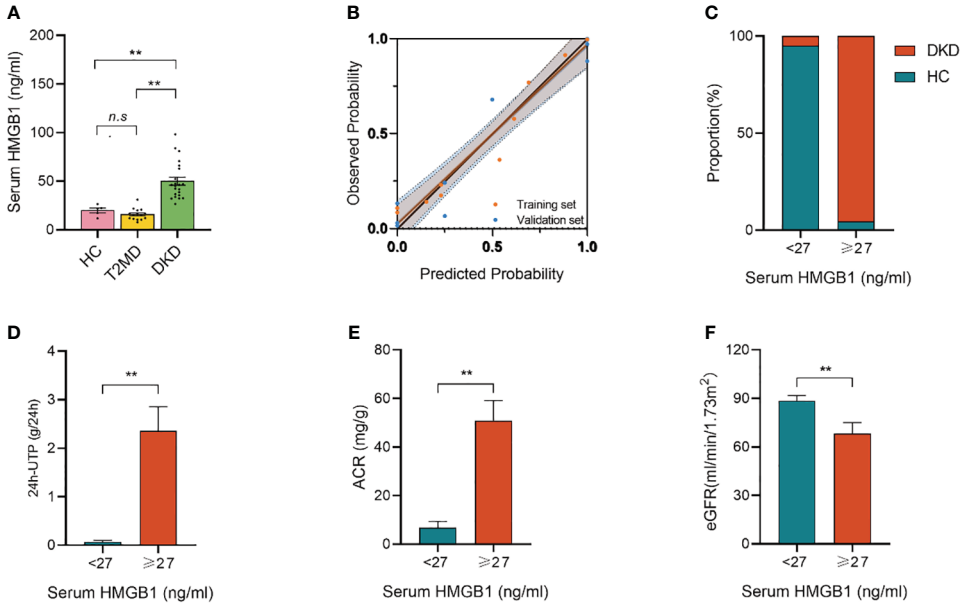

FIGURE 6
Validation set from another independent center. **(A)** serum HMGB1 levels in different groups; **(B)** Calibration plot comparing the observed and predicted probabilities for kidney function decline from the logistic regression for the study and validation set; **(C)** Proportion of DKD population with serum HMGB1 ≥27 ng/ml or <27 ng/ml; **(D)** 24h-UTP levels in serum HMGB1 ≥27 ng/ml or <27 ng/ml; **(E)** ACR levels in serum HMGB1 ≥27 ng/ml or <27 ng/ml; **(F)** eGFR levels in serum HMGB1 ≥27 ng/ml or <27 ng/ml. **P < 0.01, n.s. = no significance.

cross-sectional study, and we did not perform continuous HMGB1 measurements and long-term follow-up of the kidneys; therefore, we could not determine the causal relationship between HMGB1 and disease and the response of HMGB1 in DKD after drug treatment. Thus, a cohort study to explore whether improving serum HMGB1 levels through pharmacological targeting will affect the prognosis of DKD would be a better option to reflect the true relationship between HMGB1 and DKD and evaluate its predictive value. Second, the study population was derived from only two centers; therefore, the results should be validated in more central studies. Finally, the study population included only adults from China; thus, this association should be confirmed in other ethnic and age groups.

5 Conclusions

In conclusion, this is the first study to report that serum and urine HMGB1 levels are significantly increased in patients with DKD and are closely related to disease progression and renal inflammation. When the serum HMGB1 was ≥27 ng/ml, the risk of DKD progression increased sharply, suggesting that serum HMGB1 could be used as a potential biomarker for the progression of DKD. Further research on the detailed role of HMGB1 in the pathogenesis of DKD is required to guide its clinical treatment and management.

Data availability statement

The raw data supporting the conclusions of this article will be made available by the authors, without undue reservation.

Ethics statement

The studies involving humans were approved by Ethics Committee of Guang'anmen Hospital of the Chinese Academy of Traditional Chinese Medicine and China-Japan Friendship Hospital. The studies were conducted in accordance with the local legislation and institutional requirements. The participants provided their written informed consent to participate in this study.

Author contributions

TL: Data curation, Formal analysis, Investigation, Software, Visualization, Writing – original draft, Writing – review & editing. HZ: Data curation, Writing – original draft. YW: Data curation, Formal Analysis, Investigation, Writing – original draft. PQ: Data curation, Methodology, Writing – original draft. YMW: Data curation, Methodology, Writing – original draft. XW: Data curation, Investigation, Writing – original draft. TZ: Data curation,

Formal analysis, Project administration, Writing – original draft. LY: Data curation, Methodology, Writing – review & editing. HM: Data curation, Formal analysis, Writing – review & editing. LP: Conceptualization, Writing – review & editing. YZ: Conceptualization, Funding acquisition, Writing – review & editing. PL: Funding acquisition, Supervision, Writing – review & editing.

Funding

The author(s) declare financial support was received for the research, authorship, and/or publication of this article. This study was supported by the National Nature Science Foundation of China (82374419, 82174296, 82074393, 82305210).

Conflict of interest

The authors declare that the research was conducted in the absence of any commercial or financial relationships that could be construed as a potential conflict of interest.

Publisher's note

References

1. Koye DN, Shaw JE, Reid CM, Atkins RC, Reutens AT, Magliano DJ. Incidence of chronic kidney disease among people with diabetes: a systematic review of observational studies. *Diabetes Med.* (2017) 34:887–901. doi: 10.1111/dme.13324

2. Kalantar-Zadeh K, Jafar TH, Nitsch D, Neuen BL, Perkovic V. Chronic kidney disease. *Lancet.* (2021) 398:786–802. doi: 10.1016/S0140-6736(21)00519-5

3. Alicic RZ, Rooney MT, Tuttle KR. Diabetic kidney disease: challenges, progress, and possibilities. *Clin J Am Soc Nephrol.* (2017) 12:2032–45. doi: 10.2215/CJN.11491116

4. Macisaac RJ, Ekinci EI, Jerums G. Markers of and risk factors for the development and progression of diabetic kidney disease. *Am J Kidney Dis.* (2014) 63:S39–62. doi: 10.1053/j.ajkd.2013.10.048

5. Anders HJ, Huber TB, Isermann B, Schiffer M. CKD in diabetes: diabetic kidney disease versus nondiabetic kidney disease. *Nat Rev Nephrol.* (2018) 14:361–77. doi: 10.1038/s41581-018-0001-y

6. Tuttle KR, Agarwal R, Alpers CE, Bakris GL, Brosius FC, Kolkhof P, et al. Molecular mechanisms and therapeutic targets for diabetic kidney disease. *Kidney Int.* (2022) 102:248–60. doi: 10.1016/j.kint.2022.05.012

7. Perkins BA, Ficociello LH, Ostrander BE, Silva KH, Weinberg J, Warram JH, et al. Microalbuminuria and the risk for early progressive renal function decline in type 1 diabetes. *J Am Soc Nephrol.* (2007) 18:1353–61. doi: 10.1681/ASN.2006080872

8. MacIsaac RJ, Ekinci EI, Jerums G. 'Progressive diabetic nephropathy. How useful is microalbuminuria?: contra'. *Kidney Int.* (2014) 86:50–7. doi: 10.1038/ki.2014.98

9. MacIsaac RJ, Ekinci EI. Progression of diabetic kidney disease in the absence of albuminuria. *Diabetes Care.* (2019) 42:1842–4. doi: 10.2337/dci19-0030

10. Skupien J, Smiles AM, Valo E, Ahluwalia TS, Gyorgy B, Sandholm N, et al. Variations in risk of end-stage renal disease and risk of mortality in an international study of patients with type 1 diabetes and advanced nephropathy. *Diabetes Care.* (2019) 42:93–101. doi: 10.2337/dc18-1369

11. Rossing K, Christensen PK, Hovind P, Tarnow L, Rossing P, Parving HH. Progression of nephropathy in type 2 diabetic patients. *Kidney Int.* (2004) 66:1596–605. doi: 10.1111/j.1523-1755.2004.00925.x

12. Gutiérrez OM, Shlipak MG, Katz R, Waikar SS, Greenberg JH, Schrauben SJ, et al. Associations of plasma biomarkers of inflammation, fibrosis, and kidney tubular injury with progression of diabetic kidney disease: A cohort study. *Am J Kidney Dis.* (2022) 79:849–857.e841. doi: 10.1053/j.ajkd.2021.09.018

13. Khanijou V, Zafari N, Coughlan MT, MacIsaac RJ, Ekinci EI. Review of potential biomarkers of inflammation and kidney injury in diabetic kidney disease. *Diabetes Metab Res Rev.* (2022) 38:e3556. doi: 10.1002/dmrr.3556

14. Pichler R, Afkarian M, Dieter BP, Tuttle KR. Immunity and inflammation in diabetic kidney disease: translating mechanisms to biomarkers and treatment targets. *Am J Physiol Renal Physiol.* (2017) 312:F716–f731. doi: 10.1152/ajprenal.00314.2016

15. Niewczas MA, Pavkov ME, Skupien J, Smiles A, Md Dom ZI, Wilson JM, et al. A signature of circulating inflammatory proteins and development of end-stage renal disease in diabetes. *Nat Med.* (2019) 25:805–13. doi: 10.1038/s41591-019-0415-5

16. Waijer SW, Sen T, Arnott C, Neal B, Kosterink JGW, Mahaffey KW, et al. Association between TNF receptors and KIM-1 with kidney outcomes in early-stage diabetic kidney disease. *Clin J Am Soc Nephrol.* (2022) 17:251–9. doi: 10.2215/CJN.08780621

17. Fan Y, Ye Z, Tang Y. Serum HMGB1 and soluble urokinase plasminogen activator receptor levels aid diagnosis and prognosis prediction of sepsis with acute respiratory distress syndrome. *biomark Med.* (2023) 17:231–9. doi: 10.2217/bmm-2022-0899

18. Goldstein RS, Bruchfeld A, Yang L, Qureshi AR, Gallowitsch-Puerta M, Patel NB, et al. Cholinergic anti-inflammatory pathway activity and High Mobility Group Box-1 (HMGB1) serum levels in patients with rheumatoid arthritis. *Mol Med.* (2007) 13:210–5. doi: 10.2119/2006-00108.Goldstein

19. Zhu B, Zhu Q, Li N, Wu T, Liu S, Liu S. Association of serum/plasma high mobility group box 1 with autoimmune diseases: A systematic review and meta-analysis. *Med (Baltimore).* (2018) 97:e11531. doi: 10.1097/MD.0000000000011531

20. Liu T, Li Q, Jin Q, Yang L, Mao H, Qu P, et al. Targeting HMGB1: A potential therapeutic strategy for chronic kidney disease. *Int J Biol Sci.* (2023) 19:5020–35. doi: 10.7150/ijbs.87964

21. Hossny E, El-Ghoneimy D, Soliman DA, Ashour A. Diagnostic value of serum high-mobility group box-1 in pediatric systemic lupus erythematosus. *Int J Rheum Dis.* (2019) 22:1402–9. doi: 10.1111/1756-185X.13556

22. Nakamura T, Sato E, Fujiwara N, Kawagoe Y, Ueda Y, Suzuki T, et al. Positive association of serum levels of advanced glycation end products and high mobility group box-1 with asymmetric dimethylarginine in nondiabetic chronic kidney disease patients. *Metabolism.* (2009) 58:1624–8. doi: 10.1016/j.metabol.2009.05.018

23. Burbano C, Gómez-Puerta JA, Muñoz-Vahos C, Vanegas-García A, Rojas M, Vásquez G, et al. HMGB1(+) microparticles present in urine are hallmarks of nephritis in patients with systemic lupus erythematosus. *Eur J Immunol.* (2019) 49:323–35. doi: 10.1002/eji.201847747

24. 2. Classification and diagnosis of diabetes. *Diabetes Care.* (2016) 39 Suppl 1:S13–22. doi: 10.2337/dc16-S005

25. Tuttle KR, Bakris GL, Bilous RW, Chiang JL, de Boer IH, Goldstein-Fuchs J, et al. Diabetic kidney disease: a report from an ADA Consensus Conference. *Am J Kidney Dis.* (2014) 64:510–33. doi: 10.1053/j.ajkd.2014.08.001

26. Doshi SM, Friedman AN. Diagnosis and management of type 2 diabetic kidney disease. *Clin J Am Soc Nephrol.* (2017) 12:1366–73. doi: 10.2215/CJN.11111016

27. KDIGO clinical practice guideline for the diagnosis, evaluation, prevention, and treatment of Chronic Kidney Disease-Mineral and Bone Disorder (CKD-MBD). *Kidney Int Suppl.* (2009) 113):S1–130. doi: 10.1038/ki.2009.188

28. Durrleman S, Simon R. Flexible regression models with cubic splines. *Stat Med.* (1989) 8:551–61. doi: 10.1002/sim.4780080504

29. Coca SG, Nadkarni GN, Huang Y, Moledina DG, Rao V, Zhang J, et al. Plasma biomarkers and kidney function decline in early and established diabetic kidney disease. *J Am Soc Nephrol.* (2017) 28:2786–93. doi: 10.1681/ASN.2016101101

30. Liu C, Debnath N, Mosoyan G, Chauhan K, Vasquez-Rios G, Soudant C, et al. Systematic review and meta-analysis of plasma and urine biomarkers for CKD outcomes. *J Am Soc Nephrol.* (2022) 33:1657–72. doi: 10.1681/ASN.2022010098

31. Ignatiadis M, Sledge GW, Jeffrey SS. Liquid biopsy enters the clinic - implementation issues and future challenges. *Nat Rev Clin Oncol.* (2021) 18:297–312. doi: 10.1038/s41571-020-00457-x

32. Rolfo C, Russo A. Moving forward liquid biopsy in early liver cancer detection. *Cancer Discovery.* (2023) 13:532–4. doi: 10.1158/2159-8290.CD-22-1439

33. Brown MA, Li Z, Cao KL. Biomarker development for axial spondyloarthritis. *Nat Rev Rheumatol*. (2020) 16:448–63. doi: 10.1038/s41584-020-0450-0

34. Mann M, Kumar C, Zeng WF, Strauss MT. Artificial intelligence for proteomics and biomarker discovery. *Cell Syst*. (2021) 12:759–70. doi: 10.1016/j.cels.2021.06.006

35. Siwy J, Mischak H, Beige J, Rossing P, Stegmayr B. Biomarkers for early detection of kidney disease: a call for pathophysiological relevance. *Kidney Int*. (2021) 99:1240–1. doi: 10.1016/j.kint.2021.02.008

36. Currie GE, von Scholten BJ, Mary S, Flores Guerrero JL, Lindhardt M, Reinhard H, et al. Urinary proteomics for prediction of mortality in patients with type 2 diabetes and microalbuminuria. *Cardiovasc Diabetol*. (2018) 17:50. doi: 10.1186/s12933-018-0697-9

37. Lindhardt M, Persson F, Zürbig P, Stalmach A, Mischak H, de Zeeuw D, et al. Urinary proteomics predict onset of microalbuminuria in normoalbuminuric type 2 diabetic patients, a sub-study of the DIRECT-Protect 2 study. *Nephrol Dial Transplant*. (2017) 32:1866–73. doi: 10.1093/ndt/gfw292

38. Kobayashi H, Looker HC, Satake E, Saulnier PJ, Md Dom ZI, O'Neil K, et al. Results of untargeted analysis using the SOMAscan proteomics platform indicates novel associations of circulating proteins with risk of progression to kidney failure in diabetes. *Kidney Int*. (2022) 102:370–81. doi: 10.1016/j.kint.2022.04.022

39. Colombo M, McGurnaghan SJ, Blackbourn LAK, Dalton RN, Dunger D, Bell S, et al. Comparison of serum and urinary biomarker panels with albumin/creatinine ratio in the prediction of renal function decline in type 1 diabetes. *Diabetologia*. (2020) 63:788–98. doi: 10.1007/s00125-019-05081-8

40. Mohamed R, Rafikova O, O'Connor PM, Sullivan JC. Greater high-mobility group box 1 in male compared with female spontaneously hypertensive rats worsens renal ischemia-reperfusion injury. *Clin Sci (Lond)*. (2020) 134:1751–62. doi: 10.1042/CS20200575

41. Mohammadi L, Han DD, Xu F, Huang A, Derakhshandeh R, Rao P, et al. Chronic E-cigarette use impairs endothelial function on the physiological and cellular levels. *Arterioscler Thromb Vasc Biol*. (2022) 42:1333–50. doi: 10.1161/ATVBAHA.121.317749

42. Li Y, Yuan Y, Huang ZX, Chen H, Lan R, Wang Z, et al. GSDME-mediated pyroptosis promotes inflammation and fibrosis in obstructive nephropathy. *Cell Death Differ*. (2021) 28:2333–50. doi: 10.1038/s41418-021-00755-6

43. Chen R, Kang R, Tang D. The mechanism of HMGB1 secretion and release. *Exp Mol Med*. (2022) 54:91–102. doi: 10.1038/s12276-022-00736-w

44. Tang D, Kang R, Zeh HJ, Lotze MT. The multifunctional protein HMGB1: 50 years of discovery. *Nat Rev Immunol*. (2023) 23(12):824–841. doi: 10.1038/s41577-023-00894-6

45. Kang R, Chen R, Zhang Q, Hou W, Wu S, Cao L, et al. HMGB1 in health and disease. *Mol Aspects Med*. (2014) 40:1–116. doi: 10.1016/j.mam.2014.05.001

46. Dong H, Zhang L, Liu S. Targeting HMGB1: an available therapeutic strategy for breast cancer therapy. *Int J Biol Sci*. (2022) 18:3421–34. doi: 10.7150/ijbs.73504

47. Pellegrini L, Foglio E, Pontemezzo E, Germani A, Russo MA, Limana F. HMGB1 and repair: focus on the heart. *Pharmacol Ther*. (2019) 196:160–82. doi: 10.1016/j.pharmthera.2018.12.005

48. Bruchfeld A, Qureshi AR, Lindholm B, Barany P, Yang L, Stenvinkel P, et al. High Mobility Group Box Protein-1 correlates with renal function in chronic kidney disease (CKD). *Mol Med*. (2008) 14:109–15. doi: 10.2119/2007-00107.Bruchfeld

49. Jin X, Rong S, Yuan W, Gu L, Jia J, Wang L, et al. High mobility group box 1 promotes aortic calcification in chronic kidney disease via the wnt/β-catenin pathway. *Front Physiol*. (2018) 9. doi: 10.3389/fphys.2018.00665

50. Abdulahad DA, Westra J, Bijzet J, Dolff S, van Dijk MC, Limburg PC, et al. Urine levels of HMGB1 in Systemic Lupus Erythematosus patients with and without renal manifestations. *Arthritis Res Ther*. (2012) 14:R184. doi: 10.1186/ar4015

51. Jog NR, Blanco I, Lee I, Putterman C, Caricchio R. Urinary high-mobility group box-1 associates specifically with lupus nephritis class V. *Lupus*. (2016) 25:1551–7. doi: 10.1177/0961203316644331

52. Yan XX, Lu L, Peng WH, Wang LJ, Zhang Q, Zhang RY, et al. Increased serum HMGB1 level is associated with coronary artery disease in nondiabetic and type 2 diabetic patients. *Atherosclerosis*. (2009) 205:544–8. doi: 10.1016/j.atherosclerosis.2008.12.016

53. Biscetti F, Tinelli G, Rando MM, Nardella E, Cecchini AL, Angelini F, et al. Association between carotid plaque vulnerability and high mobility group box-1 serum levels in a diabetic population. *Cardiovasc Diabetol*. (2021) 20:114. doi: 10.1186/s12933-021-01304-8

54. Zhao ZB, Marschner JA, Iwakura T, Li C, Motrapu M, Kuang M, et al. Tubular epithelial cell HMGB1 promotes AKI-CKD transition by sensitizing cycling tubular cells to oxidative stress: A rationale for targeting HMGB1 during AKI recovery. *J Am Soc Nephrol*. (2023) 34:394–411. doi: 10.1681/ASN.0000000000000024

55. Tesch G, Sourris KC, Summers SA, McCarthy D, Ward MS, Borg DJ, et al. Deletion of bone-marrow-derived receptor for AGEs (RAGE) improves renal function in an experimental mouse model of diabetes. *Diabetologia*. (2014) 57:1977–85. doi: 10.1007/s00125-014-3291-z

56. Leelahavanichkul A, Huang Y, Hu X, Zhou H, Tsuji T, Chen R, et al. Chronic kidney disease worsens sepsis and sepsis-induced acute kidney injury by releasing High Mobility Group Box Protein-1. *Kidney Int*. (2011) 80:1198–211. doi: 10.1038/ki.2011.261

57. VanPatten S, Al-Abed Y. High mobility group box-1 (HMGb1): current wisdom and advancement as a potential drug target. *J Med Chem*. (2018) 61:5093–107. doi: 10.1021/acs.jmedchem.7b01136

58. Xue J, Suarez JS, Minaai M, Li S, Gaudino G, Pass HI, et al. HMGB1 as a therapeutic target in disease. *J Cell Physiol*. (2021) 236:3406–19. doi: 10.1002/jcp.30125

59. Yang H, Wang H, Andersson U. Targeting inflammation driven by HMGB1. *Front Immunol*. (2020) 11:484. doi: 10.3389/fimmu.2020.00484

60. Li Z, Fu WJ, Chen XQ, Wang S, Deng RS, Tang XP, et al. Autophagy-based unconventional secretion of HMGB1 in glioblastoma promotes chemosensitivity to temozolomide through macrophage M1-like polarization. *J Exp Clin Cancer Res*. (2022) 41:74. doi: 10.1186/s13046-022-02291-8

61. Zickert A, Palmblad K, Sundelin B, Chavan S, Tracey KJ, Bruchfeld A, et al. Renal expression and serum levels of high mobility group box 1 protein in lupus nephritis. *Arthritis Res Ther*. (2012) 14:R36. doi: 10.1186/ar3747

frontiers | Frontiers in Immunology

TYPE Review
PUBLISHED 13 March 2024
DOI 10.3389/fimmu.2024.1333170

OPEN ACCESS

EDITED BY
Xu-jie Zhou,
Peking University, China

REVIEWED BY
InKyeom Kim,
Kyungpook National University, Republic of Korea
Alexandre A. da Silva,
University of Mississippi Medical Center, United States

*CORRESPONDENCE
Ke-zhen Yang
ykz1996@zju.edu.cn
Jun Wang
wangjunee@yeah.net
Qing-guo Liu
liuqingguo888@vip.sina.com

†These authors have contributed equally to this work and share first authorship

RECEIVED 04 November 2023
ACCEPTED 15 February 2024
PUBLISHED 13 March 2024

CITATION
Hao X-m, Liu Y, Hailaiti D, Gong Y, Zhang X-d, Yue B-n, Liu J-p, Wu X-l, Yang K-z, Wang J and Liu Q-g (2024) Mechanisms of inflammation modulation by different immune cells in hypertensive nephropathy.
Front. Immunol. 15:1333170.
doi: 10.3389/fimmu.2024.1333170

Mechanisms of inflammation modulation by different immune cells in hypertensive nephropathy

Xiao-min Hao[1†], Yu Liu[1†], Dilizhawaer Hailaiti[2], Yu Gong[3], Xu-dong Zhang[4], Bing-nan Yue[3], Ji-peng Liu[3], Xiao-li Wu[3], Ke-zhen Yang[5*], Jun Wang[1*] and Qing-guo Liu[3*]

[1]Dongzhimen Hospital, Beijing University of Chinese Medicine, Beijing, China, [2]School of Basic Medicine, Xinjiang Second Medical College, Karamay, China, [3]School of Acupuncture-Moxibustion and Tuina, Beijing University of Chinese Medicine, Beijing, China, [4]Department of Chinese Medicine, Beijing Jishuitan Hospital, Beijing, China, [5]Department of Rehabilitation Medicine, Sir Run Shaw Hospital, Zhejiang University School of Medicine, Hangzhou, China

Hypertensive nephropathy (HTN) is the second leading cause of end-stage renal disease (ESRD) and a chronic inflammatory disease. Persistent hypertension leads to lesions of intrarenal arterioles and arterioles, luminal stenosis, secondary ischemic renal parenchymal damage, and glomerulosclerosis, tubular atrophy, and interstitial fibrosis. Studying the pathogenesis of hypertensive nephropathy is a prerequisite for diagnosis and treatment. The main cause of HTN is poor long-term blood pressure control, but kidney damage is often accompanied by the occurrence of immune inflammation. Some studies have found that the activation of innate immunity, inflammation and acquired immunity is closely related to the pathogenesis of HTN, which can cause damage and dysfunction of target organs. There are more articles on the mechanism of diabetic nephropathy, while there are fewer studies related to immunity in hypertensive nephropathy. This article reviews the mechanisms by which several different immune cells and inflammatory cytokines regulate blood pressure and renal damage in HTN. It mainly focuses on immune cells, cytokines, and chemokines and inhibitors. However, further comprehensive and large-scale studies are needed to determine the role of these markers and provide effective protocols for clinical intervention and treatment.

KEYWORDS

hypertensive nephropathy, hypertension, immunity, inflammation, cytokines

1 Introduction

Hypertension is a major public health concern (1), affecting approximately 30% of adults. It is a major contributor to cardiovascular disease morbidity and mortality (2) and is strongly associated with chronic kidney disease(CKD) (3–7). The global prevalence of hypertension-induced chronic CKD exceeds 23.6 million,is characterized by a high degree of hypertension, and severely affects the patient's quality of life (8, 9). As hypertension progresses, it eventually leads to hypertensive nephropathy(HTN) with irreversible glomerular injury, glomerulosclerosis, tubular atrophy, and interstitial fibrosis (10, 11), which is the second leading cause of end-stage renal disease (12). According to previous studies, the treatment of HTN is relatively limited to controlling blood pressure and regulating lifestyle habits (13, 14). Once the patient develops end-stage renal disease(ESRD), blood pressure control program should be implemented. Notably, dialysis and kidney transplantation are the only available approaches (15), and the treatment of HTN and ESRD is limited. In addition, the incidence of HTN and ESRD is expected to increase in the coming decades (16), placing a heavy burden on healthcare resources.

HTN is first diagnosed based on hypertension and CKD; however, secondary hypertension must be excluded. Hypertension affects the renal vasculature, glomeruli, and tubular interstitium. In general, renal immune cell aggregation promotes an immune-inflammatory response, which in turn disrupts renal blood pressure regulation. Although a large number of studies have been published on HTN in the past, the pathogenesis of hypertension and HTN remains unclear, despite the prevalence of hypertension and associated CKD. Hypertension is closely associated with a continuously activated immune system, which can cause target organ damage and dysfunction, eventually leading to the development of complications such as HTN (17) (Figure 1). The first step in innate immune activation that causes hypertension is the pathogen recognition receptor (PRR), which senses a pathogen-associated molecular pattern (PAMP) or damage-associated molecular pattern (DAMP) from stressed or injured tissues and is thus activated to initiate host defense and inflammation (18). Determining the mechanisms by which different immune cells and their subtypes regulate inflammation could help identify new strategies for treating this disease and preventing its progression.

2 Relationship between hypertension and kidney disease

Renal injury is a common complication of essential hypertension and is most commonly observed 5–10 years after the onset of hypertension (19). It is also a major cause of kidney disease deterioration. Blood pressure affects the course of kidney disease. A study evaluating ambulatory blood pressure in African Americans found that occult hypertension may be associated with the development of chronic kidney disease (20). Further, insidious hypertension may be associated with the onset of CKD (20). This suggests that regulating blood pressure reduces the risk of hypertension and is also a key factor in reducing the cardiovascular burden of kidney disease (21).

The pathogenesis of CKD is complex, encompassing vascular, glomerular, and tubulointerstitial injuries, and is influenced by environmental and genetic factors, including the severity and duration of hypertension. Remodeling small input arteries is a hallmark of HTN in humans.Hypertension leads to injury and subsequent apoptosis of podocytes, which form the final filtration barrier of the glomerulus, ultimately leading to glomerulosclerosis (22–25).

2.1 Small vessel injury

The progression of hypertension leads to changes in small arteries, resulting in intraglomerular hemodynamics changes. A clinical study found that hypertension combined with renal small artery hyalinosis was closely associated with proteinuria and that the accumulation of hyalinized material in the small renal arteries was more likely to lead to hypertensive kidney damage (26). Renal sympathetic nerve activity is usually increased in pathophysiological conditions such as hypertension and chronic and ESRD. Numerous studies (27) have confirmed that elevated sympathetic nerve levels in patients with hypertension lead to deterioration of renal function and abnormal cardiovascular homeostasis due to activation of the renin–angiotensin system (RAS) and renal vascular injury (28, 29). Angiotensin II (Ang II) is most closely related to the RAS (30). Once hypertension occurs, the RAS becomes hyperactivated *in vivo*, potentially leading to glomerulosclerosis and interstitial fibrosis (31). Overproduction of Ang II in the kidney directly constricts vascular endothelial cells (ECs), causing changes in diastolic and contractile substances that are involved in hypertension and kidney injury. In hypertensive rats, the miRNA-mediated mTOR signaling pathway may play a role in Ang II-induced renal artery endothelial cell injury by driving glycolysis and activating autophagy (32).

2.2 Glomerular injury

Glomerular injury is a prominent feature of hypertensive nephropathy (33). Any change primarily involving small blood vessels eventually translates into glomerular injury (24). In some clinical studies, patients with a history of hypertension showed a significant reduction in glomerular number (34) and an increase in glomerular volume compared with patients with normal blood pressure (35). Podocytes are epithelial cells that form a glomerular barrier to prevent protein loss (36–39). Podocyte injury is involved in RAS activation and is an essential factor in the progression of HTN and diabetic nephropathy (40). Ang II is a central active molecule of the RAS, plays a role in regulating hypertension-induced inflammation in organ damage (41, 42), and can directly contribute to podocyte injury (43, 44). Podocyte injury was positively correlated with mean arterial pressure,

10.3389/fimmu.2024.1333170

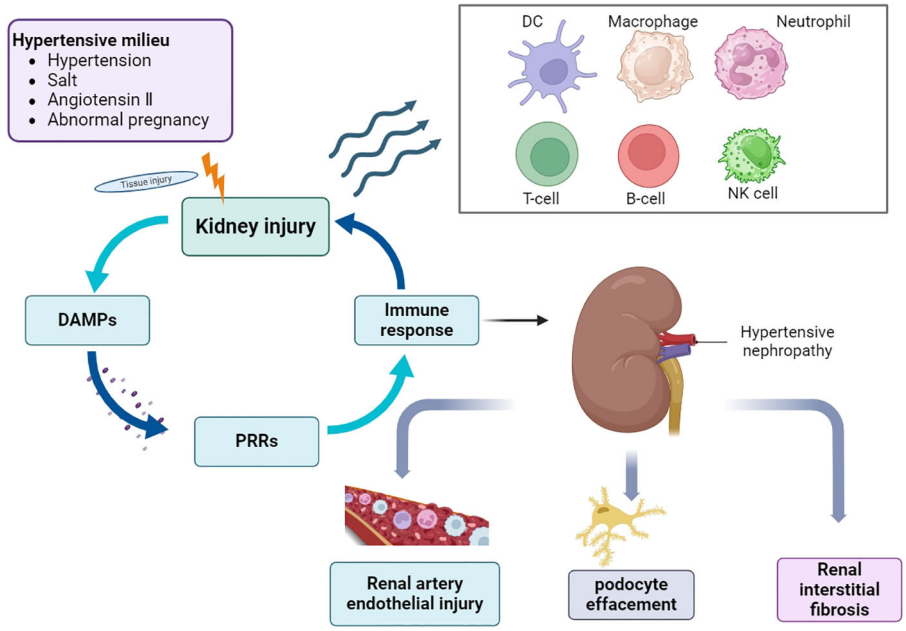

FIGURE 1
Overview of the pathogenesis of HTN. In the environment of hypertension, hypertension, high salt, angiotensin II and abnormal pregnancy activate a variety of signaling cascades, which promote the recruitment and activation of immune cells, cause the occurrence and development of inflammation, and eventually lead to a series of pathological changes of HTN. DAMPs, damage-associated molecular patterns; PRRs, pattern recognition receptors; DC, dendritic cells; NK cells, natural killer cells.

suggesting that higher blood pressure was more likely to cause glomerular injury (45). Hypertensive disease causes podocyte damage and apoptosis, leading to glomerulosclerosis (46). As a pro-apoptotic protein, septin4 is an important marker of organ damage. Recent studies have shown that septin4 promotes hypertensive kidney injury by activating the acetylation of K174 (K174Q). Septin4–K174R is one of the renoprotective factors that ameliorates Ang II-induced hypertensive kidney injury (47). In addition, an increase in blood pressure leads to arterial stiffness, which eventually affects the arteries and causes glomerular lesions (48).

Vascular endothelial growth factor (VEGF), produced by podocytes, is a significant regulator of vascular biology and plays a key role in glomerular development and function (49). Further, it has been reported in various types of glomerulonephritis, including diabetic nephropathy, which is usually associated with increased VEGF-A (50).

2.3 Renal tubulointerstitial injury

Sustained hypertension causes renal tubular cell damage and tubulointerstitial fibrosis (TIF). In patients with hypertension, numerous scattered inflammatory cells may trigger TIF (51). Renal interstitial injury is a dynamic and heterogeneous structure involving a variety of molecules, such as collagen, glycosaminoglycans, and glycoproteins. Notably, type I, III, V, VI, VII, and XV collagen are all expressed in the kidney under physiological conditions. The expression of type III procollagen and type V collagen is significantly increased in spontaneously hypertensive rats(SHR) kidneys, suggesting that these collagens play a role in hypertension-induced renal fibrosis (52). Further, complement C3 expression was significantly increased in the renal mesenchymal tissues of SHR, inducing the synthesis and overgrowth of mesenchymal cells (53). Similar results were confirmed in a clinical study in which enhanced interstitial complement C3 expression in patients with HTN was significantly associated with interstitial macrophage density, serum creatinine levels, interstitial fibrosis, glomerulosclerosis, and arteriopathy scores (54). The results of another clinical study revealed (55) that mast cells were mainly present in the renal tubulointerstitium and increased in number in human HTN, suggesting the involvement of renal mast cells in the progression of HTN.

3 Role of immune cells in HTN

The complex role of immune system in hypertension was proposed as early as the 1960s (56). Hypertension is a chronic inflammatory disease, and hypertensive stimuli lead to the accumulation of pro-inflammatory cells, such as macrophages and T lymphocytes, which affect the development and progression of hypertension (57). In renal diseases, inflammation, immune cell aggregation, and cell death form a vicious cycle of fibrous matrix deposition that destroys renal tissue structure and ultimately leads to renal dysfunction (58). Immune cells can maintain renal homeostasis and attenuate renal damage. In

addition, immunosuppressive agents have been used to treat kidney disease (59). The cells of the innate immune system in renal immunity include dendritic cells (DCs), macrophages/monocytes, natural killer (NK) cells, T cells, B cells, and neutrophils. HTN is an inflammatory disease caused by metabolic disorders in nature (60), which can be manifested as an increase in lymphocyte count (61), thereby increasing the risk of HTN.

3.1 DCs and macrophages

Considerable overlap has been reported between DCs and macrophages regarding cell origin morphology, function, and cell surface antigen expression (62). As innate immune cells, DCs and macrophages can act as sentinels and messengers and are closely related to individual development and the triggering of inflammatory responses. Simultaneously, they complement each other in their surveillance functions (63). DCs focus on antigen presentation, whereas macrophages play a role in clearing dead cells and repairing damaged tissues. These cells induce and regulate the inflammatory response and protect the kidney from infection (64).

DCs form a dendritic network that spans the barrier surface and entire organs, including the kidney, performing important sentinel and messenger functions (65). DCs are the most potent antigen-presenting cells (APCs) in the body, located in the interstitial space of the renal tubules, with immature DCs located closer to the vasculature (66). CD103+ cells mainly activate cytotoxic T cells (67), whereas CD11b+ cells activate CD4+ T cells and produce inflammatory chemokines (68). Notably, DCs are the effectors of renal inflammation, as depletion of CD11c+ cells ameliorates antibody-induced inflammation in the glomerular basement membrane (69). Renal DCs mediate the transfer of T cells to the kidney in an antigen-dependent manner during bacterial infection, suggesting that renal DCs not only monitor systemic infections but are also crucial in localized infections and autoimmunity (70). Similar findings were observed in Ang II-induced hypertension. Renal mid-renal DCs also present antigens to T cells under appropriate instructions (71). In hypertensive mice (72), activated DCs improved sensitivity to hypertension; however, only responsive T lymphocytes can trigger activation. In another mouse experiment (73), mice lacking CD70 did not aggregate T (EM) T-cells and did not develop hypertension to the point of attenuated kidney injury under high-salt conditions or a second Ang II challenge. In addition, typical FLT3L-dependent DCs promote T-cell activation in the kidney, leading to oxidative stress, fluid retention, and elevated blood pressure (74).

Macrophages participate in the innate immune response, immune surveillance, and the maintenance of renal homeostasis (75, 76). Macrophages have various functions in different microenvironments (77), responding differently depending on the nature and duration of renal injury (78–80). Macrophage phenotypes are influenced by the microenvironment, ranging from pro-inflammatory (termed classical M1-type activation) to anti-inflammatory or pro-catabolic (termed selective M2-type activation) (81, 82). The main functions are maintenance of homeostasis and phagocytosis to remove various foreign bodies (83, 84). M1 macrophages favor the clearance of infections and promote immune responses (85). M2 macrophages have a wide range of functions that inhibit inflammation and promote tissue repair (86). In the kidneys, immune activation significantly increases the number of macrophages, leading to the infiltration of monocyte-derived macrophages involved in inflammation in the stenotic kidney and the promotion of fibrosis, especially during the chronic phase of kidney disease (87–89). As previously mentioned (54), inflammation with complement C3 activation and macrophage infiltration and their interaction may play an important role in the pathogenesis of human HTN. There are also data confirming (90) that increased macrophage infiltration is closely correlated with increased YM1/Chi3l3 expression, suggesting that YM1/Chi3l3 may be a biomarker for HTN. Recent evidence shows (91) that VEGFC inhibits inflammasome activation by promoting high salt-induced autophagy in macrophages to ameliorate hypertensive kidney injury.

3.2 Neutrophils

Neutrophils are the first line of defense in the innate immune system and help maintain blood vessel tone (92). A study found that neutrophils in the aorta increased after 7 days of Ang II-induced hypertension (93). An increase in neutrophil count can aggravate the risk of chronic renal failure. However, direct evidence to confirm the role of neutrophils in HTN remains lacking.

3.3 T-lymphocytes

T-lymphocytes are immune cells with the greatest phenotypic and functional diversity. Growing evidence suggests that T cells are involved in the development and progression of HTN. Further, the FASL/FAS (CD95L-CD95) pathway is activated in the kidneys of hypertensive rats, and cytotoxic T lymphocytes (CTLs) kill target cells through this apoptotic pathway. Activation of the FAS/FASL pathway may also be a mechanism underlying renal tubular epithelial cell loss and mesangial fibrosis, which are prominent renal characteristics of hypertensive kidneys (94). Earlier studies (95) also found lymphocytic infiltration in the renal interstitial space in patients with hypertensive renal injury. Some studies have reported (96) that lymphocytes can reduce sodium excretion during Ang II-dependent hypertension by regulating NOS3 and COX-2 expression in the kidneys. Notably, the main source of interferon (IFN)-γ and TNF are CTLs, and mice lacking any of these cytokines showed attenuated hypertension and renal injury in the presence of hypertensive stimuli (97, 98), which aligns with the pathogenic role of CTLs. CTLs play a critical role in hypertension. However, only the CD8+ T-cell population is antigenically activated in the kidneys of hypertensive mice, which may be the main site of immune activation in hypertension (99). This study also found that Cd8 mice had an approximately 50% reduction in the hypertensive response to Ang II or deoxycorticosterone acetate (DOCA) and salt treatment. CD8+ mice had fewer kidney leukocytes than wild-type mice, thinner small renal arteries, and less endothelial dysfunction (99). In a recent study, during DOCA- and salt-

induced hypertension, CD8+ T cells acted directly on renal distal tubules to maintain renal retention (100). Therefore, CTLs may influence the blood pressure by enhancing renal reabsorption of sodium and water.

Activation of the immune system contributes to the pathogenesis of hypertension and the progression of chronic kidney disease. An imbalance in the helper T cell subpopulation is associated with Ang II-induced hypertensive kidney injury (101). T regulatory (Treg) cells are key regulators that mediate immunity and are involved in the activation and proliferation of auto T cells, which play an essential role in autoimmune diseases, immune homeostasis, graft tolerance, and immune regulation of tumors (102). In addition, Tregs exert an inhibitory effect on inflammation by secreting the cytotoxic factors, perforin, and granzyme.

The discovery of Tregs has led to a better understanding of CKD and HTN pathogenesis. Notably, the number of Treg cells in the serum of patients with CKD is significantly decreased, and the percentage of Th17 cells, serum IL-17 levels, and ratio of Th17/Treg cells are increased with the progression of CKD (103). Further studies found that transferring Tregs from healthy mice to mice treated for kidney injury attenuated the condition (104). Moreover, macrophages work synergistically with Tregs to attenuate kidney injury by enhancing chemokine expression (105). Tregs also reduce kidney injury by inhibiting macrophage activation and reducing pro-inflammatory cytokines (106). Clinical and basic data have shown that the Th17 pathway has specific effects on hypertensive kidney injury, ultimately leading to kidney injury (107–109). The Th17 pathway has been shown to affect hypertension (110) specifically.

3.4 NK and NKT cells

A study found that NK cells play an important role in Ang II-induced vascular dysfunction (111). A laboratory study confirmed that the long-term infusion of IL-17 into pregnant rats results in NK cell activation and proliferation (112). In another study (113), CD1d-dependent NKT cell activation was protective against Ang II-induced cardiac remodeling. However, the specific mechanisms underlying hypertension and concomitant renal disease require further investigation.

3.5 B cells and antibody-secreting cells

B cells play a role in hypertension by producing antibodies. For example, the B cell/IgG pair is closely associated with Ang II-induced hypertension and vascular remodeling in mice (114). It has been reported (4, 114) that B-cell activation and IgG production are closely associated with the pathogenesis of hypertension and end-organ damage. Targeting B cells may be able to ameliorate renal lipid peroxidative damage in patients with hyperhomocysteinemia (HHcy) and HTN (115).

Inflammation is a natural and necessary response of the body to stimuli. It is responsible for migrating immune system cells to the stimulus target after a series of steps facilitated and coordinated by cytokines, chemokines, and acute-phase proteins (58). Activation of the immune system is involved in the pathogenesis of hypertension and contributes to CKD progression (116). The accumulation of immune cells in the kidneys promotes a chronic inflammatory response that disrupts blood pressure regulation (117). Inflammation is a key factor in the pathogenesis of hypertension and cardiovascular diseases. Some studies have found that inflammation, immune cell infiltration, and alterations in chemokines and cytokines characterize hypertensive kidney damage (118, 119).

4 Cytokines and HTN

4.1 Definition and function of cytokines

Cytokines are small proteins involved in the development and activity of the immune system, have a wide range of biological activities, and help coordinate the body's response to infection (120, 121). Hypertension is associated with the aggregation of T cells and monocytes/macrophages in the blood vessels and kidneys, which produce potent cytokines that affect vascular and renal function (122). Innate immune cells express several receptors that recognize microorganisms, induce rapid defense, and delay cellular responses. Toll-like receptors on the cell surface and endosomal membranes monitor extracellular microbes and activate multiple host defense signaling pathways (123). The NF-κB and interferon regulatory factor (IRF) pathways downstream of these receptors induce the expression of pro-inflammatory cytokines TNF-α, IL-1β, and IL-6, among others (Table 1).

TABLE 1 Cytokines involved in HTN pathogenesis.

Cytokines	Cell Source	Functions in kidney disease	References
TNF-α	Macrophages, monocytes, T cells	Increase the permeability of vascular endothelial cells	(124, 125)
IL-1	Monocytes, macrophages, fibroblasts epithelial cells	Accelerate renal fibrosis	(126–129)
IL-6	T cells, macrophages, fibroblasts	Accelerate renal immune damage	(130, 131)
IFN	T cells, NK cells	Aggravate glomerular injury	(132, 133)
IL-10	T cells	Improve vascular injury	(134–136)
IL-17	T cells	Reduce kidney inflammation	(137, 138)
TGF-β	Macrophages, T cells	Accelerate renal fibrosis	(139–141)

4.2 Role of cytokines inHTN

TNF-α, a typical macrophage factor appearing earliest during the inflammatory response, is another cytokine released by immune cells (142). TNF-α activates neutrophils and lymphocytes, increases the permeability of vascular endothelial cells, regulates tissue metabolism, and promotes cytokine synthesis and release (143, 144). When inflammatory lesions occur in the kidney, mononuclear macrophages are infiltrated and can express and secrete large amounts of TNF-α, promoting the secretion of IL-6 by the tethered cells. Many experimental studies have found that TNF-α contributes to the proliferation of tethered cells and stroma and the widening of tethered zones, which promotes the onset and development of inflammation. For example, TNF deficiency in mice attenuates the Ang II-induced hypertensive response and renal injury (97, 116, 124). TNF is toxic to glomerular epithelial cells (125, 145), regulates blood pressure, and ameliorates the extent of renal injury (146–149). Inflammatory factors such as TNF-α, IL-1β and MCP-1 were significantly expressed in the kidney of SHR (150). In humans, the effect of TNF on blood pressure is more complex. For example, in patients with heart failure, TNF antagonism does not improve blood pressure or symptoms (151, 152).

In contrast, in animal models of CKD, TNF elevates renal and systemic FGF23 levels, which may be involved in CKD (153). Similarly, in an animal model of diabetic nephropathy, it was found that macrophage-produced TNF-α plays a role in diabetic kidney injury, mainly reducing albuminuria, plasma creatinine, histopathological changes, renal macrophage recruitment, and plasma inflammatory cytokine levels (154). In a mouse study (116), TNF in the kidney elevated blood pressure by reducing NO production. In other experiments, TNF-α was downregulated through Cyp2c23 and upregulated through sEH (148), activation of NF-κB-mediated pathways (147), and increased renal cortical NF-kappa B activity (149) that are involved in renal damage caused by multiple causes of hypertension. In rats (146), the direct infusion of TNF inhibitors into the renal interstitium attenuated salt-induced blood pressure elevation and renal damage. Another study confirmed (126) that during prolonged administration of Ang II and hypertension on a high-salt diet, TNF receptor 2 may mediate the inflammatory response to renal injury without activating TNF receptor 1. Therefore, TNF-α is an essential mediator of hypertension and kidney injury.

IL-1 acts as an inflammatory cytokine with two active isoforms, IL-1α and IL-1β, which are recognized by IL-1 receptor. NLRP3 is an inflammatory vesicle that promotes the maturation and secretion of IL-1β and IL-18 (127–129, 155). IL-1β can act on pericytes to accelerate renal fibrosis (156) and activate helper T cell 17 (TH17) cells in the kidneys (157). Activation of NLRP3 inflammatory vesicles causes elevated blood pressure and/or kidney injury (158–161), exacerbating cardiovascular risk (128). The guanidinylation of apolipoprotein C3 (ApoC3) activates NLRP3 inflammatory vesicles in human monocytes (162). Guanidinylated ApoC3 (gApoC3) accumulates in the kidneys and plasma of patients with CKD to promote inflammation. gApoC3 promotes renal fibrosis and impedes vascular regeneration (163). Mechanistically, NLRP3 directly promotes the epithelial-to-mesenchymal transition of renal tubular epithelial cells, independent of inflammatory vesicles, by inducing phosphorylation and activity of SMAD3 (164). In SHR, BCL6 attenuates renal inflammation by negatively regulating NLRP3 transcription (165). In a recent study (91), VEGFC was shown to inhibit the activation of NLRP3 inflammatory vesicles by promoting autophagy to ameliorate sensitized hypertension and nephritis, which may be a potential therapeutic target for HTN. We found that the infusion of exogenous IL-1 promotes urinary sodium excretion (166–168). Further, IL-1 is involved in developing pulmonary or systemic hypertension through several other mechanisms (169, 170). Several studies have also reported the use of IL-1 inhibitors (171). For example, the IL-1 receptor antagonist anakinra attenuates hypertension and renal fibrosis but does not affect inflammation and leukocyte infiltration in saline-induced hypertensive mice (1K/DOCA/salt) (172). Therefore, investigating the renal-specific mechanisms of IL-1 in hypertension is crucial.

IL-6, known for its pro-inflammatory effects, is one of the most studied cytokines in renal disease and plays a role in systemic inflammation (121, 130). IL-6 has been reported to be involved in hypertension-induced kidney injury (131, 173). IL-6 induces B-cell differentiation and antibody production as a pro-inflammatory response, causes T-cell proliferation and differentiation, and regulates the immune response. IL-6 promotes the expression of cell adhesion molecules by inducing cytokine production of acute-phase response proteins, which leads to the aggregation of inflammatory cells. The expression of IL-6 is directly proportional to the number of glomeruli in glomerular disease. In addition, it stimulates the production of platelets by tethered cells activating factors and other inflammatory mediators, exacerbating renal immune damage. Notably, the risk of cardiovascular death, myocardial infarction, and stroke is associated with decreased glomerular filtration rate (eGFR) and elevated IL-6 levels (174). IL-6 levels in CKD are involved in atherosclerosis (175, 176). Notably, the results of these studies are mutually contradictory. Other studies also reported conflicting findings, such as that IL-6 levels at baseline or changes during the observation period do not show a consistent and significant correlation with renal function in older adults (177). Recently, drug studies on IL-6 and IL-6 receptors have also gained momentum (121, 132, 178–180).

IFN is an inflammatory cytokine produced by T lymphocytes and macrophages that enhances sodium transport by activating intrarenal Ang II production to stimulate transport proteins (133) indirectly. Therefore, IFN deficiency attenuates the response to Ang II-induced chronic hypertension (98) and exacerbates glomerular injury (181). IRF is a multifunctional transcription factor, and IRF-4 deficiency improves renal function, albuminuria, and attenuates renal injury and fibrosis but does not affect blood pressure (182). IRF-4 is a multifunctional transcription factor.

Cytokines in the kidneys act indirectly by inducing other inflammatory mediators and their direct effects on tissue cells. NF-κB is a critical transcription factor in regulating the inflammatory response and the expression of many pro-inflammatory genes (183). The complex hypertensive environment (i.e., hypertension, oxidative stress, glomerular leakage of free fatty acids, and activated RAS) can

exacerbate renal inflammation and the progression of HTN by activating the NF-κB signaling system (184, 185). During glomerular disease progression, NF-κB activation triggers an inflammatory cascade that produces inflammatory factors, such as IL-10 and MCP-1.Studies have found (186) that TGF-β/SMAD and NF-κB signaling pathways play an important role in HTN, and SMAD7, as a downstream inhibitor of these two pathways, can inhibit proteinuria and serum creatinine, and improve glomerular filtration rate, thereby alleviating the condition of HTN. In a recent study (187), ubiquitin-specific protease 25 (USP25) inhibited TGF-β-induced SMAD4 ubiquitination, which reduced the expression of renal fibrosis and renal injury related genes and alleviated renal injury caused by HTN. It has also been confirmed (134) that exercise training may prevent and alleviate renal abnormalities in hypertensive patients by down-regulating TGF-β signaling. Renal fibrosis is an important pathological feature of hypertensive renal injury, which is related to the up-regulation of pro-fibrotic factor TGF-β1 (150).

IL-10 is strongly associated with inflammation in the kidney (135, 136, 188). For example, IL-10 ameliorates hypertension-induced renal and vascular injury (189), and genetic polymorphisms in IL-10 are also protective against diabetic nephropathy (139). MCP-1 promotes chemotaxis of monocytes or macrophages to reach damaged renal tissues, resulting in sustained cytokine activation and localized protease disruption of the renal basement membrane. MCP-1 increases the production of IL-8 and TGF-β1 by affecting the inflammatory response of diseased renal tissues. TGF-β, a cytokine that can regulate cellular proliferation, plays a role in the process of membranous nephropathy, diabetic nephropathy, and renal fibrosis (140, 141, 190).

Chemokine ligand 16 (CXCL16) plays a role in Ang II-induced renal injury and fibrosis by regulating macrophage and T cell infiltration and fibroblast aggregation (191). During RAS-activated hypertension, the chemokine CCL5 attenuates renal injury and fibrosis by reducing the number of infiltrating macrophages in the kidneys (137).

IL-17 is also involved in Ang II-induced hypertension and vascular function (138). In a mouse study (192), IL-17A and IL-17RA antibodies (but not IL-17F) reduced blood pressure and attenuated renal and vascular inflammation. Notably, in other experimental models of kidney injury, IL-17 deficiency exacerbated disease progression (193–195). In a recent transcriptomics study (196), genes upregulated in the renal tubules of patients with HTN were associated with IFN-γ, NF-κB, IL-12, and Wnt signaling pathways, all of which are involved in the inflammatory response, providing a broader perspective on the pathogenesis and treatment of human HTN. Although the number of immune cells is small, the released cytokines play key roles in renal changes involved in fibrosis, glomerular injury, and sodium transport (58).

5 Oxidative stress and HTN

The signaling pathways between oxidative stress and HTN are complex in the pathophysiology of HTN (197, 198). In the kidney, ROS exists in arterioles, glomerular and tubular cells and podocytes, etc. Vasoactive substances and metabolic factors stimulate the production of cellular inflammation and ROS, inducing NADPH oxidase or mitochondrial production (199). The endoplasmic reticulum (ER) is a key player in the redox pathophysiology of the cardiovascular system that maintains protein homeostasis. ER stress (ERS) is typically characterized by impaired protein and lipid synthesis and disturbed intracellular calcium levels (200–202). Excessive ERS damages glomerular mesangial cells, podocytes, and tubular epithelial cells (203–205). However, ERS activity may impair renal function and worsen renal damage during CKD development. Oxidative stress affects T-cell activation and function (206). Septin4 is a non-histone protein that promotes apoptosis, is regulated by SIRT2, and is a marker of organ damage (207–210). SIRT2 deficiency increases oxidative stress and alters mitochondrial morphology (211). Notably, SIRT2–septin4 axis prevents hypertensive kidney injury by attenuating apoptosis and oxidative stress. SIRT2 attenuated oxidative stress in podocytes through deacetylation of septin4-K174, ameliorating hypertension-induced kidney injury in mice. Therefore, septin4-K174R (mimicking deacetylation via SIRT2) may be a new target for alleviating renal injury in hypertension (47), which may help design precise therapeutic regimens and develop targeted drugs in the future. Some studies have demonstrated that SIRT3 is involved in hypertensive kidney injury by inhibiting the epithelial–mesenchymal transition (EMT) and ameliorating hypertension-induced kidney injury in mice (212, 213). Another study in rats (214) suggested that cagliflozin regulates renal EMT and oxidative stress through the SIRT3 pathway, thereby inhibiting high-salt diet-induced hypertensive renal fibrosis.

6 Interaction of immune cells and inflammatory factors in HTN

Modern medical research has found that many glomerular diseases are immune-mediated inflammatory lesions. The involvement of various inflammatory mediators, such as inflammatory cytokines and complement factors based on immune response, leads to glomerular injury and the development of corresponding clinical symptoms (215). The immune system plays an important role in developing hypertension and related endpoints, such as the associated end-organ damage. Sodium provides a strong stimulus for the development of hypertension. High concentrations of extracellular natriuretic ions have been reported to directly activate the inflammatory response in APCs, leading to hypertension, T-cell activation, and ultimately vascular and renal injury (216). APCs respond to hypertension-stimulated inflammatory processes, and DCs, macrophages, and B cells are the classical APCs of the immune system, which coordinate the immune response by activating T cells through antigen-MHT receptor complexes and expressing cytokines, among others (217). Large amounts of sodium-activated DCs produce IL-1β and promote the production of IL-17A and IFN-γ by T cells, which in turn lead to mediated hypertension and end-organ

dysfunction, indicating that the mechanistic link between salt, inflammation, and hypertension includes increased oxidative stress and IsoLG production in DCs (218). Macrophages and T cells play important roles in developing HTN-induced kidney disease (219). Pro-inflammatory cytokines, tumor necrosis factor-α, IL-6, and IL-1β have been implicated in the pathogenesis of Ang II-induced target organ damage (220). For example, as mentioned previously, the deletion of CXCL16 affects the expression of pro-inflammatory cytokines in the kidney. TGF-β1, a key pro-fibrotic cytokine, causes renal damage and tubulointerstitial fibrosis. One study showed that CXCL16 deficiency caused a significant reduction in Ang II-induced TGF-β1 gene expression, which may be an alternative mechanism for developing renal fibrosis.

GPR97, a member of the G protein-coupled receptor subfamily, modulates the inflammatory response (221, 222). GPR97 exacerbates AKI by regulating Sema3A. GPR97 was expressed in tubular epithelial cells in mice with AKI (223). Recent animal experiments have also found (224) that GPR97 causes renal injury and tubulointerstitial fibrosis (TIF) in deoxycorticosterone acetate (DOCA)/salt-induced hypertensive mice by regulating TGF-β signaling. Therefore, GPR97 leads to TIF in patients with hypertension, indicating that it may be a novel therapeutic target for delaying or attenuating renal injury in hypertension.

7 Strategies for prevention and treatment of HTN

HTN, as a cross-discipline, presents difficulties and challenges in diagnosis and intervention. Patients with HTN should monitor and manage their blood pressure and set appropriate control goals in their daily lives, make assessments before treatment, choose appropriate antihypertensive medications to actively prevent complications (225–229). Moreover, lifestyle modification is important to improve the progression and prognosis of HTN. In addition to genetic and environmental interactions, appropriate lifestyle changes, such as weight loss, healthy diet, reduction of dietary sodium, increased physical activity, and cessation of smoking and excessive alcohol consumption, should be implemented according to the recommendations of the hypertension guidelines (230). However, these non-pharmacological interventions alone are insufficient for HTN treatment. For patients with HTN, salt restriction should be the priority as patients with advanced renal disease who excrete a low sodium load exhibit significant salt and water retention (227, 231). Simultaneously, attention should be paid to the intake of adequate amounts of vegetables and fruits that can protect kidneys from renal injury (232).

8 Discussion

In conclusion, inflammation mediates the end-organ damage associated with hypertension. Although reducing blood pressure is crucial, preventing the localized inflammation accompanying this disease, resulting in damage to the vital target organs, should be prioritized (122). In recent years, an increasing number of studies have been published on the pathogenesis of HTN; however, the specific mechanisms are still not fully understood. This review was conducted based on previous studies on the role of immune cells, inflammatory cytokines, and related components in HTN. We analyzed the results at the molecular level to reveal some of the relevant mechanisms to better understand the development of HTN. Future research needs to fill the existing gaps and add more evidence and therapeutic strategies for the prevention and treatment of HTN and avoiding hypertension-related complications.

Hypertension and kidney disease are strongly co-related, and this link should be used effectively to prevent hypertension or treat it at an early stage. Although hypertension is very common today, complications due to hypertension are not encouraging, and many problems remain unresolved. In future studies, antihypertensive drugs, immunosuppressive drugs, and life management must be considered to identify more effective therapeutic targets for HTN.

Although this review focused on inflammatory markers, it is insufficient because the relationship between immunity and inflammation is complex. As the next step, the mechanism of HTN must be explored to alleviate or solve renal injury caused by hypertension.

Author contributions

XH: Writing – original draft. YL: Writing – review & editing. DH: Conceptualization, Writing – review & editing. YG: Writing – review & editing. XZ: Writing – review & editing. BY: Methodology, Writing – review & editing. JL: Writing – review & editing. XW: Writing – review & editing. KY: Writing – review & editing. JW: Supervision, Writing – review & editing. QL: Resources, Writing – review & editing.

Funding

The author(s) declare financial support was received for the research, authorship, and/or publication of this article. This study was funded by the National Natural Science Foundation of China (grant no. 82074553).

Acknowledgments

The authors thank the patients for consenting to the publication of this report.

Conflict of interest

The authors declare that the research was conducted in the absence of any commercial or financial relationships that could be construed as a potential conflict of interest.

Publisher's note

References

1. Visseren FLJ, Mach F, Smulders YM, Carballo D, Koskinas KC, Bäck M, et al. 2021 ESC Guidelines on cardiovascular disease prevention in clinical practice. *Eur Heart J*. (2021) 42:3227–337. doi: 10.1093/eurheartj/ehab484

2. Poulter NR, Prabhakaran D, Caulfield M. Hypertension. *Lancet (London England)*. (2015) 386:801–12. doi: 10.1016/S0140-6736(14)61468-9

3. NCD Risk Factor Collaboration (NCD-RisC). Worldwide trends in hypertension prevalence and progress in treatment and control from 1990 to 2019: a pooled analysis of 1201 population-representative studies with 104 million participants. *Lancet (London England)*. (2021) 398:957–80. doi: 10.1016/S0140-6736(21)01330-1

4. Drummond GR, Vinh A, Guzik TJ, Sobey CG. Immune mechanisms of hypertension. *Nat Rev Immunol*. (2019) 19:517–32. doi: 10.1038/s41577-019-0160-5

5. Pan X, Shao Y, Wu F, Wang Y, Xiong R, Zheng J, et al. FGF21 prevents angiotensin II-induced hypertension and vascular dysfunction by activation of ACE2/angiotensin-(1-7) axis in mice. *Cell Metab*. (2018) 27:1323–37.e5. doi: 10.1016/j.cmet.2018.04.002

6. Brouwers S, Sudano I, Kokubo Y, Sulaica EM. Arterial hypertension. *Lancet (London England)*. (2021) 398:249–61. doi: 10.1016/S0140-6736(21)00221-X

7. Carey RM, Moran AE, Whelton PK. Treatment of hypertension: A review. *JAMA*. (2022) 328:1849–61. doi: 10.1001/jama.2022.19590

8. Kakitapalli Y, Ampolu J, Madasu SD, Sai Kumar MLS. Detailed review of chronic kidney disease. *Kidney Dis (Basel Switzerland)*. (2020) 6:85–91. doi: 10.1159/000504622

9. Global, regional, and national incidence, prevalence, and years lived with disability for 354 diseases and injuries for 195 countries and territories, 1990–2017: a systematic analysis for the Global Burden of Disease Study 2017. *Lancet (London England)*. (2018) 392:1789–858. doi: 10.1016/S0140-6736(18)32279-7

10. Nangaku M. Chronic hypoxia and tubulointerstitial injury: a final common pathway to end-stage renal failure. *J Am Soc Nephrol*. (2006) 17:17–25. doi: 10.1681/ASN.2005070757

11. Coresh J, Byrd-Holt D, Astor BC, Briggs JP, Eggers PW, Lacher DA, et al. Chronic kidney disease awareness, prevalence, and trends among U.S. adults, 1999 to 2000. *J Am Soc Nephrol*. (2005) 16:180–8. doi: 10.1681/ASN.2004070539

12. Charles C, Ferris AH. Chronic kidney disease. *Primary Care*. (2020) 47:585–95. doi: 10.1016/j.pop.2020.08.001

13. Cai A, Calhoun DA. Resistant hypertension: an update of experimental and clinical findings. *Hypertension (Dallas Tex: 1979)*. (2017) 70:5–9. doi: 10.1161/HYPERTENSIONAHA.117.08929

14. *2017 ACC/AHA/AAPA/ABC/ACPM/AGS/APhA/ASH/ASPC/NMA/PCNA Guideline for the Prevention, Detection, Evaluation, and Management of High Blood Pressure in Adults: Executive Summary: A Report of the American College of Cardiology/American Heart Association Task Force on Clinical Practice Guidelines* (Accessed 23rd October 2023).

15. Hart PD, Bakris GL. Hypertensive nephropathy: prevention and treatment recommendations. *Expert Opin Pharmacother*. (2010) 11:2675–86. doi: 10.1517/14656566.2010.485612

16. Johansen KL, Chertow GM, Gilbertson DT, Ishani A, Israni A, Ku E, et al. US renal data system 2022 annual data report: epidemiology of kidney disease in the United States. *Am J Kidney Dis*. (2023) 81:A8–A11. doi: 10.1053/j.ajkd.2022.12.001

17. Lopez Gelston CA, Mitchell BM. Recent advances in immunity and hypertension. *Am J Hypertens*. (2017) 30:643–52. doi: 10.1093/ajh/hpx011

18. Bomfim GF, Rodrigues FL, Carneiro FS. Are the innate and adaptive immune systems setting hypertension on fire? *Pharmacol Res*. (2017) 117:377–93. doi: 10.1016/j.phrs.2017.01.010

19. Lin L, Ren J, Wang C, Mei M, Zheng L, Yang J. A set of urinary peptides can predict early renal damage in primary hypertension. *J Hypertens*. (2023) 41:1653–60. doi: 10.1097/HJH.0000000000003539

20. Mwasongwe S, Min YI, Booth JN, Katz R, Sims M, Correa A, et al. Masked hypertension and kidney function decline: the Jackson Heart Study. *J Hypertens*. (2018) 36:1524–32. doi: 10.1097/HJH.0000000000001727

21. Ameer OZ. Hypertension in chronic kidney disease: What lies behind the scene. *Front Pharmacol*. (2022) 13:949260. doi: 10.3389/fphar.2022.949260

22. Kretzler M, Koeppen-Hagemann I, Kriz W. Podocyte damage is a critical step in the development of glomerulosclerosis in the uninephrectomised-desoxycorticosterone hypertensive rat. *Virchows Archiv: Int J Pathol*. (1994) 425:181–93. doi: 10.1007/BF00230355

23. Wei SY, Wang YX, Zhang QF, Zhao SL, Diao TT, Li JS, et al. Multiple mechanisms are involved in salt-sensitive hypertension-induced renal injury and interstitial fibrosis. *Sci Rep*. (2017) 7:45952. doi: 10.1038/srep45952

24. Nagase M, Shibata S, Yoshida S, Nagase T, Gotoda T, Fujita T. Podocyte injury underlies the glomerulopathy of Dahl salt-hypertensive rats and is reversed by aldosterone blocker. *Hypertension (Dallas Tex: 1979)*. (2006) 47:1084–93. doi: 10.1161/01.HYP.0000222003.28517.99

25. Shankland SJ. The podocyte's response to injury: role in proteinuria and glomerulosclerosis. *Kidney Int*. (2006) 69:2131–47. doi: 10.1038/sj.ki.5000410

26. Zamami R, Kohagura K, Miyagi T, Kinjyo T, Shiota K, Ohya Y. Modification of the impact of hypertension on proteinuria by renal arteriolar hyalinosis in nonnephrotic chronic kidney disease. *J Hypertens*. (2016) 34:2274–9. doi: 10.1097/HJH.0000000000001091

27. Sata Y, Head GA, Denton K, May CN, Schlaich MP. Role of the sympathetic nervous system and its modulation in renal hypertension. *Front Med*. (2018) 5:82. doi: 10.3389/fmed.2018.00082

28. Campese VM, Mitra N, Sandee D. Hypertension in renal parenchymal disease: why is it so resistant to treatment? *Kidney Int*. (2006) 69:967–73. doi: 10.1038/sj.ki.5000177

29. DiBona GF, Kopp UC. Neural control of renal function. *Physiol Rev*. (1997) 77:75–197. doi: 10.1152/physrev.1997.77.1.75

30. Kobori H, Nangaku M, Navar LG, Nishiyama A. The intrarenal renin-angiotensin system: from physiology to the pathobiology of hypertension and kidney disease. *Pharmacol Rev*. (2007) 59:251–87. doi: 10.1124/pr.59.3.3

31. Kashiwagi M, Shinozaki M, Hirakata H, Tamaki K, Hirano T, Tokumoto M, et al. Locally activated renin-angiotensin system associated with TGF-beta1 as a major factor for renal injury induced by chronic inhibition of nitric oxide synthase in rats. *J Am Soc Nephrol: JASN*. (2000) 11:616–24. doi: 10.1681/ASN.V114616

32. Liu Y, Jiang Y, Li W, Han C, Qi Z. MicroRNA and mRNA analysis of angiotensin II-induced renal artery endothelial cell dysfunction. *Exp Ther Med*. (2020) 19:3723–37. doi: 10.3892/etm.2020.8613

33. Durvasula RV, Shankland SJ. The renin-angiotensin system in glomerular podocytes: mediator of glomerulosclerosis and link to hypertensive nephropathy. *Curr Hypertens Rep*. (2006) 8:132–8. doi: 10.1007/s11906-006-0009-8

34. Keller G, Zimmer G, Mall G, Ritz E, Amann K. Nephron number in patients with primary hypertension. *N Engl J Med*. (2003) 348:101–8. doi: 10.1056/NEJMoa020549

35. Hill GS, Heudes D, Jacquot C, Gauthier E, Bariéty J. Morphometric evidence for impairment of renal autoregulation in advanced essential hypertension. *Kidney Int*. (2006) 69:823–31. doi: 10.1038/sj.ki.5000163

36. Zhou D, Wang Y, Gui Y, Fu H, Zhou S, Wang Y, et al. Non-canonical Wnt/calcium signaling is protective against podocyte injury and glomerulosclerosis. *Kidney Int*. (2022) 102:96–107. doi: 10.1016/j.kint.2022.02.029

37. Nagata M. Podocyte injury and its consequences. *Kidney Int*. (2016) 89:1221–30. doi: 10.1016/j.kint.2016.01.012

38. Sun H, Li H, Yan J, Wang X, Xu M, Wang M, et al. Loss of CLDN5 in podocytes deregulates WIF1 to activate WNT signaling and contributes to kidney disease. *Nat Commun*. (2022) 13:1600. doi: 10.1038/s41467-022-29277-6

39. Seccia TM, Caroccia B, Calò LA. Hypertensive nephropathy. Moving from classic to emerging pathogenetic mechanisms. *J Hypertens*. (2017) 35:205–12. doi: 10.1097/HJH.0000000000001170

40. Fu EL, Evans M, Clase CM, Tomlinson LA, van Diepen M, Dekker FW, et al. Stopping renin-angiotensin system inhibitors in patients with advanced CKD and risk of adverse outcomes: A nationwide study. *J Am Soc Nephrol: JASN*. (2021) 32:424–35. doi: 10.1681/ASN.2020050682

41. Angiotensin II as an inflammatory mediator: evolving concepts in the role of the renin angiotensin system in the failing heart. Available online at: https://pubmed.ncbi.nlm.nih.gov/12085982/ (Accessed 26th October 2023).

42. Ruiz-Ortega M, Rupérez M, Esteban V, Rodríguez-Vita J, Sánchez-López E, Carvajal G, et al. Angiotensin II: a key factor in the inflammatory and fibrotic response in kidney diseases. *Nephrol Dialysis Transplant*. (2006) 21:16–20. doi: 10.1093/ndt/gfi265

43. Ma Y, Yang Q, Zhong Z, Liang W, Zhang L, Yang Y, et al. Role of c-Abl and nephrin in podocyte cytoskeletal remodeling induced by angiotensin II. *Cell Death Dis*. (2018) 9:185. doi: 10.1038/s41419-017-0225-y

44. Yang Q, Hu J, Yang Y, Chen Z, Feng J, Zhu Z, et al. Sirt6 deficiency aggravates angiotensin II-induced cholesterol accumulation and injury in podocytes. *Theranostics*. (2020) 10:7465–79. doi: 10.7150/thno.45003

45. Naik AS, Le D, Aqeel J, Wang SQ, Chowdhury M, Walters LM, et al. Podocyte stress and detachment measured in urine are related to mean arterial pressure in healthy humans. *Kidney Int*. (2020) 98:699–707. doi: 10.1016/j.kint.2020.03.038

46. Yu D, Petermann A, Kunter U, Rong S, Shankland SJ, Floege J. Urinary podocyte loss is a more specific marker of ongoing glomerular damage than proteinuria. *J Am Soc Nephrol*. (2005) 16:1733–41. doi: 10.1681/ASN.2005020159

47. Zhang Y, Zhang N, Zou Y, Song C, Cao K, Wu B, et al. Deacetylation of septin4 by SIRT2 (Silent mating type information regulation 2 homolog-2) mitigates damaging of hypertensive nephropathy. *Circ Res*. (2023) 132:601–24. doi: 10.1161/CIRCRESAHA.122.321591

48. Hill GS. Hypertensive nephrosclerosis. *Curr Opin Nephrol Hypertens*. (2008) 17:266–70. doi: 10.1097/MNH.0b013e3282f88a1f

49. Eremina V, Quaggin SE. The role of VEGF-A in glomerular development and function. *Curr Opin Nephrol Hypertens*. (2004) 13:9–15. doi: 10.1097/00041552-200401000-00002

50. Wolf G, Chen S, Ziyadeh FN. From the periphery of the glomerular capillary wall toward the center of disease: podocyte injury comes of age in diabetic nephropathy. *Diabetes*. (2005) 54:1626–34. doi: 10.2337/diabetes.54.6.1626

51. Costantino VV, Gil Lorenzo AF, Bocanegra V, Vallés PG. Molecular mechanisms of hypertensive nephropathy: renoprotective effect of losartan through hsp70. *Cells*. (2021) 10:3146. doi: 10.3390/cells10113146

52. Stanchev S, Stamenov N, Kirkov V, Dzhambazova E, Nikolov D, Paloff A. Differential collagen expression in kidney and heart during hypertension. *Bratislava Med J*. (2020) 121:73–8. doi: 10.4149/BLL_2020_011

53. Chen L, Fukuda N, Matsumoto T, Abe M. Role of complement 3 in the pathogenesis of hypertension. *Hypertens Res*. (2020) 43:255–62. doi: 10.1038/s41440-019-0371-y

54. Cui J, Wan J, You D, Zou Z, Chen Y, Li Z, et al. Interstitial complement C3 activation and macrophage infiltration in patients with hypertensive nephropathy. *Clin Nephrol*. (2017) 88:328–37. doi: 10.5414/CN109154

55. Welker P, Krämer S, Groneberg DA, Neumayer HH, Bachmann S, Amann K, et al. Increased mast cell number in human hypertensive nephropathy. *Am J Physiol Renal Physiol*. (2008) 295:F1103–1109. doi: 10.1152/ajprenal.00374.2007

56. White FN, Grollman A. AUTOIMMUNE FACTORS ASSOCIATED WITH INFARCTION OF THE KIDNEY. *Nephron*. (1964) 1:93–102. doi: 10.1159/000179322

57. Crowley SD, Jeffs AD. Targeting cytokine signaling in salt-sensitive hypertension. *Am J Physiol Renal Physiol*. (2016) 311:F1153–8. doi: 10.1152/ajprenal.00273.2016

58. Petreski T, Piko N, Ekart R, Hojs R, Bevc S. Review on inflammation markers in chronic kidney disease. *Biomedicines*. (2021) 9:182. doi: 10.3390/biomedicines9020182

59. Zhang L, Wang F, Wang L, Wang W, Liu B, Liu J, et al. Prevalence of chronic kidney disease in China: a cross-sectional survey. *Lancet (London England)*. (2012) 379:815–22. doi: 10.1016/S0140-6736(12)60033-6

60. Venkatraghavan L, Tan TP, Mehta J, Arekapudi A, Govindarajulu A, Siu E. Neutrophil Lymphocyte Ratio as a predictor of systemic inflammation - A cross-sectional study in a pre-admission setting. *F1000Research*. (2015) 4:123. doi: 10.12688/f1000research.6474.1

61. Pang L, Ding Z, Chai H, Shuang W. The causal relationship between immune cells and different kidney diseases: A Mendelian randomization study. *Open Med*. (2023) 18:20230877. doi: 10.1515/med-2023-0877

62. Rogers NM, Ferenbach DA, Isenberg JS, Thomson AW, Hughes J. Dendritic cells and macrophages in the kidney: a spectrum of good and evil. *Nat Rev Nephrol*. (2014) 10:625–43. doi: 10.1038/nrneph.2014.170

63. Higaki A, Mogi M. Dendritic cells as potential initiators of immune-mediated hypertensive disorders. *Hypertens Res*. (2022) 45:527–9. doi: 10.1038/s41440-021-00830-y

64. Brähler S, Zinselmeyer BH, Raju S, Nitschke M, Suleiman H, Saunders BT, et al. Opposing roles of dendritic cell subsets in experimental GN. *J Am Soc Nephrol*. (2018) 29:138–54. doi: 10.1681/ASN.2017030270

65. Jiao J, Dragomir AC, Kocabayoglu P, Rahman AH, Chow A, Hashimoto D, et al. Central role of conventional dendritic cells in regulation of bone marrow release and survival of neutrophils. *J Immunol (Baltimore Md.: 1950)*. (2014) 192:3374–82. doi: 10.4049/jimmunol.1300237

66. Hildner K, Edelson BT, Purtha WE, Diamond M, Matsushita H, Kohyama M, et al. Batf3 deficiency reveals a critical role for CD8alpha+ dendritic cells in cytotoxic T cell immunity. *Sci (New York N.Y.)*. (2008) 322:1097–100. doi: 10.1126/science.1164206

67. Dudziak D, Kamphorst AO, Heidkamp GF, Buchholz VR, Trumpfheller C, Yamazaki S, et al. Differential antigen processing by dendritic cell subsets. *vivo Sci (New York N.Y.)*. (2007) 315:107–11. doi: 10.1126/science.1136080

68. Hochheiser K, Engel DR, Hammerich L, Heymann F, Knolle PA, Panzer U, et al. Kidney dendritic cells become pathogenic during crescentic glomerulonephritis with proteinuria. *J Am Soc Nephrol*. (2011) 22:306–16. doi: 10.1681/ASN.2010050548

69. Yatim KM, Gosto M, Humar R, Williams AL, Oberbarnscheidt MH. Renal dendritic cells sample blood-borne antigen and guide T-cell migration to the kidney by means of intravascular processes. *Kidney Int*. (2016) 90:818–27. doi: 10.1016/j.kint.2016.05.030

70. Vinh A, Chen W, Blinder Y, Weiss D, Taylor WR, Goronzy JJ, et al. Inhibition and genetic ablation of the B7/CD28 T-cell costimulation axis prevents experimental hypertension. *Circulation*. (2010) 122:2529–37. doi: 10.1161/CIRCULATIONAHA.109.930446

71. Kirabo A, Fontana V, de Faria APC, Loperena R, Galindo CL, Wu J, et al. DC isoketal-modified proteins activate T cells and promote hypertension. *J Clin Invest*. (2014) 124:4642–56. doi: 10.1172/JCI74084

72. Itani HA, Xiao L, Saleh MA, Wu J, Pilkinton MA, Dale BL, et al. CD70 exacerbates blood pressure elevation and renal damage in response to repeated hypertensive stimuli. *Circ Res*. (2016) 118:1233–43. doi: 10.1161/CIRCRESAHA.115.308111

73. Lu X, Rudemiller NP, Privratsky JR, Ren J, Wen Y, Griffiths R, et al. Classical dendritic cells mediate hypertension by promoting renal oxidative stress and fluid retention. *Hypertension (Dallas Tex: 1979)*. (2020) 75:131–8. doi: 10.1161/HYPERTENSIONAHA.119.13667

74. Viehmann SF, Böhner AMC, Kurts C, Brähler S. The multifaceted role of the renal mononuclear phagocyte system. *Cell Immunol*. (2018) 330:97–104. doi: 10.1016/j.cellimm.2018.04.009

75. Rodriguez-Iturbe B, Pons H, Johnson RJ. Role of the immune system in hypertension. *Physiol Rev*. (2017) 97:1127–64. doi: 10.1152/physrev.00031.2016

76. Müller S, Kohanbash G, Liu SJ, Alvarado B, Carrera D, Bhaduri A, et al. Single-cell profiling of human gliomas reveals macrophage ontogeny as a basis for regional differences in macrophage activation in the tumor microenvironment. *Genome Biol*. (2017) 18:234. doi: 10.1186/s13059-017-1362-4

77. Wise AF, Williams TM, Kiewiet MBG, Payne NL, Siatskas C, Samuel CS, et al. Human mesenchymal stem cells alter macrophage phenotype and promote regeneration via homing to the kidney following ischemia-reperfusion injury. *Am J Physiol Renal Physiol*. (2014) 306:F1222–1235. doi: 10.1152/ajprenal.00675.2013

78. Lech M, Gröbmayr R, Ryu M, Lorenz G, Hartter I, Mulay SR, et al. Macrophage phenotype controls long-term AKI outcomes–kidney regeneration versus atrophy. *J Am Soc Nephrol*. (2014) 25:292–304. doi: 10.1681/ASN.2013020152

79. Ma R, Jiang W, Li Z, Sun Y, Wei Z. Intrarenal macrophage infiltration induced by T cells is associated with podocyte injury in lupus nephritis patients. *Lupus*. (2016) 25:1577–86. doi: 10.1177/0961203316646861

80. Dai X, Mao C, Lan X, Chen H, Li M, Bai J, et al. Acute Penicillium marneffei infection stimulates host M1/M2a macrophages polarization in BALB/C mice. *BMC Microbiol*. (2017) 17:177. doi: 10.1186/s12866-017-1086-3

81. Tang PMK, Nikolic-Paterson DJ, Lan HY. Macrophages: versatile players in renal inflammation and fibrosis. *Nat Rev Nephrol*. (2019) 15:144–58. doi: 10.1038/s41581-019-0110-2

82. Das A, Sinha M, Datta S, Abas M, Chaffee S, Sen CK, et al. Monocyte and macrophage plasticity in tissue repair and regeneration. *Am J Pathol*. (2015) 185:2596–606. doi: 10.1016/j.ajpath.2015.06.001

83. Rosenberger CM, Finlay BB. Phagocyte sabotage: disruption of macrophage signalling by bacterial pathogens. *Nat Rev Mol Cell Biol*. (2003) 4:385–96. doi: 10.1038/nrm1104

84. Gordon S, Plüddemann A. Tissue macrophages: heterogeneity and functions. *BMC Biol*. (2017) 15:53. doi: 10.1186/s12915-017-0392-4

85. Huen SC, Cantley LG. Macrophage-mediated injury and repair after ischemic kidney injury. *Pediatr Nephrol (Berlin Germany)*. (2015) 30:199–209. doi: 10.1007/s00467-013-2726-y

86. Saad A, Herrmann SMS, Crane J, Glockner JF, McKusick MA, Misra S, et al. Stent revascularization restores cortical blood flow and reverses tissue hypoxia in atherosclerotic renal artery stenosis but fails to reverse inflammatory pathways or glomerular filtration rate. *Circ Cardiovasc Interv*. (2013) 6:428–35. doi: 10.1161/CIRCINTERVENTIONS.113.000219

87. Misharin AV, Morales-Nebreda L, Reyfman PA, Cuda CM, Walter JM, McQuattie-Pimentel AC, et al. Monocyte-derived alveolar macrophages drive lung fibrosis and persist in the lung over the life span. *J Exp Med*. (2017) 214:2387–404. doi: 10.1084/jem.20162152

88. Gloviczki ML, Keddis MT, Garovic VD, Friedman H, Herrmann S, McKusick MA, et al. TGF expression and macrophage accumulation in atherosclerotic renal artery stenosis. *Clin J Am Soc Nephrol*. (2013) 8:546–53. doi: 10.2215/CJN.06460612

89. Cavalcante PAM, Alenina N, Budu A, Freitas-Lima LC, Alves-Silva T, Agudelo JSH, et al. Nephropathy in hypertensive animals is linked to M2 macrophages and increased expression of the YM1/chi3l3 protein. *Mediators Inflamm*. (2019) 2019:9086758. doi: 10.1155/2019/9086758

90. Wu Q, Meng W, Zhu B, Chen X, Fu J, Zhao C, et al. VEGFC ameliorates salt-sensitive hypertension and hypertensive nephropathy by inhibiting NLRP3 inflammasome via activating VEGFR3-AMPK dependent autophagy pathway. *Cell Mol Life Sci*. (2023) 80:327. doi: 10.1007/s00018-023-04978-3

91. Morton J, Coles B, Wright K, Gallimore A, Morrow JD, Terry ES, et al. Circulating neutrophils maintain physiological blood pressure by suppressing bacteria and IFNgamma-dependent iNOS expression in the vasculature of healthy mice. *Blood*. (2008) 111:5187–94. doi: 10.1182/blood-2007-10-117283

92. Lu X, Crowley SD. Actions of immune cells in the hypertensive kidney. *Curr Opin Nephrol Hypertens*. (2020) 29:515–22. doi: 10.1097/MNH.0000000000000635

93. Sanders PW, Wang PX. Activation of the Fas/Fas ligand pathway in hypertensive renal disease in Dahl/Rapp rats. *BMC nephrol.* (2002) 3:1. doi: 10.1186/1471-2369-3-1

94. Sommers SC, Relman AS, Smithwick RH. Histologic studies of kidney biopsy specimens from patients with hypertension. *Am J Pathol.* (1958) 34:685–715.

95. Crowley SD, Song YS, Lin EE, Griffiths R, Kim HS, Ruiz P. Lymphocyte responses exacerbate angiotensin II-dependent hypertension. *Am J Physiol Regulatory Integr Comp Physiol.* (2010) 298:R1089–1097. doi: 10.1152/ajpregu.00373.2009

96. Sriramula S, Haque M, Majid DSA, Francis J. Involvement of tumor necrosis factor-alpha in angiotensin II-mediated effects on salt appetite, hypertension, and cardiac hypertrophy. *Hypertension (Dallas Tex: 1979).* (2008) 51:1345–51. doi: 10.1161/HYPERTENSIONAHA.107.102152

97. Saleh MA, McMaster WG, Wu J, Norlander AE, Funt SA, Thabet SR, et al. Lymphocyte adaptor protein LNK deficiency exacerbates hypertension and end-organ inflammation. *J Clin Invest.* (2015) 125:1189–202. doi: 10.1172/JCI76327

98. Trott DW, Thabet SR, Kirabo A, Saleh MA, Itani H, Norlander AE, et al. Oligoclonal CD8+ T cells play a critical role in the development of hypertension. *Hypertension (Dallas Tex: 1979).* (2014) 64:1108–15. doi: 10.1161/HYPERTENSIONAHA.114.04147

99. Liu Y, Rafferty TM, Rhee SW, Webber JS, Song L, Ko B, et al. CD8+ T cells stimulate Na-Cl co-transporter NCC in distal convoluted tubules leading to salt-sensitive hypertension. *Nat Commun.* (2017) 8:14037. doi: 10.1038/ncomms14037

100. Shao J, Nangaku M, Miyata T, Inagi R, Yamada K, Kurokawa K, et al. Imbalance of T-cell subsets in angiotensin II-infused hypertensive rats with kidney injury. *Hypertension (Dallas Tex: 1979).* (2003) 42:31–8. doi: 10.1161/01.HYP.0000075082.06183.4E

101. Scheinecker C, Göschl L, Bonelli M. Treg cells in health and autoimmune diseases: New insights from single cell analysis. *J Autoimmunity.* (2020) 110:102376. doi: 10.1016/j.jaut.2019.102376

102. Zhu X, Li S, Zhang Q, Zhu D, Xu Y, Zhang P, et al. Correlation of increased Th17/Treg cell ratio with endoplasmic reticulum stress in chronic kidney disease. *Medicine.* (2018) 97:e10748. doi: 10.1097/MD.0000000000010748

103. Lu J, Zhang J, Chen M, Chen C, Li Z, Liao P. Regulatory T cells as a novel candidate for cell-based therapy in kidney disease. *Front Physiol.* (2020) 11:621. doi: 10.3389/fphys.2020.00621

104. Zhang N, Schröppel B, Lal G, Jakubzick C, Mao X, Chen D, et al. Regulatory T cells sequentially migrate from inflamed tissues to draining lymph nodes to suppress the alloimmune response. *Immunity.* (2009) 30:458–69. doi: 10.1016/j.immuni.2008.12.022

105. Mahajan D, Wang Y, Qin X, Wang Y, Zheng G, Wang YM, et al. CD4+CD25+ regulatory T cells protect against injury in an innate murine model of chronic kidney disease. *J Am Soc Nephrol.* (2006) 17:2731–41. doi: 10.1681/ASN.2005080842

106. Higaki A, Mahmoud AUM, Paradis P, Schiffrin EL. Role of interleukin-23/interleukin-17 axis in T-cell-mediated actions in hypertension. *Cardiovasc Res.* (2021) 117:1274–83. doi: 10.1093/cvr/cvaa257

107. Wang Z, Wang J, Yang P, Song X, Li Y. Elevated Th17 cell proportion, related cytokines and mRNA expression level in patients with hypertension-mediated organ damage: a case control study. *BMC Cardiovasc Disord.* (2022) 22:257. doi: 10.1186/s12872-022-02698-3

108. Taylor LE, Gillis EE, Musall JB, Baban B, Sullivan JC. High-fat diet-induced hypertension is associated with a proinflammatory T cell profile in male and female Dahl salt-sensitive rats. *Am J Physiol Heart Circ Physiol.* (2018) 315:H1713–23. doi: 10.1152/ajpheart.00389.2018

109. Mehrotra P, Patel JB, Ivancic CM, Collett JA, Basile DP. Th-17 cell activation in response to high salt following acute kidney injury is associated with progressive fibrosis and attenuated by AT-1R antagonism. *Kidney Int.* (2015) 88:776–84. doi: 10.1038/ki.2015.200

110. Kossmann S, Schwenk M, Hausding M, Karbach SH, Schmidgen MI, Brandt M, et al. Angiotensin II-induced vascular dysfunction depends on interferon-γ-driven immune cell recruitment and mutual activation of monocytes and NK-cells. *Arterioscler Thromb Vasc Biol.* (2013) 33:1313–9. doi: 10.1161/ATVBAHA.113.301437

111. Travis OK, White D, Pierce WA, Ge Y, Stubbs CY, Spradley FT, et al. Chronic infusion of interleukin-17 promotes hypertension, activation of cytolytic natural killer cells, and vascular dysfunction in pregnant rats. *Physiol Rep.* (2019) 7:e14038. doi: 10.14814/phy2.14038

112. Wang HX, Li WJ, Hou CL, Lai S, Zhang YL, Tian C, et al. CD1d-dependent natural killer T cells attenuate angiotensin II-induced cardiac remodelling via IL-10 signalling in mice. *Cardiovasc Res.* (2019) 115:83–93. doi: 10.1093/cvr/cvy164

113. Chan CT, Sobey CG, Lieu M, Ferens D, Kett MM, Diep H, et al. Obligatory role for B cells in the development of angiotensin II-dependent hypertension. *Hypertension (Dallas Tex: 1979).* (2015) 66:1023–33. doi: 10.1161/HYPERTENSIONAHA.115.05779

114. Du X, Ma X, Tan Y, Shao F, Li C, Zhao Y, et al. B cell-derived anti-beta 2 glycoprotein I antibody mediates hyperhomocysteinemia-aggravated hypertensive glomerular lesions by triggering ferroptosis. *Signal Transduct Target Ther.* (2023) 8:103. doi: 10.1038/s41392-023-01313-x

115. Zhang J, Patel MB, Griffiths R, Mao A, Song Ys, Karlovich NS, et al. Tumor necrosis factor-α produced in the kidney contributes to angiotensin II-dependent hypertension. *Hypertension (Dallas Tex: 1979).* (2014) 64:1275–81. doi: 10.1161/HYPERTENSIONAHA.114.03863

116. Mattson DL. Immune mechanisms of salt-sensitive hypertension and renal end-organ damage. *Nat Rev Nephrol.* (2019) 15:290–300. doi: 10.1038/s41581-019-0121-z

117. Crowley SD, Frey CW, Gould SK, Griffiths R, Ruiz P, Burchette JL, et al. Stimulation of lymphocyte responses by angiotensin II promotes kidney injury in hypertension. *Am J Physiol Renal Physiol.* (2008) 295:F515–524. doi: 10.1152/ajprenal.00527.2007

118. Ren J, Crowley SD. Role of T-cell activation in salt-sensitive hypertension. *Am J Physiol Heart Circulatory Physiol.* (2019) 316:H1345–53. doi: 10.1152/ajpheart.00096.2019

119. Yazdi AS, Ghoreschi K. The interleukin-1 family. *Adv Exp Med Biol.* (2016) 941:21–9. doi: 10.1007/978-94-024-0921-5_2

120. Rose-John S. Interleukin-6 family cytokines. *Cold Spring Harbor Perspect Biol.* (2018) 10:a028415. doi: 10.1101/cshperspect.a028415

121. McMaster WG, Kirabo A, Madhur MS, Harrison DG. Inflammation, immunity, and hypertensive end-organ damage. *Circ Res.* (2015) 116:1022–33. doi: 10.1161/CIRCRESAHA.116.303697

122. Wenzel UO, Ehmke H, Bode M. Immune mechanisms in arterial hypertension. *Recent advances Cell Tissue Res.* (2021) 385:393–404. doi: 10.1007/s00441-020-03409-0

123. Majid DSA. Tumor necrosis factor-α and kidney function: experimental findings in mice. *Adv Exp Med Biol.* (2011) 691:471–80. doi: 10.1007/978-1-4419-6612-4_48

124. Bertani T, Abbate M, Zoja C, Corna D, Perico N, Ghezzi P, et al. Tumor necrosis factor induces glomerular damage in the rabbit. *Am J Pathol.* (1989) 134:419–30.

125. Gómez-Chiarri M, Ortíz A, Lerma JL, López-Armada MJ, Mampaso F, González E, et al. Involvement of tumor necrosis factor and platelet-activating factor in the pathogenesis of experimental nephrosis in rats. *Lab Invest.* (1994) 70:449–59.

126. Xiao H, Lu M, Lin TY, Chen Z, Chen G, Wang WC, et al. Sterol regulatory element binding protein 2 activation of NLRP3 inflammasome in endothelium mediates hemodynamic-induced atherosclerosis susceptibility. *Circulation.* (2013) 128:632–42. doi: 10.1161/CIRCULATIONAHA.113.002714

127. Duewell P, Kono H, Rayner KJ, Sirois CM, Vladimer G, Bauernfeind FG, et al. NLRP3 inflammasomes are required for atherogenesis and activated by cholesterol crystals. *Nature.* (2010) 464:1357–61. doi: 10.1038/nature08938

128. Folco EJ, Sukhova GK, Quillard T, Libby P. Moderate hypoxia potentiates interleukin-1β production in activated human macrophages. *Circ Res.* (2014) 115:875–83. doi: 10.1161/CIRCRESAHA.115.304437

129. Rajamäki K, Lappalainen J, Oörni K, Välimäki E, Matikainen S, Kovanen PT, et al. Cholesterol crystals activate the NLRP3 inflammasome in human macrophages: a novel link between cholesterol metabolism and inflammation. *PloS One.* (2010) 5:e11765. doi: 10.1371/journal.pone.0011765

130. Zhang W, Wang W, Yu H, Zhang Y, Dai Y, Ning C, et al. Interleukin 6 underlies angiotensin II-induced hypertension and chronic renal damage. *Hypertension (Dallas Tex: 1979).* (2012) 59:136–44. doi: 10.1161/HYPERTENSIONAHA.111.173328

131. Hashmat S, Rudemiller N, Lund H, Abais-Battad JM, Van Why S, Mattson DL. Interleukin-6 inhibition attenuates hypertension and associated renal damage in Dahl salt-sensitive rats. *Am J Physiol Renal Physiol.* (2016) 311(3):F555–61. doi: 10.1152/ajprenal.00594.2015

132. Kamat NV, Thabet SR, Xiao L, Saleh MA, Kirabo A, Madhur MS, et al. Renal transporter activation during angiotensin-II hypertension is blunted in interferon-γ-/- and interleukin-17A-/- mice. *Hypertension (Dallas Tex: 1979).* (2015) 65:569–76. doi: 10.1161/HYPERTENSIONAHA.114.04975

133. Markó L, Kvakan H, Park JK, Qadri F, Spallek B, Binger KJ, et al. Interferon-γ signaling inhibition ameliorates angiotensin II-induced cardiac damage. *Hypertension (Dallas Tex: 1979).* (2012) 60:1430–6. doi: 10.1161/HYPERTENSIONAHA.112.199265

134. Lv W, Booz GW, Wang Y, Fan F, Roman RJ. Inflammation and renal fibrosis: Recent developments on key signaling molecules as potential therapeutic targets. *Eur J Pharmacol.* (2018) 820:65–76. doi: 10.1016/j.ejphar.2017.12.016

135. Steen EH, Wang X, Balaji S, Butte MJ, Bollyky PL, Keswani SG. The role of the anti-inflammatory cytokine interleukin-10 in tissue fibrosis. *Adv Wound Care.* (2020) 9:184–98. doi: 10.1089/wound.2019.1032

136. Sziksz E, Pap D, Lippai R, Béres NJ, Fekete A, Szabó AJ, et al. Fibrosis related inflammatory mediators: role of the IL-10 cytokine family. *Mediators Inflamm.* (2015) 2015:764641. doi: 10.1155/2015/764641

137. Madhur MS, Lob HE, McCann LA, Iwakura Y, Blinder Y, Guzik TJ, et al. Interleukin 17 promotes angiotensin II-induced hypertension and vascular dysfunction. *Hypertension (Dallas Tex: 1979).* (2010) 55:500–7. doi: 10.1161/HYPERTENSIONAHA.109.145094

138. Saleh MA, Norlander AE, Madhur MS. Inhibition of Interleukin 17-A but not Interleukin-17F Signaling Lowers Blood Pressure and Reduces End-organ Inflammation in Angiotensin II-induced Hypertension. *JACC. Basic to Trans science.* (2016) 1:606–16. doi: 10.1016/j.jacbts.2016.07.009

139. Mou X, Zhou DY, Zhou DY, Ma JR, Liu YH, Chen HP, et al. Serum TGF-β1 as a biomarker for type 2 diabetic nephropathy: A meta-analysis of randomized controlled trials. *PloS One.* (2016) 11:e0149513. doi: 10.1371/journal.pone.0149513

140. Isaka Y. Targeting TGF-β Signaling in kidney fibrosis. *Int J Mol Sci.* (2018) 19:2532. doi: 10.3390/ijms19092532

141. Sutariya B, Jhonsa D, Saraf MN. TGF-β: the connecting link between nephropathy and fibrosis. *Immunopharmacol Immunotoxicol*. (2016) 38:39–49. doi: 10.3109/08923973.2015.1127382

142. Wallach D. The tumor necrosis factor family: family conventions and private idiosyncrasies. *Cold Spring Harbor Perspect Biol*. (2018) 10:a028431. doi: 10.1101/cshperspect.a028431

143. Vanamee ÉS, Faustman DL. Structural principles of tumor necrosis factor superfamily signaling. *Sci Signaling*. (2018) 11:eaao4910. doi: 10.1126/scisignal.aao4910

144. Guzik TJ, Hoch NE, Brown KA, McCann LA, Rahman A, Dikalov S, et al. Role of the T cell in the genesis of angiotensin II induced hypertension and vascular dysfunction. *J Exp Med*. (2007) 204:2449–60. doi: 10.1084/jem.20070657

145. Huang B, Cheng Y, Usa K, Liu Y, Baker MA, Mattson DL, et al. Renal tumor necrosis factor α Contributes to hypertension in Dahl salt-sensitive rats. *Sci Rep*. (2016) 6:21960. doi: 10.1038/srep21960

146. Venegas-Pont M, Manigrasso MB, Grifoni SC, LaMarca BB, Maric C, Racusen LC, et al. Tumor necrosis factor-alpha antagonist etanercept decreases blood pressure and protects the kidney in a mouse model of systemic lupus erythematosus. *Hypertension (Dallas Tex: 1979)*. (2010) 56:643–9. doi: 10.1161/HYPERTENSIONAHA.110.157685

147. Elmarakby AA, Quigley JE, Pollock DM, Imig JD. Tumor necrosis factor alpha blockade increases renal Cyp2c23 expression and slows the progression of renal damage in salt-sensitive hypertension. *Hypertension (Dallas Tex: 1979)*. (2006) 47:557–62. doi: 10.1161/01.HYP.0000198545.01860.90

148. Elmarakby AA, Quigley JE, Imig JD, Pollock JS, Pollock DM. TNF-alpha inhibition reduces renal injury in DOCA-salt hypertensive rats. *Am J Physiol Regulatory Integr Comp Physiol*. (2008) 294:R76–83. doi: 10.1152/ajpregu.00466.2007

149. Xu SB, Xu B, Ma ZH, Huang MQ, Gao ZS, Ni JL. Peptide 17 alleviates early hypertensive renal injury by regulating the Hippo/YAP signalling pathway. *Nephrol (Carlton Vic.)*. (2022) 27:712–23. doi: 10.1111/nep.14066

150. Mann DL, McMurray JJV, Packer M, Swedberg K, Borer JS, Colucci WS, et al. Targeted anticytokine therapy in patients with chronic heart failure: results of the Randomized Etanercept Worldwide Evaluation (RENEWAL). *Circulation*. (2004) 109:1594–602. doi: 10.1161/01.CIR.0000124490.27666.B2

151. Chung ES, Packer M, Lo KH, Fasanmade AA, Willerson JTAnti-TNF Therapy Against Congestive Heart Failure Investigators. Randomized, double-blind, placebo-controlled, pilot trial of infliximab, a chimeric monoclonal antibody to tumor necrosis factor-alpha, in patients with moderate-to-severe heart failure: results of the anti-TNF Therapy Against Congestive Heart Failure (ATTACH) trial. *Circulation*. (2003) 107:3133–40. doi: 10.1161/01.CIR.0000077913.60364.D2

152. Egli-Spichtig D, Imenez Silva PH, Glaudemans B, Gehring N, Bettoni C, Zhang MYH, et al. Tumor necrosis factor stimulates fibroblast growth factor 23 levels in chronic kidney disease and non-renal inflammation. *Kidney Int*. (2019) 96:890–905. doi: 10.1016/j.kint.2019.04.009

153. Awad AS, You H, Gao T, Cooper TK, Nedospasov SA, Vacher J, et al. Macrophage-derived tumor necrosis factor-α mediates diabetic renal injury. *Kidney Int*. (2015) 88:722–33. doi: 10.1038/ki.2015.162

154. Singh P, Bahrami L, Castillo A, Majid DSA. TNF-α type 2 receptor mediates renal inflammatory response to chronic angiotensin II administration with high salt intake in mice. *Am J Physiol Renal Physiol*. (2013) 304:F991–999. doi: 10.1152/ajprenal.00525.2012

155. Leaf IA, Nakagawa S, Johnson BG, Cha JJ, Mittelsteadt K, Guckian KM, et al. Pericyte MyD88 and IRAK4 control inflammatory and fibrotic responses to tissue injury. *J Clin Invest*. (2017) 127:321–34. doi: 10.1172/JCI87532

156. Pindjakova J, Hanley SA, Duffy MM, Sutton CE, Weidhofer GA, Miller MN, et al. Interleukin-1 accounts for intrarenal Th17 cell activation during ureteral obstruction. *Kidney Int*. (2012) 81:379–90. doi: 10.1038/ki.2011.348

157. Ridker PM, Everett BM, Thuren T, MacFadyen JG, Chang WH, Ballantyne C, et al. Antiinflammatory therapy with canakinumab for atherosclerotic disease. *N Engl J Med*. (2017) 377:1119–31. doi: 10.1056/NEJMoa1707914

158. Wen Y, Liu Y, Tang T, Lv L, Liu H, Ma K, et al. NLRP3 inflammasome activation is involved in Ang II-induced kidney damage via mitochondrial dysfunction. *Oncotarget*. (2016) 7:54290–302. doi: 10.18632/oncotarget.11091

159. Krishnan SM, Dowling JK, Ling YH, Diep H, Chan CT, Ferens D, et al. Inflammasome activity is essential for one kidney/deoxycorticosterone acetate/salt-induced hypertension in mice. *Br J Pharmacol*. (2016) 173:752–65. doi: 10.1111/bph.13230

160. Shirasuna K, Karasawa T, Usui F, Kobayashi M, Komada T, Kimura H, et al. NLRP3 deficiency improves angiotensin II-induced hypertension but not fetal growth restriction during pregnancy. *Endocrinology*. (2015) 156:4281–92. doi: 10.1210/en.2015-1408

161. Zewinger S, Reiser J, Jankowski V, Alansary D, Hahm E, Triem S, et al. Apolipoprotein C3 induces inflammation and organ damage by alternative inflammasome activation. *Nat Immunol*. (2020) 21:30–41. doi: 10.1038/s41590-019-0548-1

162. Schunk SJ, Hermann J, Sarakpi T, Triem S, Lellig M, Hahm E, et al. Guanidinylated apolipoprotein C3 (ApoC3) associates with kidney and vascular injury. *J Am Soc Nephrol: JASN*. (2021) 32:3146–60. doi: 10.1681/ASN.2021040503

163. Wang W, Wang X, Chun J, Vilaysane A, Clark S, French G, et al. Inflammasome-independent NLRP3 augments TGF-β signaling in kidney epithelium. *J Immunol (Baltimore Md.: 1950)*. (2013) 190:1239–49. doi: 10.4049/jimmunol.1201959

164. Chen D, Xiong XQ, Zang YH, Tong Y, Zhou B, Chen Q, et al. BCL6 attenuates renal inflammation via negative regulation of NLRP3 transcription. *Cell Death Dis*. (2017) 8:e3156. doi: 10.1038/cddis.2017.567

165. Schreiner GF, Kohan DE. Regulation of renal transport processes and hemodynamics by macrophages and lymphocytes. *Am J Physiol*. (1990) 258:F761–767. doi: 10.1152/ajprenal.1990.258.4.F761

166. Kohan DE, Merli CA, Simon EE. Micropuncture localization of the natriuretic effect of interleukin 1. *Am J Physiol*. (1989) 256:F810–813. doi: 10.1152/ajprenal.1989.256.5.F810

167. Takahashi H, Nishimura M, Sakamoto M, Ikegaki I, Nakanishi T, Yoshimura M. Effects of interleukin-1 beta on blood pressure, sympathetic nerve activity, and pituitary endocrine functions in anesthetized rats. *Am J Hypertens*. (1992) 5:224–9. doi: 10.1093/ajh/5.4.224

168. Shi P, Diez-Freire C, Jun JY, Qi Y, Katovich MJ, Li Q, et al. Brain microglial cytokines in neurogenic hypertension. *Hypertension (Dallas Tex: 1979)*. (2010) 56:297–303. doi: 10.1161/HYPERTENSIONAHA.110.150409

169. Voelkel NF, Tuder RM, Bridges J, Arend WP. Interleukin-1 receptor antagonist treatment reduces pulmonary hypertension generated in rats by monocrotaline. *Am J Respir Cell Mol Biol*. (1994) 11:664–75. doi: 10.1165/ajrcmb.11.6.7946395

170. Nowak KL, Chonchol M, Ikizler TA, Farmer-Bailey H, Salas N, Chaudhry R, et al. IL-1 inhibition and vascular function in CKD. *J Am Soc Nephrol: JASN*. (2017) 28:971–80. doi: 10.1681/ASN.2016040453

171. Ling YH, Krishnan SM, Chan CT, Diep H, Ferens D, Chin-Dusting J, et al. Anakinra reduces blood pressure and renal fibrosis in one kidney/DOCA/salt-induced hypertension. *Pharmacol Res*. (2017) 116:77–86. doi: 10.1016/j.phrs.2016.12.015

172. Scheller J, Chalaris A, Schmidt-Arras D, Rose-John S. The pro- and anti-inflammatory properties of the cytokine interleukin-6. *Biochim Et Biophys Acta*. (2011) 1813:878–88. doi: 10.1016/j.bbamcr.2011.01.034

173. Batra G, Ghukasyan Lakic T, Lindbäck J, Held C, White HD, Stewart RAH, et al. Interleukin 6 and cardiovascular outcomes in patients with chronic kidney disease and chronic coronary syndrome. *JAMA Cardiol*. (2021) 6:1440–5. doi: 10.1001/jamacardio.2021.3079

174. Hassan MO, Duarte R, Dickens C, Dix-Peek T, Naidoo S, Vachiat A, et al. Interleukin-6 gene polymorhisms and interleukin-6 levels are associated with atherosclerosis in CKD patients. *Clin Nephrol*. (2020) 93:82–6. doi: 10.5414/CNP92S114

175. Desjardins MP, Sidibé A, Fortier C, Mac-Way F, Marquis K, De Serres S, et al. Association of interleukin-6 with aortic stiffness in end-stage renal disease. *J Am Soc Hypertension: JASH*. (2018) 12:5–13. doi: 10.1016/j.jash.2017.09.013

176. Salimi S, Shardell MD, Seliger SL, Bandinelli S, Guralnik JM, Ferrucci L. Inflammation and trajectory of renal function in community-dwelling older adults. *J Am Geriatrics Society*. (2018) 66:804–11. doi: 10.1111/jgs.15268

177. Chen W, Yuan H, Cao W, Wang T, Chen W, Yu H, et al. Blocking interleukin-6 trans-signaling protects against renal fibrosis by suppressing STAT3 activation. *Theranostics*. (2019) 9:3980–91. doi: 10.7150/thno.32352

178. Rovin BH, van Vollenhoven RF, Aranow C, Wagner C, Gordon R, Zhuang Y, et al. A multicenter, randomized, double-blind, placebo-controlled study to evaluate the efficacy and safety of treatment with sirukumab (CNTO 136) in patients with active lupus nephritis. *Arthritis Rheumatol (Hoboken N.J.)*. (2016) 68:2174–83. doi: 10.1002/art.39722

179. Pergola PE, Devalaraja M, Fishbane S, Chonchol M, Mathur VS, Smith MT, et al. Ziltivekimab for treatment of anemia of inflammation in patients on hemodialysis: results from a phase 1/2 multicenter, randomized, double-blind, placebo-controlled trial. *J Am Soc Nephrol: JASN*. (2021) 32:211–22. doi: 10.1681/ASN.2020050595

180. Fukuda M, Sawa N, Hoshino J, Ohashi K, Motoaki M, Ubara Y. Tocilizumab preserves renal function in rheumatoid arthritis with AA amyloidosis and end-stage kidney disease: Two case reports. *Clin Nephrol*. (2021) 95:54–61. doi: 10.5414/CN109971

181. Gao Y, Liu B, Guo X, Nie J, Zou H, Wen S, et al. Interferon regulatory factor 4 deletion protects against kidney inflammation and fibrosis in deoxycorticosterone acetate/salt hypertension. *J Hypertens*. (2023) 41:794–810. doi: 10.1097/HJH.0000000000003401

182. Lawrence T. The nuclear factor NF-kappaB pathway in inflammation. *Cold Spring Harbor Perspect Biol*. (2009) 1:a001651. doi: 10.1101/cshperspect.a001651

183. Hirohama D, Fujita T. Evaluation of the pathophysiological mechanisms of salt-sensitive hypertension. *Hypertens Res*. (2019) 42:1848–57. doi: 10.1038/s41440-019-0332-5

184. Yan Y, Zhou XE, Xu HE, Melcher K. Structure and physiological regulation of AMPK. *Int J Mol Sci*. (2018) 19:3534. doi: 10.3390/ijms19113534

185. Liu GX, Li YQ, Huang XR, Wei LH, Zhang Y, Feng M, et al. Smad7 inhibits AngII-mediated hypertensive nephropathy in a mouse model of hypertension. *Clin Sci (London England: 1979)*. (2014) 127:195–208. doi: 10.1042/CS20130706

186. Zhao Y, Chen X, Lin Y, Li Z, Su X, Fan S, et al. USP25 inhibits renal fibrosis by regulating TGFβ-SMAD signaling pathway in Ang II-induced hypertensive mice. *Biochim Et Biophys Acta Mol Basis Dis*. (2023) 1869:166713. doi: 10.1016/j.bbadis.2023.166713

187. Huang CC, Lin YY, Yang AL, Kuo TW, Kuo CH, Lee SD. Anti-renal fibrotic effect of exercise training in hypertension. *Int J Mol Sci*. (2018) 19:613. doi: 10.3390/ijms19020613

188. Wen Y, Crowley SD. Renal effects of cytokines in hypertension. *Curr Opin Nephrol Hypertens*. (2018) 27:70–6. doi: 10.1097/MNH.0000000000000385

189. Naing C, Htet NH, Basavaraj AK, Nalliah S. An association between IL-10 promoter polymorphisms and diabetic nephropathy: a meta-analysis of case-control studies. *J Diabetes Metab Disord*. (2018) 17:333–43. doi: 10.1007/s40200-018-0349-3

190. Xia Y, Entman ML, Wang Y. Critical role of CXCL16 in hypertensive kidney injury and fibrosis. *Hypertension (Dallas Tex: 1979)*. (2013) 62:1129–37. doi: 10.1161/HYPERTENSIONAHA.113.01837

191. Rudemiller NP, Patel MB, Zhang JD, Jeffs AD, Karlovich NS, Griffiths R, et al. C-C motif chemokine 5 attenuates angiotensin II-dependent kidney injury by limiting renal macrophage infiltration. *Am J Pathol*. (2016) 186:2846–56. doi: 10.1016/j.ajpath.2016.07.015

192. Mohamed R, Jayakumar C, Chen F, Fulton D, Stepp D, Gansevoort RT, et al. Low-dose IL-17 therapy prevents and reverses diabetic nephropathy, metabolic syndrome, and associated organ fibrosis. *J Am Soc Nephrol: JASN*. (2016) 27:745–65. doi: 10.1681/ASN.2014111136

193. Hamour S, Gan PY, Pepper R, Florez Barros F, Wang HH, O'Sullivan K, et al. Local IL-17 production exerts a protective role in murine experimental glomerulonephritis. *PLoS One*. (2015) 10:e0136238. doi: 10.1371/journal.pone.0136238

194. Krebs CF, Lange S, Niemann G, Rosendahl A, Lehners A, Meyer-Schwesinger C, et al. Deficiency of the interleukin 17/23 axis accelerates renal injury in mice with deoxycorticosterone acetate+angiotensin ii-induced hypertension. *Hypertension (Dallas Tex: 1979)*. (2014) 63:565–71. doi: 10.1161/HYPERTENSIONAHA.113.02620

195. Tang R, Lin W, Shen C, Hu X, Yu L, Meng T, et al. Single-cell transcriptomics uncover hub genes and cell-cell crosstalk in patients with hypertensive nephropathy. *Int Immunopharmacol*. (2023) 125:111104. doi: 10.1016/j.intimp.2023.111104

196. Guzik TJ, Touyz RM. Oxidative stress, inflammation, and vascular aging in hypertension. *Hypertension (Dallas Tex: 1979)*. (2017) 70:660–7. doi: 10.1161/HYPERTENSIONAHA.117.07802

197. Case AJ, Tian J, Zimmerman MC. Increased mitochondrial superoxide in the brain, but not periphery, sensitizes mice to angiotensin II-mediated hypertension. *Redox Biol*. (2017) 11:82–90. doi: 10.1016/j.redox.2016.11.011

198. Mennuni S, Rubattu S, Pierelli G, Tocci G, Fofi C, Volpe M. Hypertension and kidneys: unraveling complex molecular mechanisms underlying hypertensive renal damage. *J Hum Hypertens*. (2014) 28:74–9. doi: 10.1038/jhh.2013.55

199. Rainbolt TK, Saunders JM, Wiseman RL. Stress-responsive regulation of mitochondria through the ER unfolded protein response. *Trends Endocrinol metabolism: TEM*. (2014) 25:528–37. doi: 10.1016/j.tem.2014.06.007

200. Young CN. Endoplasmic reticulum stress in the pathogenesis of hypertension. *Exp Physiol*. (2017) 102:869–84. doi: 10.1113/EP086274

201. Zito E. ERO1: A protein disulfide oxidase and H2O2 producer. *Free Radical Biol Med*. (2015) 83:299–304. doi: 10.1016/j.freeradbiomed.2015.01.011

202. Inagi R. Endoplasmic reticulum stress in the kidney as a novel mediator of kidney injury. *Nephron. Exp Nephrol*. (2009) 112:e1–9. doi: 10.1159/000210573

203. Chiang CK, Hsu SP, Wu CT, Huang JW, Cheng HT, Chang YW, et al. Endoplasmic reticulum stress implicated in the development of renal fibrosis. *Mol Med (Cambridge Mass.)*. (2011) 17:1295–305. doi: 10.2119/molmed.2011.00131

204. He F, Chen S, Wang H, Shao N, Tian X, Jiang H, et al. Regulation of CD2-associated protein influences podocyte endoplasmic reticulum stress-mediated apoptosis induced by albumin overload. *Gene*. (2011) 484:18–25. doi: 10.1016/j.gene.2011.05.025

205. Larbi A, Kempf J, Pawelec G. Oxidative stress modulation and T cell activation. *Exp Gerontol*. (2007) 42:852–8. doi: 10.1016/j.exger.2007.05.004

206. Edison N, Curtz Y, Paland N, Mamriev D, Chorubczyk N, Haviv-Reingewertz T, et al. Degradation of Bcl-2 by XIAP and ARTS promotes apoptosis. *Cell Rep*. (2017) 21:442–54. doi: 10.1016/j.celrep.2017.09.052

207. Larisch S, Yi Y, Lotan R, Kerner H, Eimerl S, Tony Parks W, et al. A novel mitochondrial septin-like protein, ARTS, mediates apoptosis dependent on its P-loop motif. *Nat Cell Biol*. (2000) 2:915–21. doi: 10.1038/35046566

208. Gottfried Y, Rotem A, Lotan R, Steller H, Larisch S. The mitochondrial ARTS protein promotes apoptosis through targeting XIAP. *EMBO J*. (2004) 23:1627–35. doi: 10.1038/sj.emboj.7600155

209. Edison N, Zuri D, Maniv I, Bornstein B, Lev T, Gottfried Y, et al. The IAP-antagonist ARTS initiates caspase activation upstream of cytochrome C and SMAC/Diablo. *Cell Death Differ*. (2012) 19:356–68. doi: 10.1038/cdd.2011.112

210. Liu G, Park SH, Imbesi M, Nathan WJ, Zou X, Zhu Y, et al. Loss of NAD-dependent protein deacetylase sirtuin-2 alters mitochondrial protein acetylation and dysregulates mitophagy. *Antioxidants Redox Signaling*. (2017) 26:849–63. doi: 10.1089/ars.2016.6662

211. He P, Li Z, Yue Z, Gao H, Feng G, Wang P, et al. SIRT3 prevents angiotensin II-induced renal tubular epithelial-mesenchymal transition by ameliorating oxidative stress and mitochondrial dysfunction. *Mol Cell Endocrinol*. (2018) 460:1–13. doi: 10.1016/j.mce.2017.04.027

212. Lin JR, Zheng YJ, Zhang ZB, Shen WL, Li XD, Wei T, et al. Suppression of endothelial-to-mesenchymal transition by SIRT (Sirtuin) 3 alleviated the development of hypertensive renal injury. *Hypertension (Dallas Tex: 1979)*. (2018) 72:350–60. doi: 10.1161/HYPERTENSIONAHA.118.10482

213. Wang Z, Zhai J, Zhang T, He L, Ma S, Zuo Q, et al. Canagliflozin ameliorates epithelial-mesenchymal transition in high-salt diet-induced hypertensive renal injury through restoration of sirtuin 3 expression and the reduction of oxidative stress. *Biochem Biophys Res Commun*. (2023) 653:53–61. doi: 10.1016/j.bbrc.2023.01.084

214. Hallan SI, Øvrehus MA, Bjørneklett R, Aasarød KI, Fogo AB, Ix JH. Hypertensive nephrosclerosis: wider kidney biopsy indications may be needed to improve diagnostics. *J Internal Med*. (2021) 289:69–83. doi: 10.1111/joim.13146

215. Ertuglu LA, Kirabo A. Dendritic cell epithelial sodium channel in inflammation, salt-sensitive hypertension, and kidney damage. *Kidney360*. (2022) 3:1620–9. doi: 10.34067/KID.0001272022

216. Kambayashi T, Laufer TM. Atypical MHC class II-expressing antigen-presenting cells: can anything replace a dendritic cell? Nature Reviews. *Immunology*. (2014) 14:719–30. doi: 10.1038/nri3754

217. Barbaro NR, Foss JD, Kryshtal DO, Tsyba N, Kumaresan S, Xiao L, et al. Dendritic cell Amiloride-sensitive channels mediate sodium-induced inflammation and hypertension. *Cell Rep*. (2017) 21:1009–20. doi: 10.1016/j.celrep.2017.10.002

218. Luft FC, Dechend R, Müller DN. Immune mechanisms in angiotensin II-induced target-organ damage. *Ann Med*. (2012) 44:S49–54. doi: 10.3109/07853890.2011.653396

219. Mehta PK, Griendling KK. Angiotensin II cell signaling: physiological and pathological effects in the cardiovascular system. *Am J Physiol Cell Physiol*. (2007) 292:C82–97. doi: 10.1152/ajpcell.00287.2006

220. Zugasti O, Bose N, Squiban B, Belougne J, Kurz CL, Schroeder FC, et al. Activation of a G protein-coupled receptor by its endogenous ligand triggers the innate immune response of Caenorhabditis elegans. *Nat Immunol*. (2014) 15:833–8. doi: 10.1038/ni.2957

221. Causton B, Ramadas RA, Cho JL, Jones K, Pardo-Saganta A, Rajagopal J, et al. CARMA3 is critical for the initiation of allergic airway inflammation. *J Immunol (Baltimore Md.: 1950)*. (2015) 195:683–94. doi: 10.4049/jimmunol.1402983

222. Fang W, Wang Z, Li Q, Wang X, Zhang Y, Sun Y, et al. Gpr97 exacerbates AKI by mediating sema3A signaling. *J Am Soc Nephrol: JASN*. (2018) 29:1475–89. doi: 10.1681/ASN.2017080932

223. Wu JC, Wang XJ, Zhu JH, Huang XY, Liu M, Qiao Z, et al. GPR97 deficiency ameliorates renal interstitial fibrosis in mouse hypertensive nephropathy. *Acta Pharmacologica Sinica*. (2023) 44:1206–16. doi: 10.1038/s41401-022-01041-y

224. Fu EL, Clase CM, Evans M, Lindholm B, Rotmans JI, Dekker FW, et al. Comparative effectiveness of renin-angiotensin system inhibitors and calcium channel blockers in individuals with advanced CKD: A nationwide observational cohort study. *Am J Kidney Dis*. (2021) 77:719–729.e1. doi: 10.1053/j.ajkd.2020.10.006

225. Unger T, Borghi C, Charchar F, Khan NA, Poulter NR, Prabhakaran D, et al. 2020 International Society of Hypertension global hypertension practice guidelines. *J Hypertens*. (2020) 38:982–1004. doi: 10.1097/HJH.0000000000002453

226. Rovin BH, Adler SG, Barratt J, Bridoux F, Burdge KA, Chan TM, et al. KDIGO 2021 clinical practice guideline for the management of glomerular diseases. *Kidney Int*. (2021) 100:S1–S276. doi: 10.1016/j.kint.2021.05.021

227. Chen TK, Knicely DH, Grams ME. Chronic kidney disease diagnosis and management: A review. *JAMA*. (2019) 322:1294–304. doi: 10.1001/jama.2019.14745

228. Yang X, Zhou B, Zhou L, Cui L, Zeng J, Wang S, et al. Development and validation of prediction models for hypertensive nephropathy, the PANDORA study. *Front Cardiovasc Med*. (2022) 9:794768. doi: 10.3389/fcvm.2022.794768

229. Kokubo Y, Padmanabhan S, Iwashima Y, Yamagishi K, Goto A. Gene and environmental interactions according to the components of lifestyle modifications in hypertension guidelines. *Environ Health Prev Med*. (2019) 24:19. doi: 10.1186/s12199-019-0771-2

230. Sun N, Mu J, Li YWorking Committee of Salt evaluation, Blood Pressure Management, Chinese Medical Association Hypertension Professional Committee, Hypertension Group, Chinese Society of Cardiology. An expert recommendation on salt intake and blood pressure management in Chinese patients with hypertension: A statement of the Chinese Medical Association Hypertension Professional Committee. *J Clin Hypertension (Greenwich Conn.)*. (2019) 21:446–50. doi: 10.1111/jch.13501

231. Goraya N, Simoni J, Jo C, Wesson DE. Dietary acid reduction with fruits and vegetables or bicarbonate attenuates kidney injury in patients with a moderately reduced glomerular filtration rate due to hypertensive nephropathy. *Kidney Int*. (2012) 81:86–93. doi: 10.1038/ki.2011.313

232. Caillon A, Paradis P, Schiffrin EL. Role of immune cells in hypertension. *Br J Pharmacol*. (2019) 176:1818–28. doi: 10.1111/bph.14427

frontiers | Frontiers in Immunology

TYPE Original Research
PUBLISHED 08 April 2024
DOI 10.3389/fimmu.2024.1365591

OPEN ACCESS

EDITED BY
Xu-Jie Zhou,
Peking University, China

REVIEWED BY
Vasiliki Karava,
Aristotle University of Thessaloniki, Greece
Xingyu He,
University of Cincinnati, United States

*CORRESPONDENCE
Tao Ling
ling_tao2022@163.com
Xiaozhu Liu
xiaozhuliu2021@163.com

RECEIVED 04 January 2024
ACCEPTED 25 March 2024
PUBLISHED 08 April 2024

CITATION
Chen Y, Nie Y, Wu J, Li C, Zheng L, Zhu B, Min Y, Ling T and Liu X (2024) Association between systemic inflammatory indicators with the survival of chronic kidney disease: a prospective study based on NHANES. *Front. Immunol.* 15:1365591. doi: 10.3389/fimmu.2024.1365591

Association between systemic inflammatory indicators with the survival of chronic kidney disease: a prospective study based on NHANES

Yuan Chen[1], Yanfang Nie[1], Jiaying Wu[1], Chunsheng Li[1], Lu Zheng[1], Bixiu Zhu[1], Yu Min[2], Tao Ling[3]* and Xiaozhu Liu[4]*

[1]Department of Nephrology, Taizhou Central Hospital (Taizhou University Hospital), Taizhou, Zhejiang, China, [2]Department of Biotherapy and National Clinical Research Center for Geriatrics, Cancer Center, West China Hospital, Sichuan University, Sichuan, China, [3]Department of Pharmacy, Suqian First Hospital, Suqian, China, [4]Department of Critical Care Medicine, Beijing Shijitan Hospital, Capital Medical University, Beijing, China

Background: systemic inflammation disorders were observed in chronic kidney disease (CKD). Whether the systemic inflammatory indicators could be optimal predictors for the survival of CKD remains less studied.

Methods: In this study, participants were selected from the datasets of the National Health and Nutrition Examination Survey (NHANES) between 1999 to 2018 years. Four systemic inflammatory indicators were evaluated by the peripheral blood tests including systemic immune-inflammation index (SII, platelet*neutrophil/lymphocyte), neutrophil-to-lymphocyte ratio (NLR), platelet-to-lymphocyte ratio (PLR), lymphocyte-to-monocyte ratio (LMR). Kaplan-Meier curves, restricted cubic spline (RCS), and Cox regression analysis were used to evaluate the association between the inflammatory index with the all-cause mortality of CKD. Receiver operating characteristic (ROC) and concordance index (C-index) were used to determine the predictive accuracy of varied systemic inflammatory indicators. Sensitive analyses were conducted to validate the robustness of the main findings.

Results: A total of 6,880 participants were included in this study. The mean age was 67.03 years old. Among the study population, the mean levels of systemic inflammatory indicators were 588.35 in SII, 2.45 in NLR, 133.85 in PLR, and 3.76 in LMR, respectively. The systemic inflammatory indicators of SII, NLR, and PLR were all significantly positively associated with the all-cause mortality of CKD patients, whereas the high value of LMR played a protectable role in CKD patients. NLR and LMR were the leading predictors in the survival of CKD patients [Hazard ratio (HR) =1.21, 95% confidence interval (CI): 1.07-1.36, p = 0.003 (3rd quartile), HR = 1.52, 95%CI: 1.35-1.72, p<0.001 (4th quartile) in NLR, and HR = 0.83, 95%CI: 0.75-0.92, p<0.001 (2nd quartile), HR = 0.73, 95%CI: 0.65-0.82, p<0.001 (3rd quartile), and = 0.74, 95%CI: 0.65-0.83, p<0.001 (4th quartile) in LMR], with a C-index of 0.612 and 0.624, respectively. The RCS curves showed non-linearity between systemic inflammatory indicators and all-cause mortality risk of the CKD population.

Conclusion: Our study highlights that systemic inflammatory indicators are important for predicting the survival of the U.S. population with CKD. The systemic inflammatory indicators would add additional clinical value to the health care of the CKD population.

KEYWORDS

chronic kidney disease, systemic inflammatory index, all-cause mortality, NHANES, prospective study

Introduction

Currently, chronic kidney disease (CKD) is an important contributor to morbidity, impaired health-related quality of life (HRQOL), and premature death from noncommunicable diseases, is defined as a reduced glomerular filtration rate (GFR), increased urinary albumin excretion, or both, and is a major public health issue (1–3). In 2017, it was estimated that the prevalence of CKD was estimated as 9.1% with approximately 700 million cases in the world's population (1). In the United States, half of the population is projected to develop the disease throughout their lifetime, and more than 30 million people already have CKD (4). Population with CKD are at remarkably increased risk of cardiovascular disease, and mortality compared to the general population (4). Notably, CKD resulted in 1.2 million deaths and attributed to an additional 1.4 million deaths from cardiovascular disease (1). Therefore, epidemiological studies are warranted to determine new biomarkers for high-risk CKD subpopulation, which would help nephrologists to make timely clinical management decisions.

Systemic inflammatory disorders were frequently observed in CKD patients (5–7). The pro-inflammation condition contributes to the deterioration of kidney function (8–10). The epidemiological and genetic associations between serum levels of systemic inflammation with the incidence and progress of CKD have been established (7, 11–13). Historically, prognostic factors determined in cardiovascular disease (CVD) were prevalent among patients with CKD. However, it might not fully reflect the increased mortality rates among the CKD population. Notably, recent review literature suggested that even low-grade inflammation would play a decisive role in the all-cause mortality of these patients (14). For this reason, identifying the representative but simple systemic inflammatory indicators for predicting survival among CKD patients would bring considerable cost-benefits in clinical practice (4, 14, 15). Of note, several composite inflammatory indicators, including but not limited to systemic immune-inflammation index (SII), neutrophil-to-lymphocyte ratio (NLR), platelet-to-lymphocyte ratio (PLR), and lymphocyte-to-monocyte ratio (LMR), have been validated to be feasible in predicting the prognosis of various cancers and inflammatory diseases (16–19). These composite indicators, comprising biomarkers easily available in clinical settings such as peripheral lymphocytes, platelets, neutrophils, and monocytes, offer a comprehensive reflection of both local immune status and systemic inflammation condition (20–23). Whether these newly developed indicators presented equivalent predictive value in CKD has not been fully investigated. To date, the available evidence regarding this issue was mainly conducted with single center experience or especially interest in the single inflammatory indicator (24, 25). Moreover, whether the conclusions could be generalized to other countries or regions remains unclear.

To fill the mentioned research gaps, we aim to conduct a prospective study to evaluate the association between varied systemic inflammatory indicators with all-cause mortality among the CKD population in the U.S., based on a large-scale, population-based cohort. Besides, we also compared the predictive value of each inflammatory index.

Materials and methods

Data source

The National Health and Nutrition Examination Survey (NHANES) is a representative, ongoing, repeated series of epidemiological surveys regarding the health and nutritional conditions of the noninstitutionalized civilian population in the U.S. The survey contains a wide range of indicators of health and well-being by utilizing a combination of self-reported records and objective physical examinations. Detailed information on NHANES can be found elsewhere (https://www.cdc.gov/nchs/nhanes/). The National Center for Health Statistics Ethics Review Board has approved the NHANES study because the data from NHANES is anonymous and publicly available. All participants provided informed consent. We reported this study following the reporting of observational studies in epidemiology (STROBE) criteria (26).

Study population

Adult participants were selected from the NHANES database within ten cycles of the surveys (1999–2000 to 2017–2018). Participants with a history of CKD were included in the present

study. To evaluate the association between inflammatory indicators with the survival of participants with CKD, participants without records for blood tests were further excluded. Meanwhile, to reduce the adverse causality between systemic inflammatory indicators and CKD mortality, participants who died within two years were excluded. The specific inclusion and exclusion criteria are summarized in Figure 1.

Definition of systemic inflammatory-related indicators

Blood tests were collected by using the automated hematology analysis devices in each cycle of the survey. Considering the clinical accessibility, generalizability, established validity, and comprehensive reflection of the immune as well as inflammatory status of the CKD population, four systemic inflammatory-related indicators of interest were analyzed, including the SII, NLR, PLR, and LMR. Previous studies have validated their effectiveness in predicting outcomes and informing treatment strategies, making them attractive candidates for investigation in our specific research context.

$$SII = \frac{Platelet * Neutrophil}{Lymphocyte}$$

$$NLR = \frac{Neutrophil}{Lymphocyte}$$

$$PLR = \frac{Platelet}{Lymphocyte}$$

$$LMR = \frac{Lymphocyte}{Monocyte}$$

CKD definition

The participants with CKD were diagnosed based on two aspects. On the one hand, the participants had a self-reported history of CKD. On the other hand, eGFR< 60 mL/min/1.73m^2 was additionally used to diagnose the CKD. The eGFR was calculated according to the Chronic Kidney Disease Epidemiology Collaboration algorithm (27).

Covariates definition

The selection of study variables was based on previous literature in evaluating the survival of CKD. A series of covariates were controlled including the socioeconomic characteristics included sex (male or female), age at interview, race (Hispanic, non-Hispanic white, non-Hispanic black, and other race), marital status (not married, married or living with partner), educational level (≤ high school, college, and > college), and family income-poverty ratio (<1.3, 1.3 – 3.5, and >3.5). Besides, the personalized habits and comorbidities include smoking status (never, now, and ever), diabetes mellitus, hypertension, hyperlipidemia, congestive heart failure, and self-reported history of dialysis during the past 12 months. In addition, physical and laboratory examinations included body mass index (BMI), estimated glomerular filtration rate (eGFR), blood urea nitrogen (BUN), alanine transaminase (ALT), aspartate transaminase (AST), glycohemoglobin (HbA1c), and albumin (ALB) were controlled.

Study outcome

The primary outcome was the all-cause mortality of participants with CKD. The survival data for the population were

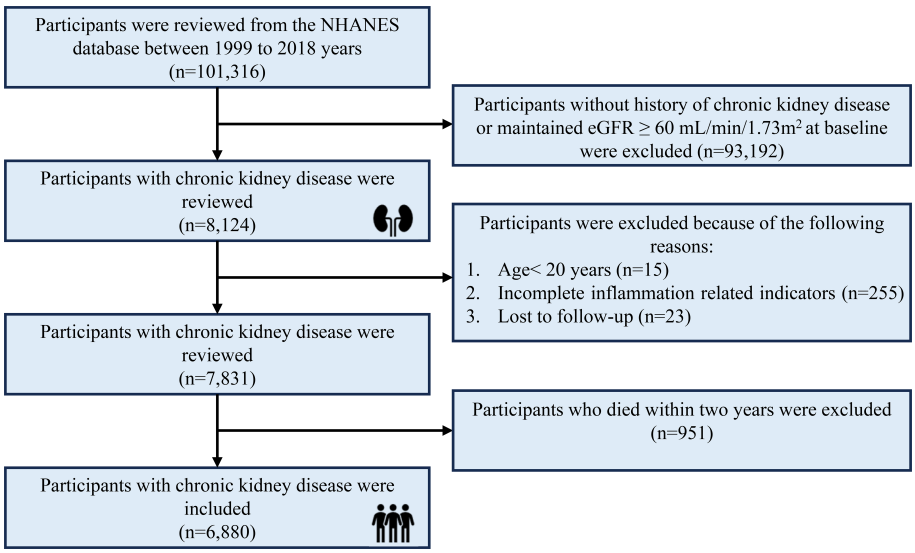

FIGURE 1
The selection process of participants in this study.

obtained from the NHANES public-use linked mortality file as of December 31, 2019, which was correlated with the National Center for Health Statistics (NCHS) with the National Death Index (NDI) through a probability matching algorithm. Additionally, the ICD-10 (International Statistical Classification of Diseases, 10th revision) was applied to identify the underlying causes of mortality. The primary mortality outcome considered in our study was all-cause mortality. The duration of mortality follow-up was calculated from the date when the diagnosis of CKD was initially taken to either the date of the patient's death or December 31, 2019 (28).

Statistical analysis

The continuous variables were presented as mean ± standard deviation (SD). The categorical variables were presented as numbers (percentages, %). The demographic characteristics were compared by using the Student's t-test or One-way analysis of variance for continuous variables and the Chi-squared test was conducted for categorical variables, respectively. Univariate and multivariable Cox regression analyses were conducted to evaluate the associations between varied inflammatory indicators with all-cause mortality of the CKD population. Model 1 served as the crude model with no adjustments. Additionally, adjustments for age, sex, and race were made in Model 2. In the fully adjusted model, covariates including age, sex, race, marital status, educational level, family income-poverty ratio, smoking status, hypertension, hyperlipidemia, diabetes mellitus, congestive heart failure, BMI, eGFR, BUN, ALT, AST, HbA1c, and ALB were adjusted. Meanwhile, Kaplan-Meier (KM) curves were utilized to display the different survival probabilities among the CKD population with varied levels of systemic inflammatory indicators. To assess the potential nonlinear associations of systemic inflammatory indicators with CKD mortality and to capture the variation in risk across the entire continuum of relations, restricted cubic splines (RCS) with 4 knots were employed. Compared with the conventional simple imputation, the random forest imputation method can not only consider the relationships between variables by using a predictive model, leading to more accurate imputations but also provide estimates of variable importance, aiding in understanding the relative importance of different features in the imputation process (29, 30). Thus, to strike a balance between maximizing data completeness and minimizing potential biases introduced by imputation, variables with missing data were interpolated using the random forest interpolation method.

The area under the curve (AUC) of time-dependent receiver operating characteristic (ROC) and concordance index (C-index) were used to compare the predictive accuracy of each inflammatory indicator in predicting the survival of the CKD population.

We performed the sensitivity analyses to check the robustness of the main findings. As dialysis might significantly influence the levels of systemic inflammatory indicators as well as the survival of the CKD population, we reevaluated the association between systemic inflammatory indicators with the all-cause mortality of the CKD population by further adjusting the covariate of history of renal dialysis during the past 12 months.

All statistical analyses were conducted using the R software (version 4.3.2). A two-tailed P-value of< 0.05 was considered as statistically significant.

Results

Baseline information of the participants with CKD

There were 6,880 participants included in the current study during the ten cycles of surveys (1999 – 2018). The mean age of the study population was 67.03 years old. A slightly higher proportion of females than males was observed (3,490 cases vs. 3,390 cases). More than half of the study population was non-Hispanic White (3,571 cases, 51.99%). Less than 20% of the population has an educational level of college. Over 60% of the population had a history of hypertension and nearly half of the study population had hyperlipidemia condition. There were 13.72% and 47.9% of the participants still smoking or drinking in the year of the interview. Compared with the survivors during the follow-up, non-survivors presented characteristics of males, older age, lower BMI, lower levels of eGFR, ALB but higher BUN and HbA1c (all $p<0.001$). Additionally, survivors showed lower serum levels of SII (541.34 ± 368.46 vs. 666.25 ± 522.15, $p<0.001$), NLR (2.25 ± 1.32 vs. 2.77 ± 1.62, $p<0.001$), PLR (127.65 ± 54.50 vs. 144.13 ± 70.41, $p<0.001$), but higher LMR (3.99 ± 1.99 vs. 3.38 ± 2.08, $p<0.001$). The study population with clinical characteristics of older age and non-Hispanic whites tended to present higher levels of pro-inflammation conditions when compared with other groups. The specific clinical information of the study population can be found in Table 1 and the comparisons of varied levels of quartile of inflammatory indicators among the CKD population can be found in Supplementary Tables S1–S4.

Association between systemic inflammatory indicators with all-cause mortality of CKD

The RCS analysis suggested non-linear associations of four systemic inflammatory indicators with the all-cause mortality of participants with CKD (All $p< 0.001$). The inflection point of the RCS curve was identified at 588 in SII, 134 in PLR, 2.4 in NLR, and 3.8 in LMR, respectively (Figure 2).

Besides, the four systemic inflammatory indicators were calculated as categorical variables. The KM curves showed significantly different survival patterns among participants with varied quartiles of systemic inflammatory indicators (All $p< 0.0001$) (Figure 3). Consistently, the higher the quartile of systemic inflammatory indicators (SII, PLR, and NLR) the participants were, the lower survival probabilities were observed. By contrast, the high quartile of levels of LMR predicted an increased survival rate in the CKD population.

10.3389/fimmu.2024.1365591

TABLE 1 The baseline information of the CKD population in this study.

Variable	Total (n = 6,880)	Survivors (n = 4,291)	Non-survivors (n = 2,589)	P [a]
Age	67.03 ± 13.98	62.29 ± 14.23	74.87 ± 9.22	**<.001**
BMI	29.65 ± 6.59	30.15 ± 6.75	28.81 ± 6.24	**<.001**
eGFR	50.62 ± 25.79	54.44 ± 28.33	44.29 ± 19.33	**<.001**
BUN	7.02 ± 3.28	6.49 ± 2.90	7.90 ± 3.68	**<.001**
ALT	22.28 ± 27.56	22.95 ± 17.28	21.17 ± 39.02	**0.009**
AST	25.17 ± 12.83	25.14 ± 13.22	25.23 ± 12.15	0.776
HbA1c	6.05 ± 1.18	6.03 ± 1.17	6.07 ± 1.20	0.171
ALB	41.42 ± 3.38	41.71 ± 3.31	40.95 ± 3.44	**<.001**
SII	588.35 ± 436.92	541.34 ± 368.46	666.25 ± 522.15	**<.001**
NLR	2.45 ± 1.46	2.25 ± 1.32	2.77 ± 1.62	**<.001**
PLR	133.85 ± 61.49	127.65 ± 54.50	144.13 ± 70.41	**<.001**
LMR	3.76 ± 2.05	3.99 ± 1.99	3.38 ± 2.08	**<.001**
Sex				**<.001**
Female	3,490 (50.73)	2,263 (52.74)	1,227 (47.39)	
Male	3,390 (49.27)	2,028 (47.26)	1,362 (52.61)	
Race				**<.001**
Hispanics	1,040 (15.12)	746 (17.39)	294 (11.36)	
Non-Hispanics White	3,571 (51.9)	1,907 (44.44)	1,664 (64.27)	
Non-Hispanics Black	1,920 (27.91)	1,357 (31.62)	563 (21.75)	
Other	349 (5.07)	281 (6.55)	68 (2.63)	
Education level				**<.001**
≤ High school	3,862 (56.13)	2,162 (50.38)	1,700 (65.66)	
College	1,766 (25.67)	1,225 (28.55)	541 (20.90)	
> College	1,252 (18.2)	904 (21.07)	348 (13.44)	
Marital status				**<.001**
Not married	3,202 (46.54)	1,839 (42.86)	1,363 (52.65)	
Married or living with partner	3,678 (53.46)	2,452 (57.14)	1,226 (47.35)	
Family income-poverty ratio				**<.001**
<1.3	1,924 (27.97)	1,139 (26.54)	785 (30.32)	
1.3-3.5	3,291 (47.83)	1,945 (45.33)	1,346 (51.99)	
>3.5	1,665 (24.2)	1207 (28.13)	458 (17.69)	
Hypertension				**<.001**
No	2,398 (34.85)	1,600 (37.29)	798 (30.82)	
Yes	4,482 (65.15)	2,691 (62.71)	1,791 (69.18)	
Hyperlipidemia				**0.023**
No	3,554 (51.66)	2,171 (50.59)	1,383 (53.42)	
Yes	3,326 (48.34)	2,120 (49.41)	1,206 (46.58)	
Diabetes mellitus				**<.001**

(Continued)

TABLE 1 Continued

Variable	Total (n = 6,880)	Survivors (n = 4,291)	Non-survivors (n = 2,589)	P [a]
No	4,957 (72.05)	3,168 (73.83)	1,789 (69.10)	
Yes	1,736 (25.23)	1,004 (23.40)	732 (28.27)	
Borderline	187 (2.72)	119 (2.77)	68 (2.63)	
CHF				**<.001**
No	6,187 (89.93)	4,013 (93.52)	2,174 (83.97)	
Yes	693 (10.07)	278 (6.48)	415 (16.03)	
Smoking status				**<.001**
Never	3,418 (49.68)	2,283 (53.20)	1,135 (43.84)	
Now	944 (13.72)	641 (14.94)	303 (11.70)	
Ever	2,518 (36.6)	1,367 (31.86)	1,151 (44.46)	
Alcohol Use				**<.001**
Never	1,892 (27.64)	944 (22.18)	948 (36.62)	
Now	3,279 (47.9)	2,304 (54.14)	975 (37.66)	
Ever	1,674 (24.46)	1,008 (23.68)	666 (25.72)	

Continuous variables are reported as the mean value with the standard deviation (SD) and categorical variables are reported as the frequency with the percentage in parentheses. [a] Bold value means statistically significant.

CKD, chronic kidney disease; BMI, body mass index; eGFR, estimated glomerular filtration rate; BUN, blood urea nitrogen; ALT, alanine transaminase; AST, aspartate transaminase; HbA1c, glycosylated hemoglobin; ALB, albumin; SII, systemic immune-inflammation index; NLR, neutrophil-to-lymphocyte ratio; PLR, platelet-to-lymphocyte ratio; LMR, lymphocyte-to-monocyte ratio. CHF, congestive heart failure.

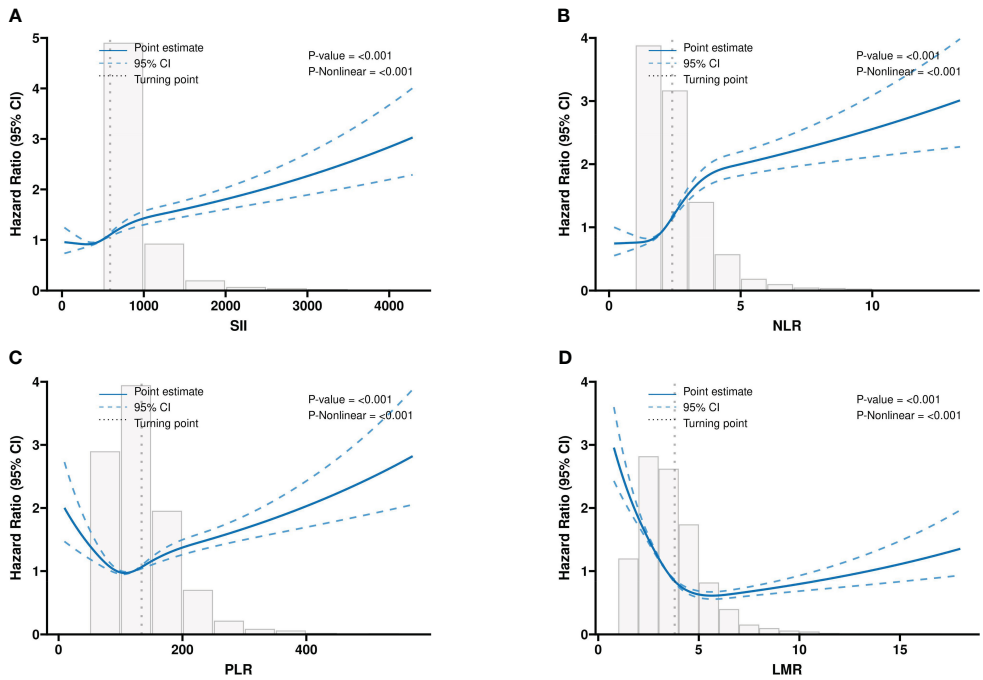

FIGURE 2
The multivariable-adjusted restricted cubic spline (RCS) curves show dose-effect relationships between different systemic inflammatory indicators with the survival of the CKD population. **(A)** SII; **(B)** NLR; **(C)** PLR; **(D)** LMR. CKD: chronic kidney disease; SII: systemic immune-inflammation index; NLR: neutrophil-to-lymphocyte ratio; PLR: platelet-to-lymphocyte ratio; LMR: lymphocyte-to-monocyte ratio. Adjusted for the effects of age, Sex, race, marital status, educational level, family income-poverty ratio, smoking status, hypertension, hyperlipidemia, diabetes mellitus, CHF, BMI, eGFR, BUN, ALT, AST, HbA1c, and ALB.

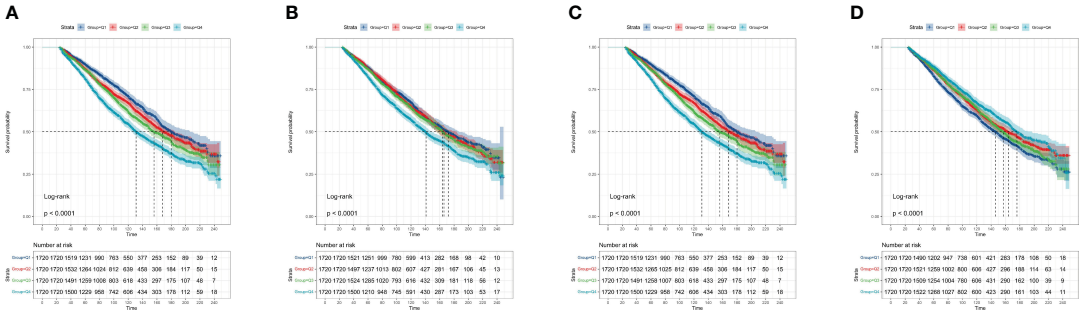

FIGURE 3
The Kaplan-Meier curves display the association between different systemic inflammatory indicators with the survival of the CKD population. **(A)** SII; **(B)** NLR; **(C)** PLR; **(D)** LMR. CKD: chronic kidney disease; SII: systemic immune-inflammation index; NLR: neutrophil-to-lymphocyte ratio; PLR: platelet-to-lymphocyte ratio; LMR: lymphocyte-to-monocyte ratio.

Furthermore, we conducted multivariate Cox regression analyses to evaluate the independent role of varied systemic inflammatory indicators in all-cause mortality among CKD participants (Supplementary Tables S5–S8). As shown in Figure 4, SII was observed as a significant predictor in all-cause mortality of CKD participants [hazard ratio (HR) = 1.13, 95% confidence interval (CI): 0.99-1.27 in 2nd quartile, p = 0.056; HR = 1.13, 95% CI: 1.00-1.28 in 3rd quartile, p = 0.039; HR =1.39, 95%CI: 1.24-1.57 in 4th quartile, p< 0.001] (Figure 4A). Similarly, high quartile levels of NLR were observed as a significant predictor in all-cause mortality of CKD participants [HR = 1.21, 95%CI: 1.07-1.36 in 3rd quartile, p = 0.003; HR = 1.52, 95%CI: 1.35 – 1.72 in 4th quartile, p< 0.001] (Figure 4B). Regarding the PLR, participants at the fourth quartile of the index showed a significantly higher risk for mortality (HR = 1.22, 95%CI: 1.10 – 1.37, p< 0.001) (Figure 4C). Additionally, higher quartile levels of LMR showed a protectable role in the

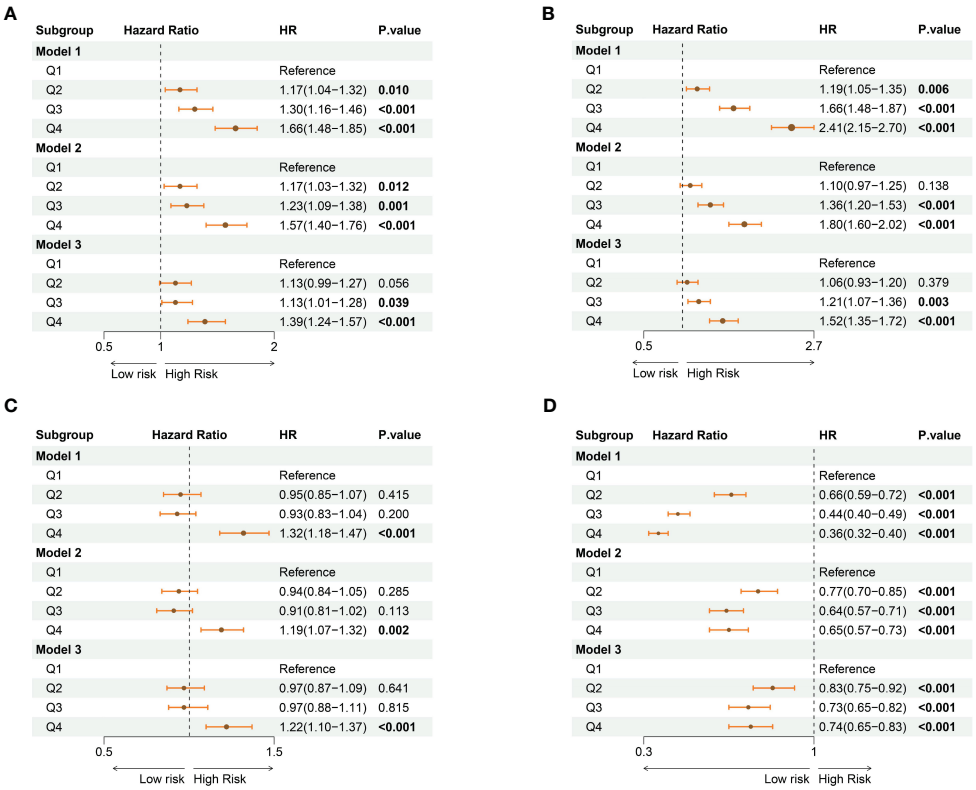

FIGURE 4
The forest plots show the association between varied levels of quartiles of systemic inflammatory indicators with the risk for all-cause mortality among the CKD population. **(A)** SII; **(B)** NLR; **(C)** PLR; **(D)** LMR. CKD: chronic kidney disease; SII: systemic immune-inflammation index; NLR: neutrophil-to-lymphocyte ratio; PLR: platelet-to-lymphocyte ratio; LMR: lymphocyte-to-monocyte ratio. Model 1: no adjustments; Model 2: adjusted for age, sex, and race Model 3: adjusted for age, sex, race, marital status, educational level, family income-poverty ratio, smoking status, hypertension, hyperlipidemia, diabetes mellitus, congestive heart failure, BMI, eGFR, BUN, ALT, AST, HbA1c, and ALB.

survival of CKD participants HR = 0.83, 95%CI: 0.75-0.92 in 2nd quartile, p< 0.001; HR = 0.73, 95%CI: 0.65-0.82 in 3rd quartile, p< 0.001; HR = 0.74, 95%CI: 0.65-0.83 in 4th quartile, p< 0.001] (Figure 4D).

Predictive accuracy of systemic inflammatory indicators with survival of CKD population

The AUCs of time-dependent ROCs showed that the LMR index maintained the highest predictive value in determining the all-cause mortality of the CKD population (AUC=0.621), followed by the NLR index (AUC=0.613), compared with the rest indicators (Figure 5 and Supplementary Table S9). Consistently, the highest C-index was observed in the LMR index (C-index = 0.624) but the lowest C-index was observed in the PLR index (C-index = 0.537) for predicting the survival of the CKD population (Supplementary Table S5). With the combination of other significant clinical factors, the C-index reached 0.789 in the LMR index, 0.785 in the NLR index, 0.779 in SII, and 0.768 in PLR, respectively (Supplementary Table S5).

Stratified and sensitive analyses

There were some interactions among the levels of ALB, family income poverty ratio in SII, NLR, and LMR, and ALT in the PLR index (Supplementary Figures S1–S4). The subgroup analyses showed that features of sex, age at the interview, comorbidity status, family income-poverty ratio, and eGFR status would affect the predictive value of systemic inflammatory indicators on the survival of the CKD population (Supplementary Figures S1–S4). In addition, the LMR index showed a more pronounced predictive value in the stage III CKD subpopulation, while SII showed a stronger association with the stage IV CKD subpopulation (Supplementary Tables S10–S11). However, the predictive values of systemic inflammatory indicators were compromised in the stage V CKD subpopulation (Supplementary Table S12). To verify the robustness of the main findings, we further controlled the clinical information on renal dialysis during the past 12 months before the survey. Consistently, the sensitive analysis supported the significant association between systemic inflammatory indicators and with survival of the CKD population (Supplementary Tables S13–S16).

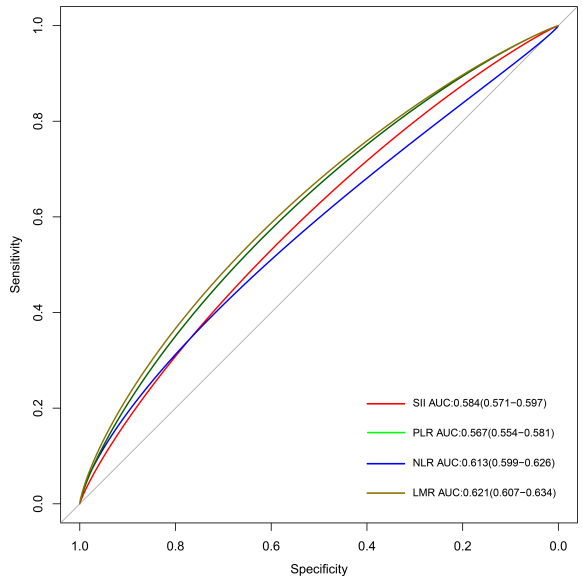

FIGURE 5
The time-dependent ROC curves for displaying the predictive abilities of different systemic inflammatory indicators. SII: systemic immune-inflammation index; NLR: neutrophil-to-lymphocyte ratio; PLR: platelet-to-lymphocyte ratio; LMR: lymphocyte-to-monocyte ratio; ROC: receiver operating characteristic.

Discussion

In the current study, we determined positive associations between systemic inflammatory indicators with the all-cause mortality of the CKD population. In particular, NLR and LMR showed the leading prediction value in clinical outcomes of the CKD population. To the best of our knowledge, this is one of few studies to evaluate the role of systemic inflammatory indicators in the prognosis of the CKD population based on one large-scale, population-based cohort.

To date, CKD remains one of the leading diseases for causing additional comorbidities and premature mortality. Determining new simple prognostic biomarkers would help clinicians make tailored management decisions on this population. Chronic inflammation disorders have been observed in the CKD population, especially in the late-stage group. Therefore, systemic inflammatory indicators derived from frequent blood tests were considered to be a feasible tool in predicting the survival of the CKD population. For instance, one single center-based study revealed that systemic inflammatory indicators presented optimal survival prediction value in acute coronary syndrome patients with CKD, with AUCs between 0.638 and 0.706. Notably, in another large multi–center longitudinal study settled in China, Lai et al. further validated the utility of SII in predicting the total and cause–specific mortality among patients with CKD. In our works, we also observed strong correlations between high levels of pro-inflammatory condition indicators with worse survival probabilities among the CKD population.

Interestingly, NLR and LMR but not SII showed the best predictive powers in predicting the all-cause mortality of the CKD population. The NLR, a surrogate marker for systemic inflammation, has recently gained increasing public interest. Emerging evidence suggested that NLR was associated with several comorbidities, including insulin resistance and CVD (31, 32). Consistently, high levels of NLR were also determined to be related to the occurrence, and poor nutritional status as well as worse prognosis of CKD (33–37). Of note, Yoshitomi and colleagues observed that CKD patients with high NLR showed a nearly 1.7-fold increased risk for poor renal outcome when compared with the low NLR group in Japan (35). Similar associations were also determined in end-stage CKD patients

(37). Nevertheless, the single-center-based experience with a small sample size limited the generalization of findings on this topic. In the current study, we filled this gap and further validated the utility of monitoring the serum NLR in predicting the prognosis of the U.S. population with CKD. Historically, the main possible underlying mechanism regarding the relationship between NLR and the prognosis of the CKD population was thought to be an increase in chronic inflammation. Previous studies have demonstrated a strong association between NLR and inflammatory markers such as TNF-α, CRP, and albumin, suggesting that high NLR reflects chronic inflammatory conditions in CKD patients (38, 39). Novelty, we observed that the high levels of LMR showed a protectable role in the clinical outcome of the CKD population. While the studies evaluating the role of LMR in the prognosis of CKD were limited, compelling evidence has proved the consistent beneficial role of high levels of LMR in other diseases, including but not limited to stroke and cancers (40–42). Recently, peripheral lymphocyte counts have been discovered to have a cell protective effect and contribute to cellular function improvement (42, 43). However, the peripheral monocytes and neutrophils could induce increasing levels of matrix metalloproteinase-9 (MMP-9) and further cause systemic inflammation (44). Furthermore, it was reported that neutrophils could induce free oxygen radicals (45, 46), which was speculated to be associated with reduced renal function and subsequent worse clinical outcomes. different from the promising predictive roles of LMR and NLR on the progress of CKD, only the last quartile level of PLR was observed to be associated with a worse prognosis of the CKD population. Elevated serum levels of platelet indicated endothelial injury and chronic inflammatory condition (47). However, platelet abnormalities were frequently observed in the CKD population, which showed complex implications in the pathophysiology progress of CKD (47). The altered platelet function would result in either platelet hyper- or hypo-reactivity, which might contribute to thrombotic or hemorrhagic complications in CKD (47–49). A recent meta-analysis showed antiplatelet therapy would reduce myocardial infarction and increase major bleeding. However, it did not appear to reduce causes and cardiovascular death among people with CKD and those treated with dialysis (50). A deep understanding of the etiology underlying platelet dysfunction during the CKD progression may contribute to the design of targeted novel antiplatelet treatment strategies, specifically tailored to patients with CKD (47, 48, 50, 51).

There are some strengths worth highlighting. First, this is a prospective, representative, large-scale population-based study based on the U.S. population. Second, we systemic analyzed the predictive value of four systemic inflammatory indicators for all-cause mortality among CKD participants, which provides new evidence for the pivotal role of systemic inflammatory disorders among CKD participants. Third, we excluded the participants who died within 2 years after the interview to reduce the causality bias. Besides, the sensitive analysis also supported the main findings we determined.

Admittedly, some limitations need to be addressed in future works. First, while a series of covariates have been adjusted to determine the association between systemic inflammatory indicators with the survival of CKD participants, some residual confounders such as the duration and cycles of the dialysis, and the history of kidney transplantation with the immunosuppression therapy. As the majority of the CKD population in our study was at stage III, the determined associations between systemic inflammatory indicators and survival of the CKD population might not be impaired. Nevertheless, our findings should be interpreted cautiously due to the diagnosis of CKD was based on the self-reported condition and baseline levels of eGFR. Second, the data was derived from the NHANES program, which could not fully reflect the prevalence and stage of the CKD population. The predictive value of systemic inflammatory indicators in the CKD population at different stages is worth investigating in future works. Moreover, we only analyzed the data of systemic inflammatory indicators at the baseline of the surveys, whether the trajectories of these indicators showed a more pivotal role in predicting the survival of CKD participants needs further exploration. Future well-designed, longitudinal, prospective studies are warranted to validate our findings.

Conclusion

In this study, we observed the significant associations between systemic inflammatory indicators with all-cause mortality of CKD in the U.S. population. Besides, the SII showed the highest prediction value in identifying the high-risk subpopulation with CKD when compared with rest indices. Our findings would help the nephrologists to make dynamic monitoring of the long-term follow-up among the CKD population with simple serum inflammatory levels.

Data availability statement

The original contributions presented in the study are included in the article/Supplementary Material. Further inquiries can be directed to the corresponding authors.

Ethics statement

All survey protocols were approved by the National Center for Health Statistics Review Board in the U.S.A. All participants provided written informed consent before participation.

Author contributions

YC: Conceptualization, Data curation, Formal analysis, Funding acquisition, Investigation, Methodology, Project administration, Resources, Software, Supervision, Validation, Visualization, Writing – original draft, Writing – review & editing. YN: Conceptualization, Data curation, Formal analysis, Investigation, Methodology, Project administration, Resources, Validation, Visualization, Writing – original draft, Writing – review & editing. JW: Conceptualization, Data curation, Formal analysis, Investigation, Methodology, Visualization, Writing –

original draft, Writing – review & editing. CL: Conceptualization, Formal analysis, Investigation, Project administration, Resources, Software, Visualization, Writing – original draft, Writing – review & editing. LZ: Conceptualization, Formal analysis, Investigation, Project administration, Resources, Software, Validation, Visualization, Writing – original draft, Writing – review & editing. BZ: Conceptualization, Investigation, Project administration, Resources, Software, Visualization, Writing – original draft, Writing – review & editing. YM: Data curation, Methodology, Conceptualization, Resources, Visualization, Writing – original draft, Writing – review & editing. TL: Conceptualization, Data curation, Formal analysis, Funding acquisition, Investigation, Methodology, Project administration, Resources, Software, Supervision, Validation, Visualization, Writing – original draft, Writing – review & editing. XL: Conceptualization, Data curation, Formal analysis, Funding acquisition, Investigation, Methodology, Project administration, Resources, Software, Supervision, Validation, Visualization, Writing – original draft, Writing – review & editing.

Funding

The author(s) declare financial support was received for the research, authorship, and/or publication of this article. This research was supported by the Suqian Sci&Tech Program (Grant No: KY202312).

Acknowledgments

We thank Prof. Hanlei Song for checking the method section and revising the discussion section during the revision process.

Conflict of interest

The authors declare that the research was conducted in the absence of any commercial or financial relationships that could be construed as a potential conflict of interest.

Publisher's note

All claims expressed in this article are solely those of the authors and do not necessarily represent those of their affiliated organizations, or those of the publisher, the editors and the reviewers. Any product that may be evaluated in this article, or claim that may be made by its manufacturer, is not guaranteed or endorsed by the publisher.

Supplementary material

The Supplementary Material for this article can be found online at: https://www.frontiersin.org/articles/10.3389/fimmu.2024.1365591/full#supplementary-material

References

1. GBD Chronic Kidney Disease Collaboration. Global, regional, and national burden of chronic kidney disease, 1990-2017: a systematic analysis for the Global Burden of Disease Study 2017. *Lancet (London England).* (2020) 395:709–33. doi: 10.1016/S0140-6736(20)30045-3

2. Fletcher BR, Damery S, Aiyegbusi OL, Anderson N, Calvert M, Cockwell P, et al. Symptom burden and health-related quality of life in chronic kidney disease: A global systematic review and meta-analysis. *PloS Med.* (2022) 19:e1003954. doi: 10.1371/journal.pmed.1003954

3. Jha V, Garcia-Garcia G, Iseki K, Li Z, Naicker S, Plattner B, et al. Chronic kidney disease: global dimension and perspectives. *Lancet (London England).* (2013) 382:260–72. doi: 10.1016/S0140-6736(13)60687-X

4. Luo S, Grams ME. Epidemiology research to foster improvement in chronic kidney disease care. *Kidney Int.* (2020) 97:477–86. doi: 10.1016/j.kint.2019.11.010

5. Cobo G, Lindholm B, Stenvinkel P. Chronic inflammation in end-stage renal disease and dialysis. *Nephrol dialysis Transplant Off Publ Eur Dialysis Transplant Assoc - Eur Renal Assoc.* (2018) 33:iii35–40. doi: 10.1093/ndt/gfy175

6. Drawz P, Rahman M. Chronic kidney disease. *Ann Internal Med.* (2015) 162:Itc1–16. doi: 10.7326/AITC201506020

7. Ebert T, Neytchev O, Witasp A, Kublickiene K, Stenvinkel P, Shiels PG. Inflammation and oxidative stress in chronic kidney disease and dialysis patients. *Antioxidants Redox Signaling.* (2021) 35:1426–48. doi: 10.1089/ars.2020.8184

8. Watson EL, Baker LA, Wilkinson TJ, Gould DW, Xenophontos S, Graham-Brown M, et al. Inflammation and physical dysfunction: responses to moderate intensity exercise in chronic kidney disease. *Nephrol dialysis Transplant Off Publ Eur Dialysis Transplant Assoc - Eur Renal Assoc.* (2022) 37:860–8. doi: 10.1093/ndt/gfab333

9. Zhao X, Wang T, Zhou L. Dose-response analysis of systemic immune-inflammation index and risk of chronic kidney disease. *Int J Surg (London England).* (2023) 110(3):1843–5. doi: 10.1097/JS9.0000000000001007

10. Zoccali C, Mallamaci F. Innate immunity system in patients with cardiovascular and kidney disease. *Circ Res.* (2023) 132:915–32. doi: 10.1161/CIRCRESAHA.122.321749

11. Guo W, Song Y, Sun Y, Du H, Cai Y, You Q, et al. Systemic immune-inflammation index is associated with diabetic kidney disease in Type 2 diabetes mellitus patients: Evidence from NHANES 2011-2018. *Front endocrinol.* (2022) 13:1071465. doi: 10.3389/fendo.2022.1071465

12. Kawalec A, Stojanowski J, Mazurkiewicz P, Choma A, Gaik M, Pluta M, et al. Systemic immune inflammation index as a key predictor of dialysis in pediatric chronic kidney disease with the use of random forest classifier. *J Clin Med.* (2023) 12:6911. doi: 10.3390/jcm12216911

13. Li H, Li M, Liu C, He P, Dong A, Dong S, et al. Causal effects of systemic inflammatory regulators on chronic kidney diseases and renal function: a bidirectional Mendelian randomization study. *Front Immunol.* (2023) 14:1229636. doi: 10.3389/fimmu.2023.1229636

14. Mihai S, Codrici E, Popescu ID, Enciu AM, Albulescu L, Necula LG, et al. Inflammation-related mechanisms in chronic kidney disease prediction, progression, and outcome. *J Immunol Res.* (2018) 2018:2180373. doi: 10.1155/2018/2180373

15. Major RW, Cockwell P, Nitsch D, Tangri N. The next step in chronic kidney disease staging: individualized risk prediction. *Kidney Int.* (2022) 102:456–9. doi: 10.1016/j.kint.2022.06.012

16. Chen JH, Zhai ET, Yuan YJ, Wu KM, Xu JB, Peng JJ, et al. Systemic immune-inflammation index for predicting prognosis of colorectal cancer. *World J gastroenterol.* (2017) 23:6261–72. doi: 10.3748/wjg.v23.i34.6261

17. Zhang Y, Xing Z, Zhou K, Jiang S. The predictive role of systemic inflammation response index (SIRI) in the prognosis of stroke patients. *Clin Interventions aging.* (2021) 16:1997–2007. doi: 10.2147/CIA.S339221

18. Karimi A, Shobeiri P, Kulasinghe A, Rezaei N. Novel systemic inflammation markers to predict COVID-19 prognosis. *Front Immunol.* (2021) 12:741061. doi: 10.3389/fimmu.2021.741061

19. Chen L, Xia S, Zuo Y, Lin Y, Qiu X, Chen Q, et al. Systemic immune inflammation index and peripheral blood carbon dioxide concentration at admission predict poor prognosis in patients with severe traumatic brain injury. *Front Immunol.* (2022) 13:1034916. doi: 10.3389/fimmu.2022.1034916

20. Hu B, Yang XR, Xu Y, Sun YF, Sun C, Guo W, et al. Systemic immune-inflammation index predicts prognosis of patients after curative resection for hepatocellular carcinoma. *Clin Cancer Res an Off J Am Assoc Cancer Res.* (2014) 20:6212–22. doi: 10.1158/1078-0432.CCR-14-0442

21. Zahorec R. Neutrophil-to-lymphocyte ratio, past, present and future perspectives. *Bratislavske lekarske listy*. (2021) 122:474–88. doi: 10.4149/BLL_2021_078

22. Gasparyan AY, Ayvazyan L, Mukanova U, Yessirkepov M, Kitas GD. The platelet-to-lymphocyte ratio as an inflammatory marker in rheumatic diseases. *Ann Lab Med*. (2019) 39:345–57. doi: 10.3343/alm.2019.39.4.345

23. Misiewicz A, Dymicka-Piekarska V. Fashionable, but what is their real clinical usefulness? NLR, LMR, and PLR as a promising indicator in colorectal cancer prognosis: A systematic review. *J Inflamm Res*. (2023) 16:69–81. doi: 10.2147/JIR.S391932

24. Lai W, Xie Y, Zhao X, Xu X, Yu S, Lu H, et al. Elevated systemic immune inflammation level increases the risk of total and cause-specific mortality among patients with chronic kidney disease: a large multi-center longitudinal study. *Inflammation Res Off J Eur Histamine Res Soc [et al]*. (2023) 72:149–58. doi: 10.1007/s00011-022-01659-y

25. Shi S, Kong S, Ni W, Lu Y, Li J, Huang Y, et al. Association of the systemic immune-inflammation index with outcomes in acute coronary syndrome patients with chronic kidney disease. *J Inflamm Res*. (2023) 16:1343–56. doi: 10.2147/JIR.S397615

26. von Elm E, Altman DG, Egger M, Pocock SJ, Gøtzsche PC, Vandenbroucke JP. The Strengthening the Reporting of Observational Studies in Epidemiology (STROBE) statement: guidelines for reporting observational studies. *Lancet (London England)*. (2007) 370:1453–7. doi: 10.1016/S0140-6736(07)61602-X

27. Levey AS, Stevens LA, Schmid CH, Zhang YL, Castro AF 3rd, Feldman HI, et al. A new equation to estimate glomerular filtration rate. *Ann Internal Med*. (2009) 150:604–12. doi: 10.7326/0003-4819-150-9-200905050-00006

28. Cao C, Cade WT, Li S, McMillan J, Friedenreich C, Yang L. Association of balance function with all-cause and cause-specific mortality among US adults. *JAMA otolaryngology– Head Neck surgery*. (2021) 147:460–8. doi: 10.1001/jamaoto.2021.0057

29. Li J, Guo S, Ma R, He J, Zhang X, Rui D, et al. Comparison of the effects of imputation methods for missing data in predictive modelling of cohort study datasets. *BMC Med Res methodology*. (2024) 24:41. doi: 10.1186/s12874-024-02173-x

30. Shah AD, Bartlett JW, Carpenter J, Nicholas O, Hemingway H. Comparison of random forest and parametric imputation models for imputing missing data using MICE: a CALIBER study. *Am J Epidemiol*. (2014) 179:764–74. doi: 10.1093/aje/kwt312

31. Azab B, Chainani V, Shah N, McGinn JT. Neutrophil-lymphocyte ratio as a predictor of major adverse cardiac events among diabetic population: a 4-year follow-up study. *Angiology*. (2013) 64:456–65. doi: 10.1177/0003319712455216

32. Marra A, Bondesan A, Caroli D, Grugni G, Sartorio A. The neutrophil to lymphocyte ratio (NLR) positively correlates with the presence and severity of metabolic syndrome in obese adults, but not in obese children/adolescents. *BMC endocrine Disord*. (2023) 23:121. doi: 10.1186/s12902-023-01369-4

33. Lin CH, Li YH, Wang YY, Chang WD. Higher neutrophil-to-lymphocyte ratio was associated with increased risk of chronic kidney disease in overweight/obese but not normal-weight individuals. *Int J Environ Res Public Health*. (2022) 19(13):8077. doi: 10.3390/ijerph19138077

34. Han Q, Lin S, He F, Zhang R, Xie X, Qing F, et al. A high neutrophil to lymphocyte ratio is associated with poor nutritional status in chronic kidney disease patients. *Br J Nutr*. (2022) 128:1990–6. doi: 10.1017/S000711452100516X

35. Yoshitomi R, Nakayama M, Sakoh T, Fukui A, Katafuchi E, Seki M, et al. High neutrophil/lymphocyte ratio is associated with poor renal outcomes in Japanese patients with chronic kidney disease. *Renal failure*. (2019) 41:238–43. doi: 10.1080/0886022X.2019.1595645

36. Kocyigit I, Eroglu E, Unal A, Sipahioglu MH, Tokgoz B, Oymak O, et al. Role of neutrophil/lymphocyte ratio in prediction of disease progression in patients with stage-4 chronic kidney disease. *J Nephrol*. (2013) 26:358–65. doi: 10.5301/jn.5000152

37. Woziwodzka K, Dziewierz A, Pawica M, Panek A, Krzanowski M, Gołasa P, et al. Neutrophil-to-lymphocyte ratio predicts long-term all-cause mortality in patients with chronic kidney disease stage 5. *Folia Med Cracoviensia*. (2019) 59:55–70. doi: 10.24425/fmc.2019.131380

38. Malhotra R, Marcelli D, von Gersdorff G, Grassmann A, Schaller M, Bayh I, et al. Relationship of neutrophil-to-lymphocyte ratio and serum albumin levels with C-reactive protein in hemodialysis patients: results from 2 international cohort studies. *Nephron*. (2015) 130:263–70. doi: 10.1159/000437005

39. Turkmen K, Guney I, Yerlikaya FH, Tonbul HZ. The relationship between neutrophil-to-lymphocyte ratio and inflammation in end-stage renal disease patients. *Renal failure*. (2012) 34:155–9. doi: 10.3109/0886022X.2011.641514

40. Gong P, Liu Y, Gong Y, Chen G, Zhang X, Wang S, et al. The association of neutrophil to lymphocyte ratio, platelet to lymphocyte ratio, and lymphocyte to monocyte ratio with post-thrombolysis early neurological outcomes in patients with acute ischemic stroke. *J Neuroinflamm*. (2021) 18:51. doi: 10.1186/s12974-021-02090-6

41. Tan D, Fu Y, Tong W, Li F. Prognostic significance of lymphocyte to monocyte ratio in colorectal cancer: A meta-analysis. *Int J Surg (London England)*. (2018) 55:128–38. doi: 10.1016/j.ijsu.2018.05.030

42. Nishijima TF, Muss HB, Shachar SS, Tamura K, Takamatsu Y. Prognostic value of lymphocyte-to-monocyte ratio in patients with solid tumors: A systematic review and meta-analysis. *Cancer Treat Rev*. (2015) 41:971–8. doi: 10.1016/j.ctrv.2015.10.003

43. Macrez R, Ali C, Toutirais O, Le Mauff B, Defer G, Dirnagl U, et al. Stroke and the immune system: from pathophysiology to new therapeutic strategies. *Lancet Neurology*. (2011) 10:471–80. doi: 10.1016/S1474-4422(11)70066-7

44. Yamamoto Y, Osanai T, Nishizaki F, Sukekawa T, Izumiyama K, Sagara S, et al. Matrix metalloprotein-9 activation under cell-to-cell interaction between endothelial cells and monocytes: possible role of hypoxia and tumor necrosis factor-α. *Heart vessels*. (2012) 27:624–33. doi: 10.1007/s00380-011-0214-5

45. Gustafsson A, Asman B. Increased release of free oxygen radicals from peripheral neutrophils in adult periodontitis after Fc delta-receptor stimulation. *J Clin periodontol*. (1996) 23:38–44. doi: 10.1111/j.1600-051X.1996.tb00502.x

46. Winterbourn CC, Kettle AJ, Hampton MB. Reactive oxygen species and neutrophil function. *Annu Rev Biochem*. (2016) 85:765–92. doi: 10.1146/annurev-biochem-060815-014442

47. Baaten C, Schröer JR, Floege J, Marx N, Jankowski J, Berger M, et al. Platelet abnormalities in CKD and their implications for antiplatelet therapy. *Clin J Am Soc Nephrol CJASN*. (2022) 17:155–70. doi: 10.2215/CJN.04100321

48. Daugirdas JT, Bernardo AA. Hemodialysis effect on platelet count and function and hemodialysis-associated thrombocytopenia. *Kidney Int*. (2012) 82:147–57. doi: 10.1038/ki.2012.130

49. Lutz P, Jurk P. Platelets in advanced chronic kidney disease: two sides of the coin. *Semin Thromb hemostasis*. (2020) 46:342–56. doi: 10.1055/s-0040-1708841

50. Natale P, Palmer SC, Saglimbene VM, Ruospo M, Razavian M, Craig JC, et al. Antiplatelet agents for chronic kidney disease. *Cochrane Database systematic Rev*. (2022) 2:Cd008834. doi: 10.1002/14651858.CD008834.pub4

51. Abdelmaguid A, Roberts LN, Tugores L, Joslin JR, Hunt BJ, Parmar K, et al. Evaluation of novel coagulation and platelet function assays in patients with chronic kidney disease. *J Thromb haemostasis JTH*. (2022) 20:845–56. doi: 10.1111/jth.15653

frontiers | Frontiers in Immunology

TYPE Original Research
PUBLISHED 24 April 2024
DOI 10.3389/fimmu.2024.1342350

OPEN ACCESS

EDITED BY
Xu-jie Zhou,
Peking University, China

REVIEWED BY
Juan Antonio Moreno,
University of Cordoba, Spain
Kim Cuong Cap,
Houston Methodist Research Institute,
United States

*CORRESPONDENCE
Xiao-gang Du
cqmudxg@163.com
Wei Ren
weiren67@sina.com

†These authors have contributed equally to this work

RECEIVED 21 November 2023
ACCEPTED 02 April 2024
PUBLISHED 24 April 2024

CITATION
Jiang X-s, Liu T, Xia Y-f, Gan H, Ren W and Du X-g (2024) Activation of the Nrf2/ARE signaling pathway ameliorates hyperlipidemia-induced renal tubular epithelial cell injury by inhibiting mtROS-mediated NLRP3 inflammasome activation. *Front. Immunol.* 15:1342350. doi: 10.3389/fimmu.2024.1342350

Activation of the Nrf2/ARE signaling pathway ameliorates hyperlipidemia-induced renal tubular epithelial cell injury by inhibiting mtROS-mediated NLRP3 inflammasome activation

Xu-shun Jiang[1†], Ting Liu[2†], Yun-feng Xia[1], Hua Gan[1], Wei Ren[3*] and Xiao-gang Du[1,4*]

[1]Department of Nephrology, The First Affiliated Hospital of Chongqing Medical University, Chongqing, China, [2]Department of Cardiology, The First Affiliated Hospital of Chongqing Medical University, Chongqing, China, [3]Department of Endocrinology, The First Affiliated Hospital of Chongqing Medical University, Chongqing, China, [4]The Chongqing Key Laboratory of Translational Medicine in Major Metabolic Diseases, The First Affiliated Hospital of Chongqing Medical University, Chongqing, China

Dyslipidemia is the most prevalent independent risk factor for patients with chronic kidney disease (CKD). Lipid-induced NLRP3 inflammasome activation in kidney-resident cells exacerbates renal injury by causing sterile inflammation. Nuclear factor erythroid 2-related factor 2 (Nrf2) is a transcription factor that modulates the cellular redox balance; however, the exact role of Nrf2 signaling and its regulation of the NLRP3 inflammasome in hyperlipidemia-induced kidney injury are poorly understood. In this study, we demonstrated that activation of the mtROS–NLRP3 inflammasome pathway is a critical contributor to renal tubular epithelial cell (RTEC) apoptosis under hyperlipidemia. In addition, the Nrf2/ARE signaling pathway is activated in renal tubular epithelial cells under hyperlipidemia conditions both *in vivo* and *in vitro*, and Nrf2 silencing accelerated palmitic acid (PA)-induced mtROS production, mitochondrial injury, and NLRP3 inflammasome activation. However, the activation of Nrf2 with tBHQ ameliorated mtROS production, mitochondrial injury, NLRP3 inflammasome activation, and cell apoptosis in PA-induced HK-2 cells and in the kidneys of HFD-induced obese rats. Furthermore, mechanistic studies showed that the potential mechanism of Nrf2-induced NLRP3 inflammasome inhibition involved reducing mtROS generation. Taken together, our results demonstrate that the Nrf2/ARE signaling pathway attenuates hyperlipidemia-induced renal injury through its antioxidative and anti-inflammatory effects through the downregulation of mtROS-mediated NLRP3 inflammasome activation.

KEYWORDS

Nrf2, mitochondrial ROS, NLRP3 inflammasome, hyperlipidemia, renal tubular epithelial cells

1 Introduction

Dyslipidemia is a common metabolic disorder in patients with chronic kidney disease (CKD), including diabetic kidney disease (DKD), and is an independent risk factor for the progression of CKD (1). It is now generally accepted that excess lipid accumulation in the kidney critically contributes to the pathogenesis of diabetic nephropathy (DN) and is closely associated with a progressive decline in renal function (2, 3). In proteinuric kidney disease, including DN, FFA-bound albumin is filtered through the injured glomeruli and reabsorbed by the proximal tubule, which may promote the progression of renal tubular cell damage and tubulointerstitial fibrosis (4, 5).

The NOD-like receptor protein 3 (NLRP3) inflammasome is a cytosolic multiprotein complex that contains NLRP3, apoptosis-related speck protein (ASC), and cysteine aspartate-1 precursor (pro-caspase-1). Moreover, the NLRP3 assembly activates caspase-1, thereby mediating the maturation and secretion of the proinflammatory cytokines IL-1β and IL-18. Previous studies have implicated the activated NLRP3 inflammasome in the pathogenesis of many kidney diseases, including acute kidney injury (AKI), crystal-related nephropathy, and CKD (6). In addition to the key role of the NLRP3 inflammasome in immune cells, previous studies have also demonstrated inflammasome activation in nonimmune cells in the kidney, such as podocytes (7) and renal tubular epithelial cells (8), in kidney disease. Activation of the NLRP3 inflammasome in kidney-resident cells drives sterile inflammation and promotes kidney dysfunction in the context of CKD. It has been reported that the NLRP3 inflammasome is activated in response to sterile stimuli such as hyperglycemia (8), hyperlipidemia (9), angiotensin II (10), and aldosterone (11) in renal tubular epithelial cells. However, the exact mechanism by which hyperlipidemic conditions induce NLRP3 inflammasome activation in renal tubular epithelial cells still needs to be clarified.

Nuclear factor erythroid 2-related factor 2 (Nrf2) is a master regulator that modulates the cell redox balance in response to oxidative stress. Under normal conditions, Nrf2 localizes to the cytoplasm by interacting with Kelch ECH-associated protein 1 (Keap1), a physiological inhibitor of Nrf2 that facilitates Nrf2 ubiquitination and degradation. Under oxidative stress conditions, Nrf2 is released from Keap1, translocates into the nucleus, binds to antioxidant response elements (AREs), and promotes the transcription of antioxidant genes, including NADPH quinine oxidoreductase 1 (NQO1) and heme oxygenase-1 (HO-1) (12). Previous studies have verified that the Nrf2/ARE pathway plays a protective role in diverse human diseases, including inflammatory diseases (13), Parkinson's disease (14), cardiovascular diseases (15), atherosclerosis (16), AKI, and CKD (17). Liu et al. reported that knocking out Nrf2 enhanced susceptibility to ischemic AKI and caused significantly worse renal function, tissue damage, vascular permeability, and mortality in Nrf2 knockout mice following renal I/R than in wild-type mice (18). Alaofi et al. showed that activation of the Nrf2 pathway ameliorated the progression of streptozotocin (STZ)-induced DN in rats (19). However, the potential role that Nrf2/ARE signaling pathways play in the pathogenesis of CKD with dyslipidemia has still not been fully elucidated.

In this study, we aimed to explore the role of the Nrf2/ARE signaling pathway and its regulation of mitochondrial ROS production and NLRP3 inflammasome activation in hyperlipidemia-induced renal tubular epithelial cell injury.

2 Materials and methods

2.1 Cell culture and treatment

Human proximal tubular cells (HK-2 cells) were cultured in DMEM/F-12 medium supplemented with 10% fetal bovine serum (FBS) in a humidified incubator containing 5% CO_2 at 37°C. Transient transfection of HK-2 cells with small interfering RNA (siRNA) was conducted with Lipofectamine 2000 (Invitrogen, CA, USA), and siRNAs (Nrf2 siRNA F: 5′-GCCCAUUGAUGUUUCUGAUTT-3′, R: 5′-AUCAGAAACGAAAUCAAUGGGCTT-3′; scrambled siRNA F: 5′-UUCUCCGAACGUGUCACGUTT-3′, R: 5′-ACGUGACACGU UCGGAGAATT-3′) were synthesized by GenePharma Company (Shanghai, China). For the overexpression of Nrf2, cells were transfected with Nrf2-pcDNA3.1-3xflag-C plasmids (Fenghbio, Hunan, China) using Lipofectamine 2000 reagent. MCC950 (10 μM), Mito Tempol (100 μM), or tBHQ (30 μM) was added to the culture medium for 2 h before exposure to palmitic acid (PA) media.

2.2 Animals

Male Sprague–Dawley rats (n = 24, aged 4 weeks) were obtained from the Animal Center of Chongqing Medical University and housed under pathogen-free conditions with free access to food and water. The rats were divided randomly into the following three groups: a control group, a high-fat diet (HFD) group, and a HFD group treated with tBHQ. The control group rats were fed a normal chow diet (#D12450B; 10 kcal% fat; Research Diet), and the HFD group was fed a Western high-fat diet (#D12451; 45 kcal% fat; Research Diet). The HFD-fed rats in the treatment group were intraperitoneally injected with tBHQ (50 mg/kg, every other day for 12 weeks; Sigma–Aldrich, USA), whereas the control group rats were injected with an equal volume of normal saline. All groups of rats were sacrificed at 20 weeks of age, and blood and kidney tissue samples were obtained for further experimental analysis. All animal experiments were performed in strict accordance with the Ethics Committee of Chongqing Medical University.

2.3 Patients and tissue samples

Kidney tissue samples were collected from the Pathology Department of the First Affiliated Hospital of Chongqing Medical University. For the control group, kidney tissues were collected from six patients who underwent nephrectomy for renal trauma with no other evidence of renal disease. Kidney tissues were collected from eight CKD patients with hyperlipidemia who underwent renal biopsy. Informed consent was obtained from all patients, and the experiments were approved by the Ethics

Committee of The First Affiliated Hospital of Chongqing Medical University. Nrf2 and NLRP3 expression was measured by immunofluorescence and immunohistochemistry.

2.4 Measurement of mitochondrial reactive oxygen species production and the mitochondrial membrane potential (ΔΨm)

To measure mitochondrial ROS, HK-2 cells were seeded on slides in 12-well culture plates. After treatment, live HK-2 cells were stained with 10 μM DCFH-DA and 50 nM MitoTracker Red for 30 min at 37°C or incubated with MitoSOX™ Red fluorescent probe (5 μM, M36008, Invitrogen, USA) at 37°C for 20 min. Moreover, 4-μm-thick frozen sections were stained with 5 μM MitoSOX™ Red fluorescent probe for 20 min at 37°C in the dark. After being washed three times with phosphate-buffered saline (PBS), the stained HK-2 cells and frozen kidney sections were immediately visualized under a fluorescence microscope. The mitochondrial membrane potential was evaluated by using JC-1 dye (Beyotime, China), and live HK-2 cells or frozen kidney sections were incubated with JC-1 staining solution for 20 min at 37°C in the dark. After the cells were washed three times with PBS, images were subsequently acquired with a fluorescence microscope.

2.5 Immunohistochemical staining

Paraffin-embedded renal tissue samples were sliced into 4-mm-thick sections. After deparaffinization in xylene and rehydration in a series of graded alcohols, the target antigens of the tissues were retrieved by microwaving for 15 min in 10 mmol/L sodium citrate buffer (pH 6.0), and endogenous peroxidases were inactivated by 0.3% H_2O_2 for 15 min at room temperature. After being washed, the sections were blocked in normal goat serum buffer for 15 min and then incubated with the following primary antibodies at 4°C overnight: rabbit anti-Nrf2 (1:200, Abcam), rabbit anti-HO-1 (1:200, Abcam), rabbit anti-NQO-1 (1:200, Abcam), rabbit anti-NLRP3 (1:200, CST), rabbit anti-caspase1 (1:200, CST), rabbit anti-IL-18 (1:200, Abcam), and mouse anti-8-OHdG (1:200, Santa Cruz). The sections were washed with PBS, incubated with a biotinylated secondary antibody (Zhongshan Golden Bridge Inc., China) for 30 min, incubated using a 3,3′-diaminobenzidine (DAB) kit for 3–5 min, counterstained with hematoxylin, dehydrated in ethanol, and visualized using a Nikon Eclipse 80i microscope. Quantification of the stained distribution area (area) and the integrated optical density (IOD) of the target protein in each IHC image was performed using ImageJ software. The average optical density (AOD = IOD/area) was used in this study for statistical analysis.

2.6 Immunofluorescence staining

HK-2 cells were seeded on slides in 12-well culture plates. After various treatments, the cells were stained with MitoTracker Red at 37°C for 30 min in the dark, fixed with 4% paraformaldehyde for 10 min, and permeabilized in 0.1% Triton X-100 for 15 min at room temperature. After blocking with 5% BSA buffer, the cells were subsequently incubated with the indicated primary antibodies against NLRP3 (1:200), 8-OHdG (1:200), or Nrf2 (1:200) at 4°C overnight. After washing three times with PBS, the cells were incubated with the corresponding FITC-conjugated secondary antibodies and stained with DAPI. The images were captured using a fluorescence microscope.

2.7 Western blot analysis

Proteins from kidney tissues or HK-2 cells were electrophoretically separated on 8%–10% SDS–polyacrylamide gels and then transferred to PVDF membranes (Millipore, USA). The membranes were blocked with 5% nonfat milk and incubated overnight at 4°C with the following primary antibodies: rabbit anti-NLRP3 (1:1,000, CST), rabbit anti-caspase1 (1:1,000, CST), rabbit anti-IL-18 (1:1,000, Abcam), rabbit anti-Nrf2 (1:1,000, Abcam), rabbit anti-HO-1 (1:5,000, Abcam), rabbit anti-NQO-1 (1:5,000, Abcam), rabbit anti-cleaved-caspase3 (1:1,000, CST), and mouse anti-β-actin (1:5,000, Sungene Biotech). Finally, the membranes were washed three times with TBST and then incubated with the corresponding horseradish peroxidase (HRP)-conjugated secondary antibodies for 1 h, after which the protein bands were visualized using an electrochemiluminescence detection system (GE Healthcare, Piscataway, NJ, USA).

2.8 Analysis of cell apoptosis

Cell apoptosis was detected using an Annexin V-FITC/PI apoptosis assay kit (Sungene Biotech, China). In brief, after double-staining with annexin V and propidine iodide (PI), the number of apoptotic cells was measured by flow cytometry analysis. To assess the extent of renal apoptosis, terminal deoxynucleotidyl transferase dUTP nick end-labeling (TUNEL) staining (*In Situ* Cell Death Detection Kit, POD, Roche) was performed on frozen kidney sections, and the number of TUNEL-positive cells per 0.25 mm^2 was calculated.

2.9 Statistical analysis

All data are expressed as means ± SEM. Qualitative data were analyzed using Student's *t*-test for comparisons between two groups or one-way analysis of variance (ANOVA) followed by Tukey's posttest for comparisons among multiple groups. A value of $P < 0.05$ was considered to indicate statistical significance.

3 Results

3.1 Activation of the NLRP3 inflammasome mediated high-lipid-induced tubular epithelial cell apoptosis

To evaluate the activation of the NLRP3 inflammasome in PA-induced tubular epithelial cells, we determined the expression levels

of NLRP3, mature caspase-1, and the proinflammatory cytokine IL-18, which are used as markers of inflammasome activation. As shown in Figures 1A–H, the protein expression of NLRP3, mature caspase-1, and IL-18 was significantly upregulated in HK-2 cells following PA stimulation in a dose- and time-dependent manner, as determined by western blot analyses. Moreover, immunofluorescence analysis revealed that PA induced an increase in NLRP3 protein expression compared to that in control cells (Figure 1I).

Next, we detected the expression of NLRP3 in the kidney tissue of CKD patients with hyperlipidemia. First, H&E and PAS staining revealed marked glomerular mesangial expansion and increased mesangial matrix in the kidneys of CKD patients with hyperlipidemia (Figure 1J). Masson's trichrome staining revealed that renal fibrosis was enhanced in the kidneys of CKD patients with hyperlipidemia (Figure 1J). Subsequently, immunofluorescence analysis and immunohistochemical staining revealed that the expression of NLRP3 was significantly upregulated in the kidneys of CKD patients with hyperlipidemia (Figures 1K–N). Finally, we investigated the role of NLRP3 inflammasome activation in PA-induced HK-2 cell apoptosis. Flow cytometry showed that MCC950 (a NLRP3 antagonist) treatment significantly ameliorated PA-induced cell apoptosis (Figures 1O, P). Taken together, these results indicated that high lipid levels

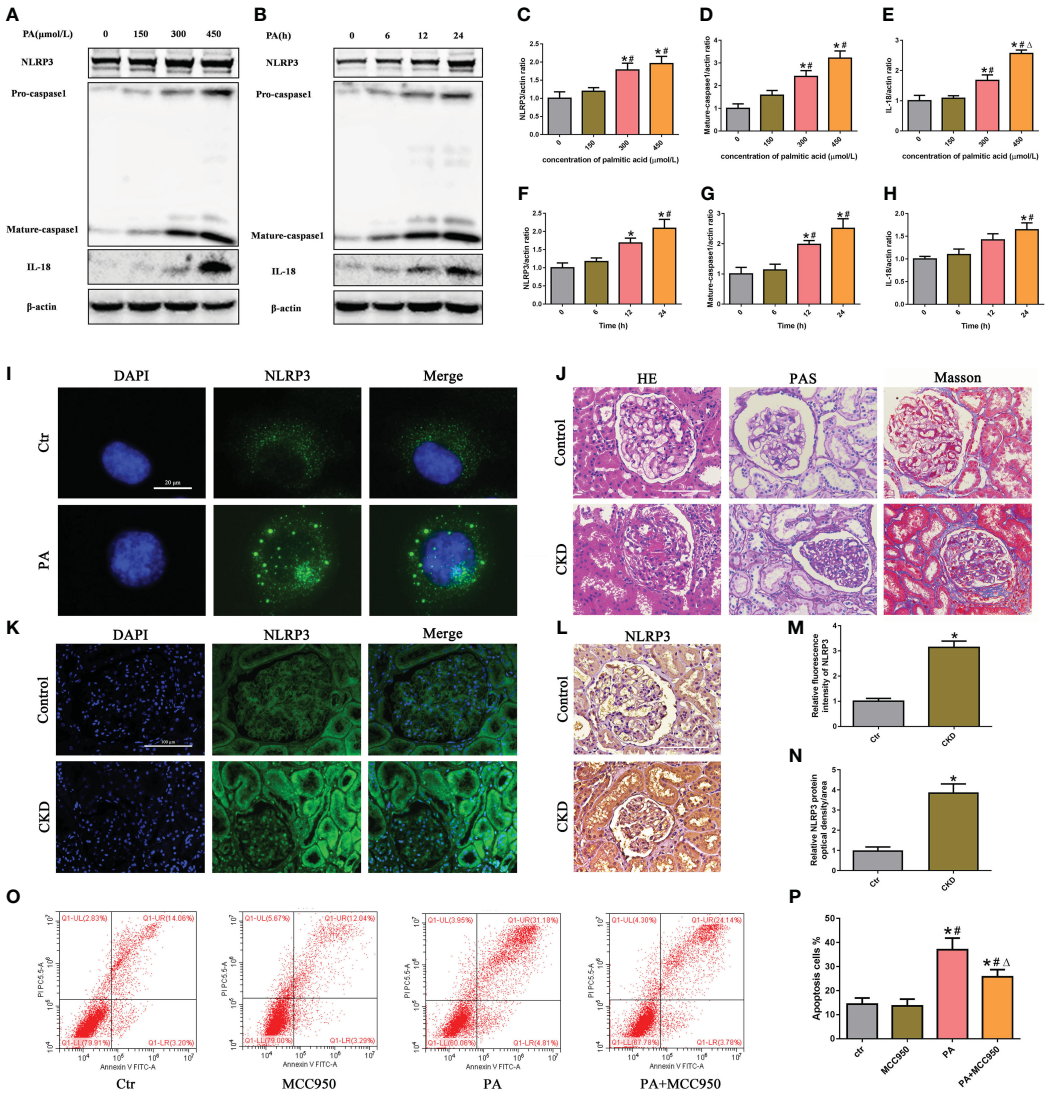

FIGURE 1
Activation of the NLRP3 inflammasome mediated high-lipid-induced tubular epithelial cell apoptosis. **(A, B)** Western blot analyses of the protein expression of NLRP3, caspase-1, and IL-18 in HK-2 cells after treatment with different concentrations of palmitic acid (PA) for 24 h or treatment with 300 μmol/L PA for different durations. **(C–H)** Quantification of NLRP3, caspase-1, and IL-18 expression in **(A, B)** ($n = 3$; $^{*}P < 0.05$ vs. 0 μmol/L or 0 h, $^{\#}P < 0.05$ vs. 150 μmol/L or 6 h, and $^{\Delta}P < 0.05$ vs. 300 μmol/L). **(I)** Representative images of immunofluorescence staining for NLRP3 in HK-2 cells. **(J)** Representative images of kidney sections subjected to H&E, PAS, and Masson staining. **(K)** Representative image of immunofluorescence staining for NLRP3 in kidney sections. **(L)** Representative images of immunohistochemical staining for NLRP3 in kidney sections. **(M)** Quantification analysis of the fluorescence intensities of NLRP3 **(K)** ($n = 6$, $^{*}P < 0.05$ vs. control group). **(N)** Quantification analysis of IHC staining for NLRP3 in **(L)** ($n = 6$, $^{*}P < 0.05$ vs. control group). **(O)** Flow cytometry analysis of cell apoptosis in HK-2 cells. **(P)** Quantification analysis of apoptotic cells in **(O)** ($n = 3$; $^{*}P < 0.05$ vs. control group, $^{\#}P < 0.05$ vs. MCC950 group, and $^{\Delta}P < 0.05$ vs. PA group).

induced NLRP3 inflammasome activation, which promoted tubular epithelial cell apoptosis.

3.2 Role of mtROS in PA-induced mitochondrial damage and NLRP3 inflammasome activation in HK-2 cells

Mitochondria are major sources of ROS and are also targets of ROS. To investigate the role of mtROS in mitochondrial damage, HK-2 cells were treated with the mitochondrion-targeted antioxidant Mito Tempol. Immunofluorescence analysis revealed that Mito Tempol treatment significantly attenuated the production of mtROS (Figures 2A, E) and reversed the loss of (the mitochondrial membrane potential) $\Delta\Psi m$ in HK-2 cells under PA stimulation (Figures 2B, F). Nuclear and mitochondrial DNA oxidative damage can be assessed by immunofluorescence staining for nuclear and nonnuclear 8-OHdG, respectively (20). As shown in Figure 2C, immunofluorescence analysis demonstrated that PA induced an increase in the colocalization of 8-OHdG and mitochondria or nuclei, suggesting that PA induced mitochondrial and nuclear DNA oxidative damage in HK-2 cells. However, Mito Tempol treatment significantly ameliorated PA-induced oxidative damage to mitochondrial and nuclear DNA in HK-2 cells.

Mitochondrial damage plays a pivotal role in NLRP3 inflammasome activation, and previous studies revealed that

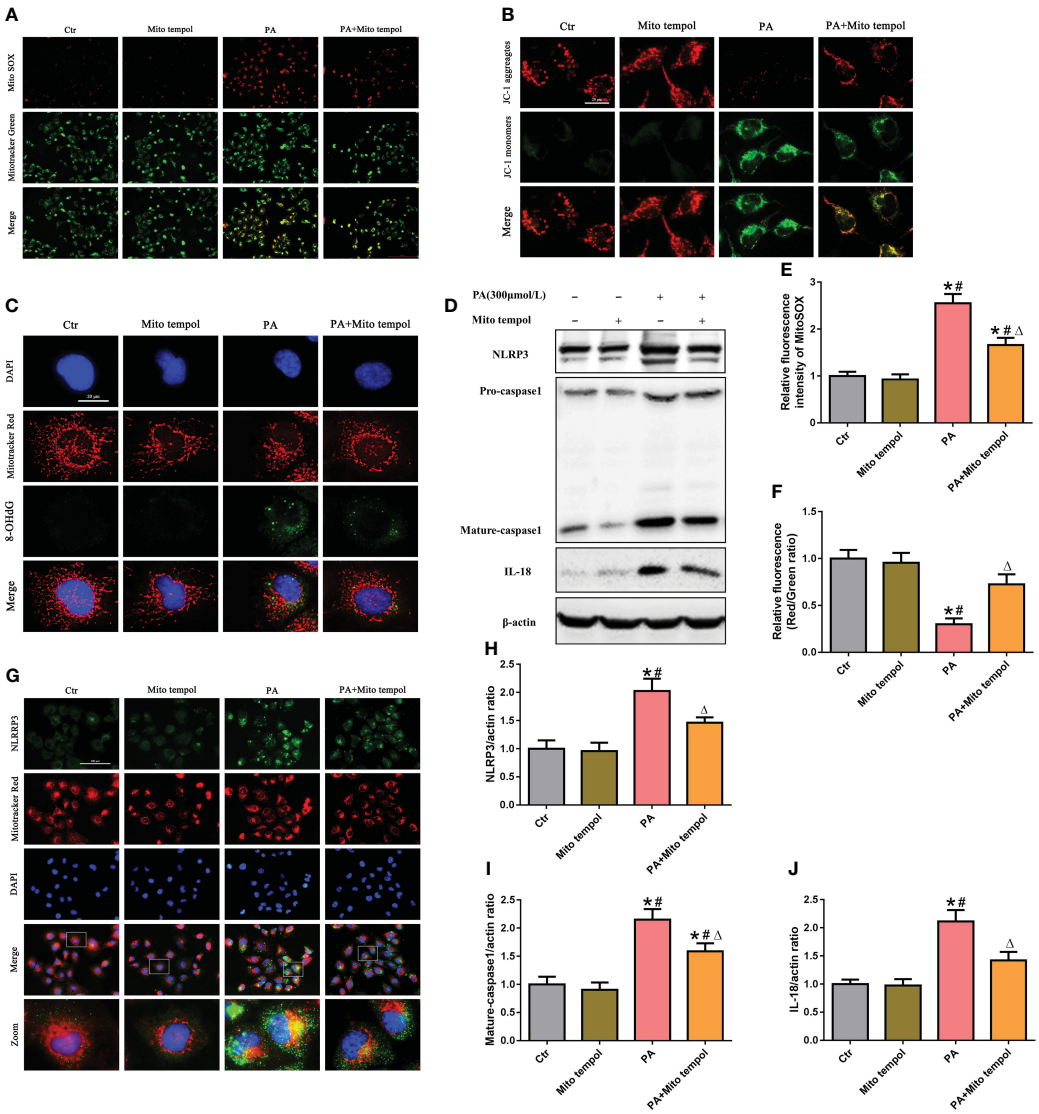

FIGURE 2
Role of mtROS in PA-induced mitochondrial damage and NLRP3 inflammasome activation in HK-2 cells. **(A)** Representative fluorescence images of MitoSOX and MitoTracker Green staining in different groups. **(B)** Representative fluorescence images of JC-1 staining in different groups. **(C)** Representative images of immunofluorescence double-labeled 8-OHdG and mitochondria (MitoTracker Red) in different groups. **(D)** Western blot analyses of the protein expression of NLRP3, caspase-1, and IL-18 in HK-2 cells. **(E, F)** Quantification of the fluorescence intensities of MitoSOX and JC-1 in **(A)** and **(B)** ($n = 3$; $^{*}P < 0.05$ vs. control group, $^{\#}P < 0.05$ vs. Mito Tempol group, and $^{\Delta}P < 0.05$ vs. PA group). **(G)** Representative images of immunofluorescence double-labeled NLRP3 and mitochondria (MitoTracker Red) in the different groups. **(H–J)** Quantification of NLRP3, caspase-1, and IL-18 expression in **(D)** ($n = 3$; $^{*}P < 0.05$ vs. control group, $^{\#}P < 0.05$ vs. Mito Tempol group, and $^{\Delta}P < 0.05$ vs. PA group).

mtROS generated by damaged mitochondria are critically involved in NLRP3 inflammasome activation (21). Similarly, our Western blot analysis showed that Mito Tempol treatment significantly prevented the PA-induced increase in the expression of NLRP3, caspase-1, and IL-18 (Figures 2D, H–J). As mitochondria can serve as a molecular platform for the assembly of NLRP3 inflammasome components (22, 23), which subsequently mediate the maturation and secretion of proinflammatory cytokines, we explored the subcellular localization of NLRP3 inflammasome components under PA stimulation conditions and found that NLRP3 was located in the cytoplasm but not within mitochondria in control cells. However, stimulation with PA led to the recruitment of NLRP3 within mitochondria, as demonstrated by the increasing overlap of NLRP3 in the mitochondria (Figure 2G). However, Mito Tempol treatment inhibited PA-induced NLRP3 upregulation and recruitment within mitochondria (Figure 2G). These results suggested that PA-induced NLRP3 inflammasome activation was dependent on mitochondrial ROS generation.

3.3 The Nrf2/ARE signaling pathway was activated in high-lipid-induced tubular epithelial cells

To determine the effects of PA exposure on the Nrf2/ARE signaling pathway, we measured the expression of Nrf2, HO-1, and NQQ-1 in HK-2 cells and found that they were noticeably increased in a dose-dependent manner under PA stimulation (Figure 3A–D). Additionally, we observed the expression and location of Nrf2 in HK-2 cells. Immunostaining revealed that PA treatment increased the Nrf2 fluorescence intensity and increased the colocalization of Nrf2 with the nucleus, indicating that Nrf2 translocated from the cytoplasm to the nucleus (Figures 3E, F). Furthermore, we detected the expression of Nrf2 in the kidney tissue of CKD patients with hyperlipidemia. As shown in Figures 3G–J, immunohistochemical staining and immunofluorescence analysis revealed that the expression of Nrf2 was significantly upregulated in the kidneys of CKD patients with hyperlipidemia. These results demonstrated that high lipid concentrations activate the Nrf2/ARE signaling pathway in tubular epithelial cells.

3.4 Silencing of Nrf2 enhanced mtROS production and mitochondrial damage in PA-treated HK-2 cells

To determine the role of the Nrf2/ARE signaling pathway in mtROS production and mitochondrial function in PA-treated HK-2 cells, siRNA was used to silence Nrf2. Immunoblot analysis indicated that Nrf2 siRNA successfully suppressed the protein expression of Nrf2 (Figures 4A, B), and Nrf2 silencing significantly decreased the protein expression of Nrf2, HO-1, and NQO-1 in HK-2 cells treated with or without PA (Figures 4C–F). In addition, immunofluorescence staining showed that silencing Nrf2 significantly exacerbated mtROS production (Figures 4G, H) and the loss of $\Delta\Psi m$ (Figures 4I, J) in HK-2 cells cultured in PA media. These data suggested that inhibiting the Nrf2/ARE signaling pathway exacerbated PA-induced mtROS production and mitochondrial damage in HK-2 cells.

3.5 Activation of the Nrf2/ARE signaling pathway ameliorated PA-induced mtROS production and mitochondrial damage in HK-2 cells

We next investigated the effect of tBHQ, a well-characterized Nrf2 activator, on the Nrf2 signaling pathway in HK-2 cells. HK-2 cells were treated with tBHQ at different concentrations (0–50 μM), and as expected, tBHQ dose-dependently increased the protein level of Nrf2 (Figures 5A–D). Consistently, the protein levels of Nrf2 downstream targets, including HO-1 and NQQ-1, were increased in response to tBHQ (Figures 5A–D). Next, we incubated HK-2 cells with PA in the absence or presence of 30 μM tBHQ for 24 h and found that tBHQ ameliorated PA-induced mitochondrial ROS production (Figures 5F, G), mitochondrial injury (Figures 5H, I), and mitochondrial DNA oxidative damage (Figure 5J). Similarly, transfection of HK-2 cells with an Nrf2 overexpression plasmid (Figure 5E) significantly attenuated mitochondrial ROS production (Figures 5F, G) and reversed PA-induced mitochondrial membrane potential collapse (Figures 5H, I) and mitochondrial DNA oxidative damage (Figure 5J).

3.6 The Nrf2/ARE signaling pathway inhibited PA-induced mtROS-dependent NLRP3 inflammasome activation in HK-2 cells

To further investigate the possible role of Nrf2 in NLRP3 inflammasome activation, PA-stimulated HK-2 cells were pretreated with tBHQ, as shown in Figures 6A, F–H. tBHQ treatment markedly inhibited the activation of the NLRP3 inflammasome in PA-treated HK-2 cells, as characterized by decreased NLRP3, caspase-1. and IL-18 levels. Moreover, we found that tBHQ significantly inhibited PA-induced colocalization of NLRP3 and MitoTracker (Figure 6B) and ameliorated PA-induced cell apoptosis in HK-2 cells (Figures 6C, D), demonstrating that the Nrf2/ARE signaling pathway plays a protective role in PA-induced cell apoptosis by inhibiting NLRP3 inflammasome activation in HK-2 cells. Next, we studied the underlying mechanism of the inhibitory effects of the Nrf2/ARE signaling pathway on NLRP3 inflammasome activation. Considering the regulatory effect of the Nrf2/ARE pathway on mtROS production, HK-2 cells were pretreated with Mito Tempol or/and Nrf2 siRNA, and knockdown of Nrf2 significantly increased the PA-induced expression of NLRP3, mature caspase-1, and IL-18 (Figure 6E). However, the enhancing effect of Nrf2 siRNA on NLRP3 inflammasome activation was markedly reversed by Mito Tempol intervention (Figures 6E, I–K). Collectively, these results indicated that Nrf2-induced NLRP3 inflammasome inhibition was dependent on mtROS production.

10.3389/fimmu.2024.1342350

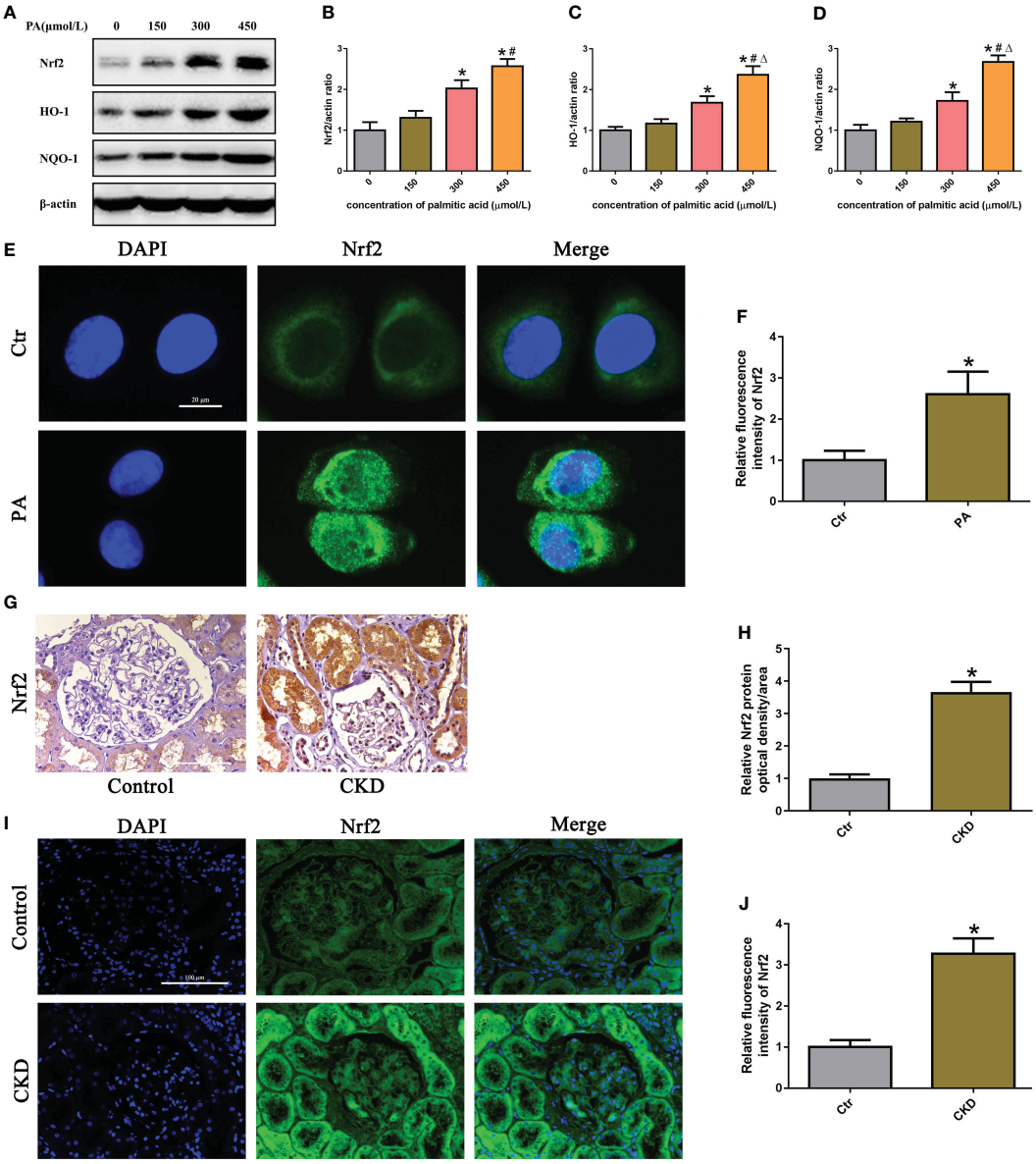

FIGURE 3
The Nrf2/ARE signaling pathway was activated in high-lipid-induced tubular epithelial cells. **(A)** Western blot analyses of the protein expression of Nrf2, HO-1, and NQO-1 in HK-2 cells. **(B–D)** Quantification of Nrf2, HO-1, and NQO-1 expression in **(A)** ($n = 3$; $^{*}P < 0.05$ vs. 0 μmol/L, $^{\#}P < 0.05$ vs. 150 μmol/L, and $^{\Delta}P < 0.05$ vs. 300 μmol/L). **(E)** Representative images of immunofluorescence staining for Nrf2 in HK-2 cells. **(F)** Quantification analysis of the fluorescence intensities of Nrf2 in **(E)** ($n = 3$, $^{*}P < 0.05$ vs. control group). **(G)** Representative images of immunohistochemical staining for Nrf2 in kidney sections. **(H)** Quantification analysis of IHC staining for Nrf2 in **(G)** ($n = 6$, $^{*}P < 0.05$ vs. control group). **(I)** Representative images of immunofluorescence staining for Nrf2 in kidney sections. **(J)** Quantification analysis of the fluorescence intensities of Nrf2 in **(I)** ($n = 6$, $^{*}P < 0.05$ vs. control group).

3.7 Activation of the Nrf2/ARE signaling pathway improved biochemical characteristics and morphological changes and ameliorated renal injury in HFD-induced obese rats

As shown in Figures 7A–F, compared with those in LFD-fed rats, body weight, blood urea nitrogen (BUN), serum creatinine (SCr), urine protein, total cholesterol (TC), and triglyceride (TG) levels were significantly greater in HFD-fed rats; however, tBHQ intervention significantly attenuated these parameters, except for body weight, relative to those in HFD-fed rats. Oil red O staining showed that abnormal lipid accumulation was notably increased in renal proximal tubule cells of HFD-fed rats; however, tBHQ treatment markedly attenuated lipid deposition in renal proximal tubule cells in HFD-fed rats (Figure 7G). Additionally, H&E and PAS staining of the kidneys of HFD-fed rats revealed enhanced glomerular hypertrophy, mesangial proliferation, mesangial matrix deposition, and notable disruption of tubular epithelial cells compared to those of LFD-fed rats (Figures 7H, I). Masson trichrome staining revealed marked renal fibrosis in HFD-fed rats (Figure 7J); however, these changes were dramatically limited by

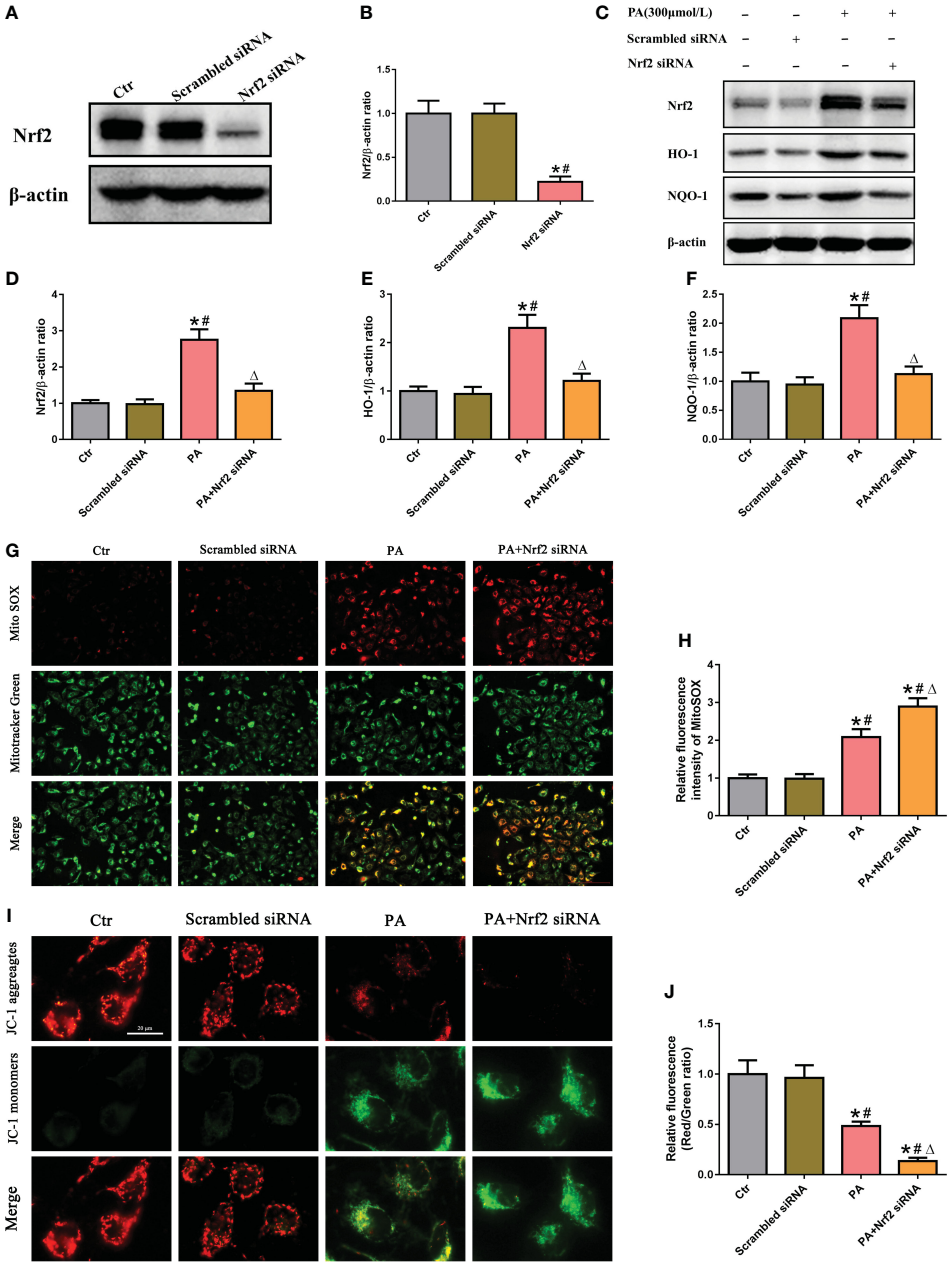

FIGURE 4
Silencing of Nrf2 enhanced mtROS production and mitochondrial damage in PA-treated HK-2 cells. **(A)** Western blot analyses of the protein expression of Nrf2 in HK-2 cells after transfection with scrambled siRNA or Nrf2 siRNA. **(B)** Quantification analysis of Nrf2 expression in **(A)** ($n = 3$; $^{*}P < 0.05$ vs. control group and $^{\#}P < 0.05$ vs. scrambled siRNA group). **(C)** Western blot analyses of the protein expression of Nrf2, HO-1, and NQO-1 in different groups. **(D–F)** Quantification analysis of Nrf2, HO-1, and NQO-1 expression in **(C)** ($n = 3$; $^{*}P < 0.05$ vs. control group, $^{\#}P < 0.05$ vs. scrambled siRNA group, and $^{\Delta}P < 0.05$ vs. PA group). **(G)** Representative fluorescence images of MitoSOX and MitoTracker Green staining in different groups. **(H)** Quantification of the fluorescence intensities of MitoSOX in **(G)** ($n = 3$; $^{*}P < 0.05$ vs. control group, $^{\#}P < 0.05$ vs. scrambled siRNA group, and $^{\Delta}P < 0.05$ vs. PA group). **(I)** Representative fluorescence images of JC-1 staining in different groups. **(J)** Quantification of the fluorescence intensities of JC-1 in **(I)** ($n = 3$; $^{*}P < 0.05$ vs. control group, $^{\#}P < 0.05$ vs. scrambled siRNA group, and $^{\Delta}P < 0.05$ vs. PA group).

tBHQ treatment. Moreover, mtROS generation (Figures 7K, O), ΔΨm loss (Figures 7L, P), and DNA oxidative damage (Figures 7M, Q) were enhanced in the kidneys of HFD-fed rats but markedly attenuated after tBHQ treatment. Furthermore, TUNEL staining demonstrated that the number of apoptotic cells (indicated by the arrow) was significantly reversed by tBHQ treatment (Figures 7N, R). Overall, these data demonstrated that tBHQ improved renal function in HFD-induced obese rats.

3.8 The Nrf2/ARE pathway inhibited NLRP3 inflammasome activation in the kidneys of HFD-induced obese rats

Finally, we investigated the role of the Nrf2/ARE pathway in the activation of the NLRP3 inflammasome in HFD-induced obese rats. Immunoblot analysis demonstrated that the expression of Nrf2, HO-1, NQO-1, NLRP3, mature-caspase-1, and IL-18 was significantly

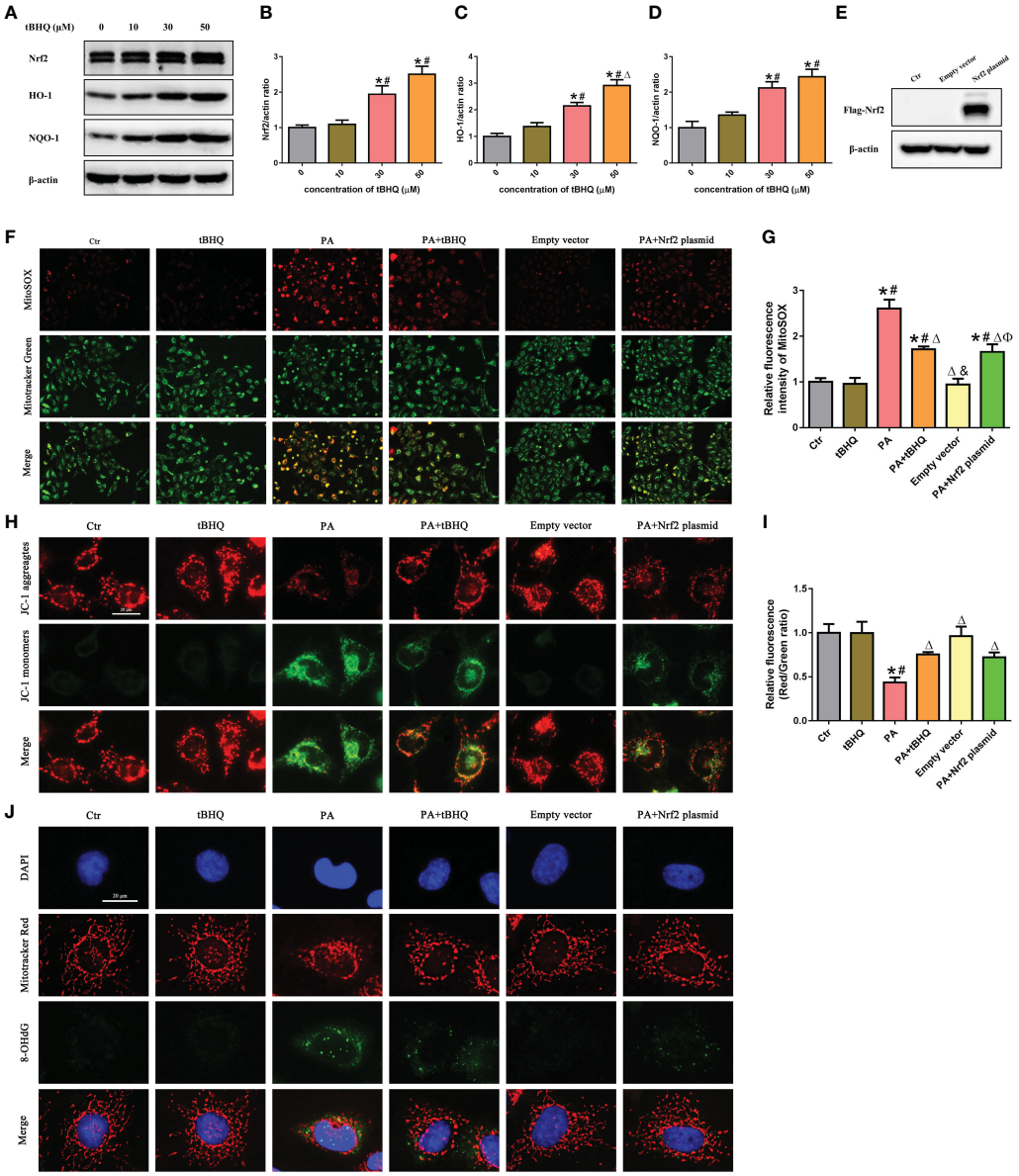

FIGURE 5
Activation of the Nrf2/ARE signaling pathway ameliorated PA-induced mtROS production and mitochondrial damage in HK-2 cells. **(A)** Western blot analyses of the protein expression of Nrf2, HO-1, and NQO-1 in HK-2 cells after being treated with various concentrations of tBHQ (0, 10, 30, and 50 μM). **(B–D)** Quantification analysis of Nrf2, HO-1, and NQO-1 expression in **(A)** ($n = 3$; $^{*}P < 0.05$ vs. 0 μmol/L, $^{\#}P < 0.05$ vs. 10 μmol/L A group, and $^{\Delta}P < 0.05$ vs. 30 μmol/L group). **(E)** Western blot analyses of the protein expression of Flag-Nrf2 in HK-2 cells after being transfected with or without empty plasmid or Nrf2 overexpression plasmid. **(F)** HK-2 cells were treated with 300 μmol/L PA for 24 h after being pretreated with tBHQ or transfected with Nrf2 overexpression plasmid and then stained with Mito SOX (red) and MitoTracker (green). **(G)** Quantification of the fluorescence intensities of MitoSOX in **(F)** ($n = 3$; $^{*}P < 0.05$ vs. control group, $^{\#}P < 0.05$ vs. tBHQ group, $^{\Delta}P < 0.05$ vs. PA group, $^{\&}P < 0.05$ vs. PA + tBHQ group, and $^{\Phi}P < 0.05$ vs. empty vector group). **(H)** HK-2 cells were treated with 300 μmol/L PA for 24 h after being pretreated with tBHQ or transfected with Nrf2 overexpression plasmid and then stained with probe JC-1. **(I)** Quantification of the fluorescence intensities of JC-1 in **(H)** ($n = 3$; $^{*}P < 0.05$ vs. control group, $^{\#}P < 0.05$ vs. tBHQ group, and $^{\Delta}P < 0.05$ vs. PA group). **(J)** HK-2 cells were treated with 300 μmol/L PA for 24 h after being pretreated with tBHQ or transfected with Nrf2 overexpression plasmid and then stained with MitoTracker (red) and an antibody against 8-OHdG.

upregulated in the HFD group compared to the LFD group (Figures 8A, C). Additionally, the expression of Nrf2, HO-1, and NQQ-1 was significantly greater in HFD-fed rats after tBHQ intervention (Figures 8A, C). However, the HFD-induced increase in the expression of NLRP3, mature caspase-1, and IL-18 was significantly attenuated following treatment with tBHQ (Figures 8A,C). Subsequently, immunohistochemical staining (Figures 8B, D) also supported the above-mentioned results, indicating that the upregulation of the Nrf2/ARE pathway inhibited the activation of the NLRP3 inflammasome in the kidneys of HFD-induced obese rats.

10.3389/fimmu.2024.1342350

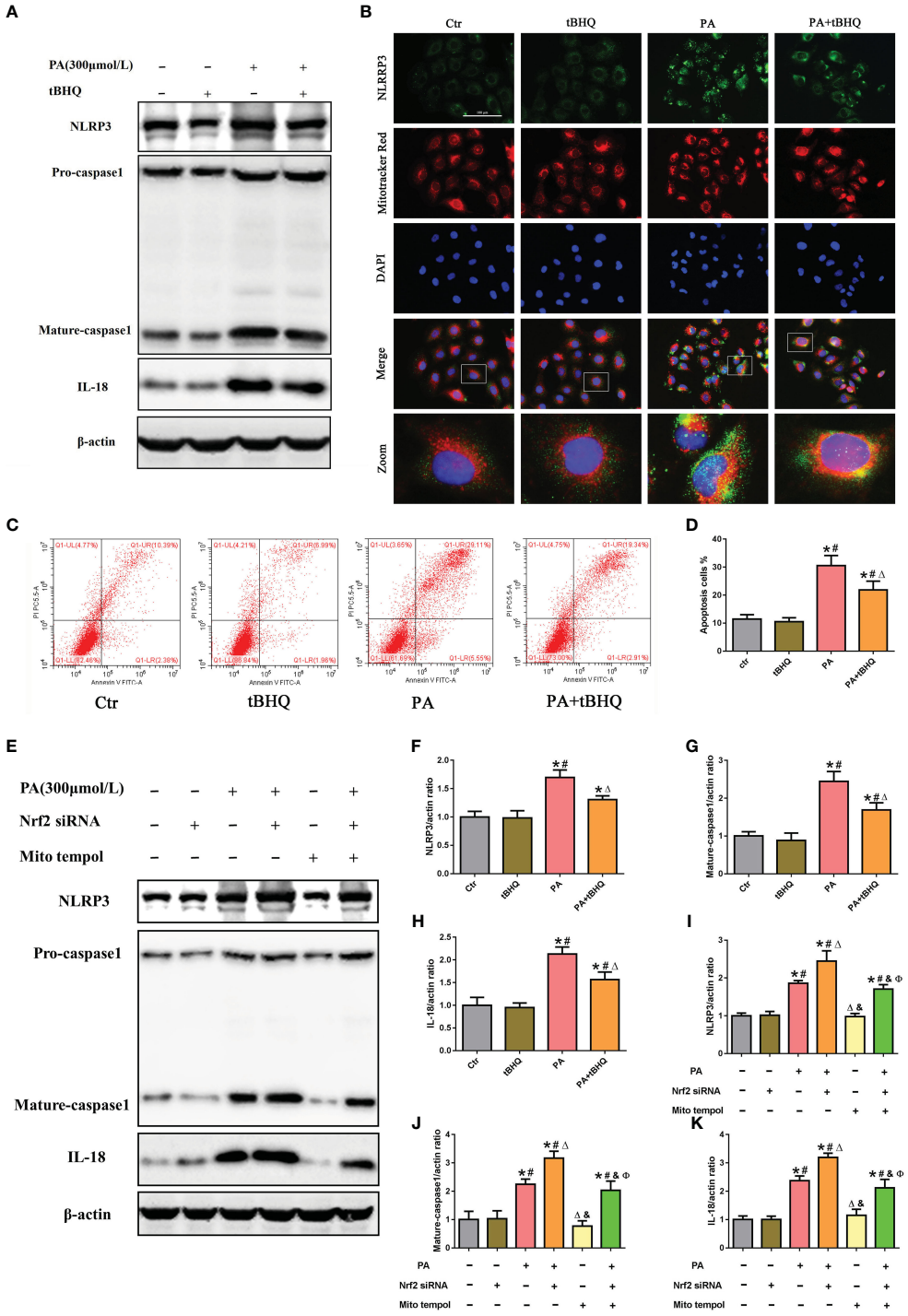

FIGURE 6
The Nrf2/ARE signaling pathway inhibited palmitic acid (PA)-induced mitochondrial ROS-dependent NLRP3 inflammasome activation in HK-2 cells. **(A)** Western blot analyses of the protein expression of NLRP3, caspase-1, and IL-18 in HK-2 cells after being pretreated with 30 μM tBHQ and then stimulated with 300 μmol/L PA for 24(h) **(B)** Representative images of immunofluorescence double-labeled NLRP3 and mitochondria (MitoTracker Red) in different groups. **(C)** Flow cytometry analysis of cell apoptosis in different groups. **(D)** Quantification analysis of apoptotic cells in **(C)** (n = 3; $^{*}P$ < 0.05 vs. control group, $^{\#}P$ < 0.05 vs. tBHQ group, and $^{\Delta}P$ < 0.05 vs. PA group). **(E)** Western blot analyses of the protein expression of NLRP3, caspase-1, and IL-18 in HK-2 cells after being pretreated with Mito Tempol or Nrf2 siRNA and then stimulated with 300 μmol/L PA for 24 (h) **(F–H)** Quantification analysis of NLRP3, caspase-1, and IL-18 expression in **(A)** (n = 3; $^{*}P$ < 0.05 vs. control group, $^{\#}P$ < 0.05 vs. tBHQ group, and $^{\Delta}P$ < 0.05 vs. PA group). **(I–K)** Quantification analysis of NLRP3, caspase-1, and IL-18 expression in **(E)** (n = 3; $^{*}P$ < 0.05 vs. control group, $^{\#}P$ < 0.05 vs. Nrf2 siRNA group, $^{\Delta}P$ < 0.05 vs. PA group, $^{\&}P$< 0.05 vs. PA + Nrf2 siRNA group, and $^{\Phi}P$< 0.05 vs. Mito Tempol group).

10.3389/fimmu.2024.1342350

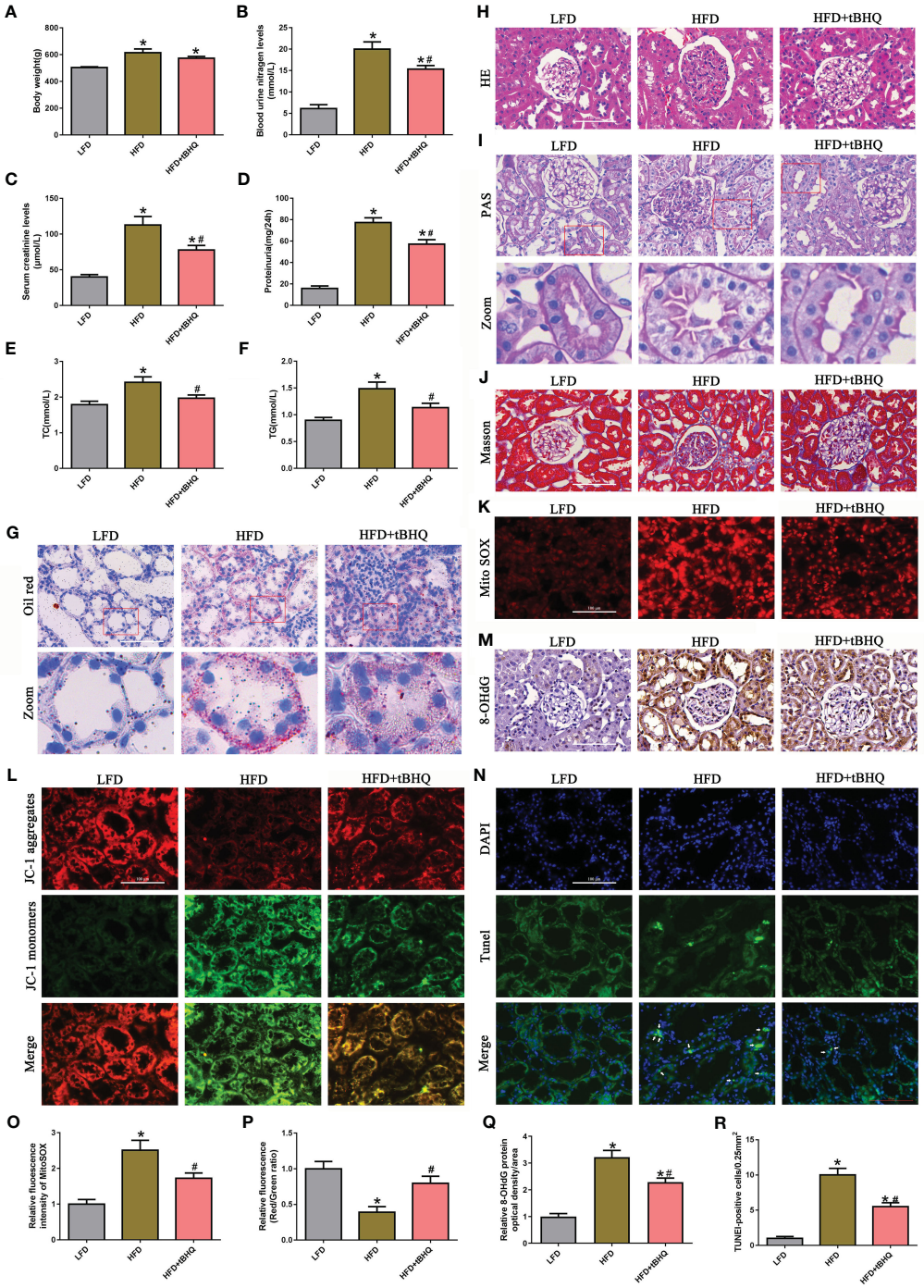

FIGURE 7
Activation of Nrf2/ARE signaling pathway improved the biochemical characteristics and morphological changes and ameliorated renal injury in high-fat diet (HFD)-induced obese rats. **(A–F)** Effects of tBHQ on body weight, BUN, SCr, urine protein, and TC and TG levels in HFD-induced obese rats ($n = 6$; $^{*}P < 0.05$ vs. LFD group and $^{\#}P < 0.05$ vs. HFD group). **(G)** Representative images of Oil red O staining in kidney sections (×400). **(H–J)** Representative images of kidney sections subjected to H&E, PAS, and Masson staining. **(K)** Representative fluorescence images of kidney sections subjected to Mito SOX staining. **(L)** Representative fluorescence images of kidney sections subjected to JC-1 staining. **(M)** Representative image of immunohistochemical staining with 8-OHdG in kidney sections. **(N)** Kidney sections stained with TUNEL, apoptotic cells (arrowhead) are shown. **(O)** Quantification of the fluorescence intensities of Mito SOX in **(K)** ($n = 6$; $^{*}P < 0.05$ vs. LFD group and $^{\#}P < 0.05$ vs. HFD group). **(P)** Quantification of the fluorescence intensities of JC-1 in **(L)** ($n = 6$; $^{*}P < 0.05$ vs. LFD group and $^{\#}P < 0.05$ vs. HFD group). **(Q)** Quantification analysis of 8-OHdG expression in **(M)** ($n = 6$; $^{*}P < 0.05$ vs. LFD group and $^{\#}P < 0.05$ vs. HFD group). **(R)** Quantification analysis of TUNEL-positive cells in **(N)** ($n = 6$; $^{*}P < 0.05$ vs. LFD group and $^{\#}P < 0.05$ vs. HFD group).

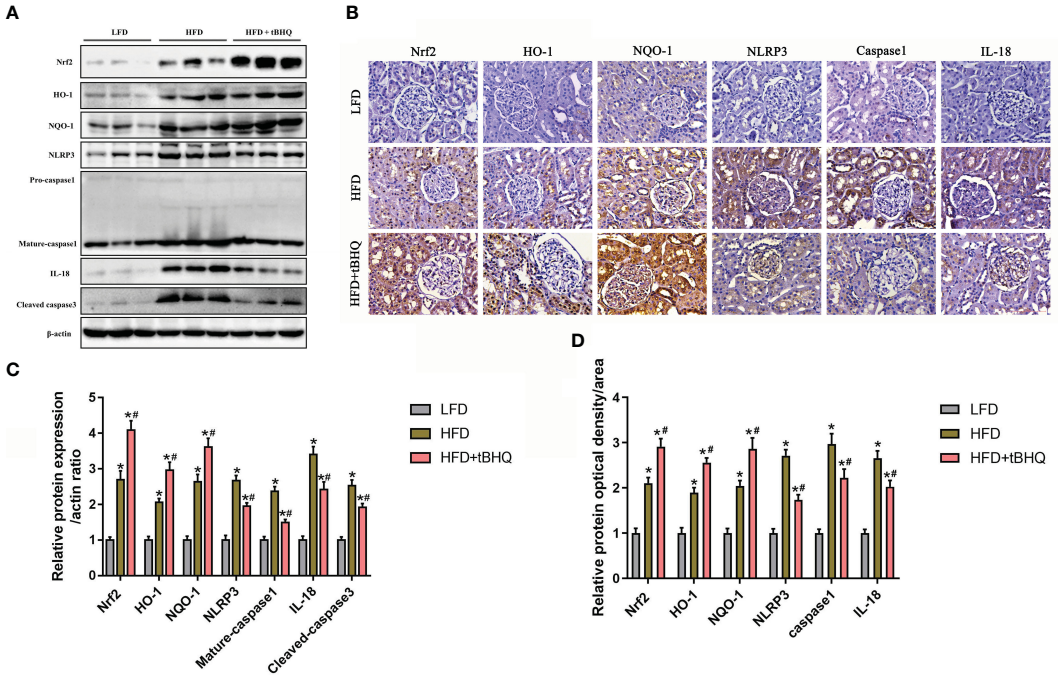

FIGURE 8
The Nrf2/ARE pathway inhibited NLRP3 inflammasome activation in the kidneys of high-fat diet (HFD)-induced obese rats. **(A)** Western blot analyses of the protein expression of Nrf2, HO-1, NQQ-1, NLRP3, caspase-1, and IL-18 in the kidneys of low-fat diet (LFD), HFD, and HFD rats treated with tBHQ. **(B)** Representative images of immunohistochemical staining for Nrf2, HO-1, NQQ-1, NLRP3, caspase-1, and IL-18 in kidney sections. **(C)** Quantification analysis of Nrf2, HO-1, NQQ-1, NLRP3, caspase-1, and IL-18 expression in **(A)** ($n = 6$; $^{*}P < 0.05$ vs. LFD group and $^{\#}P < 0.05$ vs. HFD group). **(D)** Quantification analysis of Nrf2, HO-1, NQQ-1, NLRP3, caspase-1, and IL-18 expression in **(B)** ($n = 6$; $^{*}P < 0.05$ vs. LFD group and $^{\#}P < 0.05$ vs. HFD group).

4 Discussion

Yamagata et al. reported that the hazard ratio of proteinuria increased in CKD patients with hyperlipidemia of both genders, suggesting that serum lipid status abnormalities are considered independent risk factors for CKD progression (24). Previous findings have shown that ectopic lipid deposition in the kidney can cause structural and functional changes in proximal tubule cells, which contribute to the pathophysiology of kidney disease (25). Several underlying mechanisms have been linked to impaired autophagy flux, endoplasmic reticulum stress, oxidative stress, and inflammation (26, 27).

Numerous studies have demonstrated that the NLRP3 inflammasome is a key mechanism involved in the development of a wide variety of human kidney diseases, including AKI, CKD, glomerulonephritis, and obesity-related kidney disease (6, 28). Recently, research has revealed that high lipid levels activate the CD36–NLRP3 inflammasome axis and promote the release of the inflammatory cytokines IL-1β and IL-18, which induce FFA-related renal tubular injury (9). In the present study, we also found that high lipid levels activated the NLRP3 inflammasome both *in vivo* and *in vitro*, which induced tubular epithelial cell apoptosis. However, the exact mechanism of NLRP3 inflammasome activation in hyperlipidemia-induced kidney injury has not yet been defined. Previous research has revealed that the NLRP3 inflammasome can be activated by various cellular signals, including reactive oxygen species (ROS), oxidized DNA, potassium efflux, calcium influx, and lysosomal damage (29, 30). Emerging evidence indicates that mitochondrial dysfunction plays a major role in the activation of the NLRP3 inflammasome. Furthermore, the production of ROS from damaged mitochondria was proposed to promote the deubiquitylation of NLRP3 and subsequently contribute to NLRP3 inflammasome activation (31). Moreover, previous research has shown that mitochondria can function as a platform for assembling NLRP3 inflammasome components to enable the activation of caspase-1 (22, 23). In this study, we observed that the NLRP3 inflammasome was activated both *in vivo* and *in vitro* and was accompanied by increased translocation of NLRP3 to the mitochondria in HK-2 cells treated with PA. Moreover, the mitochondrion-targeted antioxidant Mito Tempol decreased the activation of the NLRP3 inflammasome and the recruitment of NLRP3 within mitochondria by reducing mitochondrial ROS generation and DNA oxidative damage. These results indicated that mitochondrial ROS and oxidized DNA are the signals for triggering the NLRP3 inflammasome in high-lipid-induced renal tubular injury. Thus, targeting the

mechanism preserving the mitochondrial redox balance and thereby inhibiting NLRP3 inflammasome activation in CKD patients with hyperlipidemia may be an attractive therapeutic approach.

The Nrf2/ARE pathway is considered a pivotal antioxidant defense system that plays a key role in regulating the status of cellular oxidative stress. Numerous studies have described the association of the Nrf2/ARE pathway with kidney diseases. Wang et al. showed that activation of the Nrf2 signaling pathway ameliorates sepsis-induced AKI (32). Moreover, Jiang et al. suggested that Nrf2 plays a crucial role in ameliorating streptozotocin-induced renal damage in DKD mice and that genetic deletion of Nrf2 significantly increased ROS generation and oxidative DNA damage and accelerated renal injury in STZ-induced DKD mice (33). In the present study, we demonstrated that the Nrf2/ARE signaling pathway is activated in HK-2 cells under high lipid conditions and that the expression of Nrf2 was also notably upregulated in the kidneys of CKD patients with hyperlipidemia. In addition, Nrf2 silencing exacerbated PA-induced mtROS production and mitochondrial damage; however, Nrf2 activation with tBHQ or Nrf2 overexpression plasmids significantly alleviated cell injury by reducing mtROS production, improving mitochondrial membrane potential, and ameliorating oxidative DNA damage in HK-2 cells, and these effects were further verified in the kidneys of HFD-induced obese rats after tBHQ intervention.

The Nrf2/ARE pathway is a pivotal antioxidant defense system, and its effect on hyperlipidemia-induced renal inflammation and the potential underlying mechanism remain unclear. Recently, numerous studies have focused on Nrf2 signaling and the NLRP3 inflammasome. It has been demonstrated that activation of Nrf2 signaling negatively regulates NLRP3 inflammasome activity in diabetic retinopathy (34) and cerebral ischemia–reperfusion injury (35). In kidney research, Szeto et al. demonstrated that the stabilization of endogenous Nrf2 by minocycline attenuated NLRP3 inflammasome activation in diabetic nephropathy (36). Mahmoud et al. showed that Nrf2/ARE/HO-1 signaling suppressed the NF-κB/NLRP3 inflammasome axis and improved kidney function in methotrexate (MTX)-induced nephrotoxicity (37). Here we demonstrated that Nrf2/ARE antioxidant signaling plays a key role in the activation of the NLRP3 inflammasome in hyperlipidemia-induced renal injury. When HK-2 cells were exposed to high-lipid media, Nrf2 activation induced by tBHQ markedly mitigated PA-induced NLRP3 inflammasome activation; in contrast, Nrf2 knockdown significantly enhanced PA-induced NLRP3 inflammasome activation in HK-2 cells, suggesting that Nrf2/ARE signaling plays a potential role in negatively regulating NLRP3 inflammasome activation in high-lipid-induced HK-2 cells. Nonetheless, the underlying mechanism by which Nrf2/ARE signaling negatively regulates NLRP3 inflammasome activation remains unclear. Therefore, we further found that the enhancing effect of Nrf2 siRNA on NLRP3 inflammasome activation was markedly reversed by Mito Tempol in HK-2 cells, demonstrating that the potential mechanism of Nrf2-induced NLRP3 inflammasome inhibition was dependent on reducing mtROS production. However, the influence of the Nrf2/ARE pathway on other inflammatory signaling pathways, such as the NF-κB pathway, JAK-STAT pathway, and MAPK pathway, should be clarified in a future work.

tBHQ, a well-characterized Nrf2 activator, can maintain the stability of the Nrf2 protein through inhibition of Keap1-mediated ubiquitination. Previous studies have revealed that tBHQ plays a protective role against hypoxic–ischemic brain damage (38), cisplatin-induced nephrotoxicity (39), and hepatic ischemia/reperfusion (I/R) injury (40) by activating Nrf2-mediated antioxidative signaling pathways. In our study, we also found that tBHQ attenuated hyperlipidemia-induced renal injury, and the potential protective mechanism of tBHQ involved inhibiting mtROS–NLRP3 inflammasome activation *via* the upregulation of Nrf2/ARE-related antioxidant signaling. Accordingly, we proposed that the Nrf2/ARE antioxidant signaling–mitochondrial ROS–NLRP3 inflammasome pathway is involved in hyperlipidemia-induced renal injury. Furthermore, other Nrf2 agonists, such as bardoxolone methyl, are being evaluated in ongoing clinical trials for kidney disease, including DKD (41), Alport syndrome (AS), and autosomal dominant polycystic kidney disease (ADPKD) (42), providing great therapeutic potential and expectations for the future of Nrf2 agonist development for kidney diseases.

Finally, we showed that the Nrf2/ARE signaling pathway was activated under high lipid conditions both *in vitro* and *in vivo*. Therefore, why did the activation of the Nrf2 antioxidant response fail to protect against tubular cell damage under high lipid conditions? We believe that activation of the Nrf2 antioxidant response plays a key role in preventing mtROS production, preserving mitochondrial function and inhibiting NLRP3 inflammasome activation during the early stage of high-lipid-induced tubular cell damage. However, at the late stage of high-lipid-induced cell damage, the Nrf2-mediated protective mechanism is saturated by persistent and excessive ROS, resulting in NLRP3 inflammasome activation and tubular cell and renal damage.

5 Conclusion

In summary, we demonstrated that hyperlipidemia induced Nrf2/ARE signaling activation, mitochondrial ROS production, and NLRP3 inflammasome activation. Activation of the mtROS–NLRP3 inflammasome pathway is a critical contributor to renal tubular epithelial cell injury in CKD patients with hyperlipidemia. Activation of Nrf2/ARE antioxidant signaling protects against high-lipid-induced renal tubular epithelial cell damage by inhibiting mtROS-mediated NLRP3 inflammasome activation (Figure 9). Thus, our findings

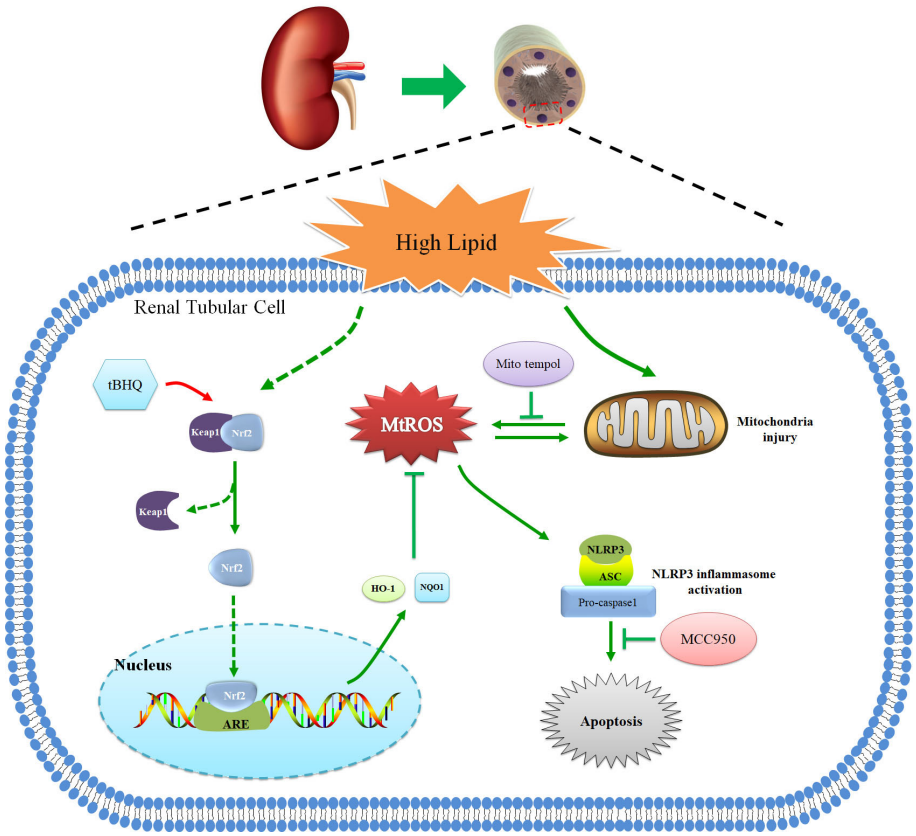

FIGURE 9
Schematic diagram of Nrf2/ARE signaling pathway, mitochondrial ROS, and NLRP3 inflammasome in renal tubular epithelial cells under high lipid conditions. Activation of Nrf2/ARE antioxidant signaling protects against high-lipid-induced renal tubular epithelial cell damage by inhibiting mtROS-mediated NLRP3 inflammasome activation.

highlight the potential for the pharmacological activation of the Nrf2/ARE antioxidant pathway, such as through the use of tBHQ as a therapeutic approach against oxidative stress and inflammation in CKD patients with hyperlipidemia.

Data availability statement

The original contributions presented in the study are included in the article/supplementary material. Further inquiries can be directed to the corresponding authors.

Ethics statement

The studies involving humans were approved by The Ethics Committee of The First Affiliated Hospital of Chongqing Medical University. The studies were conducted in accordance with the local legislation and institutional requirements. The participants provided their written informed consent to participate in this study. The animal study was approved by The Ethics Committee of The First Affiliated Hospital of Chongqing Medical University. The study was conducted in accordance with the local legislation and institutional requirements.

Author contributions

X-sJ: Funding acquisition, Data curation, Formal Analysis, Investigation, Writing – original draft. TL: Investigation, Methodology, Software, Writing – review & editing. Y-fX: Software, Data curation, Formal Analysis, Resources, Writing – review & editing. HG: Data curation, Formal Analysis, Resources, Software, Writing – review & editing. WR: Conceptualization, Supervision, Writing – review & editing. X-gD: Conceptualization, Supervision, Funding acquisition, Writing – review & editing.

Funding

The author(s) declare financial support was received for the research, authorship, and/or publication of this article. This study was funded by the National Natural Science Foundation of China (no. 82200799), the Natural Science Foundation of Chongqing Science and

Technology Commission of China (no. cstc2019jcyj-msxmX0504), and In-hospital Cultivation Fund of the First Affiliated Hospital of Chongqing Medical University (no. PYJJ2021-11).

Conflict of interest

The authors declare that the research was conducted in the absence of any commercial or financial relationships that could be construed as a potential conflict of interest.

Publisher's note

References

1. Hager MR, Narla AD, Tannock LR. Dyslipidemia in patients with chronic kidney disease. *Rev endocrine Metab Disord.* (2017) 18:29–40. doi: 10.1007/s11154-016-9402-z

2. Srivastava SP, Shi S, Koya D, Kanasaki K. Lipid mediators in diabetic nephropathy. *Fibrogenesis Tissue Repair.* (2014) 7:12. doi: 10.1186/1755-1536-7-12

3. Chen SC, Tseng CH. Dyslipidemia, kidney disease, and cardiovascular disease in diabetic patients. *Rev Diabetes Stud.* (2013) 10:88–100. doi: 10.1900/RDS.2013.10.88

4. Kamijo A, Kimura K, Sugaya T, Yamanouchi M, Hase H, Kaneko T, et al. Urinary free fatty acids bound to albumin aggravate tubulointerstitial damage. *Kidney Int.* (2002) 62:1628–37. doi: 10.1046/j.1523-1755.2002.00618.x

5. Thomas ME, Harris KP, Walls J, Furness PN, Brunskill NJ. Fatty acids exacerbate tubulointerstitial injury in protein-overload proteinuria. *Am J Physiol Renal Physiol.* (2002) 283:F640–647. doi: 10.1152/ajprenal.00001.2002

6. Komada T, Muruve DA. The role of inflammasomes in kidney disease. *Nat Rev Nephrol.* (2019) 15:501–20. doi: 10.1038/s41581-019-0158-z

7. Zhang C, Boini KM, Xia M, Abais JM, Li X, Liu Q, et al. Activation of Nod-like receptor protein 3 inflammasomes turns on podocyte injury and glomerular sclerosis in hyperhomocysteinemia. *Hypertension.* (2012) 60:154–62. doi: 10.1161/HYPERTENSIONAHA.111.189688

8. Han Y, Xu X, Tang C, Gao P, Chen X, Xiong X, et al. et al: Reactive oxygen species promote tubular injury in diabetic nephropathy: The role of the mitochondrial ros-txnip-nlrp3 biological axis. *Redox Biol.* (2018) 16:32–46. doi: 10.1016/j.redox.2018.02.013

9. Li LC, Yang JL, Lee WC, Chen JB, Lee CT, Wang PW, et al. Palmitate aggravates proteinuria-induced cell death and inflammation via CD36-inflammasome axis in the proximal tubular cells of obese mice. *Am J Physiol Renal Physiol.* (2018) 315:F1720–31. doi: 10.1152/ajprenal.00536.2017

10. Wang J, Wen Y, Lv LL, Liu H, Tang RN, Ma KL, et al. Involvement of endoplasmic reticulum stress in angiotensin II-induced NLRP3 inflammasome activation in human renal proximal tubular cells. *vitro. Acta Pharmacol Sin.* (2015) 36:821–30. doi: 10.1038/aps.2015.21

11. Ding W, Guo H, Xu C, Wang B, Zhang M, Ding F. Mitochondrial reactive oxygen species-mediated NLRP3 inflammasome activation contributes to aldosterone-induced renal tubular cells injury. *Oncotarget.* (2016) 7:17479–91. doi: 10.18632/oncotarget.v7i14

12. Yu C, Xiao JH. The keap1-nrf2 system: A mediator between oxidative stress and aging. *Oxid Med Cell Longev.* (2021) 2021:6635460. doi: 10.1155/2021/6635460

13. Ahmed SM, Luo L, Namani A, Wang XJ, Tang X. Nrf2 signaling pathway: Pivotal roles in inflammation. *Biochim Biophys Acta Mol Basis Dis.* (2017) 1863:585–97. doi: 10.1016/j.bbadis.2016.11.005

14. Fão L, Mota SI, Rego AC. Shaping the Nrf2-ARE-related pathways in Alzheimer's and Parkinson's diseases. *Ageing Res Rev.* (2019) 54:100942. doi: 10.1016/j.arr.2019.100942

15. Syed AM, Ram C, Murty US, Sahu BD. A review on herbal Nrf2 activators with preclinical evidence in cardiovascular diseases. *Phytother Res.* (2021) 35(9):5068–102. doi: 10.1002/ptr.7137

16. Mimura J, Itoh K. Role of Nrf2 in the pathogenesis of atherosclerosis. *Free Radic Biol Med.* (2015) 88:221–32. doi: 10.1016/j.freeradbiomed.2015.06.019

17. Nezu M, Suzuki N, Yamamoto M. Targeting the KEAP1-NRF2 system to prevent kidney disease progression. *Am J Nephrol.* (2017) 45:473–83. doi: 10.1159/000475890

18. Liu M, Grigoryev DN, Crow MT, Haas M, Yamamoto M, Reddy SP, et al. Transcription factor Nrf2 is protective during ischemic and nephrotoxic acute kidney injury in mice. *Kidney Int.* (2009) 76:277–85. doi: 10.1038/ki.2009.157

19. Alaofi AL. Sinapic acid ameliorates the progression of streptozotocin (STZ)-induced diabetic nephropathy in rats via NRF2/HO-1 mediated pathways. *Front Pharmacol.* (2020) 11:1119. doi: 10.3389/fphar.2020.01119

20. Valavanidis A, Vlachogianni T, Fiotakis C. 8-hydroxy-2′ -deoxyguanosine (8-OHdG): A critical biomarker of oxidative stress and carcinogenesis. *J Environ Sci Health Part C.* (2009) 27:120–39. doi: 10.1080/10590500902885684

21. Yu JW, Lee MS. Mitochondria and the NLRP3 inflammasome: physiological and pathological relevance. *Arch Pharm Res.* (2016) 39:1503–18. doi: 10.1007/s12272-016-0827-4

22. Zhou R, Yazdi AS, Menu P, Tschopp J. A role for mitochondria in NLRP3 inflammasome activation. *Nature.* (2010) 469:221–5. doi: 10.1038/nature09663

23. Traba J, Sack MN. The role of caloric load and mitochondrial homeostasis in the regulation of the NLRP3 inflammasome. *Cell Mol Life sciences: CMLS.* (2017) 74:1777–91. doi: 10.1007/s00018-016-2431-7

24. Yamagata K, Ishida K, Sairenchi T, Takahashi H, Ohba S, Shiigai T, et al. Risk factors for chronic kidney disease in a community-based population: a 10-year follow-up study. *Kidney Int.* (2007) 71:159–66. doi: 10.1038/sj.ki.5002017

25. de Vries AP, Ruggenenti P, Ruan XZ, Praga M, Cruzado JM, Bajema IM, et al. Fatty kidney: emerging role of ectopic lipid in obesity-related renal disease. *Lancet Diabetes Endocrinol.* (2014) 2:417–26. doi: 10.1016/S2213-8587(14)70065-8

26. Yamamoto T, Takabatake Y, Takahashi A, Kimura T, Namba T, Matsuda J, et al. High-Fat diet-Induced lysosomal dysfunction and impaired autophagic flux contribute to lipotoxicity in the kidney. *J Am Soc Nephrol.* (2016) 28(5):1534–51. doi: 10.1681/ASN.2016070731

27. Ruan XZ, Varghese Z, Moorhead JF. An update on the lipid nephrotoxicity hypothesis. *Nat Rev Nephrol.* (2009) 5:713–21. doi: 10.1038/nrneph.2009.184

28. Ke B, Shen W, Fang X, Wu Q. The NLPR3 inflammasome and obesity-related kidney disease. *J Cell Mol Med.* (2018) 22:16–24. doi: 10.1111/jcmm.13333

29. Wu X, Zhang H, Qi W, Zhang Y, Li J, Li Z, et al. et al: Nicotine promotes atherosclerosis via ROS-NLRP3-mediated endothelial cell pyroptosis. *Cell Death Dis.* (2018) 9:171. doi: 10.1038/s41419-017-0257-3

30. Kelley N, Jeltema D, Duan Y, He Y. The NLRP3 inflammasome: an overview of mechanisms of activation and regulation. *Int J Mol Sci.* (2019) 20(13):3328. doi: 10.3390/ijms20133328

31. Juliana C, Fernandes-Alnemri T, Kang S, Farias A, Qin F, Alnemri ES. Non-transcriptional priming and deubiquitination regulate NLRP3 inflammasome activation. *J Biol Chem.* (2012) 287:36617–22. doi: 10.1074/jbc.M112.407130

32. Wang Y, Feng F, Liu M, Xue J, Huang H. Resveratrol ameliorates sepsis-induced acute kidney injury in a pediatric rat model via Nrf2 signaling pathway. *Exp Ther Med.* (2018) 16:3233–40. doi: 10.3892/etm

33. Jiang T, Huang Z, Lin Y, Zhang Z, Fang D, Zhang DD. The protective role of Nrf2 in streptozotocin-induced diabetic nephropathy. *Diabetes.* (2010) 59:850–60. doi: 10.2337/db09-1342

34. Li S, Yang H, Chen X. Protective effects of sulforaphane on diabetic retinopathy: activation of the Nrf2 pathway and inhibition of NLRP3 inflammasome formation. *Exp Anim.* (2019) 68:221–31. doi: 10.1538/expanim.18-0146

35. Hou Y, Wang Y, He Q, Li L, Xie H, Zhao Y, et al. Nrf2 inhibits NLRP3 inflammasome activation through regulating Trx1/TXNIP complex in cerebral ischemia reperfusion injury. *Behav Brain Res.* (2018) 336:32–9. doi: 10.1016/j.bbr.2017.06.027

36. Shahzad K, Bock F, Al-Dabet MM, Gadi I, Nazir S, Wang H, et al. et al: Stabilization of endogenous Nrf2 by minocycline protects against Nlrp3-inflammasome induced diabetic nephropathy. *Sci Rep.* (2016) 6:34228. doi: 10.1038/srep34228

37. Mahmoud AM, Hussein OE, Abd El-Twab SM, Hozayen WG. Ferulic acid protects against methotrexate nephrotoxicity via activation of Nrf2/ARE/HO-1 signaling and PPARgamma, and suppression of NF-kappaB/NLRP3 inflammasome axis. *Food Funct.* (2019) 10:4593–607. doi: 10.1039/C9FO00114J

38. Zhang J, Tucker LD, Yan D, Lu Y, Yang L, Wu C, et al. : Tert-butylhydroquinone post-treatment attenuates neonatal hypoxic-ischemic brain damage in rats. *Neurochem Int.* (2018) 116:1–12. doi: 10.1016/j.neuint.2018.03.004

39. Perez-Rojas JM, Guerrero-Beltran CE, Cruz C, Sanchez-Gonzalez DJ, Martinez-Martinez CM, Pedraza-Chaverri J. Preventive effect of tert-butylhydroquinone on cisplatin-induced nephrotoxicity in rats. *Food Chem Toxicol.* (2011) 49:2631–7. doi: 10.1016/j.fct.2011.07.008

40. Zeng XP, Li XJ, Zhang QY, Liu QW, Li L, Xiong Y, et al. Tert-butylhydroquinone protects liver against ischemia/reperfusion injury in rats through nrf2-activating anti-oxidative activity. *Transplant Proc*. (2017) 49:366–72. doi: 10.1016/j.transproceed.2016.12.008

41. Kanda H, Yamawaki K. Bardoxolone methyl: drug development for diabetic kidney disease. *Clin Exp Nephrol*. (2020) 24:857–64. doi: 10.1007/s10157-020-01917-5

42. Yamawaki K, Kanda H, Shimazaki R. Nrf2 activator for the treatment of kidney diseases. *Toxicol Appl Pharmacol*. (2018) 360:30–7. doi: 10.1016/j.taap.2018.09.030

frontiers | Frontiers in Immunology

TYPE Review
PUBLISHED 14 May 2024
DOI 10.3389/fimmu.2024.1365422

OPEN ACCESS

EDITED BY
Xu-jie Zhou,
Peking University, China

REVIEWED BY
Laisel Martinez,
University of Miami, United States
Mark Ewing,
Onze Lieve Vrouwe Gasthuis (OLVG), Netherlands

*CORRESPONDENCE
Liming Liang
liangliming1023@163.com

†These authors have contributed equally to this work

RECEIVED 04 January 2024
ACCEPTED 30 April 2024
PUBLISHED 14 May 2024

CITATION
Zhang Y, Kong X, Liang L and Xu D (2024) Regulation of vascular remodeling by immune microenvironment after the establishment of autologous arteriovenous fistula in ESRD patients. *Front. Immunol.* 15:1365422. doi: 10.3389/fimmu.2024.1365422

Regulation of vascular remodeling by immune microenvironment after the establishment of autologous arteriovenous fistula in ESRD patients

Yifei Zhang†, Xianglei Kong†, Liming Liang* and Dongmei Xu

Department of Nephrology, The First Affiliated Hospital of Shandong First Medical University & Shandong Provincial Qianfoshan Hospital, Shandong Institute of Nephrology, Jinan, Shandong, China

Autogenous arteriovenous fistula (AVF) is the preferred dialysis access for receiving hemodialysis treatment in end-stage renal disease patients. After AVF is established, vascular remodeling occurs in order to adapt to hemodynamic changes. Uremia toxins, surgical injury, blood flow changes and other factors can induce inflammatory response, immune microenvironment changes, and play an important role in the maintenance of AVF vascular remodeling. This process involves the infiltration of pro-inflammatory and anti-inflammatory immune cells and the secretion of cytokines. Pro-inflammatory and anti-inflammatory immune cells include neutrophil (NEUT), dendritic cell (DC), T lymphocyte, macrophage (Mφ), etc. This article reviews the latest research progress and focuses on the role of immune microenvironment changes in vascular remodeling of AVF, in order to provide a new theoretical basis for the prevention and treatment of AVF failure.

KEYWORDS

arteriovenous fistula, immune microenvironment, inflammation, vascular remodeling, chronic kidney disease

Introduction

Chronic kidney disease (CKD) is a global public health problem. The prevalence of CKD in Chinese adults was 8.2% in the analysis of the results of the Sixth Chronic Disease and Risk Factor Surveillance in China (1), while the prevalence of dialysis in China was 419 cases per million population (2). The three main types of vascular access for hemodialysis (HD) include autogenous arteriovenous fistula (AVF), graft arteriovenous fistula (AVG),

and central venous catheter (CVC). AVF refers to artificial formation of a straight line between the proximal artery and the superficial vein at the subcutaneous distance during surgery. AVF has the advantages of lower medical cost, fewer complications, lower infection rate, lower mortality rate and higher patency rate compared with AVG or CVC (3). However, immaturity of newly formed AVF and dysfunction of established AVF are two common clinical challenges (4). The National Institutes of Health reported that 60% of AVF failed to mature after surgery and could not be successfully used for dialysis treatment (5). The hemodialysis arteriovenous fistula maturity (HFM) study showed that the rate of AVF dysfunction at 1 year was 24% (4). The results of our center showed that the 1-year AVF dysfunction rate was 14.4% (6).

The maturation of AVF is the process that makes AVF suitable for providing prescription dialysis. After the construction of AVF, the veins are affected by injury factors such as inflammation and oxidative stress, and exposed to high flow, high shear stress (WSS), high pressure and oxygen-rich arterial blood environment, which requires adaptive remodeling of AVF to mature, that is, the venous cavity dilation and wall thickening are the main characteristics, resulting in venous arterialization changes. Finally, adaptive vascular remodeling related to the acquisition of arteriovenous dual features was formed (7). The immaturity of AVF means that it cannot be used successfully for HD within 6 months after its creation despite surgical intervention. AVF dysfunction is a multifactorial process in which upstream and downstream events work together to lead to lumen stenosis and even secondary thrombosis due to neointimal hyperplasia (NIH). The upstream event refers to the injury of vascular endothelial cell (EC) and vascular smooth muscle cell (VSMC) caused by surgical trauma, hemodynamic shear stress, and uremic toxins. Downstream events refer to responses to vascular damage, including oxidative stress, inflammation, migration and proliferation of fibroblast, SMC, and myofibroblast (8). Activation of EC can increase the expression of growth factors, promote the migration and proliferation of VSMC from the medium to the intima and make it quickly form a new endometrium layer (9, 10). And EC injury, in turn, promotes the release of inflammatory mediators and the recruitment of inflammatory cells, thereby activating smooth muscle cells and fibroblasts and promoting the fibrosis process (11). Fibrosis is an outcome of the dysregulated tissue repair process in response to various types of tissue injury (12). And the degree of fibrosis after AVF surgery is related to the immaturity of AVF. AVF fibrosis can be attributed to excessive extracellular matrix (ECM) synthesis by activated VSMAs and myofibroblasts and/or insufficient ECM degradation by matrix metalloproteinases (MMP). Excessive fibrosis may reduce vessel wall compliance, and AVF patients with intermediate fibrosis have less increase in venous diameter during reconstruction (13). When the vessel wall loses compliance due to excessive ECM deposition, the NIH becomes obstructive (possibly less compressible under high blood flow) and stenotic.

Therefore, fibrotic remodeling and NIH, which in combination significantly increase the risk of AVF failure (14). Our previous study have shown that in the inferior vena cava of adenine-induced chronic kidney disease rats with aortocaval fistulas, in addition to the disordered EC and SMC, inflammatory cells such as macrophage (Mφ) are also present in the major cellular components of NIH (15). In conclusion, inflammation plays an important role in the vascular remodeling process of AVF.

The establishment of AVF can trigger the body's immune response, including chronic infiltration of immune cells and secretion of inflammatory cytokines (16). The balance between pro-inflammatory and anti-inflammatory responses is necessary for vascular remodeling of AVF, and excessive or insufficient inflammation can lead to AVF failure (16). Since the infiltration of immune cells plays a key role in the vascular remodeling of AVF, it is of great significance to study the changes and roles of immune cells in the vascular remodeling of AVF. In the past, T lymphocyte and Mφ were considered to be key molecules in chronic inflammation of vascular diseases such as atherosclerosis and AVF failure (17). However, recent evidence strongly suggests that neutrophil (NEUT) and dendritic cell (DC) are also involved in the development of vascular disease, such as AVF failure (16, 18). T lymphocyte, Mφ, NEUT, DC and other immune cells participate in the vascular remodeling process of AVF, and the inflammatory response mediated by the above inflammatory cells is the core of the vascular remodeling process (19). This article reviews the role of immune microenvironment in vascular remodeling of AVF.

Immune cells are involved in vascular remodeling of AVF

Immaturity of AVF refers to the lack of outward remodeling that, despite radiologic or surgical intervention (i.e., endovascular or open procedure management), cannot be successfully used for dialysis after its creation (20). AVF dysfunction is a very general term, and because it does not specifically address the cause of dysfunction, it has been replaced by three terms: thrombotic flow-related dysfunction, non-thrombotic flow-related dysfunction, and infectious dysfunction. Thrombotic flow-related dysfunction is associated with the risk of thrombosis or specific complications that can reduce blood flow to AVF, threaten prescribed dialysis lumen flow and/or cause clinical signs and symptoms such as stenosis or thrombosis. In contrast, non-thrombotic flow-related dysfunction may or may not threaten blood flow or patency, but is associated with clinical signs and symptoms, such as aneurysms and steal syndrome. The above three terms distinguish AVF dysfunction due to stenosis or thrombosis from dysfunction due to other causes (21). Therefore, the dysfunction discussed in this paper refers to thrombotic flow-related dysfunction associated with vascular remodeling.

In the early stages after AVF establishment, the vein is exposed to a high flow, high shear stress, high pressure, and oxygen-rich arterial environment, leading to "maturation" of both the arterial inflow limb and venous outflow limb. Adaptation of the vein to the increased flow and shear stress of the arterial environment requires dilation by outward remodeling of the venous wall (Poiseuille's law), whereas increases in pressure and tensile stress result in wall thickening (Laplace's law) (22). WSS is significantly elevated, causing the initial venous cavity to dilate through mechanical stretching, and activating EC to produce large amounts of nitric oxide (NO), stimulating MMP-2, 9 (23), triggering ECM

degradation, resulting in continuous dilation of the lumen (24). However, wall thickening is an adaptation of blood vessel walls to pressure, involving the thickening of all vascular layers through ECM deposition and cell proliferation and migration (25). Thus, AVF maturation is an adaptive vascular remodeling associated with the acquisition of dual arteriovenous characteristics. In the later period after AVF establishment, during maintenance HD therapy, repeated treatment placed the region in a state of turbulence, low flow, low wall shear stress, and increased transwall pressure. The normal physiological mechanism of AVF is not clear, but the intima thickening of AVF can maintain sufficient pressure (26).

AVF failure occurs through two different mechanisms: early failure is secondary to lack of outward remodeling and inability to support HD, i.e. AVF immaturity; Late failure is due to uncontrolled pathological process of intimal thickening, uncontrolled NIH, negative or introversion remodeling leading to previously normal intimal thickening, lumen narrowing, and reduced patency rate (17). The formation of NIH can lead to secondary thrombosis and aggravate AVF stenosis (27). The histological features of NIH is characterized by a large number of constricted SMC, myofibroblast, fibroblast, and Mφ, ultimately narrowing the venous outflow tract, and resulting in reduced blood flow (28). However, both NIH and atherosclerosis share partially similar histopathological features: the observed intimal hyperplasia is almost the same, and both are characterized by smooth muscle cell migration and proliferation and ECM deposition (29, 30). Therefore, it can be speculated that there may be chronic inflammation in the NIH of AVF.

The inflammatory response of AVF can be divided into two parts: one is surgical trauma stoma and local hypoxia, which causes local inflammatory response by activating molecular signal transduction such as hypoxia-inducible factor (HIF). Secondly, the presence of uremia in CKD patients promotes oxidative stress, leading to phagocyte activation, oxygen free radical release, lipid peroxidation, and ultimately an increase in systemic inflammatory response (28). Early and late inflammation after AVF establishment plays an important role in the regulation of vascular remodeling. Damage to vascular EC or SMC can induce local immune cell migration (28), as well as damage associated with molecular patterns (DAMP) secretion, which further activates the immune system, recruitment of immune cells, and causes inflammation (31). Thus, inflammation during vascular remodeling in AVF involves a coordinated interaction between blood vessel walls and circulating immune cells (32). In the AVF mouse model, the experimental group lacked radio-protective 105 protein (RP105), also known as CD180- a cell surface protein of various inflammatory cells that has been shown to impair Toll-like receptor (TLR)-4 signaling, thereby reducing outward venous remodeling (33). In a balloon induced rat model of carotid artery injury, NIH was increased in nude mice lacking T lymphocyte, while adoptive transfer of $CD4^+$and $CD8^+$ lymphocytes in mice after carotid artery injury was associated with decreased NIH (34). Studies in rodent models lacking macrophage colony-stimulating factors found that the Mφ of experimental mice were reduced, and therefore their outward remodeling was attenuated compared to wild-type mice (32). Conversely, adoptive transfer of regulatory T lymphocyte (Treg) has been shown to reduce the incidence of myocardial hypertrophy and fibrosis, as well as the infiltration and remodeling of immune cells (35). In the MISRA's laboratory, systematic Mφ depletion of a mouse model of AVF with sodium clodronate resulted in a decrease in the number of circulating Mφ and an improvement in AVF stenosis (28, 36). This contradiction may be related to the different roles of T lymphocyte and Mφ in vascular remodeling of AVF (17, 37). Welt and Edelman discovered in 2000 that NEUT played a role in the NIH in balloon-injured arteries of the rabbit model (38). While, Takahashi and Lee discovered in 2003 that DC play a role in the NIH after rat carotid balloon injury (16, 39). Studies have shown that elevated levels of C-reactive protein (CRP), a marked of the systemic inflammatory response produced by the liver in response to pro-inflammatory cytokines, increase the risk of AVF failure, and inhibiting the inflammatory response with prednisolone can promote venous outward remodeling and increase AVF patency in a murine AVF model (40). These findings suggest that appropriate local wall inflammation is positively correlated with AVF vascular remodeling, while systemic inflammation is negatively correlated with AVF vascular remodeling (41). These results suggest that local inflammation driven by immune cells is a necessary condition for vascular remodeling in AVF, and the balance of inflammatory and anti-inflammatory responses is related to the type and number of immune cells infiltrating the AVF site (16). Therefore, immune cells such as T lymphocyte, Mφ, NEUT, and DC play different roles in AVF vascular remodeling (17).

Different types of immune cells are involved in vascular remodeling of AVF

Macrophages: play a dual role through polarization

Mφ, DC and monocyte constitute the mononuclear phagocytic system, which is the regulator of tissue homeostasis, growth, development and regeneration (42). The monocyte-to-lymphocyte ratio (MLR) is defined as the absolute number of monocytes divided by the absolute number of lymphocytes. Several studies have found a positive correlation between MLR and AVF immaturity (43). The release of macrophage migration inhibitor factor (MIF) up-regulates tumor necrosis factor (TNF) -α, interleukin (IL) -6, IL-8 and MCP-1 and other inflammatory cytokines, causing the migration and proliferation of inflammatory cells and promoting NIH (19). MCP-1 is involved in the infiltration and activation of monocyte/Mφ, and the intermediate early response gene X-1 (IEX-1) regulates MCP-1, IEX-1 knockout mice reduce MCP-1 and NIH (44), directly blocking MCP-1 inhibition of NIH in different animal models (45). Mφ produce MMP and reactive oxygen species (ROS). MMP can damage elastin fibers such as the inner elastic lamina and promote the dilation of blood vessel walls in a pig model of AVF

stenosis (46). However, MMP also promotes the deposition of ECM in NIH and leads to subsequent thrombosis in NIH by breaking down proteins in the ECM (47). However, ROS can alter vascular reactivity, recruit more pro-inflammatory Mφ, and promote vascular remodeling in conjunction with MMP (48). In a mouse model of AVF, injection of sodium clodronate promote Mφ depletion and decreased the proliferation of VSMC activity during venous remodeling (39).

Mφ is a highly plastic type of cell. In a specific tissue with a specific phenotype and function, the process by which Mφ responds to the stimuli from the immune microenvironment is called polarization (49). Mφ is typically found in two distinct subsets: classically activated or M1Mφ, which is pro-inflammatory and polarized by the secretion of IFN-γ by Th1 cells; M2Mφ has anti-inflammatory and immunomodulatory effects and is polarized by IL-4 secreted by Th2 cells and IL-10 and TGF-β secreted by Treg cell (50). Studies have shown that inflammation caused by M1-like Mφ is associated with vein graft failure, participating in the formation of new blood vessels and disrupting the integrity of blood vessels. M2-like Mφ aggregation is associated with SMC proliferation and vascular wall thickening, promoting vascular stability and maturation (42, 51).

Classically activated macrophages

M1Mφ produces pro-inflammatory cytokines such as IL-6, IL-12, IL-23, interferon (IFN)-γ and TNF-α and inducible nitric oxide synthase (iNOS). Unlike circulating inflammatory cells, which contribute to systemic inflammation, M1-like Mφ acts within tissues, promoting local inflammation (42). M1-like Mφ produces iNOS, which can reduce vascular remodeling and NIH. Therefore, M1-like Mφ can inhibit AVF maturation and promote AVF function maintenance (17).

Vicariously activated macrophages

M2Mφ produces IL-10, transforming growth factor (TGF) -β, arginase (Arg)-1, and other anti-inflammatory cytokines, which have anti-inflammatory and tissue remodeling functions. The appearance of M2-like Mφ is a characteristic of the inflammation resolution period and a necessary condition for vascular graft re-endothelialization, which can promote vascular graft remodeling and facilitate wound healing and tissue reconstruction (52). Studies about the AVF in wild-type C57BL/6J and CD44 knockout mice have shown that CD44 regulates venous wall thickening during AVF maturation by promoting the accumulation of M2-like Mφ in the adaptive venous wall (53). IL-10 and TGF-β play an important role in maintaining vascular integrity: IL-10 and TGF-β produced by M2-like Mφ are more frequently present in stable plaques as major anti-inflammatory mediators (54). Studies have shown that blocking core fucosylation, downstream of TGF-β, can reduce markers of renal fibrosis. Although the mechanisms of renal fibrosis and AVF dysfunction differ, there is significant overlap. In addition, changes in glycosylation have been shown to affect cell proliferation, transformation, migration, and apoptosis (28). Arg-1 promotes VSMC proliferation and inhibits inflammation: M2-like Mφ infiltration plays a key role in regulating VSMCS proliferation and vascular wall thickening during AVF maturation, so Arg-1 may be involved in AVF maturation; However, in the rat model of common carotid artery injury, Arg-1 also promotes the formation of NIH, and therefore, Arg-1 may have an adverse effect on AVF function maintenance. However, arterial remodeling is different from AVF, Arg-1 may play a critical regulatory role in the balance between vascular wall thickening and NIH formation, and thus may be beneficial or harmful in AVF function maintenance (55).

When inflammation occurs, Mφ polarizes into M1-like Mφ, producing pro-inflammatory mediators that effectively control and clear infection and remove dead cells, but can lead to tissue damage if the M1 phase persists. Therefore, M2-like Mφ secretes a large amount of anti-inflammatory mediators, inhibits inflammatory responses, promotes tissue repair, vascular remodeling, and maintains homeostasis (37). For example, in a mouse model of CKD with AVF, iNOS, a marker of pro-inflammatory M1-like Mφ, was first increased, followed by Arg-1, a marker of anti-inflammatory M2-like Mφ (56). Thus, the balance of M1-like Mφ and M2-like Mφ polarization determines the fate of the organ in inflammation or injury. Revealing the polarization and recruitment process of M1-like Mφ and M2-like Mφ may provide a new therapeutic approach for regulating the balance of phenotype, quantity and distribution of vascular remodeling in AVF.

T lymphocyte: function by regulating Mφ

T lymphocyte plays a role in acquired immunity and are also involved in the regulation of inflammation. APC processing antigens are presented to major histocompatibility complex (MHC) molecules, which then activate $CD8^+$ T lymphocyte with MHC- I molecules, and $CD4^+$ T lymphocyte with MHC - II molecules (48, 57). After activation, $CD8^+$T lymphocyte has antigen-specific cytotoxicity, also known as cytotoxic T lymphocyte (CTL) (58). Unlike $CD8^+$T lymphocyte, $CD4^+$T lymphocyte activates and differentiates into different subsets, distinguished by the production of specific cytokine and effector functions, including helper (Th) and regulatory T (Treg) lymphocytes (59). $CD4^+$ lymphocyte and $CD8^+$T lymphocyte play a major role in the initiation and continuation of the inflammatory cascade, and can also regulate other immune cells through the inflammatory response, such as secreting cytokines to regulate the inflammatory state of Mφ (34). In AVF of athymic rnu nude rats lacking mature T lymphocytes and euthymic control animals, the presence of $CD4^+$T lymphocyte was consistent with the presence of Mφ, and the absence of mature T lymphocyte showed a tendency of decreasing Mφ infiltration (60). Therefore, T lymphocyte regulate the accumulation of Mφ in mature venous walls, thereby controlling adaptive remodeling (50).

Helper (Th)T lymphocyte

Th lymphocyte can be divided into different subgroups according to the type of cytokine they secrete: Th1 lymphocyte has a pro-inflammatory effects, and Th2 lymphocyte has an anti-inflammatory effects. Analysis of clinical specimens of atherosclerosis and graft atherosclerosis vessels shows that in the pathogenesis of T lymphocyte mediated vascular injury and remodeling, the Th1-dominant response leads to intimal

thickening and lumen stenosis, while the Th2-dominant response leads to arterial dilation and lumen ectasia (61).

Th1 lymphocyte produces pro-inflammatory cytokines such as IFN-γ, IL-2 and TNF-β. However, the direction of Th lymphocyte differentiation is influenced by different cytokines and chemokines, especially IL-12. IFN-γ is the signature cytokine of Th1 lymphocyte and can be promoted by IL-12. Promote Th1 lymphocyte differentiation by increasing IL-12 production and inhibit Th2 lymphocyte differentiation by inhibiting IL-4 (62). Studies have shown that the percentage and absolute number of activated $CD4^+$T lymphocyte in peripheral blood produce IFN-γ are higher in patients with hypertension than in patients with normal blood pressure (32). There is a positive feedback relationship between IFN-γ and IL-12 production and Th1 lymphocyte differentiation, making Th lymphocyte differentiation balance closer to Th1 lymphocyte differentiation. The cumulative effects of these cytokines promote the transformation of the immune microenvironment from anti-inflammatory to pro-inflammatory, resulting in the accumulation of inflammatory cells and their secretions and inhibiting AVF maturation. Th2 lymphocyte produces anti-inflammatory cytokines such as IL-4, IL-5, IL-10 and IL-13. IL-4 is the signature cytokine of Th2 lymphocyte, which can promote Th2 lymphocyte differentiation and up-regulate the expression of IL-5, thus inhibiting Th1 lymphocyte differentiation and IFN-γ production. This cascade promotes the resolution of inflammation, which promotes the maturation of AVF (16). In addition, Th lymphocyte can regulate the inflammatory state of Mφ. Th1 lymphocyte promotes the polarization of Mφ toward the proinflammatory phenotype and activate other inflammatory cells. Th2 lymphocyte promotes Mφ polarization to the anti-inflammatory phenotype (63, 64). In atherosclerosis, IFN-γ destabilizes plaque stability and recruits Mφ to promote polarization of the M1-like phenotype (65). Studies have shown that M2-like Mφ is required for AVF maturation. taken together, Th2 lymphocyte may promote AVF maturation by inhibiting Th1 lymphocyte differentiation and inducing M2-like Mφ polarization (53).

Regulatory T (Treg) lymphocyte

Treg lymphocyte is anti-inflammatory T lymphocyte characterized by CD25 and Foxp3 labeling, secreting anti-inflammatory cytokines such as IL-10, IL-35 and TGF -β, inhibiting innate and acquired immune responses, regulating the duration and amplitude of inflammatory responses, and thus maintaining immune tolerance and immune homeostasia (66). Treg lymphocyte secretes anti-inflammatory cytokines to inhibite inflammatory cells including not only Th1 lymphocyte, CTL and M1-like Mφ, but also inhibit anti-inflammatory Th2 lymphocyte and induce M2-like Mφ polarization of anti-inflammatory cells, promote inflammation lysis, tissue healing and vascular remodeling, thus promote AVF maturation (67). In $CD4^+$T lymphocyte, IL-10 is thought to be produced primarily by Treg lymphocyte. Uncontrolled secretion of IFN-γ by Th1 lymphocyte may lead to severe tissue damage, and inhibition of the spatio-temporal dependent balance between IFN-γ secretion by Th1 lymphocyte and IL-10 secretion by Treg lymphocyte may enable an effective immune response with limited tissue damage (68, 69). However, due to reduced IFN-γ production, recruitment of monocytes and effector T lymphocyte in the lesion was also reduced (70). These studies suggest that depletion of Th1 lymphocyte is induced by Treg lymphocyte and promotes AVF maturation (71). TGF-β inhibited the production of MCP-1, and the secretion of proinflammatory cytokines was significantly reduced after monocytes were treated with Treg lymphocyte (16). Treg lymphocyte expressed surface marker such as co-stimulator, $CD4^+$ $CD25^+$ $FoxP3^+$, and these elevated markers maintened the mechanism of inhibiting inflammation, and promoted AVF maturation (72). IL-2 helps maintain Foxp3 expression through IL-2Rα/CD25 signaling, thereby promoting Treg lymphocyte function (73). Co-stimulator takes part in IL-10-mediated inhibition of effector T lymphocyte, lack of Co-stimulator can lead to decrease in the number and function of Foxp3 Treg lymphocyte, and accelerate the progression of atherosclerosis (65). The accumulation of inflammatory immune cells on the blood vessel wall leads to thickening of intima and inflammation, which leads to lumen narrowing and thrombosis (74). By regulating Treg lymphocyte, the balance between effector T lymphocyte and Treg lymphocyte is coordinated to promote anti-inflammatory changes in the blood vessel wall, thereby inhibiting the immune response and promoting AVF maturation (67).

Cytotoxic T Lymphocyts (CTL)

CTL lymphocytes is a type of T lymphocyte characterized by $CD8^+$ labeling and secrete perforin, granzyme B(GzmB), IFN-g, and TNF-a. Perforin forms pores in the target cell membrane, through which granzyme can enter and induce apoptosis (75). CTL lymphocyte is more cytotoxic than $CD4^+$T lymphocyte, can induce vascular wall apoptosis, and inhibit immune cell function under certain conditions (60, 76). Unlike $CD4^+$ T lymphocyte, the function of $CD8^+$ T lymphocyte does not depend on Mφ. Studies have shown that $CD8^+$ T lymphocyte is locally activated after vein graft surgery in $CD4^+$ or $CD8^+$ T lymphocytopenia mice, and play an important role in protecting the patency of vein graft. When $CD8^+$ T lymphocyte was present, the graft vein was unobstructed. However, $CD8^+$ T lymphocyte was lacking, graft occlusion was observed, and apoptosis was increased. Therefore, $CD8^+$T lymphocyte can reduce NIH and improve graft vein patency (77). In atherosclerosis, $CD8^+$T lymphocyte mediated VSMC death leads to plaque instability, but $CD8^+$T lymphocyte induced apoptosis limits NIH after arterial injury (74). However, most of the $CD8^+$T lymphocyte on the venous wall were inactivated, suggesting that $CD8^+$T lymphocyte may not be the primary regulatory cells of venous remodeling (51).

Dendritic cell (DC)

DC generally belongs to a class of innate lymphoid cell, defined as cell that express high levels of MHC II and the cell surface integrin CD11c (78, 79). DC is a professional antigen-presenting cell (APC) with antigen-presenting, pro-inflammatory, and anti-inflammatory functions to initiate antigen-specific immune responses, induce immune tolerance, and regulate immune homeostasis. It plays a role in both innate and adaptive immunity (16). DC acts as an APC to control the activation and phenotype of T lymphocyte (80). In the AVF formation region, chronically

activated DC continues to express CD83 and CD86, and these surface molecules act as co-stimulatory molecules to activate other DC, thereby activating naive T lymphocyte to become effector T lymphocyte, promoting effector T lymphocyte proliferation and harmful T lymphocytes apoptosis (16). The appearance of DC in atherosclerosis is similar, and the stability of plaque is negatively correlated with the accumulation of DC, suggesting that DC may regulate local inflammatory response and promote plaque vulnerability (16, 81). Blocking $CD11c^+$ activity during plaque formation may have therapeutic effects (80). $Fasin^+$ is a surface marker of mature DC, while human leukocyte antigen (HLA-DR) and trigger receptor expressed on myeloid cells-1 (TREM-1) are surface markers of associated autoimmune diseases and indicators of progressive inflammation, respectively (69). In AVF with chronic, unresolved inflammation, these markers are found to be upregulated (16). Reducing the expression of HLA-DR, and TREM-1, CD83 and CD86, is a multifactorial anti-inflammatory therapeutic mechanism of DC during AVF maturation (16). Central chemokine receptor 7 (CCR7) is a chemokine of $CD11c^+$. Studies have shown that high expression of CCR7 can lead to increased DC migration, subsequent thrombolysis, and promote AVF maturation (16). DC controls excessive inflammation in acquired immunity by secreting anti-inflammatory cytokines IL-10 and TGF-β (82). TGF-β inhibited the proliferation, activation and differentiation of pro-inflammatory T lymphocyte, and promoted the apoptosis of pro-inflammatory T lymphocyte. However, studies have shown that interfering with TGF-β type II receptor signaling in $CD11c^+$ promotes the formation of atherosclerotic lesions and the expansion of activating effect T lymphocyte (80). These results suggest that DC-T lymphocyte interaction and anti-inflammatory function of DC play a role in AVF maturation and functional maintenance, and that DC can target different stages of AVF vascular remodeling, and can be used to help regulate AVF vascular remodeling in the clinic.

Neutrophil

Neutrophil (NEUT) is myeloid white blood cells that accounting for 50%-70% of all circulating white blood cells (83). It is a component of the innate immune system and can also regulate the immune microenvironment through direct intercellular contact or soluble media communication with Mφ, DC, T lymphocyte, and B lymphocyte (83, 84). Traditionally, NEUT was thought to be present only in the acute phase of inflammation and only to play a role in eliminating pathogens. However, studies have shown that the function of NEUT is not limited to infection, it also plays a role in different types of inflammation (infection and sterility) (85, 86). NEUT synthesises and releases a variety of grain proteins, including MMP, neutrophil elastase (NE), lactoferrin, and pro-inflammatory and anti-inflammatory cytokines (86). Researches have shown that when EC and SMC are co-cultured and exposed to increased shear stress in AVF, gene expression of lactoferrin increases (87). Misra et al (88) investigated the change of protein expression in venous stenosis was studied by protein spectrometry, and lactoferrin expression was significantly increased. In a study of late AVF failure in chronic HD patients, NE and lactoferrin levels were positively correlated with AVF stenosis, and elevated NE levels were also found to be an independent predictor of late AVF failure (18). The neutrophil-lymphocyte ratio (NLR), defined as the absolute number of NEUT divided by the absolute number of lymphocytes, is a strong inflammatory indicator similar to MLR and is associated with coronary atherosclerosis and restenosis (89, 90). In another study of late AVF failure in chronic HD patients, AVF stenosis was found that patients with elevated NLR levels, and the severity of stenosis was positively correlated with NLR levels. It was also found that elevated NLR levels were an independent predictor of late AVF failure (91). In studies of AVF maturation, NLR measured in the blood before surgery was found to be a potential biomarker for predicting AVF maturation. This NLR-associated AVF maturation may be due to the necessary early local pro-inflammatory response in the vascular wall (92). In addition to being a pro-inflammatory cell in cardiovascular disease, there is evidence that NEUT also contributes to tissue repair (93). In an experimental model of restenosis, blocking NEUT in diseased arteries promoted the development of NIH and inhibited damaged intima repair (94). NEUT and its granuloprotein are believed to guide immune cells, especially monocytes, into atherosclerotic lesions and directly affect the occurrence of atherogenesis (95). In a rabbit model of arterial balloon injury, the infiltration of NEUT prior to NIH was found, but no Mφ was found (38). In a mouse model of vascular inflammation, NEUT-secreted chemoattractant proteins can immobilize EC and induce firm monocyte adhesion (96). In addition, granuloprotein directly activates Mφ in human and mice, inducing the secretion of pro-inflammatory cytokines that have been shown to promote atherosclerosis (93). Studies have shown that in patients with various cardiovascular diseases, NE levels in the blood are elevated, NE is abundant in human atherosclerotic plaques, and that NE/proteinase 3 double knockout mice reduced atherosclerotic lesions (97–99). These findings suggest that NEUT plays a role in vascular remodeling in AVF.

B lymphocyte

By reviewing the relevant literature, it has not been found that B lymphocyte plays a role in vascular remodeling of AVF (Figure 1).

Drug treatment strategies targeting immune cells to regulate inflammation

Immunotherapy can promote the maturation and functional maintenance of AVF. Immunotherapy refers to the treatment of disease by activating or suppressing the immune system, which is characterized by altering the infiltration of immune cells and the expression of related cytokines (100). Most immunomodulators belong to biological drugs, which are characterized by their large volume, low stability, poor permeability to the lesion site, and limited ability to cross cell membranes. However, AVF anastomosis is a local vascular injury that must be treated effectively with a high enough concentration of the drug at the anastomosis (36). Local delivery systems can be used for high anastomotic concentrations with

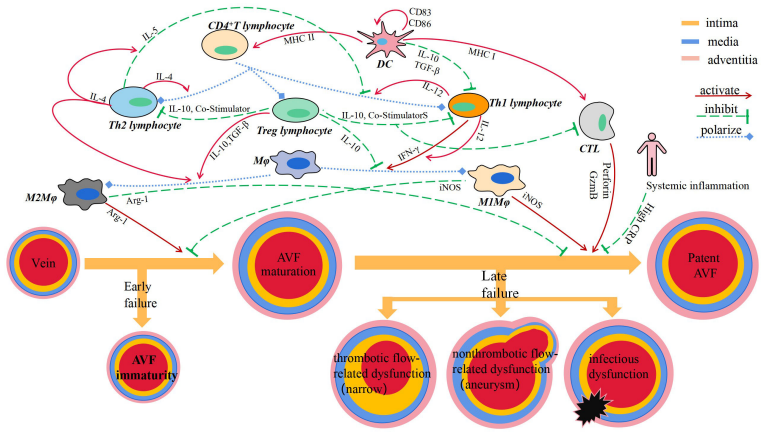

FIGURE 1
Immune cells and secreted cytokines are involved in vascular remodeling of AVF.

minimal systemic toxicity. Administration strategies include direct administration to the endothelium, administration to the adventitia, administration to the entire vessel wall, or the use of mechanical support devices (22). The drug delivery methods of liposomes include hydrogels, living cells, particles, inorganic materials, polymeric micelles, drug crystal and carrier proteins (101).

Targeting macrophage regulates inflammation

In addition to their LDL cholesterol lowering effects, statins have anti-inflammatory effects (102), and are composed of cyclodextrin particles (MP) with reliable and sustained drug release properties. Clinical studies have shown that the use of high-dose statins reduces the risk of AVF failure and can improve AVF patency (103). Studies have shown that in the mouse (C57Bl/6J) AVF model, simvastatin (SV)-loaded cyclodextrin polymer (CDP) intervention can inhibit the accumulation of Mφ in the intima tissue of AVF outflow tract, reduce the gene expression of vascular endothelial growth factor (VEGF)-A and MMP-9, improve vascular remodeling, and reduce the formation of NIH. Thus, it can promote the maturation of AVF and maintain its patency (104, 105).

Prednisolone is a commonly used anti-inflammatory drug in clinic. Liposomes have been shown to facilitate the selective delivery of drugs to inflammatory tissues with highly permeable microvessels that are then engulfed by Mφ in the inflammatory tissue (106). Therefore, liposomes drugs can selectively target AVF after anastomosis, which is often the cause of AVF failure. The mouse AVF model showed that prednisolone was coated with lipids to form liposomal prednisolone (L-Pred), which was swallowed by Mφ after intravenous injection, reduced the infiltration of Mφ, inhibited the inflammatory response and MMP activity in Mφ, alleviated the local inflammatory response of mouse AVF, stimulated outward remodeling, and promoted the maturation of AVF (40).

Human resistance CX3CR1 VHH molecule (CX3CR1 VHH, BI, 655088), CX3CR1 is a specific receptor fractalkine, belonging to the chemokine receptor superfamily. CX3CR1, expressed in monocytes, mediates the infiltration of Mφ into blood vessels, and is increased in clinical AVF specimens with stenosis and in mouse models of CKD with AVF. In a humanized mouse AVF model carried human CX3CR1 gene, inhibition of CX3CR1 with anti-human CX3CR1 VHH molecule reduced Mφ aggregation and procytokine production, promoted vascular remodeling and decreased NIH (107), and promoted AVF maturation and function maintenance.

Sirolimus can inhibit the proliferation of Mφ and the phosphorylation of Akt1-mTORC1 signaling pathway in Mφ at the mature stage of AVF, resulting in the continuous reduction of VSMC in late AVF (39). Sirolimus can also induce the expression of Foxp3, promote the differentiation and upregulation of Treg lymphocytes, which secrete IL-10 and TGF-β, inhibit the inflammation associated with AVF failure, and help improve the AVF patency (108). Thus, sirolimus promotes AVF maturation and functional maintenance while reducing vessel wall thickening, but has no effect on vessel diameter expansion. Since sirolimus in clinically used in coronary stents to protect lumen diameter and reduce restenosis after stenting. Sirolimus should reduce the NIH potential in AVF (109).

Targeting T lymphocyte regulates inflammation

The combination of tacrolimus and sirolimus may be more effective in reducing the incidence of vascular stenosis, which may be related to the fact that tacrolimus specifically acts on T lymphocyte while sirolimus inhibits Mφ.

Cyclosporine A (CsA) can inhibit the function of T lymphocyte and reduce the accumulation of Mφ, thereby regulating venous adaptive remodeling and promoting AVF maturation. In mouse models of AVF, CsA selectively blocked the proliferation and differentiation of $CD4^+$T lymphocyte, thereby inhibiting INF-γ and IL-2 secretion, which are necessary for other inflammatory cells, including Mφ, and ultimately leading to reduced vessel wall thickening and increased AVF outward remodeling in wild-type mice. However, these effects were eliminated in T lymphocyte deficient nude mice, indicating that the effect of CsA on Mφ aggregation and adaptive remodeling is T lymphocyte (50).

Programmed death ligand (PD-L)-1, a ligand that binds to programmed cell death (PD)-1, is specifically expressed on T lymphocyte, thereby increasing Treg lymphocyte and M2-like Mφ and decreasing Th lymphocyte and M1-like Mφ. In a mouse model of aortic - inferior vena cava AVF, administration of anti-PD-L1 antibodies inhibited PD-L1 activity, thickened AVF wall, increased thrombosis, and reduced AVF patency. The effect of anti-PD-L1 antibody on T lymphocyte deficient nude mice was weakened, but T lymphocyte transplantation could restore it, suggesting that the effect of anti-PD-L1 antibody on venous remodeling is also dependent on T lymphocyte. The above studies suggest that PD-L1 can specifically regulate T lymphocyte, and T lymphocyte can regulate Mφ in venous remodeling, thereby increasing the thickness of blood vessel wall and the patency of AVF, thereby promoting AVF vascular remodeling (51) (Table 1).

TABLE 1 Drug treatment strategies targeting immune cells to regulate inflammation.

Drug	Clinical trials and results
Targeting macrophage regulates inflammation	
Statin	The use of high-dose statins reduces the risk of AVF failure and can improve AVF patency
Prednisolone	–
anti-human CX3CR1 VHH molecule	–
Sirolimus	Sirolimus in clinically used in coronary stents to protect lumen diameter and reduce restenosis after stenting.
Targeting T lymphocyte regulates inflammation	
Tacrolimus	The combination of tacrolimus and sirolimus may be more effective in reducing the incidence of vascular stenosis
Cyclosporine A	–
Programmed death ligand-1	–

Conclusion

In summary, $CD4^+$T lymphocyte and Mφ are important regulators during AVF maturation and function maintenance. $CD8^+$T lymphocyte, NUET and DC are also involved. However, due to the diversity of immune cell functions, many of their roles in AVF maturation and functional maintenance are unknown. Current evidence suggests that Th2 lymphocyte contributes to increase blood flow and outward remodeling during AVF maturation, and M2-like Mφ contributes to venous wall thickening; In AVF function maintenance, Th1 lymphocyte and M1φ involved in decreasing NIH and promoting long-term patency of AVF. Th2 lymphocyte, Treg lymphocyte, and M2-like Mφ are required for AVF maturation and are associated with AVF, narrowing; Both Th1 lymphocyte and M1-like Mφ are associated with immaturity of AVF and also promote the maintenance of AVF function. Therefore, maintaining the function of targeted immune cells, especially $CD4^+$ T lymphocyte and Mφ, is of great significance for AVF reconstitution during AVF maturation.

Author contributions

YZ: Writing – original draft. XK: Writing – original draft. LL: Writing – review & editing. DX: Writing – review & editing, Conceptualization.

Funding

The author(s) declare financial support was received for the research, authorship, and/or publication of this article. This study was funded by the National Natural Science Foundation of China (82000728), the Cultivating Fund of Youth Science Foundation from Shandong First Medical University (202201–082), the China Primary Health Care Foundation (HT202112220001), and the Program for Qilu Health Excellent Young Talents from the Health Commission of Shandong Province (A001358). The funders had no role in the study design, data collection and analysis, decision to publish, or preparation of the manuscript.

Conflict of interest

The authors declare that the research was conducted in the absence of any commercial or financial relationships that could be construed as a potential conflict of interest.

Publisher's note

References

1. Wang L, Xu X, Zhang M, Hu C, Zhang X, Li C, et al. Prevalence of chronic kidney disease in China: results from the sixth China chronic disease and risk factor surveillance. *JAMA Intern Med.* (2023) 183:298–310. doi: 10.1001/jamainternmed.2022.6817

2. Murphy D, McCulloch CE, Lin F, Banerjee T, Bragg-Gresham JL, Eberhardt MS, et al. Trends in prevalence of chronic kidney disease in the United States. *Ann Intern Med.* (2016) 165:473–81. doi: 10.7326/M16–0273

3. Santoro D, Benedetto F, Mondello P, Pipitò N, Barillà D, Spinelli F, et al. Vascular access for hemodialysis: current perspectives. *Int J Nephrol Renovasc Dis.* (2014) 7:281–94. doi: 10.2147/IJNRD.S46643

4. Huber TS, Berceli SA, Scali ST, Neal D, Anderson EM, Allon M, et al. Arteriovenous fistula maturation, functional patency, and intervention rates. *JAMA Surg.* (2021) 156:1111–8. doi: 10.1001/jamasurg.2021.4527

5. Al-Jaishi AA, Oliver MJ, Thomas SM, Lok CE, Zhang JC, Garg AX, et al. Patency rates of the arteriovenous fistula for hemodialysis: a systematic review and meta-analysis. *Am J Kidney Dis*. (2014) 63:464–78. doi: 10.1053/j.ajkd.2013.08.023

6. Kong X, Tang L, Liang L, Cao W, Zhang L, Yong W, et al. Clinical outcomes following the surgery of new autologous arteriovenous fistulas proximal to the failed ones in end-stage renal disease patients: a retrospective cohort study. *Ren Fail*. (2019) 41:1036–44. doi: 10.1080/0886022X.2019.1696210

7. Rothuizen TC, Wong C, Quax PH, van Zonneveld AJ, Rabelink TJ, Rotmans JI. Arteriovenous access failure: more than just intimal hyperplasia? *Nephrol Dial Transplant*. (2013) 28:1085–92. doi: 10.1093/ndt/gft068

8. Kaygin MA, Halici U, Aydin A, Dag O, Binici DN, Limandal HK, et al. The relationship between arteriovenous fistula success and inflammation. *Ren Fail*. (2013) 35:1085–8. doi: 10.3109/0886022X.2013.815100

9. Cunnane CV, Cunnane EM, Walsh MT. A review of the hemodynamic factors believed to contribute to vascular access dysfunction. *Cardiovasc Eng Technol*. (2017) 8:280–94. doi: 10.1007/s13239–017-0307–0

10. Chiu JJ, Chien S. Effects of disturbed flow on vascular endothelium: pathophysiological basis and clinical perspectives. *Physiol Rev*. (2011) 91:327–87. doi: 10.1152/physrev.00047.2009

11. Xiao Y, Vazquez-Padron RI, Martinez L, Singer HA, Woltmann D, Salman LH. Role of platelet factor 4 in arteriovenous fistula maturation failure: What do we know so far? *J Vasc Access*. (2024) 25:390–406. doi: 10.1177/11297298221085458

12. Henderson NC, Rieder F, Wynn TA. Fibrosis: from mechanisms to medicines. *Nature*. (2020) 587:555–66. doi: 10.1038/s41586–020-2938–9

13. Martinez L, Duque JC, Tabbara M, Paez A, Selman G, Hernandez DR, et al. Fibrotic venous remodeling and nonmaturation of arteriovenous fistulas. *J Am Soc Nephrol*. (2018) 29:1030–40. doi: 10.1681/ASN.2017050559

14. Applewhite B, Gupta A, Wei Y, Yang X, Martinez L, Rojas MG, et al. Periadventitial beta-aminopropionitrile-loaded nanofibers reduce fibrosis and improve arteriovenous fistula remodeling in rats. *Front Cardiovasc Med*. (2023) 10:1124106. doi: 10.3389/fcvm.2023.1124106

15. Du J, Liang L, Liu S, Yang X, Cao S, Zhang H, et al. Neointimal hyperplasia in the inferior vena cava of adenine-induced chronic kidney disease rats with aortocaval fistulas. *Clin Exp Nephrol*. (2020) 24:1007–14. doi: 10.1007/s10157–020-01927–3

16. Samra G, Rai V, Agrawal DK. Innate and adaptive immune cells associate with arteriovenous fistula maturation and failure. *Can J Physiol Pharmacol*. (2022) 100:716–27. doi: 10.1139/cjpp-2021–0731

17. Matsubara Y, Kiwan G, Fereydooni A, Langford J, Dardik A. Distinct subsets of T cells and macrophages impact venous remodeling during arteriovenous fistula maturation. *JVS Vasc Sci*. (2020) 1:207–18. doi: 10.1016/j.jvssci.2020.07.005

18. Oh DJ, Lee JH, Kwon YE, Choi HM. Relationship between arteriovenous fistula stenosis and circulating levels of neutrophil granule proteins in chronic hemodialysis patients. *Ann Vasc Surg*. (2021) 77:226–35. doi: 10.1016/j.avsg.2021.05.056

19. Gameiro J, Ibeas J. Factors affecting arteriovenous fistula dysfunction: A narrative review. *J Vasc Access*. (2020) 21:134–47. doi: 10.1177/1129729819845562

20. Lee T, Mokrzycki M, Moist L, Maya I, Vazquez M, Lok CE. Standardized definitions for hemodialysis vascular access. *Semin Dial*. (2011) 24:515–24. doi: 10.1111/j.1525-139X.2011.00969.x

21. Lok CE, Huber TS, Lee T, Shenoy S, Yevzlin AS, Abreo K, et al. KDOQI clinical practice guideline for vascular access: 2019 update. *Am J Kidney Dis*. (2020) 75:S1–S164. doi: 10.1053/j.ajkd.2019.12.001

22. Hu H, Patel S, Hanisch JJ, Santana JM, Hashimoto T, Bai H, et al. Future research directions to improve fistula maturation and reduce access failure. *Semin Vasc Surg*. (2016) 29:153–71. doi: 10.1053/j.semvascsurg.2016.08.005

23. Tronc F, Mallat Z, Lehoux S, Wassef M, Esposito B, Tedgui A. Role of matrix metalloproteinases in blood flow-induced arterial enlargement: interaction with NO. *Arterioscler Thromb Vasc Biol*. (2000) 20:E120–126. doi: 10.1161/01.atv.20.12.e120

24. Chan CY, Chen YS, Ma MC, Chen CF. Remodeling of experimental arteriovenous fistula with increased matrix metalloproteinase expression in rats. *J Vasc Surg*. (2007) 45:804–11. doi: 10.1016/j.jvs.2006.12.063

25. Hu K, Guo Y, Li Y, Lu C, Cai C, Zhou S, et al. Oxidative stress: An essential factor in the process of arteriovenous fistula failure. *Front Cardiovasc Med*. (2022) 9:984472. doi: 10.3389/fcvm.2022.984472

26. Tellides G, Pober JS. Inflammatory and immune responses in the arterial media. *Circ Res*. (2015) 116:312–22. doi: 10.1161/CIRCRESAHA.116.301312

27. Roy-Chaudhury P, Kruska L. Future directions for vascular access for hemodialysis. *Semin Dial*. (2015) 28:107–13. doi: 10.1111/sdi.12329

28. Brahmbhatt A, Remuzzi A, Franzoni M, Misra S. The molecular mechanisms of hemodialysis vascular access failure. *Kidney Int*. (2016) 89:303–16. doi: 10.1016/j.kint.2015.12.019

29. Hofstra L, Tordoir JH, Kitslaar PJ, Hoeks AP, Daemen MJ. Enhanced cellular proliferation in intact stenotic lesions derived from human arteriovenous fistulas and peripheral bypass grafts. Does it correlate with flow parameters? *Circulation*. (1996) 94:1283–90. doi: 10.1161/01.cir.94.6.1283

30. Ross R. The pathogenesis of atherosclerosis: a perspective for the 1990s. *Nature*. (1993) 362:801–9. doi: 10.1038/362801a0

31. Rai V, Agrawal DK. The role of damage- and pathogen-associated molecular patterns in inflammation-mediated vulnerability of atherosclerotic plaques. *Can J Physiol Pharmacol*. (2017) 95:1245–53. doi: 10.1139/cjpp-2016–0664

32. Petrie JR, Guzik TJ, Touyz RM. Diabetes, hypertension, and cardiovascular disease: clinical insights and vascular mechanisms. *Can J Cardiol*. (2018) 34:575–84. doi: 10.1016/j.cjca.2017.12.005

33. Bezhaeva T, Wong C, de Vries MR, van der Veer EP, van Alem CMA, Que I, et al. Deficiency of TLR4 homologue RP105 aggravates outward remodeling in a murine model of arteriovenous fistula failure. *Sci Rep*. (2017) 7:10269. doi: 10.1038/s41598–017-10108–4

34. Mukhopadhyay S, Gabre J, Chabasse C, Bromberg JS, Antalis TM, Sarkar R. Depletion of CD4 and CD8 positive T cells impairs venous thrombus resolution in mice. *Int J Mol Sci*. (2020) 21:1650. doi: 10.3390/ijms21051650

35. Idris-Khodja N, Mian MO, Paradis P, Schiffrin EL. Dual opposing roles of adaptive immunity in hypertension. *Eur Heart J*. (2014) 35:1238–44. doi: 10.1093/eurheartj/ehu119

36. Lee T, Misra S. New insights into dialysis vascular access: molecular targets in arteriovenous fistula and arteriovenous graft failure and their potential to improve vascular access outcomes. *Clin J Am Soc Nephrol*. (2016) 11:1504–12. doi: 10.2215/CJN.02030216

37. Shapouri-Moghaddam A, Mohammadian S, Vazini H, Taghadosi M, Esmaeili SA, Mardani F, et al. Macrophage plasticity, polarization, and function in health and disease. *J Cell Physiol*. (2018) 233:6425–40. doi: 10.1002/jcp.26429

38. Welt FG, Edelman ER, Simon DI, Rogers C. Neutrophil, not macrophage, infiltration precedes neointimal thickening in balloon-injured arteries. *Arterioscler Thromb Vasc Biol*. (2000) 20:2553–8. doi: 10.1161/01.atv.20.12.2553

39. Guo X, Fereydooni A, Isaji T, Gorecka J, Liu S, Hu H, et al. Inhibition of the akt1-mTORC1 axis alters venous remodeling to improve arteriovenous fistula patency. *Sci Rep*. (2019) 9:11046. doi: 10.1038/s41598–019-47542–5

40. Wong C, Bezhaeva T, Rothuizen TC, Metselaar JM, de Vries MR, Verbeek FP, et al. Liposomal prednisolone inhibits vascular inflammation and enhances venous outward remodeling in a murine arteriovenous fistula model. *Sci Rep*. (2016) 6:30439. doi: 10.1038/srep30439

41. Gorecka J, Fereydooni A, Gonzalez L, Lee SR, Liu S, Ono S, et al. Molecular targets for improving arteriovenous fistula maturation and patency. *Vasc Investig Ther*. (2019) 2:33–41. doi: 10.4103/VIT.VIT_9_19

42. Du Cheyne C, Tay H, De Spiegelaere W. The complex TIE between macrophages and angiogenesis. *Anat Histol Embryol*. (2020) 49:585–96. doi: 10.1111/ahe.12518

43. Hu S, Wang D, Ma T, Yuan F, Zhang Y, Gao X, et al. Association between preoperative monocyte-to-lymphocyte ratio and late arteriovenous fistula dysfunction in hemodialysis patients: A cohort study. *Am J Nephrol*. (2021) 52:854–60. doi: 10.1159/000519822

44. Brahmbhatt A, NievesTorres E, Yang B, Edwards WD, Roy Chaudhury P, Lee MK, et al. The role of Iex-1 in the pathogenesis of venous neointimal hyperplasia associated with hemodialysis arteriovenous fistula. *PloS One*. (2014) 9:e102542. doi: 10.1371/journal.pone.0102542

45. Shih CM, Huang CY, Liao LR, Hsu CP, Tsao NW, Wang HS, et al. Nickel ions from a corroded cardiovascular stent induce monocytic cell apoptosis: Proposed impact on vascular remodeling and mechanism. *J Formos Med Assoc*. (2015) 114:1088–96. doi: 10.1016/j.jfma.2014.03.007

46. Roy-Chaudhury P, Khan R, Campos B, Wang Y, Kurian M, Lee T, et al. Pathogenetic role for early focal macrophage infiltration in a pig model of arteriovenous fistula (AVF) stenosis. *J Vasc Access*. (2014) 15:25–8. doi: 10.5301/jva.5000151

47. Wang X, Khalil RA. Matrix metalloproteinases, vascular remodeling, and vascular disease. *Adv Pharmacol*. (2018) 81:241–330. doi: 10.1016/bs.apha.2017.08.002

48. McMaster WG, Kirabo A, Madhur MS, Harrison DG. Inflammation, immunity, and hypertensive end-organ damage. *Circ Res*. (2015) 116:1022–33. doi: 10.1161/CIRCRESAHA.116.303697

49. Sica A, Mantovani A. Macrophage plasticity and polarization: *in vivo* veritas. *J Clin Invest*. (2012) 122:787–95. doi: 10.1172/JCI59643

50. Matsubara Y, Kiwan G, Liu J, Gonzalez L, Langford J, Gao M, et al. Inhibition of T-cells by cyclosporine A reduces macrophage accumulation to regulate venous adaptive remodeling and increase arteriovenous fistula maturation. *Arterioscler Thromb Vasc Biol*. (2021) 41:e160–74. doi: 10.1161/ATVBAHA.120.315875

51. Matsubara Y, Gonzalez L, Kiwan G, Liu J, Langford J, Gao M, et al. PD-L1 (Programmed death ligand 1) regulates T-cell differentiation to control adaptive venous remodeling. *Arterioscler Thromb Vasc Biol*. (2021) 41:2909–22. doi: 10.1161/ATVBAHA.121.316380

52. Tang D, Chen S, Hou D, Gao J, Jiang L, Shi J, et al. Regulation of macrophage polarization and promotion of endothelialization by NO generating and PEG-YIGSR modified vascular graft. *Mater Sci Eng C Mater Biol Appl*. (2018) 84:1–11. doi: 10.1016/j.msec.2017.11.005

53. Kuwahara G, Hashimoto T, Tsuneki M, Yamamoto K, Assi R, Foster TR, et al. CD44 promotes inflammation and extracellular matrix production during arteriovenous fistula maturation. *Arterioscler Thromb Vasc Biol*. (2017) 37:1147–56. doi: 10.1161/ATVBAHA.117.309385

54. Yang S, Yuan HQ, Hao YM, Ren Z, Qu SL, Liu LS, et al. Macrophage polarization in atherosclerosis. *Clin Chim Acta*. (2020) 501:142–6. doi: 10.1016/j.cca.2019.10.034

55. Peyton KJ, Ensenat D, Azam MA, Keswani AN, Kannan S, Liu XM, et al. Arginase promotes neointima formation in rat injured carotid arteries. *Arterioscler Thromb Vasc Biol*. (2009) 29:488–94. doi: 10.1161/ATVBAHA.108.183392

56. Miki K, Kumar A, Yang R, Killeen ME, Delude RL. Extracellular activation of arginase-1 decreases enterocyte inducible nitric oxide synthase activity during systemic inflammation. *Am J Physiol Gastrointest Liver Physiol*. (2009) 297:G840–848. doi: 10.1152/ajpgi.90716.2008

57. Konjar S, Veldhoen M. Dynamic metabolic state of tissue resident CD8 T cells. *Front Immunol*. (2019) 10:1683. doi: 10.3389/fimmu.2019.01683

58. Larosa DF, Orange JS. 1. Lymphocytes. *J Allergy Clin Immunol*. (2008) 121:S364–369. doi: 10.1016/j.jaci.2007.06.016

59. Weaver CT, Harrington LE, Mangan PR, Gavrieli M, Murphy KM. Th17: an effector CD4 T cell lineage with regulatory T cell ties. *Immunity*. (2006) 24:677–88. doi: 10.1016/j.immuni.2006.06.002

60. Duque JC, Martinez L, Mesa A, Wei Y, Tabbara M, Salman LH, et al. CD4(+) lymphocytes improve venous blood flow in experimental arteriovenous fistulae. *Surgery*. (2015) 158:529–36. doi: 10.1016/j.surg.2015.02.018

61. Wang Y, Burns WR, Tang PC, Yi T, Schechner JS, Zerwes HG, et al. Interferon-gamma plays a nonredundant role in mediating T cell-dependent outward vascular remodeling of allogeneic human coronary arteries. *FASEB J*. (2004) 18:606–8. doi: 10.1096/fj.03-0840fje

62. Ou HX, Guo BB, Liu Q, Li YK, Yang Z, Feng WJ, et al. Regulatory T cells as a new therapeutic target for atherosclerosis. *Acta Pharmacol Sin*. (2018) 39:1249–58. doi: 10.1038/aps.2017.140

63. Tang Q, Adams JY, Tooley AJ, Bi M, Fife BT, Serra P, et al. Visualizing regulatory T cell control of autoimmune responses in nonobese diabetic mice. *Nat Immunol*. (2006) 7:83–92. doi: 10.1038/ni1289

64. Engelbertsen D, Andersson L, Ljungcrantz I, Wigren M, Hedblad B, Nilsson J, et al. T-helper 2 immunity is associated with reduced risk of myocardial infarction and stroke. *Arterioscler Thromb Vasc Biol*. (2013) 33:637–44. doi: 10.1161/ATVBAHA.112.300871

65. Foks AC, Lichtman AH, Kuiper J. Treating atherosclerosis with regulatory T cells. *Arterioscler Thromb Vasc Biol*. (2015) 35:280–7. doi: 10.1161/ATVBAHA.114.303568

66. Vignali DA, Collison LW, Workman CJ. How regulatory T cells work. *Nat Rev Immunol*. (2008) 8:523–32. doi: 10.1038/nri2343

67. Kearley J, Barker JE, Robinson DS, Lloyd CM. Resolution of airway inflammation and hyperreactivity after in *vivo* transfer of CD4+CD25+ regulatory T cells is interleukin 10 dependent. *J Exp Med*. (2005) 202:1539–47. doi: 10.1084/jem.20051166

68. Cope A, Le Friec G, Cardone J, Kemper C. The Th1 life cycle: molecular control of IFN-gamma to IL-10 switching. *Trends Immunol*. (2011) 32:278–86. doi: 10.1016/j.it.2011.03.010

69. Subramanian M, Tabas I. Dendritic cells in atherosclerosis. *Semin Immunopathol*. (2014) 36:93–102. doi: 10.1007/s00281-013-0400-x

70. Fang D, Zhu J. Molecular switches for regulating the differentiation of inflammatory and IL-10-producing anti-inflammatory T-helper cells. *Cell Mol Life Sci*. (2020) 77:289–303. doi: 10.1007/s00018–019-03277–0

71. Dimayuga PC, Chyu KY, Lio WM, Zhao X, Yano J, Zhou J, et al. Reduced neointima formation after arterial injury in CD4-/- mice is mediated by CD8+CD28hi T cells. *J Am Heart Assoc*. (2013) 2:e000155. doi: 10.1161/JAHA.113.000155

72. Albany CJ, Trevelin SC, Giganti G, Lombardi G, Scottà C. Getting to the heart of the matter: the role of regulatory T-cells (Tregs) in cardiovascular disease (CVD) and atherosclerosis. *Front Immunol*. (2019) 10:2795. doi: 10.3389/fimmu.2019.02795

73. Fontenot JD, Rasmussen JP, Gavin MA, Rudensky AY. A function for interleukin 2 in Foxp3-expressing regulatory T cells. *Nat Immunol*. (2005) 6:1142–51. doi: 10.1038/ni1263

74. Gottschalk RA, Corse E, Allison JP. Expression of Helios in peripherally induced Foxp3+ regulatory T cells. *J Immunol*. (2012) 188:976–80. doi: 10.4049/jimmunol.1102964

75. Lord SJ, Rajotte RV, Korbutt GS, Bleackley RC. Granzyme B: a natural born killer. *Immunol Rev*. (2003) 193:31–8. doi: 10.1034/j.1600-065X.2003.00044.x

76. Gravano DM, Hoyer KK. Promotion and prevention of autoimmune disease by CD8+ T cells. *J Autoimmun*. (2013) 45:68–79. doi: 10.1016/j.jaut.2013.06.004

77. Simons KH, de Vries MR, Peters HAB, Jukema JW, Quax PHA, Arens R. CD8+ T cells protect during vein graft disease development. *Front Cardiovasc Med*. (2019) 6:77. doi: 10.3389/fcvm.2019.00077

78. Steinman RM, Witmer MD. Lymphoid dendritic cells are potent stimulators of the primary mixed leukocyte reaction in mice. *Proc Natl Acad Sci U.S.A*. (1978) 75:5132–6. doi: 10.1073/pnas.75.10.5132

79. Metlay JP, Witmer-Pack MD, Agger R, Crowley MT, Lawless D, Steinman RM. The distinct leukocyte integrins of mouse spleen dendritic cells as identified with new hamster monoclonal antibodies. *J Exp Med*. (1990) 171:1753–71. doi: 10.1084/jem.171.5.1753

80. Gil-Pulido J, Zernecke A. Antigen-presenting dendritic cells in atherosclerosis. *Eur J Pharmacol*. (2017) 816:25–31. doi: 10.1016/j.ejphar.2017.08.016

81. Zernecke A. Dendritic cells in atherosclerosis: evidence in mice and humans. *Arterioscler Thromb Vasc Biol*. (2015) 35:763–70. doi: 10.1161/ATVBAHA.114.303566

82. Anzai T. Inflammatory mechanisms of cardiovascular remodeling. *Circ J*. (2018) 82:629–35. doi: 10.1253/circj.CJ-18–0063

83. Mayadas TN, Cullere X, Lowell CA. The multifaceted functions of neutrophils. *Annu Rev Pathol*. (2014) 9:181–218. doi: 10.1146/annurev-pathol-020712–164023

84. Kolaczkowska E, Kubes P. Neutrophil recruitment and function in health and inflammation. *Nat Rev Immunol*. (2013) 13:159–75. doi: 10.1038/nri3399

85. Amulic B, Cazalet C, Hayes GL, Metzler KD, Zychlinsky A. Neutrophil function: from mechanisms to disease. *Annu Rev Immunol*. (2012) 30:459–89. doi: 10.1146/annurev-immunol-020711–074942

86. Mantovani A, Cassatella MA, Costantini C, Jaillon S. Neutrophils in the activation and regulation of innate and adaptive immunity. *Nat Rev Immunol*. (2011) 11:519–31. doi: 10.1038/nri3024

87. Heydarkhan-Hagvall S, Chien S, Nelander S, Li YC, Yuan S, Lao J, et al. DNA microarray study on gene expression profiles in co-cultured endothelial and smooth muscle cells in response to 4- and 24-h shear stress. *Mol Cell Biochem*. (2006) 281:1–15. doi: 10.1007/s11010–006-0168–6

88. Misra S, Fu AA, Puggioni A, Glockner JF, McKusick MA, Bjarnason H, et al. Proteomic profiling in early venous stenosis formation in a porcine model of hemodialysis graft. *J Vasc Interv Radiol*. (2009) 20:241–51. doi: 10.1016/j.jvir.2008.10.004

89. Arbel Y, Finkelstein A, Halkin A, Birati EY, Revivo M, Zuzut M, et al. Neutrophil/lymphocyte ratio is related to the severity of coronary artery disease and clinical outcome in patients undergoing angiography. *Atherosclerosis*. (2012) 225:456–60. doi: 10.1016/j.atherosclerosis.2012.09.009

90. Turak O, Ozcan F, Isleyen A, Tok D, Sokmen E, Buyukkaya E, et al. Usefulness of the neutrophil-to-lymphocyte ratio to predict bare-metal stent restenosis. *Am J Cardiol*. (2012) 110:1405–10. doi: 10.1016/j.amjcard.2012.07.003

91. Yilmaz H, Bozkurt A, Cakmak M, Celik HT, Bilgic MA, Bavbek N, et al. Relationship between late arteriovenous fistula (AVF) stenosis and neutrophil-lymphocyte ratio (NLR) in chronic hemodialysis patients. *Ren Fail*. (2014) 36:1390–4. doi: 10.3109/0886022X.2014.945183

92. Bashar K, Zafar A, Ahmed K, Kheirelseid EA, Healy D, Clarke-Moloney M, et al. Can a neutrophil-lymphocyte ratio derived from preoperative blood tests predict arteriovenous fistula maturation? *Ann Vasc Surg*. (2016) 35:60–7. doi: 10.1016/j.avsg.2016.02.020

93. Silvestre-Roig C, Braster Q, Ortega-Gomez A, Soehnlein O. Neutrophils as regulators of cardiovascular inflammation. *Nat Rev Cardiol*. (2020) 17:327–40. doi: 10.1038/s41569–019-0326–7

94. Soehnlein O, Kai-Larsen Y, Frithiof R, Sorensen OE, Kenne E, Scharffetter-Kochanek K, et al. Neutrophil primary granule proteins HBP and HNP1–3 boost bacterial phagocytosis by human and murine macrophages. *J Clin Invest*. (2008) 118:3491–502. doi: 10.1172/JCI35740

95. Doring Y, Drechsler M, Soehnlein O, Weber C. Neutrophils in atherosclerosis: from mice to man. *Arterioscler Thromb Vasc Biol*. (2015) 35:288–95. doi: 10.1161/ATVBAHA.114.303564

96. Ortega-Gomez A, Salvermoser M, Rossaint J, Pick R, Brauner J, Lemnitzer P, et al. Cathepsin G controls arterial but not venular myeloid cell recruitment. *Circulation*. (2016) 134:1176–88. doi: 10.1161/CIRCULATIONAHA.116.024790

97. Kosar F, Varol E, Ayaz S, Kütük E, Oğuzhan A, Diker E. Plasma leukocyte elastase concentration and coronary artery disease. *Angiology*. (1998) 49:193–201. doi: 10.1177/000331979804900305

98. Dollery CM, Owen CA, Sukhova GK, Krettek A, Shapiro SD, Libby P. Neutrophil elastase in human atherosclerotic plaques: production by macrophages. *Circulation*. (2003) 107:2829–36. doi: 10.1161/01.CIR.0000072792.65250.4A

99. Wen G, An W, Chen J, Maguire EM, Chen Q, Yang F, et al. Genetic and pharmacologic inhibition of the neutrophil elastase inhibits experimental atherosclerosis. *J Am Heart Assoc*. (2018) 7:e008187. doi: 10.1161/JAHA.117.008187

100. Galluzzi L, Chan TA, Kroemer G, Wolchok JD, López-Soto A. The hallmarks of successful anticancer immunotherapy. *Sci Transl Med*. (2018) 10:eaat7807. doi: 10.1126/scitranslmed.aat7807

101. He W, Xing X, Wang X, Wu D, Mitragotri S. Nanocarrier-Mediated cytosolic delivery of biopharmaceuticals. *Advanced Funct Materials*. (2020) 30:1910566. doi: 10.1002/adfm.201910566

102. Goldstein JL, Brown MS. A century of cholesterol and coronaries: from plaques to genes to statins. *Cell*. (2015) 161:161–72. doi: 10.1016/j.cell.2015.01.036

103. Chang HH, Chang YK, Lu CW, Huang CT, Chien CT, Hung KY, et al. Statins improve long term patency of arteriovenous fistula for hemodialysis. *Sci Rep*. (2016) 6:22197. doi: 10.1038/srep22197

104. Zhao C, Zuckerman ST, Cai C, Kilari S, Singh A, Simeon M, et al. Periadventitial delivery of simvastatin-loaded microparticles attenuate venous neointimal hyperplasia associated with arteriovenous fistula. *J Am Heart Assoc*. (2020) 9:e018418. doi: 10.1161/JAHA.120.018418

105. Cui J, Kessinger CW, Jhajj HS, Grau MS, Misra S, Libby P, et al. Atorvastatin reduces *in vivo* fibrin deposition and macrophage accumulation, and improves primary patency duration and maturation of murine arteriovenous fistula. *J Am Soc Nephrol*. (2020) 31:931–45. doi: 10.1681/ASN.2019060612

106. Farokhzad OC, Langer R. Impact of nanotechnology on drug delivery. *ACS Nano*. (2009) 3:16–20. doi: 10.1021/nn900002m

107. Misra S, Kilari S, Yang B, Sharma A, Wu CC, Vazquez-Padron RI, et al. Anti human CX3CR1 VHH molecule attenuates venous neointimal hyperplasia of arteriovenous fistula in mouse model. *J Am Soc Nephrol*. (2021) 32:1630–48. doi: 10.1681/ASN.2020101458

108. Chapman NM, Chi H. mTOR signaling, Tregs and immune modulation. *Immunotherapy*. (2014) 6:1295–311. doi: 10.2217/imt.14.84

109. Schofer J. Sirolimus-eluting stents for treatment of patients with long atherosclerotic lesions in small coronary arteries: double-blind, randomised controlled trial (E-SIRIUS). *Lancet*. (2003) 362:1093–9. doi: 10.1016/S0140-6736(03)14462-5

frontiers | Frontiers in Immunology

TYPE Original Research
PUBLISHED 23 May 2024
DOI 10.3389/fimmu.2024.1361343

OPEN ACCESS

EDITED BY
Xu-jie Zhou,
Peking University, China

REVIEWED BY
Guochun Chen,
Central South University, China
Yang Li,
Peking University, China

*CORRESPONDENCE
Hui-Yao Lan
hylan@cuhk.edu.hk
Anping Xu
xuanping@mail.sysu.edu.cn

†These authors have contributed equally to this work

RECEIVED 25 December 2023
ACCEPTED 30 April 2024
PUBLISHED 23 May 2024

CITATION
Yang H, Li J, Huang X-r, Bucala R, Xu A and Lan H-Y (2024) Macrophage-derived macrophage migration inhibitory factor mediates renal injury in anti-glomerular basement membrane glomerulonephritis. *Front. Immunol.* 15:1361343. doi: 10.3389/fimmu.2024.1361343

Macrophage-derived macrophage migration inhibitory factor mediates renal injury in anti-glomerular basement membrane glomerulonephritis

Hui Yang[1,2†], Jinhong Li[3†], Xiao-ru Huang[2,4], Richard Bucala[5], Anping Xu[1*] and Hui-Yao Lan[2,4*]

[1]Department of Nephrology, Sun Yat-Sen Memorial Hospital, Sun Yat-Sen University, Guangzhou, China, [2]Department of Medicine and Therapeutics, Li Ka Shing Institute of Health Sciences, Lui Che Woo Institute of Innovative Medicine, The Chinese University of Hong Kong, Hong Kong, Hong Kong SAR, China, [3]Department of Nephrology, The Seventh Affiliated Hospital of Sun Yat-sen University, SunYat-sen University, Shenzhen, China, [4]Departments of Nephrology and Pathology, Guangdong Provincial Hospital, Southern Medical University, Guangzhou, China, [5]Department of Internal Medicine, Yale University School of Medicine, New Haven, CT, United States

Macrophages are a rich source of macrophage migration inhibitory factor (MIF). It is well established that macrophages and MIF play a pathogenic role in anti-glomerular basement membrane crescentic glomerulonephritis (anti-GBM CGN). However, whether macrophages mediate anti-GBM CGN via MIF-dependent mechanism remains unexplored, which was investigated in this study by specifically deleting MIF from macrophages in $MIF^{f/f-lysM-cre}$ mice. We found that compared to anti-GBM CGN induced in $MIF^{f/f}$ control mice, conditional ablation of MIF in macrophages significantly suppressed anti-GBM CGN by inhibiting glomerular crescent formation and reducing serum creatinine and proteinuria while improving creatine clearance. Mechanistically, selective MIF depletion in macrophages largely inhibited renal macrophage and T cell recruitment, promoted the polarization of macrophage from M1 towards M2 via the CD74/NF-κB/p38MAPK-dependent mechanism. Unexpectedly, selective depletion of macrophage MIF also significantly promoted Treg while inhibiting Th1 and Th17 immune responses. In summary, MIF produced by macrophages plays a pathogenic role in anti-GBM CGN. Targeting macrophage-derived MIF may represent a novel and promising therapeutic approach for the treatment of immune-mediated kidney diseases.

KEYWORDS

macrophages, MIF, T cells, anti-GBM crescentic glomerulonephritis, inflammation

1 Introduction

Anti-glomerular basement membrane crescentic glomerulonephritis (anti-GBM CGN) is an autoimmune glomerular disease that progresses rapidly. It is characterized by glomerular crescentic formation and the presence of autoantibodies that target specific epitopes on the a3 chain of type IV collagen (1–3). The development of anti-GBM CGN involves different cellular components, such as macrophages, lymphocytes, intrinsic renal cells, and a complex network of cytokines (4, 5). Despite extensive research, the precise mechanisms underlying this disease are still not fully understood.

Macrophages play a crucial role in the development of anti-GBM GN by infiltrating the affected kidneys and contributing to inflammation and fibrosis (6). Recent studies have shown that depletion of macrophages or inhibiting the production of cytokines by macrophages can alleviate kidney injury in anti-GBM CGN (7–9). The severity of the disease is associated with the infiltration and activation of macrophages, which can exhibit different phenotypes depending on the local environment. Pro-inflammatory M1 macrophages promote renal injury, whereas anti-inflammatory M2 macrophages offer protection against kidney diseases (6, 10–14).

Macrophage migration inhibitory factor (MIF) is a versatile proinflammatory cytokine that plays a crucial role in triggering the release of multiple downstream cytokines and facilitating the recruitment of leukocytes to inflammatory organs by binding to CD74 (15, 16). In the pathogenesis of murine autoimmune glomerulonephritis (GN), including anti-GBM CGN, MIF has been identified as a key player, influencing both the inflammatory and adaptive immune responses (17–21). Recent research demonstrated that mice lacking the MIF gene were protected from renal injury in a murine CGN model. Additionally, studies involving bone marrow reconstitution revealed that the absence of MIF from both bone marrow-derived and non-myeloid-derived sources improves experimental anti-GBM GN (22). However, further investigation is required to establish the specific contribution of macrophage-derived MIF in the context of anti-GBM CGN.

In order to investigate the potential role of macrophage-derived MIF in anti-GBM CGN and to uncover the underlying mechanisms, we utilized genetic techniques to create a conditional knockout of MIF specifically in macrophages. Through comprehensive evaluations, we determined the role of macrophage-derived MIF in the development of anti-GBM CGN. In addition, we also aimed to elucidate the underlying mechanisms of macrophage-derived MIF in the pathogenesis of anti-GBM CGN.

2 Results

2.1 Characterization of macrophage-specific MIF deficient mouse

To evaluate the pathogenic role of macrophage-derived MIF, we employed a Cre-loxP strategy to generate mice with a specific deletion of MIF within their macrophages. To confirm the efficiency of MIF deletion, bone marrow was isolated from $MIF^{f/f\text{-}lysM\text{-}cre}$ mice, control $MIF^{f/f}$ mice, and MIF KO littermates. The isolated bone marrow cells were cultured and induced to differentiate into macrophages. As shown in Figure 1A, the deficiency of macrophage-derived MIF led to a notable reduction in MIF secretion by BMDM (Figure 1A). Additionally, MIF and CD74 mRNA expression were significantly lower in macrophages of $MIF^{f/f\text{-}lysM\text{-}cre}$ mice compared with $MIF^{f/f}$ mice under basal conditions (Figures 1B, C). Furthermore, TNF-a treatment for 24 hours significantly increased MIF protein expression in macrophages derived from $MIF^{f/f}$ mice but not in macrophages from $MIF^{f/f\text{-}lysM\text{-}cre}$ mice (Figure 1D). These results demonstrated the successful deletion of MIF from macrophages in $MIF^{f/f\text{-}lysM\text{-}cre}$ mice.

2.2 Selective MIF depletion in macrophages ameliorates experimental anti-GBM GN

To examine the involvement of macrophage-derived MIF in experimental anti-GBM CGN, we conducted experiments using both $MIF^{f/f}$ and $MIF^{f/f\text{-}lysM\text{-}cre}$ mice. The mice were induced to develop anti-GBM CGN, and the renal injuries were evaluated. Notably, the $MIF^{f/f\text{-}lysM\text{-}cre}$ mice showed a significant inhibition in renal injuries such as segmental glomerular capillary necrosis and crescent formation compared to the anti-GBM GN $MIF^{f/f}$ mice (Figures 2A, B). Renal dysfunction such as the urine albumin/creatinine ratio (Figure 2C), serum creatinine levels (Figure 2D), and creatinine clearance (Figure 2E) were also significantly improved in $MIF^{f/f\text{-}lysM\text{-}cre}$ mice compared to the anti-GBM CGN $MIF^{f/f}$ mice. These findings indicate that macrophage-derived MIF plays a pathogenic role in anti-GBM CGN.

2.3 Deletion of macrophage MIF inhibits macrophage and T cell infiltration in a mouse model of anti-GBM CGN

We next examined macrophage-derived MIF on cellular immune response during anti-GBM CGN. Immunohistochemistry detected that a massive F4/80+ macrophages infiltrating the anti-GBM CGN in $MIF^{f/f}$ mice, which was largely inhibited in $MIF^{f/f\text{-}lysM\text{-}cre}$ mice (Figures 3A-C). Moreover, the infiltration of glomerular and interstitial CD3+ T cells in $MIF^{f/f\text{-}lysM\text{-}cre}$ GN mice was also significantly lower than in $MIF^{f/f}$ GN mice (Figures 3D-F). These findings demonstrate that selective depletion of MIF in macrophages suppresses the infiltration of macrophages and T cells in the kidney during anti-GBM GN.

2.4 Deletion of macrophage MIF suppresses antigen-specific antibody production in a mouse model of anti-GBM CGN

Immunofluorescence was used to assess the glomerular deposition of sheep anti-mouse GBM antibody, mouse IgG, and complement component C3 in MIFf/f and MIFf/f-lysM-cre mice (Figure 4A). Interestingly, there was no significant difference in the

glomerular deposition of these markers between the two groups, indicating that macrophage-specific MIF depletion did not affect immune complex deposition in inflamed glomeruli. However, as demonstrated in Figure 4B, the serum levels of mouse anti-sheep IgG antibodies were notably reduced in $MIF^{f/f\text{-}lysM\text{-}cre}$ GN mice compared to $MIF^{f/f}$ GN mice. This was associated with significant reduction in serum MIF levels in $MIF^{f/f\text{-}lysM\text{-}cre}$ GN mice compared to $MIF^{f/f}$ GN mice (Figure 4C). These results indicate that macrophage-specific MIF depletion reduced systemic MIF levels and selectively inhibited the antigen-specific antibody production without influencing the immune complex deposition in the inflamed glomeruli.

2.5 Deletion of macrophage MIF enhances macrophage polarization from M1 to M2 through in a mouse model of anti-GBM CGN

To investigate the impact of macrophage-derived MIF on macrophage polarization in the kidneys of mice with anti-GBM CGN, we utilized flow cytometry to determine the populations of M1 (F4/80+CD86+) and M2 (F4/80+CD206+) macrophages. Notably, $MIF^{f/f\text{-}lysM\text{-}cre}$ GN mice exhibited a significantly decreased M1 macrophages while increasing the M2 macrophages compared to $MIF^{f/f}$ GN mice (Figures 5A, B; Supplementary Figure S1). Furthermore, real-time PCR analysis revealed that selective MIF depletion in macrophages led to a significant inhibition of pro-inflammatory cytokines including MCP-1 and IL-1β while increasing the anti-inflammatory cytokine IL-10 in CGN mice (Figures 5C–E). These findings indicate that selective depletion of MIF in macrophages results in a shift in macrophage polarization from the pro-inflammatory M1 phenotype towards the anti-inflammatory M2 phenotype in experimental anti-GBM CGN. Moreover, this shift is associated with reduced pro-inflammatory cytokine expression and increased anti-inflammatory cytokine expression.

2.6 Deletion of macrophage MIF promotes Treg but inhibits Th1 and Th17 immune responses in a mouse model of anti-GBM CGN

We next examined whether disrupted macrophage MIF influences T cell immunity as it is well-established that Th1 and Th17 are pathogenic whereas Treg is protective in anti-GBM CGN (23–26). In light of this, we investigated the impact of selective MIF depletion in macrophages on the immune differentiation of CD4+ T cells, specifically focusing on Th1 ($CD4^+IFN\gamma^+$), Th2 ($CD4^+IL\text{-}4^+$),

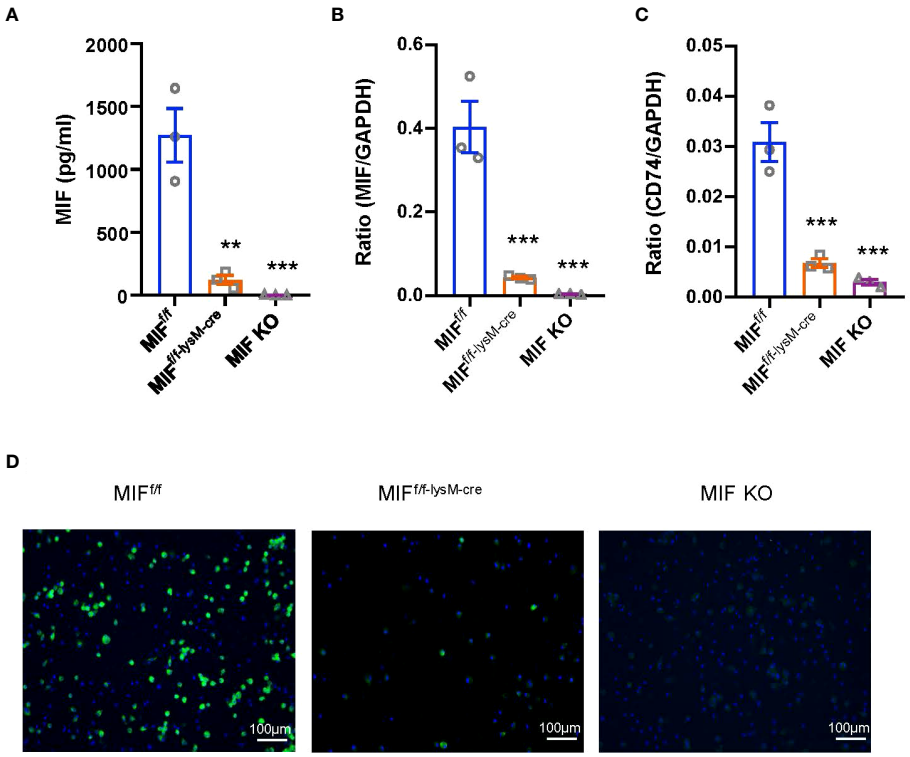

FIGURE 1
Characterization of $MIF^{f/f\text{-}lysM\text{-}cre}$ mice. **(A)** Bone marrow-derived macrophages (BMDMs) were isolated from $MIF^{f/f}$, $MIF^{f/f\text{-}lysM\text{-}cre}$ and MIF KO mice. Enzymelinked immunosorbent assay (ELISA) show that $MIF^{f/f\text{-}lysM\text{-}cre}$ and MIF KO mice inhibit MIF expression by BMDMs. **(B, C)** RNA was isolated from cells for quantitative reverse transcription-PCR (qRT-PCR) quantitation of MIF and CD74. **(D)** Immunofluorescence staining for MIF(green) with nuclear DAPI (blue) counterstain in macrophages stimulated with TNF-a (10ng/ml for 24hours). Each bar represents mean±SEM. Each dot represents one mouse. $^{**}P < 0.01$, $^{***}P < 0.001$ compared with $MIF^{f/f}$ mice; GAPDH, glyceraldehyde-3-phosphate dehydrogenase.

10.3389/fimmu.2024.1361343

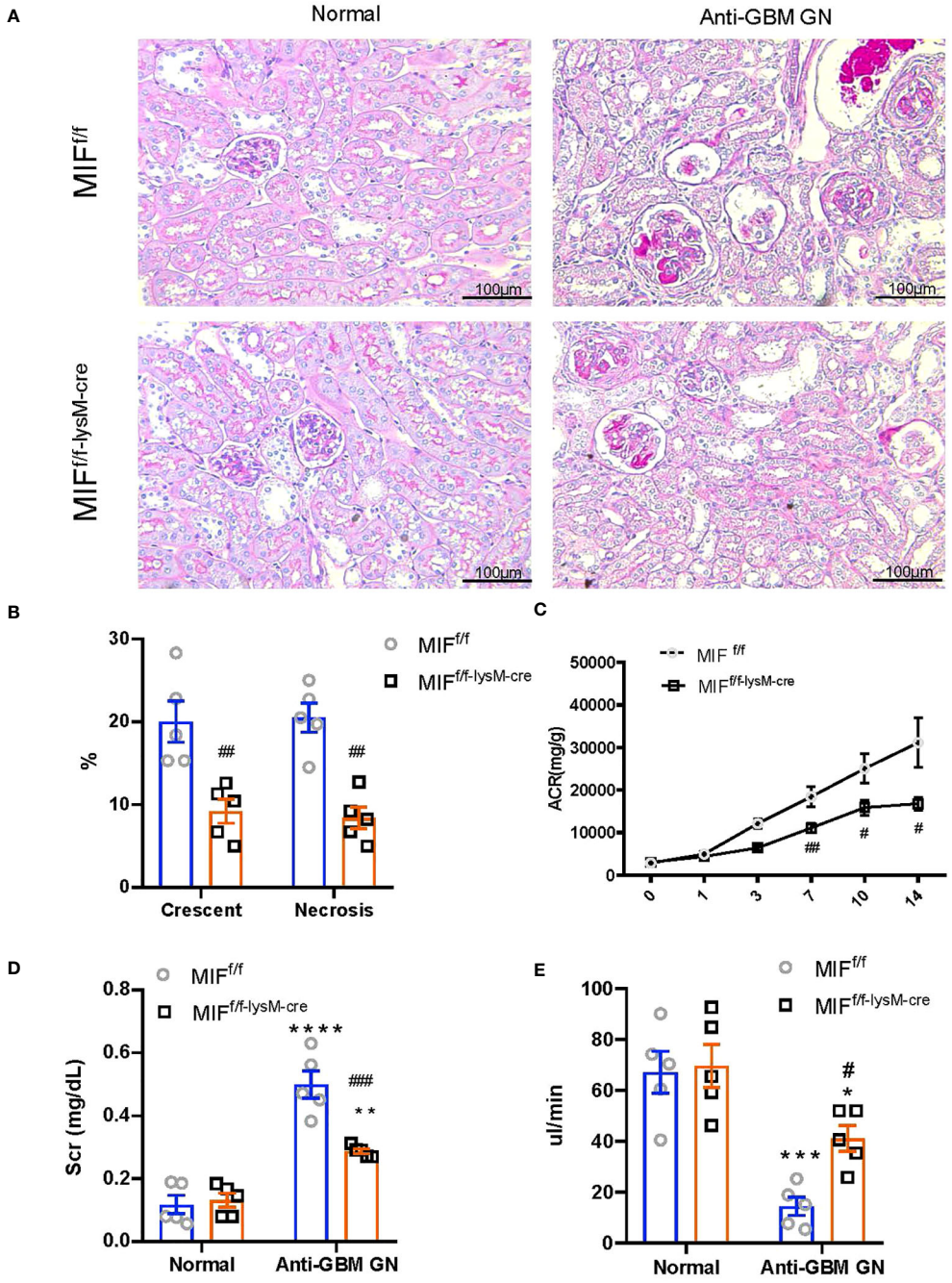

FIGURE 2
Selective MIF depletion in macrophages ameliorates experimental anti-GBM GN. **(A)** Representative images in PAS sections (magnification X200). **(B)** Semi-quantitative analysis of histology. **(C)** Urine albumin creatinine ration (ACR) over the disease course. **(D)** plasma creatinine. **(E)** Creatinine clearance. Each bar represents mean±SEM. Each dot represents one mouse. *p <0.05, **p <0.01, ***p< 0.001, ****p< 0.0001 versus corresponding control; $^{\#}$p<0.05, $^{\#\#}$p < 0.01, $^{\#\#\#}$p< 0.001 versus corresponding MIF$^{f/f}$.

Th17 ($CD4^+IL\text{-}17a^+$) and Treg ($CD4^+CD25^+FoxP3^+$) subpopulations. Flow cytometry analysis revealed that selective MIF depletion in macrophages led to a significant reduction in Th1 ($CD4^+IFN\gamma^+$) and Th17 ($CD4^+IL\text{-}17a^+$) cells in the anti-GBM CGN kidney (Figures 6A, C; Supplementary Figures S2A, C). Conversely, there was an increase in Treg population ($CD4^+CD25^+FoxP3^+$), however, the Th2 (CD4+IL-4+) immune response remained unaffected (Figures 6D, B; Supplementary Figure S3, Supplementary Figure S2B). These findings indicate that selective MIF depletion in macrophages enhances the Treg immune response while inhibiting the Th1 and Th17 immune responses in experimental anti-GBM CGN. This shift in immune cell differentiation may contribute to the amelioration of renal injury observed in this context.

2.7 *Deletion of macrophage MIF* inhibits Anti-GBM GN by inactivating M1 macrophages via CD74/NF-κB and p38 MAPK-dependent mechanisms *in vivo* and *in vitro*

We next examined the mechanisms through which specific deletion of macrophage MIF inhibits anti-GBM GN induced in MIF $^{f/f}$ and MIF $^{f/f\text{-lysM-cre}}$ mice. Western blot analysis revealed that there was a marked upregulation of CD74 and activation of NF-κB/p65 and p38 MAPK signaling and expression of iNOS in the diseased kidney of MIF $^{f/f}$ mice (Figure 7). In contrast, selective MIF depletion from macrophages significantly inhibited the expression of CD74 and phosphorylation of NF-κB/p65 and p38 MAPK, as well as expression of iNOS in MIFf/f-lysM-cre GN mice (Figure 7). All of these findings indicated that MIF may promote anti-GBM GN by activating M1 macrophages through the CD74/NF-kB/p38 MAPK signaling. This was further demonstrated *in vitro* in cultured BMDM from MIF WT and MIF KO mice. We found that addition of TNF-α largely promoted iNOS-producing M1 macrophages in MIF WT BMDM by activating CD74/NF-κB/p38 MAPK signaling, which was blocked in BMDM lacking MIF (Figure 8). Thus,

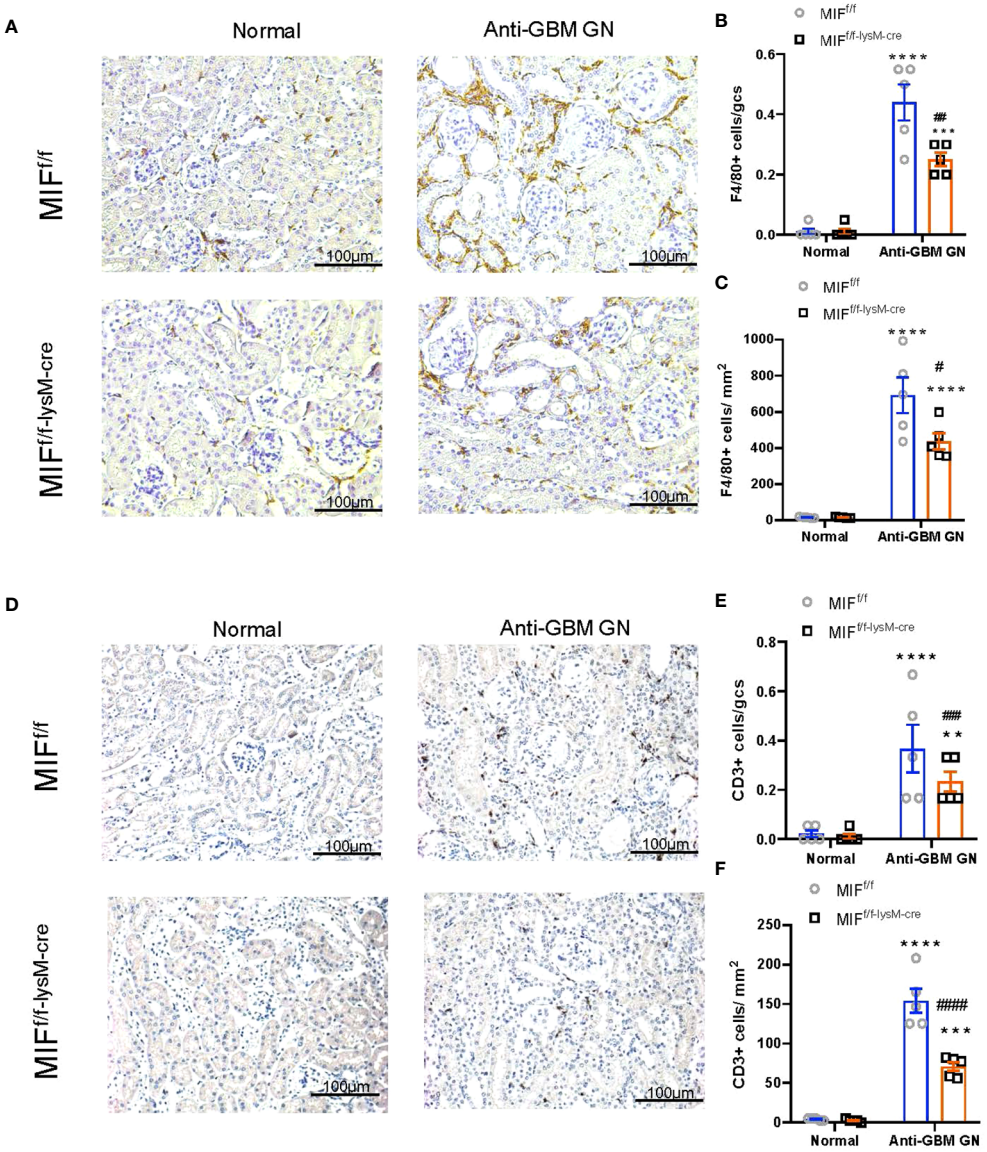

FIGURE 3
Selective MIF depletion in macrophages reduces macrophage and T cell recruitment in experimental anti-GBM GN. **(A)** Immunohistochemical staining for F4/80-positive macrophages in the kidney with anti-GBM crescentic GN on Day 14 after disease induction. **(B, C)** Summary data for macrophages in glomerulus and tubulointerstitium. **(D)** Immunohistochemical staining for CD3-positive T cells in the kidney with anti-GBM crescentic GN on Day 14 after disease induction. **(E, F)** Summary data for T cells in glomerulus and tubulointerstitium. Original magnification 200X. Each bar represents mean±SEM. Each dot represents one mouse. **p <0.01, ***p< 0.001, ****p< 0.0001 versus corresponding control; $^{\#}$p<0.05, $^{\#\#}$p < 0.01, $^{\#\#\#}$p< 0.001, $^{\#\#\#\#}$p<0.0001 versus corresponding MIF$^{f/f}$.

macrophage-derived MIF may mediate anti-GBM GN by promoting M1 macrophage activation via the CD74/NK-κB/p38 MAPK-dependent mechanism.

3 Discussion

MIF has been implicated in the pathogenesis of various diseases, including infectious diseases, inflammatory diseases, immune diseases such as rheumatoid arthritis, septic shock, and cardiovascular disease (20, 23–26). Previous studies have also demonstrated the importance of MIF in kidney-related conditions like acute kidney injury (AKI), chronic kidney disease (CKD), diabetic nephropathy, autosomal dominant polycystic kidney disease (ADPKD), and vasculitides (27–35).In glomerulonephritis, inhibition of MIF by neutralizing antibodies has shown renal protective in IgA nephritis and in rats with crescentic GN (36–38). Additionally, systemic MIF knockout (KO) can also suppress lupus nephritis and anti-GBM CGN (17, 19–22). However, it should be noted that systemic MIF KO models cannot distinguish the source of functional MIF since MIF is released by both macrophages and other intrinsic cells within the kidney. To address this, we generated mice with a macrophage-specific MIF KO and investigated the role and mechanisms of macrophage-derived MIF in a mouse model of anti-GBM GN. The results demonstrated that mice with macrophage-specific deletion of MIF were protected from the development of anti-GBM CGN. These findings highlight the crucial role of macrophage-derived MIF in the pathogenesis of anti-GBM CGN, shedding light on the specific contribution of macrophage-derived MIF in this disease context.

It is well-established that macrophages play a crucial role in the progressive renal injury associated with glomerular crescentic formation (6–8, 10, 11, 39). It is reported that MIF regulates macrophage activation via Toll-like receptor 4 (TLR4) (40). Thus,

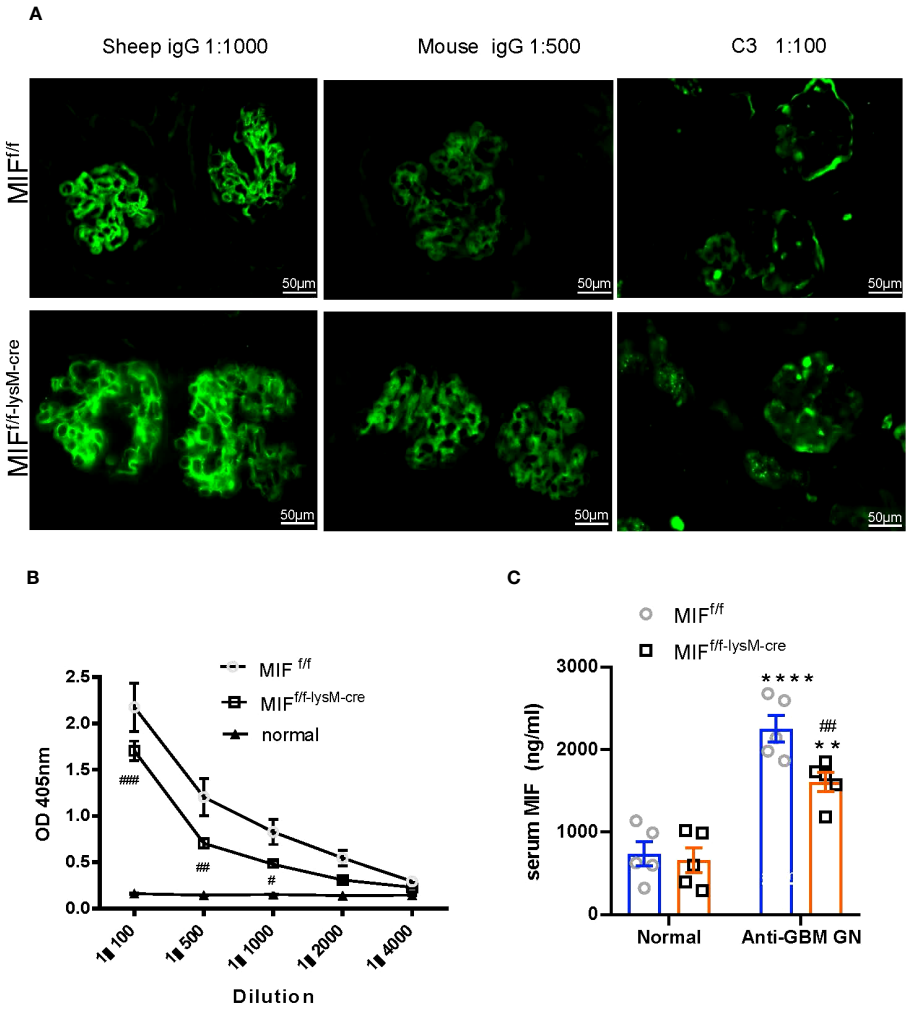

FIGURE 4
Selective MIF depletion in macrophages attenuates plasma levels of mouse anti-sheep IgG antibody and serum MIF production, which does not affect immune complex deposition in inflamed glomeruli. **(A)** Immunofluorescence staining for the deposition of sheep IgG, mouse IgG and mouse C3 in the kidney glomeruli with anti-GBM crescentic GN on Day 14 after disease induction. Plasma mouse anti-sheep IgG **(B)** and serum MIF **(C)** were determined using ELISA kits according to the manufacturer's protocol. Original magnification 200X. Each bar represents mean±SEM. Each dot represents one mouse. **p <0.01, ****p< 0.0001 versus corresponding control; $^{\#}$p<0.05, $^{\#\#}$p < 0.01, $^{\#\#\#}$p< 0.001 versus corresponding MIF$^{f/f}$.

deletion of macrophage TLR4 inhibits anti-GBM cGN (39). It is also well defined that MIF is pathogenic in immunologically-mediated kidney disease as mice lacking MIF are protected against lupus mice and anti-GBM GN (17, 22). Similarly, systemic or bone marrow disruption of MIF also inhibits cardiac remodeling by suppressing myocardial leukocyte infiltration and the expression of inflammatory mediators (41). Findings from the present study added new information that macrophages may mediate anti-GBM CGN via MIF-dependent mechanism as selective depletion of macrophage MIF protected against anti-GBM CGN by inhibiting macrophage infiltration and promoting macrophage polarization from the pro-inflammatory M1 phenotype towards the anti-inflammatory M2 phenotype. These results suggest that macrophage-derived MIF may have a critical role in modulating macrophage activation and function in the pathogenesis of anti-GBM CGN.

Furthermore, an intriguing aspect of our findings is that the specific depletion of MIF in macrophages appears to confer kidney protection in crescentic GN by promoting renal Treg cells while suppressing Th1 and Th17 immune responses. The involvement of Th1 and Th17 immune responses in the pathogenesis of anti-GBM GN is well-established (42–44), whereas Treg cells are known to have a protective role (44, 45). In murine crescentic glomerulonephritis, Treg cells have been shown to regulate the Th1 immune response (45). Additionally, recent studies have highlighted the important role of cytokines and chemokines in the cross-regulation of Th1 and Th17 immune responses in experimental anti-GBM GN (46).

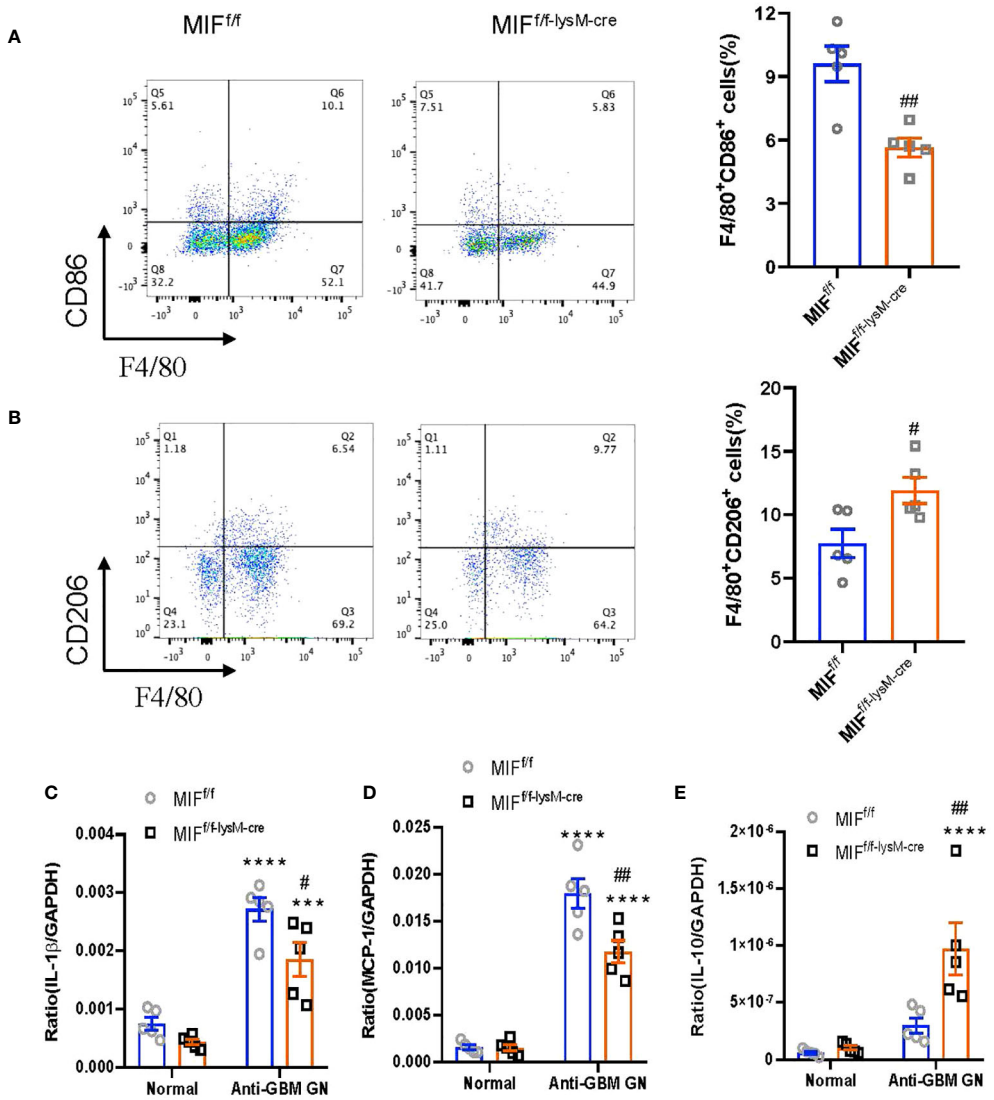

FIGURE 5
Selective MIF depletion in macrophages promotes macrophage polarization from M1 towards M2. **(A)** Representative flow cytometry plots and quantification of renal singlets analyzed for M1 (F4/80+CD86+). **(B)** Representative flow cytometry plots and quantification of renal singlets analyzed for M2 (F4/80+CD206+). Reverse transcription-PCR (RT-PCR) was performed on whole mouse kidney total RNA with anti-GBM crescentic GN on Day 14 after disease induction. **(C–E)** IL-1 β, monocyte chemoattractant protein-1 (MCP-1) and IL-10mRNA expression were normalized with GAPDH mRNA. Each bar represents mean±SEM. Each dot represents one mouse. ****p< 0.0001 versus corresponding control; #p<0.05, ##p < 0.01 versus corresponding MIF$^{f/f}$.

Interestingly, MIF has been shown to enhance the acquisition of a Th17 cell-like phenotype in spondylarthritis (47). Based on these findings, it is reasonable to speculate that selective depletion of MIF in macrophages may protect against anti-GBM crescentic GN by suppressing Th1/Th17 while promoting Treg immune responses.

CD74 is identified as main receptor of MIF (48). The binding of MIF to CD74 triggers the activation of mitogen-activated protein kinase (MAPK) and NK-kB signaling (49, 50). It has been reported that M1 macrophage activation in anti-GBM GN is NF-κB-dependent (51) and M1-mediated NF-κB signaling can release cytokines including IL-1β, IL-6, TNF-α and granulocyte colony-stimulating factors (G-CSF) (52). The present study unraveled that deletion of macrophage MIF ameliorated anti-GBM GN by shifting the M1 macrophages to M2 macrophages via the CD74/NK-kB/p38 MAPK-dependent mechanism. Importantly, deletion of macrophage MIF inhibited the Th1 and Th17 immune responses, while increasing Treg. These findings also suggest that macrophage-derived MIF may play a regulatory role in T cell immunity during the development of anti-GBM GN, although the mechanisms remain largely unclear.

In summary, macrophage-derived MIF plays an important role in anti-GBM CGN. Mechanistically, as shown in Figure 9,

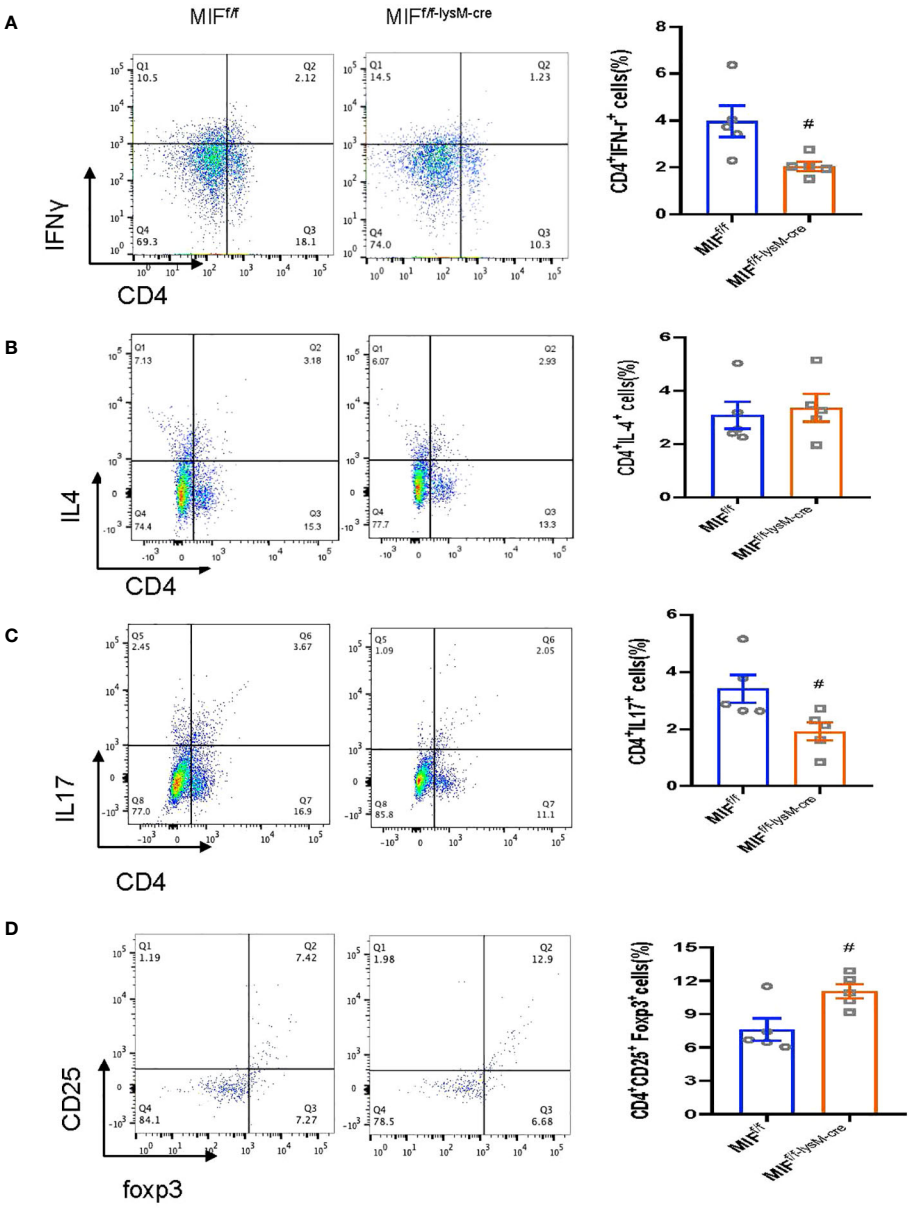

FIGURE 6
Selective MIF depletion in macrophages downregulates renal Th1/Th17 response and upregulates renal Treg response in experimental anti-GBM GN. Flow cytometry analysis of renal infiltrated CD4+IFNγ+Th1 cells **(A)**, CD4+ IL-4+Th2 cells **(B)**, CD4+ IL-17+Th17 cells **(C)** and CD4+CD25+ Foxp3 +Treg **(D)**. CD4+CD25+ Foxp3+Treg is Gated on CD4+ T cells. Each bar represents mean±SEM. Each dot represents one mouse. #p<0.05 versus corresponding $MIF^{f/f}$.

10.3389/fimmu.2024.1361343

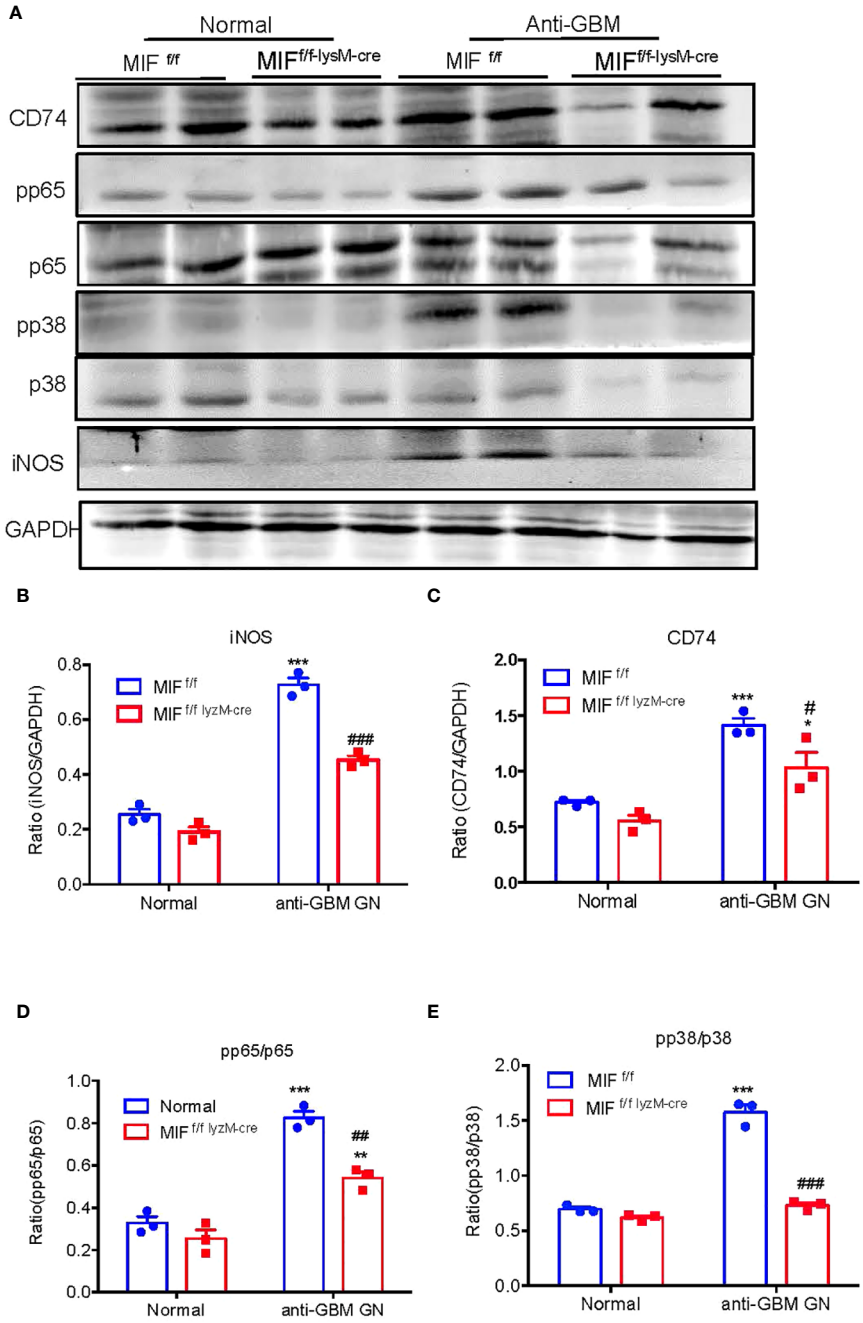

FIGURE 7
Selective MIF depletion in macrophages ameliorates experimental anti- GBM GN by inactivating NF-kB and p38/MAPK signaling and inhibiting M1 macrophages activation. **(A)** Western blots. **(B–E)** Statistics data of the protein expression (iNOS, CD74, pp65/p65 and pp38/p38). Each bar represents mean ± SEM. Each dot represents one mouse. *p <0.05, ***p<0.001 versus corresponding control; $^{\#}$p<0.05, $^{\#\#}$p < 0.01, $^{\#\#\#}$p< 0.001 versus corresponding MIF$^{f/f}$.

macrophage-derived MIF may mediate anti-GBM CGN by promoting proinflammatory M1 macrophage infiltration and activation via the NK-κB and p38 MAPK pathways and promoting the Th1/Th17 immune responses while suppressing the Treg population. These findings are in line with our previous studies that T cell-mediated immunity plays a crucial role in anti-GBM disease, despite not necessarily impacting the glomerular deposition of immune complexes (44).

4 Materials and methods

4.1 Generation of macrophage-specific MIF deletion mice

To generate mice with myeloid-specific MIF deletion (MIF$^{f/f-lysM-cre}$), we utilized C57BL/6 mice carrying MIF genes with homozygous loxP-flanked regions (MIF$^{f/f}$), which were

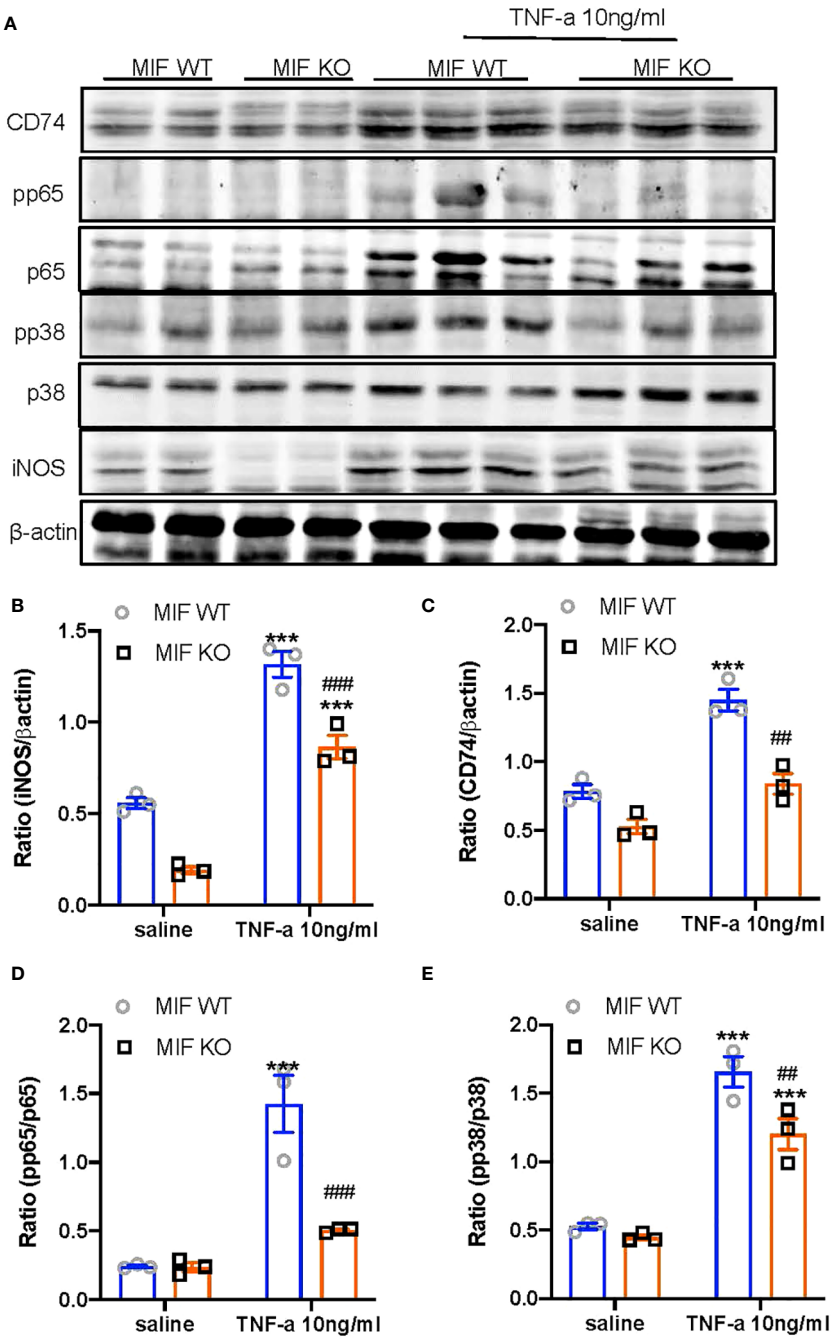

FIGURE 8
Bone marrow-derived macrophages (BMDM) lacking MIF show inhibition of MIF signaling and M1 macrophage activation in response to TNFa *in vitro*. **(A)** Western blots; **(B–E)** Statistics data of the protein expression (CD74, pp65/p65, pp38/p38, INOS). Results show that bone marrow-derived macrophages (BMDMs) isolated MIF KO mice inhibit TNF-α (10ng/ml)-induced upregulation of MIF signaling by downregulating CD74 expression and activation of NF-kB/p65 and p38/MAPK, there by inhibiting M1 macrophage activation by suppressing iNOS expression. Each bar represents mean±SEM. Each dot represents one mouse. ***P < 0.001 compared with MIF WT mice; $^{\#\#}$P < 0.01, $^{\#\#\#}$p< 0.001 compared with MIF WT mice treated with TNF-a 10ng/ml.

previously described (53). Lysozyme M promoter-driven cre (lysM-cre) mice were obtained from the Jackson Laboratory in the USA. The MIF$^{f/f}$ mice were crossed with lysM-cre mice to obtain the desired genotype. The genotypes of the resulting littermates were confirmed using PCR with specific primers recommended by the Jackson Laboratory. All mice used in the study were maintained under specific pathogen-free conditions at a temperature of 25°C and a 12-hour light-dark cycle. They were housed in our animal facility and provided with standard food and water ad libitum.

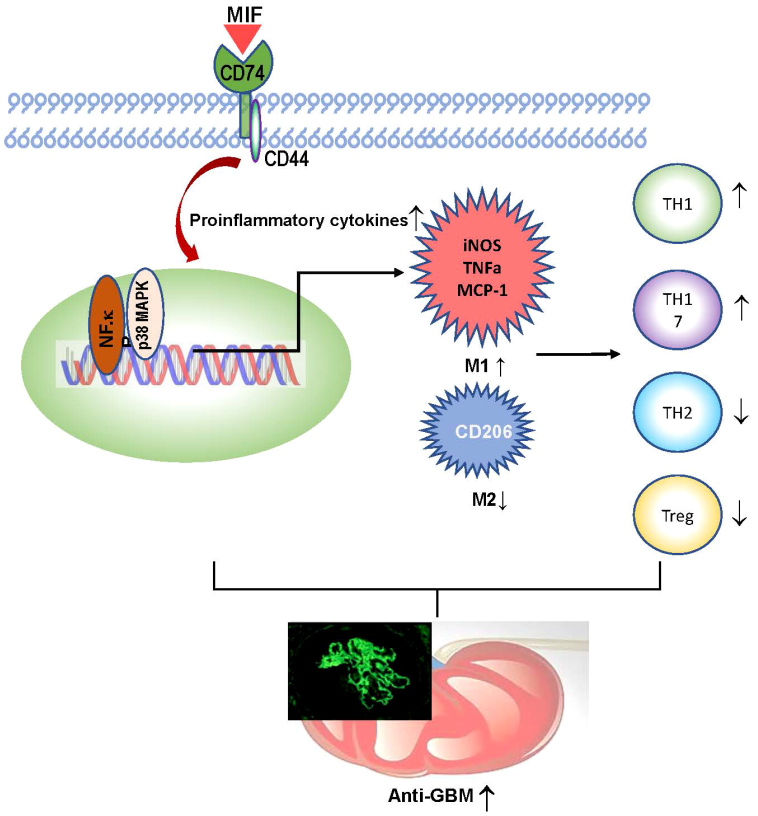

FIGURE 9
Mechanisms of MIF mediate experimental anti-GBM GN.

4.2 Isolation and culture of bone marrow-derived macrophages

To culture bone marrow-derived macrophages (BMDMs), bone marrow cells were isolated from the tibias and femurs of $MIF^{f/f}$, $MIF^{f/f-lysM-cre}$, and MIF knockout (KO) mice. These cells were then cultured in Dulbecco modified Eagle medium (DMEM) supplemented with 50 ng/ml macrophage colony-stimulating factor (M-CSF) for 7 days, following a previously established protocol (54). After the 7-day culture period, BMDMs were stimulated with TNF-α (10 ng/ml) for 24 hours and proteins were collected for western blot analysis.

4.3 Real-time PCR analysis

Total RNA was extracted from either diseased kidney tissue or cultured cells using the RNeasy Isolation Kit (Qiagen, Valencia, CA) following the manufacturer's protocol. RT-PCR was conducted following established methods (44, 55). The mRNA expression levels of the target genes were normalized to glyceraldehyde-3-phosphate dehydrogenase (GAPDH) as an internal control. The primer sequences for mouse MIF, CD74, MCP-1, IL-1β, IL-10, and GAPDH were previously reported (44, 55, 56).

4.4 Induction of anti-GBM glomerulonephritis in mice

The mouse model of anti-glomerular basement membrane crescentic glomerulonephritis (anti-GBM cGN) was established using male $MIF^{f/f}$ and $MIF^{f/f-lysM-cre}$ mice (8–12 weeks old), following a well-established protocol (44). Herein, the procedure involved the following steps: Firstly, groups of $MIF^{f/f}$ and $MIF^{f/f-lysM-cre}$ mice received a flank subcutaneous immunization with normal sheep IgG mixed with Freund's complete adjuvant (Sigma Aldrich, St. Louis, Missouri, USA) five days prior to the initiation of the experiment. Anti-GBM cGN was induced by administering sheep anti-mouse GBM IgG via tail vein injection at a dose of 60 μg/g of body weight (referred to as day 0). On day 14, the mice were sacrificed using a lethal dose of ketamine and xylazine mixture. Age-matched normal male MIFf/f and MIFf/f–lysM–cre mice (n = 5 per group) were included as normal control counterparts. All animal experiments were conducted in compliance with the

guidelines approved by the Animal Experimentation Ethics Committee at the Chinese University of Hong Kong.

4.5 Measurement of proteinuria and creatinine

Analysis of proteinuria: Urinary samples were collected at various time points, including before and after the induction of anti-GBM disease on days 0, 1, 3, 7, and 14. Proteinuria analysis was performed following the manufacturer's protocols, as described previously (44). Urinary albumin excretion was quantified as total urinary albumin/creatinine ratio (expressed as micrograms per milligram). Measurement of urinary and serum creatinine levels was conducted using an enzymatic kit (Stanbio Laboratory, Boerne, USA).

4.6 Renal pathology and immunohistochemistry

Renal pathology assessment was conducted on methyl Carnoy's fixed, paraffin-embedded tissue sections (4μm thick). The sections were stained with periodic acid Schiff (PAS) to visualize the renal structures. Glomerular crescents and necrosis were quantified by examining 50 glomeruli per diseased kidney section and calculating the percentage of affected glomeruli. Immunohistochemistry was performed on paraffin sections stained with monoclonal an anti-F4/80 antibody (Serotec, Oxford, UK) to detect macrophages, and a rabbit anti-mouse polyclonal CD3+ antibody (SP7) (Abcam, Cambridge, UK) to identify total T cells. The number of positive cells for CD3 and F4/80 was counted in 20 glomeruli and expressed as cells per glomerular cross-section (gcs). In the tubulointerstitium, positive cells were counted under high-intensity fields (400× magnification) using a 0.0625 mm^2 graticule fitted in the microscope eyepiece. The cell count was then reported as cells per square millimeter ($mm^{2)}$.

4.7 Immunofluorescence

To assess the presence of MIF-expressing macrophages in the kidney, immunofluorescence staining was performed. Acetone-fixed bone marrow-derived macrophages (BMDMs) were cultured with the MIF antibody (sc-20121; Santa Cruz) followed by incubation with a fluorescein isothiocyanate anti-rabbit secondary antibody, as previously described (54). To evaluate immune deposition in the glomeruli, direct immunofluorescence was conducted using FITC-conjugated polyclonal antibodies specific to sheep IgG, mouse IgG, and complement C3, following established protocols (38).

4.8 Enzyme-linked immunosorbent assay

Plasma levels of mouse anti-sheep IgG were quantified using a method previously described (56). The concentration of serum MIF was determined using ELISA kits (R&D Systems, Minneapolis, USA) according to the manufacturer's instructions.

4.9 Flow cytometry analysis

Kidney single cells were prepared and subjected to flow cytometry analysis following a previously described protocol (44, 56). Single-cell suspensions were treated with IC Fixation Buffer and Permeabilization Buffer (eBioscience) to allow intracellular staining. The suspended kidney cells were then incubated with specific conjugated antibody cocktails in the dark for 30 minutes on ice. Negative controls included cells treated with irrelevant antibodies (isotype). Cells were also incubated with only one specific conjugated antibody. The antibodies used in this study were as follows: F4/80-Pacific blue (BioLegend, Catalog: 123124), CD86-APC (BioLegend, Catalog: 10512), CD206-Alexa 647 (Serotec, Catalog: MCA2235), CD4-FITC (eBioscience, Catalog: 11–0042-86), IFNγ-APC (eBioscience, Catalog: 17–7311-82), IL-4-PE (eBioscience, Catalog: 12–7041-82), IL-17a-PE (eBioscience, Catalog: 12–7177-81), CD25-PE (eBioscience, Catalog: 12–0251-83), and Foxp3-APC (eBioscience, Catalog: 12–0251-83). Flow cytometry analysis was performed using a FACS Calibar instrument and analyzed using the CellQuest Pro Analysis software (BD Biosciences, Franklin Lakes, New Jersey, USA).

4.10 Western blot analysis

Western blotting was performed as described previously (55, 57–59). Proteins from BMDMs and the kidney cortex were extracted with RIPA lysis buffer. After blocking nonspecific binding with 5% BSA, membranes were incubated overnight at 4 ° C with the primary antibodies against rabbit anti-iNOS (Abcam ab-15323), rabbit anti-iNOS (Abcam ab-178945), goat anti-CD74 (Santa Cruz, sc-5438), mouse anti-CD74 (Santa Cruz, sc-6267), goat anti-CD74 (Santa Cruz, sc-5438), rabbit anti-phosphorylated NF-kB p65 (Cell Signaling, #3031), rabbit anti-phosphorylated NF-kB p65 (Cell Signaling, #3033s), mouse anti-NF-kB p65 (Cell Signaling, #6965), rabbit anti-NF-kB p65 (Cell Signaling, # 8242S), rabbit anti-pp38 (Cell signaling, #9211), rabbit anti-pp38 (Cell signaling, # 4631L), rabbit anti-p38 (Cell signaling, #9212), rabbit anti-p38 (Cell signaling, # 8690S), mouse anti-ß-actin (Santa Cruz, sc-69879), mouse anti-GAPDH(proteintech, #60004–1-Ig).Then the membranes were incubated with IRDye800-conjugated secondary antibody (Rockland Immunchemicals). Signals were scanned using the Odyssey IR imaging system (LI-COR Biosciences). Image J software (National Institutes of Health) was used for quantitative analysis of images.

4.11 Statistical analysis

Statistical analysis was conducted using Prism 9.0 GraphPad Software (GraphPad Software, La Jolla, California, USA). Data obtained from the study were presented as the mean ± standard

error of the mean (SEM). Two-group comparisons were assessed using an independent sample t-test. Multiple group comparisons were performed using one-way analysis of variance (ANOVA) followed by Tukey's *post hoc* tests. A p-value less than 0.05 was considered statistically significant in this experiment.

5 Conclusions

Our study demonstrates that selective MIF depletion in macrophages ameliorates experimental anti-GBM cGN by promoting macrophage polarization from M1 towards M2, enhancing Treg while inhibiting Th1 and Th17 immune responses via CD74/NF-κB/p38 MAPK signaling. Thus, targeting macrophage-derived MIF could be a novel therapy for anti-GBM cGN.

Data availability statement

The raw data supporting the conclusions of this article will be made available by the authors, without undue reservation.

Ethics statement

The animal study was approved by The Chinese University of Hong Kong. The study was conducted in accordance with the local legislation and institutional requirements.

Author contributions

HY: Writing – original draft. JL: Writing – original draft. XH: Methodology, Writing – review & editing. RB: Methodology, Resources, Writing – review & editing. AX: Funding acquisition, Writing – review & editing. HL: Funding acquisition, Writing – review & editing.

Funding

The author(s) declare financial support was received for the research, authorship, and/or publication of this article. This research was funded by the Research Grants Council of Hong Kong (GRF 14104019, 14101121, and R4012-18); the High-Level Hospital Construction Project from Guangdong Provincial People's Hospital, Guangdong Academy of Medical Science (KJ012019108), the Guangdong-Hong Kong-Macao-Joint Labs Program (2019B121205005), the Lui Che Woo Institute of Innovative Medicine (CARE program), NIH 1R01-AR078334 (RB), Shenzhen Technology Project (JCYJ201908 09120801655, JCYJ20180307150634856), the National Natural Science Funds of China (81870481), the Guangdong Provincial Natural Science Foundation (2021A1515011625) and the Guangdong Provincial Natural Science Foundation (2022A1515012308).

Conflict of interest

The authors declare that the research was conducted in the absence of any commercial or financial relationships that could be construed as a potential conflict of interest.

Publisher's note

Supplementary material

The Supplementary Material for this article can be found online at: https://www.frontiersin.org/articles/10.3389/fimmu.2024.1361343/full#supplementary-material

References

1. Lan HY, Nikolic-Paterson DJ, Atkins RC. Involvement of activated periglomerular leukocytes in the rupture of Bowman's capsule and glomerular crescent progression in experimental glomerulonephritis. *Lab Invest*. (1992) 67:743–51.

2. McAdoo SP, Pusey CD. Anti-glomerular basement membrane disease. *Clin J Am Soc Nephrol*. (2017) 12:1162–72. doi: 10.2215/CJN.01380217

3. Shi Y, Jia XY, Gu QH, Wang M, Cui Z, Zhao MH. A modified peptide derived from goodpasture autoantigen arrested and attenuated kidney injuries in a rat model of anti-GBM glomerulonephritis. *J Am Soc Nephrol*. (2020) 31:40–53. doi: 10.1681/ASN.2019010067

4. Bolton WK, Innes DJ Jr, Sturgill BC, Kaiser DL. T-cells and macrophages in rapidly progressive glomerulonephritis: clinicopathologic correlations. *Kidney Int*. (1987) 32:869–76. doi: 10.1038/ki.1987.288

5. Tipping PG, Holdsworth SR. T cells in crescentic glomerulonephritis. *J Am Soc Nephrol*. (2006) 17:1253–63. doi: 10.1681/ASN.2005091013

6. Tang PM, Nikolic-Paterson DJ, Lan HY. Macrophages: versatile players in renal inflammation and fibrosis. *Nat Rev Nephrol*. (2019) 15:144–58. doi: 10.1038/s41581-019-0110-2

7. Fujinaka H, Yamamoto T, Takeya M, Feng L, Kawasaki K, Yaoita E, et al. Suppression of anti-glomerular basement membrane nephritis by administration of anti-monocyte chemoattractant protein-1 antibody in WKY rats. *J Am Soc Nephrol*. (1997) 8:1174–8. doi: 10.1681/ASN.V871174

8. Duffield JS, Tipping PG, Kipari T, Cailhier JF, Clay S, Lang R, et al. Conditional ablation of macrophages halts progression of crescentic glomerulonephritis. *Am J Pathol*. (2005) 167:1207–19. doi: 10.1016/S0002-9440(10)61209-6

9. Chalmers SA, Chitu V, Herlitz LC, Sahu R, Stanley ER, Putterman C. Macrophage depletion ameliorates nephritis induced by pathogenic antibodies. *J Autoimmun*. (2015) 57:42–52. doi: 10.1016/j.jaut.2014.11.007

10. Rogers NM, Ferenbach DA, Isenberg JS, Thomson AW, Hughes J. Dendritic cells and macrophages in the kidney: a spectrum of good and evil. *Nat Rev Nephrol*. (2014) 10:625–43. doi: 10.1038/nrneph.2014.170

11. Yang N, Isbel NM, Nikolic-Paterson DJ, Li Y, Ye R, Atkins RC, et al. Local macrophage proliferation in human glomerulonephritis. *Kidney Int*. (1998) 54:143–51. doi: 10.1046/j.1523-1755.1998.00978.x

12. Meng XM, Tang PM, Li J, Lan HY. Macrophage phenotype in kidney injury and repair. *Kidney Dis (Basel)*. (2015) 1:138–46. doi: 10.1159/000431214

13. Chen T, Cao Q, Wang Y, Harris DCH. M2 macrophages in kidney disease: biology, therapies, and perspectives. *Kidney Int*. (2019) 95:760–73. doi: 10.1016/j.kint.2018.10.041

14. Lee H, Fessler MB, Qu P, Heymann J, Kopp JB. Macrophage polarization in innate immune responses contributing to pathogenesis of chronic kidney disease. *BMC Nephrol*. (2020) 21:270. doi: 10.1186/s12882-020-01921-7

15. Lin SG, Yu XY, Chen YX, Huang XR, Metz C, Bucala R, et al. De novo expression of macrophage migration inhibitory factor in atherogenesis in rabbits. *Circ Res*. (2000) 87:1202–8. doi: 10.1161/01.RES.87.12.1202

16. Chen Z, Sakuma M, Zago AC, Zhang X, Shi C, Leng L, et al. Evidence for a role of macrophage migration inhibitory factor in vascular disease. *Arterioscler Thromb Vasc Biol*. (2004) 24:709–14. doi: 10.1161/01.ATV.0000119356.35748.9e

17. Hoi AY, Hickey MJ, Hall P, Yamana J, O'Sullivan KM, Santos LL, et al. Macrophage migration inhibitory factor deficiency attenuates macrophage recruitment, glomerulonephritis, and lethality in MRL/lpr mice. *J Immunol*. (2006) 177:5687–96. doi: 10.4049/jimmunol.177.8.5687

18. Lan HY, Yang N, Nikolic-Paterson DJ, Yu XQ, Mu W, Isbel NM, et al. Expression of macrophage migration inhibitory factor in human glomerulonephritis. *Kidney Int*. (2000) 57:499–509. doi: 10.1046/j.1523-1755.2000.t01-1-00869.x

19. Wang FF, Zhu LA, Zou YQ, Zheng H, Wilson A, Yang CD, et al. New insights into the role and mechanism of macrophage migration inhibitory factor in steroid-resistant patients with systemic lupus erythematosus. *Arthritis Res Ther*. (2012) 14:R103. doi: 10.1186/ar3828

20. Bilsborrow JB, Doherty E, Tilstam PV, Bucala R. Macrophage migration inhibitory factor (MIF) as a therapeutic target for rheumatoid arthritis and systemic lupus erythematosus. *Expert Opin Ther Targets*. (2019) 23:733–44. doi: 10.1080/14728222.2019.1656718

21. Kang I, Bucala R. The immunobiology of MIF: function, genetics and prospects for precision medicine. *Nat Rev Rheumatol*. (2019) 15:427–37. doi: 10.1038/s41584-019-0238-2

22. Djudjaj S, Lue H, Rong S, Papasotiriou M, Klinkhammer BM, Zok S, et al. Macrophage migration inhibitory factor mediates proliferative GN via CD74. *J Am Soc Nephrol*. (2016) 27:1650–64. doi: 10.1681/ASN.2015020149

23. Bernhagen J, Krohn R, Lue H, Gregory JL, Zernecke A, Koenen RR, et al. MIF is a noncognate ligand of CXC chemokine receptors in inflammatory and atherogenic cell recruitment. *Nat Med*. (2007) 13:587–96. doi: 10.1038/nm1567

24. Lehmann L, Novender U, Schroeder S, Pietsch T, von Spiegel T, Putensen C, et al. Plasma levels of macrophage migration inhibitory factor are elevated in patients with severe sepsis. *Intensive Care Med*. (2001) 27:1412–5. doi: 10.1007/s001340101022

25. Zernecke A, Bernhagen Jr., Weber C. Macrophage migration inhibitory factor in cardiovascular disease. *Circulation*. (2008) 117:1594–602. doi: 10.1161/CIRCULATIONAHA.107.729125

26. Averdunk LS, Goetzenich A, Bernhagen J, Bucala R, Stoppe C. The protective role of macrophage migration inhibitory factor (MIF) in acute kidney injury after cardiac surgery. *Circulation*. (2017) 136. doi: 10.26226/morressier.58f5b031d462b80296c9d416

27. Brown FG, Nikolic-Paterson DJ, Hill PA, Isbel NM, Dowling J, Metz CM, et al. Urine macrophage migration inhibitory factor reflects the severity of renal injury in human glomerulonephritis. *J Am Soc Nephrol*. (2002) 13 Suppl 1:S7–13. doi: 10.1681/ASN.V13suppl_1s7

28. Li JH, Tang Y, Lv J, Wang XH, Yang H, Tang PMK, et al. Macrophage migration inhibitory factor promotes renal injury induced by ischemic reperfusion. *J Cell Mol Med*. (2019) 23:3867–77. doi: 10.1111/jcmm.14234

29. Li J, Tang Y, Tang PMK, Lv J, Huang XR, Carlsson-Skwirut C, et al. Blocking macrophage migration inhibitory factor protects against cisplatin-induced acute kidney injury in mice. *Mol Ther*. (2018) 26:2523–32. doi: 10.1016/j.ymthe.2018.07.014

30. Bruchfeld A, Carrero JJ, Qureshi AR, Lindholm B, Barany P, Heimburger O, et al. Elevated serum macrophage migration inhibitory factor (MIF) concentrations in chronic kidney disease (CKD) are associated with markers of oxidative stress and endothelial activation. *Mol Med*. (2009) 15:70–5. doi: 10.2119/molmed.2008.00109

31. Rammos C, Hendgen-Cotta UB, Sobierajski J, Adamczyk S, Hetzel GR, Kleophas W, et al. Macrophage migration inhibitory factor is associated with vascular dysfunction in patients with end-stage renal disease. *Int J Cardiol*. (2013) 168:5249–56. doi: 10.1016/j.ijcard.2013.08.021

32. Watanabe T, Tomioka NH, Doshi M, Watanabe S, Tsuchiya M, Hosoyamada M. Macrophage migration inhibitory factor is a possible candidate for the induction of microalbuminuria in diabetic db/db mice. *Biol Pharm Bull*. (2013) 36:741–7. doi: 10.1248/bpb.b12-00741

33. Sanchez-Nino MD, Sanz AB, Ihalmo P, Lassila M, Holthofer H, Mezzano S, et al. The MIF receptor CD74 in diabetic podocyte injury. *J Am Soc Nephrol*. (2009) 20:353–62. doi: 10.1681/ASN.2008020194

34. Torres VE, Chapman AB, Devuyst O, Gansevoort RT, Grantham JJ, Higashihara E, et al. Tolvaptan in patients with autosomal dominant polycystic kidney disease. *N Engl J Med*. (2012) 367:2407–18. doi: 10.1056/NEJMoa1205511

35. Wendt M, Borjesson O, Avik A, Bratt J, Anderstam B, Qureshi AR, et al. Macrophage migration inhibitory factor (MIF) and thyroid hormone alterations in antineutrophil cytoplasmic antibody (ANCA)-associated vasculitis (AAV). *Mol Med*. (2013) 19:109–14. doi: 10.2119/molmed.2012.00352

36. Leung JC, Chan LY, Tsang AW, Liu EW, Lam MF, Tang SC, et al. Anti-macrophage migration inhibitory factor reduces transforming growth factor-beta 1 expression in experimental IgA nephropathy. *Nephrol Dial Transplant*. (2004) 19:1976–85. doi: 10.1093/ndt/gfh323

37. Yang N, Nikolic-Paterson DJ, Ng YY, Mu W, Metz C, Bacher M, et al. Reversal of established rat crescentic glomerulonephritis by blockade of macrophage migration inhibitory factor (MIF): potential role of MIF in regulating glucocorticoid production. *Mol Med*. (1998) 4:413–24. doi: 10.1007/BF03401748

38. Lan HY, Bacher M, Yang N, Mu W, Nikolic-Paterson DJ, Metz C, et al. The pathogenic role of macrophage migration inhibitory factor in immunologically induced kidney disease in the rat. *J Exp Med*. (1997) 185:1455–65. doi: 10.1084/jem.185.8.1455

39. Yang F, Chen J, Huang XR, Yiu WH, Yu X, Tang SCW, et al. Regulatory role and mechanisms of myeloid TLR4 in anti-GBM glomerulonephritis. *Cell Mol Life Sci*. (2021) 78:6721–34. doi: 10.1007/s00018-021-03936-1

40. Roger T, David J, Glauser MP, Calandra T. MIF regulates innate immune responses through modulation of Toll-like receptor 4. *Nature*. (2001) 414:920–4. doi: 10.1038/414920a

41. White DA, Su Y, Kanellakis P, Kiriazis H, Morand EF, Bucala R, et al. Differential roles of cardiac and leukocyte derived macrophage migration inhibitory factor in inflammatory responses and cardiac remodelling post myocardial infarction. *J Mol Cell Cardiol*. (2014) 69:32–42. doi: 10.1016/j.yjmcc.2014.01.015

42. Summers SA, Steinmetz OM, Li M, Kausman JY, Semple T, Edgtton KL, et al. Th1 and Th17 cells induce proliferative glomerulonephritis. *J Am Soc Nephrol*. (2009) 20:2518–24. doi: 10.1681/ASN.2009030337

43. Kitching AR, Holdsworth SR. The emergence of th17 cells as effectors of renal injury. *J Am Soc Nephrol*. (2011) 22:235–8. doi: 10.1681/ASN.2010050536

44. Yang C, Huang XR, Fung E, Liu HF, Lan HY. The regulatory T-cell transcription factor foxp3 protects against crescentic glomerulonephritis. *Sci Rep*. (2017) 7:1481. doi: 10.1038/s41598-017-01515-8

45. Paust HJ, Ostmann A, Erhardt A, Turner JE, Velden J, Mittrucker HW, et al. Regulatory T cells control the Th1 immune response in murine crescentic glomerulonephritis. *Kidney Int*. (2011) 80:154–64. doi: 10.1038/ki.2011.108

46. Paust H-J, Turner J-E, Riedel J-H, Disteldorf E, Peters A, Schmidt T, et al. Chemokines play a critical role in the cross-regulation of Th1 and Th17 immune responses in murine crescentic glomerulonephritis. *Kidney Int*. (2012) 82:72–83. doi: 10.1038/ki.2012.101

47. Nakamura A, Zeng F, Nakamura S, Reid KT, Gracey E, Lim M, et al. Macrophage migration inhibitory factor drives pathology in a mouse model of spondyloarthritis and is associated with human disease. *Sci Transl Med*. (2021) 13:eabg1210. doi: 10.1126/scitranslmed.abg1210

48. Leng L, Metz CN, Fang Y, Xu J, Donnelly S, Baugh J, et al. MIF signal transduction initiated by binding to CD74. *J Exp Med*. (2003) 197:1467–76. doi: 10.1084/jem.20030286

49. Tillmann S, Bernhagen J, Noels H. Arrest functions of the MIF ligand/receptor axes in atherogenesis. *Front Immunol*. (2013) 4:115. doi: 10.3389/fimmu.2013.00115

50. Schulze-Osthoff K, Ferrari D, Riehemann K, Wesselborg S. Regulation of NF-kappa B activation by MAP kinase cascades. *Immunobiology*. (1997) 198:35–49. doi: 10.1016/S0171-2985(97)80025-3

51. Tomita N, Morishita R, Lan HY, Yamamoto K, Hashizume M, Notake M, et al. *In vivo* administration of a nuclear transcription factor-kappaB decoy suppresses experimental crescentic glomerulonephritis. *J Am Soc Nephrol*. (2000) 11:1244–52. doi: 10.1681/ASN.V1171244

52. Murray PJ. Macrophage polarization. *Annu Rev Physiol*. (2017) 79:541–66. doi: 10.1146/annurev-physiol-022516-034339

53. Fingerle-Rowson G, Petrenko O, Metz CN, Forsthuber TG, Mitchell R, Huss R, et al. The p53-dependent effects of macrophage migration inhibitory factor revealed by gene targeting. *Proc Natl Acad Sci U.S.A*. (2003) 100:9354–9. doi: 10.1073/pnas.1533295100

54. Wang S, Meng XM, Ng YY, Ma FY, Zhou S, Zhang Y , et al. TGF-beta/Smad3 signalling regulates the transition of bone marrow-derived macrophages into myofibroblasts during tissue fibrosis. *Oncotarget*. (2016) 7:8809–22. doi: 10.18632/oncotarget.v7i8

55. Lv J, Huang Xiao R, Klug J, Fröhlich S, Lacher P, Xu A, et al. Ribosomal protein S19 is a novel therapeutic agent in inflammatory kidney disease. *Clin Sci*. (2013) 124:627–37. doi: 10.1042/CS20120526

56. Wang YY, Jiang H, Wang YC, Huang XR, Pan J, Yang C, et al. Deletion of Smad3 improves cardiac allograft rejection in mice. *Oncotarget*. (2015) 6:17016–30. doi: 10.18632/oncotarget.v6i19

57. Qin W, Chung AC, Huang XR, Meng XM, Hui DS, Yu CM, et al. TGF-β/Smad3 signaling promotes renal fibrosis by inhibiting miR-29. *J Am Soc Nephrol*. (2011) 22:1462–74. doi: 10.1681/ASN.2010121308

58. Lv LL, Tang PM-K, Li CJ, You YK, Li J, Huang X-R, et al. The pattern recognition receptor, Mincle, is essential for maintaining the M1 macrophage phenotype in acute renal inflammation. *Kidney Int*. (2017) 91:587–602. doi: 10.1016/j.kint.2016.10.020

59. Huang XR, Chung AC, Zhou L, Wang XJ, Lan HY. Latent TGF-beta1 protects against crescentic glomerulonephritis. *J Am Soc Nephrol*. (2008) 19:233–42. doi: 10.1681/ASN.2007040484

frontiers | Frontiers in Immunology

TYPE Original Research
PUBLISHED 24 May 2024
DOI 10.3389/fimmu.2024.1309447

OPEN ACCESS

EDITED BY
Xu-jie Zhou,
Peking University, China

REVIEWED BY
Feng Yu,
Peking University, China
Yiming Zhou,
Sun Yat-sen Memorial Hospital, China

*CORRESPONDENCE
Xiaoyan Huang
huangxiaoyan@pku.org.cn
Meiying Wang
wmy99wmy99@163.com
Zuhui Pu
zuhuipu@email.szu.edu.cn

†These authors have contributed equally to this work

RECEIVED 08 October 2023
ACCEPTED 30 April 2024
PUBLISHED 24 May 2024

CITATION
Mou L, Zhang F, Liu X, Lu Y, Yue M, Lai Y, Pu Z, Huang X and Wang M (2024) Integrative analysis of COL6A3 in lupus nephritis: insights from single-cell transcriptomics and proteomics. *Front. Immunol.* 15:1309447. doi: 10.3389/fimmu.2024.1309447

Integrative analysis of COL6A3 in lupus nephritis: insights from single-cell transcriptomics and proteomics

Lisha Mou[1,2†], Fan Zhang[3†], Xingjiao Liu[1], Ying Lu[2], Mengli Yue[1], Yupeng Lai[1], Zuhui Pu[4*], Xiaoyan Huang[3*] and Meiying Wang[1*]

[1]Department of Rheumatology and Immunology, Institute of Translational Medicine, The First Affiliated Hospital of Shenzhen University, Shenzhen Second People's Hospital, Shenzhen, China, [2]MetaLife Lab, Shenzhen Institute of Translational Medicine, Health Science Center, The First Affiliated Hospital of Shenzhen University, Shenzhen Second People's Hospital, Shenzhen, China, [3]Department of Nephrology, Beijing University Shenzhen Hospital, Shenzhen, China, [4]Imaging Department, The First Affiliated Hospital of Shenzhen University, Shenzhen Second People's Hospital, Shenzhen, China

Introduction: Lupus nephritis (LN), a severe complication of systemic lupus erythematosus (SLE), presents significant challenges in patient management and treatment outcomes. The identification of novel LN-related biomarkers and therapeutic targets is critical to enhancing treatment outcomes and prognosis for patients.

Methods: In this study, we analyzed single-cell expression data from LN (n=21) and healthy controls (n=3). A total of 143 differentially expressed genes were identified between the LN and control groups. Then, proteomics analysis of LN patients (n=9) and control (SLE patients without LN, n=11) revealed 55 differentially expressed genes among patients with LN and control group. We further utilizes protein-protein interaction network and functional enrichment analyses to elucidate the pivotal role of COL6A3 in key signaling pathways. Its diagnostic value is evaluate through its correlation with disease progression and renal function metrics, as well as Receiver Operating Characteristic Curve (ROC) analysis. Additionally, immunohistochemistry and qPCR experiments were performed to validate the expression of COL6A3 in LN.

Results: By comparison of single-cell and proteomics data, we discovered that COL6A3 is significantly upregulated, highlighting it as a critical biomarker of LN. Our findings emphasize the substantial involvement of COL6A3 in the pathogenesis of LN, particularly noting its expression in mesangial cells. Through comprehensive protein-protein interaction network and functional enrichment analyses, we uncovered the pivotal role of COL6A3 in key signaling pathways including integrin-mediated signaling pathways, collagen-activated signaling pathways, and ECM-receptor interaction, suggesting potential therapeutic targets. The diagnostic utility is confirmed by its correlation with disease progression and renal function metrics of the glomerular filtration rate. ROC analysis further validates the diagnostic value of COL6A3, with the area under the ROC values of 0.879 in the in-house cohort, and 0.802 and 0.915 in tubular and glomerular external cohort samples, respectively. Furthermore,

immunohistochemistry and qPCR experiments were consistent with those obtained from the single-cell RNA sequencing and proteomics studies.

Discussion: These results proved that COL6A3 is a promising biomarker and therapeutic target, advancing personalized medicine strategies for LN.

KEYWORDS

systemic lupus erythematosus, kidney disease, lupus nephritis, single-cell RNA sequencing, proteomics, COL6A3, biomarkers, diagnosis

Introduction

Lupus nephritis (LN) is as a common consequence of systemic lupus erythematosus (SLE), marked by significant mortality rates (1). Approximately 50% of SLE patients are at risk of developing LN in the future (2, 3). Current LN treatment primarily involves immunosuppressive therapy, typically employing cyclophosphamide or mycophenolate mofetil combined with glucocorticoids. However, these treatments come with a host of adverse effects, making treatment adherence challenging and leading to treatment failure and refractory LN (4, 5). Over 10% of individuals with LN develop into end-stage renal disease in ten years (6). Early diagnosis and intervention are vital for reducing end-stage renal disease risk and improving patient outcomes. The identification of novel LN-related biomarkers and therapeutic targets is critical to enhancing treatment outcomes and prognosis for patients.

Renal biopsy, the gold standard for LN diagnosis, can cause invasive damage, necessitating the exploration of non-invasive approaches. Given the systemic nature of SLE, with multiple organs affected and various positive autoantibodies present, gene expression analysis of peripheral blood cells has emerged as a valuable source of LN biomarkers due to the ease of acquisition. Developing reliable LN-related candidate biomarkers from peripheral blood may offer a less invasive and accessible method for diagnosis and monitoring disease progression.

Single-cell RNA sequencing (scRNA-seq) enables us to analyze gene expression profiling at the single-cell level, offering powerful insights into cellular heterogeneity and biological mechanisms (7, 8). ScRNA-seq is also a valuable method in studying autoimmune diseases, including LN, enabling a comprehensive characterization of the cellular landscape involved in immune inflammations (9). This technology can accurately measure gene expression within individual cells, facilitating the analysis of cell heterogeneity between disease and normal states (10).

This study used scRNA-seq and plasma proteomics to discover biomarkers and therapeutic targets in LN. We identified COL6A3 as a key biomarker in LN. By integrating non-invasive protein expression analysis of peripheral blood cells and implementing precision medicine approaches, early and effective intervention strategies can be devised to reduce the burden of LN and its potential progression to end-stage renal disease.

Methods

Data processing

ScRNA-seq data of lupus nephritis (LN) patients were obtained from PMID31110316 (11). Seurat was employed for filtering and subsequent clustering (12). The study analyzed renal and skin tissue from 21 patients with LN and 3 healthy controls. The control group consisted of individuals undergoing nephrectomy for kidney transplant donation, from whom biopsy samples of healthy skin and renal tissue were obtained. Cells with RNA feature counts and read count below 100 and 10000 respectly, were excluded as poor-quality cells. The t-distributed stochastic neighbor embedding (t-SNE) algorithm was applied for visualization (13), and batch effect correction was performed using the "RunHarmony" function (14). Cell subtypes were annotated according to cell markers from the original study (11). Differential expression analysis was performed using the Wilcoxon method to identify genes with significant expression differences (DEGs) between groups, setting adjusted *P*-values to 0.05.

Patient samples of LN for proteomics analysis

The blood samples of control (systemic lupus erythematosus (SLE) patients without LN) and LN patients were collected from Shenzhen Second People's Hospital. Enrollment criteria for LN patient inclusion criteria: (1) Persistent proteinuria: >0.5g/day, or > (+++), (2) Cylindruria: May include red blood cells, hemoglobin, granular casts, or mixed casts. Patients were recruited in October 2022. A total of 11 control and 9 LN patients were included. Blood samples were collected with the clinical information including gender, age, SLEDAI, and drug information details of participants are shown in Table 1. Participants gave written informed consent and the ethics approval number is 20220824001.

10.3389/fimmu.2024.1309447

TABLE 1 Baseline demographic and clinical characteristics of LN patients in proteomics analysis.

Clinical information	All (n=20)	SLE w/o LN (11)	LN (9)	t/Z/Fisher	*P* Value
Demographic					
Age, years	39 ± 13	34 ± 10	45 ± 13	-2.174	0.043
Female, no. (%)	20 (100.0)	11 (100.0)	9 (100.0)	NA	NA
SLEDAI Score	8 (3,16)	4 (2,8)	15 (8,19)	-2.886	0.004
BMI, kg/m^2	20.8 (18.2, 22.4)	19.8 (17.9, 21.6)	24.0 (18.4, 28.5)	-1.899	0.580
Disease duration, months	12.1 (1.0, 118.6)	36.5 (0.7, 121.7)	12.2 (1.0, 139.9)	-0.419	0.675
Clinical manifestations					
Musculoskeletal, no. (%)	6 (30.0)	1 (9.1)	5 (55.6)	NA	0.050
Serositis, no. (%)	2 (10.0)	1 (9.1)	1 (11.1)	NA	1.000
Skin rash, no. (%)	6 (30.0)	3 (27.3)	3 (33.3)	NA	1.000
Raynaud's phenomenon, no. (%)	1 (5.0)	1 (9.1)	0 (0)	NA	1.000
Laboratory assessment					
Anti-dsDNA positive, no. (%)	11 (55.0)	5 (45.5)	6 (66.7)	NA	0.406
Anti-Sm positive, no. (%)	8 (47.1)	2 (22.2)	6 (75.0)	NA	0.057
Anti-Ro positive, no. (%)	9 (50)	7 (70.0)	2 (25.0)	NA	0.153
Anti-La positive, no. (%)	3 (15.8)	2 (20.0)	1 (11.1)	NA	1.000
Anti-U1RNP positive, no. (%)	7 (41.2)	3 (33.3)	4 (50.0)	NA	0.637
Anti-β2GPI positive, no. (%)	2 (11.8)	1 (11.1)	1 (12.5)	NA	1.000
aCL positive, no. (%)	2 (11.1)	0(0)	2 (22.2)	NA	0.471
LAC positive, no. (%)	4 (40.0)	3 (50.0)	1 (25.0)	NA	1.000
Anti-CCP, U/mL	11.5 (1.6, 23.6)	11.5 (1.1, 33.4)	9.0 (2.2, 15.0)	-0.356	0.722
RF, IU/L	10.5 (2.1, 25.6)	15.0 (2.9, 41.2)	5.8 (1.4, 20.5)	-0.8	0.424
Leukocyte, 10^9/L	4.3 (2.7, 6.1)	4.1 (3.5, 6.5)	4.6 (1.9, 5.7)	-0.646	0.518
Lymphocyte, 10^9/L	1.1 (0.8, 1.6)	1.3 (0.7, 1.7)	1.1 (0.8, 1.3)	-0.532	0.595
Platelets, 10^9/L	164.5 (123.8, 221.5)	195.0 (151.0, 249.0)	156.0 (110.5, 170.5)	-1.709	0.870
ESR, mm/h	31.5 (13.8, 62.5)	28.0 (13.0, 48.0)	33.0 (14.0, 79.0)	-0.725	0.468
CRP, mg/L	3.0 (1.5, 4.2)	3.8 (1.9, 5.1)	2.2 (1.2, 3.7)	-1.244	0.214
eGFR (mL/min/1.73 m^2)	126.0 (107.8, 133.8)	131.4 (125.0, 139.8)	106.4 (85.4, 129.5)	-2.317	0.020
Urea, mmol/L	4.5 (3.1, 6.9)	3.6 (2.8, 4.9)	6.9 (4.5, 10.7)	-2.776	0.006
Uric acid, μmol/L	332.5 (261.4, 420.6)	309 (270.1, 371.4)	419.8 (235.7, 459.4)	-0.95	0.342
Cystatin C, mg/L	1.0 (0.8, 1.1)	0.8 (0.7, 1.0)	1.1 (1.0, 1.5)	-2.86	0.004
Retinol-binding protein, mg/L	40.1 (31.9, 45.8)	32.5 (22.2, 40.7)	46.2 (41.4, 56.5)	-2.889	0.004
Hematuria, no. (%)	8 (42.1)	1 (10.0)	7 (77.8)	NA	0.005
Proteinuria, no. (%)	11 (55.0)	2 (18.2)	9 (100.0)	NA	<0.001
Casts, no. (%)	1 (5.3)	0 (0)	1 (11.1)	NA	0.474
Pyuria, no. (%)	3 (15.8)	0 (0)	3 (33.3)	NA	0.087
Urine albumin (g/24h)	0.56 (0.06, 1.75)	0.06 (0.05, 0.1)	1.23 (0.66, 2.45)	-3.334	0.001
Complement C3, g/L	0.6 (0.3, 1.0)	0.8 (0.5, 1.1)	0.3 (0.1, 1.0)	-1.749	0.080

(Continued)

TABLE 1 Continued

Clinical information	All (n=20)	SLE w/o LN (11)	LN (9)	t/Z/Fisher	*P* Value
Complement C4, g/L	0.1 (0, 0.2)	0.1 (0.1, 0.2)	0.05 (0, 0.2)	-1.254	0.210
Medications					
Prednisolone, no. (%)	19 (95.0)	11 (100.0)	8 (88.9)	NA	0.450
Hydroxychloroquine, no. (%)	16 (80.0)	10 (90.9)	6 (66.7)	NA	0.285
Mycophenolate mofetil, no. (%)	5 (25.0)	2 (18.2)	3 (33.3)	NA	0.617

Descriptive statistics were employed for data presentation: normally distributed quantitative data were expressed as mean ± standard deviation, non-normally distributed quantitative data were presented as median (P25, P75), and binary categorical variables were represented as percentages. w/o, without.

Preparation of serum samples and LC-MS/MS analysis

Blood samples were obtained from both LN and control (SLE patients without LN) patients in the fasting state. Initially, cellular remnants were eliminated from the serum sample through centrifugation at 12,000 g for 10 minutes at 4°C. Subsequently, the resulting supernatant was carefully transferred to a fresh centrifuge tube. Employing the Pierce™ Top 14 Abundant Protein Depletion Spin Columns Kit, the top 14 high-abundance proteins were efficiently eliminated. Ultimately, the protein concentration was quantified using a BCA kit as per the manufacturer's stipulations. LC-MS/MS Analysis was performed by PTM BIO company. Differential expression analysis was performed using the Wilcoxon method to identify proteins with significant expression differences (DEPs) between groups, setting *P*-values to 0.05 and fold change value to >1.5.

Functional enrichment analysis of COL6A3

We performed GO functional annotation and KEGG pathway enrichment analyses on the set of proteins exhibiting differential expression among two groups in proteomics analysis: control (SLE patients without LN), and LN patients.

Protein-protein interaction network analyses of COL6A3

Potential protein interactions with COL6A3 were collected and integrated using the STRING database (https://string-db.org/). PPI network analysis was conducted with the relevant genes obtained. A confidence score greater than 0.7 was used as the threshold for significance. We then imported relevant data into Cytoscape (v3.8.2) for analysis and visualization. As hub genes, the top 10 nodes, ranked using MCC of cytoHubba, were identified from Cytoscape's cytoHubba plugins.

Validation, clinical correlation analysis, and diagnostic value analysis of COL6A3

We performed a validation of COL6A3 expression levels by an independent dataset from the Ju cohort (15). Additionally, we explored the correlation between COL6A3 expression and renal function, particularly focusing on the glomerular filtration rate, among patients with LN. To assess the diagnostic efficacy of COL6A3 in distinguishing LN patients, receiver operating characteristic curve analysis was utilized.

Immunohistochemistry

Renal samples from control individuals (patients with IgA nephropathy) and LN patients were collected from Beijing University Shenzhen Hospital and is approved by the Research Ethics Committee in Beijing University Shenzhen Hospital (approval number: [2021] No. (038-Extension 2)). Immunohistochemical staining was conducted on paraffin kidney sections using standard procedures. Briefly, kidney sections were blocked with 5% BSA in PBS and then incubated with primary antibodies (anti-Collagen VI alpha 1/2/3, 1:100, R381465, ZEN-Bio, China) for 2 hours at 37°C. After washing the sections with PBS, streptavidin-biotin complex (SA1050, SABC, BOSTER, Wuhan, China) was added and incubated for 30 minutes. Finally, the sections were washed with PBS, and color development was achieved using BCIP/NBT solution, followed by staining with nuclear fast red for 6 minutes. Images were acquired using an optical microscope (NM IL LED, Leica Microsystems, Wetzlar, Germany).

Real-time PCR analysis

Blood samples were obtained from both LN patients and healthy controls in the fasting state from Shenzhen Second People's Hospital. Total RNA from the blood was extracted using the SteadyPure Quick RNA Extraction Kit (AG21025, AG, Hunan, China). Total RNA was reverse transcribed into cDNA using a reverse transcription kit (RR036A, Takara, Japan). Real-time PCR was conducted using the SYBR Green mixture kit (QPK-201, TOYOBO, Japan), followed by Real-Time PCR performed on the QuantStudio™ 3 (Thermo Fisher SCIENTIFIC, USA). The primer sequences used are as follows:

GAPDH-F: 5'-AGATCCCTCCAAAATCAAGTGG-3';
GAPDH-R: 5'-GGCAGAGATGATGACCCTTTT-3';
COL6A3-F: 5'-CTGTTCCTCTTTGACGGCTCA-3';
COL6A3-R: 5'-CCTTGACATCATCGCTGTACTGA-3'.

Statistical analysis

All statistical analyses of single-cell and proteomics data were performed with R (Version 4.3.1). Results of the mRNA and protein expression of COL6A3 were analyzed by Prism (Version 9.4.0). $P < 0.05$ was regarded as statistically significant. The baseline demographic and clinical characteristics of LN patients in the proteomics analysis were analyzed using SPSS (Version 25.0). Descriptive statistics were employed for data presentation: normally distributed quantitative data were expressed as mean ± standard deviation, non-normally distributed quantitative data were presented as median (P25, P75), and binary categorical variables were represented as percentages. Group differences were assessed using various statistical tests, including t-tests, rank-sum tests, and Fisher's exact probability test. All hypothesis tests were two-tailed, and a *P*-value less than 0.05 was considered statistically significant.

Results

Single-cell analysis of lupus nephritis

The workflow of this study is shown in Figure 1. We first analyzed the single-cell RNA sequencing data from 21 LN patients and 3 healthy controls, leading to the identification of differentially expressed genes (DEGs). Subsequent proteomics analysis differentiated serum protein expression between control (non-LN SLE patients, n=11) and LN patients (n=9), identifying differentially expressed proteins (DEPs). Further, gene ontology and pathway analyses of DEPs were conducted. Comparative analysis of DEGs and DEPs highlighted COL6A3 as a candidate biomarker. The relationship between COL6A3 expression and renal function was examined, along with its diagnostic potential through receiver operating characteristic (ROC) curve analysis. Lastly, protein-protein interaction (PPI), functional enrichment, and gene set enrichment analyses of COL6A3 were performed, contributing to our understanding of its role in LN.

Initially, we accessed a single-cell dataset comprising 21 renal biopsies from LN patients and 3 from control participants without LN, alongside 18 skin biopsies from LN patients and 3 from control participants without LN. Following quality control, normalization, and preliminary dimensionality reduction, t-distributed stochastic neighbor embedding (t-SNE) algorithms were employed to segregate cellular clusters corresponding to both the LN and control cohorts, as illustrated in Figures 2A–F. Specifically, Figures 2A–C display both renal and skin samples, Figures 2D–F focus on renal samples.

In a consistent approach with the initial study, identical cell markers were utilized to identify six principal cell categories (Figures 2A, D). In renal samples, tubular cells emerged as the predominant cell type, whereas mesangial cells, leukocytes, endothelial cells, and fibroblasts were identified as minor cell types (Figure 2D). Visualization of both kidney and skin sample types via t-SNE is presented in Figure 2B. Figure 2E showed the kidney samples via t-SNE. Furthermore, t-SNE was also applied to visualize the scRNA-seq results for each patient (Figures 2C, F).

A total of 143 differentially expressed genes (DEGs) were identified between the LN and control groups, with 66 genes upregulated and 77 downregulated in LN (Figures 3A–D). The upregulated and downregulated genes across each cell type were illustrated in the heatmap (Figures 3C, D).

Proteomics analysis, gene ontology and pathway enrichment analyses

LC-MS/MS was used to identify the proteins in the serum of the patients grouped in control (SLE patients without LN, n=11), and LN patients (n=9). In total, 4,459 peptides were identified by the spectrogram analysis, 923 proteins were identified, and 800 of which were quantifiable. Demographic and clinical characteristics of 11 control and 9 patients diagnosed with LN were shown in Table 1. We identified 55 differentially expressed genes (DEPs) among patients with LN and the control group with $P < 0.05$ and fold change >1.5 (Figure 4A; Supplementary Figures 1A, B), of which 36 were upregulated and 19 were downregulated (Figure 4A; Supplementary Figures 1A, B).

GO enrichment analyses revealed that the main biological processes (BP) of DEPs between LN and control group were primarily related to mitotic nuclear division, sister chromatid segregation, and mitotic sister chromatid segregation, whereas the cellular components (CC) term, DEPs were mainly localized in collagen-containing extracellular matrix, platelet alpha granule, and platelet alpha granule lumen (Supplementary Figure 2). As for the molecular functions (MF) between LN and the control group, DEPs were primarily related to extracellular matrix structural constituent, microtubule binding, and chemokine activity (Supplementary Figure 2). Additionally, pathway enrichment analysis showed that DEPs between LN and the control group were primarily related to viral protein interaction with cytokine and cytokine receptor, ECM-receptor interaction, complement, and coagulation cascades (Supplementary Figure 2).

Comprehensive analysis and clinical significance of COL6A3 in LN

We conducted a comparative analysis between the 55 DEPs identified via proteomics analysis and the 143 DEGs discerned between LN and control samples through scRNA-seq analysis. Notably, COL6A3 was found to be upregulated in both the scRNA-seq and proteomics datasets, while there were no intersections found between the downregulated DEPs and DEGs (Figures 4B, C). To elucidate the distribution pattern of the central gene COL6A3, we measured its average expression levels within the scRNA-seq cohort. The analysis revealed that mesangial cells displayed the highest expression levels, underscoring their significance in LN pathology (Figure 4D). This evidence underscores the critical role of *COL6A3* in mesangial cells during LN progression by scRNA-seq analysis. The proteomics dataset also demonstrated the expression profile of COL6A3 (Figure 4E). Further analysis of the relationship between the protein

10.3389/fimmu.2024.1309447

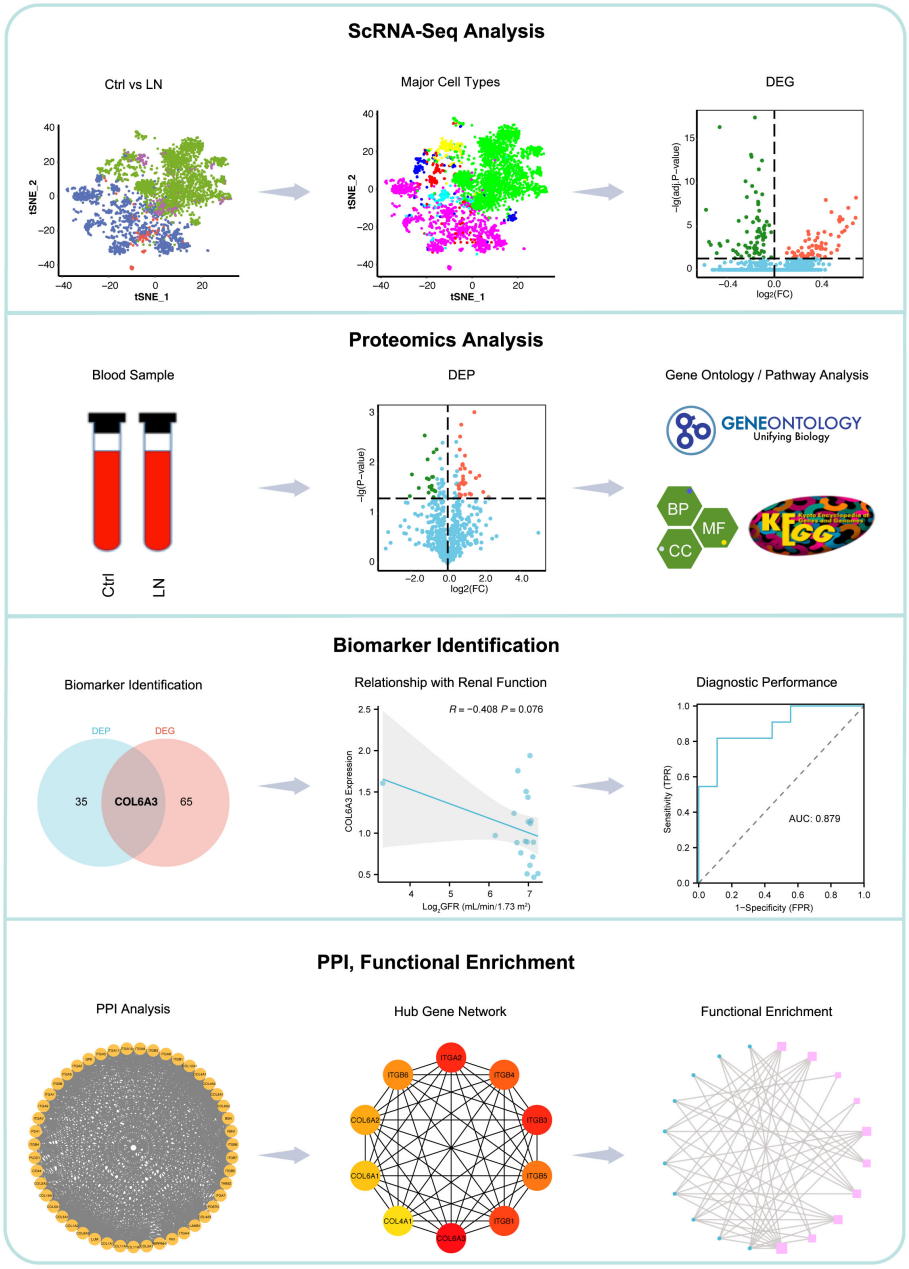

FIGURE 1
Workflow of this study. We began with single-cell RNA sequencing analysis of 21 lupus nephritis (LN) patients and 3 healthy controls to identify differentially expressed genes (DEGs). This was followed by proteomics analysis to distinguish serum protein expression between SLE patients without LN (n=11) and LN patients (n=9), identifying differentially expressed proteins (DEPs). Gene ontology and pathway analyses of DEPs were conducted. Comparative analysis of DEGs and DEPs leaded to the identification of COL6A3 as a potential biomarker. The association between COL6A3 expression and renal function was evaluated, alongside its diagnostic value using receiver operating characteristic (ROC) curve analysis. Lastly, analyses including protein-protein interaction (PPI), functional enrichment, and gene set enrichment for COL6A3 were performed to elucidate its role in LN.

expression of COL6A3 and renal function in our internal cohort revealed a negative correlation with the estimated glomerular filtration rate (GFR) (Figure 4F). Moreover, the area under the receiver operating characteristic curve (AUC) for COL6A3 was calculated, yielding a value of 0.879 within our internal cohort, indicating high diagnostic accuracy of COL6A3 in predicting LN (Figure 4G). We conducted qPCR experiments to validate the mRNA expression of COL6A3 (Figure 4H). The results were consistent with those obtained from the scRNA-seq and proteomics studies. Additionally, histological staining, including HE, PAS, MASSON, and PSAM, of LN and normal renal tissue revealed significant differences between LN and control patients (IgA nephropathy patients) (Figure 4I). Furthermore, immunohistochemistry showed a significant difference in COL6A3 expression in renal tissue between the normal and LN groups (Figure 4J).

10.3389/fimmu.2024.1309447

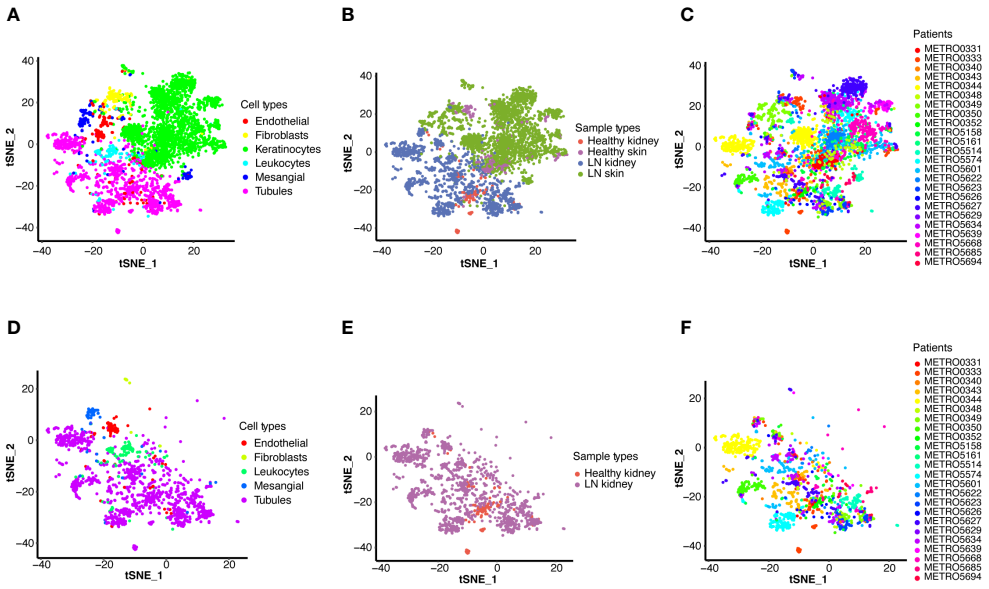

FIGURE 2
Single-cell RNA sequencing (scRNA-seq) analysis of LN. T-distributed stochastic neighbor embedding (t-SNE) plots display the major cell types in kidney and skin samples from LN patients and healthy controls **(A–C)**, and detailed cell type analysis within kidney **(D–F)**. **(A)** T-SNE analysis of the scRNA-seq data showing six major cell types in the kidney and skin samples. **(B)** T-SNE analysis of two groups, including the kidney and skin samples of healthy control and LN patients. **(C)** T-SNE analysis of the kidney and skin samples from each healthy control and LN patient. **(D)** T-SNE analysis of the scRNA-seq data showing five major cell types in the kidney samples (LN group: n=21, healthy group: n=3). **(E)** T-SNE analysis of two groups, including the kidney samples of healthy control and LN patients. **(F)** T-SNE analysis of the kidney samples from each healthy control and LN patient.

To further validate the link between *COL6A3* and clinical features, we utilized an external cohort from the Ju cohort (15). Here, the mRNA expression levels of *COL6A3* were significantly elevated in LN patients compared to healthy controls (Figures 5A, B), corroborating the negative correlation between *COL6A3* expression and estimated GFR (Figures 5C, D). Additionally, the ROC analysis demonstrated the high diagnostic capability of *COL6A3* (AUC=0.802 in tubular samples and AUC=0.915 in glomerular samples) (Figures 5E, F), aligning with our internal findings.

The PPI, functional enrichment, and gene set enrichment of COL6A3

A PPI network was then constructed based on 50 genes closely related to COL6A3 (Supplementary Figure 3A). In terms of hub genes, COL6A3 ranked first, followed by ITGA2, ITGB3, ITGB1, ITGB4, ITGB5, ITGB6, COL6A2, COL6A1, and COL4A1 (Supplementary Figure 3B). GO and KEGG enrichment analyses were performed on these genes. As a result of these results, these hub genes primarily play a role in integrin-mediated signaling pathway, collagen-activated signaling pathways, and ECM-receptor interaction (Supplementary Figure 3C).

Discussion

In exploring the complexities of lupus nephritis (LN), our study embraced an integrative methodology combining single-cell transcriptomics and plasma proteomics. We identified COL6A3 as a prominent biomarker, with a consistent upregulation observed across both methods. This concordance underscores the potential of COL6A3 in elucidating the molecular landscape of LN. Notably, the marked upregulation of COL6A3 in mesangial cells, as revealed through scRNA-seq, underscores its pivotal involvement in the disease's pathogenesis and opens potential avenues for targeted therapeutic interventions.

The advent of scRNA-seq technology has revolutionized our capacity to systematically examine cell heterogeneity and identify pathogenic cell populations, thereby enriching our understanding of autoimmune diseases' underlying mechanisms (9, 16, 17). In the context of LN, recent scRNA-seq endeavors have delineated the intricate immune cell networks (18, 19), underscoring the significance of cytokine expression profiles in mediating renal immune activity (20). This study leveraged high-throughput single-cell data to unearth biomarkers predictive of LN severity and treatment response, setting the stage for personalized therapeutic strategies.

COL6A3, encoding Collagen Type VI Alpha 3, functions primarily as a cell-binding protein, playing a pivotal role in the extracellular matrix's structural integrity and cellular interactions (21, 22). The observed inverse relationship between COL6A3 expression and estimated glomerular filtration rate (GFR) accentuates its utility in tracking disease progression. Furthermore, the diagnostic potential of COL6A3 affirmed through the area under the receiver operating characteristic curve analysis, advocates for its inclusion in non-invasive diagnostic modalities. External cohort validation, facilitated by the

10.3389/fimmu.2024.1309447

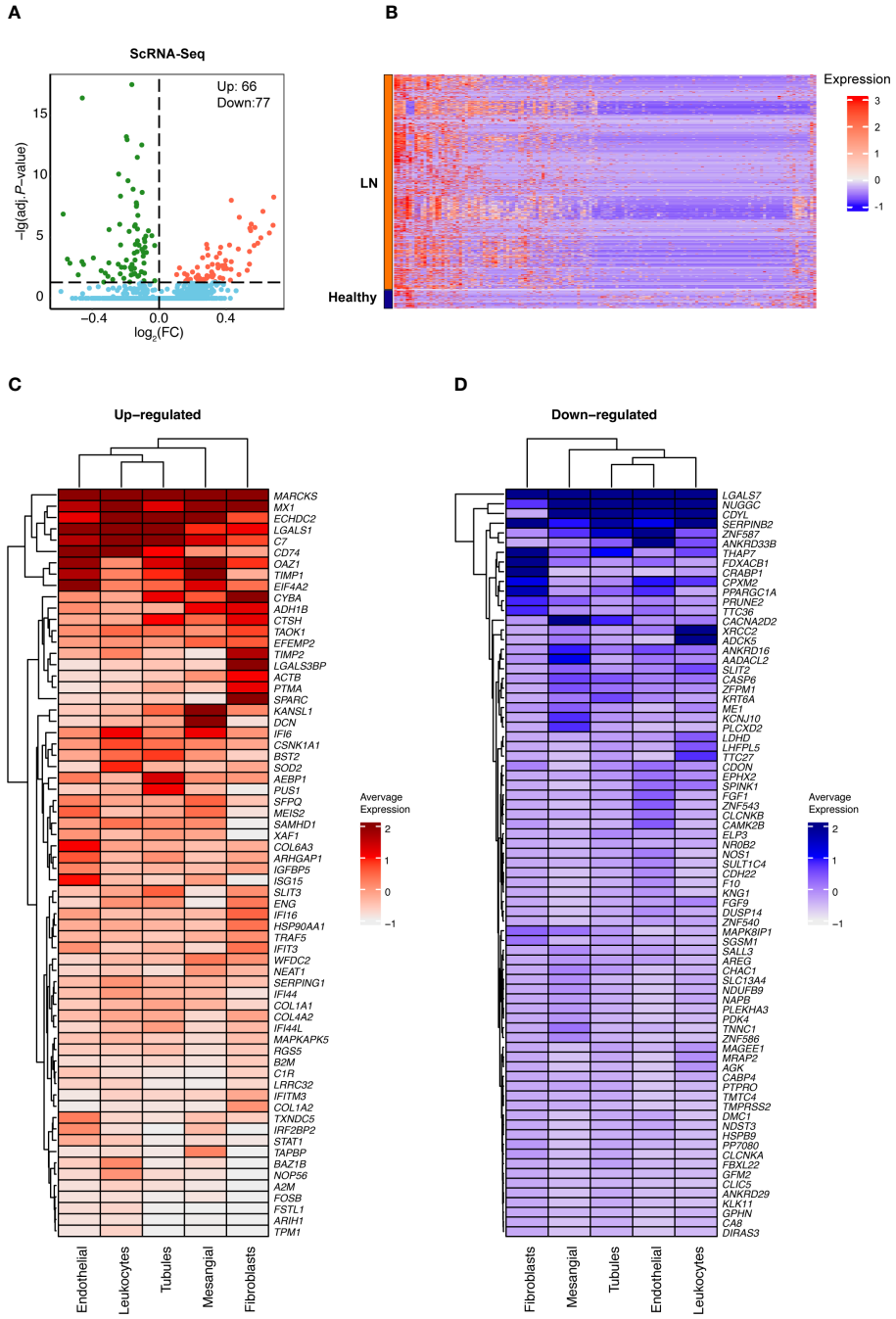

FIGURE 3
Identification of differentially expressed genes of renal scRNA-seq data in LN. **(A)** A volcano plot showed the upregulated and downregulated DEGs between LN and healthy controls. **(B)** A heatmap showed the upregulated and downregulated DEGs between LN and healthy controls. **(C)** A heatmap showed the upregulated and **(D)** downregulated DEGs between LN and healthy controls in five major cell types.

Ju cohort (15), not only reinforces COL6A3's diagnostic credibility but also exemplifies the merit of cross-cohorts analyses in biomarker substantiation.

Investigation into the protein-protein interaction (PPI) network and the functional enrichment of COL6A3 revealed its engagement in key signaling pathways, implicating integrins, collagen, and extracellular matrix (ECM) receptor interactions. These findings suggest therapeutic intervention targets, offering fresh perspectives for LN treatment strategies.

It's important to note that while COL6A3 expression was identified predominantly in mesangial cells via scRNA-seq analysis, its presence in the bloodstream, as shown in proteomics data, points towards its systemic impact, including potential roles beyond the mesangium. COL6A3's subcellular localization in the endoplasmic reticulum and vesicles, indicating a secretory pathway, suggests its ability to be secreted into the circulation, thus impacting LN pathogenesis beyond its site of predominant expression. This secretory nature allows COL6A3 to act both locally within the

10.3389/fimmu.2024.1309447

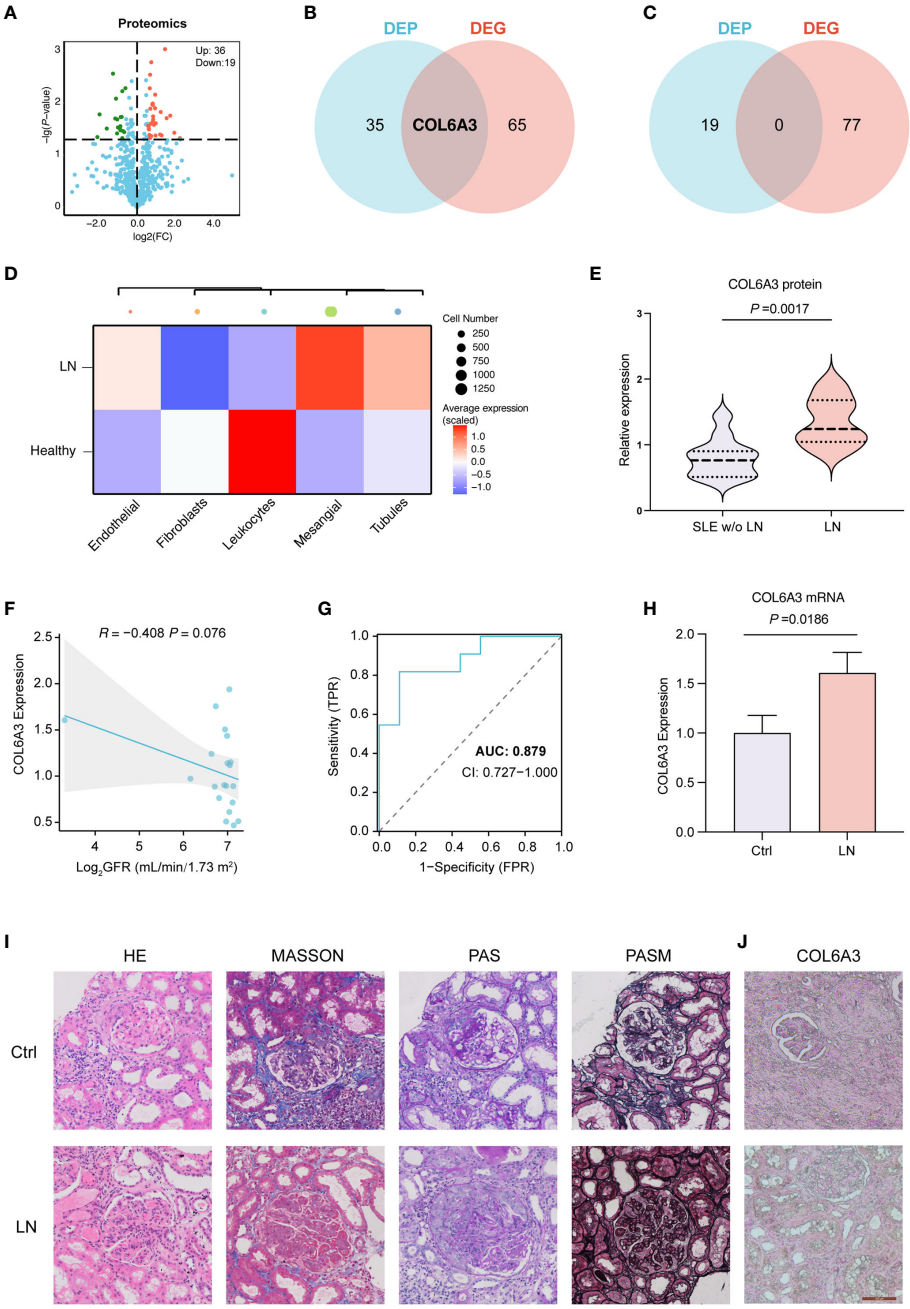

FIGURE 4
Proteomics analysis of LN. **(A)** Differentially expressed proteins (DEPs) in control (SLE without LN, n=11), and LN patients (n=9). **(B)** Venn diagrams showing the overlap of upregulated DEPs and DEGs, indicating shared and unique molecular features. **(C)** Venn diagrams showing non overlap of upregulated DEPs and DEGs. **(D)** The expression of COL6A3 in five major cell types of renal sample by scRNA-seq analysis. **(E)** The expression of COL6A3 in proteomics data. **(F)** The relationship between COL6A3 expression and estimated glomerular filtration rate (GFR) in our internal cohort. **(G)** The area under the receiver operating characteristic curve (AUC) for COL6A3 in our internal cohort. **(H)** The mRNA expression level of COL6A3 in LN (n=3) and control (healthy volunteers, n=3) examined by Real-time PCR analysis. **(I)** Hematoxylin and eosin (HE), periodic acid-Schiff (PAS), Masson's trichrome (MASSON), Picrosirius red (PSA), and periodic acid silver methenamine (PASM) staining of LN and control (IgA nephropathy) tissue. **(J)** Protein expression of COL6A3 in LN and control (IgA nephropathy, n=3) tissue analyzed by immunohistochemical staining.

kidney and systemically, which might explain its detection in blood samples and its involvement in the broader pathophysiological processes of LN.

The expression of COL6A3 and its association with immune cells, particularly M2 macrophages, has been documented in other immune-mediated diseases, indicating its broad role in immune regulation and tissue remodeling (23). Such associations have been noted in conditions like diabetic retinopathy (23) and diabetic nephropathy (24), suggesting the potential of COL6A3 as both a biomarker and therapeutic target across various diseases.

However, the profibrotic nature of COL6A3, as highlighted in its association with deteriorating kidney function in diabetic

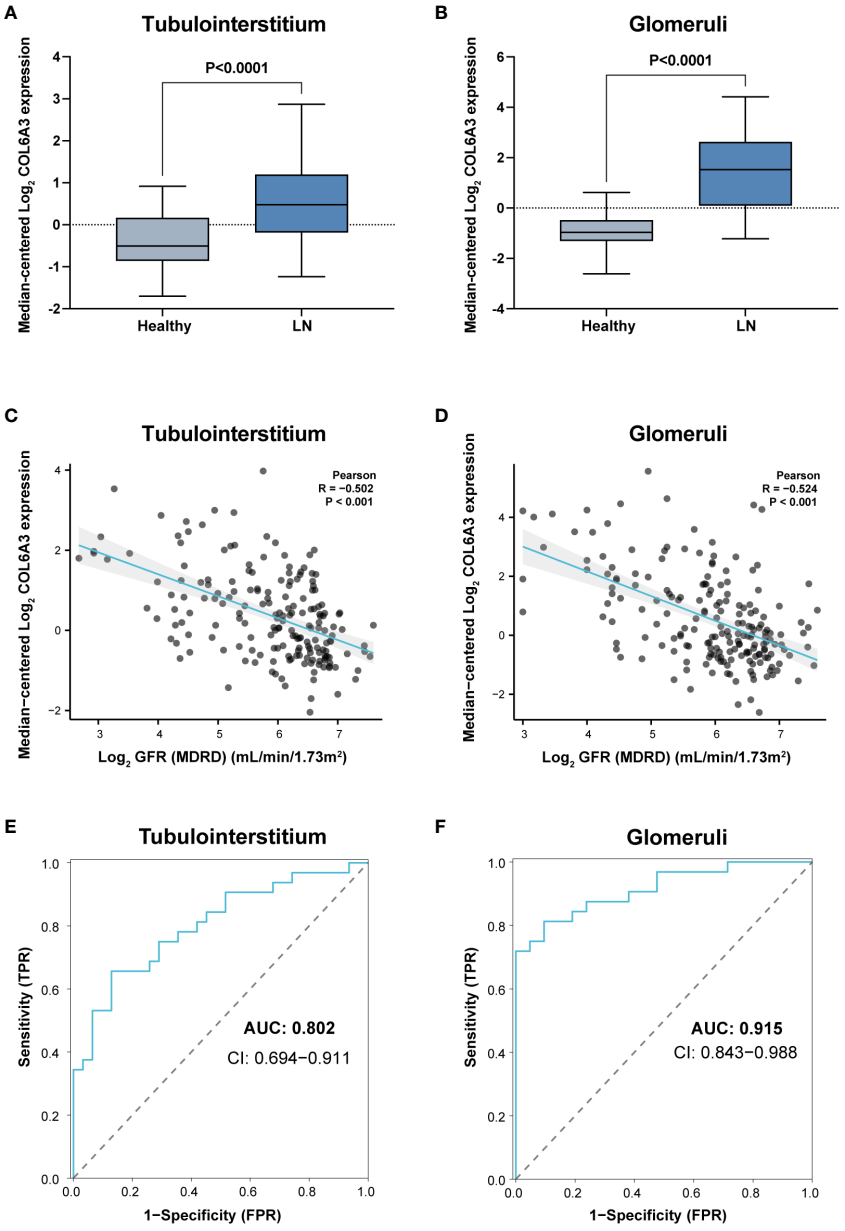

FIGURE 5
External validation of the clinical significance of COL6A3. Expression in tubulointerstitium **(A)** and glomeruli **(B)** from the Ju cohort (15) and its relationship with GFR **(C, D)**. **(E, F)** Diagnostic performance of AUC results in the Ju cohort.

nephropathy (25), aligns with its observed role in LN, suggesting a shared pathological pathway across kidney diseases. This underscores the rationale for exploring COL6A3 as a therapeutic target in a broader spectrum of kidney conditions. Moreover, the role of COL6A3 in metabolic processes, including inflammation, obesity, and insulin resistance (26, 27), extends its relevance beyond specific organ pathology, suggesting its potential involvement in the metabolic complications experienced by SLE patients.

Our findings, along with related literature, reinforce the significance of COL6A3 as a biomarker and therapeutic target in LN, prompting further research into its roles across various kidney diseases and immune regulation processes. Understanding the function of COL6A3 in the ECM, its influence on immune cell activity, and its contribution to fibrotic processes could inform the development of treatments targeting the intricate interplay of immune and fibrotic mechanisms in LN.

Nevertheless, the limitations of this study, including the reliance on available datasets and the complex pathophysiology of LN, necessitate further investigation into the role of COL6A3 in diverse and larger patient cohorts. Overcoming these challenges and translating biomarker discoveries into clinical practice will require the development of standardized assays and a deeper understanding of the biomarker's role in the multifactorial landscape of LN.

In conclusion, this study marks a significant contribution to LN research by pinpointing COL6A3 as a promising biomarker and therapeutic target, offering valuable insights into the molecular underpinnings of disease. Future research is imperative to validate these findings and investigate the clinical translational potential of COL6A3, with an aim towards enhancing diagnostics and therapeutic solutions for LN, ultimately improving patient care and outcomes.

Data availability statement

The datasets presented in this study can be found in online repositories. The names of the repository/repositories and accession number(s) can be found below: https://www.iprox.cn//page/project.html?id=IPX0006998000, IPX0006998000. The mass spectrometry proteomics data have been deposited to the ProteomeXchange Consortium (https://proteomecentral.proteomexchange.org) via the iProX partner repository (28, 29) with the dataset identifier PXD052168.

Ethics statement

The studies involving humans were approved by the Research Ethics Committee in Shenzhen Second People's Hospital and the Research Ethics Committee in Beijing University Shenzhen Hospital. The studies were conducted in accordance with the local legislation and institutional requirements. The participants provided their written informed consent to participate in this study.

Author contributions

LM: Formal analysis, Writing – original draft, Writing – review & editing. FZ: Data curation, Writing – review & editing, Writing – original draft. XL: Data curation, Writing – original draft. YLu: Formal analysis, Visualization, Writing – original draft. MY: Data curation, Writing – original draft. YLai: Data curation, Writing – original draft. ZP: Conceptualization, Project administration, Writing – review & editing. XH: Conceptualization, Data curation, Project administration, Writing – review & editing, Writing – original draft. MW: Conceptualization, Project administration, Writing – review & editing.

Funding

The author(s) declare financial support was received for the research, authorship, and/or publication of this article. This work was supported in part by the Shenzhen Science and Technology Program (No. JCYJ20190809095811254, No. JCYJ20200109140412476, No. GCZX2015043017281705), the Clinical Research Project in Shenzhen (20213357002 and 20213357028).

Conflict of interest

The authors declare that the research was conducted in the absence of any commercial or financial relationships that could be construed as a potential conflict of interest.

Publisher's note

All claims expressed in this article are solely those of the authors and do not necessarily represent those of their affiliated organizations, or those of the publisher, the editors and the reviewers. Any product that may be evaluated in this article, or claim that may be made by its manufacturer, is not guaranteed or endorsed by the publisher.

Supplementary material

The Supplementary Material for this article can be found online at: https://www.frontiersin.org/articles/10.3389/fimmu.2024.1309447/full#supplementary-material

SUPPLEMENTARY FIGURE 1
Differential protein expression between LN and controls. Heatmaps of upregulated **(A)** and downregulated **(B)** DEPs between LN and controls, providing a visual representation of protein expression differences.

SUPPLEMENTARY FIGURE 2
Gene Ontology (GO) and KEGG pathway enrichment. Analyzes of DEPs to elucidate the biological processes and pathways enriched in LN versus control groups.

SUPPLEMENTARY FIGURE 3
PPI network and functional enrichment of COL6A3. **(A)** The PPI network was constructed based on 50 genes closely related to COL6A3. **(B)** The top ten hub genes of PPI network. **(C)** Enrichment of GO and KEGG pathways for COL6A3 genes and genes associated with closed interactions.

References

1. Wang S, Wu M, Chiriboga L, Zeck B, Goilav B, Wang S, et al. Membrane attack complex (MAC) deposition in renal tubules is associated with interstitial fibrosis and tubular atrophy: a pilot study. *Lupus Sci Med.* (2022) 9:e000576. doi: 10.1136/lupus-2021–000576

2. Tanaka Y, O'Neill S, Li M, Tsai I-C, Yang Y-W. Systemic lupus erythematosus: targeted literature review of the epidemiology, current treatment, and disease burden in the asia pacific region. *Arthritis Care Res (Hoboken).* (2022) 74:187–98. doi: 10.1002/acr.24431

3. Zhang Y, Gan L, Tang J, Liu D, Chen G, Xu B. Metabolic profiling reveals new serum signatures to discriminate lupus nephritis from systemic lupus erythematosus. *Front Immunol.* (2022) 13:967371. doi: 10.3389/fimmu.2022.967371

4. Fanouriakis A, Kostopoulou M, Cheema K, Anders H-J, Aringer M, Bajema I, et al. 2019 Update of the Joint European League Against Rheumatism and European Renal Association-European Dialysis and Transplant Association (EULAR/ERA-EDTA) recommendations for the management of lupus nephritis. *Ann Rheum Dis.* (2020) 79:713–23. doi: 10.1136/annrheumdis-2020–216924

5. Rovin BH, Adler SG, Barratt J, Bridoux F, Burdge KA, Chan TM, et al. Executive summary of the KDIGO 2021 guideline for the management of glomerular diseases. *Kidney Int*. (2021) 100:753–79. doi: 10.1016/j.kint.2021.05.015

6. Hoover PJ, Costenbader KH. Insights into the epidemiology and management of lupus nephritis from the US rheumatologist's perspective. *Kidney Int*. (2016) 90:487–92. doi: 10.1016/j.kint.2016.03.042

7. Hwang B, Lee JH, Bang D. Single-cell RNA sequencing technologies and bioinformatics pipelines. *Exp Mol Med*. (2018) 50:1–14. doi: 10.1038/s12276–018-0071–8

8. Chen G, Ning B, Shi T. Single-cell rna-seq technologies and related computational data analysis. *Front Genet*. (2019) 10:317. doi: 10.3389/fgene.2019.00317

9. Zeng L, Yang K, Zhang T, Zhu X, Hao W, Chen H, et al. Research progress of single-cell transcriptome sequencing in autoimmune diseases and autoinflammatory disease: A review. *J Autoimmun*. (2022) 133:102919. doi: 10.1016/j.jaut.2022.102919

10. Papalexi E, Satija R. Single-cell RNA sequencing to explore immune cell heterogeneity. *Nat Rev Immunol*. (2018) 18:35–45. doi: 10.1038/nri.2017.76

11. Der E, Suryawanshi H, Morozov P, Kustagi M, Goilav B, Ranabothu S, et al. Tubular cell and keratinocyte single-cell transcriptomics applied to lupus nephritis reveal type I IFN and fibrosis relevant pathways. *Nat Immunol*. (2019) 20:915–27. doi: 10.1038/s41590–019-0386–1

12. Hao Y, Hao S, Andersen-Nissen E, Mauck WM, Zheng S, Butler A, et al. Integrated analysis of multimodal single-cell data. *Cell*. (2021) 184:3573–87.e29. doi: 10.1016/j.cell.2021.04.048

13. Laurens van der M, Hinton G. Visualizing Data using t-SNE. *Mach Learn Res*. (2008) 9:2579–605.

14. Korsunsky I, Millard N, Fan J, Slowikowski K, Zhang F, Wei K, et al. Fast, sensitive and accurate integration of single-cell data with Harmony. *Nat Methods*. (2019) 16:1289–96. doi: 10.1038/s41592–019-0619–0

15. Ju W, Greene CS, Eichinger F, Nair V, Hodgin JB, Bitzer M, et al. Defining cell-type specificity at the transcriptional level in human disease. *Genome Res*. (2013) 23:1862–73. doi: 10.1101/gr.155697.113

16. Stubbington MJT, Rozenblatt-Rosen O, Regev A, Teichmann SA. Single-cell transcriptomics to explore the immune system in health and disease. *Science*. (2017) 358:58–63. doi: 10.1126/science.aan6828

17. Efremova M, Vento-Tormo R, Park J-E, Teichmann SA, James KR. Immunology in the era of single-cell technologies. *Annu Rev Immunol*. (2020) 38:727–57. doi: 10.1146/annurev-immunol-090419–020340

18. Arazi A, Rao DA, Berthier CC, Davidson A, Liu Y, Hoover PJ, et al. The immune cell landscape in kidneys of patients with lupus nephritis. *Nat Immunol*. (2019) 20:902–14. doi: 10.1038/s41590–019-0398-x

19. Der E, Ranabothu S, Suryawanshi H, Akat KM, Clancy R, Morozov P, et al. Single cell RNA sequencing to dissect the molecular heterogeneity in lupus nephritis. *JCI Insight*. (2017) 2:e93009. doi: 10.1172/jci.insight.93009

20. Fava A, Rao DA, Mohan C, Zhang T, Rosenberg A, Fenaroli P, et al. Urine proteomics and renal single cell transcriptomics implicate IL-16 in lupus nephritis. *Arthritis Rheumatol*. (2022) 74:829–39. doi: 10.1002/art.42023

21. Di Martino A, Cescon M, D'Agostino C, Schilardi F, Sabatelli P, Merlini L, et al. Collagen VI in the musculoskeletal system. *Int J Mol Sci*. (2023) 24:5095. doi: 10.3390/ijms24065095

22. Karsdal MA, Nielsen SH, Leeming DJ, Langholm LL, Nielsen MJ, Manon-Jensen T, et al. The good and the bad collagens of fibrosis - Their role in signaling and organ function. *Adv Drug Deliv Rev*. (2017) 121:43–56. doi: 10.1016/j.addr.2017.07.014

23. Meng Z, Chen Y, Wu W, Yan B, Meng Y, Liang Y, et al. Exploring the immune infiltration landscape and M2 macrophage-related biomarkers of proliferative diabetic retinopathy. *Front Endocrinol (Lausanne)*. (2022) 13:841813. doi: 10.3389/fendo.2022.841813

24. Xu D, Jiang C, Xiao Y, Ding H. Identification and validation of disulfidptosis-related gene signatures and their subtype in diabetic nephropathy. *Front Genet*. (2023) 14:1287613. doi: 10.3389/fgene.2023.1287613

25. Chen J, Luo S-F, Yuan X, Wang M, Yu H-J, Zhang Z, et al. Diabetic kidney disease-predisposing proinflammatory and profibrotic genes identified by weighted gene co-expression network analysis (WGCNA). *J Cell Biochem*. (2022) 123:481–92. doi: 10.1002/jcb.30195

26. Pasarica M, Gowronska-Kozak B, Burk D, Remedios I, Hymel D, Gimble J, et al. Adipose tissue collagen VI in obesity. *J Clin Endocrinol Metab*. (2009) 94:5155–62. doi: 10.1210/jc.2009–0947

27. Gesta S, Guntur K, Majumdar ID, Akella S, Vishnudas VK, Sarangarajan R, et al. Reduced expression of collagen VI alpha 3 (COL6A3) confers resistance to inflammation-induced MCP1 expression in adipocytes. *Obes (Silver Spring)*. (2016) 24:1695–703. doi: 10.1002/oby.21565

28. Ma J, Chen T, Wu S, Yang C, Bai M, Shu K. iProX: an integrated proteome resource. *Nucleic Acids Res*. (2019) 47(D1):D1211–D1217.

29. Chen T, Ma J, Liu Y, Chen Z, Xiao N, Lu Y. iProX in 2021: connecting proteomics data sharing with big data. *Nucleic Acids Res*. (2021) 50(D1):D1522–D1527.

frontiers | Frontiers in Immunology

TYPE Original Research
PUBLISHED 06 June 2024
DOI 10.3389/fimmu.2024.1334151

OPEN ACCESS

EDITED BY
Xu-jie Zhou,
Peking University, China

REVIEWED BY
Richard Benjamin Pouw,
Sanquin Research, Netherlands
Marcin Okrój,
Intercollegiate Faculty of Biotechnology of University of Gdańsk and Medical University of Gdańsk, Poland
Kevin James Marchbank,
Newcastle University, Newcastle upon Tyne, United Kingdom

*CORRESPONDENCE
Filippo Mori
F.mori@kedrion.com

RECEIVED 06 November 2023
ACCEPTED 24 May 2024
PUBLISHED 06 June 2024

CITATION
Mori F, Pascali G, Berra S, Lazzarotti A, Panetta D, Rocchiccioli S, Ceccherini E, Norelli F, Morlando A, Donadelli R, Clivio A, Farina C, Noris M, Salvadori PA and Remuzzi G (2024) Proof of concept of a new plasma complement Factor H from waste plasma fraction.
Front. Immunol. 15:1334151.
doi: 10.3389/fimmu.2024.1334151

Proof of concept of a new plasma complement Factor H from waste plasma fraction

Filippo Mori[1]*, Giancarlo Pascali[2,3], Silvia Berra[4], Alessandra Lazzarotti[1], Daniele Panetta[5], Silvia Rocchiccioli[5], Elisa Ceccherini[5], Francesco Norelli[5], Antonio Morlando[5], Roberta Donadelli[6], Alberto Clivio[4], Claudio Farina[1], Marina Noris[6], Piero A. Salvadori[5] and Giuseppe Remuzzi[6]

[1]Research and Innovation, Kedrion Biopharma, Lucca, Italy, [2]Biosciences, Australian Nuclear Science and Technology Organisation, Lucas Heights, NSW, Australia, [3]School of Chemistry, University of New South Wales, Kensington, NSW, Australia, [4]Department of Biomedical and Clinical Sciences (DIBIC), University of Milan, Milan, Italy, [5]Istituto di Fisiologia Clinica, Consiglio Nazionale delle Ricerche, Pisa, Italy, [6]Istituto di Ricerche Farmacologiche Mario Negri IRCCS, Bergamo, Italy

Introduction: Complement factor H (FH) is a major regulator of the complement alternative pathway, its mutations predispose to an uncontrolled activation in the kidney and on blood cells and to secondary C3 deficiency. Plasma exchange has been used to correct for FH deficiency and although the therapeutic potential of purified FH has been suggested by *in vivo* experiments in animal models, a clinical approved FH concentrate is not yet available. We aimed to develop a purification process of FH from a waste fraction rather than whole plasma allowing a more efficient and ethical use of blood and plasma donations.

Methods: Waste fractions from industrial plasma fractionation (pooled human plasma) were analyzed for FH content by ELISA. FH was purified from unused fraction III and its decay acceleration, cofactor, and C3 binding capacity were characterized *in vitro.* Biodistribution was assessed by high-resolution dynamic PET imaging. Finally, the efficacy of the purified FH preparation was tested in the mouse model of C3 glomerulopathy (Cfh–/– mice).

Results: Our purification method resulted in a high yield of highly purified (92,07%), pathogen-safe FH. FH concentrate is intact and fully functional as demonstrated by *in vitro* functional assays. The biodistribution revealed lower renal and liver clearance of human FH in Cfh-/- mice than in wt mice. Treatment of Cfh-/- mice documented its efficacy in limiting C3 activation and promoting the clearance of C3 glomerular deposits.

Conclusion: We developed an efficient and economical system for purifying intact and functional FH, starting from waste material of industrial plasma fractionation. The FH concentrate could therefore constitute possible

10.3389/fimmu.2024.1334151

treatments options of patients with C3 glomerulopathy, particularly for those with FH deficiency, but also for patients with other diseases associated with alternative pathway activation.

KEYWORDS

concentrated complement factor H (FH), plasma purification, high-resolution dynamic PET, C3 glomerulopathy, membrano proliferative glomerulonephritis (MPGN)

Introduction

Complement factor H (FH) is a 155-kDa soluble glycoprotein produced in the liver and secreted into the circulation at concentrations of 250–600 µg / ml (1). It is a single polypeptide chain with a beads-in-a-string-like structure composed of 20 homologous domains named short consensus repeat (SCR) or complement control protein (CCP) domains (2). It regulates the alternative pathway (AP) of the complement system in the fluid phase as well as on cell surfaces preventing uncontrolled C3 activation and host tissue damage. Specifically, FH accelerates the dissociation of the C3 convertase (C3bBb) and C5 convertase (C3bBbC3b) (decay-accelerating activity), acts as a cofactor to factor I in the inactivation of C3b into iC3b (cofactor activity) and competes with FB in binding to C3b to prevent convertase formation. Through its C-terminal domains SCR19–20, FH binds cell surface glycosaminoglycans and C3b, thus exerting decay-accelerating activity and cofactor activity on host cell surfaces. A splice variant product of CFH gene, FHL-1, carries the first seven SCRs of FH and has complement regulatory activity in fluid phase and on the matrix of certain tissues, but it lacks the C-terminal recognition domains and is not capable to bind sialic acids on cell surfaces (3).

Genetic and acquired abnormalities causing FH deficiency or defective activity lead to an uncontrolled alternative pathway activation in the kidney and on blood cells and to secondary C3 deficiency (4). Such abnormalities are associated with different human pathologies which include kidney diseases like the atypical form of the hemolytic uremic syndrome (aHUS) (5), the membrano proliferative glomerulonephritis (MPGN) (6), and the C3 glomerulopathy, and the most common eye disease in adults, age-related macular degeneration (AMD) (7).

Before the introduction of complement-inhibitory drugs, plasma supplementation or plasma exchange was the only available treatment for FH defects, particularly in patients with aHUS and in a few cases with MPGN. With such a therapy, deficient complement regulators are supplemented (8). Plasma exchange therapy in addition removes mutant complement factors and/or autoantibodies directed against complement factors. However, the efficiency of plasma therapy in aHUS depends on the underlying genetic defect (9) and prospective clinical studies are lacking. Data on outcomes with plasma therapy in MPGN and C3G are scanty and limited to case reports (10). In addition, plasma therapy has several limitations. Some patients develop anaphylactic reactions to fresh frozen plasma, which may require cessation of any form of plasma therapy (11).

Plasma perfusions are repeated at regular intervals from twice a week to twice a month, each perfusion lasting 2–3 hours. This treatment is therefore long and recurrent for the patient. The amounts of transfused frozen fresh plasma are significant, which increases the standard risks of frozen fresh plasma perfusion.

The therapeutic potential of purified human FH for MPGN/C3G has been demonstrated with success by *in vivo* treatment in experimental mouse models of FH deficiency. Complement activity was regulated in this C3G model by different FH constructs, including the FH1–5 domains linked to either non-targeting mouse IgG or to anti-mouse properdin antibody (12) and homodimeric mini-FH constructs (13). Treatment with human complement factor H rapidly reverses renal complement deposition in factor H-deficient mice (12). Other recent studies have tested purified human FH for use in a mouse model of bacterial meningitis (13), or are exploring the production of recombinant FH for therapeutic use (14).

Therefore, for targeted treatment for diseases requiring FH, it would be desirable for a concentrate to be available; this would facilitate rapid attainment of therapeutic plasma levels with a low protein load. At present, there is no approved FH concentrate available for clinical use. Several groups developed methods to obtain a purified concentrated FH sample from human, rat, or mouse plasma mainly for research purposes (15–18). Another group used the Cohn fractionation method (19) to purify FH from a non-identified fraction of pooled plasma (20), pointing out the necessity to develop a scalable production procedure to obtain a high pure and pathogen-safe FH concentrate. This method is based on the alteration of protein solubility by modifying pH levels, temperatures, and ethanol concentrations. The process separates plasma proteins into five major fractions (Figure 1A):

1. Fraction I: Contains as much fibrinogen as possible.
2. Fraction II: Primarily consists of γ-globulins.
3. Fraction III: Composed of lipid-globulins.
4. Fraction IV: Contains α-globulins.
5. Fraction V: Comprises albumins.

10.3389/fimmu.2024.1334151

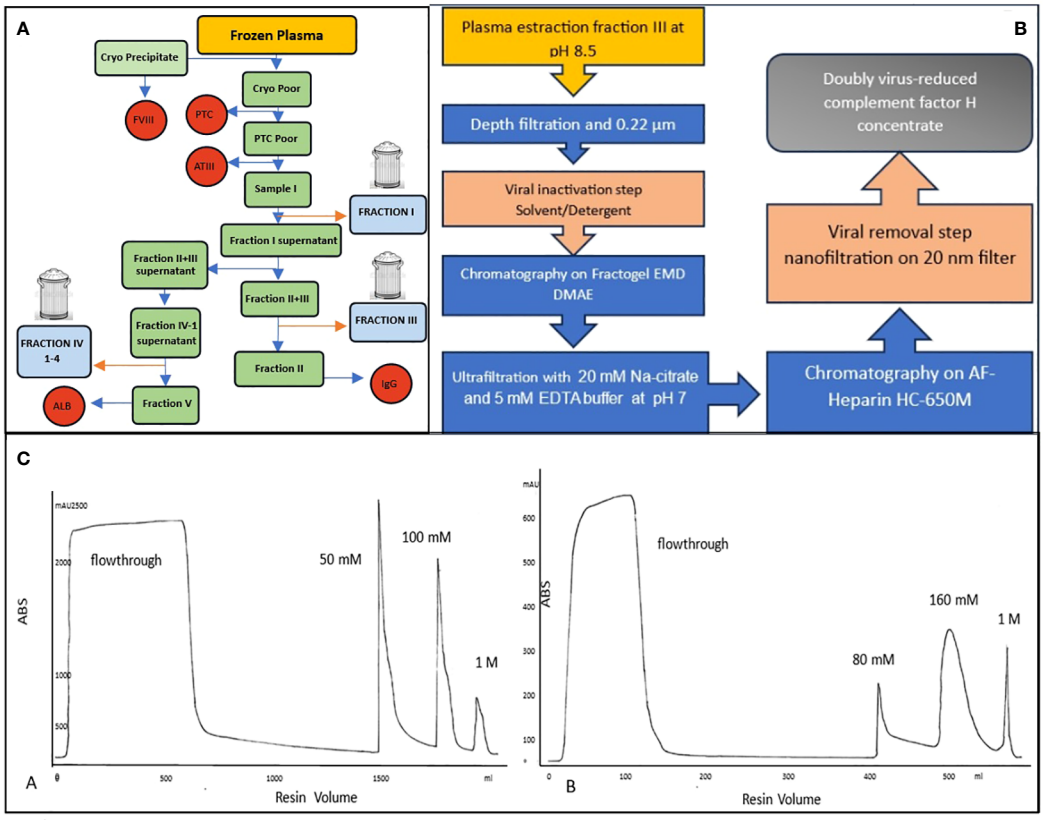

FIGURE 1
(A) Typical Cohn fractionation with 3 waste fractionations: fraction I, fraction III and fraction IV. **(B)** Flow chart of a new purification of human plasma FH, **(C)** Two chromatographic runs: Anionic exchange A=Fractogel EMD DMAE, the most of contaminants are removed in the flowthrough while FH is eluted at 50 mM NaCl. Affinity resin B=AF-Heparin HC 650M was used to further purify FH which elutes at 160mM NaCl after removing the rest of the contaminants in a washing step with 50 mM NaCl.

The plasma involved in this procedure is typically derived from human blood donations. This blood is collected from numerous donors, and the desired plasma proteins are extracted from these plasma pools through a process known as fractionation. This method has been instrumental in isolating specific proteins for various applications, particularly during wartime, when the demand for certain plasma proteins was very high. It's a testament to the innovative approaches in protein separation techniques. The Cohn method is still widely used in the industry for the purification of plasma derivatives. However, some fractions are not utilized and are discarded, including Fraction I, Fraction III, and Fraction IV (1–4). Human plasma is a precious resource and represents a very significant proportion of the cost of a plasma-derived product. Production of a new plasma therapy may limit the availability of plasma to afford existing products. The high cost of goods together with the small patient populations can make plasma therapies for rare diseases very expensive, and uneconomic.

This study aimed to identify and purify FH from a waste plasma fraction rather than from whole plasma, allowing more efficient and ethical use of blood and plasma donations. The integrity and function of FH were monitored during all the production steps by *in vitro* assay to evaluate the best purification strategy. Finally, the activity of purified FH was characterized both *in vitro* and *in vivo* in an animal model of C3G to provide the proof of concept that the new purification approach provides a fully active protein.

Materials and methods

Materials

FH antigen determination was conducted by commercial ELISA kit (HK342; Hycult Biotechnology Inc., Uden, The Netherlands). Protein concentration was determined by the Bradford Assay using a Coomassie reagent (Blue Stain Reagent, 24592; Pierce, Rockford, IL, USA). Ultradiafiltration (UDF) was performed on membranes with a 100-kDa exclusion limit (Pellicon Mini – Biomax Hydrophilic Polyethersulfone Membrane A Screen; Millipore, Billerica, MA, USA). Complement proteins, control FH, Factor I (FI), Factor B (FB), Factor D (FD) and C3b were from Merck (Merck Millipore, Billerica, MA, USA). The antibody we used for C3 staining is a polyclonal goat IgG fraction to mouse complement C3 that was obtained by immunization with the whole mouse C3. The IgG fraction is prepared from the specific goat antiserum. Thus, the antibody is expected to recognize both inactive C3 and activated C3 fragments. Chemicals were purchased from Merck and used without further purification unless stated otherwise. As far as radiolabeling of FH for subsequent *in vivo* biodistribution study is concerned, ^{18}F-fluoride was obtained from a PETrace 860 cyclotron (GE Healthcare, Uppsala, Sweden) irradiating ^{18}O-enriched water in silver body target. Radio-TLC was run on silica gel plates (S60-F254, Merck) and

radioactive spots were detected using Cyclone Plus phosphor reader (Perkin Elmer). HPLC was used to assess the purity of precursors and intermediate chemicals (Waters 1100 HPLC interfaced to a diode array UV-Vis and a Raytest GINA radio detector). Microfluidic reactions were conducted using an Advion NanoTek system; the system was controlled by version 1.4 of NanoTek software and the plumbing set-up was analog as reported in previous literature (21). The optimization reactions for the fluoroalkynes were run using the software in Automatic Discovery mode.

FH identification in plasma fractionations and purification

All waste fractions (frz I; frz III and frz IV-1–4) from industrial plasma fractionation (pooled human plasma) were analyzed by ELISA to identify the highest FH content. Thirty-five grams of the waste fraction III, which contains adjuvants (celite and perlite) were dissolved in six buffer volumes (50 mM Tris, 5 mM EDTA, and 300 KIU/ml aprotinin at pH 8.5) for a contact time of at least 30 minutes at room temperature. The soluble fraction III was filtered (3 µm) to remove celite and perlite, S/D-treated by the addition of 1% (w/v) Tween80 and 0.325% (w/v) Tri-N-Butyl-Phosphate and incubated for 30 min at RT. Subsequently, was subjected to weak Ion-exchange (AIX) resin (Fractogel EMD-DMAE, Merck) equilibrated with 50 mM Tris, 5 mM EDTA, 20 mM NaCl pH 8.5 and FH was eluted by the addition of 50 mM NaCl into the equilibration buffer used for the AIX resin. This FH-containing intermediate was adapted for subsequent Heparin affinity resin (AF-Heparin HC 650M; Tosoh Bioscience) by UDF against 20 mM Na-citrate and 5 mM EDTA pH 7. The adapted intermediate was loaded onto the Heparin affinity resin, and FH was eluted with 160 mM NaCl after a washing step with 80 mM NaCl. FH concentrate was finally pre-filtered (0.22 µm), subjected to nanofiltration using filters with pore sizes of 20 nm (Planova 20N; Asahi Kasei) and finally sterile-filtered (0.22 µm).

SDS-PAGE and Western blot

SDS-PAGE was carried out under reducing and non-reducing conditions using precast 4–12% NuPAGE Bis-Tris protein gels (Thermo, Monza Italy). For each sample, an equal amount of 1 µg was run in the gel. Protein markers were applied (Precision Plus, All Blue pre-stained; Bio-Rad, Hercules, CA, US). Gels were stained with Bio-Safe protein stain (Bio-Rad, Hercules, California, Stati Uniti), and FH purity was compared to purified human FH from commercial sources (341274; Merck).

Immunoblotting was performed by subsequent protein transfer onto nitrocellulose membrane, incubation with anti-FH Goat pAb (341276; Merck) followed by HRP-conjugated goat anti-rabbit-IgG (Merck KGaA, Darmstadt, Germany) or with OX-24 monoclonal antibody (Thermo, Monza, Italy) followed by HRP-conjugated rabbit anti-mouse-IgG (DAKO), washing and monitoring upon substrate exposure with 4Opti-CN-substrate-Kit (Bio-Rad, Hercules, California, Units States) Hercules, California, Stati Uniti) using a digital imaging system Chemidoc (Bio-Rad, Hercules, California, Units States).

Evaluation of structural integrity

To evaluate the integrity of FH during the production steps, samples were analyzed by SDS-PAGE under reducing conditions, and gels were analyzed by densitometry with TotalLab Quant software (TotalLab Ltd, Newcastle upon Tyne, UK). The integrity was calculated as a percentage of from intensity of the bands corresponding to intact or truncated form over total FH.

Native-polyacrylamide gel electrophoresis

To investigate the presence of oligomers, samples were separated using native PAGE on 4–15% Mini-PROTEAN TGX Stain-Free Protein gels (Bio-Rad, Hercules, California, Unit States) in Tris/Glycine running buffer for 5 h at 100 V. After run, stain-free gels were exposed to UV light to activate the embedded tri halo compound and make proteins fluorescent, images were acquired with ChemiDoc MP Imaging System (Bio-Rad, Hercules, California, Unit states).

Quantification of accompanying plasma proteins

C3, C4, immunoglobulin A, E, G and M (IgA; IgE, IgG; IgM), transferrin and fibrinogen were quantified using rabbit polyclonal antibodies against those proteins on a BN100 nephelometer (Siemens, Munich, Germany).

Total protein concentration was assessed by Bradford assay (Pierce, Waltham, Massachusetts, USA), according to the manufacturer's instruction, using albumin as standard.

Protein digestion for MS analysis

Samples are desalted using SPE (Solid Phase Extraction, PIERCE). One hundred and fifty µl of Ammonium bicarbonate 50 mM were added to 100 µl of a sample at pH 8.0. Twenty µg of the resulting proteins were further processed. Proteins were thus reduced with 5 mM dithiothreitol at 80°C for 20 min and alkylated for 30 min with 10 mM iodoacetamide at 37°C. Digestion was carried out by incubating overnight at 37°C in a solution containing trypsin (Roche, Germany) at 1:100 ratio with the substrate. The resulting peptide solution was loaded on a C18 cartridge in order to purify peptide solutions and filtered with 0.22 µm filter. Peptides were diluted to 100 µL by 5% ACN/0.1% FA.

HPLC- MSMS analysis

Chromatographic separation of peptides was performed using a nano-HPLC system (Thermo, Monza, Italy) in duplicates. Samples were loaded through a pre-column cartridge (PepMap-100 C18 5 µm 100 A, 0.1 × 20 mm, Thermo, Monza, Italy) and then resolved in a C18 PepMap-100 column (3 µm, 75 µm × 250 mm, Thermo,

Monza, Italy) at a flow rate of 300 nL min^{-1}. Runs were performed with eluent A H_2O (0.1% HCOOH), eluent B: 80% acetonitrile (0.1% HCOOH) 20% H_2O (0.1% HCOOH), starting with 5% of B and increasing to 35% in 40 min, then up to 100% in 1 min and isocratic for 8 min then back to the initial composition and equilibrating for 10 min.

The detection was done by an Orbitrap Q Exactive Plus high resolution mass spectrometer operated in positive ion mode. The operating parameters were optimized using standard proteins digested in the same condition as for the human samples and were as follows: spray voltage 1.9 kV, Max Spray Current:50.00 Probe Heater Temp.350°C, S-Lens RF Level:50.00, auxillary gas flow 5 arbs. Data were acquired in centroid mode across the 400–1500 m/z range. A false discovery rate (FDR) analysis was accomplished by using the integrated tools in Proteome Discover software with a confidence level of 95%. The identification of proteins are related parameters were obtained using MASCOT and Sequest-HT search engine. The mass spectrometry proteomics data have been deposited to the ProteomeXchange Consortium via the PRIDE partner repository (22) with the dataset identifier PXD050268.

Cofactor activity

The fluid-phase FH cofactor activity for cleavage of C3b by FI was assessed using purified C3b and CFI (Merck). This test was used both to monitor production steps and drive the purification procedure and on the final FH concentrate.

To test FH activity from purification intermediates containing other proteins it was necessary to further purify FH by a one-step affinity chromatography on a FH-specific antibody (5H5) with an already described method (23). Affinity-purified FH was then used to compare different purification intermediates. In this case we used as control a FH directly purified from plasma with the same method. On the contrary, when the test was performed on the final FH concentrate, this was used directly in the assay without any further purification.

Briefly, 500 ng of C3b and 125 ng of CFI were mixed with varying amounts of FH in a 20-µl reaction with PBS buffer. For affinity-purified FH from different purification intermediates, limiting amounts were used (0.5 - 1 - 2.5 ng) while for the final FH concentrate a wider range between 0.25 and 200 ng was used.

Reactions were incubated for 30 min at 37°C and stopped by the addition of reducing SDS sample buffer. Samples were analyzed by SDS-PAGE under reducing conditions followed by Coomassie staining. The cofactor activity was calculated as a decrease in the ratio between α' chain of C3b over β chain.

C3b binding assay (ELISA)

The assay was modified from a previous study (24). Microtiter plates were coated with 250 ng of C3b (Merck) in coating buffer (0.05 M carbonate-bicarbonate, pH 9.6) overnight at 4°C. After washing, plates were blocked with 3% BSA for 1 h at room temperature. Wells were incubated with purified or commercial FH (Merck) from 800 to 12.5 ng for 1 h at 37°C. Binding was detected with chicken anti-FH pAb (in-house) (23) and HRP-conjugated anti-chicken IgY (G135A - Promega, Fitchburg, WI, USA) followed by TMB (KPL, Gaithersburg, MD, USA) development. After stopping with 2 M H2SO4 the absorbance was measured at 450 nm on a Spectra Max 190 photometer (Molecular Devices, Eugene, OR).

Decay acceleration activity

The ability of FH to dissociate Bb fragments from C3 convertase complexes (C3bBb) was assessed by ELISA. Briefly, microtiter plates were coated with 250 ng of C3b (Merck) in coating buffer (0.05 M carbonate-bicarbonate, pH 9.6) overnight at 4°C. To allow the formation of C3 convertase complexes, 400 ng of FB, 30 ng of FD (Merck) and 1.5 mM NiCl2 in 10 mM phosphate buffer pH 7.2 supplemented with 25 mM NaCl and 4% BSA were added, and the plate was incubated for 2 h at 37°C. After washing, increasing concentrations of FH (from 2 µg to 0.1 ng) were added and incubated for 45 min at 37°C to allow displacement Bb fragment. The remaining C3 convertase complexes were detected by goat polyclonal antibody to human FB (341272; Merck) followed by rabbit anti-goat IgG-HRP (401515**;** Merck). The signal was revealed with ***O***-phenylenediamine (OPD), stopped with 2 M H2SO4 and the absorbance was read at 492 nm.

Radiolabeling of FH for *in vivo* biodistribution by PET imaging

In order to assess the kinetics of the purified FH *in vivo* quantitatively, a radiosynthesis procedure was devised and implemented, involving a microfluidic approach. Fluorine-18 (^{18}F, decay half-life T1/2 = 109.7 min) was selected as the radionuclide, due to favorable radiochemistry and widespread use in Positron Emission Tomography (PET) imaging. Chemicals used were purchased from Merck (Milano (MI), Italy), unless stated otherwise.

(N3-PEG)@FH precursor synthesis

One hundred twenty-five µg of human FH concentrate was dissolved in 500 µL of PBS 50 mM at pH 6.5 and stirred at room temperature for 10 minutes. In a second vial, 2.9 mg of N3-PEG (4)-COOH (IRIS Biotech GmbH, Marktredwitz, Germany) was activated using a solution of 1.1 mg of N-Hydroxysuccinimide (NHS) and 1.5 mg of (1-ethyl-3-(3-dimethylaminopropyl) carbodiimide hydrochloride) (EDC, Fluka, Brescia, Italy) in 200 µL of 2-(N-morpholino) ethanesulfonic acid (MES, Thermo, Monza, Italy) at pH 4.5.

The activation reaction was left standing at room temperature for 20 minutes. After this time, the solutions from both vials were combined and the resulting mixture was basified by 25 µL of N,N-Diisopropylethylamine (DIPEA) to a final pH of 8.5. The reaction was kept at room temperature for 2 hours without agitation. The

final product was separated from an excess of small molecular weight reagents on a Sephadex G-25 column using a 0.25 mM NaCl aqueous solution as eluent. The (N3-PEG)@FH was further purified by ultracentrifugation, suspended in water, lyophilized, and the resulting powder was analyzed by HPLC.

Microfluidic optimization of tosyl-alkyne radiolabeling

Two compounds, 5-tosyloxy-1-pentyne (PeTos) and 6-tosyloxy-1-hexyne (HeTos) were synthesized from the corresponding alcohols (25) and used in the optimization process. The system tests different temperatures, solvents, and ratios of precursor to labeling solution. The reaction mixtures were analyzed and pure [^{18}F]fluoroalkynes were obtained by heating and condensing the gaseous products. The process was efficient and precise, allowing for the production of radiochemically pure compounds.

Microfluidic synthesis of [^{18}F]fluoropentyne ([^{18}F]FPe) for CuAAC reaction

The [^{18}F]FPe was synthesized from the corresponding tosylate using a microfluidic system under optimal radiolabeling conditions. The starting [^{18}F]fluoride was captured on an ion exchange column and eluted with a solution of Kryptofix 222 (K_{222}) in acetonitrile (21). The radioactive solution and PeTos precursor solution were delivered into a microfluidic reactor, heated at 130°C, to obtain the final product in high radiochemical purity and 92 ± 3% RadioChemical Yield (RCY) (26, 27). The final product was then distilled into a second vial containing a (N3-PEG)@CFH solution, leaving unreacted fluoride and reagents in the first vial. The procedure allowed obtaining 15 ± 10MBq of [^{18}F]FPe 45 min after the start of the synthesis.

Synthesis of [^{18}F]FPe-(trN-PEG)@FH

[^{18}F]FPe was collected in a vial containing a solution of (N3-PEG)@FH in water. After distillation, the mixture was stirred at 45°C for 5 min. A solution of CuI and Tris(benzyltriazolylmethyl) amine (TBTA) in THF/H_2O was added to the reaction and stirred at 45°C for an additional 10 min. The solution residue was diluted with isotonic saline containing 1% ethanol and purified by gel filtration. The quality of [^{18}F]FPe-(trN-PEG)@FH was assessed using a HPLC interfaced to a diode array UV-Vis and a GINA radio detector.

PET/CT image acquisition and analysis

The images were acquired using an IRIS CT/PET instrument designed for high-resolution imaging of small animals (27, 28). This instrument allowed for 3D and time-resolved quantification of tracer kinetics in the entire mouse body.

All imaging procedures were performed under general anesthesia in accordance with international guidelines and Italian laws for the care and use of laboratory animals, demanded by the European Directive (Directive 86/609/EEC of 1986 and Directive 2010/63/UE) and Italian laws (D.lgs. 26/2014). Each animal was anesthetized with isoflurane and oxygen, and positioned on the imaging bed once the correct degree of anesthesia is reached (29).

Imaging protocol

[^{18}F]FPe-(trN-PEG)@FH was formulated in saline before injection, and used for *in vivo* PET imaging of both control and Cfh-/- mice. The tracer was intravenously administered to two distinct groups of mice: one consisting of C57BL6 mice and the other composed of Cfh-/- mice. The dynamic acquisition of the tracer was carried out from 5 min to 160 min post-injection. The image reconstruction was done using 3D ordered subset expectation-maximization (OSEM), with corrections for radioactive decay, random coincidences, and dead time. Low-dose micro-CT imaging was also performed after PET on the same integrated scanner. Both PET and CT images were exported in standard DICOM format after reconstruction for further image processing/quantification.

Quantitative image analysis

Analysis of PET/CT images was performed using AMIDE software v 1.0.4 three-dimensional regions of interest (ROIs) were traced on the left ventricle cavity, whole brain, liver, kidneys, gallbladder and bladder. Standardized Uptake Value (SUV) was calculated on each ROI and on each time frame, and the results were plotted against time for each animal. On each of the two groups (CTRL and Cfh-/-), average values, range, median and quartiles of organ uptake at each time point were calculated.

Animal models experimental protocols

These studies were done in the mouse model of C3 glomerulopathy in Cfh−/− mice. Comparing Cfh−/− with wild-type mice, Cfh−/− mice developed severe albuminuria starting at 8 months of age.

Study 1: single administration

Cfh−/− mice (n=4, 2–4 months old) received a single intraperitoneal injection (0.5 mg in 200 microliter PBS) of human plasma FH concentrate. Four Cfh−/− mice received PBS as controls. At baseline (before injection), and at 2 and 6 h after injection we evaluated serum C3 levels by ELISA. At 24 hours after injection, the animals were sacrificed. Blood was collected for the evaluation of serum C3 levels and human FH levels by ELISA. The kidneys were

collected for immunofluorescence analysis of C3 and C5b-9 deposition in glomerular capillaries and tubuli. Sections of kidney, liver, eye, and heart tissues were stored for future analysis by light microscopy and ultrastructural analysis by transmission electron microscope.

Study 2: multiple administrations

Four groups of Cfh−/− mice (n=4 each, 2–4 months old) have been studied as follows:

Group 1: Cfh−/− mice received two daily intraperitoneal injections (0.5 mg in 200 microliters PBS) of human plasma FH concentrate. At 48 hours (24 hours after the second injection) the animals were sacrificed. Group 2: Cfh−/− mice received three daily intraperitoneal injections (0.5 mg in 200 microliters PBS) of human plasma FH concentrate. At 72 hours (24 hours after the third injection) the animals have been sacrificed. Group 3: Cfh−/− mice received four daily intraperitoneal injections (0.5 mg in 200 microliters PBS) of human plasma FH concentrate. At 96 hours (24 hours after the fourth injection) the animals were sacrificed. Group 4: Cfh−/− mice received five daily intraperitoneal injections (0.5 mg in 200 microliters PBS) of human plasma FH concentrate. At 120 hours (24 hours after the fifth injection) the animals were sacrificed. Serum C3 levels were evaluated in all animals at baseline. At sacrifice, blood was collected for the evaluation of serum C3 levels and human FH levels. Human FH levels were also measured at baseline in 4 Cfh−/− mice as negative controls of the assay. The kidneys were collected for immunofluorescence analysis of C3 and C5b-9 deposition in glomerular capillaries and tubuli. Three wild-type C57/BL6 mice were also studied as controls.

Immunofluorescence analysis of renal tissue

Three-µm OCT-fixed frozen sections were used for the evaluation of C3 and C5b-9 staining. For C3 deposition, sections were incubated with FITC-conjugated goat anti-mouse C3 Ab (1:200; Cappel) and with Rhodamine-labeled Lens Culinaris Agglutinin (1:400) and DAPI to label kidney structures and cell nuclei, respectively. For C9 staining, rabbit anti-mouse C9 (1:1600) and Cy3-conjugated goat anti-rabbit secondary Abs (1:300) were used. Fluorescein-labeled Lens Culinaris Agglutinin (1:400) and DAPI were used to label kidney structures and cell nuclei, respectively. Isotype-matched irrelevant Abs were used as negative controls. Glomerular C3 and C9 staining was scored from 0 to 3 (0, no staining or traces (<5%); 1, staining in <25% of the glomerular tuft; 2, staining affecting 26 to 50%; 3, staining >50%). Tubular C3 and C9 staining were scored from 0 (no staining) to 1 (granular staining), 2 (linear interrupted staining), to 3 (linear staining).

Statistical analysis

In vivo animal model data analysis were reported as mean ± SD and were analyzed by one-way ANOVA (MedCal software). Values of $p < 0.05$ were considered statistically significant. For PET biodistribution data, two-tailed Welch's t-test was carried out for comparison of the organ's SUV data at each time point, between the control and diseased (Cfh-/-) group.

Results

FH process purification and characterization

Based on Cohn fractionation, the plasma proteins were separated with different ethanol concentrations and pH levels into five major fractions (19) as much as possible fibrinogen in Fraction I, y-globulins in Fraction II, lipid-globulins in Fraction III, α-globulins in Fraction IV, and albumins in Fraction V. Proteins extracted and purified from plasma have a wide range of therapeutic uses, including treatment for immune deficiencies, neurological diseases, autoimmune disorders, and bleeding disorders, among others (30). However, the demand for specific proteins can vary, and this, along with other factors as the difficulty of further purification, can lead to certain fractions being discarded (Fraction I; III and IV (1–4)). To identify in which waste fraction FH was present we analyzed the proteome of the principal unused fractionation intermediates from an industrial plasma fractionation plant. FH was found in Cohn Fraction III and its presence was confirmed by ELISA. Cohn Fraction III contains a very high concentration of FH with a recovery of 70% compared to cryo-poor plasma (Figure 1A) addressing its use as a starting material for FH purification.

Two scalable chromatography steps were applied to purify a new FH concentrate resulting in 87.96% purity (Figure 1B).

The novel process developed for the purification of human plasma FH is schematized in Figure 1C and comprises two chromatographic separations, including pathogen elimination and inactivation by Solvent – Detergent (S /D) treatment and nanofiltration.

Each step of the purification procedure was monitored for FH contents, integrity, and functionality, to choose the purification protocol that best preserves FH integrity and activity.

In the process optimization study, aprotinin was added as a protease inhibitor only in the phase of extraction of FH from fraction III. This allowed for a reduction of the percentage of degraded protein, (Supplementary Material Table S1), resulting from the analysis in SDS-PAGE (data not shown) and subsequent densitometry of the purified product obtained from samples extracted with or without aprotinin (300 KIU/ml).

The purification intermediates were analyzed by SDS-PAGE and western blot: the electrophoresis was performed in both reducing and non-reducing conditions (Supplementary Material Figure S1). The analysis reveals the presence of FH in all the intermediates, the bands corresponding to cleaved form of FH (130 and 35 KDa) are also evident upon reduction. A faint band around 35 KDa is also present in non-reducing conditions only in the filtration intermediate, probably corresponding to the splice variant FHL-1, however this band is no longer visible in subsequent purifications.

10.3389/fimmu.2024.1334151

FH obtained from different purification intermediates was analyzed by cofactor assay to monitor FH activity. Different samples were directly compared by plotting α'-chain/β chain ratio and generating a curve by linear-log regression. Figure 2 reports an example of an analysis on 4 different samples obtained during the development of the purification protocol. Two batches (#16 and #18) were produced using aprotinin in the phase of extraction of FH from fraction III and show a better activity, confirming the importance of adding this inhibitor during purification. Moreover, batch #16, which, unlike batch #18, was stored in a buffer containing glycine as a stabilizer, preserves the best activity.

Characterization of the final product

Upon completion of the process, the overall yield of the FH process purification was found to be 38.60%. The purified FH demonstrated a purity level of 92%, which is represented as the ratio of FH antigen to the total protein, with an antigen concentration of 3.093 mg/ml. Our process increases the purity by 9.1 fold compared to Cohn fraction III (starting material) and 211.6-fold over FH present in plasma (Table 1).

The purified FH was concentrated about 7 times, by a 30 KDa cut-off centrifugal concentrator Vivaspin, and tested for C3, C4, Immunoglobulin (IgA, IgM, IgE, IgG), fibrinogen, albumin, and transferrin by nephelometric analysis.

Among the analyzed proteins of three different process, complement C3 protein has the highest concentration with 255.5 ± 10.6 mg/L and Immunoglobulin A and M with respectively 12.85 ± 0.49 mg/L and 13.1 ± 0.14 mg/L (Table 2).

The results are confirmed by proteomic analysis, where different batch samples of FH (N=3, detailed results are reported in Supplementary Material Table S2) were processed and analyzed using the protocol reported in the "methods" section The mean identified proteins were 185 ± 18 (Mean ± SD) with a statistical significance of ≥ 95%. In Supplementary Material Table S3 are reported the common proteins comparing the three batches.

FH coverage was 71 ± 1,5% (Mean ± SD) by peptide analysis using Sequest HT search engine. Data are available via ProteomeXchange with identifier PXD050268.

SDS-PAGE and Western blot

The final FH concentrate was analyzed by SDS-PAGE under reducing condition (Figure 3A), the analysis revealed the presence of the cleaved form of FH and, as already observed with other methods, the presence of C3b as the major contaminant. The

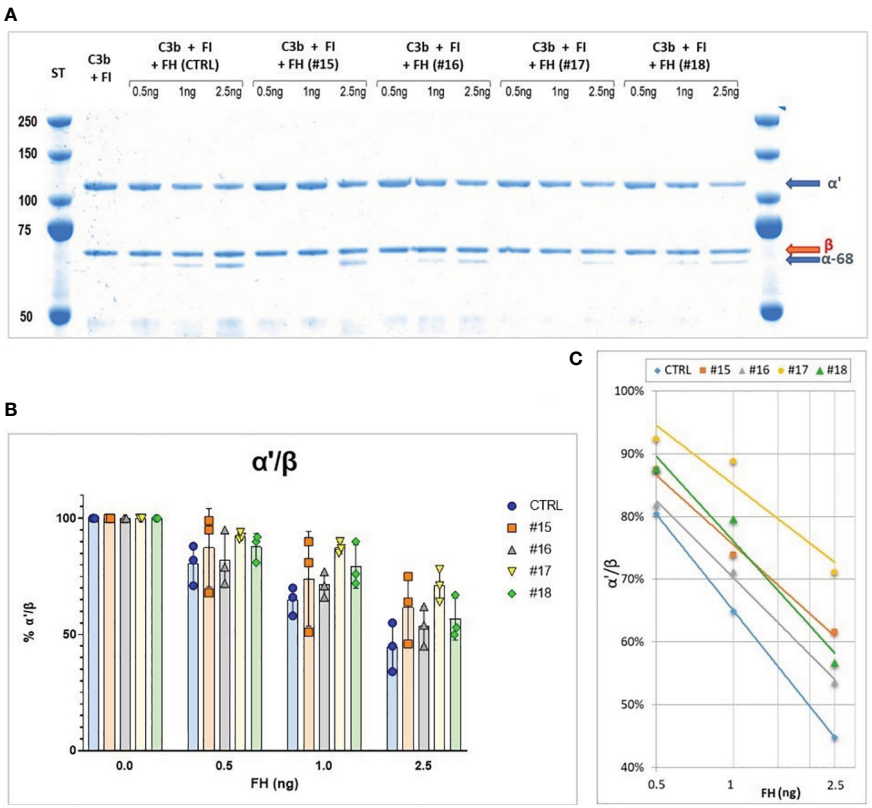

FIGURE 2
(A) SDS-PAGE and Coomassie staining of a Cofactor assay on 4 different purification intermediates (#15, #16, #17, #18) and a Control (CTRL). The samples were subjected to affinity purification with a FH-specific antibody to exclude contaminating protein before performing the test, the control was purified directly from human serum by the same affinity chromatography. **(B)** α'/β chains ratio obtained for the different samples, means and SD from three independent assays are indicated. **(C)**, Curves generated by linear-log regression from mean results.

10.3389/fimmu.2024.1334151

TABLE 1 Step Recovery and purities of complement Factor H (FH): The FH amounts are obtained by ELISA as described in Material and Methods.

FH-rich intermediates	FH amount (mg/l)	Total protein (mg/ml)	FH Purity (%)	FH Step process recovery (%)	FH process recovery (%)
Human plasma	414.00	80.00	0.52	–	–
Plasma fraction (starting material)	1000.74	7.72	12.96	–	–
Miniprofile filtration	541.34	5.55	9.74	95.03	95.03
Anion-exchange chromatography eluate	675.02	1.76	38.30	71.83	66.21
Heparin affinity chromatography eluate	1167.95	1.32	87.96	71.09	43.38
Purified FH (20N + 0.22 µm)	3093.93	2.81	92.07	100.00	38.60

The purity % is a ratio between the amount FH and total protein.

presence of the cleaved form of FH was also shown by Western Blot analysis under reducing condition with a polyclonal antibody against FH (Figure 3B). Finally, to exclude the presence of the FHL-1 splice variant, which could be confused with the lower band of the cleaved form, a non-reducing Western blot with the OX-24 antibody was performed (Figure 3C). This antibody recognizes an epitope in the SCR-5 of FH and detects also FHL-1. Under non-reducing condition the cleaved form of FH is held together by a disulfide bridge and migrates as the integral form, thus the only form visible around 35 KDa is FHL-1. This analysis excluded the presence of FHL-1 which is visible in a sample of human serum used as a control, but not in our concentrates.

TABLE 2 Nephelometric analysis of the most important contaminants.

Contaminant	Concentration (mg/ml)	Limit of Detection (mg/ml)
Factor H	2.9 ± 0.12	
Complement component C3	0.26 ± 0.01	0.0084
Complement component C4	< DL	0.0032
Immunoglobulins G	0.0044 ± 0.0004	0.0035
Immunoglobulins A	0.0128 ± 0.004	0.0035
Immunoglobulins M	0.0131 ± 0.001	0.0035
Immunoglobulins E1	< DL	0.0035
Immunoglobulins E2	< DL	0.0035
Transferrin	< DL	0.0174
Albumin	< DL	0.0177
A2-macroglobin	< DL	0.0086
Fibrinogen	< DL	0.0266
Fibronectin	< DL	0.0417

C3, IgA and IgM, are the most representative contaminant protein.

Native-polyacrylamide gel electrophoresis

It is hypothesized that FH oligomerizes when stored at high concentrations. To evaluate the presence of high molecular weight species, we conducted a Native PAGE analysis. We examined two batches of our purified FH, with concentrations of 1.5 mg/ml and 3 mg/ml respectively, along with a commercially available purified FH preparation of 1 mg/ml (as shown in Figure 3D). The results were consistent across all samples, displaying a prominent band corresponding to the monomer and fainter bands of higher molecular weight, which correspond to the oligomeric forms.

Functional analysis of purified FH

The activity of our purified FH preparation was tested in three different functional assays.

Cofactor assay

FH acts as a cofactor for FI-mediated cleavage of C3b to iC3b in the fluid phase. The cleavage products of C3b α'-chain, α68, and α43 iC3b chains can be visualized on a reducing SDS-PAGE. Purified FH displays cofactor activity, a minimum of 2.5 ng is sufficient to induce C3b cleavage, as shown by the reduction of α'-chain and the presence of α68 and α43 chains (Figure 4A). Results were comparable to those obtained with commercial FH.

C3b binding

The ability of purified FH to bind surface-bound C3b was assessed by ELISA assay. We observed a dose-dependent binding of purified FH to immobilized C3b, comparable results were obtained with the commercial FH (Figure 4B).

Decay acceleration activity

Purified FH displays a dose-dependent decay acceleration activity on C3 convertase complexes. Increasing the amount of

10.3389/fimmu.2024.1334151

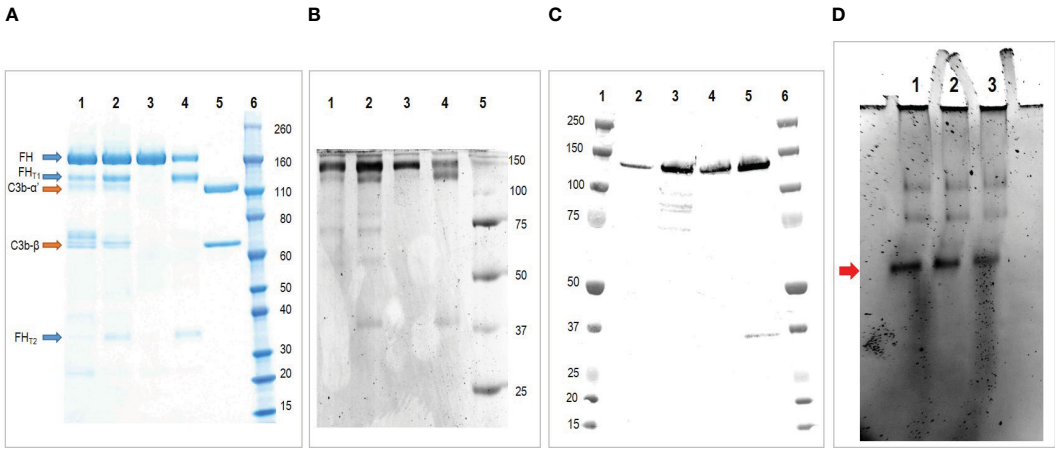

FIGURE 3
Characterization of the purified FH. **(A)** SDS-PAGE under reducing condition of purified FH. Lane 1 and 2 two batches of purified FH; Lane 3, commercial FH; Lane 4, commercial FH cleaved with trypsin; Lane 5, C3b; Lane 6, molecular weight standard. The analysis reveals the presence of FH integral form (apparent MW 170 kda) together with the larger (130 kda) and smaller (35 kda) fragments of the truncated form. Moreover it reveals the presence of C3b as major contaminant. **(B)** Western blot under reducing condition of purified FH. Lane 1 and 2 two batches of purified FH; Lane 3, commercial FH; Lane 4, commercial FH cleaved with trypsin; Lane 5, molecular weight standard. This analysis confirms the presence of FH integral form (170 kda) together with the larger (130 kda) and smaller (35 kda) fragments of the truncated form. **(C)** Western blot under non reducing condition of purified FH with antibody OX-24. Lane 1, molecular weight standard; Lane 2 and 3 two batches of purified FH; Lane 4, commercial FH; Lane 5, human serum (used as positive control); Lane 6, molecular weight standard. This analysis exclude the presence of FHL-1 in our preparations. **(D)** Native-PAGE analyses of purified FH. Lane 1, purified FH stored at 1.5 mg/ml; Lane 2, purified FH stored at 3 mg/ml; Lane 3, commercial FH stored at 1 mg/ml. The major form indicated by the arrow corresponds to the monomer, the higher molecular-weight bands denote oligomeric forms.

FH enhanced the displacement of the Bb fragment causing a decrease in the intact C3 convertase (C3bBb). The effect was comparable to that obtained with purified FH from a commercial source (Figure 4C).

Radiochemistry

As conjugation partners, [^{18}F]fluoropentyne and [^{18}F] fluorohexyne were radiolabeled using a microfluidic flow approach from respective tosylate precursors, achieving maximum radiochemical conversion (RCC) of 96 ± 9% and 81.5 ± 5% respectively. Therefore, [^{18}F]fluoropentyne was chosen and simple distillation was effective in recovering such prosthetic group in high purity, and reacted quantitatively with the azide-functionalized FCH.

[^{18}F]FPe-(trN-PEG)@FH was produced via a 2-step process, comprising the radio fluorination of the 5-tosyl-pent-1-yne under microfluidic conditions (31) (92% radiochemical yield, RCY), its purification by distillation, and a quantitative click reaction conjugation with an aqueous solution of (N_3-PEG)@FH and CuCl/TBTA in 10min at 45°C. The process led to the desired product in >95% radiochemical purity (RCP).

Animal experiments

In vivo PET imaging

Previous works have reported the tagging and imaging of FH analogues, using I-125 labelling (32) Tc-99m (33) or optical tags (34), however, these studies presents limitations in terms of imaging performance (i.e. planar scintigraphy or autoradiography), scope (i.e. identification of myocardial damage) and pharmacological assessment (i.e. using FH fragments or recombinant complement). We therefore decided to design an imaging tracer based on entire FH that can be used in PET imaging, thus improving on these aspects. The biodistribution of the labeled product imaging was assessed in CTRL and Cfh-/- mice by dynamic PET. Figure 5 shows the average tracer kinetics in the selected organs, for the two groups. The reported activities are expressed as Standardized Uptake Values (SUVs) and take into account the different weights of each animal. Indeed, control mice were heavier than Cfh-/- countermates (CTRL: 42.6 ± 3.0 g; Cfh-/-: 21.7 ± 1.6 g $p<0.001$). A different shape of activity accumulation in both the bladder and the gallbladder for the Cfh-/- mice during the first 60' post-injection is apparent in the observed curves.

The renal curves, inclusive of tracer activity for both cortical (extraction) and medullary (excretion) components, resulted significantly different in the time range of 40 min post-injection (CTRL: 0.055 ± 0.011 g/ml; Cfh-/-: 0.040 ± 0.017 g/ml, $p<0.05$, at 33.5 min post-injection; CTRL: 0.054 ± 0.012 g/ml; Cfh-/-: 0.040 ± 0.017 g/ml, $p<0.05$, at 38.5 min post-injection) Also, the uptake in the liver was different in the time range of 20–55 min post-injection (CTRL: 0.065 ± 0.034 g/ml; Cfh-/-: 0.037 ± 0.021 g/ml, $p<0.05$, at 23.5 min post-injection; CTRL: 0.051 ± 0.022 g/ml; Cfh-/-: 0.033 ± 0.015 g/ml, $p<0.05$, at 53.5 min post-injection). Intra and inter-group variability of the tracer uptake as a function of time from injection is shown in Figure 5. Apart from the gallbladder, Cfh-/- mice show much intragroup variability than control mice, with lower SUV values especially in the bladder and kidney as shown in Figure 5. Both bladder and gallbladder curve also show a delayed uptake in Cfh- mice as compared with controls. Two out of 5 Cfh-/- mice did not show any tracer uptake in the gallbladder, explaining the high variability in this group (Figure 5F). Some representative PET/CT images of the [^{18}F]FPe-(trN-PEG)@CFH are shown in Figure 6.

10.3389/fimmu.2024.1334151

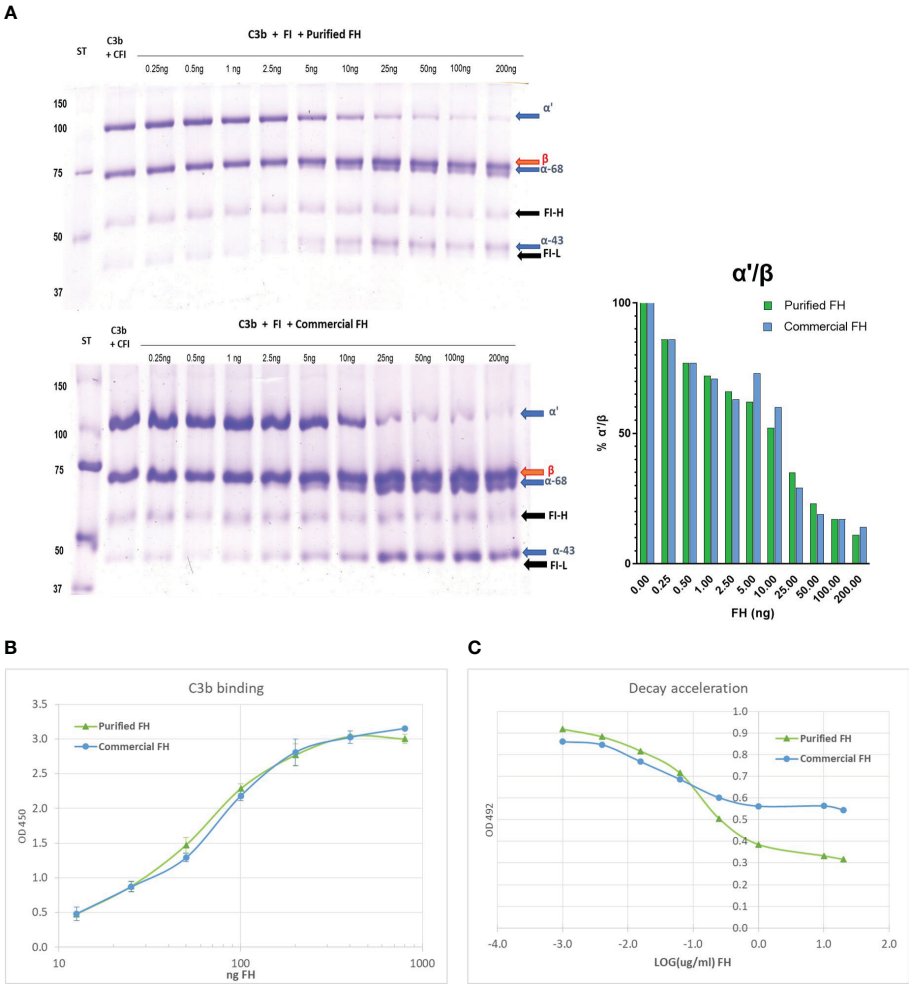

FIGURE 4
In vitro activity of the purified FH compared with a commercial FH (Merck). **(A)** Cofactor assay: C3b and FI were incubated with different amounts of purified FH, run on a reducing SDS-PAGE and stained with Coomassie. In the presence of FH, FI cleaves C3b and the degradation products iC3b-α68 and iC3b-α43 are visible. The bands corresponding to the heavy (FI-H) and light (FI-I) chain of FI are also evident in the gel. **(B)** C3b binding assay: Purified FH can bind surface-bound C3b in a dose-dependent manner, similar to commercial FH. The binding of FH to immobilized C3b was visualized in an ELISA assay by the use of an antibody to human FH. **(C)** Decay acceleration activity: Purified FH displays decay acceleration activity on C3 convertase complexes. The decay of C3bBb was enhanced by the presence of an increasing concentration of FH. The decrease of bound Bb to the intact complex was visualized by the use of an antibody to human FB. Results are presented as LOG of FH concentration.

Effect of the human FH concentrate on C3 levels in Cfh−/− mice

In Cfh−/− mice treated with a single injection of human FH concentrate, plasma C3 levels progressively increased at 2, 6, and 24 h after injection, and values were significantly higher than those recorded in the same Cfh−/− mice at baseline and at the corresponding time points in PBS treated Cfh−/− mice (Figure 7A). Similarly, C3 levels at sacrifice were significantly higher than values at baseline in Cfh−/− mice treated with daily injections of human FH concentrate and sacrificed at 48 h, 96 h, and 120 h (Figure 7B). In the group sacrificed at 72h, C3 levels increased in 2 out of 4 animals while for the other 2 animals, not enough plasma could be obtained (Figure 7B). However, at all-time points, plasma C3 values in Cfh −/− mice treated with the FH concentrate remained significantly lower than C3 values in C57/BL6 wild-type mice (909.6 ± 145.68 µg/ml). These results indicate that administration of a FH concentrate partially but significantly prevented C3 activation and consumption in the circulation of Cfh −/− mice.

Evaluation of human FH levels in CFH−/− mice

Human FH levels in plasma of 4 Cfh−/− mice at baseline were undetectable, as expected. At variance, human FH was detectable at all time points after either single or multiple injections of human FH concentrate starting from 32.64 µg/ml at 24 h to 41.01 µg/ml at 96 h concentration of FH (Supplementary Material Figure S2).

Effect of the human FH concentrate on C3 staining in the kidney of Cfh−/− mice

We observed intense staining for C3 in the glomeruli of PBS-treated Cfh−/− mice, which was significantly higher than glomerular C3 staining in wild-type mice (Figure 8A). In Cfh−/− animals treated with a daily injection of human FH concentrate and

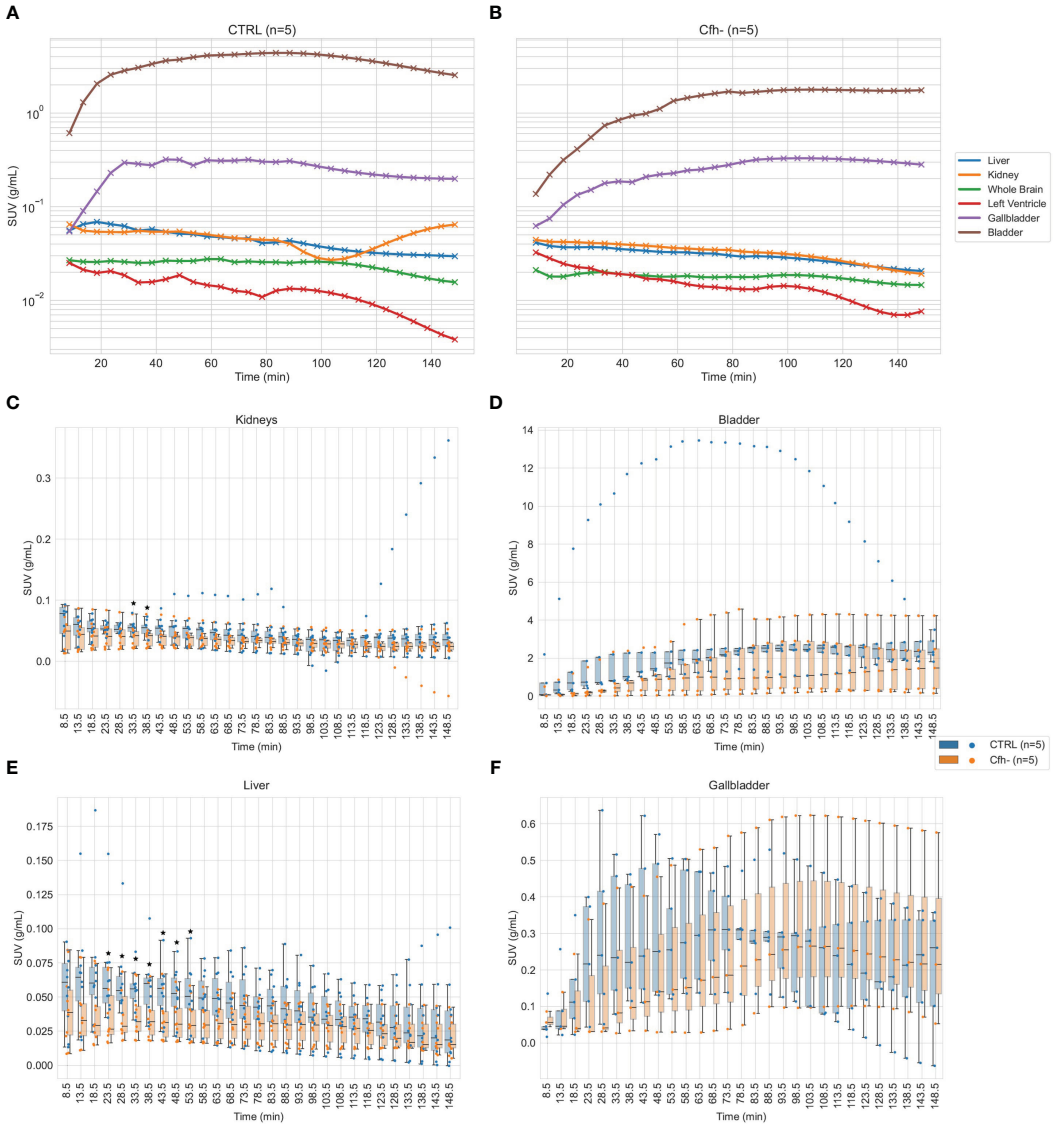

FIGURE 5
(A, B): Average tracer kinetics of the ^{18}F-labelled FH in organs, for the control group (left) and Cfh-/- group (right). Activity levels are expressed in terms of Standardized Uptake Values (SUV). **(C–F):** Organ-specific distribution of tracer uptake for kidneys (both sides) **(C)**, bladder **(D)**, liver (all ROIs) **(E)** and gallbladder **(F)**. Individual data points for each subject at each time are superimposed to boxplots for better understanding of the intragroup and intergroup variability. Statistical significance ($p<0.05$) has been marked with asterisks at the corresponding time frames.

sacrificed at 24 h, 48 h, 72 h, 96 h, and 120 h we found a progressive decrease of glomerular C3 staining, which was already significantly lower than in PBS-treated mice at 24 h (Figures 8A, B). Notably, the 120 h glomerular C3 staining in FH-treated Cfh−/− mice was not significantly different from staining in wild-type mice. These results indicate that the FH concentrate was effective in limiting C3 activation and also favored the clearance of C3 deposits from the glomerular tuft.

No tubular C3 staining was observed in PBS-treated Cfh−/− mice, while moderate peritubular C3 staining was observed in wild-type mice ($p<0.05$ vs. PBS-treated Cfh−/− mice, Figure 8C). The lack of tubular C3 staining in PBS-treated Cfh−/− mice likely reflected the massive C3 consumption in the circulation and the entrapment of C3 activation products within the glomerular structures. In Cfh−/− animals treated with a daily injection of human FH concentrate and sacrificed at 24 h, 48 h, 72 h, 96 h, and 120 h we found a progressive increase of tubular C3 staining, which was already significantly higher than in PBS-treated mice at 24h and paralleled the decrease of glomerular C3 staining. The appearance of C3 staining in the tubular compartment after FH administration in CFH -/- mice could be explained both by the mobilization of C3b inactivation products from the glomerulus due to the cofactor activity of injected FH and by the partial restoration of C3 levels in the circulation, so that C3 molecules were filtered by the glomeruli from the blood to tubular compartment.

Notably, the 72h and 120 h tubular C3 staining in FH-treated Cfh−/− mice was significantly higher than tubular C3 staining in wild-type mice (Figures 8C, D). Whether the higher-than-normal tubular staining in Cfh−/− mice treated with multiple injections of FH is due to tubular uptake of C3 activation products cleared from

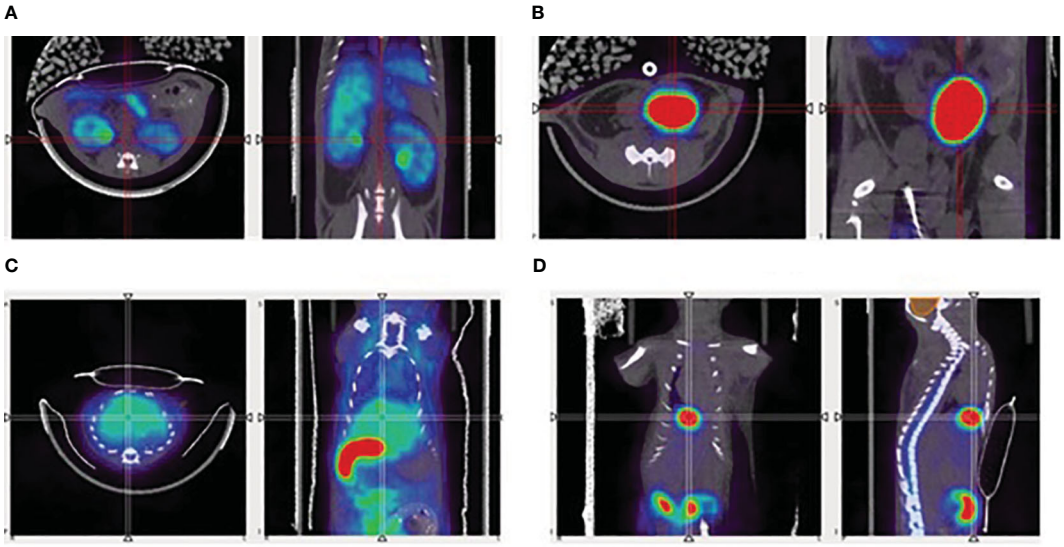

FIGURE 6
Representative PET/CT images of the ^{18}F-labelled FH, in mice, showing uptake in **(A)** kidneys, **(B)** bladder, **(C)** liver, and **(D)** gallbladder.

the glomeruli or reflects an immune response against the human FH concentrate remains to be established.

Discussion

Over the past few years, plasma collection has been significantly reduced due to the COVID-19 pandemic. This has underscored the importance of optimizing plasma use for therapeutic development, a concern that has been at the forefront for both society and the industry. Annually, over 50 million liters of collected plasma are utilized for the production of immunoglobulin and albumin. This process incurs a total expenditure exceeding US$20 billion, highlighting the scale and economic impact of this sector (35).

Utilizing plasma intended for the production of higher-value products to develop new plasma-derived therapies may not be economically viable, especially for rare disease indications. Therefore, the use of discarded plasma fractionation intermediates, which are industrial waste generated during the manufacturing of medically valuable products, for the purification of other plasma proteins needed for various therapies, offers significant added value. Firstly, the ethical implications of using plasma, a scarce and precious resource derived from donations, for therapeutic development cannot be overlooked. Secondly, the cost-effectiveness of using plasma for the development of therapies for ultra-rare diseases could be questionable compared to the use of waste plasma, given the high cost of goods and the limited patient population. Thirdly, enhancing the economic feasibility of developing plasma-derived orphan drugs could positively impact the cost of rare disease treatments, benefiting patients and national health systems. Lastly, reducing the industrial waste generated in the plasma fractionation process by reintroducing such waste into the production cycle could lessen the industry's

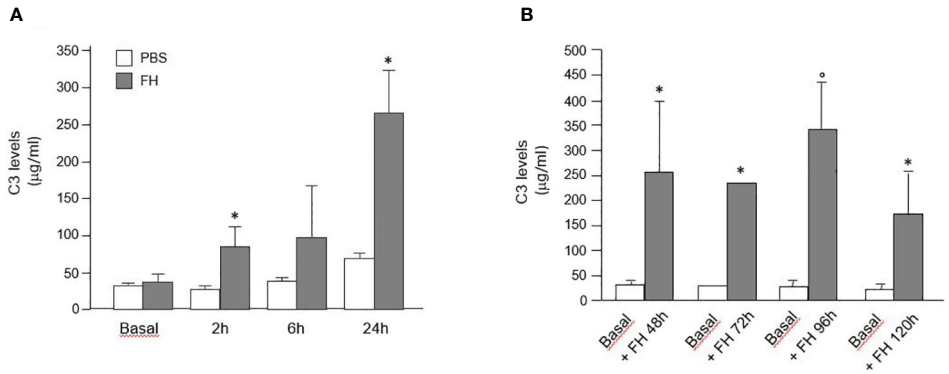

FIGURE 7
(A) Mean+SD values (µg/ml) of plasma C3 levels measured in Cfh−/− mice at baseline and at different time points after a single injection of PBS (control) or human FH concentrate. * P<0.05 versus PBS control group. **(B)** Mean+SD values (µg/ml) of plasma C3 levels were measured in Cfh−/− mice at baseline and at sacrifice (48 h, 72 h, 96 h, and 120 h) after multiple injections of a human FH concentrate. *P<0.05 versus baseline; °P<0.01 versus baseline.

10.3389/fimmu.2024.1334151

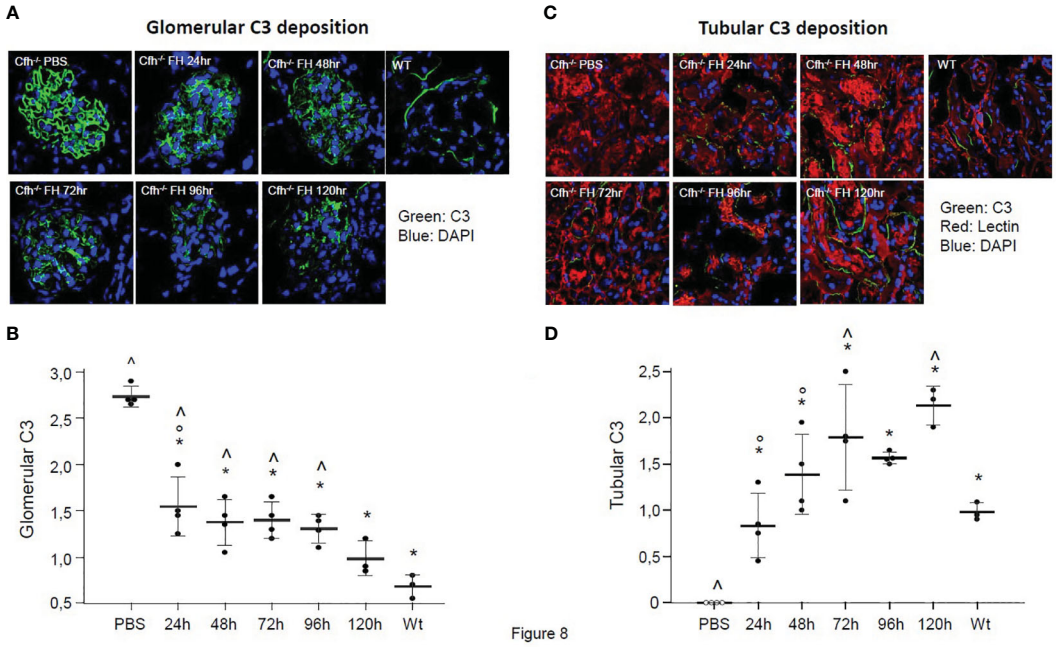

Figure 8

FIGURE 8
(A) Representative images of glomerular C3 staining (in green) in Cfh−/− mice treated with PBS or with the human FH concentrate, and in wild-type (WT) mice. Nuclei are stained by DAPI (in blue). **(B)** Results of semiquantitative evaluation of glomerular C3 staining in Cfh−/− mice treated with PBS or with the human FH concentrate, and in wild-type (WT) mice. Mean ± SD, individual values are represented as black dots. *p<0.05 versus PBS control group; ° p<0.05 versus 120 h group; ^ p<0.05 versus WT group. **(C)** Representative images of tubular C3 staining (in green) in *Cfh*$^{-/-}$ mice treated with PBS or the human FH concentrate and in wild-type (WT) mice. Nuclei are stained with DAPI (in blue), cell membranes with Rhodamine-labeled Lens Culinaris Agglutinin (in red). **(D)** Results of semiquantitative evaluation of tubular C3 staining in Cfh−/− mice treated with PBS or with the human FH concentrate, and in wild-type (WT) mice. Mean ± SD, individual values are represented as black dots. *p<0.05 versus PBS control group; ° p<0.05 versus 120 h group; ^ p<0.05 versus WT group.

environmental footprint. To address these aspects, we conducted a proteomic analysis of the primary unused fractionation intermediates from an industrial plasma fractionation plant and discovered FH in waste Fraction III (36).

We therefore developed a chromatography purification method for FH starting from this waste fraction. The purification steps were constantly monitored to obtain a product as pure and functional as possible. As FH can be cleaved by plasma proteinases during purification procedures, generating two fragments (130 and 35 kDa) we evaluated its integrity during all purification phases. Moreover, we used a cofactor assay to monitor the activity of purification intermediates, and the results were used to drive the procedure.

The purity of our final product was analyzed by proteomic analysis and by SDS-PAGE and Western blot. The presence of the splice variant FHL-1 was excluded using a specific monoclonal antibody.

The final product was further characterized with three different functional assays to ensure that the main properties of FH are preserved. Our final product is fully active as demonstrated by cofactor and decay acceleration assays and can attach to surface-bound C3b.FH circulates in plasma predominantly in the monomeric form, however, it was reported a weak tendency for dimer formation (37) which is greatly enhanced in the presence of polyanions (38). Several studies report that FH tends to oligomerize when stored at high concentrations in solution (39). In gel filtration experiments, FH migrates with an apparent size of 330,000 Da and was therefore often erroneously reported as a dimer. However, this characteristic is due to the high flexibility of the molecule which can even fold back on itself altering its mobility in agarose gel. Sedimentation equilibrium analysis by analytical ultracentrifugation demonstrated that this form corresponds to the monomer (38).

We analyzed our FH concentrate by Native PAGE and the results showed that it is predominantly in the monomeric form, with small percentages of higher molecular weight aggregates.

Before testing our product in a clinically relevant animal model, we investigated its *in vivo* biodistribution using PET/CT imaging. This was achieved by labeling the purified FH with ^{18}F, utilizing a bifunctional conjugation strategy. This strategy is based on the azide-alkyne Cu-catalyzed 1,3-dipolar cycloaddition reaction, where the azide functional group was introduced on FH and the radionuclide was incorporated in short-chain, ^{18}F-radiolabelled alkynes. Functionalization of FH was achieved by amide coupling, exploiting the lysine residues available (~80 residues in the sequence); while not chemiospecific, the average quantity and position of functionalization was sufficient to allow successful click chemistry conjugation with the radiofluorinated synthon.

Innovative reaction conditions were applied to the radiolabeling of the ^{18}F-alkynes, which were optimized using a microfluidic system, that allowed to explore multiple consecutive reaction conditions, thus achieving the best RCY with minimal use of precious starting materials. Finally, the synthesis of the [^{18}F] fluoropentyne intermediate did not require time-consuming

chromatographic purifications and allowed a simple one-pot bioconjugation reaction which included the online precursor purification by distillation and the functionalized FH coupling reaction, affording the final compound [^{18}F]FPe-(trN-PEG)@FH in good purity and yield.

Kinetics of FH distribution, as measured by imaging experiments, was shown to be different between normal and diseased mice. In particular, a point-wise comparison between the time activity curves (TACs) of the two groups revealed statistically significant differences in liver uptake in the time range of 20–55 min post-injection as well as in the kidneys in the time range of 30–40 min post injection. Even though the same statistical test did not report significant differences in the bladder and gallbladder TACs, the observed different shapes (in particular, their slope and interquartile ranges), the delayed bladder and gallbladder TACs of CFH- mice as compared to the control mice, along with the above-mentioned result about liver and kidney uptake, coherently suggest a dysfunction of the renal and hepatobiliary system in the Cfh-/- group. Also, a higher degree of intergroup variability for the [^{18}F]FPe-(trN-PEG)@FH in almost all organs was found in diseased animals, as compared to control ones. The small number of animals used for the imaging experiments (n=5 for both groups) shall be regarded as a limitation of the present study. The characterization by PET/CT imaging and, to the best of the authors' knowledge, the labelling and imaging of such an important molecule has never been reported with a PET tracer before, thus representing one of the main novelties of this study. Another limitation is the absence of a plasma stability test of the ^{18}F-labeled FH tracer, which will be performed in future experiments.

Since FH is the main regulator of the alternative pathway of complement (40), we then assessed whether the FH concentrate was effective in correcting the severe complement alternative pathway dysregulation in Cfh-/- mice, a model of C3G (41). In these animals, C3 convertase activation in the fluid phase is unrestricted, leading to C3 consumption. Finding that the reduction in serum C3 levels observed in Cfh-/- mice was significantly limited by treatment with the FH concentrate, documented *in vivo* that the product possesses the expected complement regulatory activity. Intense glomerular deposits of C3 products are observed both in Cfh-/- mice and in patients with C3G (42), and this reflects hyperactivation of the complement alternative pathway. Indeed, when we analyzed kidney tissue through immunofluorescence experiments, we found marked staining of C3 in the capillary wall in Cfh-/- mice. Treatment with the FH concentrate was able to significantly reduce glomerular C3 staining in Cfh-/- mice which was notably almost completely normalized after five daily administrations of the FH concentrate. These results indicate that the FH concentrate was effective in limiting C3 activation and also favored the clearance of C3 deposits from the glomerular tuft.

Conclusions

In summary, our findings provide important insights into the potential benefits of the use of discarded plasma fractionation intermediates for the purification of the natural complement inhibitor FH. PET/CT imaging was used to explore the *in vivo* biodistribution of FH, a protein that is part of a complex and highly regulated process and, to the best of authors' knowledge, the labeling and imaging of such an important molecule has never been reported before, thus representing a relevant novelty of this study and a promising tool for future pharmacology assessment. All the results reported suggest that the obtained FH concentrate could represent a promising therapeutic approach for patients with C3G and FH deficiency (43), but also in more common C3G/MPGN patients with C3NeF-dependent C3 convertase stabilization, since FH accelerates the decay of the C3 convertase complex (44). Administration of exogenous FH could be useful also in other conditions associated with alternative pathway dysregulation ranging from the rare hematological disease paroxysmal nocturnal hemoglobinuria, to the common blinding disease age-related macular degeneration (3) Considering the human and economic cost of plasma-derived products and the shortage of blood and its derivatives, the use of plasma waste fractions for the therapy of orphan rare diseases will represent an ethical and essential approach.

Data availability statement

The datasets presented in this study can be found in online repositories. The names of the repository/repositories and accession number(s) can be found below: PXD050268 (ProteomeXchange).

Ethics statement

The studies involving animal participants were reviewed and approved by Dr. Silvia Burchielli, Centro Biomedicina Sperimentale, Area della Ricerca del CNR, Pisa. The study was conducted in accordance with the local legislation and institutional requirements.

Author contributions

FM: Conceptualization, Data curation, Formal analysis, Investigation, Supervision, Writing – original draft, Writing – review & editing. GP: Methodology, Software, Writing – review & editing. SB: Investigation, Methodology, Writing – original draft, Writing – review & editing. AL: Investigation, Methodology, Writing – review & editing. DP: Methodology, Writing – review & editing. SR: Investigation, Methodology, Writing – review & editing. EC: Methodology, Writing – review & editing. FN: Writing – review & editing. AM: Writing – review & editing. RD: Writing – review & editing. AC: Investigation, Methodology, Writing – review & editing. CF: Data curation, Writing – review & editing, Conceptualization, Project administration, Resources. MN: Investigation, Methodology, Writing – review & editing, Formal analysis. PS: Data curation, Investigation, Methodology, Writing – review & editing. GR: Investigation, Methodology, Resources, Supervision, Validation, Writing – review & editing.

Funding

The author(s) declare financial support was received for the research, authorship, and/or publication of this article. The author (s) declare financial support was received for the research, authorship of this article. This study was funded byPOR CREO FESR 2007–2013 Activity 1.1 – Intervention Line 1.1.C.

Acknowledgments

We thank CISUP (Centre for Instrumentation Sharing - University of Pisa) for the acquisition and elaboration of the LC-HR-MS data.

Conflict of interest

Authors FM, CF, and AL were employed by Kedrion.

The remaining authors declare that the research was conducted in the absence of any commercial or financial relationships that could be construed as a potential conflict of interest.

Publisher's note

All claims expressed in this article are solely those of the authors and do not necessarily represent those of their affiliated organizations, or those of the publisher, the editors and the reviewers. Any product that may be evaluated in this article, or claim that may be made by its manufacturer, is not guaranteed or endorsed by the publisher.

Supplementary material

The Supplementary Material for this article can be found online at: https://www.frontiersin.org/articles/10.3389/fimmu.2024.1334151/full#supplementary-material

References

1. Rodríguez de Córdoba S, Esparza-Gordillo J, Goicoechea de Jorge E, Lopez-Trascasa M, Sánchez-Corral P. The human complement factor H: functional roles, genetic variations and disease associations. *Mol Immunol*. (2004) 41:355–67. doi: 10.1016/j.molimm.2004.02.005

2. Ripoche J, Day AJ, Harris TJ, Sim RB. The complete amino acid sequence of human complement factor H. *Biochem J*. (1988) 249:593–602. doi: 10.1042/bj2490593

3. Lucientes-Continente L, Márquez-Tirado B, Goicoechea de Jorge E. The factor H protein family: the switchers of the complement alternative pathway. *Immunol Rev*. (2023) 313:25–45. doi: 10.1111/imr.13166

4. Noris M, Remuzzi G. Translational mini-review series on complement factor H: therapies of renal diseases associated with complement factor H abnormalities: atypical haemolytic uraemic syndrome and membranoproliferative glomerulonephritis. *Clin Exp Immunol*. (2008) 151:199–209. doi: 10.1111/j.1365-2249.2007.03558.x

5. Gurevich E, Landau D. Pharmacological management of atypical hemolytic uremic syndrome in pediatric patients: current and future. *Pediatr Drugs*. (2023) 25: 193–202. doi: 10.1007/s40272–022-00555–6

6. Noris M, Daina E, Remuzzi G. Membranoproliferative glomerulonephritis: no longer the same disease and may need very different treatment. *Nephrology dialysis transplantation: Off Publ Eur Dialysis Transplant Assoc - Eur Renal Assoc*. (2021) 38(2): 283–290. doi: 10.1093/ndt/gfab281

7. Scholl HP, Fleckenstein M, Charbel Issa P, Keilhauer C, Holz FG, Weber BH. An update on the genetics of age-related macular degeneration. *Mol Vision*. (2007) 13:196–205.

8. Ruggenenti P, Noris M, Remuzzi G. Thrombotic microangiopathy, hemolytic uremic syndrome, and thrombotic thrombocytopenic purpura. *Kidney Int*. (2001) 60:831–46. doi: 10.1046/j.1523-1755.2001.060003831.x

9. Noris M, Caprioli J, Bresin E, Mossali C, Pianetti G, Gamba S, et al. Relative role of genetic complement abnormalities in sporadic and familial ahus and their impact on clinical phenotype. *Clin J Am Soc Nephrology: CJASN*. (2010) 5:1844–59. doi: 10.2215/cjn.02210310

10. Noris M, Remuzzi G. C3g and ig-mpgn - treatment standard. *Nephrology dialysis transplantation: Off Publ Eur Dialysis Transplant Assoc - Eur Renal Assoc*. (2023) 5(10): 1844–59 . doi: 10.1093/ndt/gfad182

11. Waters AM, Licht C. Ahus caused by complement dysregulation: new therapies on the horizon. *Pediatr Nephrol (Berlin Germany)*. (2011) 26:41–57. doi: 10.1007/s00467–010-1556–4

12. Fakhouri F, de Jorge EG, Brune F, Azam P, Cook HT, Pickering MC. Treatment with human complement factor H rapidly reverses renal complement deposition in factor H-deficient mice. *Kidney Int*. (2010) 78:279–86. doi: 10.1038/ki.2010.132

13. Kasanmoentalib ES, Valls Serón M, Engelen-Lee JY, Tanck MW, Pouw RB, van Mierlo G, et al. Complement factor H contributes to mortality in humans and mice with bacterial meningitis. *J Neuroinflamm*. (2019) 16:279. doi: 10.1186/s12974–019-1675–1

14. Michelfelder S, Parsons J, Bohlender LL, Hoernstein SNW, Niederkrüger H, Busch A, et al. Moss-produced, glycosylation-optimized human factor H for therapeutic application in complement disorders. *J Am Soc Nephrology: JASN*. (2017) 28:1462–74. doi: 10.1681/asn.2015070745

15. Kaidoh T, Fujita T, Takata Y, Natsuume-Sakai S, Takahashi M. Simplified method for purification of mouse beta 1h. *Complement (Basel Switzerland)*. (1984) 1:44–51.

16. Carron JA, Bates RC, Smith AI, Tetoz T, Arellano A, Gordon DL, et al. Factor H co-purifies with thrombospondin isolated from platelet secretate. *Biochim Biophys Acta*. (1996) 1289:305–11. doi: 10.1016/0304-4165(95)00095-X

17. Daha MR, van Es LA. Isolation, characterization, and mechanism of action of rat beta 1h. *J Immunol (Baltimore Md: 1950)*. (1982) 128:1839–43. doi: 10.4049/jimmunol.128.4.1839

18. Sim RB, DiScipio RG. Purification and structural studies on the complement-system control protein beta 1h (Factor H). *Biochem J*. (1982) 205:285–93. doi: 10.1042/bj2050285

19. Cohn EJ, Strong LE, Hughes WL, Mulford DJ, Ashworth JN, Melin M, et al. Preparation and properties of serum and plasma proteins; a system for the separation into fractions of the protein and lipoprotein components of biological tissues and fluids. *J Am Chem Soc*. (1946) 68:459–75. doi: 10.1021/ja01207a034

20. Brandstatter H, Schulz P, Polunic I, Kannicht C, Kohla G, Romisch J. Purification and biochemical characterization of functional complement factor H from human plasma fractions. *Vox sanguinis*. (2012) 103:201–12. doi: 10.1111/j.1423-0410.2012.01610.x

21. Pascali G, Berton A, DeSimone M, Wyatt N, Matesic L, Greguric I, et al. Hardware and software modifications on the advion nanotek microfluidic platform to extend flexibility for radiochemical synthesis. *Appl Radiat isotopes: including data instrumentation Methods Use agriculture industry Med*. (2014) 84:40–7. doi: 10.1016/j.apradiso.2013.10.020

22. Perez-Riverol Y, Bai J, Bandla C, García-Seisdedos D, Hewapathirana S, KamatChinathan S, et al. The pride database resources in 2022: A hub for mass spectrometry-based proteomics evidences. *Nucleic Acids Res*. (2022) 50:D543–d52. doi: 10.1093/nar/gkab1038

23. Berra S, Clivio A. Rapid isolation of pure complement factor H from serum for functional studies by the use of a monoclonal antibody that discriminates fh from all the other isoforms. *Mol Immunol*. (2016) 72:65–73. doi: 10.1016/j.molimm.2016.03.001

24. Cugno M, Berra S, Depetri F, Tedeschi S, Griffini S, Grovetti E, et al. Igm autoantibodies to complement factor H in atypical hemolytic uremic syndrome. *J Am Soc Nephrology: JASN*. (2021) 32:1227–35. doi: 10.1681/asn.2020081224

25. Mařík J, Sutcliffe JL. Click for pet: rapid preparation of [18f]Fluoropeptides using cui catalyzed 1,3-dipolar cycloaddition. *Tetrahedron Lett*. (2006) 47:6681–4. doi: 10.1016/j.tetlet.2006.06.176

26. Matesic L, Kallinen A, Greguric I, Pascali G. Dose-on-demand production of diverse (18)F-radiotracers for preclinical applications using a continuous flow microfluidic system. *Nucl Med Biol*. (2017) 52:24–31. doi: 10.1016/j.nucmedbio.2017.05.004

27. Panetta D, Belcari N, Tripodi M, Burchielli S, Salvadori P, Del Guerra A. Performance evaluation of the ct component of the iris pet/ct preclinical tomograph. *Nucl Instruments Methods Phys Res Section A: Accelerators Spectrometers Detectors Associated Equip*. (2015) 805: 134–44. doi: 10.1016/j.nima.2015.08.044

28. Belcari N, Camarlinghi N, Ferretti S, Iozzo P, Panetta D, Salvadori PA, et al. Nema nu-4 performance evaluation of the iris pet/ct preclinical scanner. *IEEE Trans Radiat Plasma Med Sci*. (2017) 1:301–9. doi: 10.1109/TRPMS.2017.2707300

29. Panetta D, Guzzardi MA, La Rosa F, Granziera F, Terlizzi D, Kusmic C, et al. High-resolution cardiac positron emission tomography/computed tomography for small animals. *J Vis Exp*. (2022) 16: 190. doi: 10.3791/64066

30. Brodniewicz-Proba T. Human plasma fractionation and the impact of new technologies on the use and quality of plasma-derived products. *Blood Rev*. (1991) 5:245–57. doi: 10.1016/0268–960X(91)90016–6

31. Pascali G, Watts P, Salvadori PA. Microfluidics in radiopharmaceutical chemistry. *Nucl Med Biol*. (2013) 40:776–87. doi: 10.1016/j.nucmedbio.2013.04.004

32. Koskinen AR, Cheng ZZ, Pickering MC, Kairemo K, Meri T, Cook HT, et al. Distribution of exogenous complement factor H in mice. *In vivo*. *Scandinavian J Immunol*. (2018) 88:e12671. doi: 10.1111/sji.12671

33. Badar A, DeFreitas S, McDonnell JM, Yahya N, Thakor D, Razavi R, et al. Recombinant complement receptor 2 radiolabeled with [99mtc(Co)3]+: A potential new radiopharmaceutical for imaging activated complement. *PloS One*. (2011) 6: e18275. doi: 10.1371/journal.pone.0018275

34. Kamala O, Malik TH, Hallam TM, Cox TE, Yang Y, Vyas F, et al. Homodimeric minimal factor H: *in vivo* tracking and extended dosing studies in factor H deficient mice. *Front Immunol*. (2021) 12:752916. doi: 10.3389/fimmu.2021.752916

35. Hotchko M, Robert P. Recent market status and trends of fractionated plasma products. *Ann Blood*. (2018) 3. doi: 10.21037/aob

36. Zanardi A, Nardini I, Raia S, Conti A, Ferrini B, D'Adamo P, et al. New orphan disease therapies from the proteome of industrial plasma processing waste- a treatment for aceruloplasminemia. *Commun Biol*. (2024) 7:140. doi: 10.1038/s42003–024-05820–7

37. Nan R, Gor J, Perkins SJ. Implications of the progressive self-association of wild-type human factor H for complement regulation and disease. *J Mol Biol*. (2008) 375:891–900. doi: 10.1016/j.jmb.2007.11.015

38. Pangburn MK, Rawal N, Cortes C, Alam MN, Ferreira VP, Atkinson MA. Polyanion-induced self-association of complement factor H. *J Immunol (Baltimore Md: 1950)*. (2009) 182:1061–8. doi: 10.4049/jimmunol.182.2.1061

39. Perkins SJ, Nealis AS, Sim RB. Oligomeric domain structure of human complement factor H by X-ray and neutron solution scattering. *Biochemistry*. (1991) 30:2847–57. doi: 10.1021/bi00225a017

40. Lachmann PJ. The amplification loop of the complement pathways. *Adv Immunol*. (2009) 104:115–49. doi: 10.1016/s0065–2776(08)04004–2

41. Pickering MC, Cook HT, Warren J, Bygrave AE, Moss J, Walport MJ, et al. Uncontrolled C3 activation causes membranoproliferative glomerulonephritis in mice deficient in complement factor H. *Nat Genet*. (2002) 31:424–8. doi: 10.1038/ng912

42. Noris M, Remuzzi G. Glomerular diseases dependent on complement activation, including atypical hemolytic uremic syndrome, membranoproliferative glomerulonephritis, and C3 glomerulopathy: core curriculum 2015. *Am J Kidney diseases: Off J Natl Kidney Foundation*. (2015) 66:359–75. doi: 10.1053/j.ajkd.2015.03.040

43. Meuleman MS, Vieira-Martins P, El Sissy C, Audard V, Baudouin V, Bertrand D, et al. Rare variants in complement gene in C3 glomerulopathy and immunoglobulin-mediated membranoproliferative gn. *Clin J Am Soc Nephrology: CJASN*. (2023) 18:1435–45. doi: 10.2215/cjn.0000000000000252

44. Donadelli R, Pulieri P, Piras R, Iatropoulos P, Valoti E, Benigni A, et al. Unraveling the molecular mechanisms underlying complement dysregulation by nephritic factors in C3g and ic-mpgn. *Front Immunol*. (2018) 9:2329. doi: 10.3389/fimmu.2018.02329

Frontiers in Immunology

Explores novel approaches and diagnoses to treat immune disorders.

The official journal of the International Union of Immunological Societies (IUIS) and the most cited in its field, leading the way for research across basic, translational and clinical immunology.

Discover the latest Research Topics

See more →

Frontiers

Avenue du Tribunal-Fédéral 34
1005 Lausanne, Switzerland
frontiersin.org

Contact us

+41 (0)21 510 17 00
frontiersin.org/about/contact